

Topics in Organometallic Chemistry 61

Carmen Claver *Editor*

Rhodium Catalysis

 Springer

Editorial Board

M. Beller, Rostock, Germany
P.H. Dixneuf, Rennes CX, France
J. Dupont, Porto Alegre, Brazil
A. Fürstner, Mülheim, Germany
F. Glorius, Münster, Germany
L.J. Gooßen, Kaiserslautern, Germany
T. Ikariya, Tokyo, Japan
S.P. Nolan, Ghent, Belgium
J. Okuda, Aachen, Germany
L.A. Oro, Zaragoza, Spain
M. Willis, Oxford, United Kingdom
Q.-L. Zhou, Tianjin, China

Aims and Scope

The series *Topics in Organometallic Chemistry* presents critical overviews of research results in organometallic chemistry. As our understanding of organometallic structure, properties and mechanisms increases, new ways are opened for the design of organometallic compounds and reactions tailored to the needs of such diverse areas as organic synthesis, medical research, biology and materials science. Thus the scope of coverage includes a broad range of topics of pure and applied organometallic chemistry, where new breakthroughs are being achieved that are of significance to a larger scientific audience.

The individual volumes of *Topics in Organometallic Chemistry* are thematic. Review articles are generally invited by the volume editors. All chapters from *Topics in Organometallic Chemistry* are published OnlineFirst with an individual DOI. In references, *Topics in Organometallic Chemistry* is abbreviated as *Top Organomet Chem* and cited as a journal.

More information about this series at <http://www.springer.com/series/3418>

Carmen Claver

Editor

Rhodium Catalysis

With contributions by

D. Bonincontro · A.J. Burnie · R. Castarlenas · M. Cettolin ·
A.B. Cuenca · A. Cunillera · J.G. de Vries · P.A. Evans ·
E. Fernández · E.J. García-Suárez · A.D. Giuseppe ·
C. Godard · K. Kahr · P. Kalck · L.A. Oro · P. Puylaert ·
E.A. Quadrelli · A. Riisager · A. Ruiz · M. Urrutigoity



Springer

Editor

Carmen Claver
Facultat de Química
Universitat Rovira i Virgili
Tarragona, Spain

ISSN 1436-6002 ISSN 1616-8534 (electronic)
Topics in Organometallic Chemistry
ISBN 978-3-319-66663-1 ISBN 978-3-319-66665-5 (eBook)
DOI 10.1007/978-3-319-66665-5

Library of Congress Control Number: 2017953213

© Springer International Publishing AG 2018

This work is subject to copyright. All rights are reserved by the Publisher, whether the whole or part of the material is concerned, specifically the rights of translation, reprinting, reuse of illustrations, recitation, broadcasting, reproduction on microfilms or in any other physical way, and transmission or information storage and retrieval, electronic adaptation, computer software, or by similar or dissimilar methodology now known or hereafter developed.

The use of general descriptive names, registered names, trademarks, service marks, etc. in this publication does not imply, even in the absence of a specific statement, that such names are exempt from the relevant protective laws and regulations and therefore free for general use.

The publisher, the authors and the editors are safe to assume that the advice and information in this book are believed to be true and accurate at the date of publication. Neither the publisher nor the authors or the editors give a warranty, express or implied, with respect to the material contained herein or for any errors or omissions that may have been made. The publisher remains neutral with regard to jurisdictional claims in published maps and institutional affiliations.

Printed on acid-free paper

This Springer imprint is published by Springer Nature
The registered company is Springer International Publishing AG
The registered company address is: Gewerbestrasse 11, 6330 Cham, Switzerland

Preface

Rhodium coordination complexes or systems formed with rhodium in the presence of ligands, in particular phosphorus derivatives, have been extensively and successfully used as catalytic precursors in homogeneous catalysis for many years. The particular properties of both oxidation states of Rh(I) and Rh(III) allow for the successive oxidative addition, insertion, reductive elimination steps, and facilitate the activity and efficiency of the rhodium catalysts. The selectivity can be controlled and modified due to the versatility and modification possibilities of the ligands coordinated to the rhodium center. After the breakthrough of the application of $\text{RhCl}(\text{PPh}_3)_3$ as a hydrogenation catalyst, rhodium catalysis blossomed enormously and cationic rhodium(I) phosphorus systems were also applied in hydrogenation reactions, being particularly attractive due to the use of chiral ligands allowing for the enantioselective hydrogenation reaction of prochiral substrates. The main characteristic of catalytic rhodium systems is the high selectivity and enantioselectivity achieved in most of the homogeneous catalytic processes. A relevant example is the hydroformylation reaction which involves a one-carbon chain elongation by the addition of carbon monoxide and hydrogen across a C=C double bond. It is well known that this is one of the main industrial processes carried out by homogeneous catalysis concerning the formation of aldehydes from alkenes. The use of the appropriate ligands allows the control of the regioselectivity and more recently the control of the enantioselectivity.

Many relevant books and reviews have been published about rhodium-catalyzed processes. This new volume “*Rhodium catalysis*” in the series “*Topics in Organometallic Chemistry*” intends to be an update of relevant, well-known reactions, as well as a summary of the lesser known applications of rhodium catalysis in organic transformations, together with topics related with sustainability. All the chapters are authored by research experts in each one of the topics presented.

It is shown in this volume how for hydrogenation reactions the monodentate ligands provide opportunities that would have been impossible to imagine with the bidentate ligands, owing to the possibility of producing complexes based on two different ligands. Rhodium-catalyzed C–H and C–X borylation is extensively reviewed in this volume. This area has received growing interest based on the

strong influence of rhodium to activate H–B and B–B bonds, the power of the ligands that modify the rhodium center to induce high levels of chemo-, regio-, and enantioselectivity, and the unrestricted mechanisms that can be deduced with the aid of density functional theory (DFT) calculations.

The impressive advances observed in recent years in the field of asymmetric hydroformylation are examined in this volume and conclude that the key to achieving high enantioselectivities is not the type of phosphorus function involved in the coordination to the metal, but rather the particular spatial arrangement of the coordinated ligand. Supramolecular strategies which have been very successful in asymmetric hydroformylation are also considered, indicating that the control of the second coordination sphere could be the key to achieving selectivity for the more challenging substrates.

Tandem reactions demonstrate how the efficiency of the reaction is improved when operating in the absence of isolating the intermediates, leading to the formation of more complex molecules in an economic manner. It is shown in this work how the rhodium-catalyzed tandem carbonylation reactions, involving the hydroformylation of an alkene followed by the transformation of the aldehyde product with a second reagent, can yield important chemicals for organic synthesis.

Other reactions are included in this volume, for example the rhodium-catalyzed decarbonylation developed over the last 50 years which has resulted in a wide range of reported catalyst systems and reaction protocols. The applications of these rhodium-catalyzed decarbonylation reactions are surveyed and discussed, including cross-coupling reactions, tandem reactions, and alternative methodologies for process intensification. The advances in rhodium-catalyzed cyclocarbonylation reactions are also discussed, including a variety of methods for the synthesis of carbo- and heterocyclic rings of different sizes, diastereoselective and asymmetric approaches, and the application of these reactions in the total synthesis of the important natural products (+)-asteriscanolide and (–)-ingenol. Rhodium catalysis for C–S bond formation is also considered. The recent developments in the reactions of cross-coupling, C–H activation, metathesis, thiolation, carbothiolation, and hydrothiolation for the C–S bond formation catalyzed by rhodium complexes, particularly highlighting the synthetic and mechanistic aspects, are summarized.

This volume also includes a chapter discussing the role of rhodium-based catalysts in homogenous and heterogeneous catalyzed CO₂ reductions, with well-described mechanisms.

This work presents the advances, new perspectives, and applications in a variety of representative rhodium-catalyzed reactions and will therefore be useful for researchers, graduate students, and synthetic chemists at all levels in academia and industry.

Tarragona, Spain

Carmen Claver

Contents

Rhodium-Catalyzed C–B Bond Formation	1
Ana B. Cuenca and Elena Fernández	
Rhodium Catalysts for C–S Bond Formation	31
Andrea Di Giuseppe, Ricardo Castarlenas, and Luis A. Oro	
Tandem Rhodium Carbonylation Reactions	69
Philippe Kalck and Martine Urrutigoity	
Asymmetric Hydroformylation Using Rhodium	99
Anton Cunillera, Cyril Godard, and Aurora Ruiz	
Rhodium Catalyzed Decarbonylation	145
Eduardo J. García-Suárez, Klara Kahr, and Anders Riisager	
Recent Developments in Rhodium-Catalyzed Cyclocarbonylation Reactions	167
Andrew J. Burnie and P. Andrew Evans	
Rhodium-Catalysed Hydrogenations Using Monodentate Ligands	231
Mattia Cettolin, Pim Puylaert, and Johannes G. de Vries	
CO₂ Reduction Reactions by Rhodium-Based Catalysts	263
Danilo Bonincontro and Elsje Alessandra Quadrelli	
Index	283

Rhodium-Catalyzed C–B Bond Formation

Ana B. Cuenca and Elena Fernández

Abstract This chapter focuses on Rh-activation of boron-based reagents and its assistance in efficient catalytic borylation reactions. The introduction is a critical reflection of the importance that hydroborane reagents have had in reactions such as Rh-catalyzed hydroboration for the last 30 years. The next section shows a brief history of the Rh–B bond formation from Rh complexes and diboron reagents. The most relevant advances in Rh-catalyzed diboration are summarized in the following section. In the fourth section, examples of Rh-catalyzed β -boration of α,β -unsaturated substrates are collected, completing the fifth section with a description and comments about the new trends on Rh-catalyzed C–H and C–X borylation. At the end of this chapter, the authors compile a summary and their perspective for the related field from a mechanistic point of view.

Keywords Borylation • Catalysis • C–B bond • Rhodium • Stereoselectivity

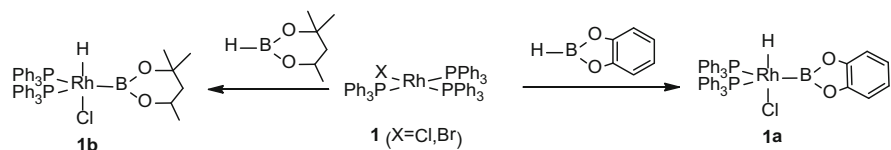
Contents

1	Introduction: 30 Years on Rh-Catalyzed Hydroboration	2
2	Activation of Diboron Reagents by Rhodium Complexes	5
2.1	Rh-Activation of Diboron Reagents by Oxidative Addition	5
2.2	Rh-Activation of Diboron Reagents by σ -Bond Metathesis	10
3	Rh-Catalyzed Diboration Reaction	11
3.1	Rh-Catalyzed Diboration Reaction of C–C Multiple Bonds	11
3.2	Rh-Catalyzed Diboration Reaction of C–X Multiple Bonds	18
4	Rh-Catalyzed β -Boration of α,β -Unsaturated Carbonyl Compounds	18

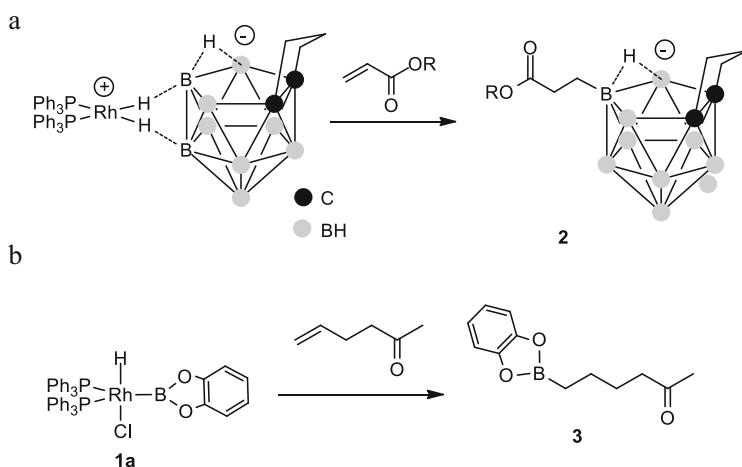
5 Rh-Catalyzed C–H and C–X (X = F, CN, OMe) Borylation with Diboron Reagents	20
6 Summary and Outlook	26
References	26

1 Introduction: 30 Years on Rh-Catalyzed Hydroboration

The first isolation of a σ -rhodium–boron complex was carried by Kono et al. [1] (Scheme 1) despite the fact that several previous attempts were conducted to react rhodium complexes with series of carboranes and polyboranes [2–6]. The hydroborane reagents selected by H. Kono and co-workers were the cyclic secondary boronate esters catecholborane (**HBcat**) and neopentylborane (**HBneop**). The complex $[\text{RhX}(\text{PPh}_3)_3]$ (X = Cl, Br) was able to activate the B–H bond of **HBcat** and **HBneop** via oxidative addition. That early key experiment led to the eventual development of rhodium-complex-catalyzed hydroboration of alkenes. The first examples of this type of catalysis (Scheme 2) corroborated the potential power of the original experiment [7, 8]. In particular the use of catecholborane, by Mannig and Noth [7], was the model on which most further experimentation has been based (Scheme 2b). Burgess and Ohlmeyer were the first to demonstrate catalytic

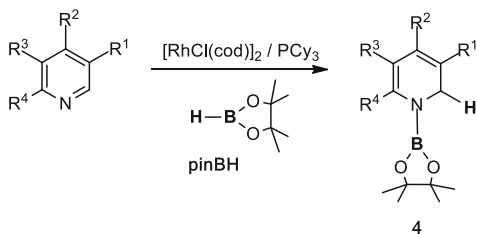


Scheme 1 First isolated σ -rhodium–boron complex

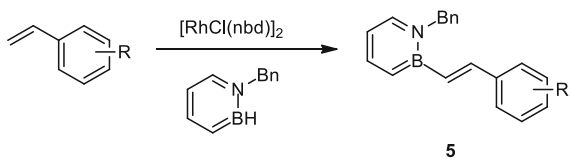


Scheme 2 First Rh-catalyzed hydroboration

Scheme 3 Rhodium-catalyzed 1,2-hydroboration of substituted pyridines



Scheme 4 Rhodium-catalyzed B–H activation of azaborines



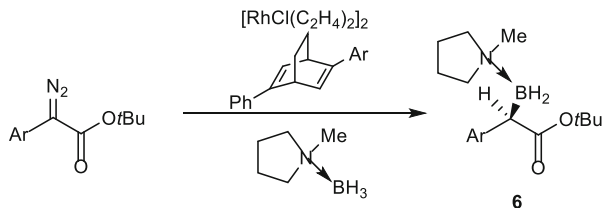
asymmetric hydroboration of alkenes [9], and since then the field has been extensively covered and much attention has been focused for the synthesis of target organoboronates with catecholborane (**HBcat**) and pinacolborane (**HBpin**) (An early review on Rh-catalyzed hydroboration: [10]), [11–26], (The more recent review on catalyzed hydroboration: [27]).

After 30 years from the discovery of the Rh-catalyzed hydroboration of unsaturated bonds [8], this section aims to gather the current trends dealing with B–H bond activation by means of this metal. One of the interesting directions is focussed on dearomatizing unactivated pyridines to gain access to 1,2-dihydropyridines via rhodium-catalyzed hydroboration with pinacolborane (**HBpin**) [28]. Interestingly, pyridine can undergo addition of pinacolborane at 50°C in the presence of $[\text{Rh}(\mu^2\text{-Cl})(\text{cod})]_2$ as catalyst precursor, giving *N*-boryl-1,2-dihydropyridine in a high yield (Scheme 3). The selective 1,2-hydroboration also takes place in the reactions of substituted pyridines.

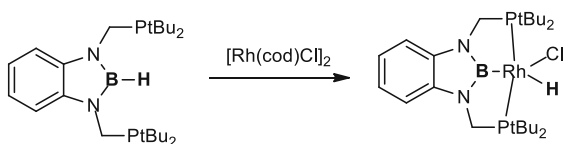
Interestingly, alkenyl pinacolboronates can be obtained as by-products from the hydroboration process of activated aryl- or alkoxyethenes with pinacolborane in the presence of Rh(I) complexes. However, in a recent work, also simple aliphatic terminal alkenes can easily react with pinacolborane at ambient temperature to afford dehydrogenative borylation compounds as the major product when *i*Pr-Foxap is used as ligand with the cationic rhodium(I) complex $[\text{Rh}(\text{cod})_2]\text{BF}_4$, in the presence of norbornene, which acts as the sacrificial hydrogen acceptor [29]. Since terminal alkenes are more easily accessible and often more desirable starting materials than terminal alkynes, the reaction represents an interesting alternative to alkyne hydroboration. Contemporarily, it has been developed the first example of catalytic B–H activation of azaborines by $[\text{Rh}(\mu^2\text{-Cl})(\text{nbd})]_2$ leading to a new family of stilbene related derivatives through dehydrogenative borylation (Scheme 4) [30]. Remarkably, it has been possible to isolate only the *trans*-BN stilbene isomer **5** among all the possible reaction products obtained under the optimized conditions.

The Rh(I) neutral catalyst precursor $[\text{Rh}(\mu^2\text{-Cl})(\text{cod})]_2$ and its analogue $[\text{Rh}(\mu^2\text{-Cl})(\text{C}_2\text{H}_4)_2]_2$, have recently shown to be able to catalyze the asymmetric B–H insertion of α -diazo carbonyl compounds with easily available amine–borane

Scheme 5 Rhodium-catalyzed asymmetric B–H insertion reactions of α -diazooesters



Scheme 6 Synthesis of an Rh-PBP pincer complex

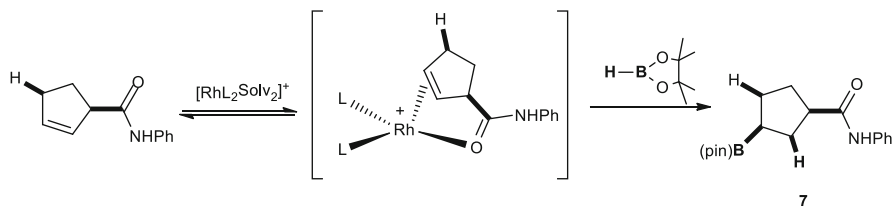


adducts using a newly developed C_1 -symmetric chiral diene as ligand (Scheme 5) [31]. Rh(I)-carbene directed B–H insertion example represents an attractive and promising approach for synthesis of highly enantioenriched organoboron compounds, allowing for the efficient construction of α -boryl esters and ketones with excellent enantioselectivities (up to 99% ee) under exceptionally mild conditions.

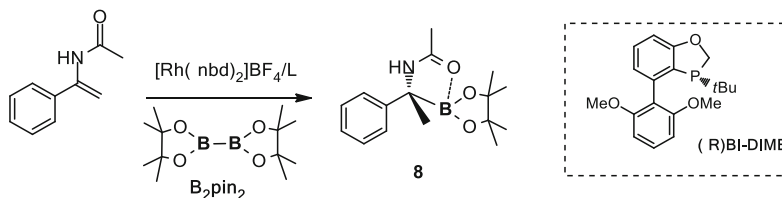
The application of a B–H reagent as a tridentate PBP ligand to Rh has also been disclosed. The PBP ligand seems to be a strong σ -donor ligand for the metal complex which can be easily achieved by hydroboration of the diamineborane to $[\text{Rh}(\mu^2\text{-Cl})(\text{cod})]_2$. Considering the very strong *trans*-influence of the boryl ligand, a low-coordinated species having a vacant site in the position *trans* to the boryl ligand may be stabilized (Scheme 6) [32].

Current interest is also devoted to the directed Rh-catalyzed hydroboration reaction to gain more insights about selective C–B formation via a two-point binding mechanism, depending on the polifunctionality of the alkene [33–35]. The main characteristics of the two-point binding mechanism imply that the substrate has two coordinating groups, the alkene and another functional group that can chelate the substrate to the Rh(I) catalyst leading to favored intermediates that end up with a selective hydroborated product (Scheme 7). But also the same substrate directed hydroboration can be performed in an enantioselective way towards the synthesis of chiral α -amino tertiary boronic esters by rhodium-catalyzed hydroboration of α -arylenamides using the diboron reagent bis(pinacolato)diboron ($\mathbf{B}_2\text{pin}_2$), as the boron source (Scheme 8) [36]. Interestingly, the transformation seems to proceed through hydroboration over diboration of acyl imine pathway, despite the use of a diboron reagent.

During the last three decades, the use of pinacolborane (\mathbf{HBpin}) has replaced catecholborane (\mathbf{HBcat}) as the borane reagent due to the more enhanced stability of the resulted organoboronate compounds (First report on the use of \mathbf{HBpin} : [37]), [38]. But now the use of diboron reagents, such as bis(pinacolato)diboron ($\mathbf{B}_2\text{pin}_2$) [39], is becoming even more convenient and therefore the following sections are focussed on the activation of the diboron reagents by Rh complexes [40] and their application to other reactions such as diboration, β -boration, and C–X or C–H borylations.



Scheme 7 Model two-point binding mechanism for Rh-catalyzed reaction



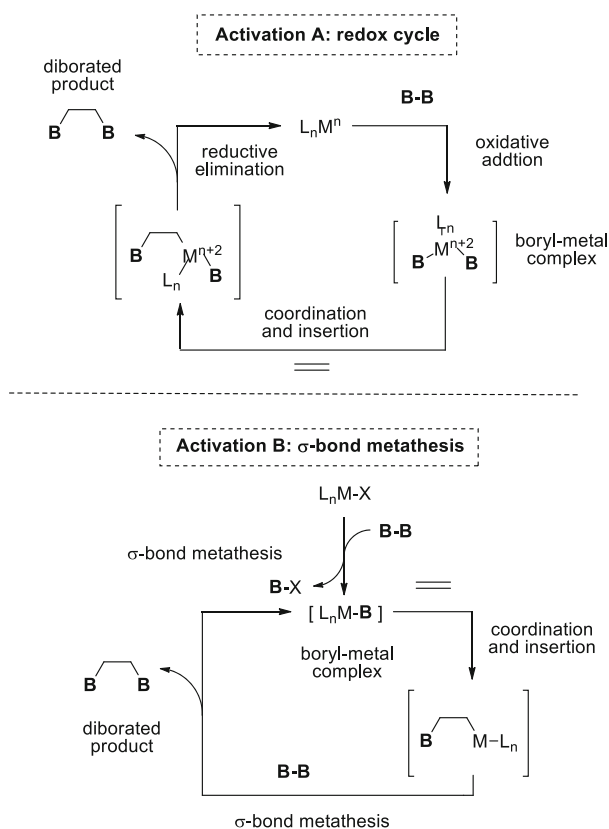
Scheme 8 Remarkable Markovnikov selectivity and enantioselectivity to form chiral tertiary boronic esters by Rh-catalyzed hydroboration

2 Activation of Diboron Reagents by Rhodium Complexes

Rh-promoted borylation reactions with diboron reagents are a powerful tool for facile synthesis of various types of organodiboronate compounds. From a mechanistic point of view, the activation of diboron reagents by Rh complexes can be divided mainly into two categories. One comprises a redox process of the Rh (I) center via oxidative addition of the B–B bonds to form bisborylrhodium complexes (activation A, Scheme 9) and the other approach implies generation of borylrhodium species by σ -bond metathesis pathway between the Rh–X bond and the B–B bond (activation B, Scheme 9). In this case the oxidation state of the rhodium center does not change during the catalytic cycle.

2.1 Rh-Activation of Diboron Reagents by Oxidative Addition

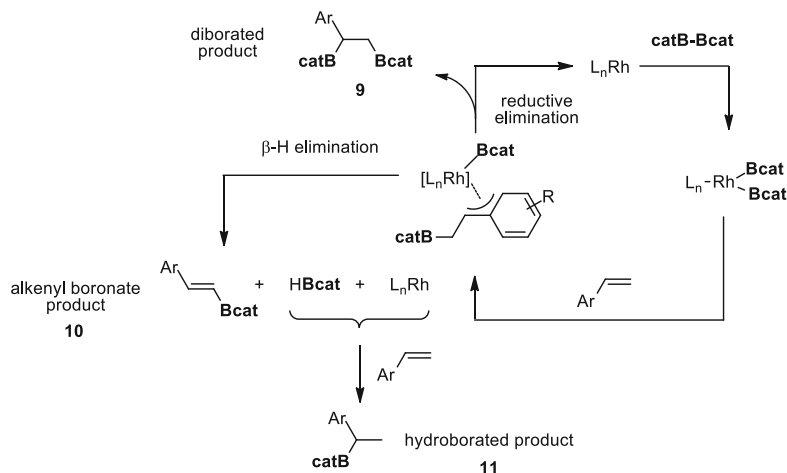
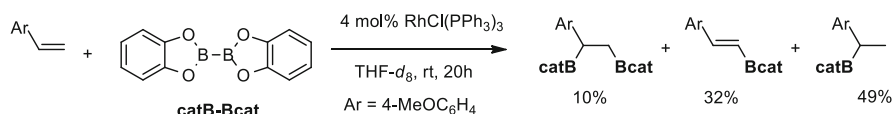
Marder, Westcott, and Baker described in 1995, for the first time, a $[\text{RhCl}(\text{PPh}_3)_3]$ -catalyzed diboration of 4-methoxy styrene using B_2cat_2 . Since this exceptional discovery, many examples of the extraordinary ability that this metal has to activate diboron reagents have been nicely illustrated [41]. The corresponding diborated compound **9** was formed in modest yield because of the simultaneous significant generation of alkenylboronate **10** (via dehydrogenative borylation process) and the hydroborated product **11**. The proposed catalytic cycle (Scheme 10) involved generation of bisborylrhodium complex via oxidative addition, which should



Scheme 9 Activation modes of diboron reagents by Rh complexes and subsequent reactivity with alkenes

undergo then to alkene insertion, followed by reductive elimination to create the new C–B bond. Competitive fast β -hydride elimination will account for the observation of **10** and **HBCat**, which can participate in the Rh-catalyzed hydroboration generation of monoborylalkane **11**. The rhodium-catalyzed diboration of olefins became more efficient than the double hydroboration protocol of the same substrates [42] and therefore opened a nonexisting platform to generate a chemoselective route towards the diborated product as well as made possible to run the reaction in an enantioselective manner by selection of the appropriate chiral phosphine in the Rh(I) complex [43, 44].

Although, as pointed out, oxidative addition of the B–B bond in **B₂cat₂** was proposed as a key step, former evidence for this process came as well from the groups of Marder and Norman [45]. A number of different tetra(alkoxy)diboron reagents were activated via initial dissociation of a phosphine ligand in the metal complex and subsequent oxidative addition by either $[RhCl(PPh_3)_3]$ or $[Rh(\mu^2-Cl)(PPh_3)_2]_2$. A series of Rh(III) complexes were nicely evidenced by multinuclear

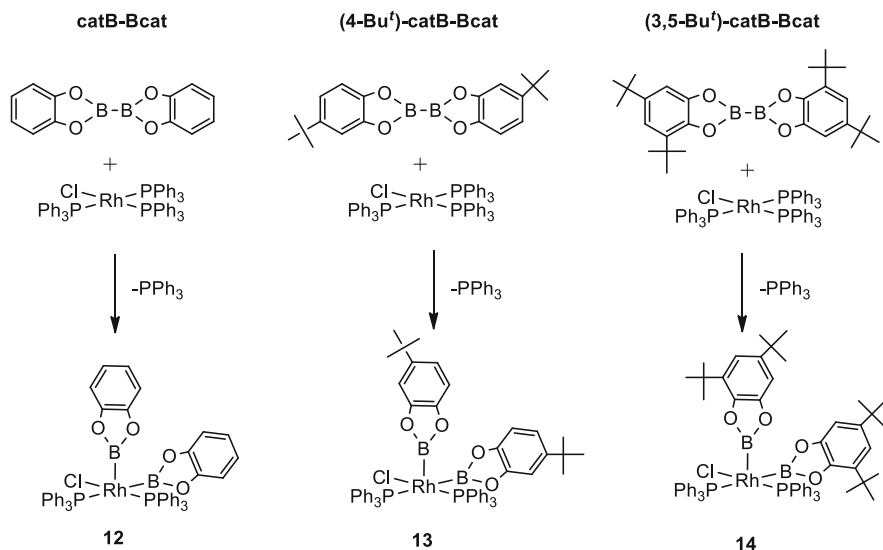


Scheme 10 $[\text{RhCl}(\text{PPh}_3)_3]$ -catalyzed diboration of vinylarenes and side formation of alkenylboronate and hydroborated products

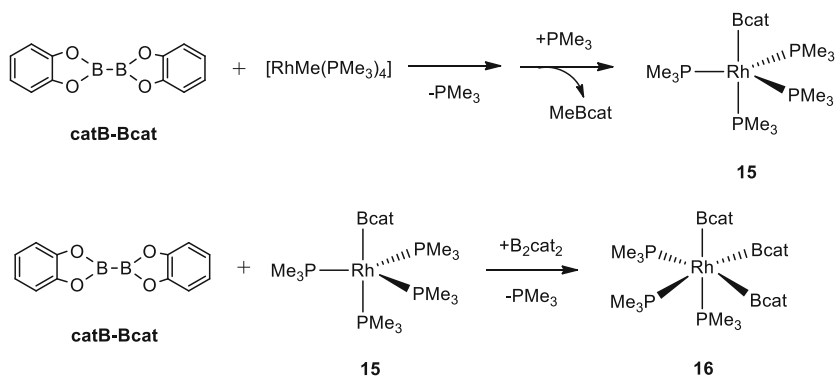
NMR spectroscopy after oxidative addition of **B₂cat₂** and its diborane analogous (**4-Bu^t**)-**B₂cat₂** and (**3,5-Bu^t**)-**B₂cat₂** (Scheme 11). The authors realized that catechol-based diboron reagents, which have shorter B–B bonds than **B₂pin₂**, are nonetheless easier to oxidatively add to Rh(I). It has to be noted that the bis(boryl) complex $[\text{RhCl}(\text{Bcat})_2(\text{PPh}_3)_2]$ (**12**) was previously detected by the slow reactivity of $[\text{Rh}(\mu^2\text{-Cl})(\text{PPh}_3)_2]_2$ with an excess of **HBcat**, through the intermediate $[\text{RhCl}(\text{H})(\text{Bcat})(\text{PPh}_3)_2]$ [46].

Likewise, addition of **B₂cat₂** to the electron-rich complex $[\text{RhMe}(\text{PMe}_3)_4]$ was thought to proceed via initial dissociation of a trimethyl-phosphine ligand followed by oxidative addition of the B–B bond. A subsequent reductive elimination step generated MeBcat along with the boryl complex $[\text{Rh}(\text{Bcat})(\text{PMe}_3)_4]$ (**15**), which has trapped the previously dissociated PMe_3 ligand (Scheme 12). Addition of a second equivalent of **B₂cat₂** proceeded smoothly to give the tris(boryl)rhodium(III) complex *fac*- $[\text{Rh}(\text{Bcat})_3(\text{PMe}_3)_3]$ (**16**) (Scheme 12). The *fac*-arrangement of the three boryl groups was justified to minimize the strong *trans*-influence of B(cat) ligands thanks to their significant σ -donor ability [47]. DFT calculations suggest that the boryl ligands prefer to occupy sites that those orbital accommodating metal *d* electron have minimal metal-boryl σ^* -antibonding character [48].

Photochemically induced oxidative addition of B–B sigma bonds has also been observed in Rh-alkene complexes. For example, $[\text{Rh}(\eta^5\text{-C}_5\text{H}_5)(\text{PMe}_3)(\text{C}_2\text{H}_4)]$, $[\text{Rh}(\eta^5\text{-C}_5\text{H}_5)(\text{PPh}_3)(\text{C}_2\text{H}_4)]$, and $[\text{Rh}(\eta^5\text{-C}_5\text{H}_4\text{CF}_3)(\text{PMe}_3)(\text{C}_2\text{H}_4)]$ led to B–B



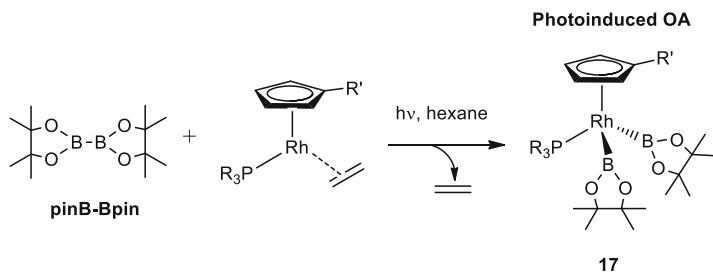
Scheme 11 $[\text{RhCl}(\text{PPh}_3)_3]$ activates B_2cat_2 and the $(4\text{-Bu}^t)\text{-B}_2\text{cat}_2$ and $(3,5\text{-Bu}^t)\text{-B}_2\text{cat}_2$ diborane analogues



Scheme 12 $[\text{RhMe}(\text{PMe}_3)_4]$ activates B_2cat_2

oxidative addition of B_2pin_2 by photolysis in hexane at -10°C to form $[\text{Rh}(\eta^5\text{-C}_5\text{H}_4\text{CF}_3)(\text{PR}_3)(\text{Bpin})_2]$ (**17**) (Scheme 13). The formulation of **17** was clearly established by NMR spectroscopy [49]. Interestingly, competition experiments using HBpin and B_2pin_2 were performed with these rhodium complexes and results suggested a slight preference for B–B oxidative addition over B–H sigma bond activation.

More recently, Fernández and Bo demonstrated that Rh(III) complexes modified with NHC ligands could activate diborane reagents and promote the diboration of cyclic systems. The reaction mechanism was explored by means of DFT



Scheme 13 Photoinduced activation of **B₂pin₂** with $[\text{Rh}(\eta^5\text{-C}_5\text{H}_5)(\text{PMe}_3)(\text{C}_2\text{H}_4)]$

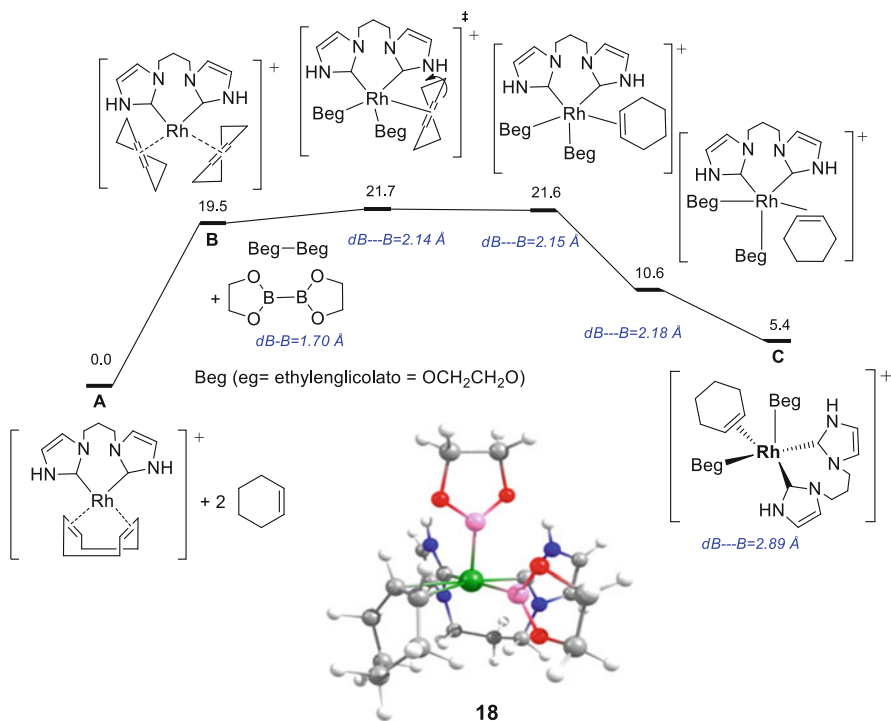
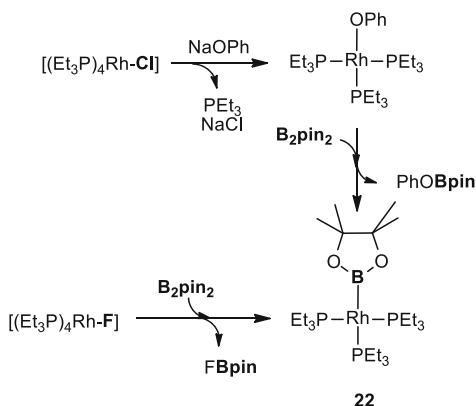


Fig. 1 Energy profile for the formation of cationic bisboryl Rh(III)-NHC complex. Electronic energy as kcal/mol. Distances between B atoms are given in Å

calculations (Fig. 1), and the oxidative addition of **B₂pin₂** or bis(neopentyl glycolato)diboron (**B₂neop₂**) to the Rh(III) system was postulated as the initial key step [50].

Scheme 16 Activation of **pinB-Bdmab** with [RhX (Et₃P)₄] (X = Me, OrBu) complex by σ -bond metathesis



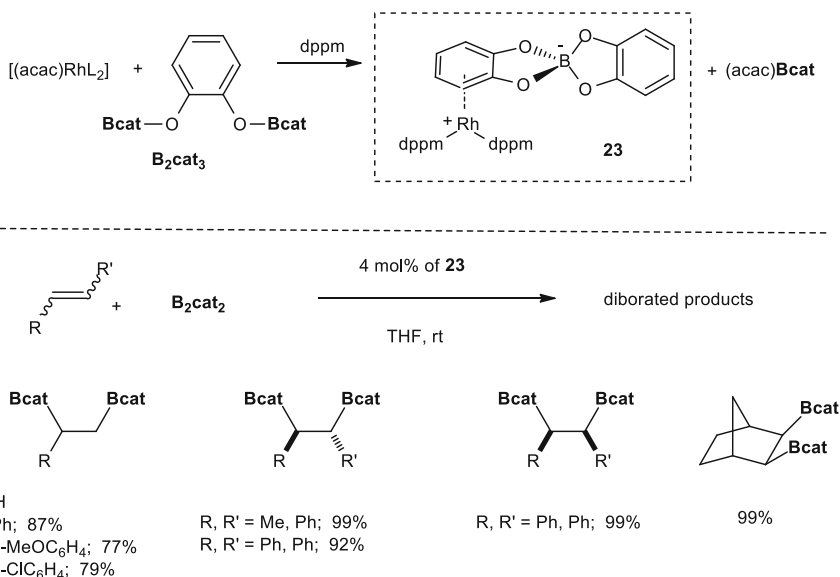
P3–Rh1–B1 might indicate the significant steric encumbrance of this complex. Similar Rh-complex **22** has been observed by Braun et al. when complexes [RhX (PEt₃)₄] (X = Cl, F) react with diboron reagents (Scheme 16) [56].

3 Rh-Catalyzed Diboration Reaction

Bis(boronate)compounds are chemical entities that possess two boronate moieties in a single molecule. These species become highly useful synthetic tools for straightforward access to complex structures, through C–B bond formation followed by homo- and heteroatom functionalization. Among the available methods to prepare them, diboration of unsaturated C–X (X = C, O or N,) bonds, by means of transition metal-promoted reactions, demonstrated to be a particularly powerful tool. In this section we describe the most remarkable developments achieved utilizing rhodium complexes in diboration reactions.

3.1 Rh-Catalyzed Diboration Reaction of C–C Multiple Bonds

From the key discovery of the Rh-diboration of olefins by Baker et al. [41], the diboration process has been focussed to improve the chemoselective issues related to the dehydrogenative borylation. Therefore, the same authors reported that use of 4 mol% of the zwitterionic η^6 -(arene)rhodium complex [Rh(η^6 -catB-cat)(dppm)] **23** allowed a more efficient addition of **B₂cat₂** to a wide range of vinylarenes, norbornene, and unstrained internal alkenes *cis* and *trans*-stilbene and *trans*- β -methylstyrene, at room temp (Scheme 17) [57]. *Syn* addition of the two

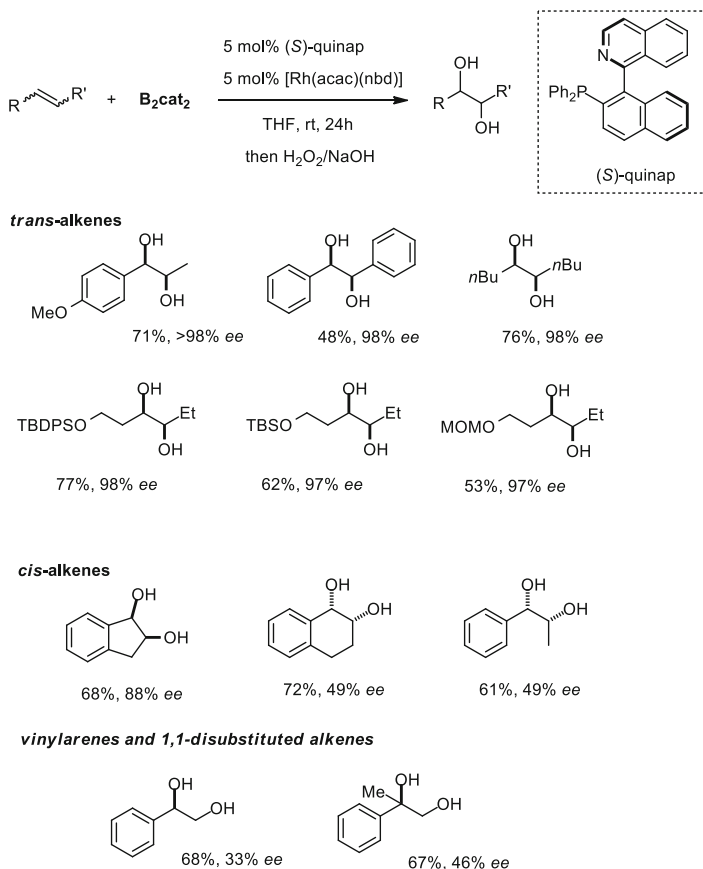


Scheme 17 $[\text{Rh}(\eta^6\text{-catB-cat})(\text{dppm})]$ -catalyzed diboration of alkenes with B_2cat_2

Bcat moieties was unambiguously determined by means of the X-ray analysis of the solid *trans*-stilbene diborated product.

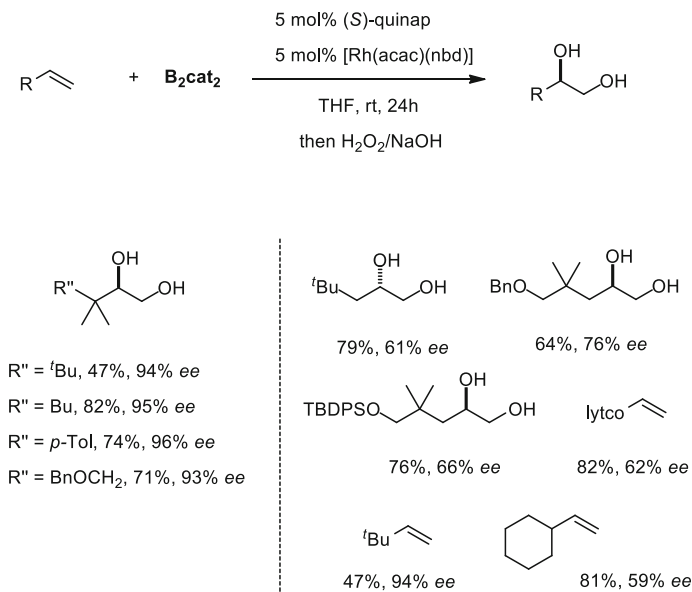
It was not until 2003 that the group of Morken developed the first example of an enantioselective diboration of alkenes catalyzed by Rh(I) complex modified with a chiral P,N-bidentate ligand [43]. The combination of (*S*)-quinap with $[\text{Rh}(\text{acac})(\text{nbd})]$ was found to be highly effective for the catalytic diboration of a wide series of internal alkenes. After subsequent oxidative work-up, the corresponding 1,2-diols were isolated in good yield and enantioselectivity. While with this particular catalysts disubstituted *trans* alkenes reacted in a highly selective fashion, *cis*-disubstituted reacted in variable enantioselection. Vinylarenes and 1,1-disubstituted alkenes underwent diboration with relatively poorer enantiocontrol (Scheme 18) [58].

Subsequent studies by the group of Fernández explored the effect of the ligand, Rh source, and electronic nature of the substrates on the diboration outcome of reluctant monosubstituted vinylarenes. The selectivity of the diboration seemed to be highly sensitive to the nature of the catalysts and the electronics of the substrate [42]. A parallel investigation about the substrate scope and different conditions for this reaction was as well undertaken by the group of Morken which established a stereoinduction model that can predict the sense and levels of enantioselectivities for the reaction of a wide range of alkenes [44]. In the latter work, unhindered monosubstituted aliphatic olefins still reacted in only moderate enantioselectivity, however, monosubstituted alkenes featuring a highly branched α -carbon reacted in significant levels of enantiocontrol (Scheme 19).



Scheme 18 [Rh(acac)(nbd)]/(S)-Quinap-catalyzed enantioselective diboration of alkenes with B_2cat_2

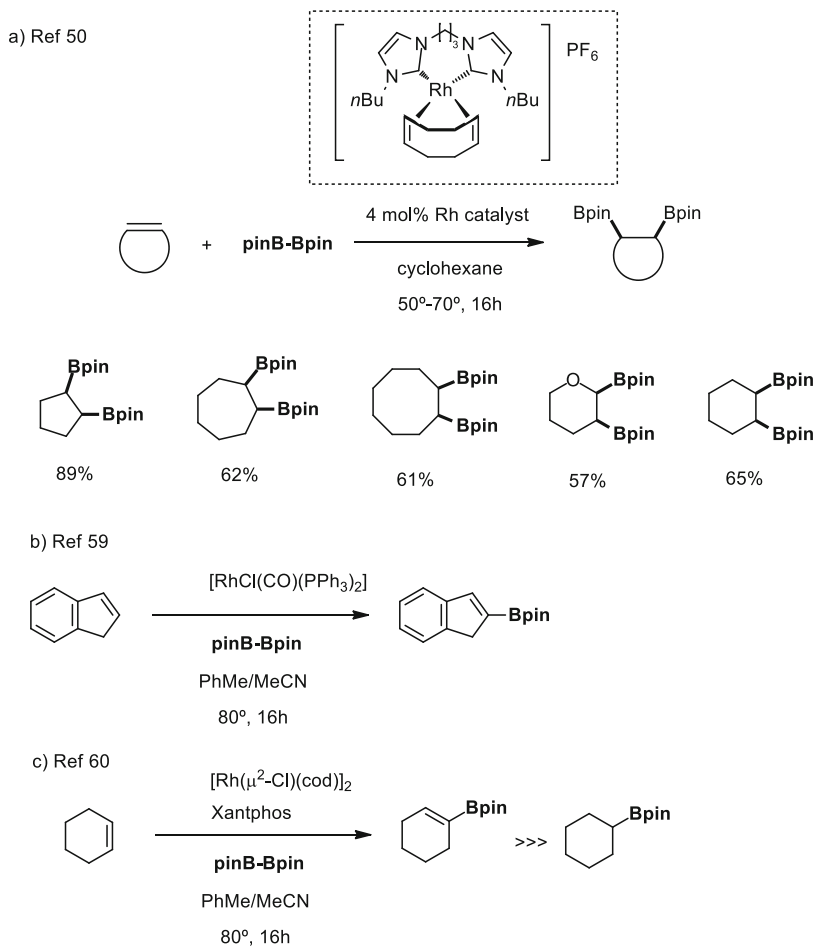
More recently Fernández and Bo demonstrated that Rh(III) complexes modified with NHC ligands could catalyze the diboration of cyclic systems with B_2pin_2 [50]. Although it has been well established that rhodium-phosphine complexes favored the dehydrogenative borylation process in the borylation of cyclic olefins, the authors found that Rh(III)-cationic complexes modified by NHC ligands promoted efficient and selective diboration of these challenging systems. The reaction takes place with a series of cyclic alkenes of different size (Scheme 20a) and the use of non-polar solvents such as pentane, hexane, or cyclohexane seems to be crucial to ensure the diboration efficacy. DFT calculations have demonstrated that, in this case, reductive elimination step results a more energetically favored step. This selective diboration of cyclic systems seems to be in contrast with the observed trend reported by other groups where the addition of B_2pin_2 to *trans*-[RhCl(CO)(PPh₃)] or [Rh(μ^2 -Cl)(cod)]₂ promoted the exclusive formation of the dehydrogenative borylated product (Scheme 20b, c) [59, 60]. Rh complexes can



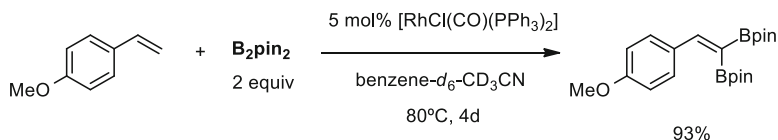
Scheme 19 Steric influence on the [Rh(acac)(nbd)]/(S)-Quinap-catalyzed enantioselective diboration of alkenes with **B₂cat₂**

catalyze the double dehydrogenative borylation that could be considered as a “formal” diboration reaction. Marder et al. observed that when the diboration of 4-vinylanisole is carried out with an excess of 2 equiv of **B₂pin₂** in the presence of 5 mol% of [RhCl(CO)(PPh₃)₂] in acetonitrile at 80°C for 4 days, the corresponding 1,1-diborylalkene is formed in almost quantitative yield (Scheme 21) [61]. - Rhodium-catalyzed diborations of (*E*)-styrylboronate esters have also been reported; however, this reaction provides a mixture of isomeric (tris)boronate compounds depending on the catalyst used [62].

Nishiyama and co-workers have suggested that, in the presence of a base, **B₂pin₂** and [Rh(OAc)₂(OH)(Phebox)] complex react through a σ-bond metathesis step to form the Rh(III)-boryl species able to promote asymmetric diboration of terminal alkenes with high enantio- and chemoselectivities [52]. The reaction works efficiently with a wide series of aryl substituted terminal alkynes, as well as with aliphatic monosubstituted olefins (Scheme 22). As a limitation of the method, 1,2-disubstituted alkenes such as β-methylstyrene, 1,2-dihydronaphthalene, or *trans*-stilbene could not be diborated under these conditions. A hypothetical transition-state model structure was also proposed to explain the stereochemical outcome of the diboration. Similar protocol can be, as well, applied to the asymmetric synthesis of optically active 3-amino-1,2-diols prepared from *N*-acyl-protected allylamines [63].

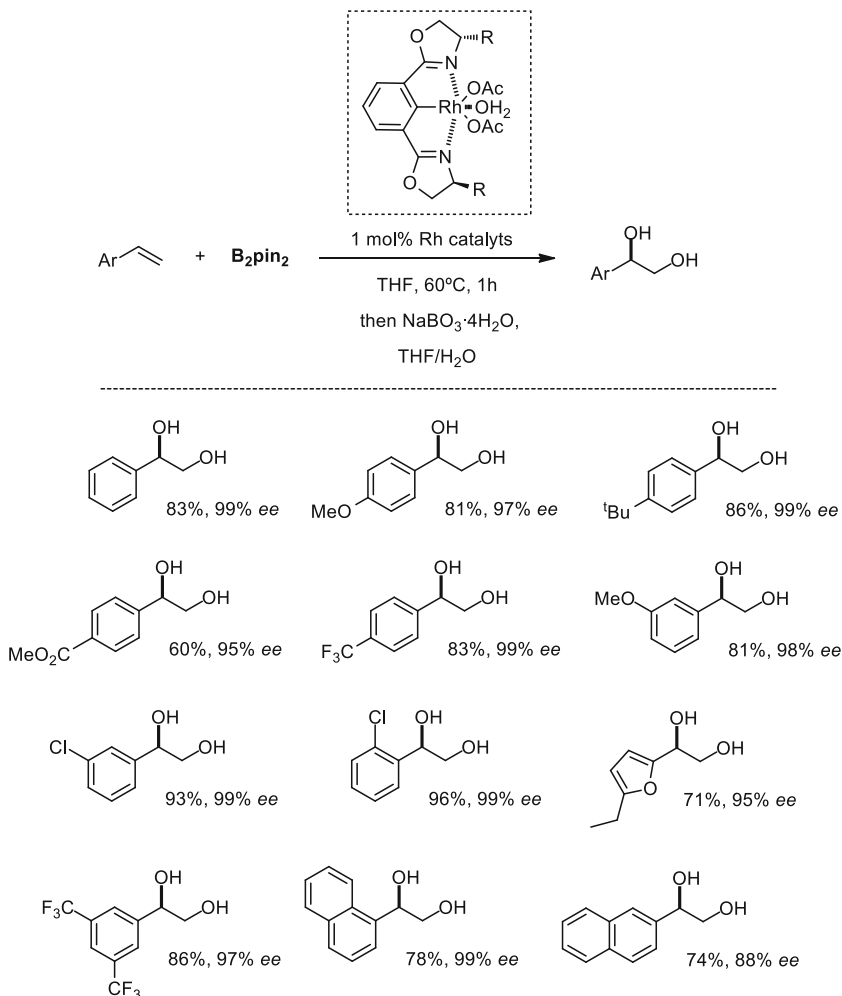


Scheme 20 Rh-NHC mediated 1,2-diboration reaction of cyclic alkenes with **B₂pin₂** and comparison with Rh complexes that favored the dehydrogenative borylation of cyclic alkenes



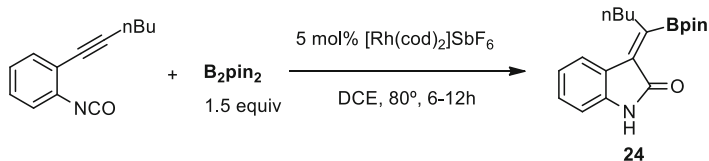
Scheme 21 Rh-catalyzed double dehydrogenative borylation of vinylarenes

Rh complexes also accomplish the diboration of alkynes. Therefore, 2-alkynylaryl isocyanates react with **B₂pin₂** in the presence of the cationic rhodium(I) catalyst [Rh(cod)₂]⁺SbF₆⁻ to produce the borylated 3-alkylideneoxindoles **24** in a stereoselective way (Scheme 23) [64]. The carbon–boron linkage formed can

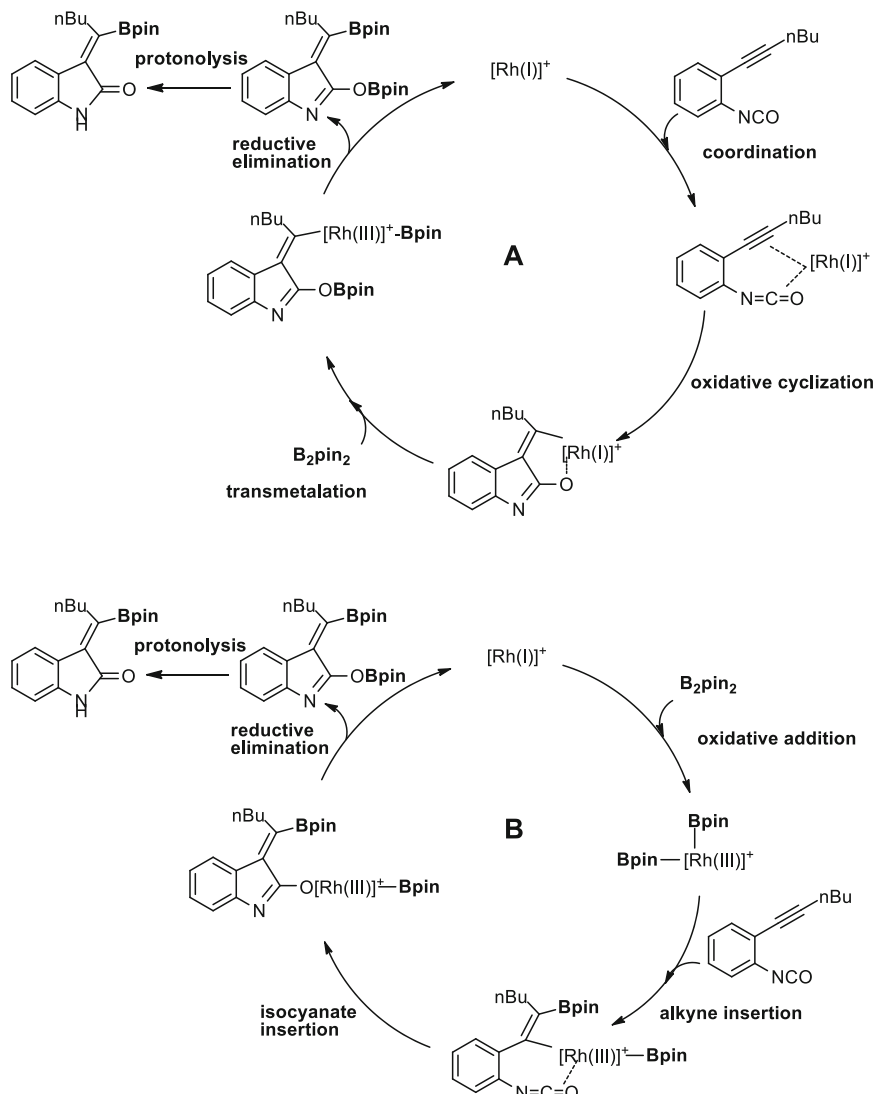


Scheme 22 [Rh(Phebox-ip)]-catalyzed asymmetric diboration/oxidation of olefins with **B₂pin₂**

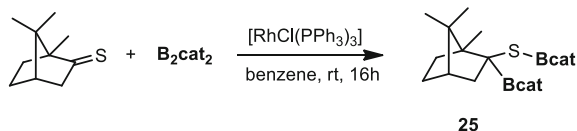
be further transformed via reactions such as a cross-coupling and a halogenation reaction [65]. Interestingly, the authors of this important achievement have suggested two plausible mechanisms, the catalytic cycle **A** where the substrate binds the rhodium(I) to generate the chelate complex, which then forms the oxa-rhodacycle by oxidative cyclization. A subsequent reaction with **B₂pin₂** produces the borylrhodium(III) species via transmetalation. Finally, reductive elimination affords the diboronate intermediate along with the starting cationic rhodium (I) species to complete the catalytic cycle **A** (Scheme 24). Protonolysis occurs during aqueous workup to end up with the desired product. Another mechanism, **B**, has also been conceivable that involves oxidative addition of the B–B bond onto the cationic rhodium(I) complex furnishing a diboryl-rhodium(III) intermediate,



Scheme 23 $[\text{Rh}(\text{cod})_2]\text{SbF}_6$ -catalyzed borylative cyclization of 2-alkynylaryl isocyanates with B_2pin_2



Scheme 24 Plausible mechanisms for the $[\text{Rh}(\text{cod})_2]\text{SbF}_6$ -catalyzed borylative cyclization of 2-alkynylaryl isocyanates with B_2pin_2



Scheme 25 [RhCl(PPh₃)₃]-catalyzed diboration of (1*R*)-(-)-thiocamphor with **B₂pin₂**

followed by a sequential addition onto the alkyne moiety and the isocyanate moiety, finishing with the reductive elimination (Scheme 24).

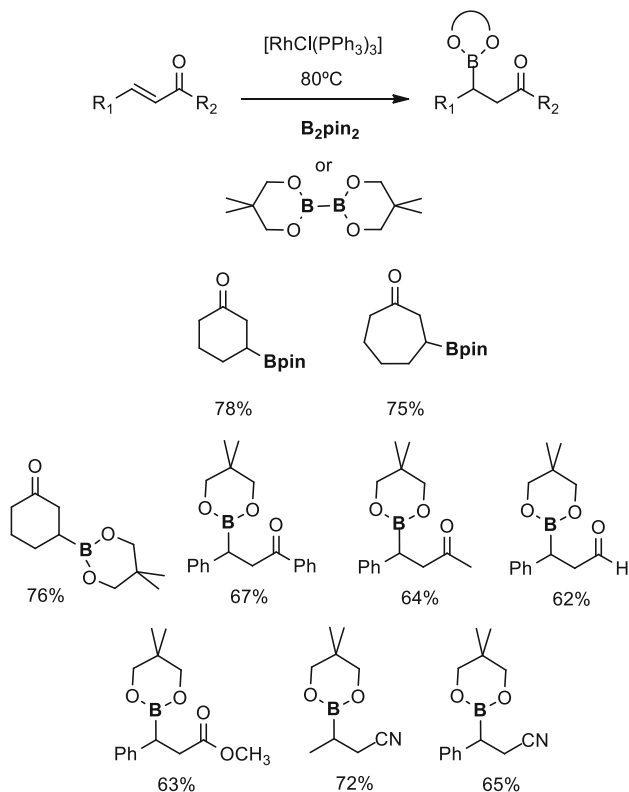
3.2 *Rh-Catalyzed Diboration Reaction of C–X Multiple Bonds*

The Rh-catalyzed diboration of C=S bond with **B₂cat₂** was performed with the Wilkinson's catalyst [RhCl(PPh₃)₃] and illustrated in (1*R*)-(-)-thiocamphor as substrate (Scheme 25) [66]. Nowadays it has been reported that the preformed system [Rh(Bpin)(PEt₃)₃] can react with CO₂, PhNCO, and CS₂ via the cleavage of C=X bonds (X = O, N, S). The concomitant formation of thermodynamically stable B–X bonds represents a driving force of these reactions [67–69].

4 Rh-Catalyzed β-Boration of α,β-Unsaturated Carbonyl Compounds

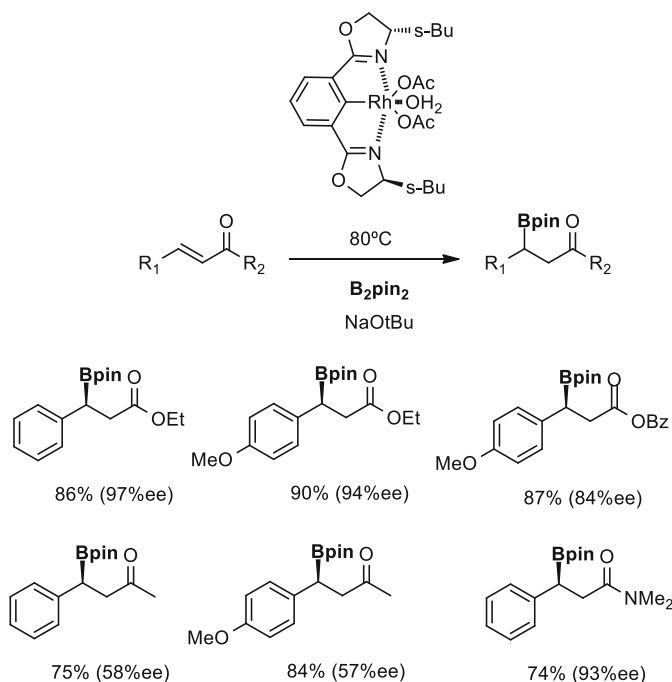
The conjugate borylative addition to α,β-unsaturated carbonyl compounds has become a real challenge since its discovery in early twenty-first century [70–74] to promote the β-borated carbonyl compound in a regio- and stereoselective way [75]. Kabalka et al. were pioneers in the rhodium-catalyzed 1,4-diboration of α,β-unsaturated carbonyl compounds and related electron deficient alkenes including esters and nitriles with **B₂pin₂** and bis(neopentyl glycolato)diboron (Scheme 26) [76].

The asymmetric conjugate borylative addition to α,β-unsaturated carbonyl compounds with Rh complexes has been developed by Nishiyama et al. [51, 77] to obtain the β-borated compounds using the chiral rhodium–bisoxazolinyphenyl catalysts, Rh(Phebox) (Scheme 27). The catalytic boration was found to proceed at 80°C within 12 h to give the desired β-borated products with high yield and enantioselectivity. The addition of a catalytic amount of NaOtBu (5 mol%) significantly accelerated the β-boration. However, in contrast to the Cu and Ni protocols reported by Yun's [78–81] and Oshima's [82], respectively, the rhodium complexes Rh(Phebox) and [RhCl(PPh₃)₃] did not require addition of protic additives. Authors relate the presence of such additives to undesirable conjugate reduction of the



Scheme 26 $[\text{RhCl}(\text{PPh}_3)_3]$ -catalyzed β -boration of α,β -unsaturated ketones, aldehydes, esters, and nitriles with B_2pin_2 and B_2neop_2

substrate. In this work, it's assumed that the borylation takes place via initial σ -bond metathesis of the diboron on rhodium(III) species and B_2pin_2 to activate the diboron, and subsequent insertion of the $\text{C}=\text{C}$ into $\text{Rh}-\text{B}$ bond.

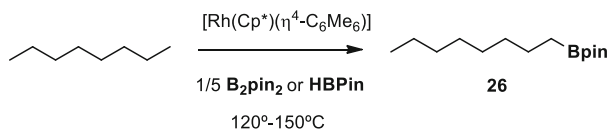


Scheme 27 [Rh(Phebox)]-catalyzed asymmetric β -boration/oxidation of olefins with B_2pin_2

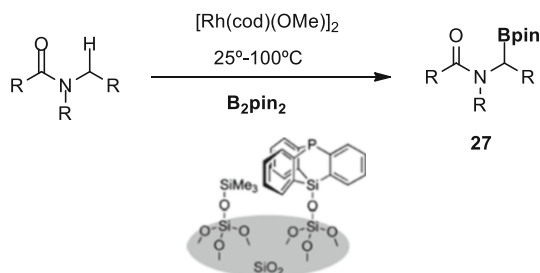
5 Rh-Catalyzed C–H and C–X (X = F, CN, OMe) Borylation with Diboron Reagents

The direct borylation of C–H bonds is usually achieved in the presence of specific organometallic complexes. Since the pioneer work by Hartwig and co-workers on the stoichiometric borylation by irradiation of $[\text{Fe}(\text{CO})_2(\text{Cp})(\text{Bcat})]$, in benzene, which resulted in the formation of PhBcat (2-phenyl-1,3,2-benzodioxaborole) [83], the development of alternative active thermal C–H borylations, mainly described by the groups of Hartwig [84, 85] and Smith [86, 87] using $[\text{Rh}(\eta^4\text{-C}_6\text{Me}_6)(\text{Cp}^*)]$ ($\text{Cp}^* = 1,2,3,4,5$ pentamethylcyclopentadiene) and $[\text{Ir}(\mu^2\text{-X})(\text{cod})_2]$ (X = Cl or OMe) in combination with substituted bipyridine or phenanthroline ligands, has become an important progress in this area [88]. Marder et al. demonstrated that $[\text{RhCl}(\text{P}i\text{Pr}_3)_2\text{N}_2]$ was able to catalyze the borylation of benzene with HBPin [89].

The real conceptual breakthrough about the potential of the unoccupied *p*-orbital of a covalent boryl ligand, coordinated to Rh, in order to activate C–H bonds was postulated by Hartwig demonstrating that rhodium complexes generated in situ from $[\text{Rh}(\text{Cp}^*)(\eta^4\text{-C}_6\text{Me}_6)]$, $[\text{Rh}(\text{Cp}^*)(\text{C}_2\text{H}_4)_2]$, or $[\text{RhCl}_2(\text{Cp}^*)]_2$ and either HBPin or B_2pin_2 catalyzed the uniquely regioselective conversion of alkanes into



Scheme 28 $[\text{Cp}^*\text{Rh}(\eta^4\text{-C}_6\text{Me}_6)]$ -catalyzed borylation of alkanes with **HBPin** or **B₂pin₂**

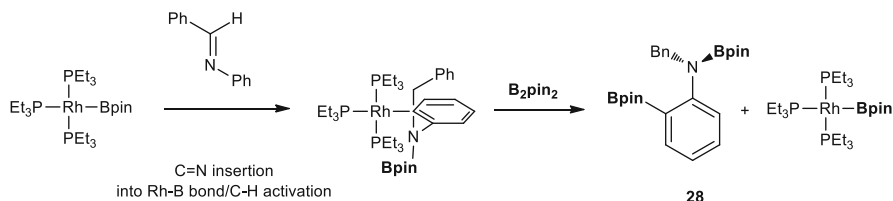


Scheme 29 $[\text{Rh}((\mu^2\text{-OMe})(\text{cod}))_2]$ -catalyzed $\text{C}(\text{sp}^3)\text{-H}$ borylation of amides, ureas, and 2-aminopyridine derivatives at the α position to the N atom with **B₂pin₂**

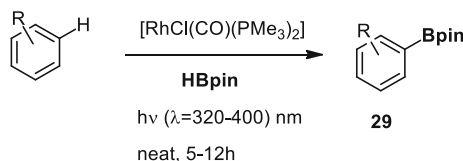
terminal alkylboronate esters (Scheme 28) [90]. In addition, Rh catalysts exhibited concomitant benzylic borylation activity towards alkylarenes, which is predominant in some cases [89, 91, 92].

Metal-catalyzed *ortho*-selective borylations have also been developed in the recent literature. The Rh-catalyzed C–H borylations using *ortho* directing groups such as nitrogen heterocycles have been reported by the group of Sawamura. The authors describe that immobilized phosphine–Rh system, prepared from silica-supported bridgehead monophosphines and $[\text{Rh}(\mu^2\text{-OH})(\text{cod}))_2]$, has enabled *ortho*-selective C–H borylation for a wide range of arenes containing different nitrogen-based directing groups. Furthermore, the reaction showed significant tolerance towards steric hindrance around the reacting C–H bond [93]. The same group has developed the direct $\text{C}(\text{sp}^3)\text{-H}$ borylation of amides, ureas, and 2-aminopyridine derivatives at α position respect to the N atom, which gives the corresponding α -aminoalkylboronates **27**, with a heterogeneous catalyst system consisting of $[\text{Rh}((\mu^2\text{-OMe})(\text{cod}))_2]$ and a silica-supported triarylphosphine ligand (Silica-TRIP) that features an immobilized triptycene-type cage structure with a bridgehead P atom (Scheme 29). The reaction occurs not only at terminal C–H bonds but also at internal secondary C–H bonds under mild reaction conditions (25–100°C, 0.1–0.5 mol% Rh) [94, 95].

Braun and co-workers have also investigated the reactivity of $[\text{Rh}(\text{Bpin})(\text{PEt}_3)_3]$ towards a number of ketimines and aldimines. Some of the resulting insertion (into the Rh–B bond) products underwent C–H activation to generate the corresponding rhodium aryl species. Such complexes were subsequently treated with **B₂pin₂** to give unique diborated products through a possible mechanism involving B–B



Scheme 30 Activation of **B₂pin₂** with Rh-aryl species and further C–H activation

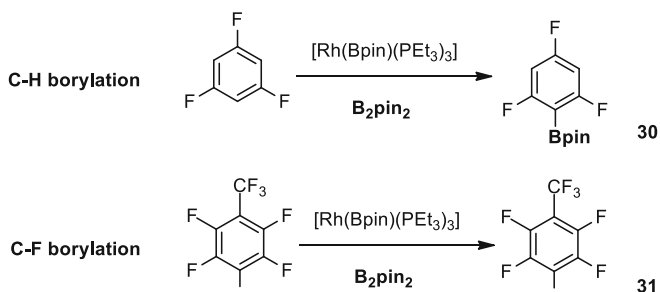


Scheme 31 Activation of **HBpin** with Rh-aryl species and further C–H activation

oxidative addition and reductive elimination (Scheme 30) [96]. **B₂pin₂** has also been activated by $[\text{Rh}(\text{Bpin})(\text{PEt}_3)_3]$ in the presence of SCF_3 -functionalized arenes to accomplish their selective borylation [97].

Beller et al. have developed a straightforward and convenient photocatalytic protocol for the borylation of a range of aromatic and heteroaromatic compounds under mild conditions with the Rh complex *trans*- $[\text{RhCl}(\text{CO})(\text{PMe}_3)_2]$ and **HBpin** as the boron reagent (Scheme 31) [98]. Under the optimized conditions, the catalyst loading can be reduced to 0.1 mol% of *trans*- $[\text{RhCl}(\text{CO})(\text{PMe}_3)_2]$ leading to a turnover number of 700. It represents the highest productivity for any rhodium complex under photocatalytic conditions. The catalytic system has some limitations since heterocycles such as pyridine and 2,6-lutidine did not lead to borylated products with **HBpin** and **B₂pin₂** as the boron source in the presence of *trans*- $[\text{RhCl}(\text{CO})(\text{PMe}_3)_2]$, and neither *N*-boryldihydropyridine derivatives were observed. The photochemical reactions of $[\text{RhTp}'(\text{PMe}_3)_2\text{H}_2]$ ($\text{Tp}' = \text{tris}(3,5\text{-dimethylpyrazolyl})\text{borate}$) with **HBpin** are under current development [99].

Borylations of aryl halides with boron reagents play also a fundamental role in C–B bond formation [100]. The replacement of a C–F bond by a boryl group as a viable entity is particularly beneficial for further conversions. The first borylation of a C–F bond was reported by Marder and Perutz et al. [101] The reaction of pentafluoropyridine at $[\text{Rh}(\text{SiPh}_3)(\text{PMe}_3)_3]$ gave the C–F activation products: $[\text{Rh}(2\text{-C}_5\text{NF}_4)(\text{PMe}_3)_3]$ and $[\text{Rh}(4\text{-C}_5\text{NF}_4)(\text{PMe}_3)_3]$. Subsequent treatment with **B₂cat₂** resulted in the formation of pyridyl boronic ester derivatives. A catalytic C–F borylation using the highly reactive rhodium boryl complex $[\text{Rh}(\text{Bpin})(\text{PEt}_3)_3]$ as catalyst has also been reported [102]. In that case the Rh complex activates selectively the C–F bond at the 2-position of pentafluoropyridine to yield $[\text{Rh}(2\text{-C}_5\text{NF}_4)(\text{PEt}_3)_3]$. Further reactivity with **B₂pin₂** gave access to the 2,3,4,5-tetrafluoropyridyl boronic ester. DFT calculations showed that the C–F bond



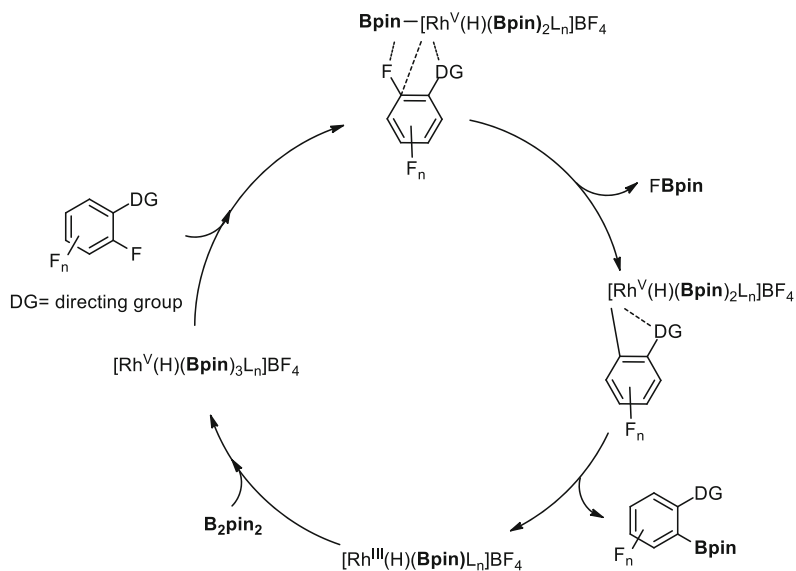
Scheme 32 [Rh(Bpin)(PEt₃)₃]-catalyzed C–H and C–F borylation with **B₂pin₂**

cleavage step proceeds via a four centered boryl-assisted transition state in which C–F bond cleavage occurs over the Rh–B bond. On treatment of pentafluoropyridine with **B₂pin₂**, in the presence of [Rh(Bpin)(PEt₃)₃] or [Rh(H)(PEt₃)₃] as catalyst, 2-Bpin-C₅NF₄ can be synthesized by C–F borylation at the 2-position. Using 2,3,5,6-tetrafluoropyridine, **B₂pin₂**, and catalytic amounts of [Rh(H)(PEt₃)₃] led to a C–H borylation reaction at the 4-position (Scheme 32) [103].

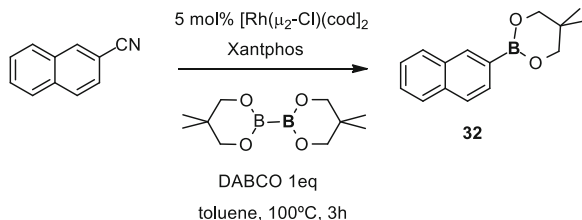
An *ortho*-selective C–F bond borylation between N-heterocycle-substituted polyfluoroarenes and **B₂pin₂** with simple and commercially available [Rh(cod)₂]BF₄ as a catalyst has recently been reported. The reaction proceeds under mild reaction conditions with high efficiency and broad substrate scope, even towards monofluoroarene, thus providing a facile access to a wide range of borylated fluoroarenes that are useful for photoelectronic materials. Preliminary mechanistic studies reveal that an Rh(III)/(V) catalytic cycle via a key intermediate rhodium(III) hydride complex [Rh(H)Ln(Bpin)] may be involved in the reaction (Scheme 33) [104].

The reaction of aryl cyanides with diboron reagents in the presence of a rhodium/Xantphos catalyst and DABCO affords arylboronic esters via carbon–cyano bond cleavage (Scheme 34). The reaction involves an unprecedented C–CN bond activation that is promoted by a borylrhodium complex. In addition, the reaction offers a new strategy for the synthesis of complex boronic acid derivatives wherein a cyano group can now be utilized as a boron equivalent [105]. A proposed mechanism for this rhodium-catalyzed nitrile borylation is outlined in Scheme 35. The reaction of the rhodium precatalyst [Rh(μ²-Cl)(cod)]₂ with diboron **B₂neop₂** initially generates a borylrhodium species. The formation of B(neop)-Cl (neop = neopentylglycolate) was confirmed by ¹¹B NMR. The addition of Rh-**B(neop)** to the nitrile then forms an iminylrhodium species which is followed by E/Z isomerization. β-Aryl elimination generates an arylrhodium and the boryl cyanide, and eventually a new transmetalation affords the borylated product and regenerates the Rh-**B(neop)**. The *ortho*-directing ability of the cyano group also allows a reactivity pattern that cannot be achieved using other borylation methodologies.

To clarify the dominant mechanism of this reaction, a density functional theory study on borylation of PhCN and BnCN catalyzed by [Rh(XantPhos)(B(nep))] (nep = neopentylglycolate, XantPhos = 4,5-Bis-(diphenylphosphino)-9,9-

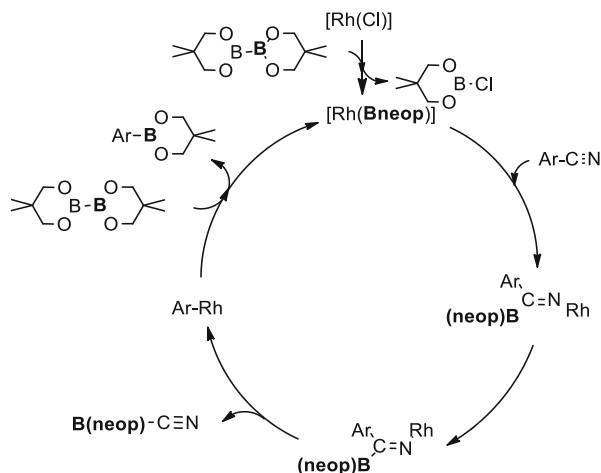


Scheme 33 Proposed mechanism for the $[\text{Rh}(\text{cod})_2]\text{BF}_4$ -catalyzed *ortho*-C–F bond borylation with B_2pin_2

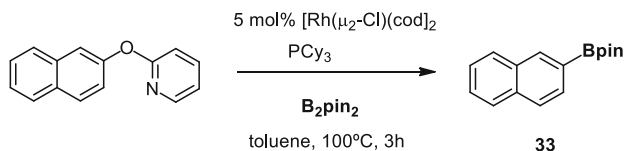


Scheme 34 $[\text{Rh}(\mu_2\text{-Cl})(\text{cod})_2]$ -catalyzed C–CN bond borylation with B_2neop_2

dimethylxanthene) has been conducted by Fu et al. [106]. The computational results indicated that the deinsertion mechanism (2,1-insertion of the Rh–B bond into the triple C–N bond occurs first followed by the insertion of the metal center into C–CN bond) is favored over oxidative addition, β -carbon elimination, and the initial C–H bond activation mechanism within all the investigated reactions. The activation of the C–CN bond is a facile step in the deinsertion mechanism, and the oxidative addition of the diboron reagent is the rate determining step. On this basis, the mechanism of borylation of PhCN catalyzed by a similar Ir–B complex ($[\text{Ir}(\text{Xantphos})(\text{B}(\text{nep}))]$) was also examined. The deinsertion mechanism was found to be the most favorable. The overall energy barrier of the Ir–B complex-catalyzed borylation of benzonitriles was slightly higher than that of the same Rh–B complex-catalyzed reaction (by 1.1 kcal/mol), indicating that $[\text{Ir}(\text{Xantphos})(\text{B}(\text{nep}))]$ could act as an alternative catalyst for borylation of nitriles. An alternative study based on



Scheme 35 Proposed mechanism for the $[\text{Rh}((\mu^2\text{-Cl})(\text{cod}))_2]$ -catalyzed C–CN bond borylation with B_2neop_2

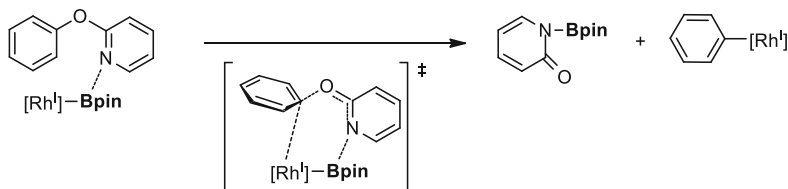


Scheme 36 $[\text{Rh}((\mu^2\text{-Cl})(\text{cod}))_2]$ -catalyzed C–OR bond borylation with B_2pin_2

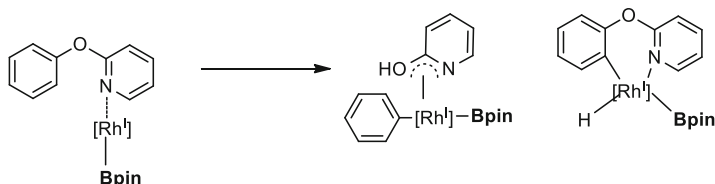
the stoichiometric reaction between complex $[\text{RhCl}(\text{Xantphos})_2]$ and B_2pin_2 in benzene, resulted in the formation of the rhodium(III) derivative $[\text{RhHCl}(\text{Bpin})(\text{xantphos})_2]$ and the corresponding PhBpin . This experiment helps to understand the proposed species in the mechanism of the rhodium-mediated decyanative borylation indicating the plausible occurrence of the oxidative addition of B_2pin_2 to the Rh complex in this borylative reaction [107].

Similarly, Chatani et al. [108] have also reported the rhodium-catalyzed reaction of aryl 2-pyridyl ethers with a diboron reagent resulting in the formation of arylboronic ester derivatives via activation of the C(aryl)–O bonds (Scheme 36). The straightforward synthesis of 1,2-disubstituted arenes was enabled through catalytic *ortho*-C–H bond functionalization directed by the 2-pyridyloxy group followed by substitution of this group with a boryl group. Several control experiments revealed that the presence of an sp^2 nitrogen atom at the 2-position of the substrate and the use of a boron-based reagent were crucial for the activation of the relatively inert C(aryl)–O bond of aryl 2-pyridyl ethers (Scheme 37).

a) via N-B interaction



b) via N-Rh interaction



Scheme 37 $[\text{Rh}(\mu^2\text{-Cl})(\text{cod})_2]$ -catalyzed C–OR bond borylation with **B₂pin₂**: plausible mechanisms for the C–OPy bond cleavage

6 Summary and Outlook

After 30 years from the discovery of the Rh-catalyzed C–B bond formation from unsaturated bonds [8], the development of the field has intensively been growing. Three are the essential pillars which uphold the current and future directions: (a) the strong influence of the metal itself to activate H–B and B–B bonds, both from oxidative addition and σ -bond metathesis, (b) the power of the ligands that modify the Rh center to induce high levels of chemo-, regio-, and enantioselectivity, and (c) the unrestricted mechanisms that can be interpreted to answer the real evidences, such as the complementary ways to understand the syn addition approaches as well as the non-conventional *trans*-borylations [109–114], by the aid of density functional theory (DFT) calculations.

Acknowledgement The authors acknowledged all the students, postdocs, and colleagues in our papers in references section, all the friends to discuss chemistry with, and all the funding resources, principally AllyChem.

References

1. Kono H, Ito K, Nagai Y (1975) *Chem Lett* 4:1095
2. Paxson TE, Hawthorne MF (1974) *J Am Chem Soc* 96:4674
3. Siedle AR (1975) *J Organomet Chem* 90:249
4. Klanberg F, Wegner PA, Parshall GW, Mutttries EL (1968) *Inorg Chem* 7:2072

5. Sneath RL, Todd LJ (1973) *Inorg Chem* 12:44
6. Davison A, Traficante DD, Wreford SS (1974) *J Am Chem Soc* 96:2802
7. Mannig D, Noth H (1985) *Angew Chem Int Ed Engl* 24:878
8. Hewes JD, Kriemendahl CW, Marder TB, Hawthorne MF (1984) *J Am Chem Soc* 106:5757
9. Burgess K, Ohlmeyer MJ (1988) *J Org Chem* 53:5178
10. Burgess K, Ohlmeyer MJ (1991) *Chem Rev* 91:1179
11. Beletskaya I, Pelter A (1997) *Tetrahedron* 53:4957
12. Crudden CM, Edwards D (2003) *Eur J Org Chem* 24:4695
13. Fu GC (2004) *Transition metals for organic synthesis*, pp 193–198
14. Carroll AM, O'Sullivan TP, Guiry PJ (2005) *Adv Synth Catal* 347:609
15. Vogels CM, Westcott SA (2005) *Curr Org Chem* 9:687
16. Brown JM (2005) *Modern rhodium catalyzed reactions*, pp 33–53
17. Vogels ChM, Westcott SA (2006) *Leading edge organometallic chemistry research*, pp 133–148
18. Mingos D, Miachel P, Crabtree RH (2007) *Compr Organomet Chem III* 10:839
19. Miyaura N (2008) *Bull Chem Soc Jap* 81:1535
20. Coyne AG, Guiry PJ (2008) *Modern reduction methods*, pp 65–86
21. Westcott SA, Baker RT (2008) *Modern reduction methods*, pp 297–319
22. Thomas SP, Aggarwal VK (2009) *Angew Chem Int Ed* 48:1896
23. Guiry PJ (2009) *ChemCatChem* 1:233
24. Brown JM, Guyen BN (2011) *Sci Synth Stereoselective Synth* 1:295
25. Ojima I, Athan AA, Chaterpaul SJ, Kaloko JJ, Teng Y-HG (2013) *Organometallics in synthesis: fourth manual* 135
26. Huang S, Xie Y, Wu S, Jia M, Wang J, Xu W, Fang H (2013) *Curr Org Synth* 10:683
27. Chang Chong Ch, Kinio R (2015) *ACS Catal* 5:3238
28. Oshima K, Ohmura T, Suginome M (2012) *J Am Chem Soc* 134:3699
29. Morimoto M, Miura T, Murakami M (2015) *Angew Chem Int Ed* 54:12659
30. Brown AN, Zakharov LN, Mikulas T, Dixon DA, Liu S-Y (2014) *Org Lett* 16:3340
31. Chen D, Zhang X, Qi W-Y, Xu B, Xu M-H (2015) *J Am Chem Soc* 137:5268
32. Hasegawa M, Segawa Y, Yamashita M, Nozaki K (2012) *Angew Chem Int Ed* 51:6956
33. Hoang GL, Yang Z-D, Smith SM, Pal R, Miska JL, Perez DE, Pelter LSW, Zeng XC, Takacs JM (2015) *Org Lett* 17:940
34. Yang Z-D, Pal R, Hoang GL, Zeng XC, Takacs JM (2014) *ACS Catal* 4:763
35. Smith SM, Hoang GL, Pal R, Bani Khaled MO, Pelter LSW, Zeng XC, Takacs JM (2012) *Chem Commun* 48:12180
36. Hu N, Zhao G, Zhang Y, Liu X, Li G, Tang W (2015) *J Am Chem Soc* 127:6746
37. Pereira S, Srebnik M (1996) *J Am Chem Soc* 37:3283
38. Matteson DS (2004) *Sci Synth* 6:5
39. Braunschweig H, Dewhurst RD, Mozo S (2015) *ChemCatChem* 7:1630
40. Szabo KL (2014) *Sci Synth Multicomponent React* 2:345
41. Baker RT, Nguyen P, Marder TB, Westcott SA (1995) *Angew Chem Int Ed* 34:1336
42. Ramírez J, Segarra AM, Fernández E (2005) *Tetrahedron Asymmetry* 16:1289
43. Morgan JB, Miller SP, Morken JP (2003) *J Am Chem Soc* 125:8702
44. Trudeau S, Morgan JB, Shrestha M, Morken JP (2005) *J Org Chem* 70:9538
45. Nguyen P, Lesley G, Taylor NJ, Marder TB, Pickett NL, Clegg W, Elsegood MRJ, Norman NC (1994) *Inorg Chem* 33:4623
46. Baker RT, Calabrese JC, Westcott SA, Nguyen P, Marder TB (1993) *J Am Chem Soc* 115:4367
47. Dai C, Stringer G, Marder TB, Scott AJ, Clegg W, Norman NC (1997) *Inorg Chem* 36:272
48. Lam KC, Lam WH, Lin Z, Marder TB, Norman NC (2004) *Inorg Chem* 43:2541
49. Câmpian MV, Harris JL, Jasim N, Perutz RN, Marder TB, Whitwood AC (2006) *Organometallics* 25:5093
50. Pubill-Ulldemolins C, Poyatos M, Bo C, Fernández E (2013) *Dalton Trans* 14:746

51. Shiomi T, Adachi T, Toribatake K, Zhou L, Nishiyama, H (2009) *Chem Commun* 5987
52. Toribatake K, Nishiyama H (2003) *Angew Chem Int Ed* 52:11011
53. Iwadate N, Suginome M (2010) *J Am Chem Soc* 132:2548
54. Miralles N, Cid J, Cuenca AB, Carbó JJ, Fernández E (2015) *Chem Commun* 51:1193
55. Borner C, Brandhorst K, Kleeberg C (2015) *Dalton Trans* 44:8600
56. Teltewskoi M, Panetier JA, Macgregor SA, Braun T (2013) *Angew Chem Int Ed* 49:3947
57. Dai C, Robins EG, Scott AJ, Clegg W, Yufit DS, Howard JAK, Marder TB (1998) *Chem Commun* 1983
58. Miller SP, Morgan JB, Nepveux FJ, Morken JP (2006) *Org Lett* 6:131
59. Mkhaliid IA, Coapes RB, Edes SN, Coventry DN, Souza FES, Thomas RLL, Hall JJ, Bi S-W, Lin Z, Marder TB (2008) *Dalton Trans* 1055
60. Kondoh A, Jamison TF (2010) *Chem Commun* 46:907
61. Coapes RB, Souza FES, Thomas RL, Hall JJ, Marder TB (2003) *Chem Commun* 614
62. Nguyen P, Coapes RB, Woodward AD, Taylor NJ, Burke JM, Howard JAK, Marder TB (2002) *J Organomet Chem* 652:77
63. Toribatake K, Miyata S, Naganawa Y, Nishiyama H (2015) *Tetrahedron* 71:3203
64. Miura T, Takahashi Y, Murakami M (2008) *Org Lett* 10:1743
65. Youn SW (2009) *Eur J Org Chem* 2009(16):2597
66. Carter CAG, Vogels CM, Harrison DJ, Gagnon MKJ, Norman DW, Langler RF, Baker RT, Westcott SA (2001) *Organometallics* 20:2130
67. Kallaene SI, Braun T, Teltewskoi M, Braun B, Herrmann R, Laubenstein R (2015) *Chem Commun* 51:14613
68. Kallaene SI, Braun T, Braun B, Mebs S (2014) *Dalton Trans* 43:6786
69. Teltewskoi M, Kallaene SI, Braun T, Herrmann R (2013) *Eur J Inorg Chem* 33:5762
70. Lawson YG, Lesley MJG, Norman NC, Rice C, Craig R, Marder TB (1997) *Chem Commun* 2051
71. Ali HA, Goldberg I, Srebnik M (2001) *Organometallics* 20:3962
72. Ito H, Yamanaka H, Tateiwa J, Hosomi A (2000) *Tetrahedron Lett* 4:6821
73. Takahashi K, Ishiyama T, Miyaura N (2000) *Chem Lett* 31:982
74. Takahashi K, Ishiyama T, Miyaura N (2001) *J Organomet Chem* 625:47
75. Fernández E, Whiting A (2015) *Synthesis and application of organoboron compounds*. Springer, Heidelberg, Chapters 1 and 3
76. Kabalka GW, Das BC, Das S (2002) *Tetrahedron Lett* 43:2323
77. Toribatake K, Zhou L, Tsunuta A, Nishiyama H (2013) *Tetrahedron* 69:3551
78. Mun S, Lee J-E, Yun J (2006) *Org Lett* 8:4887
79. Lee J-E, Yun J (2008) *Angew Chem Int Ed* 47:145
80. Sim H-S, Feng X, Yun J (2009) *Chem Eur J* 15:1939
81. Chea H, Sim H-S, Yun J (2009) *Adv Synth Catal* 351:855
82. Hirano K, Yorimitsu H, Oshima K (2007) *Org Lett* 9:5031
83. Waltz KM, He X, Muhoro C, Hartwig JF (1995) *J Am Chem Soc* 117:11357
84. Ishiyama T, Takagi J, Ishida K, Miyaura N, Anastasi NR, Hartwig JF (2001) *J Am Chem Soc* 124:390
85. Hartwig JF, Cook KS, Hapke M, Incarvito CD, Fan Y, Webster CE, Hall MB (2005) *J Am Chem Soc* 127:2538
86. Cho J-Y, Tse MK, Holmes D, Maleczka RE, Smith MR (2002) *Science* 295:305
87. Paul S, Chotana GA, Holmes D, Reichle RC, Maleczka RE, Smith MR (2006) *J Am Chem Soc* 128:15552
88. Mkhaliid IA, Barnard JH, Marder TB, Murphy JM, Hartwig JF (2010) *Chem Rev* 110:890
89. Shimada S, Batsanov AS, Howard JAK, Marder TB (2001) *Angew Chem Int Ed* 40:2168
90. Chen H, Schlecht S, Semple TC, Hartwig JF (2000) *Science* 287:1995
91. Cho JY, Iverson CN, Smith MR (2000) *J Am Chem Soc* 122:12868
92. Mertins K, Zapf A, Beller M (2004) *J Mol Catal A Chem* 207:21
93. Kawamori S, Miyazaki T, Ohmiya H, Iwai T, Sawamura M (2011) *J Am Chem Soc* 133:19310

94. Kawamorita S, Miyazaki T, Iwai T, Ohmiya H, Sawamura M (2012) *J Am Chem Soc* 134:12924
95. Iwai T, Murakami R, Harada T, Kawamorita S, Sawamura M (2014) *Adv Synth Catal* 356:1563
96. Källäne SI, Braun T, Braun B, Mebs S (2014) *Dalton Trans* 43:6786
97. Källäne SI, Braun T (2014) *Angew Chem Int Ed* 53:9311
98. Bheeter ChB, Chowdhury AD, Adam R, Jackstell R, Beller M (2015) *Org Biomol Chem* 13:10336
99. Procacci B, Jiao Y, Evans ME, Jones WD, Perutz RN, Whitwood AC (2015) *J Am Chem Soc* 137:1258
100. Murata M (2012) *Heterocycles* 85:1795
101. Lindup RJ, Marder TB, Perutz RN, Whitwood AC (2007) *Chem Commun* 3664
102. Teltewskoi M, Panetier JA, Macgregor SA, Braun T (2019) *Angew Chem Int Ed* 49:3947
103. Källäne SI, Teltewskoi M, Braun T, Braun B (2015) *Organometallics* 34:11156
104. Guo W-H, Min Q-Q, Gu J-W, Zhang X (2015) *Angew Chem Int Ed* 54:9075
105. Tobisu M, Kinuta H, Kita Y, Remond E, Chatani N (2012) *J Am Chem Soc* 134:115
106. Jiang Y-Y, Yu H-Z, Fu Y (2013) *Organometallics* 32:926
107. Esteruelas AA, Oliván M, Vélez A (2015) *J Am Chem Soc* 137:12321
108. Kinuta H, Tobisu M, Chatani N (2015) *J Am Chem Soc* 137:1593
109. Ohmura T, Yamamoto Y, Miyaara M (2000) *J Am Chem Soc* 122:4990
110. Cid J, Carbó JJ, Fernández E (2012) *Chem Eur J* 18:1512
111. Barbeyron B, Benedetti E, Cossy J, Vasseur JJ, Arseniyadis S, Smietana M (2014) *Tetrahedron* 70:8431
112. Lin Z (2008) *Struct Bond Contemp Met Boron Chem* 130:123
113. Kays D, Aldridge S (2008) *Struct Bond Contemp Met Boron Chem* 130:29
114. Johnson HC, Torry-Harris R, Ortega L, Theron R, McIndoe JS, Weller AS (2014) *Catal Sci Technol* 4:3486

Rhodium Catalysts for C–S Bond Formation

Andrea Di Giuseppe, Ricardo Castarlenas, and Luis A. Oro

Abstract Sulfur-containing molecules are commonly found in chemical biology, organic synthesis, and materials chemistry. The preparation of these compounds through traditional methods usually required harsh reaction conditions. The use of transition-metal-based catalysts has allowed the development of more efficient and sustainable synthetic processes. Rhodium-catalyzed C–S bond formation through the reaction between sulfur sources such as S_8 , thiols, or disulfides with organic substrates such as alkynes, allenes, and aryl/alkyl halides is one of the most important methods in the synthesis of thioethers. Here, we summarize recent efforts in the reactions of cross coupling, C–H activation, metathesis, thiolation, carbothiolation, and hydrothiolation for the C–S bond formation catalyzed by rhodium complexes, particularly highlighting the synthetic and mechanistic aspects.

Keywords Alkynes • Allenes • Carbothiolation • C–H activation • Cross coupling • Halides • Hydrothiolation • Thioethers • Thiolation

Contents

1	Introduction	33
1.1	Rhodium-Catalyzed C–S Bond Formation Reactions	33
2	Substitution Reactions	34
2.1	Cross-Coupling Reactions	35
2.2	C–S Coupling via C–H Activation	39
2.3	Metathesis of Thioethers and Disulfides	49

3	Catalytic Addition of S–X on Unsaturated Substrates	51
3.1	Addition of S–S and S–C	53
3.2	Hydrothiolation of Unsaturated Substrates	56
	References	64

Abbreviations

(S)-	(R,R)-1,2-Bis[(R)-4,5-dihydro-3H-binaphtho(1,2-c:2',1'-e)
BIPHANE	phosphepino]benzene
AMLA	Ambiphilic metal ligand activation
Ar ^F	3,5-(CF ₃) ₂ C ₆ H ₃
Bz	Benzyl
CMD	Concerted metalation deprotonation
Cod	Cyclooctadiene
Coe	Cyclooctene
Cp*	Pentamethylcyclopentadienyl
DCE	Dichloroethane
DDQ	2,3-Dichloro-5,6-dicyano-1,4-benzoquinone
DMA	Dimethylacetamide
DMF	Dimethylformamide
DMSO	Dimethylsulfoxide
DPEPhos	Bis[(2-diphenylphosphino)phenyl] ether
Dppb	1,4-Bis(diphenylphosphino)butane
dppBz	1,2-Bis(diphenylphosphino)benzene
Dppe	1,2-Bis(diphenylphosphino)ethane
dppf	1,1'-Ferrocenediyl-bis(diphenylphosphine)
Dppp	1,3-Bis(diphenylphosphino)propane
Dpppe	1,5-Bis(diphenylphosphino)pentane
e.e.	Enantiomeric excess
IPr	1,3-Bis-(2,6-diisopropylphenyl)imidazol-2-carbene
Nbd	2,5-Norbornadiene
OAc	Acetate
O ^t Bu	<i>tert</i> -Butoxide
OTf	Triflate
r.t.	Room temperature
^t AmOH	2-Methyl-2-butanol
THF	Tetrahydrofuran
Tp	Hydrotris(1-pyrazolyl)borate
Tp*	Hydrotris(3,5-dimethylpyrazol-1-yl)borate

1 Introduction

Sulfur is contained in many synthetic reagents, functional materials, or agrochemicals and represents an essential element for all type of life as it is present in amino acids, vitamins, and cofactors [1]. Several bioactive drugs including β -lactam and sulfonamide antibiotics, nonsteroidal anti-inflammatory agents/analgesics, diuretics, antidiabetics, antiulcer, and antipsychotics contain this oligoelement [1–9]. An increasing demand of these molecules has entailed the development of new efficient and selective synthetic methods via C–S bond formation. From this point of view, catalysis is one of the fundamental pillars of sustainable chemistry, and the design and application of new catalysts and catalytic systems are simultaneously achieving the dual goals of environmental protection and economic benefit [10, 11].

Among all branches of catalysis, transition-metal-based catalysts had always been a mainstay of industrial chemistry, and nowadays a number of outstanding catalytic systems have been developed. In particular, the last 3 decades have witnessed a huge increase in catalytic systems for C–heteroatom bond formation [12–30]. In contrast, the development of catalytic systems able to mediate C–S coupling is relatively scarce. One of the reasons for this underdevelopment is the consideration of sulfurated compounds as potent poisons for organometallic catalysts [31]. The overcome of this established belief has changed this trend, and only recently an amount of transition-metal catalytic systems for C–S bond formation has impressively emerged [32–44]. Among these catalysts, rhodium complexes represent one of the most interesting systems principally due to its tunability that allows the thiofunctionalization of a broad range of substrates using a wide variety of sulfur sources. Particularly, rhodium catalysts are the perfect examples where a high degree of control of the chemo-, stereo-, and regioselectivity can be achieved due to an in-depth understanding of the mechanistic issues that allow for a rational design of the organometallic catalysts.

This review outlines the recent advances in the catalytic C–S bond formation mediated by rhodium complexes with a special attention on the mechanism of the reaction. Transformations which are the topics of other chapter of this volume are not included in this review.

1.1 Rhodium-Catalyzed C–S Bond Formation Reactions

As introduced above, rhodium compounds are really flexible catalysts for C–S bond-forming transformations. A regrouping in two big families of reactions can be formally established: (1) substitution and (2) addition reactions. The former includes all type of transformations in which a C–X bond is transformed into a C–S functionality through the formal substitution of the X (a halogen or a hydrogen) by a thio-substituent arising from the appropriate sulfur source S–Y with concomitant formation of X–Y as a by-product (Fig. 1a). Transformations included in this family

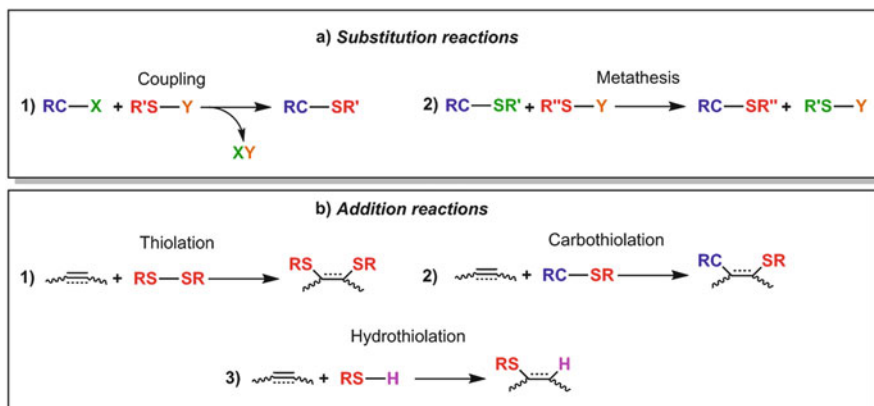


Fig. 1 C-S bond formation catalyzed by Rh: substitution reactions (a) and addition reactions (b)

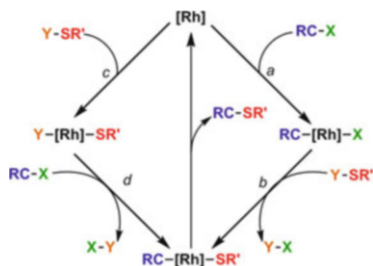
are the cross-coupling reactions and the metathesis of thioethers. Substrates involved include alkynes, aromatic compounds bearing a directing group, molecules with an activated $C(sp^2)$ -H or $C(sp^3)$ -H (including heterocycles), halogenated compounds, and thioethers, while the sulfur sources are thiols, disulfides, and α -thioketones.

In the second family of reactions, an appropriate sulfur source S-Y is added into an unsaturation of the substrate. In contrast to the substitution reactions, the hybridization of the carbon where the addition occurs changes from sp^x to sp^{x+1} , and more importantly, a 100% atom efficiency is obtained with no by-product formation, leading to substantial practical advantages in terms of green chemistry. Typical substrates used for these transformations are alkynes and allenes, while the sulfur sources include disulfides, thioethers, and thiols. Depending on the type of thio-substrate added, the reactions are, respectively, named thiolation, carbothiolation, and hydrothiolation (Fig. 1b).

2 Substitution Reactions

The substitution reactions are a widely recognized approach for the coupling of two organic substrates by the construction of new C-C and C-X bonds and the elimination of a small molecule. Depending on the substrates, the following classification can be established for C-S bond formation reactions promoted by rhodium: (1) cross coupling between organic halides with thiols, disulfides (or oligosulfide), or elemental sulfur, (2) coupling via C-H activation between non pre-functionalized organic compounds containing relative acidic C-H bond or bearing directing groups and disulfides or α -thio-substituted ketones as the sulfur source, and (3) metathesis between two sulfurated substrates.

Fig. 2 General reaction mechanism of cross-coupling Rh-catalyzed C–S bond formation

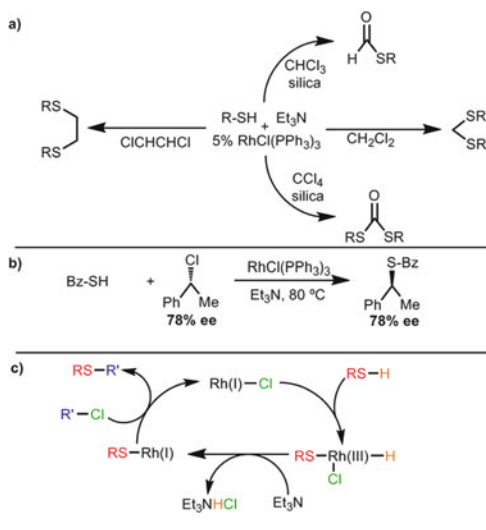


2.1 Cross-Coupling Reactions

The transition-metal-catalyzed cross coupling is a very powerful tool for the creation of C–C and C–heteroatom bonds [45–52]. A general mechanistic framework is described in Fig. 2. In the first step of the cycle, the Rh^I precursor activates the C–X bond leading to a RC–Rh^{III}–X species (step a). The transmetalation by the sulfur-containing substrate Y–SR' provides RC–Rh^{III}–SR' simultaneously to the elimination of YX (step b). In some cases an additive (bases, phosphine, silane) is required for trapping of the Y and X fragments. In the last step, a C–S reductive elimination gives the coupling product and regenerates the starting Rh^I species. Alternatively, the sulfur-containing compound can add first (c) and subsequent reaction with the halogenated substrate yields RC–Rh^{III}–SR' (d) that evolves by the same pathway.

The formation of C–S bonds by metal-catalyzed cross-coupling reactions was studied for the first time by Migita in 1978 for the Pd-catalyzed coupling of aryl halides with thiols [53]. Starting from this pioneering work, a lot of new catalytic systems have been developed using several metals such as Pd, Cu, Ni, Fe, Mn, Co, In, Ag, Bi, or La [54–70]. The development of rhodium-based catalysts for the formation of C–S bonds via cross coupling is relatively recent. The first work was published by Tanaka and coworkers in 2005 [71]. In this report the coupling of thiols and polychloroalkanes in the presence of trimethylamine using RhCl(PPh₃)₃ was reported. This reaction serves as a convenient new method to produce formaldehyde dithioacetals and ethylenedithioethers. It was interestingly found that the reaction of thiols and tri- or tetra-chlorinated alkanes such as CHCl₃ and CCl₄ gives thioformate and a dithiocarbonic ester, respectively, presumably through hydrolysis of corresponding polythiomethanes by silica gel (Fig. 3a). The reaction of benzyl mercaptan with (R)-(1-chloroethyl)benzene was investigated to gain mechanistic insights, revealing a complete inversion of configuration in the formed sulfide (Fig. 3b). The mechanism proposed in Fig. 3c justifies this observation. The first step is the oxidative addition of the thiol to afford a hydride–thiolate–rhodium(III) species. Elimination of HCl by treatment with Et₃N furnishes rhodium(I)–thiolate intermediates, which reacted with alkyl halides in an S_N2 fashion, thereby furnishing sulfides and regenerating the rhodium(I) active species.

Fig. 3 Coupling of thiols and polychloroalkanes catalyzed by $\text{RhCl}(\text{PPh}_3)_3$ in the presence of trimethylamine [71]



The heterogeneous version of this reaction was developed by Cai and coworkers by supporting of the Wilkinson's catalyst on MCM 41 derivatized with diphosphine ligand [72]. This system achieves the coupling of thiols with polychloroalkanes or alkyl halides at 30 °C or 80 °C in the presence of triethylamine, yielding a variety of formaldehyde dithioacetals, ethylenedithioethers, and unsymmetric thioethers in good to excellent yields. The catalyst was easily recycled by simple filtration of the reaction solution and reused for ten consecutive trials without significant loss of activity.

Tanaka and coworkers expanded their methodology to the catalytic enantioselective synthesis of planar-chiral dithiaparacyclophanes [73, 74]. A catalytic system based on the cationic $[\text{Rh}(\text{cod})_2]\text{BF}_4$ complex and the chiral diphosphine (S)-BINAPHANE was efficient for the catalytic coupling of dithiols and 1,4-bis(bromomethyl)benzenes, yielding dithiaparacyclophanes with enantiomeric excess (e.e.) up to 49% (Fig. 4) [73]. This method represents the first example of asymmetric synthesis of planar-chiral cyclophanes through catalytic enantioselective construction of the *ansa* chains.

An enhancement of this reaction was disclosed by the same research group. A reductive coupling of disulfides with alkyl halides mediated by Wilkinson's catalyst in presence of triethylamine was developed. Molecular hydrogen was used as a reducing agent. This reaction serves as a convenient method to produce unsymmetrical sulfides from disulfides instead of odoriferous thiols (Fig. 5a) [75]. The in situ formation of thiols was demonstrated by the reaction of didodecyl disulfide with molecular hydrogen in the presence of 3% $\text{RhCl}(\text{PPh}_3)_3$ at 100 °C (Fig. 5b). Noteworthy, in spite of $\text{RhCl}(\text{PPh}_3)_3/\text{H}_2$ being a powerful hydrogenating system, the presence of olefins seems to be tolerated. The reaction of (p-TolS)₂ with cinnamyl bromide provides the desired cinnamyl sulfide in 76% yield, and almost no hydrogenated phenylpropyl sulfide was generated (Fig. 5c).



Fig. 4 Enantioselective coupling of dithiols with dibromides catalyzed by $[\text{Rh}(\text{cod})_2]\text{BF}_4/(\text{S})\text{-BINAP}$ [73]

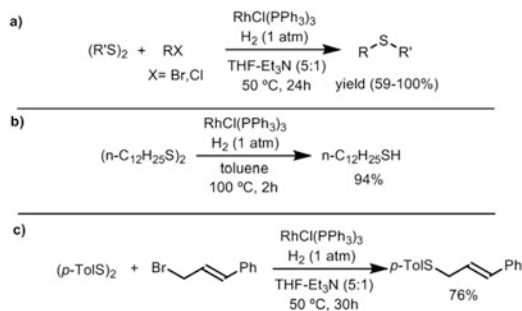


Fig. 5 Reductive coupling of disulfides with alkyl halides mediated by Wilkinson's catalyst in the presence of triethylamine and H_2 [75]

The examples showed above are all referred to $\text{C}(\text{sp}^3)\text{-X}$ coupling with a thio-compound. It should be pointed out that nucleophilic substitution on the $\text{C}(\text{sp}^3)$ atoms occurs readily and usually does not require a catalyst. However, the formation of $\text{C}(\text{sp}^2)\text{-S}$ bonds is more challenging and a metallic catalyst is often required. In this context, Yamaguchi and coworkers reported that a catalytic system composed of $\text{RhH}(\text{PPh}_3)_3$, dppbz, and an excess of triphenylphosphine is efficient for the reaction between aryl fluorides and aliphatic and aromatic disulfides (Fig. 6a) [76]. The reaction proceeds in high yield when electron-withdrawing groups are present in the aryl fluoride, while fluorobenzene is inert. The use of polyfluorobenzenes leads to the production of polyaryltiolation products, with a marked preference for the formation of *p*-difluoride derivatives (Fig. 6b). Interestingly, the reaction of 1-bromo-4-chloro-3-fluorobenzene with di(*p*-tolyl) disulfide provides selectively the fluorine-substituted product indicating that, in this reaction conditions, the reactivity of aryl fluoride is higher than bromide and chloride counterparts. Triphenylphosphine is fundamental for the reaction acting as a trap of fluoride. In fact, extremely unstable sulfenium fluoride R-SF is formally formed in the reaction. The presence of PPh_3 is crucial to make the reaction thermodynamically favorable converting this compound into more stable products such as triphenylphosphine difluoride and disulfide [40].

A slight modification of the reaction conditions, as the change of dppbz for dppe and THF instead of $\text{C}_6\text{H}_5\text{Cl}$ as solvent, allowed for the coupling of aromatic and aliphatic acid fluorides with disulfides providing the corresponding thioesters (Fig. 7) [77]. Also in this case, fluoride seems to be more reactive than chloride

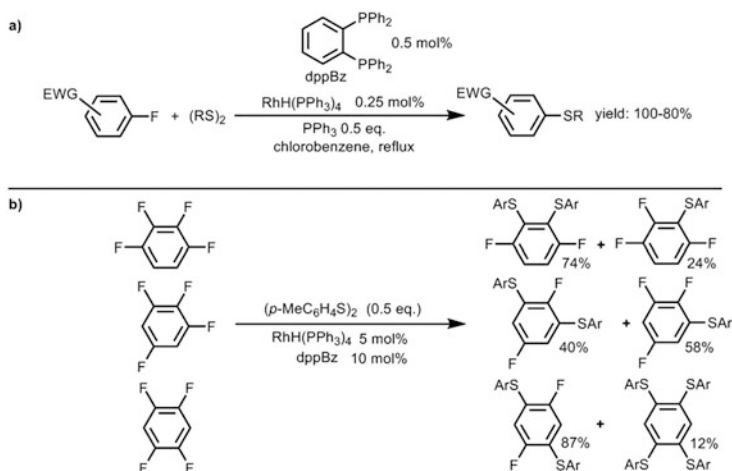


Fig. 6 Reaction between aryl fluorides and disulfides catalyzed by $\text{RhH}(\text{PPh}_3)_3$ and dppbz in the presence of an excess of triphenylphosphine [76]

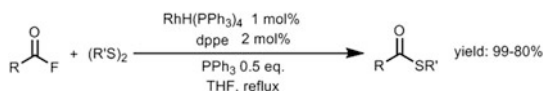


Fig. 7 Reaction between acid fluorides and disulfides catalyzed by $\text{RhH}(\text{PPh}_3)_3$ and dppe in the presence of an excess of triphenylphosphine [77]

as demonstrated in the reaction of benzoyl fluoride/chloride with di(*p*-tolyl)disulfide in which the former gave the respective thioester in higher yield than the last.

Thiols and disulfides are not the only sulfur source available. In this context, elemental sulfur is attractive because it is cheap, readily available, and easy to handle. Yamaguchi reported the coupling of pentafluorobenzenes with S_8 to give bis(4-substituted 2,3,5,6-tetrafluorophenyl) sulfides in the presence of a catalytic system composed of $\text{RhH}(\text{PPh}_3)_4/\text{dppBz}$ and a stoichiometric amount of tributylsilane as fluoride scavenger (Fig. 8a) [78]. An organic trisulfide and a tetrasulfide were also examined, which exhibited notable substrate specificity. Di-tert-butyl tetrasulfide reacted only with very poor aryl monofluorides (containing two electron-withdrawing groups) and 2-fluorobenzothiazole, while di-tert-butyl trisulfide reacted with aryl monofluorides (Fig. 8b). The authors ascribe this difference of reactivity to the variation in S–S bond energy. In fact, elemental sulfur with lower S–S bond energy reacts with the most reactive aryl fluoride (pentafluorobenzenes), while increasing the S–S bond energy (trisulfide > tetrasulfide) results in reactivity with less activated aryl fluorides. A similar correlation will be discussed below for other thiolation reactions.

Aryl fluorides are not the exclusivity for these transformations; also the other aryl halides (chloride, bromide, iodide) are suitable substrates for this reaction [79, 80]. Lee and coworkers have shown that the dimeric complex $[\text{RhCl}(\text{cod})_2]_2$

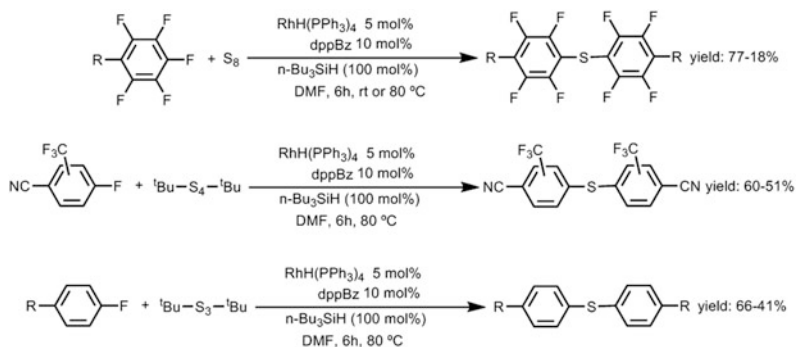


Fig. 8 Reaction between aryl fluoride and S_8 or oligosulfide mediated by $\text{RhH(PPh}_3)_4/\text{dppBz}$ in the presence of $n\text{-Bu}_3\text{SiH}$ [78]

(with 1 equiv. of PPh_3) is able to catalyze the cross coupling of aryl iodide with both aromatic and aliphatic thiols in the presence of a strong base such as NaO^tBu leading to asymmetric diaryl and aryl alkyl thioethers in good to excellent yields (73–99%) [79]. In similar conditions, Ozerov and coworkers extended the precedent work to the use of aryl chlorides and bromides using the pincer complex $(\text{POCOP})\text{Rh}(\text{H})\text{Cl}$ as a catalyst (Fig. 9) [80]. In this brilliant paper, the mechanism of the process was unveiled due to an in-depth study of each elementary step and the isolation of some intermediates involved in the reaction (Fig. 9b). In the first step, the active Rh^{I} species $(\text{POCOP})\text{Rh}$ (**b**) (unobserved) is generated by dehydrochlorination of **a** with NaO^tBu . The oxidative addition of the aryl halide to this unsaturated fragment generates $(\text{POCOP})\text{Rh}(\text{Ar})(\text{X})$ (**c**). The transmetalation of **c** with the in situ produced NaSR provides the aryl-thiolate– Rh^{III} species **d**. Then, C–S reductive elimination gives rise to the Rh^{I} sulfur adduct $(\text{POCOP})\text{Rh}(\text{ArSR})$ (**e**) that after the final thioether, dissociation regenerates the initial active fragment **b**.

2.2 C–S Coupling via C–H Activation

As showed above cross coupling of halogenated substrate with sulfur source, such as thiol disulfides or elemental sulfur, is a powerful tool for the synthesis of thioethers under a variety of conditions (*vide supra*). However, these methodologies present an important drawback, the prefunctionalization of the substrates. This inconvenience can be overcome by using catalytic systems able to directly functionalize the C–H bonds. Transition-metal-mediated C–H activation is nowadays one of the most important methodologies for the formation of carbon–carbon and carbon–heteroatom bonds with application both in academic and industrial chemistry [81–92]. During the past decade, this approach has been applied to the

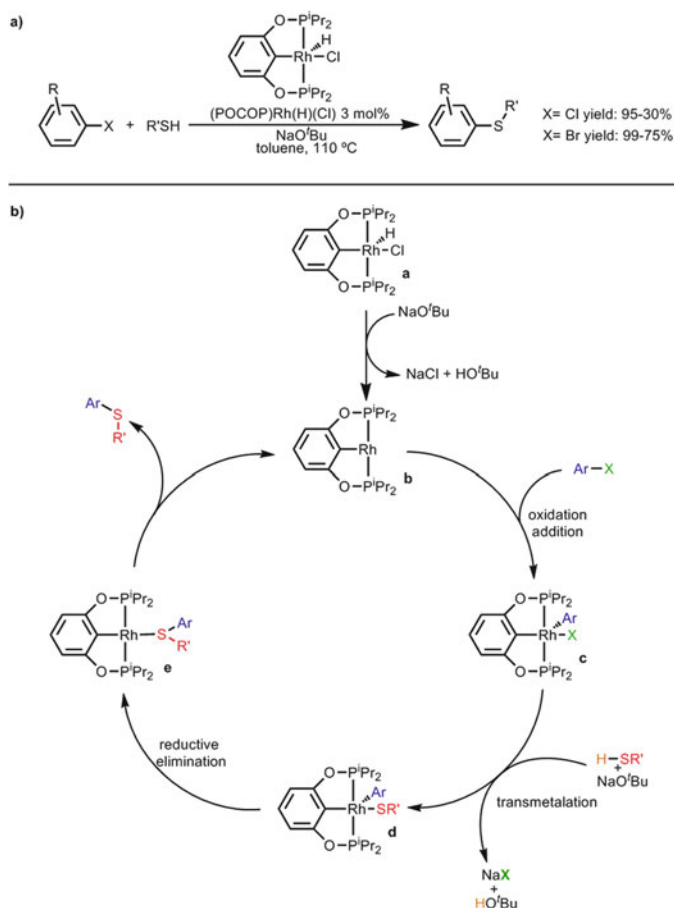
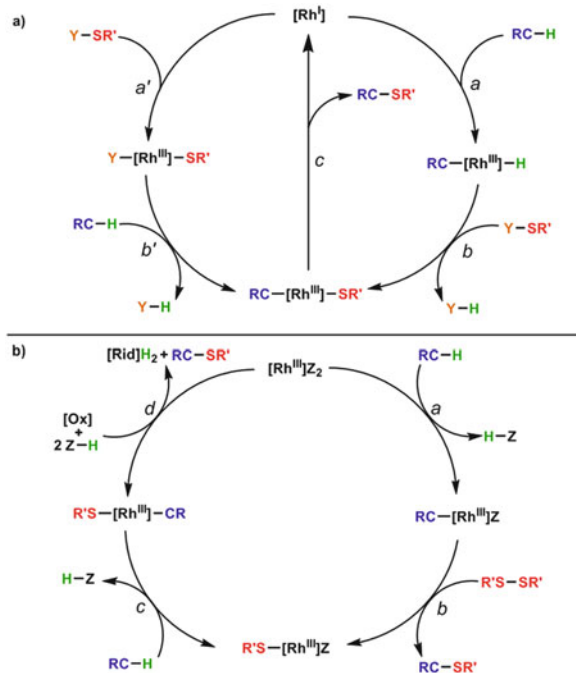


Fig. 9 Cross coupling of aryl chlorides or bromides with thiols catalyzed by $(\text{POCOP})\text{Rh(H)Cl}$ in the presence of NaO'Bu [80]

direct thiolation of unfunctionalized substrates using different transition metals such as Pd, Cu, Ru, etc. [93–99].

In the field of the C–H activation, rhodium catalysts have a prominent place, and several systems able to mediate the direct thiolation of C–H bonds have been developed. Two main families can be encountered: (1) the Yamaguchi systems based on the Rh^{I} complex $\text{RhH}(\text{PPh}_3)_4$ and (2) the systems based on the Rh^{III} complex $[\text{RhCp}^*\text{Cl}_2]_2$ for the thiolation of aromatic substrates bearing a directing group. The general mechanism of these two catalysts is showed in Fig. 10. In the case of the systems based on $\text{RhH}(\text{PPh}_3)_4$, the C–H bond oxidatively adds to the Rh^{I} precursor (step a) or, alternatively, it is the Y–S bond (a'), leading to the activated Rh^{III} species C–Rh–H or Y–Rh–S, respectively (Fig. 10a). These species further react with a Y–S or C–H bond (step b or b) to provide thiolate– Rh^{III} –alkyl/alkynyl intermediates with the simultaneous elimination of Y–H. This fundamental step can

Fig. 10 General mechanisms of reaction for the formation of C–S bond via C–H activation mediated by $\text{RhH}(\text{PPh}_3)_4$ (a) or $[\text{RhCp}^*\text{Cl}_2]_2$ (b)



take place either by the formation of oxidized $[\text{Rh}^{\text{V}}(\text{RC})(\text{R}'\text{S})(\text{Y})(\text{H})]$ intermediate followed by the reductive elimination of Y-H or by a non-oxidative process via electrophilic substitution, base-mediated (AMLA or CMD) or σ -bond metathesis [100–102]. The final reductive coupling of the C–S bond (c) gives rise to the wanted thiolated substrate $\text{RC-SR}'$ and regenerates the starting Rh^{I} species. In the case of the $[\text{RhCp}^*\text{Cl}_2]_2$ -based systems, the mechanism is quite different (Fig. 10b). After an activation step in which the chlorido ligands are substituted by more labile anions (Z) (typically triflate), the Rh^{III} species undergo the activation of the C–H bond to form a C– Rh^{III} derivative with concomitant elimination of HZ (step a). This fundamental step can occur by several mechanisms that depend on the substrate and the reaction conditions [100–102]. The reaction of C– Rh^{III} with disulfides via a Rh^{V} intermediate or by nucleophilic substitution-like reaction affords the coupled product $\text{RC-SR}'$ (step b). Then, Rh^{III} -thiolate intermediate can activate another molecule of substrate leading to a C– $\text{Rh}^{\text{III}}-\text{S}$ (step c), which after reductive elimination step affords another molecule of thioether $\text{RC-SR}'$ (step d). The catalytic cycle is closed by the regeneration of the initial Rh^{III} active species through the oxidation of the final Rh^{I} complex obtained in step d.

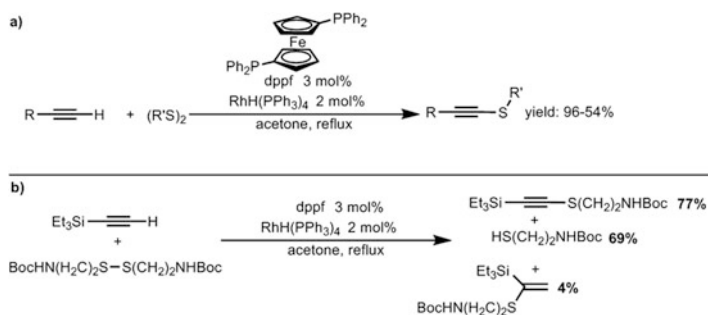


Fig. 11 Alkylthiolation reaction of 1-alkynes with disulfides catalyzed by $RhH(PPh_3)_4/dppf$ in acetone [103]

Rhodium(I) Catalytic Systems for C–S Coupling via C–H Activation

The first paper on the direct thiolation of organic substrates via C–H activation mediated by rhodium was presented in 2005 by Yamaguchi and coworkers, who disclosed the thiolation of 1-alkynes with disulfides [103]. Aryl, alkyl, and silyl 1-alkynes were reacted with dialkyl/diaryl disulfides under the catalyst system $RhH(PPh_3)_3/dppf$ in acetone. 1-alkyl/arylthio-1-alkynes were obtained in high yield with the simultaneous elimination of thiol (Fig. 11a). Remarkably, this catalytic system is highly chemoselective. In fact, rhodium(I) complexes are efficient catalysts for the addition of disulfides or thiols to alkynes (see Sect. 3). However, in this case the competition between C–H substitution and addition is completely displaced for the former, and only traces of hydrothiolation products were found, as demonstrated with the reaction of trimethylsilylacetylene and bis[2-(*t*-butoxycarbonylamino)ethyl] disulfide (Fig. 11b).

A slight modification of the above catalytic system allowed the α -thiolation of different substrates containing relative acidic C–H bonds (pK_a 16–18), such as nitroalkanes (and cyclo-nitroalkanes), diethyl malonate, and 1,2-diphenyl-1-ethanone with different disulfides (Fig. 12) [104]. In this report, the dppf is replaced with dppe and the DMA is used as solvent instead of acetone. Noteworthy, this reaction achieves good conversion only when is performed under air atmosphere. In fact, in these conditions thiols are oxidized to disulfide converting the reaction exergonic, then thermodynamically favored.

These reactions, as well as the other thiolation, developed by Yamaguchi with $RhH(PPh_3)_4$, turned out to be in equilibrium that suggest the easy reversibility of the C–S bond cleavage/formation. For this reason, depending on the reaction conditions, it is possible to control the transfer of a thio-group from an organosulfurated compound to another organic substrate. Following this approach, Yamaguchi and coworkers developed many transfer reactions for the thiolation of different types of substrates using in each case an appropriate sulfur source. The methylthiolation of α -phenyl ketones and α -phenylthio ketones was obtained using *p*-cyano- α -methylthioacetophenone as sulfur source in the presence of a catalytic

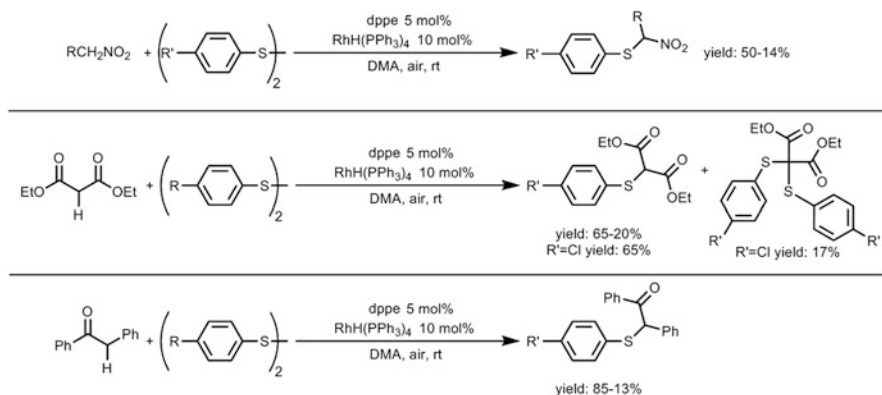


Fig. 12 Alkylthiolation reaction of 1-alkynes with disulfides catalyzed by $\text{RhH}(\text{PPh}_3)_4/\text{dppe}$ in acetone [104]

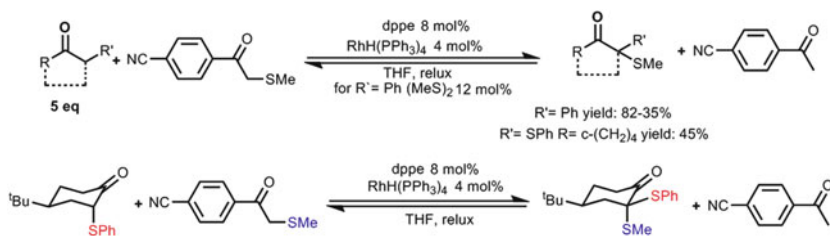


Fig. 13 Methylthiolation of α -phenyl ketones and α -phenylthio ketones with *p*-cyano- α -methylthioacetophenone catalyzed by $\text{RhH}(\text{PPh}_3)_4/\text{dppe}$ in THF [105, 106]

amount of $\text{RhH}(\text{PPh}_3)_4$ and dppe (Fig. 13) [105, 106]. Interestingly, the reaction of diastereomeric 4-(*tert*-butyl)-2-phenylthiocyclohexanones gave selectively an axial 2-methylthiolated product (Fig. 13).

The same catalytic system can be used for the α -methylation reaction of unactivated ketone giving α -methylthio ketones (Fig. 14a) [107]. In this case the use of *p*-cyano- α -methylthioacetophenone as SMe source is not effective, while good results have been obtained with 1,2-diphenyl-2-methylthio-1-ethanone. Interestingly, the methylthiolation in unsymmetric ketones takes place initially into the more substituted α -carbon, and then a rearrangement to the products thiolated at the less substituted carbons takes place (Fig. 14b). This probably indicates that the former to be the kinetic product and the latter the thermodynamic. Other substrates such as aldehydes, phenylacetate, and phenylacetone nitrile have been α -methylthiolated in the same reaction conditions (Fig. 14c).

The usefulness of this catalytic system was also demonstrated in the thioderivatization of heteroarenes such as 1,3-benzothiazoles, 1,3-benzoxazoles, and benzothiophene that give 2-phenylthio derivatives, and the monocyclic heteroaromatics, 1-methyl-1,2,3,4-tetrazole and 2-cyanothiophene, were converted

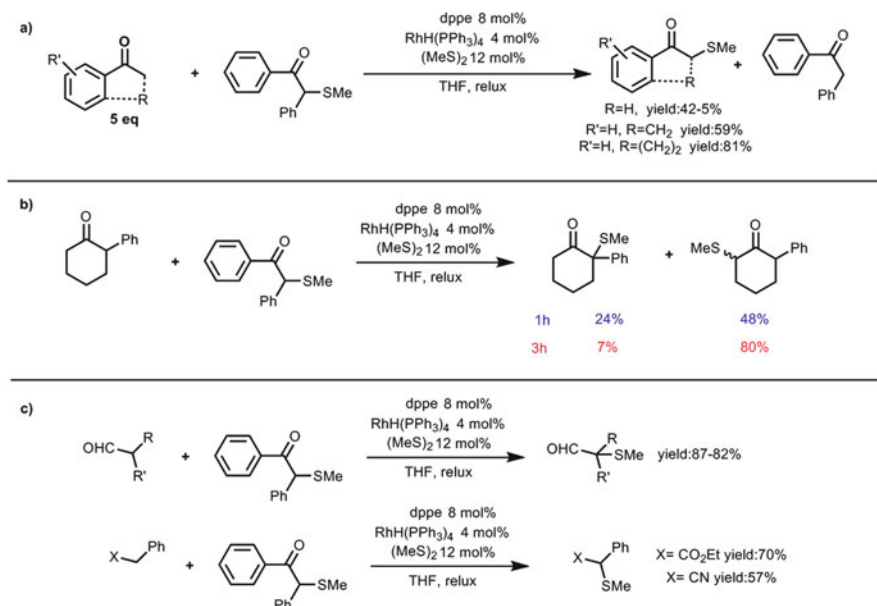


Fig. 14 Methylthiolation of unactivated ketones aldehydes, phenylacetate, and phenylacetonitrile with 1,2-diphenyl-2-methylthio-1-ethanone catalyzed by $\text{RhH(PPh}_3)_4/\text{dppe}$ in THF [107]

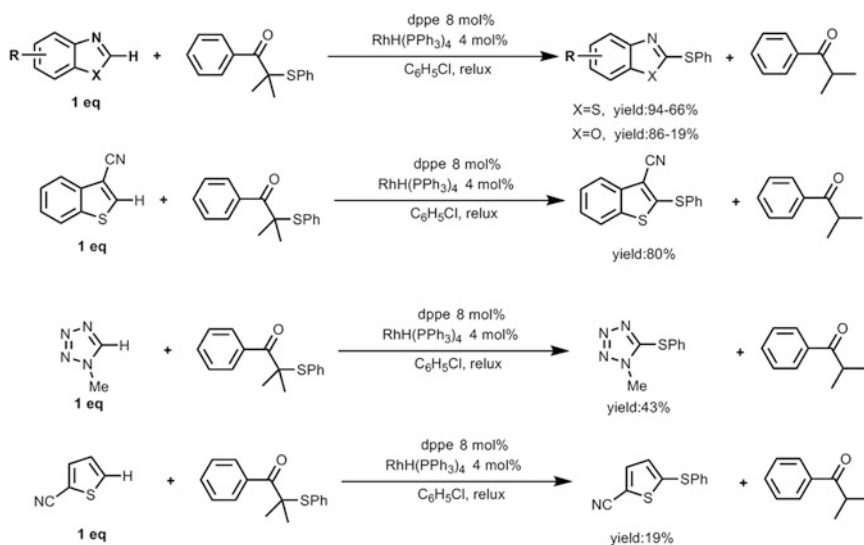


Fig. 15 Phenylthiolation of heteroarenes with α -(phenylthio)isobutyrophenone catalyzed by $\text{RhH(PPh}_3)_4/\text{dppe}$ in $\text{C}_6\text{H}_5\text{Cl}$ [108]

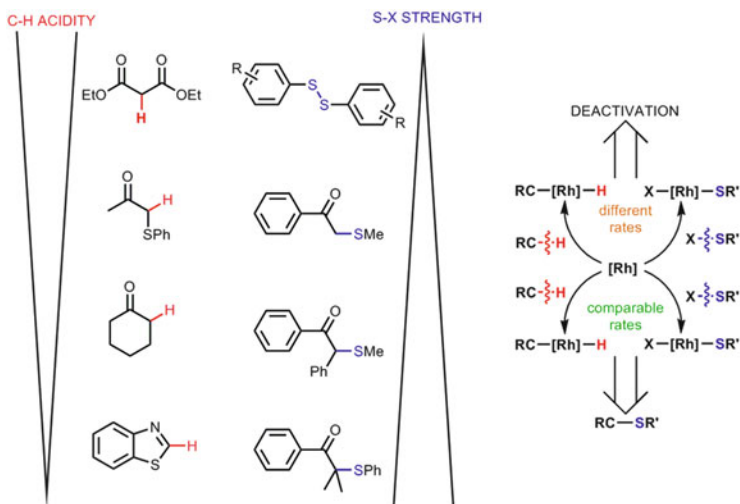


Fig. 16 C–H bond acidity of the substrate vs C–S strength of the S–X bond in the reaction of thiolation mediated by $\text{RhH}(\text{PPh}_3)_4$

into the 5-phenylthio compounds (Fig. 15) [108]. In this case the author found that the best sulfur source was α -(phenylthio)isobutyrophenone.

As it has been demonstrated with the above examples, the use of an appropriate phenylthio transfer reagent is crucial for the efficient catalyzed conversion of heteroaromatic C–H bonds into C–S bonds. An interesting correlation between the acidity of the C–H of the substrates and the strength of the S–X bond of the thio-source was found. Therefore, relatively acidic compounds such as nitroalkanes or malonate (pK_a 16–18) reacted with diaryl disulfides in the presence of O_2 , while 1-alkynes with a moderate acidic proton (pK_a 21) reacted with disulfides, and less acidic ketones and heteroarenes (pK_a 27) interact with different types of thioethers. These observations suggest an inverse correlation between the strength of the S–X bond and the acidity of the C–H proton (Fig. 16). Authors suggest that the favorable combination of substrates and sulfurating reagents is ascribable to kinetic reasons [104]. In fact, when a rhodium complex activates C–H and S–S bonds at comparable rates, thiolation reactions should proceed smoothly. Instead, if the C–H bond activation is much slower than S–S bond activation, the catalyst preferentially interacts with the S–S bond, which retards the total reaction deactivating the catalyst (Fig. 16). For this reason, the wise choice of an appropriate combination of substrate and sulfur source results fundamental to enhance the reaction rate and to drive the reaction to completion before catalyst deactivation.

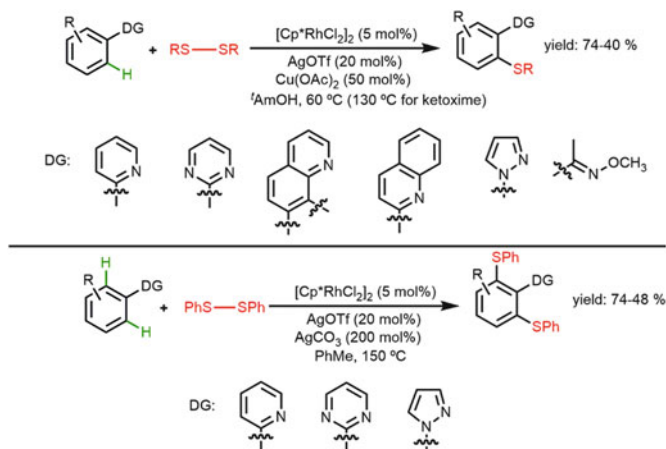


Fig. 17 Direct sulfenylation of arene via C–H activation mediated by $[\text{Cp}^*\text{RhCl}_2]_2/\text{AgOTf}/\text{Cu}(\text{OAc})_2$ in ${}^t\text{AmOH}$ [112]

Rhodium(III) Catalytic Systems for C–S Coupling via C–H Activation

Aromatic compounds represent one of the most abundant starting materials available for organic synthesis. However, the high stability of the aromatic $\text{C}(\text{sp}^2)\text{--H}$ bonds makes their functionalization really challenging. In the last years, Rh-based systems have been broadly exploited and used for its excellent catalytic properties in C–H bond activation and subsequent C–C or C–X formation [83, 109–111]. In particular, complexes containing the $[\text{Cp}^*\text{Rh}^{\text{III}}]$ have been extensively used in the selective C–H activation of aromatic compound bearing directing groups such as pyridine, oxime, and hydrazine, among others.

Catalytic systems based on these species have been just recently applied in the field of the C–S bond formation. In 2014 Li and coworkers reported the first example of Rh^{III} -catalyzed direct C–H thiolation using aryl and alkyl disulfides as sulfur source (Scheme 17) [112]. In this work, the catalytic system $[\text{Cp}^*\text{RhCl}_2]_2/\text{AgOTf}/\text{Cu}(\text{OAc})_2$ in ${}^t\text{AmOH}$ at 60°C is efficient in the mono-thiolation of several arenes containing pyridines, benzo[h]quinolone, bicyclic quinolone, pyrimidine, pyrazole, and ketoximes. In addition, modification of the reaction conditions allows for a double C–H activation/thioesterification process that affords dithioethers in moderate to good yields (Fig. 17). The broad substrate scope and high efficiency of the direct C–S coupling provide a straightforward way for selective preparation of sulfur-containing heterocycles not easily accessible by conventional cross-coupling reactions.

A mechanism coherent to that explained above was proposed by the authors (Fig. 18). In the first step of the reaction, the chlorido ligands of $[\text{Cp}^*\text{RhCl}_2]_2$ (**a**) are eliminated using AgOTf providing a more active cationic species containing the fragment $[\text{Cp}^*\text{Rh}]\text{OTf}_2$ (**b**). The pyridine framework coordinates to this Rh^{III} precursor directing the activation of the C–H bond of the arene leading to the

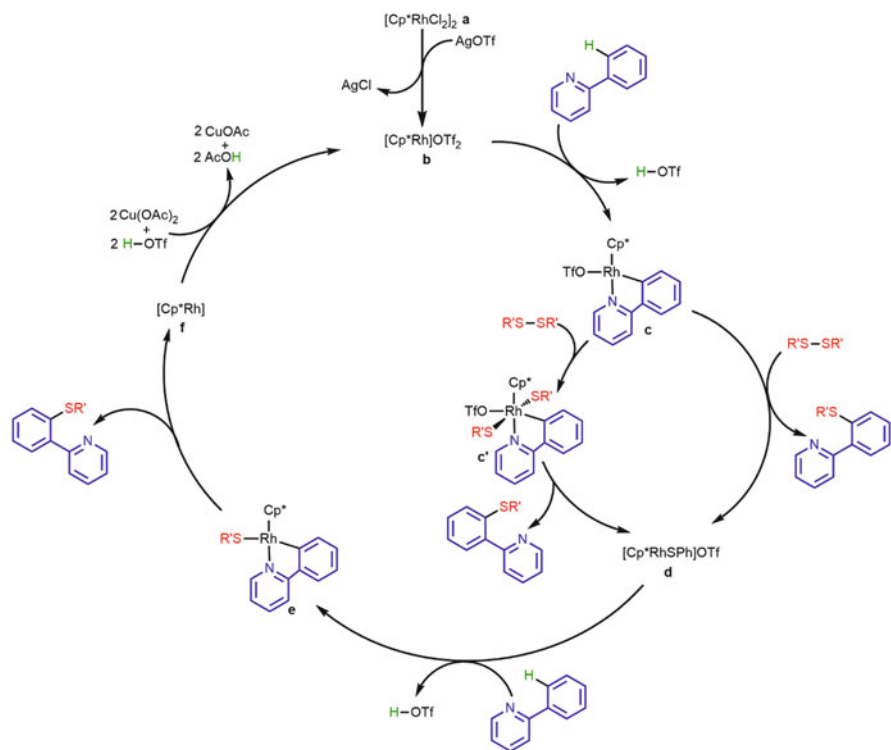


Fig. 18 Catalytic cycle for the direct sulfenylation of phenylpyridine mediated by $[\text{Cp}^*\text{RhCl}_2]_2/\text{AgOTf}/\text{Cu}(\text{OAc})_2$ [112]

rhodacycle **c**. This derivative can be synthesized independently and prove to catalyze efficiently the thiolation of phenylpyridine with $(\text{PhS})_2$, “bold” demonstrating that effectively is an intermediate of this transformation. Compound **c** reacts with disulfide to afford the phenylthiolated phenylpyridine and the $\text{PhS-Rh}^{\text{III}}$ species **d**, via a nucleophilic-addition-type reaction (path a) or, alternatively, via an oxidative pathway with the Rh^{V} intermediate **c'** (path b). Complex **d** reacts with another molecule of substrate leading to the five-membered rhodacycle **e**, which then undergoes reductive elimination to afford another molecule of organic product together with a rhodium(I) species **f**. Oxidation of **f** to **b** by the reduction of Cu^{II} to Cu^{I} completes the catalytic cycle.

Following the same catalytic approach, the direct thiolation of other type of substrates has been studied. Zhu and coworkers report in 2015 a convenient and efficient method for sulfuration and olefination of aromatic ketazines via rhodium-catalyzed oxidative C–H bond activation [113]. The catalytic system is composed of $[\text{Cp}^*\text{RhCl}_2]_2$ as precatalyst, AgOTf for the activation of the Rh complex, and $\text{Cu}(\text{OAc})_2$ as final oxidant. The selective phenylthio-etherification of a range of substituted ketazines using phenyl disulfides takes place in DCE at 60°C (Fig. 19). The proposed mechanism according to experimental results of kinetic

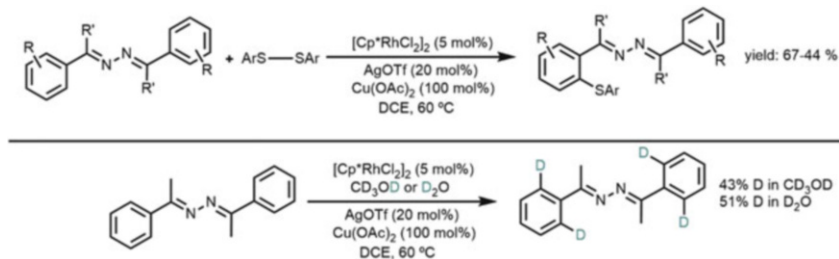


Fig. 19 Selective mono-phenyl thiosulfonylation of ketazines catalyzed by $[\text{Cp}^*\text{RhCl}_2]_2/\text{AgOTf}/\text{Cu}(\text{OAc})_2$ in DCE [113]

isotopic effect is similar to that described for the previous $\text{Cp}^*\text{Rh}^{\text{III}}$ system (Fig. 18). Notably, H/D exchange experiments revealed that all the four *ortho*-positions on aryl are deuterated, which demonstrated that the catalytic system, thanks to the key role of the directing group, is able to activate each of these C–H bonds (Fig. 19). However, the authors have been able to find adequate reaction conditions for the selective mono-thiolation to occur.

The usefulness of this catalytic system was also demonstrated in the selective C7-thiolation of indoles with disulfides [114]. Indole and indoline scaffolds are ubiquitous structural motifs found in a multitude of pharmaceutical compounds, particularly 7-substituted indoles and indolines. Wang and coworkers elegantly showed that the catalytic C7-thiolation of indolines is achievable by using a readily available and easily removable pyrimidyl group as a directing group. In the optimal conditions, the catalytic system, composed of $[\text{Cp}^*\text{RhCl}_2]_2$, AgOTf, and AgCO_3 (as oxidant) in toluene at 130°C , is able to mediate the thioetherification of a broad type of 1-(pyrimidin-2-yl)indoline derivatives with diphenyl disulfides (Fig. 20a). Notably, the choice of the N-protecting group was found to be crucial for this reaction. In fact, it was demonstrated that acetyl or *N,N*-dimethylcarbamoyl directing group did not deliver the corresponding product under the standard conditions of the pyrimidyl derivatives. Finally, the utility of this C7-thiolation reaction was further highlighted by its successful conversion of indolines into indoles. Oxidation with DDQ and removing of the pyrimidyl group with NaOEt afford 7-(phenylthio)-1*H*-indole in 97% yield (Fig. 20b). Also in this case, the proposed catalytic cycle perfectly fits with that showed in Fig. 18.

Alkyl and aromatic disulfides are not the only sulfur source suitable for the C–S formation by rhodium-catalyzed oxidative C–H bond activation. Li and coworkers have recently reported the selective catalytic trifluoromethylthiolation of indoles using *N*-(trifluoromethylthio)saccharin as a source of trifluoromethylthio group ($-\text{SCF}_3$) (Fig. 21) [115]. The catalytic system developed for this reaction contains $[\text{Cp}^*\text{RhCl}_2]_2$, AgSbF_6 , and $\text{Zn}(\text{OTf})_2$. In the opinion of the authors, this last reactive acts as Lewis base for the activation of the *N*-(trifluoromethylthio)saccharin. In fact, when $\text{Zn}(\text{OTf})_2$ is replaced by $\text{Cu}(\text{OTf})_2$, the product yield decreased sharply, which may indicate that the oxidizing power is not relevant in this reaction system. The selective C-2 trifluoromethylthiolation of indoles *N*-derivatized by

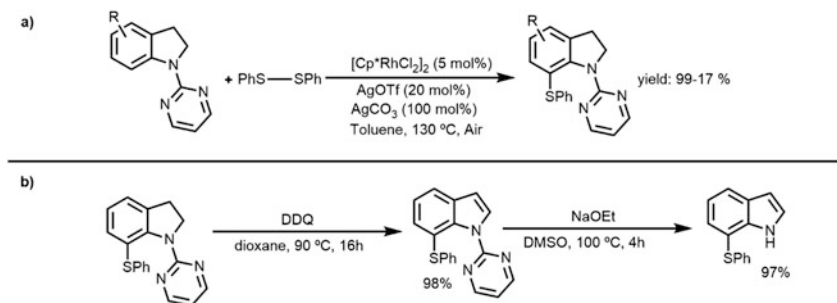


Fig. 20 (a) Selective C7-thiolation of indolines with PhSSPh catalyzed by $[\text{Cp}^*\text{RhCl}_2]_2/\text{AgOTf}/\text{AgCO}_3$ in toluene; (b) conversion of N-protected indolines into indoles [114]

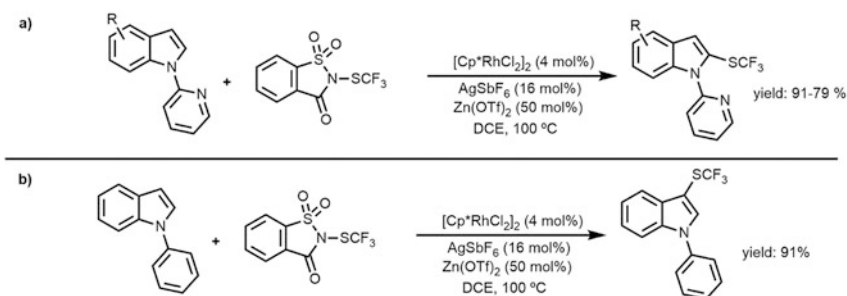


Fig. 21 Selective C2-trifluoromethylthiolation of indolines with *N*-(trifluoromethylthio)saccharin catalyzed by $[\text{Cp}^*\text{RhCl}_2]_2/\text{AgSbF}_6/\text{Zn}(\text{OTf})_2$ [115]

2-pyridyl group that acts both as N-protecting and directing groups is operative in DCE at 100 °C (Fig. 21a). Arene functionality is not limited to indoles. Trifluoromethylthiolation of 2-phenylpyridine and 2-(1*H*-pyrrol-1-yl)pyridine also occurred in moderate to high yield (Fig. 21a). Remarkably, when 1-phenyl-1*H*-indole was used as a substrate under the standard conditions, the functionalization occurred exclusively at the 3-position (Fig. 21b). This is a demonstration that the selectivity is correlated to the N-substituent. In fact, in the presence of an N-directing group, the reaction occurred via a C–H activation pathway, while, as demonstrated previously by the same research group, in the absence of such a group, the reaction is Lewis acid catalyzed [116].

2.3 Metathesis of Thioethers and Disulfides

The works discussed above account for the reaction of RC–X (X = halogen) or RC–H bonds with an adequate sulfur source (Y–SR') for the formation of thioethers of type RC–SR'. Another approach for synthesis of new thioethers consists in the

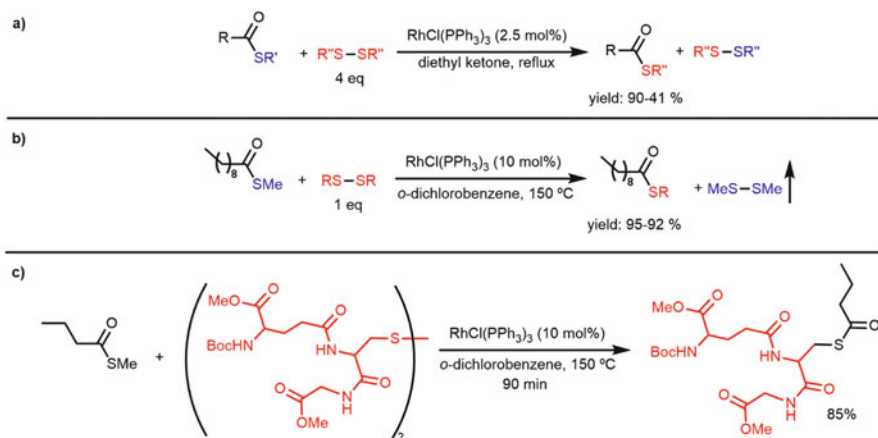


Fig. 22 Alkythio exchange reaction of thioesters and disulfides [117]

interchange of their thio-groups of two previously sulfurated products (see Fig. 1). This type of transformation is really interesting for the study of fundamental processes in the catalytic C–S bond formation and also extends the available synthetic methods for the synthesis of thio-compounds.

Catalysts able to mediate this type of reaction should have the capacity to establish an equilibrium between the thiolated reagents and the thio-interchanged products, through the activation of their C–S bonds. As showed in Sect. 2.2.1, Yamaguchi and coworkers have demonstrated that $\text{RhH}(\text{PPh}_3)_4$ is able to activate C–S bonds establishing equilibria between different types of thio-compounds; thus it was a promising candidate for the metathesis of different sulfur-containing compounds.

Alkoxy exchange between esters is a fundamental reaction catalyzed by acid or base. In contrast, the exchange reaction of the sulfur analogs in similar conditions does not proceed. However, Yamaguchi and coworkers reported the alkythio metathesis of thioesters and disulfides mediated by Rh^{I} complexes [117]. The treatment of a thioester and a dialkyl disulfide (4 eq) in refluxing diethyl ketone in the presence of $\text{RhCl}(\text{PPh}_3)_3$ (or $\text{RhH}(\text{PPh}_3)_4$) (2.5 mol%) for 1.5 h gave an alkythio-exchanged thioester (and mixed disulfides) in good to excellent yields (Fig. 22a). The species involved in this reaction are in equilibrium; thus an excess of reactives must be added to shift the equilibrium to the wanted products. However, the use of *S*-methyl thioester shifts the equilibrium to the exchanged thioester using one equivalent of disulfide, since dimethyl disulfide formed can be removed by evaporation (Fig. 22b). This method was effectively applied in a molecule of remarkable biological interests as the glutathione disulfide that was thioesterified with *S*-methyl butanethioate in good yield (Fig. 22c).

A similar catalytic system composed of $\text{RhH}(\text{PPh}_3)_4$ and dppe is able to mediate the metathesis of α -organothioketones with disulfides [118]. Similar to previously described for C–H activation reactions, the metathesis process is affected by the

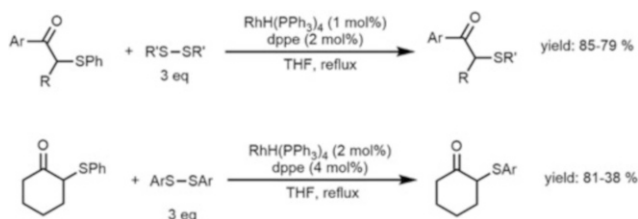


Fig. 23 Organothio exchange reaction of α -organothio ketones with disulfides catalyzed by $\text{RhH}(\text{PPh}_3)_4/\text{dppe}$ in THF at reflux [118]

structure of the substrate: α -phenylthio and α -alkylthio aryl ketones react effectively with diaryl and dialkyl disulfides, while α -phenylthio dialkyl ketones react only with diaryl disulfides (Fig. 23).

In the two examples of metathesis showed above, a thioether (C–S) reacts with a disulfide (S'–S') to afford the exchange products C–S' and S–S'. In contrast, the metathesis of two sulfurated organic products CS/C'S' can undergo two modes of reactivity to yield CS'/C'S and CC'/SS' derivatives. The control of the reaction mode using a single metal complex is an interesting challenge. Yamaguchi reported that an appropriate choice of the ligands can totally change the reactivity of a catalytic system shifting from CS'/C'S to CC'/SS' metathesis products [119]. In the presence of a catalytic amount of $\text{RhH}(\text{PPh}_3)_4$ and the chelating bisphosphine dppe, two 1-alkylthioalkynes exchange alkylthio groups to give equilibrium mixtures of four 1-alkylthioalkynes (CS'/C'S). In contrast, when a monodentate phosphine such as (*p*-OMePh)₃P or MePh₂P is used, 1,3-butadiynes and disulfides are obtained (CC'/SS') (Fig. 24a). A feasible explanation for this interesting ligand effect consists in the proposal of a reaction mechanism involving a Rh(V) intermediate (Fig. 24b). Two thioalkynes undergo oxidative addition within a rhodium(I) intermediate (**a**) to give an octahedral rhodium(V) species (**b** and **c**) bearing two alkynyl and two alkylthio ligands. In the opinion of the authors, the *trans*-effect of the different ligands together with the geometrical constrain of the dppe ligand leads to complex **b** in which the alkynyl groups are disposed in *trans*-configuration and the thiolated ligand in *cis*. This configuration does not allow the reductive elimination of the two alkynyl groups to form butadiyne, and only alkylthio exchange proceeds. In the case of monophosphine complex, the two phosphines take the *trans*-configuration, allowing the reductive elimination to form butadiyne or alkylthio-exchanged products.

3 Catalytic Addition of S–X on Unsaturated Substrates

The addition of sulfur–hydrogen, sulfur–carbon, or sulfur–sulfur (S–Y) bond to an acetylenic hydrocarbon represents a powerful tool for the synthesis of vinyl thioethers. This 100% atom-economical methodology meets the demands for the

35, 38, 39, 42, 43]. Also in this transformation, rhodium complexes have a prominent role, providing catalytic systems with very high activity and selectivity in hydrothiolation, thiolation, and carbthiolation of alkynes and allenes. In the case of rhodium, both of these transformations are stereoselective and proceed via a *syn*-addition. However, the regioselectivity of the reaction may change and depends on the metal complex, in particular on the stereoelectronic properties of the ligands that can totally change the final composition of the reaction products. The origin of the selectivity and the role of the ligand in this transformation are more extensively explained in the following sections.

3.1 Addition of S–S and S–C

As shown in Fig. 11, when disulfides were used as substrates in the Rh^{I} -catalyzed reaction with terminal alkynes, 1-alkyl/arylthio-1-alkynes were obtained. Yamaguchi and coworkers have reported a slight modification of this catalytic system leads to a total change of the chemoselectivity. In fact, they showed that the system composed of $\text{RhH}(\text{PPh}_3)_4$ /phosphine with the addition of a small amount of triflic acid leads to 1,2-disubstituted alkenes of *Z* configuration (Fig. 26a) [121]. It should be emphasized that while *E*-bis(thio)-substituted alkenes can be easily obtained under nucleophilic conditions, selective formation of *Z*-isomers has been a challenge for a long time. The catalytic system developed is highly active for both alkylic and aromatic disulfides (including cystine) as well as a wide range of different terminal alkynes with different functional groups (hydroxyl, tert-butyltrimethylsilyloxy, ester, or nitrile). In all cases the products were obtained with good to excellent yield, with outstanding *Z*-stereoselectivity (no trace of other isomers was detected). The reaction mechanism can explain the impressive stereoselectivity obtained (Fig. 26b). In the first step, the oxidative addition of the S–S bond to the Rh^{I} takes place leading to the S– Rh^{III} –S complex **a**. Coordination (**b**) and insertion of alkyne into the M–S bond (**c**) and, finally, reductive elimination of the product furnish the final *Z*-1,2-dithiolated alkenes and regenerate the initial Rh^{I} species. The addition of the disulfides in this mechanism is strictly *syn*; then *Z*-1,2-disubstituted alkene is the only isomer that can be formed.

Noteworthy, when allenes were treated with disulfides in the same catalytic conditions, a 1:1 mixture of (*E*)-2-alkylthio-1,3-dienes and (*E*)-2-alkylthio-2-alkene was found (Fig. 27a) [122]. The reaction can be applied to various combinations of monosubstituted allenes and aliphatic disulfides. The proposed catalytic cycle that explains the formation of these two products in 1:1 ratio is showed in Fig. 27b. The oxidative addition of the disulfide to the initial Rh^{I} complex (**a**) gives the dithiolate– Rh^{III} complex **b**. Allene insertion into the Rh–S bond yields the π -allyl complex **c**. Subsequent β -hydride elimination leads to the diene product and the hydride– Rh^{III} –thiolate complex **d**. The formation of the diene instead of the 1,2-dithiolated product **z** is an evidence that in this step of the catalytic cycle, the β -hydride elimination is faster than the reductive elimination with the other thiolate

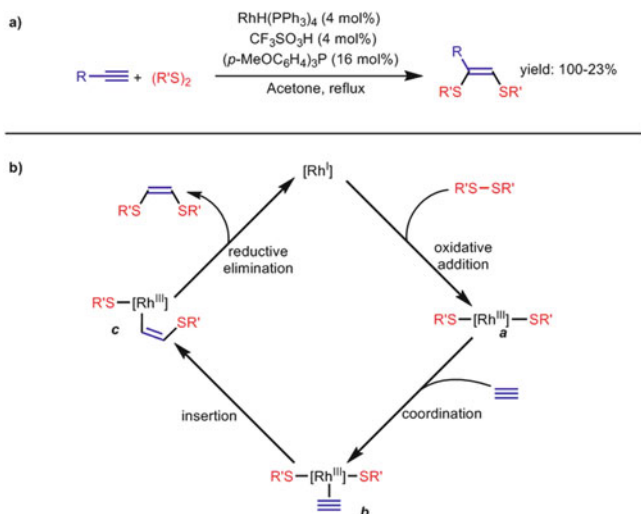


Fig. 26 (a) Addition of disulfides to terminal alkynes. (b) Putative reaction mechanism [121]

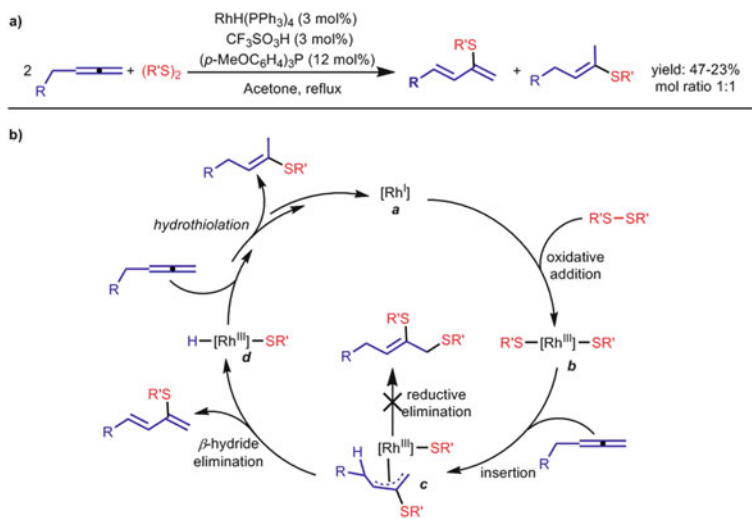


Fig. 27 (a) Reaction between allenes and disulfides catalyzed by $\text{RhH}(\text{PPh}_3)_4$; (b) reaction mechanism [122]

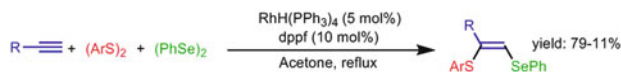
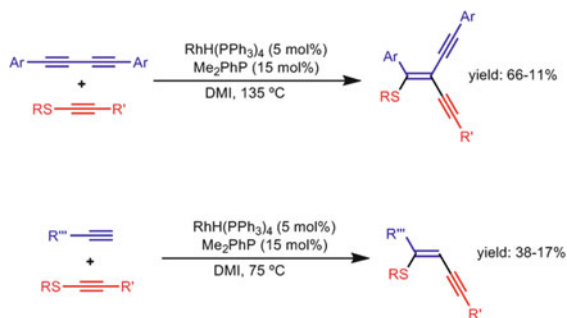


Fig. 28 Rhodium-catalyzed 1-seleno-2-thiolation of 1-alkynes [123]

Fig. 29 Carbothiolation of diynes and terminal alkynes with 1-1-alkylthio-1-alkynes catalyzed by RhH(PPh₃)₄ [124]



group. Complex **d** then reacts with another molecule of allene (the mechanism of hydrothiolation is described in the next section) giving the (*E*)-2-alkylthio-2-alkane and regenerating the initial Rh^I species.

The addition of seleno- and thio-groups on alkynes can be obtained in similar conditions. RhH(PPh₃)₄ and dppf catalyze the regio- and stereoselective additions of diaryl disulfides and diaryl diselenides to 1-alkynes giving (*Z*)-1-arylseleno-2-arylthio-1-alkenes in moderate to good yields (Fig. 28) [123]. The authors have found that the nature of phosphine and, in particular, the appropriate carbon chain length are fundamental for activity and selectivity of the reaction. In fact, when dppp or dppb was used instead of dppf, the reaction took place in lower yield and selectivity. Dppe and dpppe did not catalyze the reaction.

Another important reaction catalyzed by Rh complexes is the carbothiolation of alkynes. Yamaguchi reported that the catalytic system, RhH(PPh₃)₄/Me₂PhP, is able to mediate the carbothiolation reaction of 1-alkylthio-1-alkynes into symmetric diynes (Fig. 29) [124]. The reactions proceed via *syn*-addition to the triple bond. Regioselective ethynylation at the carbon 2 and thiolation into carbon 1 were observed. Terminal alkynes such as 1-decyne and (*t*-butylthio)acetylene also underwent the carbothiolation but in lower yield than diynes. In this case, the C–C bond formation occurs at C-1 (and C–S at C-2), confirming that for all type of substrates studied, the ethynylation is directed to the less hindered atom of the unsaturated moiety of the substrate.

Another interesting example of Rh-catalyzed carbothiolation was reported by Willis and coworkers [125]. In this work, the efficient addition of aryl methyl sulfides (bearing a carbonyl group in *ortho*-position) to terminal alkynes catalyzed by [Rh(DPEphos)(ligand)][BAr^F₄] (ligand = nbd or *o*-xylene) was showed (Fig. 30a). The process proved to be broad in scope, tolerating a variety of steric and electronic changes to both reaction partners. Importantly, the alkenyl sulfide products were generated as single geometric isomers, suggesting a stereoselective *syn*-addition process. Similar to the reaction mentioned above (Fig. 29a), the reaction proceeds with high regioselectivity leading to the selective arylation of the terminal position of the alkyne (C-1) together with the thiolation of the C-2. The identification of the intermediates through stoichiometric and catalytic experiments allowed the authors to suggest a mechanism of reaction (Fig. 30b). In the first step,

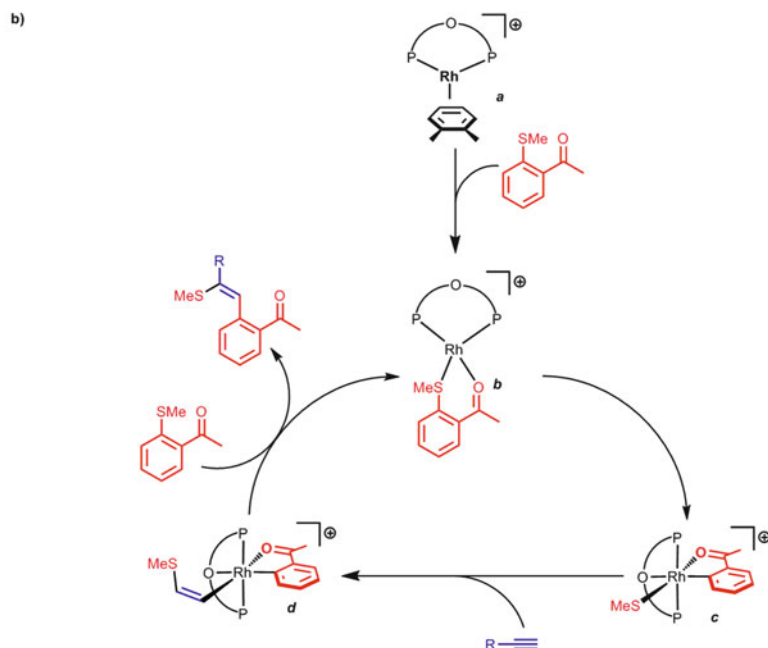
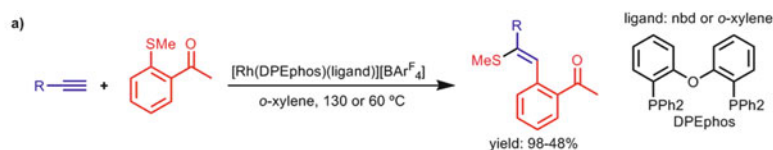


Fig. 30 (a) Rhodium-catalyzed reaction of aryl methyl sulfides and terminal alkynes. (b) Reaction mechanism [125]

the exchange between the *o*-xylene and the aryl-thiolate substrate takes place in furnishing complex **b**. The oxidative addition of the Ar–S bond to this complex leads to the Rh^{III} complex **c** that was identified as the resting state of the reaction. The addition of alkyne results in productive turnover by insertion of Rh–S bond (**d**). Subsequent reductive elimination of the thiovinyl and aryl groups results in the overall carbothiolation of the alkyne.

3.2 Hydrothiolation of Unsaturated Substrates

Hydrothiolation constitutes one of the simplest and atom-economical approaches for the introduction of sulfurated functionalities into organic frameworks. Particularly for alkyne hydrothiolation, the control of chemo-, regio-, and stereoselectivity still constitutes a motivating challenge. In this context, rhodium complexes have

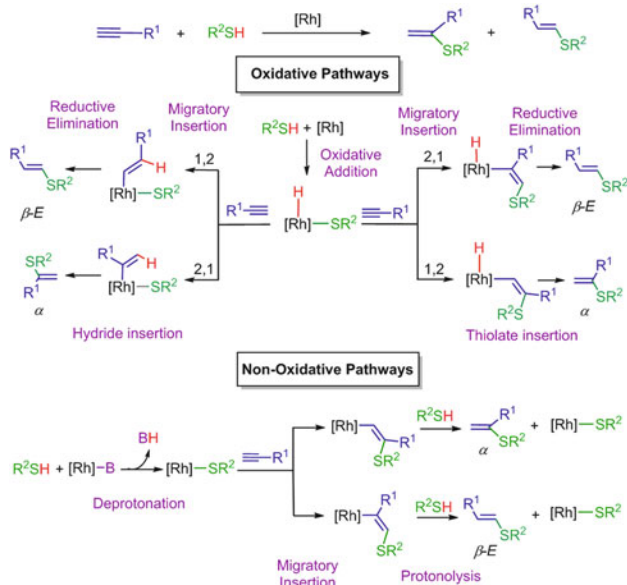
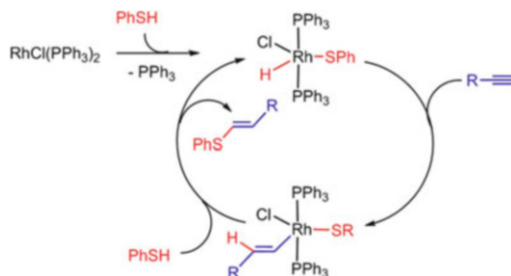


Fig. 31 Regioselectivity in rhodium-catalyzed alkyne hydrothiolation

been revealed as chameleonic species able to direct the regioselectivity upon subtle tuning of the ligands [126–146]. The established mechanisms for this transformation can be mainly divided into oxidative and non-oxidative processes (Fig. 31). The more common route starts by oxidative addition of the S–H bond of the thiol to the metallic precursor. Then, the alkyne can insert into Rh–H or Rh–S bonds with two orientations generating four catalytic pathways. Finally, the C–S reductive elimination step affords α - or β -E-vinyl sulfides. Alternatively, a non-oxidative mechanism entails the deprotonation of the thiol to generate a Rh–thiolate species. Then, alkyne insertion and protonolysis by an external thiol afford the corresponding vinyl sulfides. As clearly arising from Fig. 31, the complexity of the process needs for a rational design of the catalysts in order to obtain the desired regioselectivity. In general, the insertion of alkynes into metal–hydride bonds is favored compared to that into metal–thiolates, and 1,2-insertion is preferred over 2,1-insertion, but the metal environment can play an essential role in reversing this trend. Indeed, in some circumstances reductive elimination could be rate limiting; thus the mode of insertion plays a minor role.

The first use of rhodium catalysts for alkyne hydrothiolation was reported by the Ogawa's group [126]. The Wilkinson catalyst $\text{RhCl}(\text{PPh}_3)_3$ led predominantly to the formation of β -E vinyl sulfide. The mechanism was studied by stoichiometric NMR experiments (Fig. 32). The first step consists in the oxidative addition of thiophenol to form *trans*- $\text{HRhCl}(\text{SPh})(\text{PPh}_3)_2$. Subsequent 1,2-insertion of 1-dodecyne into rhodium–hydride bond yields a stable β -E-metal-alkenyl that undergoes reductive elimination with the thiolate ligand to generate a lineal vinyl

Fig. 32 Catalytic cycle for the formation of β -*E* vinyl sulfides proposed for Wilkinson's catalyst



sulfide. Furthermore, Love et al. have also demonstrated that alkyne insertion takes place into the metal–hydride bond, thereby ruling out a possible competing vinylidene-based pathway [127]. Wilkinson's catalyst is also effective in the oligomerization and polymerization of dithiols with dialkynes [128, 129]. Supported variants based on $\text{RhCl}(\text{PR}_3)_3$ have also been described [130, 131].

Messerle and coworkers disclosed in 2003 that neutral and cationic rhodium complexes bearing P,N and N,N ligands may act as efficient catalysts for alkyne hydrothiolation (Fig. 33) [132]. The best results were obtained for cationic complexes having P,N bidentate ligands which showed complete selectivity for the *E/Z* anti-Markovnikov vinyl sulfide products. Mechanistic studies point to a catalytic cycle initiated by oxidative addition of the thiol to generate hydride–thiolate species followed by alkyne insertion into the hydride ligand. The formation of *Z*- β -vinyl sulfide would require an isomerization of metal–alkenyl intermediates prior to reductive elimination step.

The Love's group contributes to field with an important landmark in 2005 [133]. In contrast to the previous assessment that group 9 transition-metal-based catalysts induce anti-Markovnikov selectivity, these authors elegantly showed that a reverse selectivity could be obtained by hydrotris(3,5-dimethylpyrazolyl)borate (Tp^*) rhodium precursors. Furthermore, $\text{Tp}^*\text{Rh}(\text{PPh}_3)_2$ complexes are very active, particularly with the previously unreactive aliphatic thiols, and display broad scope, tolerating a wide range of functional groups such as amines, ethers, nitriles, or silanes. The nature of the Tp moiety was found to be essential for the catalytic activity. Thus, the bis(pyrazolyl)borate precursor found to be less effective than the tris(pyrazolyl)borate analogs, indicating that a k^3 -coordination of the ligand should play an important role. Although the full mechanism has not completely been determined, the authors suggest a 1,2-insertion of the alkyne into Rh–S bonds as a key step for selectivity (Fig. 34) [134]. A year after the seminal report of Love's group, Mizobe and coworkers showed that the related precursor $\text{Tp}^*\text{Rh}(\text{coe})(\text{NCMe})$ promotes the hydrothiolation of benzyl and phenylacetylene with thiophenol [138]. In this case, a slightly different mechanism was proposed. A double addition of thiol with concomitant release of molecular hydrogen generates a dithiolate–rhodium complex as the active species. The insertion of the alkyne into a Rh–S bond is therefore the only possibility, thus generating branched vinyl sulfides by subsequent protonolysis. Reactivity studies and the X-ray structural

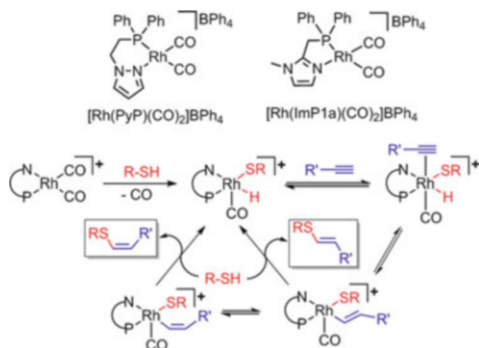


Fig. 33 Rhodium cationic systems favoring anti-Markovnikov selectivity

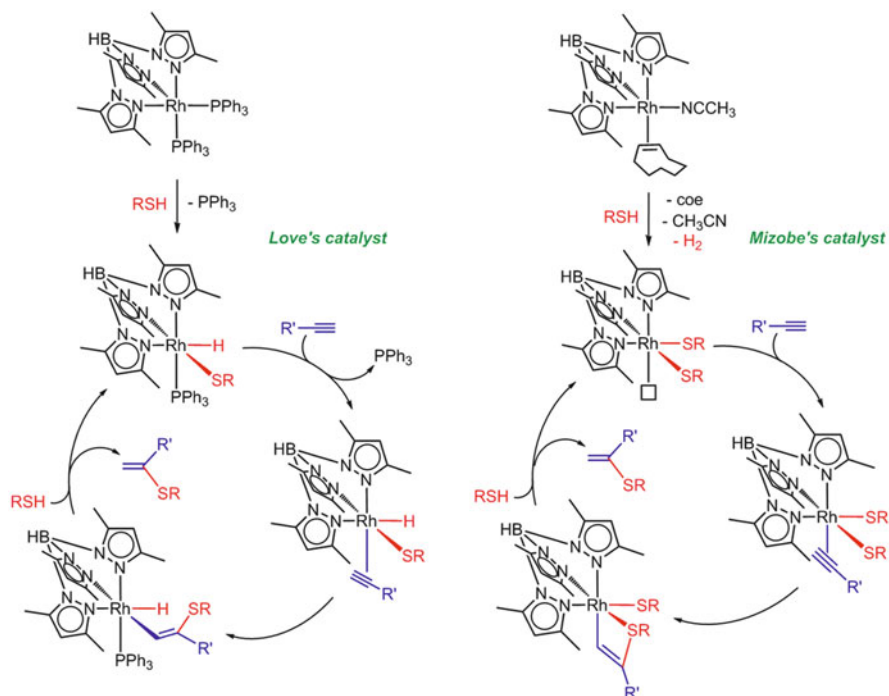


Fig. 34 Proposed catalytic cycles for Tp^*Rh precursors leading to Markovnikov-vinyl sulfides

characterization of a rhodium-alkenyl-thioether intermediate strongly support the mechanistic proposal.

Markovnikov selectivity in the formation of vinyl sulfides by alkyne hydrothiolation is also obtained with dinuclear rhodium-phosphino-carbonyl catalysts (Fig. 35) [139]. The reaction can be performed in a mixture of THF/water due to the presence of water-soluble phosphines and is possible to recycle. These results are in stark contrast with those obtained for related monomeric catalysts described

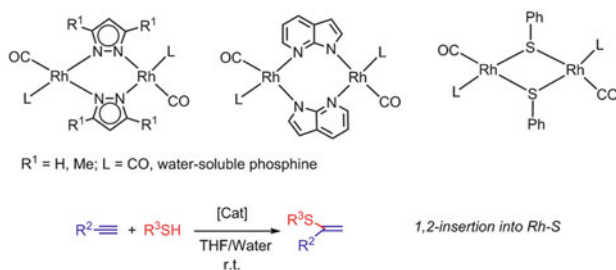


Fig. 35 Markovnikov-selective dinuclear phosphine–carbonyl catalysts

by Messerle (see above). Kinetic measurements indicate that the dinuclear species maintain its entity and the bridges are not cleaved during the catalytic process. Deuterated experiments demonstrate a *syn*-addition of the thiol over the alkynes. The authors propose a 1,2-insertion of the alkyne into the rhodium thiolate bond generated by oxidative addition as responsible for the branched selectivity.

Allenes can also participate in rhodium-mediated hydrothiolation reactions. The approach furnishes α -chiral sulfides and sulfones which are valuable building blocks in organic synthesis [140, 141]. The catalytic system composed of [RhCl(cod)]₂ and a chiral phosphine showed higher enantioselectivity for the addition of the sulfur atom to the more substituted carbon of the allene (Fig. 36). Subsequent oxidation affords the chiral sulfones in high yield. Based on deuterium-labeled experiments, the authors propose an initial oxidative addition of the thiol and subsequent hydrometalation of the more substituted double bond of the allene.

Ligand-Controlled Selectivity in Rh–NHC Catalysts

Our group has recently disclosed that rhodium(I)-N-heterocyclic carbene (NHC) catalysts efficiently perform alkyne hydrothiolation under mild conditions [143]. Substitution of a phosphine by a N-heterocyclic ligand in Wilkinson's catalyst resulted in the stabilization of the active species although with slight reduction of initial rate for thiophenol addition to phenylacetylene at room temperature (Fig. 37). Conversion with RhCl(PPh₃)₃ reaches 80% with a TOF $\frac{1}{2}$ of 300 s⁻¹, whereas 99% of conversion was observed for RhCl(IPr)(PPh₃)₂ but displaying 55 s⁻¹ of TOF $\frac{1}{2}$. Selectivity outcome also changed. The amount of α -vinyl sulfide was increased by the introduction of the carbene moiety. Other Rh–NHC complexes were tested as catalyst for this transformation. The free-phosphine dinuclear catalyst [Rh(μ -Cl)(IPr)(η^2 -ethylene)]₂ surpassed the activity of Wilkinson's catalyst maintaining the stabilizing effect of carbene. Full conversion was obtained after 1 h with anti-Markovnikov vinyl sulfide preference. The introduction of mononuclear pyridine complex RhCl(IPr)(η^2 -coe)(py), obtained by bridge cleavage with the nitrogenated ligand in the dinuclear precursor, remarkably increased the selectivity toward the Markovnikov-type adducts up to 91%, although with a decrease of activity. Indeed, both selectivity increment and activity decrease were magnified by addition of ten



Fig. 36 Asymmetric addition of thiols to allenes

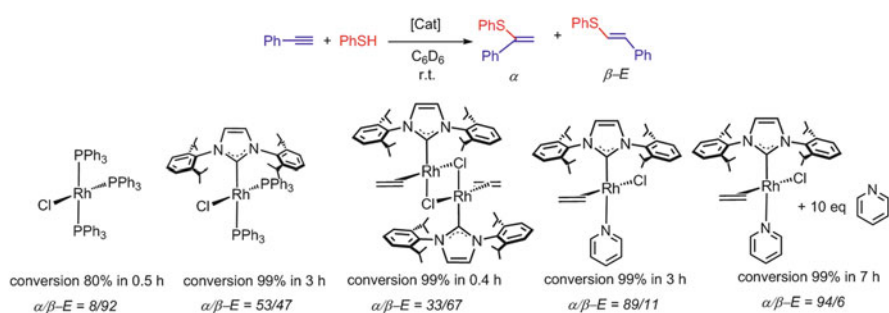


Fig. 37 Introduction of a NHC ligand into rhodium catalysts

equivalents of pyridine to the catalytic precursor. The catalyst was totally inactive in neat pyridine. The use of other nitrogenated bases does not result in an increase of selectivity, indicating that the role of pyridine is played in coordination with the metallic center. Antiradical additives do not affect catalytic outcome thus excluding radical processes as responsible for catalytic activity.

In order to shed light into the pyridine effect over selectivity in Rh–NHC-based catalysts, stoichiometric experiments and theoretical DFT calculations were performed. The first step consists in the oxidative addition of the thiol to form a hydride–thiolate–rhodium species. This type of intermediate was not possible to detect in the absence of pyridine. Then, rate-determining 1,2-alkyne insertion into R–S bond takes place to finally afford the Markovnikov thioether after reductive elimination. A likely explanation for the “pyridine effect” is as follows: the sterically hindered and strongly electron-donating NHC ligand directs the coordination of the pyridine *trans* to it, consequently blocking coordination of the alkyne in this position. Simultaneously, the *trans* influence of the hydride paves the way to a *cis* thiolate–alkyne disposition, which subsequently gives rise to the branched vinyl sulfide regioisomer. The absence of pyridine allows the alkyne to coordinate in the preferred site *trans* to IPr position, and therefore subsequent unselective migratory insertion into hydride or thiolate can occur (Fig. 38).

As previously discussed, the dinuclear precursors of type $[\text{Rh}(\mu\text{-Cl})(\text{NHC})(\eta^2\text{-olefin})]_2$ favor the formation of linear thioethers, whereas the selectivity is switched toward branched *gem*-vinyl sulfides by the mononuclear catalyst $\text{RhCl}(\text{NHC})(\text{pyridine})(\eta^2\text{-olefin})$. An equilibrium between both types of precursors is established rendering the concentration of pyridine essential for the control of regioselectivity. We hypothesized that the equilibrium shift to the mononuclear species by using a

Fig. 38 Interplay between NHC, pyridine, and hydride ligand for Markovnikov selectivity

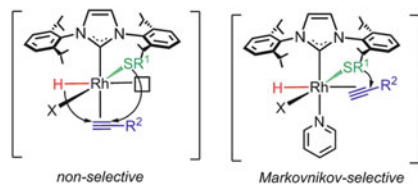
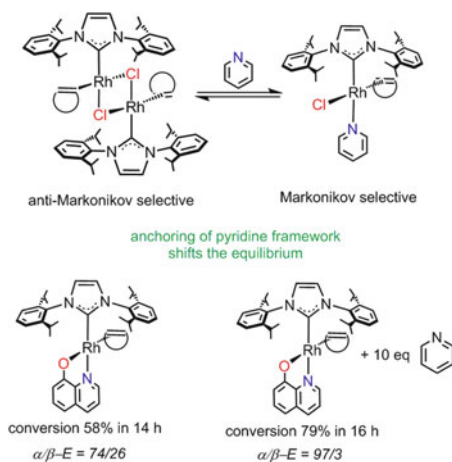


Fig. 39 Selectivity enhancement by anchorage of the N-donor ligand



chelate ligand would increase Markovnikov selectivity. Thus, we design a next generation of catalyst bearing a quinolinolate ligand (Fig. 39) [144]. The catalytic activity is lower, as observed in the aforementioned systems by the addition of pyridine. Selectivity to α -vinyl sulfides of the quinolinolate-based catalysts is high (74–80%), but, unfortunately, lower than expected. Notably, the addition of pyridine results in an increase of the selectivity up to 97%.

Theoretical DFT and experimental results revealed that a different mechanism is operative for the quinolinolate-based catalysts with regard to pyridine systems. The first step is similar for both, the oxidative addition of the acidic thiol. Then, each catalyst takes different routes but reaching the same goal, the branched vinyl sulfide (Fig. 40). Pyridine catalysts undergo 1,2-thiolate insertion with migratory insertion as rate limiting, whereas quinolinolate species evolve by hydride insertion with reductive elimination as rate limiting. These facts exemplify how subtle changes in catalytic structure may result in complete change in the operative mechanism although arriving to the same final result.

The fact that the presence of pyridine as additive is essential in quinolinolate catalysts to reach high selectivity is intriguing. In contrast to $\text{RhCl}(\text{IPr})(\eta^2\text{-olefin})$ (py) precursors, alkenyl intermediates resulting from alkyne insertion into hydride bond can be detected for quinolinolate-based catalysts (Fig. 41). However, we observed that pyridine coordinates to linear alkenyl but not to the bulkier branched one, thus disfavoring the reductive elimination of anti-Markovnikov thioether and therefore increasing Markovnikov selectivity.

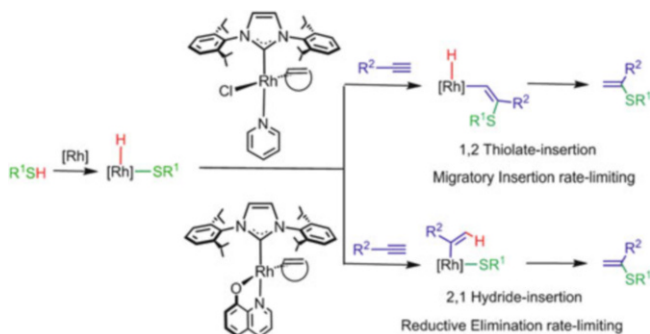


Fig. 40 Mechanistic pathways for pyridine and quinolinolate catalyst precursors



Fig. 41 Role of pyridine in selectivity

Another approach for enhancement of Markovnikov selectivity is the non-oxidative strategy depicted in Fig. 31. A deprotonation of the thiol eliminates the hydride moiety; therefore only the insertion over R–S bond is operative. We have designed dinuclear Rh–NHC precursors bearing hydroxo bridges as internal base able to achieve this task (Fig. 42) [145]. As anticipated, these catalysts display a high selectivity (up to 94%), but a decrease of activity is observed. Low-temperature experiments allow for detection of the square-planar Rh^I–thiolate intermediate. Nevertheless, as a consequence of the tendency of pyridine to coordinate *trans* to IPr [146], both thiolate and alkyne are mutually *trans* disposed; therefore insertion step is limited, making this intermediate inactive. However, these species undergo a subsequent thiol addition to generate hydride–dithiol–Rh^{III} species that can evolve in similar pathways that pyridine catalysts do, thus displaying high Markovnikov selectivity.

In view that the non-oxidative mechanism is not operative for Rh–pyridine precursors because of oxidation to Rh^{III} by the free thiol used as a substrate, we envisage that the introduction of a π -acceptor carbonyl group would reduce this step. Indeed, a pyridine moiety gives stability and flexibility to the catalytic system. With these prerequisites established, we chose a 2-hydroxymethylpyridine–Rh–CO catalyst as suitable candidate for improving selectivity (Fig. 43). This precursor displayed the higher selectivity within the family of Rh–NHC catalysts [144]. The catalytic activity is reduced at room temperature, but 98% of conversion was attained at 50°C. The effect of the carbonyl ligand, in addition to reduce Rh^{III}



Fig. 42 Mechanism for Rh-hydroxo-NHC catalyst



Fig. 43 Design of NHC-Rh-CO catalysts

oxidation by the thiol, favors a thiolate to alkyne *cis* disposition; therefore the migratory insertion, as the π -acceptor ligand, prefers to coordinate *cis* to carbene in contrast to pyridine that prefer *trans* coordination.

As showed above, the introduction of a NHC ligand into rhodium precursors has provided a fruitful family of alkyne hydrothiolation catalysts. The particular stereoelectronic properties confer stability to active species that result in an enhancement of catalytic activity. The different pathways available for this transformation render the rational design of the ligands essential for controlling selectivity. An in-depth knowledge of the precise mechanism has allowed this task to be achieved successfully. Further work is necessary in order to apply the insights gained for this model system to other hydrofunctionalization reactions.

References

- Hurlimann S, Abuhl B, Inauen W, Halter F (1994) *Aliment Pharmacol Ther* 8:193
- Fitton A, Wiseman L (1996) *Drugs* 51:460
- Patel OG, Mberu EK, Nzila AM, Macreadie IG (2004) *Trends Parasitol* 20:1
- Rendell M (2004) *Drugs* 64:1339
- Singh GS (2004) *Mini-Rev Med Chem* 4:69
- Zillich AJ, Garg J, Basu S, Bakris GL, Carter BL (2006) *Hypertension* 48:219
- Abdel-Tawab M, Zettl H, Schubert-Zsilavecz M (2009) *Curr Med Chem* 16:2042
- McCabe C, Huber A, Harmer CJ, Cowen PJ (2011) *Psychopharmacology* 217:271
- Emmert D, Campos CR, Ward D, Lu P, Namanja HA, Bohn K, Miller DS, Sharom FJ, Chmielewski J, Hrycyna CA (2014) *ACS Chem Neurosci* 5:305
- Anastas PT, Bartlett LB, Kirchhoff MM, Williamson TC (2000) *Catal Today* 55:11

11. Sheldon RA (2012) *Chem Soc Rev* 41:1437
12. Pohlki F, Doye S (2003) *Chem Soc Rev* 32:104
13. Alonso F, Beletskaya IP, Yus M (2004) *Chem Rev* 104:3079
14. Hong S, Marks TJ (2004) *Acc Chem Res* 37:673
15. Teles JH (2012) In: Hashmi A, Stephen K, Toste D (eds) *Modern gold catalyzed synthesis*. Wiley-VCH, Weinheim, p 201
16. Julian LD (2013) *Top Heterocycl Chem* 32:109
17. Rosenberg L (2013) *ACS Catal* 3:2845
18. Zeng X (2013) *Chem Rev* 113:6864
19. Koshit V, Gaikwad S, Chikkali SH (2014) *Coord Chem Rev* 265:52
20. Chen J, Cao M, Cheng B, Lu Z (2015) *Synlett* 26:2332
21. Chong CC, Kinjo R (2015) *ACS Catal* 5:3238
22. Di Giuseppe A, Castarlenas R, Oro LA (2015) *C R Chim* 18:713
23. Greenhalgh MD, Jones AS, Thomas SP (2015) *ChemCatChem* 7:190
24. Huang L, Arndt M, Goossen K, Heydt H, Goossen LJ (2015) *Chem Rev* 115:2596
25. Rodriguez-Ruiz V, Carlino R, Bezzenine-Lafolle S, Gil R, Prim D, Schulz E, Hannedouche J (2015) *Dalton Trans* 44:12029
26. Shigehisa H (2015) *Synlett* 26:2479
27. Pirnot MT, Wang Y-M, Buchwald SL (2016) *Angew Chem Int Ed Engl* 55:48
28. Ritleng V, Henrion M, Chetcuti MJ (2016) *ACS Catal* 6:890
29. Sun J, Deng L (2016) *ACS Catal* 6:290
30. Wathier M, Love JA (2016) *Eur J Inorg Chem*. doi:[10.1002/ejic.201501272](https://doi.org/10.1002/ejic.201501272)
31. Dunleavy JK (2006) *Platinum Met Rev* 50:110
32. Ogawa A (2000) *J Organomet Chem* 611:463
33. Zyk NV, Beloglazkina EK, Belova MA, Dubinina NS (2003) *Russ Chem Rev* 72:769
34. Beletskaya IP, Ananikov VP (2007) *Eur J Org Chem* 2007:3431
35. Beletskaya IP, Ananikov VP (2007) *Pure Appl Chem* 79:1041
36. Arisawa M, Yamaguchi M (2008) *Pure Appl Chem* 80:993
37. Weiss CJ, Marks TJ (2010) *Dalton Trans* 39:6576
38. Beletskaya IP, Ananikov VP (2011) *Chem Rev* 111:1596
39. Castarlenas R, Di Giuseppe A, Perez-Torrente JJ, Oro LA (2013) *Angew Chem Int Ed Engl* 52:211
40. Arisawa M (2014) *Tetrahedron Lett* 55:3391
41. Lee C-F, Liu Y-C, Badsara SS (2014) *Chem Asian J* 9:706
42. Mashkina AV (2014) *Russ Chem Rev* 83:733
43. Orlov NV (2015) *ChemistryOpen* 4:682
44. Shen C, Zhang P, Sun Q, Bai S, Hor TSA, Liu X (2015) *Chem Soc Rev* 44:291
45. Baranano D, Mann G, Hartwig JF (1997) *Curr Org Chem* 1:287
46. Denmark SE, Regens CS (2008) *Acc Chem Res* 41:1486
47. Ishii Y, Obora Y, Sakaguchi S (2009) In: Oro LA, Claver C (eds) *Iridium complexes in organic synthesis*. Wiley-VCH, Weinheim, p 251
48. Kambe N, Iwasaki T, Terao J (2011) *Chem Soc Rev* 40:4937
49. Qiao JX, Lam PYS (2011) *Synthesis* 6:829
50. De Figueiredo RM, Campagne JM, Prim D (2012) In: Cossy J, Arseniyadis S (eds) *Modern tools for the synthesis of complex bioactive*. Wiley, Hoboken, p 77
51. Wang Z-X, Liu N (2012) *Eur J Inorg Chem* 2012:901
52. Panda N, Jena AK (2015) *Org Chem Curr Res* 4:1
53. Kosugi M, Shimizu T, Migita T (1978) *Chem Lett* 7:13
54. Wong Y-C, Jayanth TT, Cheng C-H (2006) *Org Lett* 8:5613
55. Zhang Y, Ngeow KC, Ying JY (2007) *Org Lett* 9:3495
56. Murthy SN, Madhav B, Reddy VP, Nageswar YVD (2009) *Eur J Org Chem* 2009:5902
57. Reddy VP, Kumar AV, Swapna K, Rao KR (2009) *Org Lett* 11:1697
58. Reddy VP, Swapna K, Kumar AV, Rao KR (2009) *J Org Chem* 74:3189

59. Wu J-R, Lin C-H, Lee C-F (2009) *Chem Commun* 2009:4450
60. Bandaru M, Sabbavaru NM, Katla R, Yadavalli VDN (2010) *Chem Lett* 39:1149
61. Xu R, Wan J-P, Mao H, Pan Y (2010) *J Am Chem Soc* 132:15531
62. Lan M-T, Wu W-Y, Huang S-H, Luo K-L, Tsai F-Y (2011) *RSC Adv* 1:1751
63. Sayah M, Organ MG (2011) *Chem Eur J* 17:11719
64. Zhou A-X, Liu X-Y, Yang K, Zhao S-C, Liang Y-M (2011) *Org Biomol Chem* 9:5456
65. Das R, Chakraborty D (2012) *Tetrahedron Lett* 53:7023
66. Guan P, Cao C, Liu Y, Li Y, He P, Chen Q, Liu G, Shi Y (2012) *Tetrahedron Lett* 53:5987
67. Lin Y-Y, Wang Y-J, Lin C-H, Cheng J-H, Lee C-F (2012) *J Org Chem* 77:6100
68. Malik P, Chakraborty D (2012) *Appl Organomet Chem* 26:557
69. Bastug G, Nolan SP (2013) *J Org Chem* 78:9303
70. Liu T-J, Yi C-L, Chan C-C, Lee C-F (2013) *Chem Asian J* 8:1029
71. Tanaka K, Ajiki K (2005) *Org Lett* 7:1537
72. Xia J, Yao R, Cai M (2015) *Appl Organomet Chem* 29:221
73. Tanaka K, Hori T, Osaka T, Noguchi K, Hirano M (2007) *Org Lett* 9:4881
74. Hori T, Shibata Y, Tanaka K (2010) *Tetrahedron Asymmetry* 21:1303
75. Ajiki K, Hirano M, Tanaka K (2005) *Org Lett* 7:4193
76. Arisawa M, Suzuki T, Ishikawa T, Yamaguchi M (2008) *J Am Chem Soc* 130:12214
77. Arisawa M, Yamada T, Yamaguchi M (2010) *Tetrahedron Lett* 51:6090
78. Arisawa M, Ichikawa T, Yamaguchi M (2012) *Org Lett* 14:5318
79. Lai C-S, Kao H-L, Wang Y-J, Lee C-F (2012) *Tetrahedron Lett* 53:4365
80. Timpa SD, Pell CJ, Ozerov OV (2014) *J Am Chem Soc* 136:14772
81. Crabtree RH (2001) *J Chem Soc Dalton Trans* 2001:2437
82. Jia C, Kitamura T, Fujiwara Y (2001) *Acc Chem Res* 34:633
83. Lewis JC, Bergman RG, Ellman JA (2008) *Acc Chem Res* 41:1013
84. Park YJ, Park J-W, Jun C-H (2008) *Acc Chem Res* 41:222
85. Giri R, Shi B-F, Engle KM, Mangel N, Yu J-Q (2009) *Chem Soc Rev* 38:3242
86. Balcells D, Clot E, Eisenstein O (2010) *Chem Rev* 110:749
87. Jazzar R, Hitce J, Renaudat A, Sofack-Kreutzer J, Baudoin O (2010) *Chem Eur J* 16:2654
88. Cho SH, Kim JY, Kwak J, Chang S (2011) *Chem Soc Rev* 40:5068
89. Kuhl N, Hopkinson MN, Wencel-Delord J, Glorius F (2012) *Angew Chem Int Ed Engl* 51:10236
90. Gensch T, Hopkinson MN, Glorius F, Wencel-Delord J (2016) *Chem Soc Rev* 45:2900
91. McKeown BA, Lee JP, Mei J, Cundari TR, Gunnoe TB (2016) *Eur J Inorg Chem* 2016:2296
92. Yang X, Shan G, Wang L, Rao Y (2016) *Tetrahedron Lett* 57:819
93. Chen X, Hao X-S, Goodhue CE, Yu J-Q (2006) *J Am Chem Soc* 128:6790
94. Zhao X, Dimitrijevic E, Dong VM (2009) *J Am Chem Soc* 131:3466
95. Saidi O, Marafie J, Ledger AEW, Liu PM, Mahon MF, Kociok-Kohn G, Whittlesey MK, Frost CG (2011) *J Am Chem Soc* 133:19298
96. Dai C, Xu Z, Huang F, Yu Z, Gao Y-F (2012) *J Org Chem* 77:4414
97. Tran LD, Popov I, Daugulis O (2012) *J Am Chem Soc* 134:18237
98. Li J, Huang H, Liang W, Gao Q, Duan Z (2013) *Org Lett* 15:282
99. Xu C, Shen Q (2014) *Org Lett* 16:2046
100. Boutadla Y, Davies DL, Macgregor SA, Poblador-Bahamonde AI (2009) *Dalton Trans* 2009:5820
101. Lapointe D, Fagnou K (2010) *Chem Lett* 39:1119
102. Ackermann L (2011) *Chem Rev* 111:1315
103. Arisawa M, Fujimoto K, Morinaka S, Yamaguchi M (2005) *J Am Chem Soc* 127:12226
104. Arisawa M, Nihei Y, Yamaguchi M (2012) *Tetrahedron Lett* 53:5729
105. Arisawa M, Suwa K, Yamaguchi M (2009) *Org Lett* 11:625
106. Arisawa M, Toriyama F, Yamaguchi M (2011) *Heteroat Chem* 22:18
107. Arisawa M, Toriyama F, Yamaguchi M (2011) *Tetrahedron* 67:2305
108. Arisawa M, Toriyama F, Yamaguchi M (2011) *Tetrahedron Lett* 52:2344

109. Colby DA, Tsai AS, Bergman RG, Ellman JA (2012) *Acc Chem Res* 45:814
110. Patureau FW, Wencel-Delord J, Glorius F (2012) *Aldrichimica Acta* 45:31
111. Song G, Li X (2015) *Acc Chem Res* 48:1007
112. Yang Y, Hou W, Qin L, Du J, Feng H, Zhou B, Li Y (2014) *Chem Eur J* 20:416
113. Wen J, Wu A, Wang M, Zhu J (2015) *J Org Chem* 80:10457
114. Xie W, Li B, Wang B (2016) *J Org Chem* 81:396
115. Wang Q, Xie F, Li X (2015) *J Org Chem* 80:8361
116. Wang Q, Qi Z, Xie F, Li X (2015) *Adv Synth Catal* 357:355
117. Arisawa M, Kubota T, Yamaguchi M (2008) *Tetrahedron Lett* 49:1975
118. Arisawa M, Toriyama F, Yamaguchi M (2010) *Chem Pharm Bull* 58:1349
119. Arisawa M, Tagami Y, Yamaguchi M (2008) *Tetrahedron Lett* 49:1593
120. McDonald JW, Corbin JL, Newton WE (1976) *Inorg Chem* 15:2056
121. Arisawa M, Yamaguchi M (2001) *Org Lett* 3:763
122. Arisawa M, Suwa A, Fujimoto K, Yamaguchi M (2003) *Adv Synth Catal* 345:560
123. Arisawa M, Kozuki Y, Yamaguchi M (2003) *J Org Chem* 68:8964
124. Arisawa M, Igarashi Y, Tagami Y, Yamaguchi M, Kabuto C (2011) *Tetrahedron Lett* 52:920
125. Hooper JF, Chaplin AB, Gonzalez-Rodriguez C, Thompson AL, Weller AS, Willis MC (2012) *J Am Chem Soc* 134:2906
126. Ogawa A, Ikeda T, Kimura K, Hirao T (1999) *J Am Chem Soc* 121:5108
127. Fraser LR, Bird J, Wu Q, Cao C, Patrick BO, Love JA (2007) *Organometallics* 26:5602
128. Liu J-Z, Lam JWY, Jim CKW, Ng JCY, Shi J-B, Su H-M, Yeung K-F, Hong Y-N, Faisal M, Yu Y, Wong K-S, Tang B-Z (2011) *Macromolecules* 44:68
129. Yoshimura A, Nomoto A, Ogawa A (2014) *Res Chem Intermed* 40:2381
130. Yang Y, Rioux RM (2011) *Chem Commun* 47:6557
131. Zhao H, Peng J, Cai M (2012) *Catal Lett* 142:138
132. Burling S, Field LD, Messerle BA, Vuong KQ, Turner P (2003) *Dalton Trans* 2003:4181
133. Cao C, Fraser LR, Love JA (2005) *J Am Chem Soc* 127:17614
134. Shoai S (2010) Ph.D. Thesis, University of British Columbia, Canada
135. Shoai S, Bichler P, Kang B, Buckley H, Love JA (2007) *Organometallics* 26:5778
136. Field LD, Messerle BA, Vuong KQ, Turner P (2009) *Dalton Trans* 2009:3599
137. Yang J, Sabarre A, Fraser LR, Patrick BO, Love JA (2009) *J Org Chem* 74:182
138. Misumi Y, Seino H, Mizobe Y (2006) *J Organomet Chem* 691:3157
139. Kankala S, Nerella S, Vadde R, Vasam CS (2013) *RSC Adv* 3:23582
140. Pritzius AB, Breit B (2015) *Angew Chem Int Ed* 54:15818
141. Pritzius AB, Breit B (2015) *Angew Chem Int Ed Engl* 54:3121
142. Kleinhans G, Guisado-Barrios G, Liles DC, Bertrand G, Bezuidenhout DI (2016) *Chem Commun* 52:3504
143. Di Giuseppe A, Castarlenas R, Perez-Torrente JJ, Crucianelli M, Polo V, Sancho R, Lahoz FJ, Oro LA (2012) *J Am Chem Soc* 134:8171
144. Palacios L (2014) Ph.D. Thesis, Universidad de Zaragoza, Spain
145. Palacios L, Artigas MJ, Polo V, Lahoz FJ, Castarlenas R, Perez-Torrente JJ, Oro LA (2013) *ACS Catal* 3:2910
146. Palacios L, Di Giuseppe A, Castarlenas R, Lahoz FJ, Perez-Torrente JJ, Oro LA (2015) *Dalton Trans* 44:5777

Tandem Rhodium Carbonylation Reactions

Philippe Kalck and Martine Urrutigoity

Abstract This review presents the recent advances in the rhodium-catalyzed tandem carbonylation reactions involving in the main step the hydroformylation. Such reactions open huge opportunities in synthetic chemistry, since they offer a general efficient strategy to synthesize building blocks for fine chemistry, starting from abundant and low price substrates and avoiding the formation of substantial amounts of by-products. This atom-efficient tandem reaction approach shows that rhodium has a privileged place in the CO chemistry, not only to perform the hydroformylation reaction but also to functionalize the aldehyde function in a one-pot process.

Keywords CO chemistry • Rhodium • Tandem reactions involving hydroformylation

Contents

1	Introduction	70
1.1	Rhodium-Catalyzed Hydroformylation: Generalities	70
2	Isomerization-Hydroformylation	72
3	Hydroformylation-Hydrogenation	75
4	Hydroformylation-Acetalization	78
5	Hydroformylation-Wittig Olefination	81
6	Hydroaminomethylation	84
6.1	Hydroaminomethylation of Terminal and Internal Alkenes	86
6.2	Hydroaminomethylation of Arylalkenes	92
6.3	Hydroaminomethylation of Monoterpenes and Fatty Acids	93
7	Conclusion	95
	References	96

1 Introduction

Carbon monoxide has been shown to be a powerful building block to functionalize organic products, and the two main organic products obtained by carbonylation are acetic acid (11 million tons per year, 11 MT/y) from methanol [1] and aldehydes by hydroformylation of alkenes (12 MT/y) [2, 3]. The initial hard conditions of catalysis, especially the high pressures required by the cobalt carbonyl complexes, have been replaced by milder conditions due to the development of rhodium complexes whose the coordination sphere is sufficiently sophisticated to reach high reaction rate, chemoselectivity, and regioselectivity. Moreover, the modern recycling processes are efficient enough to avoid the loss of this precious metal and to have industrial units with capacities as high as 500 kT/y.

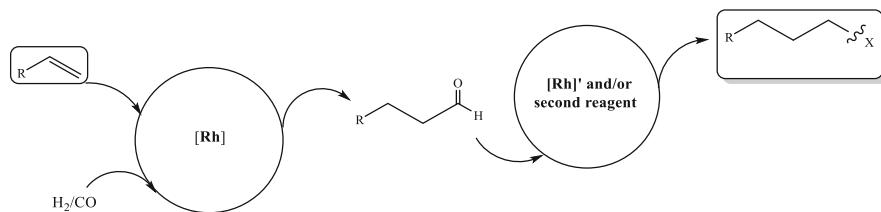
As the major problems in chemical synthesis are the handling of wastes, the search for efficient procedures, and the preservation of resources, many efforts have been devoted to improve the efficiency of the reaction, operating in one sequence, in the absence of isolating the intermediates [4]. This strategy of cascade reactions [5, 6] has been expanded until the synthesis of a given product mimics the principles of biosynthesis, including asymmetric reactions to perform natural product synthesis [7] for advancing the drug discovery and development process [8]. Using tandem (or domino) reactions, two or more bonds are produced, under identical conditions, leading to the formation of more complex molecules in an economic approach, especially since unstable intermediates are immediately transformed [9].

Due to their high reactivity, aldehydes have been also largely used in organic synthesis since they can be easily transformed into alcohols, amines, carboxylic acid derivatives, acetals, etc. The tandem reaction sequences under the hydroformylation reaction conditions have been largely explored in the 1990s, and the Eilbracht's reviews give an interesting view of the performances of the first catalytic systems able to combine hydroformylation reaction and in a second sequence C–H, C–O, C–C bond formations [10, 11].

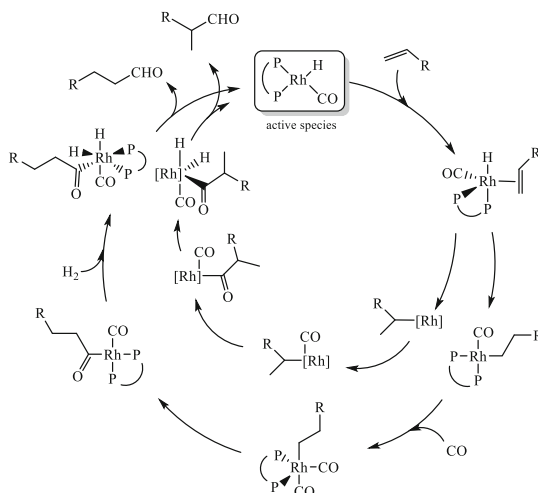
This chapter is devoted to the rhodium-catalyzed tandem carbonylation reactions, involving in the first step the hydroformylation of an alkene. Then, the produced aldehydes are generally transformed in a tandem reaction to yield important chemicals for organic synthesis. A second reagent or a second catalytic cycle operates, starting from the aldehyde as shown in Scheme 1.

1.1 Rhodium-Catalyzed Hydroformylation: Generalities

The hydroformylation reaction of an alkene mainly involves the $[\text{Rh}(\text{H})(\text{CO})_2\text{L}_2]$ precursor in which L is a phosphorus-containing ligand and more interestingly L_2 a bidentate ligand. Under the reaction conditions, this resting state produces the $[\text{Rh}(\text{H})(\text{CO})\text{L}_2]$ square-planar active species, which coordinates the alkene substrate ($\text{RCH}=\text{CH}_2$). Transfer of the hydride ligand to one carbon atom of the $\text{C}=\text{C}$ double



Scheme 1 General feature of the tandem hydroformylation/second functionalization reaction



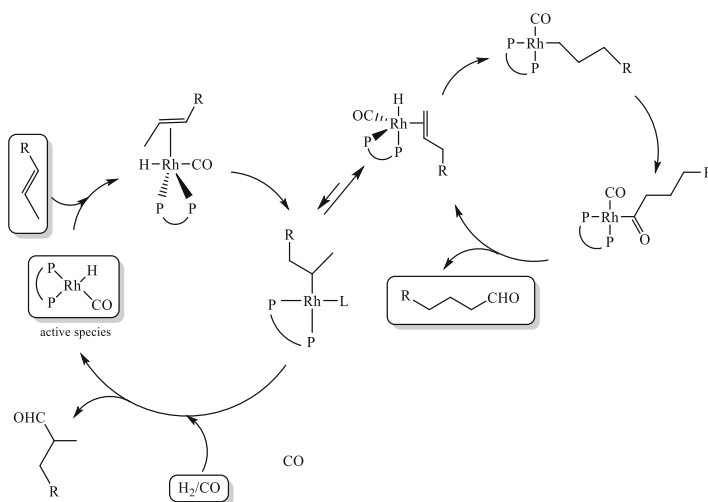
Scheme 2 Main steps for the hydroformylation of an alkene into the corresponding linear and branched aldehydes (the $\text{Rh}(\text{CO})(\text{P}\text{P})$ framework has been reduced to $[\text{Rh}]$ for the branched isomer cycle)

bond, coordination of one CO ligand followed by the migratory CO insertion in the alkyl chain, and then oxidative addition of dihydrogen give rise to the last intermediate of the catalytic cycle $[\text{Rh}(\text{H})_2(\text{COCH}_2\text{CH}_2\text{R})(\text{CO})\text{L}_2]$. Release of the aldehyde by reductive elimination of one hydride and the acyl group regenerates the active $[\text{Rh}(\text{H})(\text{CO})\text{L}_2]$ species.

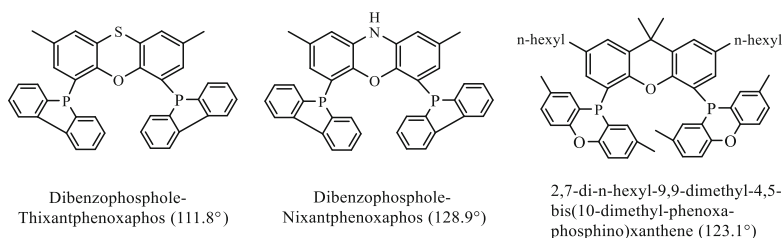
Scheme 2 shows the main steps of the hydroformylation reaction, in which a diphosphine ligand is coordinated to the rhodium metal center. In chapter Rhodium catalyzed hydroformylation (Carmen Claver), this reaction is detailed, particularly the parameters which govern the chemo-, the regio- and even the stereoselectivity of the reaction. The two catalytic cycles giving rise to the linear and the branched aldehydes are represented in two parallel ways. The discrimination between the two isomers arises in the step where the nucleophilic attack of the hydride ligand to the C_1 or C_2 carbon atoms of the coordinated $\text{C}=\text{C}$ double bond occurs, from the δ^- hydride charge induced by the two phosphorus atoms bonded to the rhodium metal center.

2 Isomerization-Hydroformylation

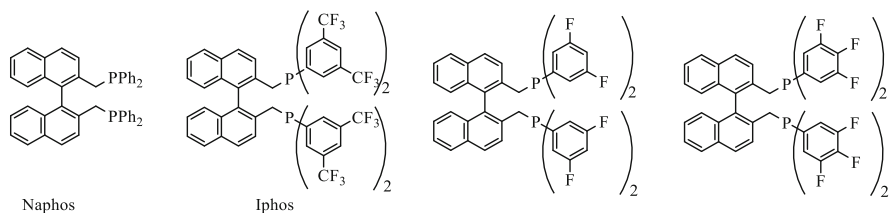
Instead of using terminal alkenes to produce aldehydes, preferably the linear ones in bulk chemistry, it is tempting from an economical point of view to start from internal alkenes or most of the time a mixture of terminal and internal alkenes such as found in Raffinate II (1-butene 64%, (*Z*)-2-butene 9%, (*E*)-2-butene 16%, traces of isobutene) after extraction of butadiene and isobutene from the C4 cut [12]. The tandem isomerization-hydroformylation reaction avoids to perform the separated isomerization reaction, since the thermodynamic mixture contains only around 5% of the terminal alkene. With an appropriate rhodium catalyst, which presents a high activity and selectivity for the hydroformylation of a terminal alkene, the tandem reaction is an elegant way to end up with terminal aldehydes [13, 14]. As previously stated [15], (1) the hydroformylation of the terminal C=C bond has to be fast compared with that of the internal one, (2) the isomerization rate must be fast compared to all hydroformylation reaction rates, and (3) the *n/i* ratio must be very high. Scheme 3 shows the two catalytic cycles in which the crucial connection line between the two catalytic cycles is the β -H elimination from the branched alkyl rhodium species to generate the terminal alkene coordinated to the metal center and the rapid formation of the terminal alkyl ligand through the hydride transfer onto the C₁ carbon atom. A diphosphine ligand has been represented on Scheme 3 since monophosphine ligands provide less attractive results in terms of selectivity for the terminal aldehyde starting from an internal alkene [16].



Scheme 3 Tandem isomerization of an internal alkene and hydroformylation into a terminal aldehyde



Scheme 4 Three crowded diphosphine ligands leading to a 96% selectivity in linear nonanal starting from (*E*)-oct-2-ene (from Refs. [18, 19])

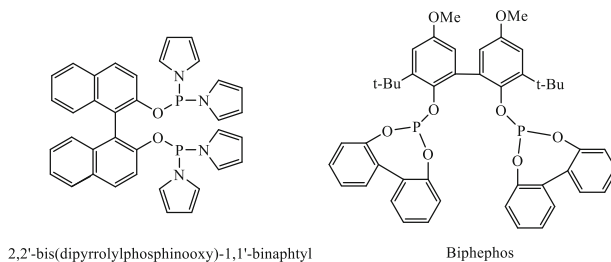


Scheme 5 Naphos, Iphos, and its difluoro- or trifluorophenyl analog ligands

The introduction of bulky chelating diphosphine ligands, with natural bite angles of around 112 and 129° [17], such as the two ligands drawn in Scheme 4, leads to performances comparable to those obtained early at an industrial scale [13]. At a low CO/H₂ pressure of 3.6 and even 2 bar and 120°C to enhance the rate of isomerization, it is possible to reach a highly selectivity in the isomerization-hydroformylation of (*E*)-oct-2-ene into nonanal, although a modest turnover frequency is observed [18].

Using the 2,7-di-*n*-hexyl-9,9-dimethyl-4,5-bis(10-dimethyl-phenoxaphosphino)xanthene ligand largely more soluble (118 mmol L⁻¹), kinetic studies reveal that for pent-2-ene, the reaction order is 0.6 in its concentration, consistent with a fast and reversible alkene coordination, and a -0.5 order in the CO pressure, indicative of a slow migratory CO insertion step justifying the use of low CO pressures (2–8 bar) [19]. Hydroformylation of pent-2-ene catalyzed by the [Rh(acac)(CO)₂]/Naphos system at 120°C and 10 bar provides a *n*/*iso* ratio of 89:11, although with modest reaction rates (TOF = 138 h⁻¹) [20]. The Iphos ligand (Scheme 5) containing electron-withdrawing substituents leads to significantly a more active and a selective catalyst, since but-2-ene and pent-2-ene give a 91:9 *n*/*iso* ratio with 66–68% yields, under the same conditions [20]. The performances are, respectively, 86:14 and 51% for oct-2-ene.

Using the 2,2'-bis(dipyrrolylphosphinoxy)1,1'-binaphthyl bulky phosphinite chelating ligand (Scheme 6) combined to the [Rh(acac)(CO)₂] complex, but-2-ene is transformed into *n*-pentanal at 120°C, 25 bar, with conversion of 90.5% in 6 h and regioselectivity *n*/*iso* = 95:5 obtained [21].



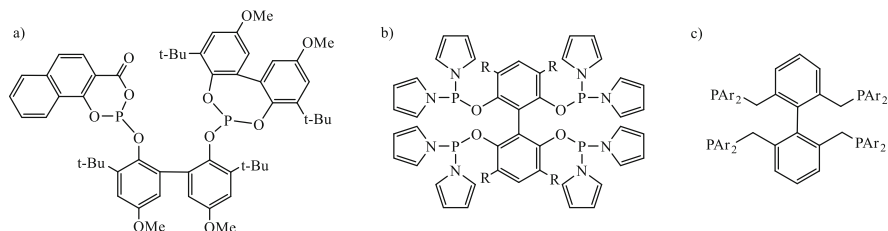
Scheme 6 2,7-di-*n*-hexyl-9,9-dimethyl-4,5-bis(10-dimethyl-phenoxaphosphino)xanthene from Ref. [21] and Biphephos from Ref. [13]

Sulfonated Naphos, which is a mixture a sodium salts of different regioisomers with a 6-8 sulfonation degree of the phenyl groups between 6 and 8, so-called Binas [22, 23], allows to perform the reaction in a biphasic water system [24]. It is necessary to adjust the pH of the water phase to 7–8 with phosphate buffer in order to obtain a 72–73% yield C₆ aldehydes starting from pent-2-ene and a *n*/iso regioselectivity of 99:1. The same performances are reached by addition of amines in water such as triethanolamine or triisooctylamine, showing that the increase in the reactivity is due to the adjustment of the pH and not to the transfer of the catalyst in the organic phase [24].

Performing the isomerization-hydroformylation of oct-4-ene to obtain *n*-nonanal in propylene carbonate instead of toluene, in the presence of [Rh(acac)(CO)₂] and five equivalents of the Biphephos diphosphite ligand (2,2'-bis[(2,2'-bisphenoxy)phosphino]-oxy-3,3',5,5'-tetra-*tert*-butyl-1,1'-biphenyl) (Scheme 6) at 125°C and 20 bar, provides 95% selectivity in *n*-nonanal [25]. Five runs can be performed, leading to the same catalytic performances. This reaction can be operated in a temperature-dependent multicomponent system (TMS) to suppress the catalyst leaching. For instance, with a cyclic carbonate/*N*-octyl-pyrrolidone/*n*-dodecane system, which gives only one phase at 125°C but two phases at room temperature, the conversion of (*E*)-oct-4-ene is 99%, with a 80% regioselectivity in *n*-nonanal, the leaching in rhodium is <0.1% and in phosphorus of 0.6% [26]. This tandem reaction applied to methyl oleate, with an original diphosphite ligand leading to the eq,eq-[Rh(H)(CO)₂L₂] precursor, allows to isomerize the C=C double bond in 9-position to give 75% of linear aldehyde selectivity [27].

The difluorophenyl analog of Iphos (Scheme 5) gives 94:6 *n*/iso ratio and 59% yield for pent-2-ene, and the trifluorophenyl analog (Scheme 5) gives 94:6–95:5 and 61–74% for both but-2-ene and pent-2-ene and even 70:30 and 41% after 31 h for oct-2-ene [20]. The unsymmetrical ligand of Scheme 7a is able to give rise to 69% of *n*-nonanal starting from a mixture containing 94% internal alkenes with high reactivity since the TOF is 4,448 h⁻¹ at 130°C and 20 bar [28].

The tetraphos ligand (R=H of Scheme 7b) added to [Rh(acac)(CO)₂] in a ligand/metal = 3:1 ratio appears as particularly efficient, presumably because of its enhanced chelating ability with regard to diphosphine ligands [29]. Indeed, at 100°C and 10 bar of a CO/H₂ gas mixture for 1 h, *n*/iso = 98:2 ratio is obtained

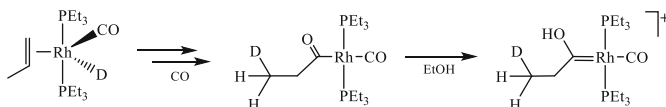


Scheme 7 Unsymmetrical diphosphite ligand (from Ref. [28]) and tetraphos ligands (from Refs. [29–31])

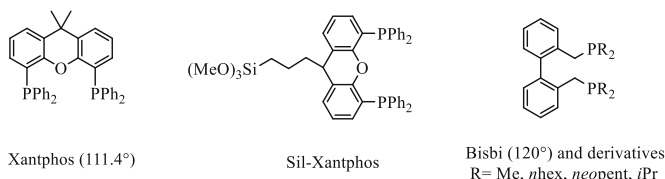
with a 1,500 turnover number (TON) for oct-2-ene and for hex-2-ene 98.8:1.2 and TON=1,700. Introduction of Cl, Me, Et, Ph, tolyl, and *p*FPh substituents in the 3,3',5,5' positions ($R \neq H$) still increases the efficiency of this isomerization for these two substrates [30]. Similarly the tetraphosphine ligand based on a biphenyl backbone (Scheme 7c) gives regioselectivities close to 99:1 at 120°C, 5 bar, for a L/Rh=4 ratio, particularly when the Ar group is the electron-withdrawing 3,5-F₂C₆H₃ substituent [31]. Analog bidentate phosphite ligands containing two bisphosphoramidite entities bound to a spiroketal backbone provide the isomerization-hydroformylation of but-2-ene and oct-2-ene with regioselectivities close to 95–97% and TONs as high as 27,000. The X-ray crystal structure of the [Rh(acac)L₂] complex, as well as infrared and ¹H, ³¹P NMR analyses of the [Rh(H)(CO)₂L₂] in situ prepared show that the P-Rh-P bite angle is 94.7°, and the phosphorus atoms occupy two equatorial positions of the trigonal bipyramid [32], as already shown for the 1,1'-biphenyl-2,2'-diyl-bis(dipyrrolylphosphoramidite) ligand [33]. Similar high-pressure NMR spectroscopic data on rhodium-crowded bidentate diphosphites are consistent with an energetically preferred bis-equatorial mode of coordination in the trigonal-bipyramidal [Rh(H)(CO)₂L₂] resting state and being efficient in this tandem reaction [34, 35].

3 Hydroformylation-Hydrogenation

Alcohols, particularly linear alcohols, have broad applications as solvents and raw materials for plasticizers and detergents. Thus, the tandem hydroformylation-hydrogenation reaction allows to directly synthesize the alcohol from an alkene, provided a specific catalytic system leads to a high selectivity at a reasonable reaction rate. In the early stages of the “oxo” reaction, the formation of alcohols has been observed. The Shell process involving the [Co(H)(CO)₃(PBu₃)] catalyst allows to produce directly butanol from propene at high temperature and pressure [36]. Working under the mild conditions of Rh-oxo synthesis, patents claim that (β-diketone)Rh [37] or [(η⁵-C₅H₅)Rh(CO)(PBu₃)] precursors [38] catalyze the formation of alcohols. Starting from the [Rh(H)(PEt₃)₃] precursor hex-1-ene is fully transformed into heptanol at 120°C and 40 bar CO/H₂ = 1:1 in ethanol, or



Scheme 8 Partial catalytic steps leading to a cationic hydroxycarbene-rhodium species in ethanol (adapted from Ref. [40]). The counter-anion is presumably EtO^-



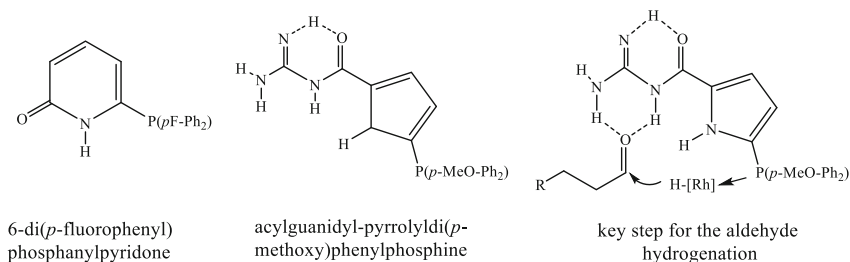
Scheme 9 Xantphos, its trimethoxysilane-*n*-propyl version, and Bisbi's derivatives (from Refs. [41, 42])

an alcoholic solvent, with an initial TOF of $2,300 \text{ h}^{-1}$ and the *n*/*iso* ratio ca 2.8:1 [39, 40]. Using D_2 -CO labeling studies, ^1H and ^{31}P NMR analyses allow to identify the $[\text{Rh}(\text{H})(\text{CO})(\text{PEt}_3)_2]$ active species. They are consistent with the protonation of the acyl intermediate by ethanol to generate an hydroxycarbene-rhodium species which reacts with H_2 to provide after reductive elimination the final alcohol (Scheme 8) [40].

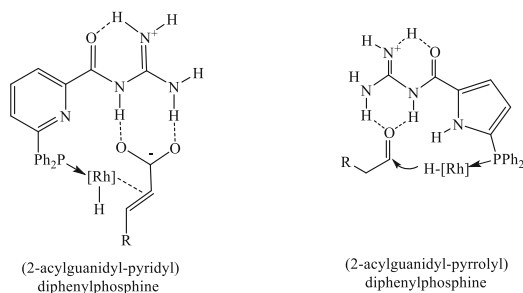
The introduction in the coordination sphere of rhodium of Xantphos-type ligands immobilized on silica (Scheme 9) transforms oct-1-ene into *n*-nonanol with 90% selectivity in the linear alcohol [41]. The reaction is carried out in toluene, since it simultaneously involves the two species $[\text{Rh}(\text{polySil-Xantphos})(\text{CO})]^+$ and $[\text{Rh}(\text{H})(\text{CO})_2(\text{polySil-Xantphos})]$. In *n*-propanol solvent, the hydrogenation activity is suppressed and 93–95% of linear aldehyde are obtained, presumably by deactivating the acidic silanols on the silica surface. By comparison the complex $[\text{Rh}(\text{H})(\text{CO})_2(\text{Xantphos})]$ is active for the hydroformylation reaction with around 25% of hydrogenation of oct-1-ene into octane, whereas the cationic $[\text{Rh}(\text{CO})(\text{Xantphos})]^+[\text{CF}_3\text{COO}]^-$ complex is active for the hydrogenation of nonanal.

The large bite angle Me-Bisbi ligand (Scheme 9) is interesting since, added to $[\text{Rh}(\text{acac})(\text{CO})_2]$, the resulting catalytic system in ethanol gives 97% of the C_{11} alcohols from dec-1-ene with a *n*/*iso* = 80:20 ratio at high temperature of 170°C [42]. The simultaneous use of PEt_3 and the wide bite angle diphosphines such as Xantphos or Diop with $[\text{Rh}(\text{acac})(\text{CO})_2]$ leads to a mixed complex very efficient to do this tandem reaction and to obtain heptanol from hex-1-ene in 90% yield with *n*/*iso* = 99:1 ratio. Similar performances are observed with oct-1-ene and dec-1-ene, as well as allyl alcohol providing butanediol [43].

This strategy of the cooperative ligand system is adopted to define the best catalytic tool able to perform the two distinct hydroformylation and hydrogenation reactions with high selectivity. Indeed, the simultaneous addition of 6-di(*p*-fluorophenyl)phosphanylpyridone and acylguanidyl-pyrrolyldi(*p*-methoxy)



Scheme 10 The two phosphanylpyridone and acylguanidyl-diphenylphosphine ligands leading to a cooperative action in the hydroformylation-hydrogenation of an alkene (from Ref. [44])



Scheme 11 The two key steps in the decarboxylative hydroformylation-hydrogenation reaction of α,β -unsaturated carboxylic acids using two supramolecular bifunctional ligands (from Ref. [45])

phenylphosphine (1:1) (Scheme 10) to $[\text{Rh}(\text{acac})(\text{CO})_2]$ leads to an efficient catalytic system to gain alcohols with 95% conversion and $n/\text{iso} = 96:4$ regioselectivity [44]. A wide range of substrates were evaluated and selectively transformed under the same operating conditions (20 bar, 80°C, toluene, 24 h). The acylguanidyl ligand is responsible for the hydrogenation step, and it is suggested that two NH bonds interact with the aldehyde to favor the Rh-H transfer to reduce the carbonyl group into the alcohol (Scheme 10).

Taking advantage of the recognition of functional groups by the acylguanidinium functionality, association of the two ligands of Scheme 11 is responsible for the novel tandem decarboxylative hydroformylation-hydrogenation of α,β -unsaturated carboxylic acids [45]. In the key step, the C=C bond coordinates to the rhodium metal center, whereas the guanidine group interacts with the two oxygen atoms of the acidic function, to remove CO_2 ; in the second key step, the aldehydic function interacts with the guanidine group to assist the hydride transfer.

The tandem hydroformylation-hydrogenation reaction has been applied to the isoprene substrate. Addition of a large excess (15:1) of the bis(diphenylphosphino) ethane ligand (dppe) to $[\text{Rh}(\text{acac})(\text{CO})_2]$ induces the classical 1,4-hydroformylation of isoprene [46], but the next step is the hydrogenation of the C=C double bond to synthesize 3-methylpentanal [47]. The reaction, performed in cumene at 100°C, 50 bar, and during 24 h, leads to 85% yield in the saturated aldehyde, and no alcohol is detected [47]. The dppe role is also to induce the oxidative addition of dihydrogen

to the 2,3-unsaturated acyl-rhodium intermediate leading to the conjugated unsaturated aldehyde, which is further rapidly hydrogenated.

4 Hydroformylation-Acetalization

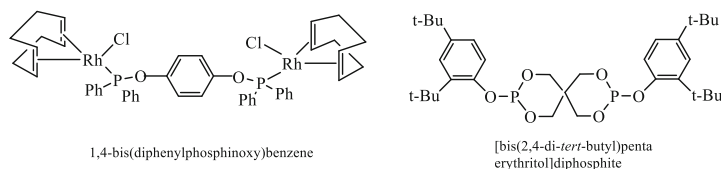
As rhodium complexes, such as $[\text{RhCl}_2(\text{MeCN})\{\text{MeC}(\text{CH}_2\text{Ph})_3\}][\text{CF}_3\text{SO}_3]$, are able to catalyze the acetalization of aldehydes or ketones under mild conditions [48], the direct synthesis of acetals from an alkene by the tandem hydroformylation-acetalization reaction is shown to be effective in the presence of $[\text{Rh}_2(\mu\text{-OMe})_2(\text{COD})_2]/10 \text{ PPh}_3$ at 60–90°C under 50 bar of a $\text{CO}/\text{H}_2 = 1:1$ gas mixture [49]. A weak acid as pyridinium *p*-toluenesulfonate or camphorsulfonate is required as well as 2,2-dimethoxypropane or triethylorthoformate to introduce the two alkoxy functions. Thus 2,5-dihydrofuran, styrene, 5-methyl-hex-5-ene-2-one, or vinylacetate are almost fully converted into the corresponding acetals (95–97%) [49].

The synthesis of the dirhodium complex bridged by a diphosphinite ligand (Scheme 12) leads to a good catalyst for the tandem reaction of hex-1-ene in methanol, operating at 30 bar, 80°C, for 8 h. It gives 99% selectivity in aldehyde for 100% conversion, although the *n*/*iso* ratio is only 46:54 [50]. This reaction has been extended with the same efficiency to styrene and its substituted analogs with donating or withdrawing substituents and cyclopentene or cyclohexene.

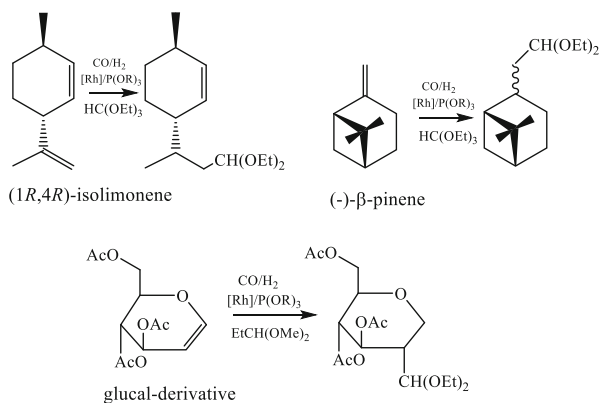
Using the crowded diphosphinite ligand drawn on Scheme 12 with $[\text{Rh}(\text{acac})(\text{CO})_2]$ results in 85% yield in acetals at 20 bar, 110°C, for 6 h, starting from various allylbenzene substrates [51].

Introducing four equivalents of $\text{P}(\text{OPh})_3$ to the two dirhodium $[\text{Rh}_2\{\mu\text{-SCR}_2\text{CH}(\text{NH}_3)^+(\text{COOH})_2(\text{CO})_4\}][\text{CF}_3\text{SO}_3]_2$ catalytic precursors (with $\text{R}=\text{H}$ cysteine bridging ligand and $\text{R}=\text{Me}$, penicillamine) allows to obtain high yields of the acetals starting from (1*R*,4*R*)-isolimonene and (–)-β-pinene with triethylorthoformate (Scheme 13) [52]. Glucal derivatives are similarly transformed into acetals using the $[\text{Rh}_2(\mu\text{-OMe})_2(\text{COD})_2]/10 \text{ P}(\text{O}-o\text{-Bu}^t\text{Ph})_3$ catalytic system (Scheme 13) [53].

The $[\text{Rh}_2\{\mu\text{-SCH}_2\text{CH}_2(\text{NHMe}_2)\}_2(\text{CO})_2(\text{PPh}_3)_2][\text{CF}_3\text{SO}_3]_2$ complex anchored to a sulfonic exchange resin catalyzes this tandem reaction in methanol with a small leaching of rhodium. Styrene is fully converted into dimethyl acetal, with ca 85% selectivity into the branched product [54]. Direct use of the $\text{RhCl}_3 \cdot 3\text{H}_2\text{O}/2 \text{ P}(\text{OPh})_3$ catalytic system leads to high yields in the acetals corresponding to styrene



Scheme 12 Dirhodium precursor with a bridging diphosphinite ligand (from Ref. [50]) and [bis(2,4-di-*tert*-butyl)pentarythritol]diphosphite (from Ref. [51])



Scheme 13 Tandem hydroformylation-acetalization of isolimonene and β-pinene (from Ref. [52]) and 3,4,6-tri-*O*-acetyl-D-glucal and related glucal derivatives (from Ref. [53])

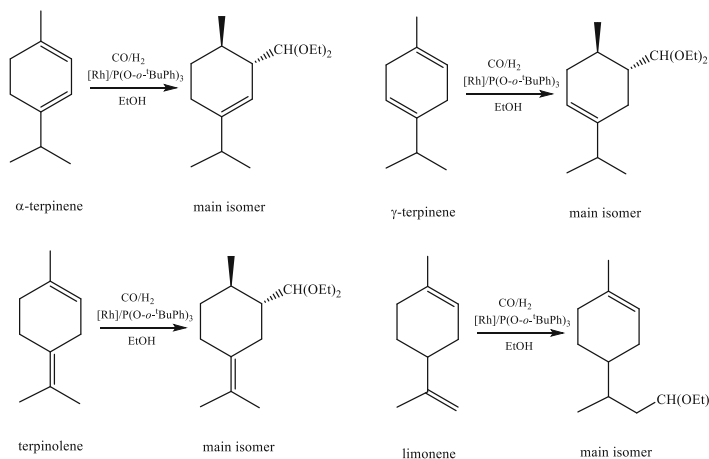
and oct-1-ene, in methanol [55] but not in triethylorthoformate, which gives exclusively aldehydes [56]. The Rh^(III) precursor (RhCl₃·3H₂O) can be anchored on mesoporous silica MCM-41 support, eventually in the presence of the H₃PW₁₂O₄₀ heteropoly acid, that increases the yield of acetals to 92%, even if the leaching of rhodium remains too high [57]. The *cis*-[Rh(CO)₂(amine)₂][PF₆] complexes, with amine being pyridine, picoline, or lutidine, transform hex-1-ene, still in methanol, under 0.9 bar of only CO at 100°C, in similar quantities of the methyl ester (by methoxycarbonylation) and the 1,1-dimethoxyheptane acetal, dihydrogen being produced by the water-gas shift reaction [58]; the reaction can be also performed with the cationic complex immobilized on poly(4-vinylpyridine) [59].

Another immobilization method involves triphenylphosphine functionalized on one phenyl in 4-position with a glycine group. The zwitterionic NH₃⁺-CH₂-COO⁻ group, allows to prepare a Brønsted acid-rhodium bifunctional catalyst to keep it in an ionic liquid [60]. No significant loss of rhodium is observed during at least 12 recycling experiments for the hydroformylation-acetalization of oct-1-ene.

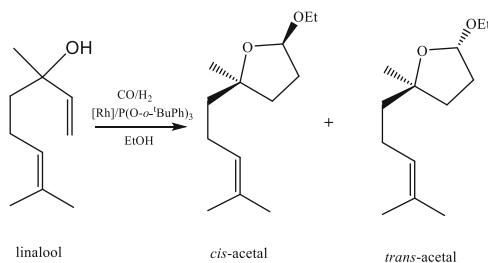
The [Rh₂(μ-OMe)₂(COD)₂]/P(*o*-Bu^tPh)₃ catalytic system (P/Rh = 20–50) is largely more active than with the PPh₃ phosphorus ligand and allows to convert in ethanol at 80°C and 80 bar (CO/H₂ = 1:1) α-terpinene, γ-terpinene, terpinolene, and limonene into the corresponding diethylacetals (Scheme 14) [61].

This procedure has been extended to the synthesis of other fragrance compounds from acyclic monoterpenes such as linalool and β-citronellene [62]. Excellent selectivity in the formation of the cyclic acetals from linalool is obtained. Two *cis*- and *trans*-stereoisomers are formed, the *cis*- being the major isomer (Scheme 15). For β-citronellene the reaction is less efficient since a mixture of aldehydes and acetals is obtained whatever the experimental conditions explored. This reaction is performed in ethanol with the bulky phosphite ligand in the absence of additional acid cocatalyst under mild conditions.

As hydroformylation of unsaturated alcohols results in cyclic hemiacetals [10, 62, 63], this tandem reaction has been explored on alkenediols, especially



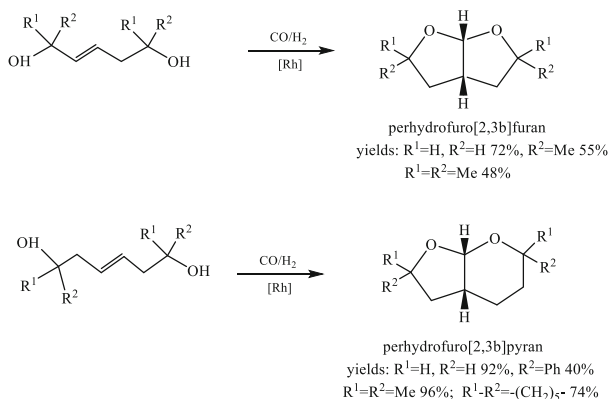
Scheme 14 Main acetal isomers obtained by hydroformylation of α -terpinene, γ -terpinene, terpinolene, and limonene with the $[\text{Rh}_2(\mu\text{-OMe})_2(\text{COD})_2]/\text{P}(\text{O-}i\text{-Bu}^t\text{Ph})_3$ catalyst in ethanol (from Ref. [61])



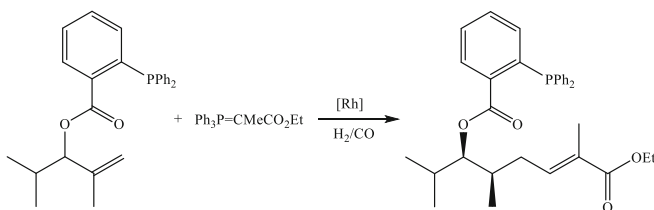
Scheme 15 The two cyclic acetals produced in ethanol by hydroformylation-acetalization of linalool (from Ref. [62])

since active pharmacodynamic compounds such as aflatoxins possess a furo[2,3*b*] skeleton [64]. Thus, operating with $[\text{Rh}_2(\mu\text{-OMe})_2(\text{COD})_2]/\text{PPh}_3$ ($P/\text{Rh} = 6$), at 120°C for 20 h under 60 bar of a $\text{CO}/\text{H}_2 = 3:1$ mixture, pent-2-ene-1,5-diol as well as hex-2-ene-1,6-diol, and some of their substituted analogs provides the corresponding perhydrofuro[2,3*b*]furans or perhydrofuro[2,3*b*]pyrans through a double acetalization-cyclization process (Scheme 16).

Concerning the mechanism of the acetal formation in methanol, especially in the absence of acid added, several studies have shown that the $[\text{Rh}(\text{COD})_2][\text{BF}_4]$ or $[\text{Rh}_2(\mu\text{-Cl})_2(\text{COD})_2]$ precursors, in the presence of a diphosphine [65] or PPh_3 ligand [66], as well as molecular hydrogen, are required to obtain a good acetal selectivity. There is a cooperative effect between the rhodium complex and the in situ formed acid HBF_4 or HCl . The hydroformylation is fast, for instance, the TOF is $1,000 \text{ h}^{-1}$ with $[\text{Rh}(\text{COD})_2][\text{BF}_4]/\text{Xantphos}$ at 30 bar and 110°C , and the acetalization is the limiting step with a $\text{TOF} = 120 \text{ h}^{-1}$ [65].



Scheme 16 Tandem hydroformylation-acetalization of α,ω -alkenediols into the corresponding bicyclic acetals (from Ref. [64])

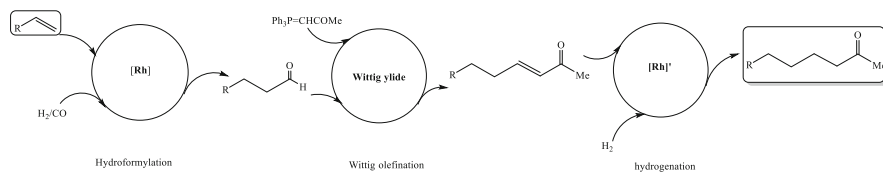


Scheme 17 Stereoselective formation of a trisubstituted C=C bond by tandem hydroformylation-Wittig reaction (from Ref. [68])

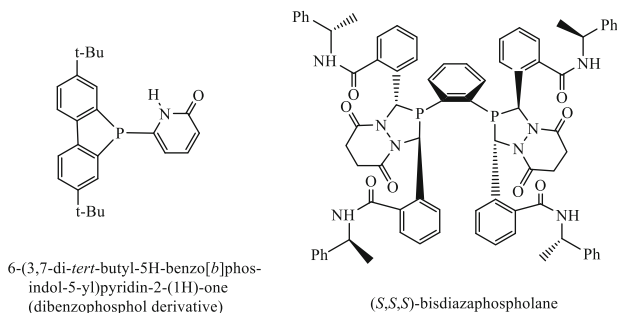
5 Hydroformylation-Wittig Olefination

The classical Wittig olefination results from the reaction of an aldehyde or a ketone with a phosphonium ylide to synthesize an alkene, coproducing a phosphine oxide [67]. This tandem reaction has been developed since the first demonstration reported that a methallyl protected alcohol could react with $\text{Ph}_3\text{P}=\text{CMeCO}_2\text{Et}$ or $\text{Ph}_3\text{P}=\text{CMeCOMe}$ and be transformed into an α,β -unsaturated carbonyl derivative with 75–78% yields. Moreover the attachment of the *ortho*-diphenylphosphanylbenzene (*o*-DPPB) group to the alcohol function transforms the corresponding trisubstituted alkene with a high *syn/anti* = 96:4 diastereoselectivity (Scheme 17) [68]. Due to the second stereogenic center formed, the diastereoselectivity is controlled by the *o*-DPPB directing group in the course of the hydroformylation reaction. The *E*-selectivity of the double bond is due to the high *E*-preference of phosphorus ylides.

The success of this tandem reaction requires working with stabilized phosphorus ylides.



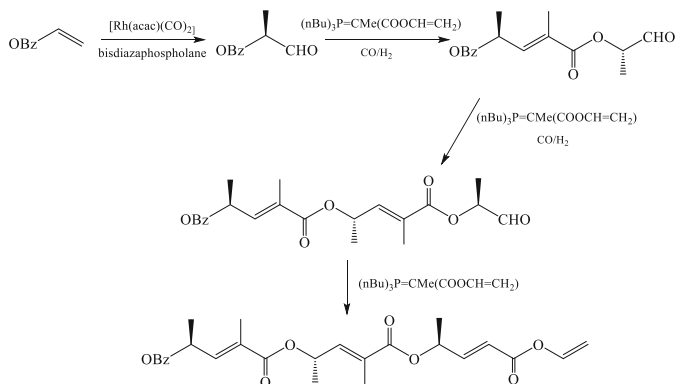
Scheme 18 Tandem reaction involving hydroformylation-Wittig olefination and hydrogenation of the unsaturated carbonyl compound



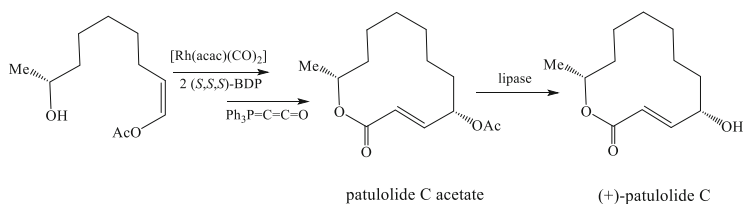
Scheme 19 Two efficient dibenzophosphole and bisdiazaphospholane ligands used in the hydroformylation-Wittig olefination tandem reaction (from Refs. [71, 72])

Saturated ketones (Scheme 18), still containing the *o*-DPPB group, are produced with 70% yield and *syn/anti* = 92:8 diastereoselectivity when the non-disubstituted $\text{Ph}_3\text{P}=\text{CHCOMe}$ ylide is introduced in the one-pot reactor [68]. The third step is the hydrogenation of the C=C double bond, catalyzed by the rhodium complex, as shown by independent tests involving $[\text{Rh}(\text{H})(\text{CO})(\text{PPh}_3)_3]$ under H_2 [69]. In this case the tandem hydroformylation-Wittig olefination-hydrogenation process is realized.

The same catalytic system involving the Xantphos or Biphephos ligands allows to obtain full conversions of N-protected allylamine into ca 85% α,β -unsaturated carbonyl compounds using $\text{Ph}_3\text{P}=\text{CHCOX}$ (X = Me, OMe, N(OMe)Me) and to reduce the amounts of the saturated ester to ca 15% [70]. Moreover, the reaction with Biphephos can be carried out at 50°C and under atmospheric pressure of a $\text{CO}/\text{H}_2 = 1:1$ gas mixture, allowing to obtain selectivity up to 98% in unsaturated carbonyl compounds. Deprotection of the nitrogen atom by elimination of the formyl or Boc group, followed by an intramolecular aza-Michael addition, gives *trans*-2,5-disubstituted pyrrolidines with a 94–97% enantiomeric excess. The scope of the reaction is done with a variety of allylamine derivatives. Various homoallylic alcohols can be transformed in 7-hydroxyenoates at 3 bar of $\text{CO}/\text{H}_2 = 1:1$, 80°C, for 16 h with $[\text{Rh}(\text{acac})(\text{CO})_2]/\text{dibenzophosphol}$ derivative (shown in Scheme 19), which gives the most satisfactory chemo- and regioselectivity. The enoates can be further cyclized through an oxa-Michael addition reaction to produce the



Scheme 20 Hydroformylation-Wittig olefination sequences with the $[\text{Rh}(\text{acac})(\text{CO})_2]/(S,S,S)$ -bisdiazaphospholane catalytic system and the allyl-substituted $(n\text{Bu})_3\text{P}=\text{CMe}(\text{COOCH}=\text{CH}_2)$ ylide (from Ref. [72])



Scheme 21 Tandem hydroformylation-Wittig olefination of 9-acetoxy-*Z*-(2*R*)-8-nonene-2-ol into patulolide acetate, transformed into (+)-patulolide C with *Pseudomonas fluorescens* lipase (from Ref. [73])

corresponding *cis*-pyrans in 87–91% yields and excellent diastereoselectivities [71].

An efficient enantioselective one-pot hydroformylation-Wittig olefination has been designed to produce γ -chiral α,β -unsaturated carbonyl compounds. The chiral bis(diazaphospholane) ligand (Scheme 19) coordinated to rhodium transforms vinylacetate into the branched aldehyde in the first step with an excellent enantioselectivity (up to 99%) followed by the Wittig olefination with stabilized ylides [72].

Multiple iterative hydroformylation-Wittig olefination sequences can be performed with successive depressurization and repressurization steps to provide an aldehyde from the diene intermediate obtained. Concerning the tandem reaction, the aldehyde resulting from the sequential reactions with the vinylbenzoate substrate and the $(n\text{Bu})_3\text{P}=\text{CMe}(\text{COOCH}=\text{CH}_2)$ ylide, leads to the 4-hydroxyvalerate trimer with three unique stereocenters in a 17% isolated yield (Scheme 20) [72].

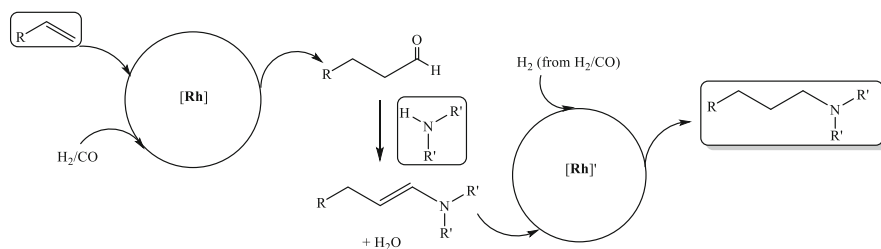
The patulolide C acetate macrolactone is synthesized by the same procedure (Scheme 21) [73]. The 9-acetoxy-*Z*-(2*R*)-8-nonene-2-ol substrate, obtained by acetoxylation of (2*R*)-8-nonyn-2-ol, is transformed at 14 bar of syn gas, at 50°C,

for 24 h and then in the presence of the $\text{Ph}_3\text{P}=\text{C}=\text{C}=\text{O}$ ylide into the corresponding 12-membered lactone, with complete *E*-selectivity. Deacetylation with a lipase proceeds in quantitative yield to give (+)-patulolide **C** with a 97% diastereoselectivity.

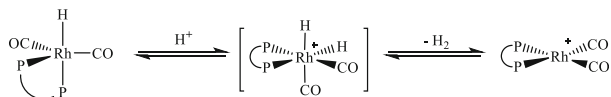
6 Hydroaminomethylation

As rhodium complexes are able to catalyze both the Hydrogenation [74] and hydroformylation reactions [75] (cf. *also part Hydroformylation-Hydrogenation of this chapter*), the hydroaminomethylation reaction (HAM), shown in Scheme 22, has been significantly investigated and some reviews have recently appeared [76, 77]. HAM represents an attractive atom economy reaction providing amines from alkenes in a one-pot way. Moreover, the reactants are generally abundant and cheap building blocks. This tandem reaction is composed of three successive steps. Aldehydes produced by the first catalytic hydroformylation reaction react with ammonia, or primary or secondary amines present in the medium, to afford the corresponding imines or enamines. The linear aldehyde is largely more reactive than the branched one in this condensation reaction. Most of the time, isomerization between imine and enamine occurs, and hydrogenation of these two intermediates in the second catalytic cycle results in the formation of the expected amines.

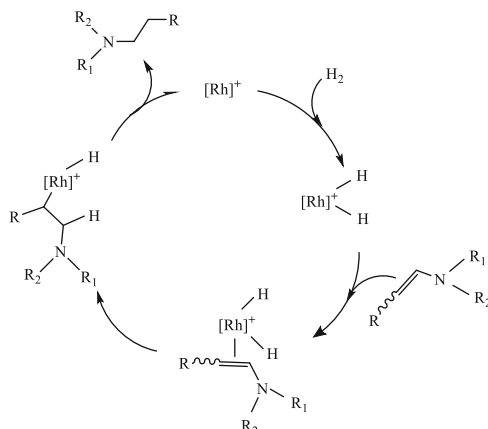
It is necessary to carefully control the design of the catalytic system in order to have not only high chemoselectivity but also regioselectivity depending of the branched or linear expected final amine. Indeed the hydrogenation reaction is the rate determining step in HAM. Recently, it has been demonstrated that an equilibrium between the neutral $[\text{Rh}(\text{H})(\text{CO})_2\text{L}_2]$ and the cationic $[\text{Rh}(\text{CO})(\text{X})\text{L}_2]^+$ species exists to perform the two catalytic cycles [78]. Presumably, the neutral rhodium-hydride species catalyzes the hydroformylation reaction, whereas the cationic species performs the hydrogenation reaction. Instead of using simultaneously a cationic and a neutral rhodium precursor in order to increase both catalytic activity and amine selectivity [79], it is preferable to have an appropriate rhodium system



Scheme 22 The two catalytic cycles involved in the tandem hydroaminomethylation reaction (only the linear products are represented)



Scheme 23 Equilibrium between the neutral rhodium-hydride complex and the cationic square-planar complex (from Ref. [78])



Scheme 24 Catalytic cycle for the hydrogenation of an enamine (the active species is just represented as $[\text{Rh}]^+$ for more clarity)

able to generate in situ the two catalytic active species which remain in equilibrium (Scheme 23).

Scheme 24 is devoted to the $\text{R-CH=CH-NR}_1\text{R}_2$ enamine hydrogenation, showing the main catalytic steps. Classically, the cationic active species, represented as $[\text{Rh}]^+$, reacts with dihydrogen by an oxidative addition reaction to give a dihydride which coordinates the enamine. The hydride transfer, and then the reductive elimination leads to the final amine, restoring the $[\text{Rh}]^+$ active species.

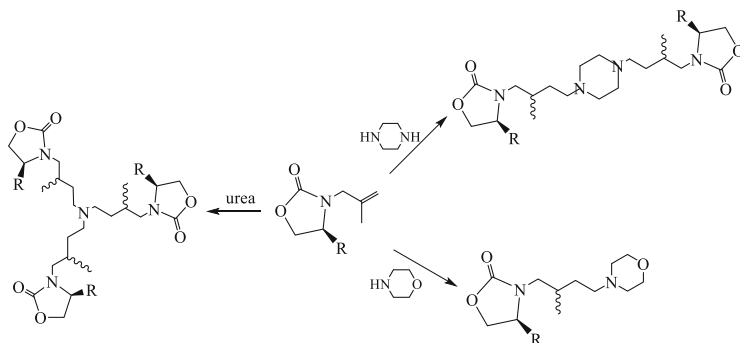
To reach good yields in amines, this tandem reaction is generally performed in the 90–130°C temperature and 30–60 bar of CO/H_2 range. These operating conditions are somewhat more severe than those for the hydroformylation reaction consistent with a rate determining step for the hydrogenation reaction of imines/enamines. The CO/H_2 composition generally varies from 1:1 to 1:5 depending on the experimental procedures.

In the following part, we analyze the various performances of the catalysts according to the nature of the alkene and in some cases that of the amine, giving the most attractive performances.

6.1 Hydroaminomethylation of Terminal and Internal Alkenes

With an efficient catalytic system, the hydroformylation reaction quickly proceeds, especially for the terminal alkenes, so no isomerization of the C=C double bond occurs. Thus the two linear and iso- (on the C2 carbon atom) aldehydes are formed, and after hydrogenation of the enamines/imines, the *n*- and iso-amines are produced. However, for most amines the two isomers possess similar physical properties, making their separation difficult for obtaining pure products. Many efforts have been made to adjust the coordination sphere of the catalyst in order to reach regioselectivities as high as 98:2 to obtain directly the linear isomer. This goal has been achieved by using diphosphine ligands. Indeed, whereas triphenylphosphine generates the $[\text{Rh}(\text{H})(\text{CO})(\text{PPh}_3)_3]$ resting state and gives rise to a 86:14 *n*/iso ratio, the use of the Xantphos ligand (Scheme 9) and $[\text{Rh}(\text{COD})_2]\text{BF}_4$ precursor combines not only the quantitative conversion of different terminal alkenes but also the fast hydrogenation of the enamine/imine (ca 97%) and a high 98:2 *n*/iso ratio [80]. The conditions are $\text{CO}/\text{H}_2 = 7:33$ bar, 125°C, and 5 h in a 1:1 toluene/methanol mixture. Using these two solvents allows to suppress the formation of *N*-formylpiperidine which is produced in pure methanol up to 15%. Introducing the $[\text{Rh}_2(-\mu\text{-Cl})_2(\text{COD})_2]$ or $[\text{Rh}(\text{acac})(\text{CO})_2]$ precursors with four equivalents of Xantphos ligand gives a lower selectivity in amines (94 and 90%, respectively). In addition the two dppe 1,2-bis(diphenylphosphino)ethane and Iphos diphosphines (Scheme 5) give rise to less interesting performances even if Iphos leads to *n*/iso ratio of 99:1. This latter ligand combined with $[\text{Rh}(\text{acac})(\text{CO})_2]$ proves to be a powerful catalyst to the one-pot synthesis of hydrazones from terminal alkenes and hydrazines since at 65°C under 10 bar CO/H_2 (1:1), the alkenes are converted in 16 h into the expected hydrazones with selectivities ranging from 85 to 99% and *n*/iso ratios of 99:1 except for functionalized alkenes (88:12–98:2) [81]. Moreover, it is possible, after catalysis, to add four equivalents of ZnCl_2 to the crude reaction mixture for obtaining by heating for several hours the corresponding indoles. Starting from pent-1-ene or allyl phenyl ether and *N*-phenylhydrazine, excellent yields of 80–85% and *n*/iso = 99:1 regioselectivity are obtained [81].

The $[\text{Rh}(\text{COD})_2]\text{BF}_4/\text{Xantphos}$ catalytic system was explored for various alkenes under the following conditions: 60 bar ($\text{CO}/\text{H}_2 = 10:50$) and 95°C for 12 h. The HAM reaction starting from pent-1-ene and piperidine, morpholine, thiomorpholine, *N*-benzylpiperazine, dimethylamine, and aniline produces the corresponding amines with the hexyl fragment. The same reaction from pent-1-ene and the primary hexylamine generates dihexylamine and, with this latter amine, the trihexylamine. For all these substrates, the conversions and chemoselectivity as well as the regioselectivity (98:2–99:1) are very attractive. The piperidine reactant has also been used with hex-1-ene, oct-1-ene, and various substituted alkenes. In all these experiments, the performances are high for the three selectivity parameters [80].



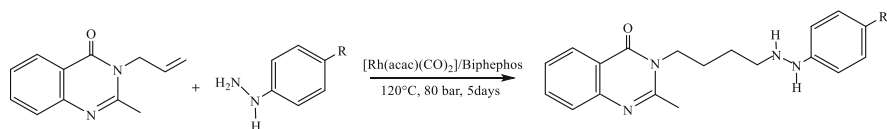
Scheme 25 Hydroaminomethylation of *N*-methylallyloxazolidinone (adapted from ref [82])

Due to the presence of their N–O functional groups, chiral amino alcohols are useful vectors to assist catalysis by chiral recognition and combinatorial approach. They can be obtained by hydrolysis of oxazolidinone moieties in which the amino alcohol is protected. Following this strategy, *N*-olefinic oxazolidinones ($R = \text{Ph}$, CH_2Ph , *i*-Pr) have been used to perform HAM with various amines.

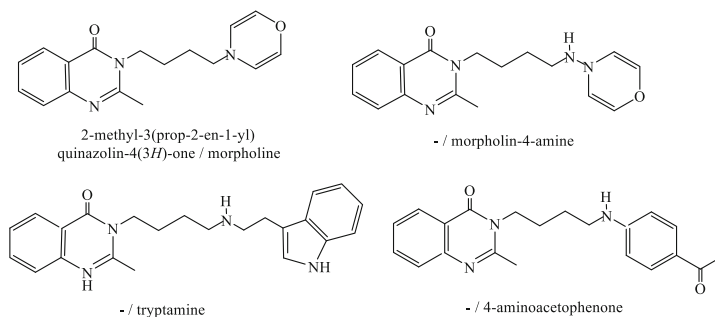
As shown in Scheme 25, the reaction with morpholine, piperazine, and urea gives the corresponding amines with high yields (79–95%) and total regioselectivity. However no chiral induction is observed during the hydroformylation step or the reduction of the imines/enamines [82]. The catalytic $[\text{Rh}_2(\mu\text{-Cl})_2(\text{COD})_2]$ precursor operates at 120°C and 60 bar ($\text{CO}/\text{H}_2 = 1:1$) in dioxane for 48–72 h. This reaction can be extended to tris(aminoethyl)amine, $\text{N}(\text{CH}_2\text{CH}_2\text{NH}_2)_3$, providing after 120 h the formation of the corresponding dendritic polyamines containing 6 oxazolidinone (no s) moieties. The same reaction involving *N*-allyloxazolidinone requires the use of the $[\text{Rh}(\text{acac})(\text{CO})_2]/\text{Biphephos}$ (cf. Scheme 6) catalytic system to obtain the linear aldehyde in *n*/*iso* = 87:13 regioselectivity in dioxane at 50°C under 20 bar ($\text{CO}/\text{H}_2 = 1:1$) for 48 h. In a second step, the reductive amination of the aldehydes is performed after adding piperazine or 1-(3,5-bis(piperazin-1-yl)methylbenzyl)piperazine and repressurizing under 60 bar ($\text{CO}/\text{H}_2 = 1:5$) to obtain the two dendritic polyamines. Their hydrolysis leads to the two corresponding aminoalcohols. These chiral aminoalcohols are used as ligands for $[\text{RuCl}_2(\text{p-cymene})]_2$ catalytic precursor in the asymmetric hydrogen transfer reaction [82].

The $[\text{Rh}(\text{acac})(\text{CO})_2]/\text{Biphephos}$ system also catalyzes the reaction of 2-methyl-3(prop-2-en-1-yl)quinazolin-4(3*H*)-one with arylhydrazines at 120°C and 80 bar ($\text{CO}/\text{H}_2 = 70:10$) for 5 days, resulting in the formation of the linear amines with yields as high as 96% and regioselectivity of around 90:10 (Scheme 26) [83].

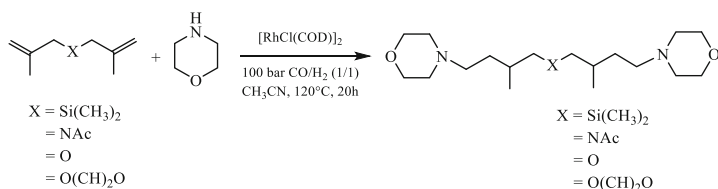
Similarly, starting from 2-methyl-3(prop-2-en-1-yl)quinazolin-4(3*H*)-one and morpholine, morpholine-4-amine, tryptamine, and 4-aminoacetophenone, $[\text{Rh}(\text{acac})(\text{CO})_2]/\text{P}(\text{OPh})_3$ produces the four linear amines represented on Scheme 27. The yields after purification by column chromatography are 89, 93, 78, and 67%, respectively [83]. This high yield method for synthesizing 3-substituted quinazolin-



Scheme 26 HAM reaction of 2-methyl-3(prop-2-en-1-yl)quinazolin-4(3H)-one with arylhydrazine (adapted from ref [83])



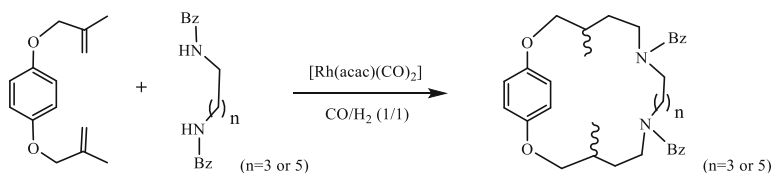
Scheme 27 Hydroaminomethylation reaction involving 2-methyl-3(prop-2-en-1-yl)quinazolin-4(3H)-one with four amines (adapted from ref [83])



Scheme 28 Hydroaminomethylation of bis(methallyl)silanes, bis(methallyl)amines, and bis(methallyl)ether (adapted from ref [86])

4(3H)-ones is of great interest since these compounds have a biological activity, particularly for the central nervous system [84, 85].

Di- or triamines can be synthesized by the reaction of alkene moieties of diallyl-ethers, diallyl-silanes, or diallyl-amines. The reaction is carried out with [Rh₂(-μ-Cl)₂(COD)₂] catalyst at 120°C and 100 bar CO/H₂ (1:1) [86]. The non-substituted allyl systems afford mixtures of n/n, n/iso, and iso/iso products with morpholine. The n/iso ratio values range from 66:34 to 28:72 depending on the heteroatom present. On the contrary, the bis(methallyl) compounds only give the n/n products, the yields being 93%, 59%, 55%, and 66% with -Si(CH₃)₂-, -O-, -O(CH₂)₂O-, -NAc groups, respectively (Scheme 28). The di- or triamines characterized by linear carbon chain between the two nitrogen atoms possess a potential biological activity [86].

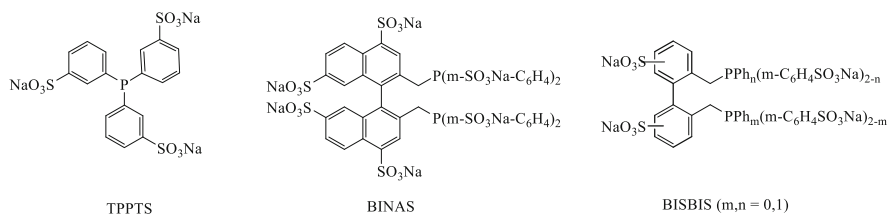


Scheme 29 Hydroaminomethylation reaction of the 1,4-bis(2-methyl-allyloxy)-benzene with *N,N'*-dibenzyl-butane ($n = 3$)- or hexane- ($n = 5$)-1,4-diamine (adapted from ref [88])

Oxa- and azamacroheterocyclic systems are of interest for various applications due to their selective binding properties toward ions and neutral molecules and as valuable building blocks for the synthesis of natural products. Azamacroheterocyclic compounds are synthesized starting from readily available dialkenes and diamines via ring-closing bis(hydroaminomethylation) reaction [87]. This method allows for wide variations in ring size, heteroatoms, and substitution patterns to obtain various macroheterocycles. Moreover, starting from *N*-benzyl-substituted systems, the synthesis of cryptands can be accomplished by subsequent hydrogenolysis of the benzyl group and successive hydroaminomethylation with α,ω -dialkenes. The application of this procedure in the synthesis of azamacroheterocycles containing hydroquinone, 1,1'-biphenyl, or (*S*)-1,1'-binaphthol units is successfully conducted since relatively high yields (59–78%) are obtained [88]. The reaction involves bis-methylallylphenyl ethers and *N*-benzyl-diamine units (Scheme 29).

Due to the generation of two new stereogenic centers, the final products are obtained as a mixture of enantiomers and diastereomers difficult to separate [88]. These azamacrocycles can be considered as ligands for asymmetric catalysis starting from tartaric acid as the chiral unit functionalized by two methylallyl moieties, which are directly involved in the HAM reaction using diamines [89]. But this procedure is less efficient than the stepwise hydroformylation-reductive amination sequence as only 32% of the 1:1 mixture of the azamacrocycle diastereoisomers are obtained in comparison with 86% in the second process.

Intramolecular HAM also provides a direct access to synthesize azaheterocycles. A novel air stable phosphine-free ionic rhodium catalyst designed by addition of the *N,N,N',N'*-tetramethylethylenediamine (TMEDA) ligand affords the cationic $[\text{Rh}(\text{CO})_2(\text{TMEDA})]^+$ species associated to the anionic $[\text{RhCl}_2(\text{CO})_2]^-$ moiety under CO atmosphere. The 2-isopropenylaniline is transformed into 1,2,3,4-tetrahydroquinoline with total chemoselectivity and 98% selectivity after optimization of the conditions (68 bar of CO/H₂ 1:1, 100°C for 48 h). This catalytic system is extended to other 2-isopropenylanilines substituted at the nitrogen atom and in the aromatic ring. The corresponding 1,2,3,4-tetrahydroquinolines are obtained in the range of 70–98% isolated yields [90]. Similarly, these ionic diamine rhodium complexes can give 2,3,4,5-tetrahydro-1*H*-2-benzazepines starting from 2-allylaniline derivatives. In this case a more sterically demanding diamine complex obtained by the combined system of $[\text{Rh}_2(\mu\text{-Cl})_2(\text{COD})_2]$ with *N,N,N',N'*-tetra(isopropyl)ethylene diamine (TIPEDA) or *N,N,N',N'*-tetra(*o*-methylbenzyl)



Scheme 30 Representation of three sulfonated phosphine ligands

ethylene diamine (MTBEDA) is needed to improve the selectivity of the reaction. The isolated yield of each product does not exceed up to 50%, depending of the nature of the 2-allylaniline [91].

Dendritic amines with neutral core structure and amine functionalities only on the periphery of the dendrimer can present interesting potential biomedical applications, especially for DNA delivery. Starting from a dendritic polyallylether obtained by allylation of hyperbranched polyglycerol [92, 93] and the morpholine-modified polyglycerol, the dendritic polyamine is obtained with a 93:7 n/iso regioselectivity, isolated in pure form after simple dialysis with an excellent 99% yield [94]. However, to obtain this high n/iso ratio, it is necessary to operate in a sequential manner: first the hydroformylation reaction at 30 bar of CO/H₂ (1:1) in toluene with the [Rh(acac)(CO)₂]/Xantphos catalytic system at 70°C for 5 days and then the hydrogenation reaction after addition of morpholine at 70 bar of CO/H₂ (1:6), at 85°C for 5 days. In fact, the one-pot HAM reaction only leads to a 50:50 n/iso ratio, presumably due to the coordination of morpholine to the rhodium catalyst, which affects the regioselectivity during the hydroformylation step.

Performing the HAM reaction in an aqueous two-phase system is an elegant approach to separate the catalyst from the organic products. Experiments performed with the TPPTS monophosphine (tris-sulfonated triphenylphosphine) or BINAS diphosphine ligands (Scheme 30) lead to attractive results, with high P/Rh ratio (425 and 140, respectively) kept to maintain the [Rh(H)(CO)L₂] species in the aqueous phase. However, the hydrogenation rate is significantly reduced [95]. This methodology can be extended to longer chain alkenes with dimethylamine, provided the CTAB (cetyltrimethylammonium bromide) cationic surfactant is introduced to increase the interfacial area between the two phases [96]. Indeed, in absence of CTAB, [RhCl(CO)(TPPTS)₂] with an excess of TPPTS (TPPTS/Rh = 32:1) converts 67% of dodec-1-ene into 17.4% C13 amines (n/iso = 86:14) with large quantities of dodecane, internal dodecenes, and aldehydes as by-products at 130°C and 30 bar (CO/H₂ = 1:1) for 6 h. Introduction of CTAB (CTAB/Rh = 5.5:1) leads to 80% conversion and 51% in C13 amines (n/iso = 88:12). Addition of the BISBIS ligand (Scheme 30) to the [RhCl(CO)(TPPTS)₂] complex (7.5:1 molar ratio) increases both conversion to 97% and amine chemoselectivity to 82% with high 99:1 regioselectivity. Presumably, the [RhH(CO)(BISBIS)] active species is formed to catalyze the reaction. Under the same catalytic conditions for a

BISBIS/[RhCl(CO)(TPPTS)₂] 5:1 ratio, hex-1-ene, oct-1-ene, dec-1-ene or tetradec-1-ene give similar high conversion rates (99.7–96.5%), high chemoselectivity (84.4–70.8%), and regioselectivity as well (97:3–99:1). Under similar conditions, dodec-1-ene reacts with diethylamine, dipropylamine, morpholine, and piperidine [97].

Addition of an acid has a positive effect on the rhodium [Rh₂(μ-Cl)₂(COD)₂]/TPPTS system, presumably due to the formation of a cationic [H-RhL_n]⁺ species suitable for the highly selective hydrogenation of imines and enamines [98]. The catalytic activity is not directly function of the p*K*_a value but rather the size of the associated anion. It is exemplified by good performances in the reaction of oct-1-ene with morpholine, either for the conversion (99%), the selectivity in amine (85–98%) provided sulfate, acetate, trifluoroacetate, methanesulfonate, p-toluenesulfonate, sulfosuccinate or even citrate anions are present. The reaction conditions [Rh₂(μ-Cl)₂(COD)₂]/TPPTS (1/64), 60 bar (CO/H₂ = 1:3), and 130°C for 4 h have been extended to the reaction of oct-1-ene with piperidine, di-*n*-butylamine, and *n*-propylamine with similar good results and more modest performances with diisopropylamine, ethanolamine, and isopropylamine [98].

Internal alkenes are less reactive than the corresponding terminal alkenes, giving a mixture of branched amines and aldol condensation by-products due to the basic conditions. In the literature all the efforts have been devoted to combine both isomerization and hydroformylation toward the linear aldehyde (see Part 2: Isomerization-Hydroformylation) in order to selectively produce the linear amine. This goal can be achieved by using crowded diphosphine ligands such as derivatives of Naphos (Scheme 5) [99]. Thus, starting from piperidine and but-2-ene, pent-2-ene, hex-2-ene, and oct-2-ene, excellent yields and selectivities to the corresponding linear amines are reached at 120°C, under 60 bar pressure (CO/H₂ = 1:5) in toluene/THF mixture, after 16 h, in presence of the [Rh(COD)₂]BF₄/Naphos system. Selectivity in amines ranges from 91 to 98% and linear amines from 78:22 to 94:6 *n*/*iso* ratios. The results from hex-3-ene are a little bit lower with values reaching 96% and 71:29. These performances can be improved by using the *t*-Bu-Xantphenoxaphos ligand since, under slightly different conditions (p_{CO} = 5 bar, p_{H2} = 33 bar, 125°C, in methanol/toluene, 16 h), 99% and 96:4 values are obtained [100]. Functionalized internal alkenes have been also examined. The presence of the CN electron-withdrawing group reduces the conversion (60%), the yield in amine (45%), and the regioselectivity in linear amine to 75:25. Conversely, the OMe electron-donating substituent leads to satisfactory results such as 95%, 84%, and 93:7, respectively [100].

Another strategy to convert cyclopentene relies on the synthesis of rhodium diphosphinite complexes anchored on polyethylene glycol (PEG). High amine selectivities with morpholine and other amines are obtained at 120°C and 28 bar CO/H₂ (1:2). After addition of hexane at room temperature, the lower PEG phase containing the rhodium catalyst can be separated from the (toluene/hexane/amine) phase. Five recycling steps show that the catalytic activity is maintained [101]. The efficient rhodium diphosphinite complex described above (Scheme 12) [102] catalyzes the reaction of cyclopentene, cyclohexene, and norbornene with high activity

and selectivity close to 99%. This catalytic system also gives good performances with linear terminal alkenes and primary or secondary amines [102].

6.2 Hydroaminomethylation of Arylalkenes

Arylethylamines represent an attracting goal because they are known to exhibit a pharmacological activity. Styrene and its derivatives offer an easy access to this class of compounds. The presence of the aromatic ring provides a trend to favor the branched isomer. High temperatures and pressures bring mainly this isomer as observed at 110°C and 110 bar with phosphine-free ligand $[\text{Rh}_2(\mu\text{-Cl})_2(\text{COD})_2]$ (6:94 n/iso ratio) [103]. 2-Vinylnaphthalene is also transformed into the corresponding secondary or tertiary amines with the same performances [104]. Interestingly, milder conditions, 80°C and 14 bar, are required to transform styrene and various *para*-substituted styrenes into the branched isopropylamine-derived products in the ratio up to 8:92 with the zwitterionic complex $[\text{Rh}^+(\text{COD})(\eta^6\text{-PhBPh}_3)^-]$ [105]. The reaction can be applied to both primary and secondary amines keeping good ratios in branched amines provided the CO/H₂ pressure is increased up to 68 bar.

The presence of phosphine ligands allows operation under mild conditions (60°C, 30 bar CO/H₂ = 1:5) as illustrated with the cationic active species generated from $[\text{Rh}(\text{COD})_2]\text{BF}_4/\text{Xantphos}$ or 1,1'-bis(diphenylphosphino)ferrocene, providing 15:85 or 12:88 n/iso regioselectivity, respectively [106]. The addition of HBF₄ is crucial to gain high yields in amines. Similar results are obtained in presence of the (*o*-diphenylphosphino-[N-(2-hydroxyethyl)-N-methyl]aniline) P,N bidentate ligand although it is necessary to operate at 80°C and 100 bar [107]. Another interesting study to reach high regioselectivity in the branched amine is related to the use of a sol-gel immobilized rhodium catalyst for the functionalization of some vinylarenes with aniline or nitrobenzene derivatives in an aqueous microemulsion [108]. A slight influence of the electronic nature of the substrates on the regioselectivity is observed. For example, the HAM of 4-chlorostyrene with aniline affords a ratio of n/iso = 2:98 instead of 6:94 with 4-methylstyrene. Ortho-substituted substrates can affect the regioselectivity due to their steric hindrance. Indeed, 2-chlorostyrene gives only a 9:91 ratio compared to 4-chlorostyrene with 2:98. This latter result can also be reached with nitrobenzene in a one-pot procedure over the course of the reaction. However, either electron-donating or electron-withdrawing substituents in *para*-position of aniline, or nitrobenzene, decrease the performance in terms of the yields (79–82% instead of 91%) and the regioselectivity in the branched isomer (n/iso = 13:87 instead of 2:98).

In a reverse strategy to reach highly linear-selective HAM of styrene, the very crowded tetraphosphine ligands (Scheme 7) are used. Starting from styrene and piperidine, the corresponding amine is obtained in a 94:6 n/iso ratio at 125°C and 40 bar (CO/H₂ = 3:1) in the polar *tert*-amyl alcohol solvent. To obtain such

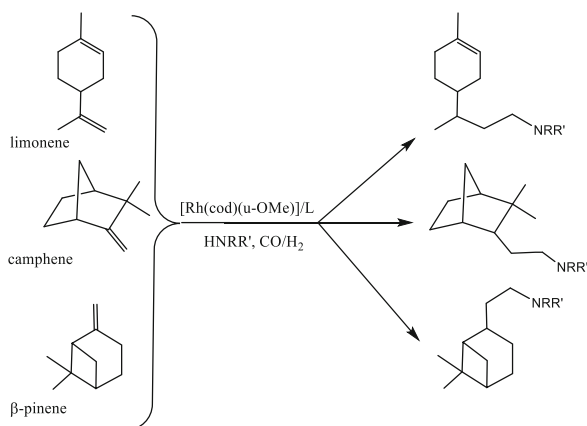
performances, the partial CO pressure needs to be high in the CO/H₂ gas mixture [109].

As expected from the Keulemans rule for the hydroformylation step [110], the condensation of piperidine to 1,1-diphenylethene (or 1-phenyl-styrene) exclusively gives the linear 3,3-diphenylamines, which constitute the basic backbone in many biological compounds like fenpiprane, diisoproamine, and prozapine. Using the [RhCl(COD)(Imes)] catalytic system (Imes being the 1,3-dimesitylimidazol-2-ylidene ligand), 99% selectivity is obtained at 125°C and 60 bar (CO/H₂ = 1:5) in toluene [111]. The same catalyst transforms under similar conditions α -methylstyrene into the corresponding linear piperidine-amine with >99:1 regioselectivity, whereas styrene gives rise to lower 21:79 regioselectivity [112]. Extension of the reaction to allylbenzenes provides good activity and n/iso selectivity of 88:12 [113] and 90:10 [114].

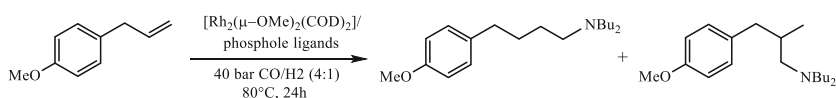
6.3 Hydroaminomethylation of Monoterpenes and Fatty Acids

This HAM reaction is a powerful method to functionalize renewable substrates. Limonene is one of the major constituents of the essential oil extracted from citric plants [115]. It can be transformed with secondary amines like diethylamine and morpholine in 81–93% yields and gives exclusively the linear product, owing to the steric hindrance of the isopropenyl group [116]. The catalytic conditions are 80 bar of CO/H₂ (1:1), 80°C, and 20 h in presence of the dimer [Rh₂(μ -Cl)₂(COD)₂] catalyst. The reaction gives an easy access to growth regulators for tobacco plants.

Seven other (*R*)-(+)-limonene-derived amines have been synthesized in good isolated yields [117]. Alkylated amines (*n*-propylamine, isopropylamine, benzylamine), cyclic amines (piperidine, piperazine, morpholine), and an aromatic one (aniline) have been used. In order to decrease the long reaction time for completion (sometimes 48 h), it is possible to improve the HAM protocol in splitting the process into two steps: hydroformylation (under a CO/H₂ mixture) and hydrogenation (only H₂). Depending on the amine used as substrate, the total reaction time is between 10 and 24 h. Higher selectivity is reached for the products of the reactions with secondary amines (79–89% isolated yield). The products were tested against *Leishmania (V) braziliensis* and some of them (the resulting amines from *n*-propylamine and aniline) demonstrated higher in vitro activity than the standard drug pentamidine. Two promising new *anti-Trypanosoma cruzi* limonene derivatives have also been identified (the resulting amines from aniline and piperazine) [118]. With the goal to transform natural products that can be extracted from renewable crops in large amounts into useful or potentially useful new chemicals, the HAM of limonene, camphene, α -pinene [119], and eugenol [120] has been carried out in presence of di-*n*-butylamine, morpholine, and *n*-butylamine to obtain the corresponding homologous amines. Moderate to good yields (73–94%) are



Scheme 31 Hydroaminomethylation of limonene, camphene, and α -pinene (from Ref. [119])

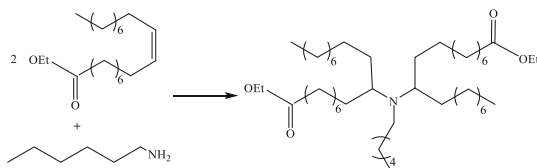


Scheme 32 HAM reaction of estragole (from Ref. [122])

reached using $[\text{Rh}_2(\mu\text{-OMe})_2(\text{COD})_2]$ as catalytic precursor in the presence or not of phosphines as ancillary ligands in toluene at 80°C under 60 bar of CO/H_2 pressure. The regioselectivity of the reaction is strongly induced by the substrate itself and the amine group is almost exclusively present in the α -carbon position (Scheme 31).

The rhodium catalyst in absence of ligands is very efficient for the HAM transformation of terpenes, notably camphene in which double bond isomerization is not a competitive reaction. The addition of the triphenylphosphine ligand can prevent isomerization but decreases the enamine/imine hydrogenation rate. Bulkier tribenzylphosphine at appropriate concentration gives better results due probably to its greater steric hindrance which disfavors the formation of the bis-ligand-metal species $[\text{Rh}(\text{H})(\text{CO})_2\text{L}_2]$ less active in the reaction [119]. All the products formed, except the final amine obtained from limonene and morpholine, are new, and the products derived from limonene have potential bioactivity.

The HAM of estragole, a bio-renewable starting material available from basil oil (90% of estragole), is reported using di-*n*-butylamine as the amine counterpart. The corresponding phenylalkylamines which can present fungicidal activities [121] are obtained in good yields (80–87%) (Scheme 32). The monophospholes are good candidates as ancillaries for the HAM, and they are a promising option because they have been more efficient in promoting the reductive amination than the classic PPh_3 ligand and resulted in less side products than the systems with phosphites [122].



Scheme 33 Double HAM involving ethyl oleate and hexylamine (from Refs. [123] and [124])

Hydrolysis of fats and oils gives rise to even-numbered aliphatic carboxylic acids and coproduces glycerol. The C18 oleic acid is widely produced from many crops.

The HAM of ethyl oleate has been recently explored with hexylamine, benzylamine, aspartic acid diethyl ester, valinol, and morpholine [123]. The reaction proceeds in toluene or 1,4-dioxane at 140°C for 20 h under a 100 bar CO/H₂ pressure in the presence of [Rh₂(μ-Cl)₂(COD)₂] precatalyst. High yields can be obtained, such as 99% with morpholine. However, diisopropylamine gives mainly the aldehyde and only 5% of the amine, since the hydrogenation step converts the two aldehyde regioisomers into the corresponding alcohols. Interestingly, two equivalents of oleic ester with the primary hexylamine results in the formation of the tertiary amine after a double hydroaminoamination reaction (Scheme 33) [123, 124].

An extension of this reaction using *S*(−) or *R*(+)-pyrrolidine-2-carboxylic acid or proline in methanol allows to combine the HAM reaction with an esterification giving rise to a diester, an interesting biopolymer precursor. Thermomorphic solvent systems involving linear alkanes as the second solvent result in yields as high as 95% in the two expected regioisomers and the separation of the catalyst with a leaching reduced to several ppm [125, 126]. Similarly, oleyl alcohol is transformed with diethylamine and the resulting amino alcohol separated in a thermomorphic process [127].

7 Conclusion

This chapter presents the recent advances in the tandem rhodium carbonylation reactions involving in the main step the hydroformylation. Such reactions open huge opportunities in synthetic chemistry. Indeed, they offer a general efficient strategy to synthesize building blocks for fine chemistry, starting from abundant and low price substrates and avoiding the formation of substantial amounts of by-products. This atom-efficient tandem reaction approach shows that rhodium has a privileged place in the CO chemistry, not only to perform the hydroformylation reaction but also to combine it with other functionalization processes.

References

1. Haynes A (2013) In: Reedijk J, Poepplmeier K (eds) *Comprehensive inorganic chemistry II: from elements to applications*, vol 6, p 1
2. Wu X-F, Fang X, Wu L, Jackstell R, Neumann H, Beller M (2014) *Acc Chem Res* 47:1041
3. Hibbel J, Wiebus E, Cornils B (2013) *Chemie Ingenieur Technik* 85:1853
4. Tietze LF (1996) *Chem Rev* 96:115
5. Nicolaou KC, Edmonds DJ, Bulger PG (2006) *Angew Chem Int Ed* 45:7134
6. Nicolaou KC, Chen JS (2009) *Chem Soc Rev* 38:2993
7. Grondal C, Jeanty M, Enders D (2010) *Nat Chem* 2:167
8. Nicolaou KC (2014) *Angew Chem Int Ed* 53:9128
9. Tietze LF (2014) *Domino reactions, concepts for efficient organic synthesis*. Wiley-VCH
10. Eilbracht P, Bärfacker L, Buss C, Hollmann C, Kitsos-Rzychon BE, Kranemann CL, Rische T, Roggenbuck R, Schmidt A (1999) *Chem Rev* 99:3329
11. Eilbracht P, Schmidt AM (2006) *Top Organomet Chem* 18:65
12. Weissermel K, Arpe H-J (1997) *Industrial organic chemistry*, 3rd edn. VCH, Weinheim
13. Billig E, Abatjoglou AG, Bryant DR, Murray RE, Maher JM (1988) US patent 4.717.775, Jan 5, 1988, to Union Carbide Corp
14. Burke PM, Garner JM, Tam W, Kreutzer KA, Teunissen AJJM, Snijder CS, Hansen CB (1999) US patent 5874641, Feb 23, 1999, to DSM/Du Pont, 1999
15. Beller M, Zimmermann B, Geissler H (1999) *Chem Eur J* 5:1301
16. Vilches-Herrera M, Domke L, Börner A (2014) *ACS Catal* 4:1706
17. Casey CP, Whiteker GT (1990) *Isr J Chem* 30:299
18. Bronger RP, Kamer PCJ, van Leeuwen PWNM (2003) *Organometallics* 22:5358
19. Bronger RP, Berman JP, Herwig J, Kamer PCJ, van Leeuwen PWNM (2004) *Adv Synth Catal* 346:789
20. Klein H, Jackstell R, Wiese K-D, Borgmann C, Beller M (2001) *Angew Chem Int Ed* 40:3408
21. Mo M, Yi T, Zheng CY, Yuan M-L, Fu H-Y, Li R-X, Chen H (2012) *Catal Lett* 142:238
22. Bahrmann H, Bergrath K, Kleiner H-J, Lappe P, Naumann C, Peters D, Regnat D (1996) *J Organometal Chem* 520:97
23. Bahrmann H, Bach H, Frohning CD, Kleiner H-J, Lappe P, Peters D, Regnat D, Herrmann WA (1997) *J Mol Catal A Chem* 116:49
24. Klein H, Jackstell R, Beller M (2005) *Chem Commun* 2283
25. Behr A, Obst D, Schulte C, Schosser T (2003) *J Mol Catal A Chem* 206:179
26. Behr A, Henze G, Obst D, Turkowski B (2005) *Green Chem* 7:645
27. Pandey S, Chikkali SH (2015) *ChemCatChem* 7:3468
28. Selent D, Hess D, Wiese K-D, Röttger D, Kunze C, Börner A (2001) *Angew Chem Int Ed* 40:1696
29. Yan Y, Zhang X, Zhang X (2006) *J Am Chem Soc* 128:16058
30. Yu S, Chie Y-M, Guan Z-H, Zhang X (2008) *Org Lett* 10:3469
31. Cai C, Yu S, Liu G, Zhang X, Zhang X (2011) *Adv Synth Catal* 353:2665
32. Jia X, Wang Z, Xia C, Ding K (2012) *Chem Eur J* 18:15288
33. van der Slot SC, Duran J, Luten J, Kamer PCJ, van Leeuwen PWNM (2002) *Organometallics* 21:3873
34. Piras I, Jennerjahn R, Jackstell R, Baumann W, Spannenberg A, Franke R, Wiese K-D, Beller M (2010) *J Organometal Chem* 695:479
35. Selent D, Franke R, Kubis C, Spannenberg A, Baumann W, Kreidler B, Börner A (2011) *Organometallics* 30:4509
36. Cornils B (1980) In: Falbe J (ed) *New syntheses with carbon monoxide*. Springer, p 1
37. Lawrenson MJ, Foster G (1968) GB patent 1.243.189, filed Dec 5, 1967, to British Petroleum Co Lim
38. Lawrenson MJ (1971) GB patent 1.254.222, priority June 24, 1969, to British Petroleum Co Lim
39. MacDougall JK, Cole-Hamilton DJ (1990) *J Chem Soc Chem Commun* 165

40. MacDougall JK, Simpson MC, Green MJ, Cole-Hamilton DJ (1996) *J Chem Soc Dalton Trans* 1161
41. Sandee AJ, Reek JNH, Kamer PCJ, van Leeuwen PWNM (2001) *J Am Chem Soc* 123:8468
42. Ichihara T, Nakano K, Katayama M, Nozaki K (2008) *Chem Asian J* 3:1722
43. Boogaerts IIF, White DFS, Cole-Hamilton DJ (2010) *Chem Commun* 46:2194
44. Fuchs D, Rousseau G, Diab L, Gellrich U, Breit B (2012) *Angew Chem Int Ed* 51:2178
45. Diab L, Gellrich U, Breit B (2013) *Chem Commun* 49:9737
46. Barros HJV, dos Santos EN, Guimaraes CC, Gusevskaya EV (2007) *Organometallics* 26:2211
47. Behr A, Reyer S, Tenhumberg N (2011) *Dalton Trans* 40:11742
48. Ott J, Ramos Tombo GM, Schmid B, Venanzi LM, Wang G, Ward TR (1989) *Tetrahedron Lett* 30:6151
49. Fernandez E, Castillon S (1994) *Tetrahedron Lett* 35:2361
50. Khan SR, Bhanage BM (2013) *Tetrahedron Lett* 54:5998
51. Alhaffar M, Suleiman R, Shakil Hussain SM, El Ali B (2011) *React Kinet Mech Catal* 104:323
52. Soulantica K, Sirol S, Koinis S, Pneumatikakis G, Kalck P (1995) *J Organometal Chem* 498: C10
53. Fernandez E, Polo A, Ruiz A, Claver C, Castillon S (1998) *Chem Commun* 1803
54. Balu  J, Bayon JC (1999) *J Mol Catal A Chem* 137:193
55. El Ali B, Tijani J, Fettouhi M (2005) *J Mol Catal A Chem* 230:9
56. El Ali B (2003) *Catal Commun* 4:621
57. El Ali B, Tijani J, Fettouhi M (2006) *Appl Catal A Gen* 303:213
58. Pardey AJ, Uzcategui GC, Hung-Low F, Rivas AB, Yanez JE, Ortega MC, Longo C, Aguirre P, Moya SA (2005) *J Mol Catal A Chem* 239:205
59. Hung-Low F, Uzcategui GC, Alvarez J, Ortega MC, Pardey AJ, Longo C (2006) *React Kinet Catal Lett* 88:143
60. Jin X, Zhao K, Cui F, Kong F, Liu Q (2013) *Green Chem* 15:3236
61. Vieira CG, Da Silva JG, Penna CAA, dos Santos EN, Gusevskaya EV (2010) *Appl Catal A Gen* 380:125
62. Vieira CG, dos Santos EN, Gusevskaya EV (2013) *Appl Catal A Gen* 466:208
63. Castillon S, Fernandez E (2000) Hydroformylation in organic synthesis. In: van Leeuwen PWNM, Claver C (eds) *Rhodium catalyzed hydroformylation*. Kluwer Academic Publisher, p 145
64. Roggenbuck R, Schmidt A, Eilbracht P (2002) *Org Lett* 4:289
65. Diebolt O, Cruzeuil C, M ller C, Vogt D (2012) *Adv Synth Catal* 354:670
66. Jin X, Zhao K, Kong F, Cui F, Liu Q, Zhang Y (2014) *Catal Lett* 144:192
67. Maryanoff BE, Reitz AB (1989) *Chem Rev* 89:863
68. Breit B, Zahn SK (1999) *Angew Chem Int Ed* 38:969
69. Breit B, Zahn SK (2005) *Tetrahedron* 61:6171
70. Farwick A, Helmchen G (2010) *Adv Synth Catal* 352:1023
71. Ruan Q, Zhou L, Breit B (2014) *Catal Commun* 53:87
72. Wong GW, Landis CR (2013) *Angew Chem Int Ed* 52:1564
73. Risi RM, Burke SD (2012) *Org Lett* 14:1180
74. van Leeuwen PWNM (2000) In: Claver C (ed) *Rhodium catalyzed hydroformylation*. Kluwer Academic Publisher
75. Oro LA, Carmona D (2007) In: de Vries JG, Elsevier CJ (eds) *The handbook of homogeneous hydrogenation*, vol 1. Wiley-VCH, Weinheim, p 3
76. Crozet D, Urrutigoity M, Kalck P (2011) *ChemCatChem* 3:1102
77. Raoufmoghaddam S (2014) *Org Biomol Chem* 12:7179
78. Crozet D, Gual A, McKay D, Dinoi C, Godard C, Urrutigoity M, Daran J-C, Maron L, Claver C, Kalck P (2012) *Chem Eur J* 18:7128
79. Hamers B, Kosciusko-Morizet E, M ller C, Vogt D (2009) *ChemCatChem* 1:103
80. Ahmed M, Seayad A, Jackstell R, Beller M (2003) *J Am Chem Soc* 125:10311
81. Ahmed M, Jackstell R, Seayad AM, Klein H, Beller M (2004) *Tetrahedron Lett* 45:869

82. Subhani MA, Müller K-S, Eilbracht P (2009) *Adv Synth Catal* 351:2113
83. El-Badry YA, El-Farargy AF, Eilbracht P (2013) *Helvetica Chim Acta* 96:1782
84. Jatav V, Mishra P, Kashaw S, Stables JP (2008) *Eur J Med Chem* 43:135
85. Jatav V, Mishra P, Kashaw S, Stables JP (2008) *Eur J Med Chem* 43:1945
86. Eilbracht P, Kranneman CL, Bärfacker L (1999) *Eur J Org Chem* 1907
87. Kranemann CL, Eilbracht P (2000) *Eur J Org Chem* 2367
88. Angelovski G, Eilbracht P (2003) *Tetrahedron* 59:8265
89. Angelovski G, Keränen MD, Eilbracht P (2005) *Tetrahedron: Asymmetry* 16:1919
90. Vieira TO, Alper H (2007) *Chem Commun* 2710
91. Okuro K, Alper H (2010) *Tetrahedron Lett* 51:4959
92. Haag R, Sunder A, Stumbé J-F (2000) *J Am Chem Soc* 122:2954
93. Garcia-Bernabé A, Krämer M, Oläh B, Haag R (2004) *Chem Eur J* 10:2822
94. Koç F, Wyszogrodzka M, Eilbracht P, Haag R (2005) *J Org Chem* 70:2021
95. Zimmermann B, Herwig J, Beller M (1999) *Angew Chem Int Ed* 38:2372
96. Wang YY, Luo MM, Chen H, Li XJ, Li YZ (2004) *Appl Catal A Gen* 272:151
97. Wang YY, Chen J, Luo MM, Chen H, Li X (2006) *J Catal Commun* 7:979
98. Behr A, Becker M, Reyer S (2010) *Tetrahedron Lett* 2438
99. Seayad A, Ahmed M, Klein H, Jackstell R, Gross T, Beller M (2002) *Science* 297:1676
100. Ahmed M, Bronger RPJ, Jackstell R, Kamer PCJ, van Leeuwen PWNM, Beller M (2006) *Chem Eur J* 12:8979
101. Khan SR, Khedkar MV, Qureshi ZS, Bagal DB, Bhanage BM (2011) *Catal Commun* 15:141
102. Khan SR, Bhanage BM (2013) *Appl Organomet Chem* 27:711
103. Rische T, Eilbracht P (1997) *Synthesis* 1331
104. Rische T, Eilbracht P (1999) *Tetrahedron* 55:7841
105. Lin Y-S, El Ali B, Alper H (2001) *Tetrahedron Lett* 42:2423
106. Routaboul L, Buch C, Klein H, Jackstell R, Beller M (2005) *Tetrahedron Lett* 46:7401
107. Kostas ID (1999) *J Chem Res (S)* 630
108. Nairoukh Z, Blum J (2014) *J Org Chem* 79:2397
109. Li S, Huang K, Zhang J, Wu W, Zhang X (2013) *Org Lett* 15:3078
110. Keulemans AIM, Kwantes A, van Bavel T (1948) *Rec Trav Chim Pays-Bas Belg* 67:298
111. Ahmed M, Buch C, Routaboul L, Jackstell R, Klein H, Spannenberg A, Beller M (2007) *Chem Eur J* 13:1594
112. Seayad AM, Selvakumar K, Ahmed M, Beller M (2003) *Tetrahedron Lett* 44:1679
113. Wu L, Fleischer I, Jackstell R, Beller M (2013) *J Am Chem Soc* 135:3989
114. Güllak S, Wu L, Liu Q, Franke R, Jackstell R, Beller M (2014) *Angew Chem Int Ed* 53:7320
115. Breitmaier E (2006) *Terpenes, flavors, fragrances, pharmaca, pheromones*. Wiley-VCH, Weinheim
116. Kranemann CL, Eilbracht P (1998) *Synthesis* 71
117. Graebin CS, Eifler-Lima VL, da Rosa RG (2008) *Catal Commun* 9:1066
118. Graebin CS, Madeira MF, Yokoyama-Yasunaka JKU, Miguel DC, Uliana SRB, Benitez D, Cerecetto H, Gonzalez M, da Rosa RG, Eifler-Lima VL (2010) *Eur J Med Chem* 45:1524
119. Melo DS, Pereira-Jr SS, dos Santos E (2012) *Appl Catal* 411:70
120. Oliveira KCB, Santos AG, dos Santos E (2012) *Appl Catal* 445:204
121. Himmele W, Pommer EH (1980) *Angew Chem Int Ed* 19:184
122. Oliveira KCB, Carvalho SN, Duarte MF, Gusevskaya EV, dos Santos EN, El Karroumi J, Gouygou M, Urrutigoity M (2015) *Appl Catal A Gen* 497:10
123. Behr A, Fiene M, Buss C, Eilbracht P (2000) *Eur J Lipid Sci Technol* 102:467
124. Behr A, Vorholt AJ (2012) Hydroformylation and related reactions of renewable resources. In: Meier MAR, Weckhuysen BM, Bruijninx PCA (eds) *Top. Organometal. Chem.*, vol 39. Springer, p 103
125. Behr A, Seidensticker T, Vorholt A (2014) *J Eur J Lipid Sci Technol* 116:477
126. Behr A, Vorholt AJ, Ostrowski KA, Seidensticker T (2014) *Green Chem* 16:982
127. Vorholt AJ, Neubert P, Behr A (2013) *Chem Ing Tech* 85:1540

Asymmetric Hydroformylation Using Rhodium

Anton Cunillera, Cyril Godard, and Aurora Ruiz

Abstract Asymmetric hydroformylation is a powerful catalytic reaction that produces chiral aldehydes from inexpensive feedstock (alkenes, *syngas*) in a single step. The elucidation of the different steps of the catalytic cycle and the characterization of the resting state, together with the discovery of several types of ligands, have made possible that nowadays a variety of chiral products incorporating a formyl unit can be enantioselectively prepared by Rh-catalyzed asymmetric hydroformylation, and that this process is now considered as a useful tool in organic synthesis.

Keywords Aldehydes • Asymmetric • Chiral ligands • Enantioselectivity • Hydroformylation • Phosphorus • Regioselectivity • Rhodium

Contents

1	Introduction	100
2	Rh-Catalyzed Hydroformylation Mechanism	102
3	Rh-Catalyzed Asymmetric Hydroformylation of Monosubstituted Alkenes	104
3.1	1,3-Diphosphite Ligands	104
3.2	Phosphine–Phosphite Ligands	108
3.3	Bisphosphacyclic Ligands	114
3.4	Bis-Phosphonite Ligands	117
3.5	Bis-Phosphinite Ligands	117
3.6	Monodentate Phosphorus-Based Ligands	118
4	Other Monosubstituted Alkene Substrates	120
5	Rh-Catalyzed Asymmetric Hydroformylation of Disubstituted Alkenes	123
5.1	Linear 1,2-Disubstituted Alkenes	123
5.2	Scaffolding [156] Ligands	125

A. Cunillera, C. Godard (✉), and A. Ruiz

Department of Physical Chemistry and Inorganic Chemistry, Universitat Rovira i Virgili,
Campus Sescelades, C/ Marcel·li Domingo s/n, 43007 Tarragona, Spain

e-mail: cyril.godard@urv.cat; mariaaurora.ruiz@urv.cat

5.3	Monocyclic 1,2-Disubstituted Alkenes	127
5.4	Bicyclic 1,2-Disubstituted Alkenes	133
5.5	1,1'-Disubstituted Alkenes	135
6	Conclusions	137
	References	139

1 Introduction

The hydroformylation of alkenes, which was originally discovered by Otto Roelen in 1938 [1–3], is nowadays one of the most important industrial applications of homogeneous catalysis (Scheme 1) [4–14]. Today, over 9 million tons of so-called oxo-products are produced per year, a number which is still rising. The majority of these oxo-products are obtained from the hydroformylation of propene **1**, which is a fraction of the steam-cracking process. The resulting products *iso*-butyraldehyde **2** and *n*-butanal **3** are important intermediates for the production of esters, acrylates, and 2-ethylhexanol [4, 5].

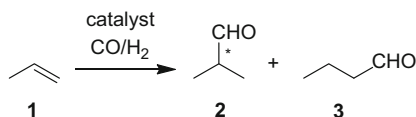
From a synthetic point of view, the reaction is a one-carbon chain elongation caused by the addition of carbon monoxide and hydrogen across the π system of a C=C double bond [15, 16]. As a pure addition reaction, the hydroformylation reaction meets all requirements of an atom-economic process [17]. Furthermore, the synthetically valuable aldehyde function is introduced, which allows subsequent skeleton expansion that may even be achieved in one-pot sequential transformations [18, 19].

In 1968, Wilkinson discovered that phosphine-modified rhodium complexes display a significantly higher activity and selectivity compared to the first generation of cobalt catalysts [20–22]. Since that time, ligand modification of the rhodium catalyst has been the method of choice in order to influence the catalyst activity and selectivity [23].

In the asymmetric hydroformylation of alkenes, the first examples of high level of enantioselectivity (*ee*'s up to 90%) were achieved by Stille and Consiglio using chiral Pt-diphosphine systems [24, 25]. However, these catalysts suffered several disadvantages such as low reaction rates, tendency to hydrogenate the substrates, and low regioselectivity to the branched products. Later, these issues were mainly overcome by the use of Rh-based catalysts [26, 27].

In the low-pressure hydroformylation of internal alkenes, the chemoselectivity (and simultaneously regioselectivity) is one of the remaining problems to be solved in industry. This issue originates from the exponential drop of alkene reactivity when

Scheme 1
Hydroformylation of propene



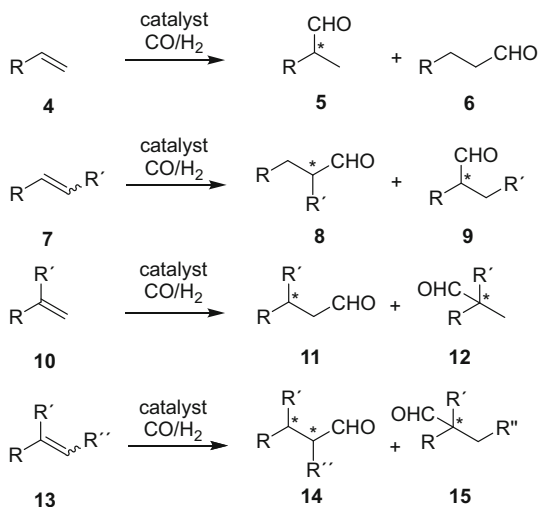
increasing the number of alkene substituents. The known hydroformylation catalysts for internal alkene hydroformylation operating under low-pressure conditions rely on the use of strong π -acceptor ligands, such as bulky phosphites and phosphobenzene systems [28–30]. However, the high activity of the corresponding rhodium catalysts is usually associated with a high tendency towards alkene isomerization, which renders a position-selective hydroformylation of an internal alkene extremely challenging, although over the last years, some examples started to appear in the literature.

The regioselectivity of the hydroformylation of alkenes is function of many factors and quantum chemical calculations have been frequently used to gain useful insights into its origin [31–50]. These include inherent substrate preferences, directing effects exerted by functional groups as part of the substrate, as well as catalyst effects. In order to appreciate substrate inherent regioselectivity trends, alkenes have to be classified according to the number and nature of their substituents (Scheme 2) [15, 16].

The regioselectivity issue usually only arises for terminal and 1,2-disubstituted alkenes **7**. For alkyl-substituted terminal alkenes **4** there is a slight preference for the linear product **6**. For terminal alkenes **4** containing an electron-withdrawing substituent, the formation of the branched product **5** is favored and is sometimes exclusive. This tendency is more or less unaffected by the catalyst structure. Both 1,1-disubstituted **10** and trisubstituted **13** alkenes generally provide only one regioisomer (**11** and **14**, respectively) based on Keuleman's rule, which states that the formyl group is usually added in order to avoid the formation of a quaternary carbon center [51].

Asymmetric hydroformylation is a very promising catalytic reaction that produces chiral aldehydes from inexpensive feedstock (alkenes, *syngas*) in a single step under essentially neutral reaction conditions. Even though asymmetric hydroformylation offers great potential for the fine chemical industry, this reaction has not yet been utilized on an industrial scale due to several technical challenges [4, 5]. Among the most

Scheme 2 Regioselective trends on hydroformylation of different alkenes



involving 20-electron intermediates for ligand/substrate exchange will not be considered. In this process, a great understanding of the mechanism has been possible due to the observation and structural characterization of the resting state of the catalyst by in situ spectroscopic techniques (HP-IR, HP-NMR) [23, 53]. For bidentate ligands (L–L), the common starting complex is the $[\text{RhH}(\text{L}-\text{L})(\text{CO})_2]$ species **16**, containing the ligand coordinated in equatorial positions (denoted eq–eq throughout the scheme) or in an apical-equatorial positions (complexes denoted eq–ax).

Dissociation of equatorial CO from **16** leads to the square-planar intermediate **17**, which associates with alkene to give complexes **18**, where the ligand can again be coordinated in two isomeric forms eq–ax and eq–eq, having a hydride in an apical position and alkene coordinated in the equatorial plane. On the basis of experimental results and theoretical calculations, it has been proposed that the regioselectivity is determined by the coordination of the alkene to the square-planar intermediate **17** to give the pentacoordinate intermediates **18** [35]. This step is also crucial in determining the enantioselectivity since the enantioface discrimination occurs between **17** and **19**, and particularly from **17** to **18**. The CO dissociation from **16** was shown to be much faster than the overall hydroformylation process, indicating that the rate of the reaction is dominated by the reaction of **17** with either CO or the alkene to form **16** or **18** [39]. It has not been established experimentally whether alkene complexation is reversible or not; although in the Scheme 3, all steps are described as reversible except the final hydrogenolysis. Experiments using deuterated substrates suggest that alkene coordination and insertion into the Rh–H bond can be reversible, certainly when the pressures are low. Complexes **18** undergo migratory insertion to give the square-planar alkyl complex **19**. This species can undergo β -hydride elimination, thus leading to isomerization or can react with CO to form the trigonal bipyramidal (TBP) complexes **20**. Thus, under low pressure of CO more isomerization may be expected. At low temperatures ($<70^\circ\text{C}$) and a sufficiently high pressure of CO (>10 bar) the insertion reaction is usually irreversible and thus the regioselectivity and the enantioselectivity in the hydroformylation of alkenes is determined at this point. Complexes **20** undergo the second migratory insertion (see Scheme 3) to form the acyl complex **21**, which can react with CO to give the saturated acyl intermediates **22** or with H_2 to give the aldehyde product and the unsaturated intermediate **17**. The reaction with H_2 involves presumably oxidative addition and reductive elimination, but for rhodium no trivalent intermediates have been observed [54]. At low hydrogen pressures and high rhodium concentrations, the formation of dirhodium dormant species such as **23** becomes significant [55].

Recently, the full catalytic cycle for mono- and bis-ligated monophosphine Rh complexes has been investigated using DFT calculations [56].

As mentioned above, the catalytic hydroformylation of alkenes is one of the largest applications of homogeneous transition metal catalysis today. Due to the robustness of the process and the wide availability of alkene substrates, enantioselective hydroformylation provides high possibilities to obtain a great variety of enantiomerically pure aldehydes. The first Rh-based systems that were reported in the asymmetric hydroformylation contained diphosphine ligands provided low to moderate enantioselectivities [26, 27]. With this type of ligand, the highest *ee* value was reported using styrene as substrate and bdpp (bis-diphenylphosphino pentane) as ligand

(*ee*'s up to 64%) [57]. Later, higher enantioselectivities were achieved using more sophisticated diphosphite and phosphine–phosphite ligands [6–16, 23]. The most successful ligands developed for this reaction were recently reviewed [58].

In the following sections, the most relevant results reported in the asymmetric Rh-catalyzed hydroformylation of alkenes are described. The reactions are classified by degree of substitution of the substrates in order to highlight the issue of the substrate/ligand compatibility in this process. For each family of substrates, the most successful ligands are described.

3 Rh-Catalyzed Asymmetric Hydroformylation of Monosubstituted Alkenes

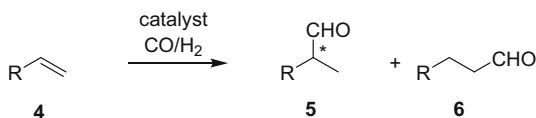
The hydroformylation of monosubstituted alkenes (Scheme 4) was extensively studied due to the interest in the synthesis of linear aldehydes (non-chiral) or the enantioselective synthesis of 2-substituted branched aldehydes using chiral hydroformylation catalysts [4–16].

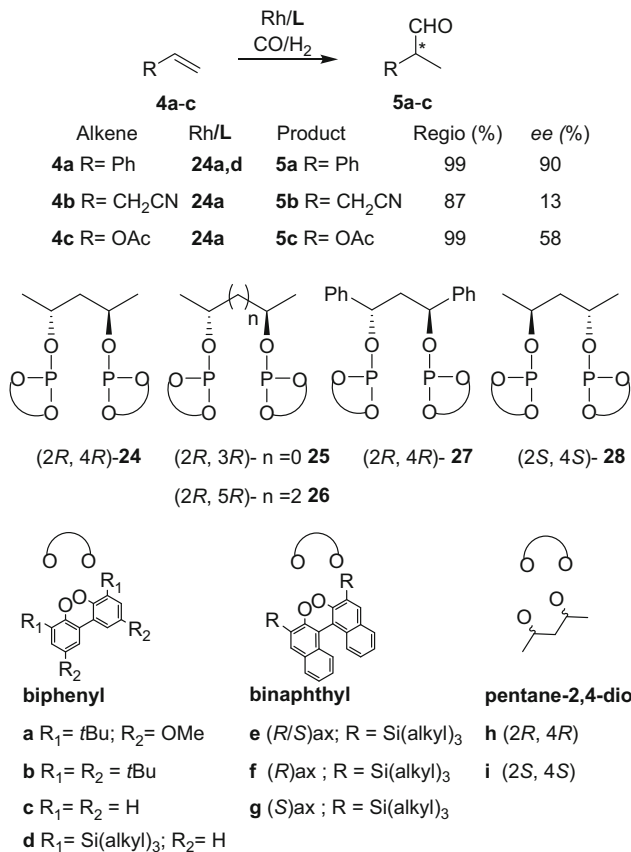
For example, the hydroformylation of vinylarenes (R=aryl) is used as a model for the synthesis of 2-aryl propionaldehydes, which are intermediates in the synthesis of 2-aryl propionic acids, the profen class of non-steroidal drugs. Nowadays, the application of the Rh-catalyzed asymmetric hydroformylation to obtain enantiomerically pure chiral aldehydes is growing. The Rh-catalyzed asymmetric hydroformylation of several other monosubstituted alkenes was successfully carried out, such as allyl cyanide and vinyl acetate [6–16]. In general, 1,3-diphosphite and phosphine–phosphite ligands provided the best results in these processes [23]. However, the use of bisphosphacyclic ligands has recently emerged as an efficient alternative [6–16].

3.1 1,3-Diphosphite Ligands

The use of diphosphite ligands was intensively studied in this process as they provide high levels of selectivity with these substrates [59]. The initial success in the rhodium-catalyzed asymmetric hydroformylation of vinylarenes came from Union Carbide with the discovery of the diphosphite ligand (2*R*, 4*R*)-pentane-2,4-diol **24** (Scheme 5) [60, 61].

Scheme 4 Asymmetric hydroformylation of monosubstituted alkenes





Scheme 5 Rh-catalyzed asymmetric hydroformylation of monosubstituted alkenes **4a–c** using ligands **24–28**

Good chemo-, regio-, and enantioselectivities (*ee* up to 90%) were obtained with (*2R, 4R*)-pentane-2,4-diol diphosphite derivatives (**24a,d**) but only when the reaction was performed around room temperature. Other research groups synthesized the series of diphosphite ligands **25–28** in order to study the effect of structural modifications on the Rh-catalyzed asymmetric hydroformylation of vinylarenes (Scheme 5) [62–66].

The influence of the bite angle of these ligands was studied with diphosphite ligands (*2R, 4R*)-pentane-2,4-diol **24**, (*2R, 3R*)-butane-2,4-diol **25**, and (*2R, 5R*)-hexane-2,4-diol **26** [63]. In general, the ligand **24**, which contains a three carbon atoms bridge, provided higher enantioselectivities than ligands **25** and **26**, which have a two and four carbon atoms bridge, respectively.

The effect of different phosphite moieties was studied with ligands **24a–g** [62–64]. In general, sterically hindered phosphite moieties are necessary to achieve high enantioselectivities. The results indicated that varying the *ortho* and *para* substituents on the biphenyl and binaphthyl moieties has also a great effect on

the asymmetric induction. The highest enantioselectivity (*ee* up to 90% at 20 bar of syngas and 25°C) in the Rh-catalyzed asymmetric hydroformylation of styrene was obtained by using ligands **24a** and **24d**.

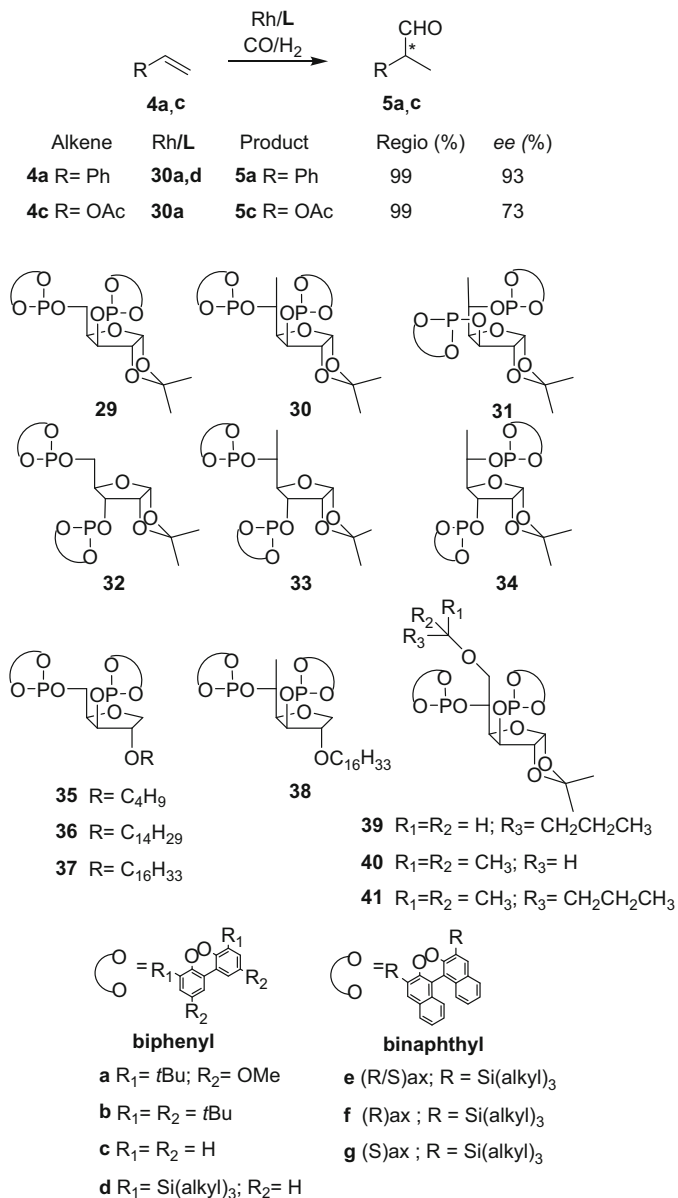
The influence of the backbone was studied comparing the results obtained with the ligands **24** and **27** [62–64]. Surprisingly, the ligand **27**, which contains a more sterically hindered phenyl group, provided lower enantioselectivity than ligand **24**.

A cooperative effect between the different chiral centers of the phosphite ligands **24f–i** and **28f–i** was demonstrated. Initially, van Leeuwen and co-workers studied the cooperative effect between the chiral ligand bridge and the axially chiral binaphthyl phosphite moieties by comparing ligands **24f,g** and **28f,g**. The hydroformylation results indicated a suitable combination for ligand **24g** (*ee*'s up to 86%) [62–64]. Later, Bakos and co-workers found a similar matched–mismatched effect between the chiral ligand bridge and the chiral phosphite moiety of the ligands **24h,i** and **28h,i** [65]. Interestingly, the hydroformylation results obtained with ligands **24a** and **24d**, that are conformationally flexible and contain axially chiral biphenyl moieties, are similar to those obtained with ligand **24g**. This indicated that diphosphite ligands containing these biphenyl moieties predominantly exist as a single atropisomer in the hydridorhodium complexes [RhH(CO)₂(diphosphite)] when bulky substituents are present in *ortho* positions [62–64]. It is therefore not necessary to use expensive conformationally rigid binaphthyl moieties.

To investigate whether a relationship exists between the solution structures of the [RhH(CO)₂(diphosphite)] species and catalytic performance, van Leeuwen and co-workers extensively studied the [RhH(CO)₂(diphosphite)] (diphosphite = **24**, **28**) species formed under hydroformylation conditions by high pressure NMR techniques (HP-NMR) [16, 23]. From these trigonal bipyramidal (TBP) complexes, two isomeric structures are possible: one containing the diphosphite coordinated in a bis-equatorial (eq–eq) fashion and one containing the diphosphite in an equatorial-axial (eq–ax) fashion (Scheme 3). The results indicated that the stability and catalytic performance of the [RhH(CO)₂(diphosphite)] (diphosphite = **24**, **28**) species strongly depend on the configuration of the pentane-2,4-diol ligand backbone and on the chiral biaryl phosphite moieties. Thus, ligands **24a**, **24d**, and **24g**, which form well-defined stable bis-equatorial (eq–eq) complexes, lead to good enantiomeric excesses. In contrast, the ligands **24i** and **28g**, which form mixtures of complexes, lead to low enantioselectivities [62–64, 67]. The ligand **24a** was also evaluated in the Rh-catalyzed asymmetric hydroformylation of allyl cyanide **4b** and vinyl acetate **4c** but low to moderate enantioselectivities (13 and 58%, respectively) were obtained with these substrates [6].

1,3-Diphosphite ligands derived from 1,2-*O*-isopropylidene- α -D-xylofuranose (**29**, **32**) and 6-deoxy-1,2-*O*-isopropylidene- α -D-glucofuranose (**30**, **31**, **33**, **34**) were successfully applied in the Rh-catalyzed asymmetric hydroformylation of vinylarenes (Scheme 6) [68–71].

The use of diphosphite ligands **30a,d** and **34a,d** in the Rh-catalyzed asymmetric hydroformylation of styrene provided the *S*- and *R*-enantiomers of the product with high enantioselectivities (*ee* up to 93%) and excellent regioselectivity (Scheme 6) [70, 71]. The ligand **30a** was also tested in the hydroformylation of vinyl acetate obtaining excellent regioselectivity (99%) with an enantioselectivity of 73% [72].



Scheme 6 Rh-catalyzed asymmetric hydroformylation of monosubstituted alkenes using ligands **29–41**

Recently, related C1-symmetry diphosphite ligands conformationally more flexible (**35–38**) or incorporating an increase in steric hindrance at the C-6 position (**39–41**) were synthesized (Scheme 6) [72, 73]. These ligands were probed in the hydroformylation of styrene **4a** and vinyl acetate **4c** with good regio- and enantioselectivity (up to 81% and 68%, respectively), but these selectivities resulted to be lower than with the ligand **30**. Therefore, the bicycle structure and the methyl substituent at C-5 position seem required to achieve high enantioselectivity in the hydroformylation of styrene and vinyl acetate when using 1,3-diphosphites derived from carbohydrates.

In summary, the results obtained in the Rh-catalyzed asymmetric hydroformylation of monosubstituted alkenes indicate that: (a) the absolute configuration of the product is governed by the configuration at the stereogenic center C-3; (b) the level of enantioselectivity is influenced by the presence of stereocenters at C-3 and C-5 positions, where the phosphorus atoms are attached; (c) bulky substituents in *ortho* positions of the biaryl phosphite moieties are necessary to achieve high levels of enantioselectivity; (d) pseudo-enantiomer ligands such as **30** and **34** afford the same level of enantioselectivity for both product enantiomers.

Interestingly, the ligands **30** and **34**, for which only $[\text{RhH}(\text{CO})_2(\text{L})]$ species with eq–eq coordination were observed by HP-NMR techniques, provided higher enantioselectivity (*ee* up to 93%) than the related ligands **31** and **33** (*ee* up to 64%), for which an equilibrium between the isomeric eq–eq and eq–ax $[\text{RhH}(\text{CO})_2(\text{L})]$ species was observed by HP-NMR and HP-IR techniques. Therefore, the presence of a single coordination isomer, in this case with ligand coordinated in an equatorial–equatorial (eq–eq) mode, was observed to produce high levels of enantioselectivity in the Rh-catalyzed asymmetric hydroformylation of styrene, as previously mentioned [70–73].

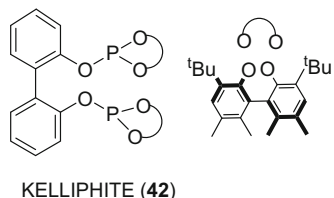
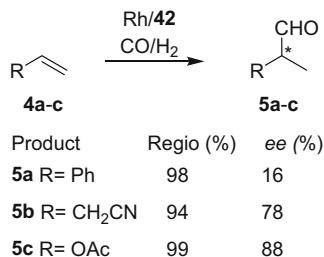
In contrast with the diphosphites previously mentioned, the KELLIPHITE ligand (**42**), which was developed by Dow Chemical Company, incorporates the chirality in the bisphenol unit, while the backbone is achiral (Scheme 7). The catalytic system containing this ligand afforded very good enantioselectivity in the rhodium-catalyzed hydroformylation of vinyl acetate and allyl cyanide, although low selectivities were obtained in the hydroformylation of styrene [74, 75].

Recently, Vidal-Ferran and co-workers reported the use of polyether binders as regulation agents (RAs) to enhance the enantioselectivity of rhodium-catalyzed transformations (Scheme 8) [76, 77]. Using rhodium complexes bearing α,ω -bisphosphite-polyether ligands, the enantiomeric excess was increased by up to 82% in the asymmetric hydroformylation of vinyl benzoate (96% *ee*). This ligand design enabled the regulation of enantioselectivity by generation of an array of catalysts that simultaneously preserve the advantages of a privileged structure and offer geometrically close catalytic sites.

3.2 Phosphine–Phosphite Ligands

The discovery of the (*R,S*)-BINAPHOS (**44**) and (*S,R*)-BINAPHOS (**45**) ligands in 1993 by Takaya and Nozaki produced a real breakthrough in the Rh-catalyzed asymmetric hydroformylation reaction (Scheme 9) [78].

Scheme 7 Rh-catalyzed asymmetric hydroformylation of monosubstituted alkenes using ligand KELLIPHITE (**42**)



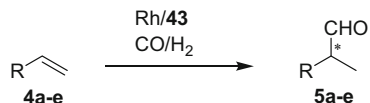
These ligands allowed for the first time an increase in the scope of this process since they provided high enantioselectivity in the Rh-catalyzed asymmetric hydroformylation of several classes of monosubstituted alkenes such as vinyl arenes, 1-heteroatom-functionalized alkenes, and disubstituted 1,3-dienes (Scheme 9), and is still currently a reference in this area [79–90]. Excellent regio- and enantioselectivity were achieved with most of these substrates, although the formation of the branched product (21%) was disfavored when but-1-ene was the substrate. In 2003, De Vries and co-workers reported the first Rh-catalyzed asymmetric hydroformylation of allylcyanide and although moderate regioselectivity was obtained (72%), the highest enantioselectivity (66%) by far was achieved using the ligand **44** [91]. As a general rule, the presence of electron-withdrawing substituents such as phenyl or heteroatoms in the alkene substrate leads to control the regioselectivity in favor of the branched product, independently of the ligand used [6].

It is noteworthy that (*R,S*)-BINAPHOS (**44**) or the (*S,R*)-BINAPHOS (**45**) ligands yield the two enantiomers of the product with high enantioselectivity; [92, 93] however, the (*R,R*)- and (*S,S*)-BINAPHOS, diastereoisomers of ligands **44** and **45**, yielded much lower enantioselectivity in this process, thus demonstrating the importance of the combination of opposite configurations at the phosphine and phosphite moieties.

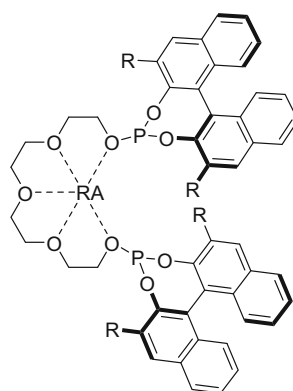
In contrast with the previously mentioned diphosphite ligands which coordinate to the Rh center in an eq–eq fashion, the BINAPHOS ligand was found to coordinate to Rh in an eq–ax mode as a single isomer in the resting state [RhH(CO)₂(L-L)] of the process [92, 93]. Recently, DFT calculations on this system demonstrated that the coordination of the ligand with the phosphite moiety in apical position is crucial for the stereoselectivity of this reaction and that the presence of a second chiral center plays a role in determining the *R* or *S* configuration of the aldehyde product [94]. They also showed that for styrene, in the stereoselectivity determining

Scheme 8

Supramolecularly regulated bisphosphite ligands with a distal regulation site reported by Vidal and co-workers



Product	Regio %	ee %
5a R = OAc	>99	99
5b R = EtCO ₂	>99	99
5c R = PhCO ₂	>99	96
5d R = Ph	80	5
5e R = CH ₂ OSiMe ₃	18	25

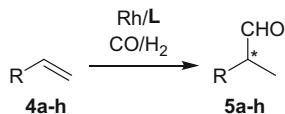


43 RA = RbBArF

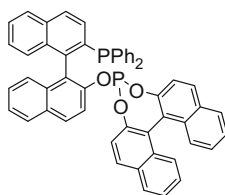
transition state, the key substrate–ligand interactions occur between the styrene and the phosphite moiety and that these interactions are repulsive in nature.

The second generation of BINAPHOS-type ligands (Scheme 10) was developed by the introduction of 3-methoxy substituents on the aryl phosphine units **46** [80, 81], and by replacement of the phosphite group by a phosphoramidite function, yielding the YANPHOS ligand (**47**) (Scheme 10) [95]. The Rh/**46** increased the regio- and enantioselectivity in the asymmetric hydroformylation of styrene, vinylfurans and thiophenes (Scheme 10). Recently, the use of (*S,R*)-Bn-YANPHOS was reported in the asymmetric hydroformylation of vinyl-heteroarenes such as pyrroles and provided excellent regio- and enantioselectivities (up to 96%) [96].

YANPHOS (**47**) (Scheme 10) provided higher enantioselectivity than the BINAPHOS ligand **44** without altering the regioselectivity in the Rh-catalyzed asymmetric hydroformylation of styrene and vinyl acetate (*ee* up to 99 and 98%, respectively). Additionally, the ligand **47** provided higher enantioselectivity than KELLIPHITE



Product	5a	5b	5c	5d	5e	5f	5g	5h
R	Ph	CH ₂ CN	OAc	C ₆ F ₅	CF ₃	Et	Phth	S(4-tolyl)
Regio (%)	90	72	86	96	95	21	89	96
ee (%)	94	66	92	98	93	83	85	74

(R,S)-BINAPHOS (**44**)(S,R)-BINAPHOS (**45**)

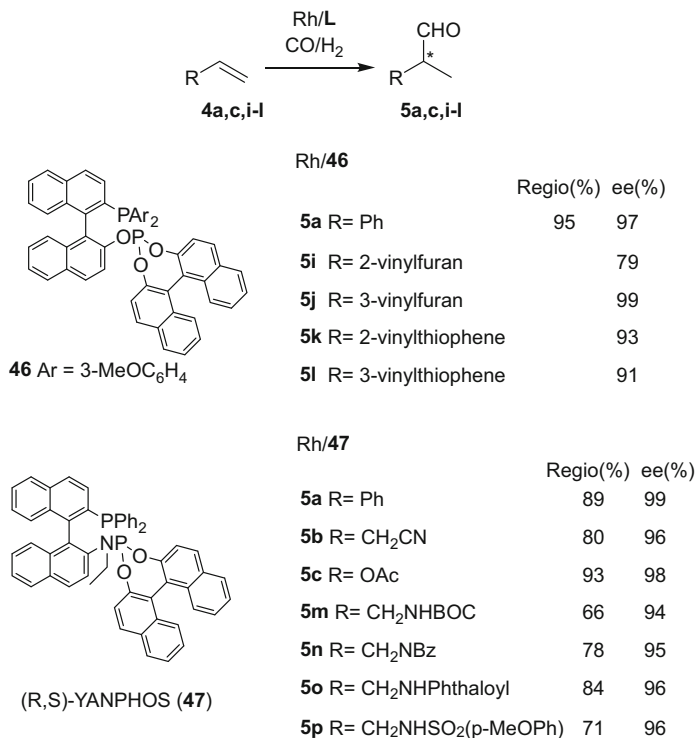
Scheme 9 Rh-catalyzed asymmetric hydroformylation of monosubstituted alkenes using (*R,S*)- and (*S,R*)-BINAPHOS (**44**) and (**45**)

(**42**) (Scheme 7), although a slight decrease in regioselectivity (80 vs 94%) was observed in the hydroformylation of allyl cyanide (ee up to 96 vs 78%) [97].

Recently, the efficiency of YANPHOS ligand **47** was again demonstrated in the Rh-catalyzed asymmetric hydroformylation of monosubstituted alkenes with *N*-allylamides, *N*-allylphthalamides, and *N*-allylsulfonamides substituents with excellent ee's (up to 96%), good regioselectivities (up to 84%), and a turnover number (TON) up to 9,700 [98].

DFT calculations on a series of chiral Rh catalysts proposed an explanation for the high enantioinduction observed for Rh-CHIRAPHITE, -BINAPINE, -diazaphospholane, and YANPHOS systems [99]. For BINAPINE and YANPHOS ligands, the main contribution to the selectivity was assigned to the naphthyl groups, while for CHIRAPHITE and diazaphospholane ligands, the ^tBu and chiral amine groups were highlighted as the key enantioinducting moieties. Importantly, in all cases, the effective placement of these groups to interact with the substrate is achieved through the coordination of phosphane moieties in the apical site of the complex.

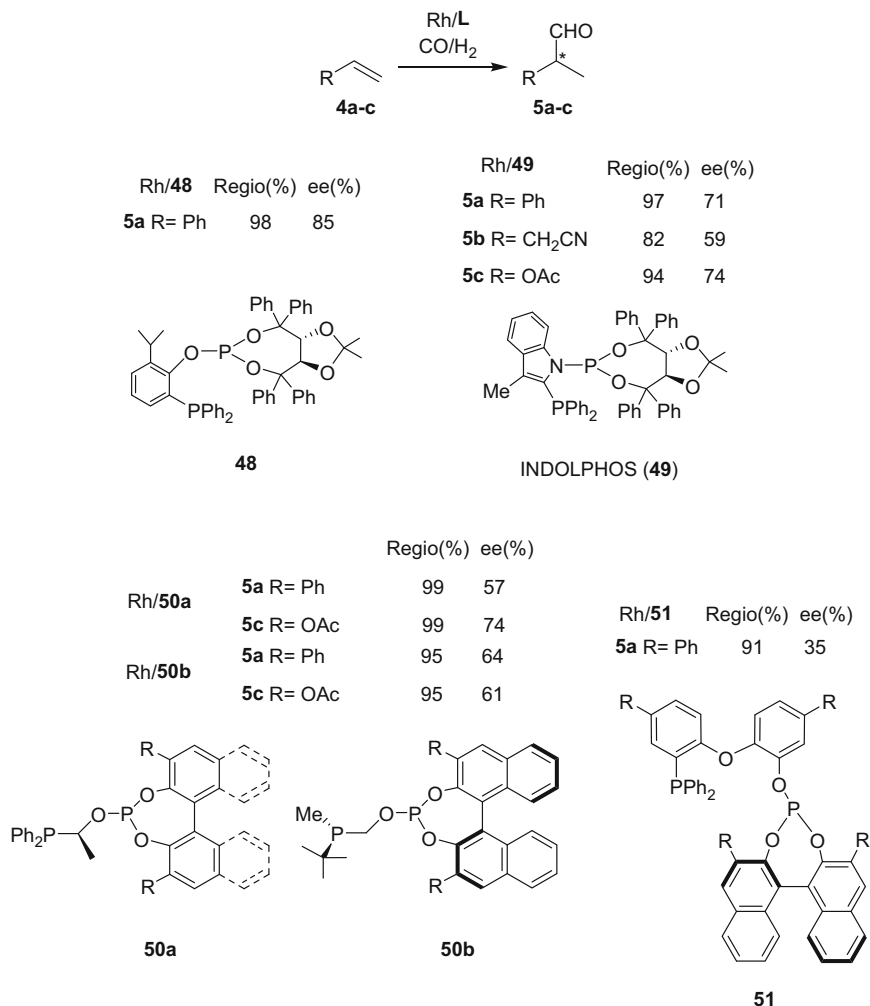
Inspired by the excellent results obtained using **44** and **45**, several new phosphine-phosphite ligands with different backbones were developed over the last years but the catalytic results using these ligands provided lower enantioselectivity (from 20 to 85%) than those previously achieved with the original BINAPHOS ligand [100–105]. Some of these ligands help to elucidate the correlation between the ee and the electronic withdrawing properties of the substituent on the alkene [106].



Scheme 10 Rh-catalyzed asymmetric hydroformylation of monosubstituted alkenes using the ligands **46** and **47**

A new family of phosphine–phosphite and phosphine–phosphoramidite ligands was constituted using a Taddol-based backbone in the phosphite or phosphoramidite moiety, respectively (ligands **48** and **49**, Scheme 11) [107, 108]. These ligands were applied in the Rh-catalyzed asymmetric hydroformylation of styrene, allyl cyanide, and vinyl acetate with excellent regioselectivities (up to 98%) and good ee's (up to 85%). Recently, the group of Vidal-Ferran reported the use of two families of small bite angle phosphine–phosphite ligands **50a** and **50b** in the hydroformylation of styrene and vinyl acetate, obtaining excellent regioselectivity but with moderate ee's (up to 74%) [109, 110]. Interestingly, the introduction of P-stereogenic center in ligands **50b** slightly increased the ee when styrene was the substrate but resulted in a lower enantioinduction in the case of vinyl acetate. The use of the large bite angle ligands **51** containing a diphenylether backbone only provided moderate ee's (up to 35%) in the Rh-catalyzed hydroformylation of styrene [111]. The synthesis of phosphine–phosphite ligands built on an α -cyclodextrin scaffold was also reported recently and provided moderate regioselectivity (ca. 75%) and ee (50%) in the Rh-catalyzed hydroformylation of styrene [112].

Reek and co-workers reported the use of supramolecular phosphine–phosphoramidite hybrid ligands in the Rh-catalyzed hydroformylation of styrene derivatives (Scheme 12)

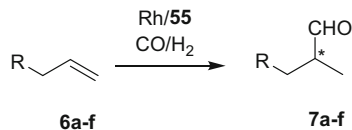


Scheme 11 Rh-catalyzed asymmetric hydroformylation of monosubstituted alkenes using Taddol-based ligands (**48** and **49**) and phosphine–phosphite ligands (**50**) and (**51**)

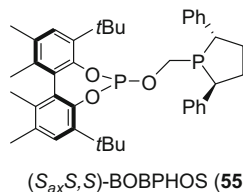
[113]. They observed that the electronic and steric properties of the M(II) (M = Zn, Ru) templates had a significant influence on the activity and selectivity of the catalytic reaction. Using styrene as substrate, ee's up to 59% were obtained using ligand **54**.

The production of chiral aldehyde from simple terminal alkyl olefins of formula $RCH_2CH=CH_2$ with high regio- and enantioselectivity has been aimed for many years and a large set of ligands was probed in this reaction. However, poor regioselectivity was usually obtained, the linear aldehyde is preferably formed in most cases, although interesting ee's were achieved, for instance, using the BINAPHOS

Scheme 13 Rh-catalyzed asymmetric hydroformylation of terminal alkyl alkenes using the BOBPPOS ligand **55**



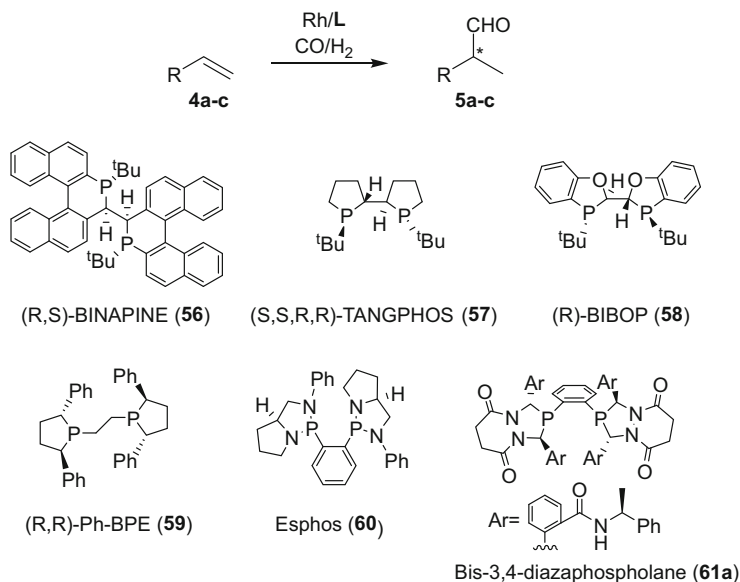
Rh/55	regio (%)	ee (%)
7a R= Ph	80	90
7b R= C ₆ F ₅	86	91
7c R= 4- <i>t</i> -BuC ₆ H ₄	75	92
7d R= Bn	70	75
7e R= Pr	75	93
7f R= CN	89	71
7g R= CONPh(Me)	82	92



reported for the allyl cyanide substrate. Recently, the ligand BIBOP **58** was reported to provide excellent results in the asymmetric hydroformylation of vinyl acetate and allylic substrates [116].

The discovery of the biphospholane scaffold as a new privileged structure for asymmetric alkene hydroformylation has triggered new research efforts for novel and improved bisphospholane-type ligands. In this context, the (*R,R*)-Ph-BPE ligand (**59**) (Scheme 14), derivative of DuPhos, was identified as an outstanding ligand for asymmetric hydroformylation since excellent regio- and enantioselectivities were achieved for styrene, allyl cyanide, and vinyl acetate as substrates with this ligand [117]. Several spacers between the two phosphorus donor atoms were evaluated and the two carbon bridge of **59** provided the highest selectivity for all three substrates [118]. Recently, both enantiomers of ligand were also utilized in the Rh-catalyzed asymmetric hydroformylation of vinylarenes using formaldehyde as a substitute of syngas providing excellent regioselectivity and enantioselectivity (up to 95%) [119]. This ligand also provided excellent results in the branched selective asymmetric hydroformylation of a wide range of 1-alkenes, including 1-dodecene, with regioselectivity up to 93% and enantioselectivity up to 96% [120].

A series of bis-2,5-diazaphospholane ligands was also probed in this process and the ESPHOS (**60**) proved to be optimal, with the best results being obtained in the hydroformylation of vinyl acetate (*ee* up to 89%) (Scheme 14) [121]. The bis-3,4-diazaphospholane ligand **61a** also provided excellent regio- and enantioselectivity (*ee* up to 96%) in this reaction (Scheme 14) [122]. Immobilization of ligand **61a**



Product	5a	5b	5c
Rh/L	R= Ph	R= CH ₂ CN	R= OAc
	Regio (%) ee(%)		
56	90 94	87 94	97 87
57	93 90	88 93	97 83
58			96 82
59	98 94	88 90	99 82
60			94 89
61a	97 82	83 87	98 96

Scheme 14 Rh-catalyzed asymmetric hydroformylation of monosubstituted alkenes using the diphosphine ligands **56–61**

onto resins and silica supports was also recently reported and provided similar performances to those of the homogenous systems with high regio- and enantioselectivity for the Rh-catalyzed hydroformylation of styrene and vinyl acetate [123]. Using these systems, excellent recyclability with only trace levels of Rh leaching was observed in batch and flow reactor conditions. It is noteworthy that silica supported systems provided poorer enantioselectivities than resin-supported catalysts. Recently, a detailed spectroscopic characterization of catalytic Rh intermediates bearing ligand **61a** was reported for the hydroformylation of octene, vinyl acetate, allyl cyanide, and 1-phenyl-1,3-butadiene [124].

This catalytic system was recently used for the continuous flow asymmetric hydroformylation of 2-vinyl-6-methoxynaphthalene during 8h of reaction using a

reactor consisting of 20 vertical bubble pipe-in-series connected by small tubing jumpers [125, 126].

Two derivatives of the ligand **61a** were also used in the synthesis of the Prelog–Djerassi Lactone via an asymmetric hydroformylation/crotylation tandem sequence in which the hydroformylation step provided 93% *ee* (Scheme 15).

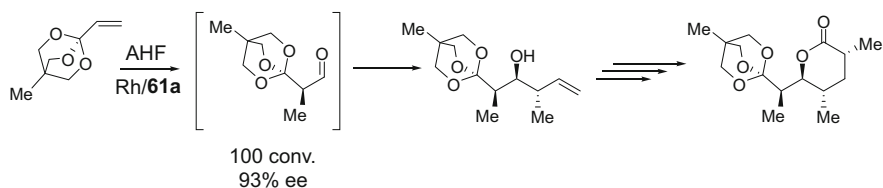
The sequential asymmetric hydroformylation/aerobic aldehyde oxidation was recently reported using the same ligand, providing an access to α -chiral carboxylic acids without racemization [127].

3.4 Bis-Phosphonite Ligands

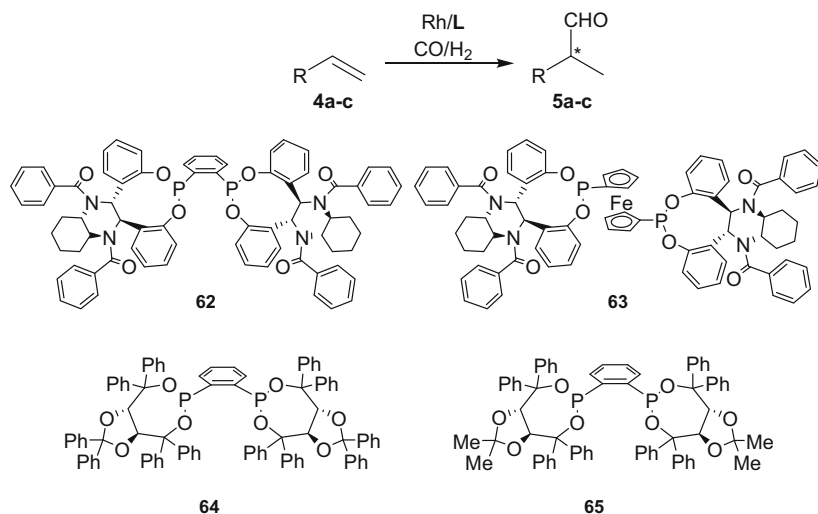
The bis-phosphonite ligand **62** provided moderate selectivities in the hydroformylation of styrene and allyl cyanide (Scheme 16). However, this ligand provided an excellent 91% *ee* in the hydroformylation of vinyl acetate [128]. The related diphosphinite ligand derived from ferrocene **63** was also reported by Ding and co-workers and its application in the Rh-catalyzed asymmetric hydroformylation of styrene and vinyl acetate provided good conversion but lower enantioselectivities in the hydroformylation of styrene and vinyl acetate (up to 55% and 83%, respectively) [129]. More recently, a family of TADDOL-derived bis-phosphonite ligands was reported, among which the ligands **64** and **65** provided excellent enantioselectivity in the asymmetric hydroformylation of styrene and derivatives [130].

3.5 Bis-Phosphinite Ligands

The diastereogenic bis-phosphinite ligands **66** and **67** were recently reported by Leitner and co-workers (Scheme 17) [131]. The Rh-catalysts bearing these binol-based ligands containing chiral phospholane units provided good regioselectivity for the branched products but only low to moderate selectivities in the hydroformylation of styrene and vinyl acetate. It is noteworthy that the diastereoisomer **67** provided higher *ee* than **66** while the opposite trend was observed in the asymmetric hydrogenation of dimethyl itaconate.



Scheme 15 Synthesis of the Prelog–Djerassi Lactone via asymmetric hydroformylation/crotylation tandem sequence in the presence of derivatives of ligand **61a**



Product	5a	5b	5c
Rh/L	R= Ph	R= CH ₂ CN	R= OAc
		Regio (%) ee(%)	
62	92 79	82 79	98 91
63	95 55		94 83
64	84 90		
65	84 91		

Scheme 16 Rh-catalyzed asymmetric hydroformylation of monosubstituted alkenes with ligands **62–65**

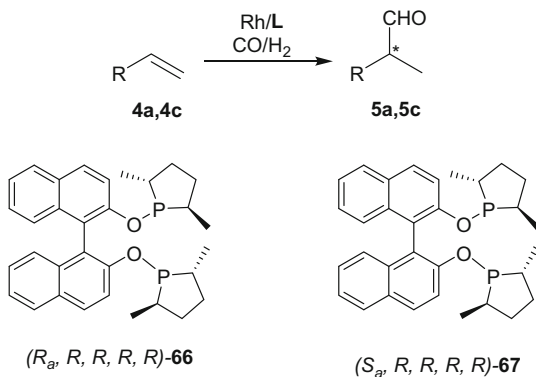
3.6 Monodentate Phosphorus-Based Ligands

Nowadays, despite the successful use of monodentate ligands in many transition metal-catalyzed processes, there are only a few reports concerning their use in asymmetric hydroformylation and achieving high enantioselectivities in this process using those ligands remains a challenge.

Recently, an Rh complex bearing the monodentate phosphoramidite ligand encapsulated in a self-assembled molecular cage **68** (Scheme 18) provided the highest enantioselectivity (74%) in the asymmetric hydroformylation of styrenes using monoligated catalyst [132]. The presence of the cage was shown to enhance the enantioinduction of the catalyst and can therefore be considered as a second coordination sphere that is reminiscent of enzymatic active sites.

The monophosphite ligand **69** was tested in the Rh-catalyzed asymmetric hydroformylation of styrene and allyl cyanide and provided moderate enantioselectivities (Scheme 19). When vinyl acetate was the substrate, very poor *ee*'s were obtained

Scheme 17 Rh-catalyzed asymmetric hydroformylation of monosubstituted alkenes with ligands **66** and **67**

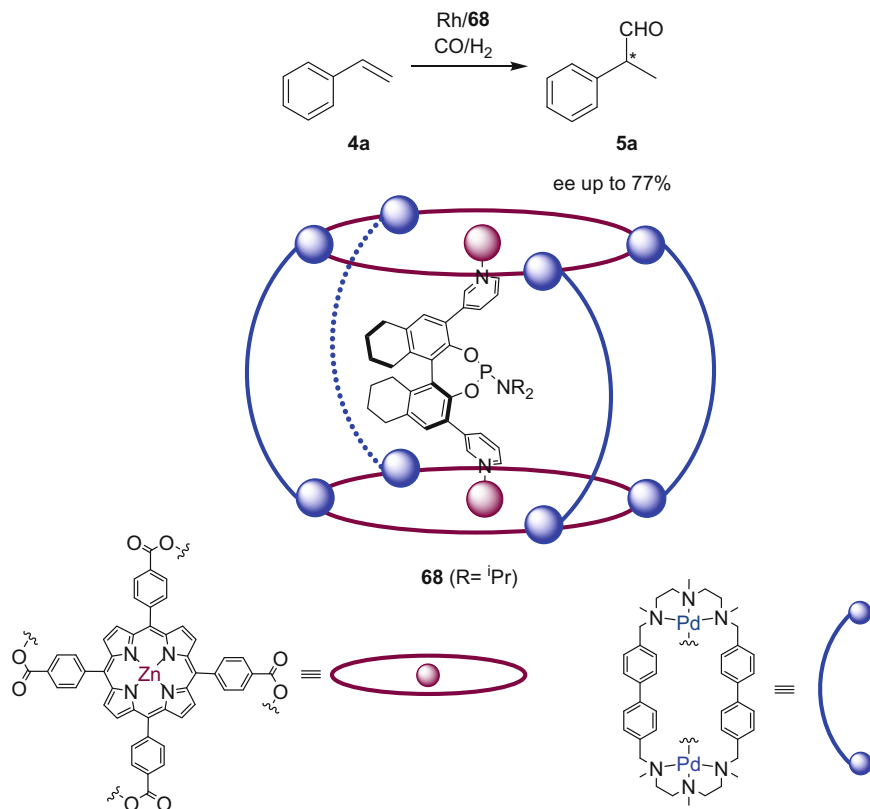


Product	5a	5c
Rh/L	R= Ph	R= OAc
	regio (%) / ee(%)	
66	84 4	
67	75 40	96 33

(Scheme 19) [74, 75]. However, in 2004, Ojima and co-workers reported the use of the phosphoramidite ligand **70** (Scheme 19), related to monophosphite **69**, in the Rh-catalyzed asymmetric hydroformylation of allyl cyanide and achieved excellent regioselectivities together with the highest enantiomeric excess (80%) ever reported for this reaction with a monodentate ligand [133].

These results, although still far from those obtained with bidentate ligands, clearly indicated that achieving high *ee*'s using monodentate ligands is possible. Later, Alexakis, Pamies, Dieguez, and co-workers reported the testing of monodentate phosphoramidite and aminophosphine libraries in the asymmetric hydroformylation of styrene derivatives [134]. However, only *ee*'s up to 50% could be achieved.

In 2005, Breit reports an alternative approach to the classical synthesis of bidentate ligands for hydroformylation by using the self-assembly of bidentate ligands based on an A-T base-pair model [135]. This method presents the advantage of allowing the rapid screening of various pairs of available monodentate ligands to obtain the most suitable combination for each substrate, overcoming the typical synthetic limitations for new bidentate ligands. Later, van Leeuwen and Reek reported the template-induced formation of chelating heterobidentate ligands by the self-assembly of two distinct monodentate ligands on a rigid bis-zinc(II)-salphen template with two identical binding sites (Scheme 20) [136, 137]. The templated heterobidentate ligand **71** induced much higher enantioselectivities (*ee* up to 74%) than any of the corresponding homobidentate ligands or non-templated mixed ligand combinations (*ee* up to 13%) in the Rh-catalyzed asymmetric hydroformylation of styrene.



Scheme 18 Rh-catalyzed asymmetric hydroformylation of styrene using Rh/monodentate phosphoramidite catalyst encapsulated in a self-assembled molecular cage

4 Other Monosubstituted Alkene Substrates

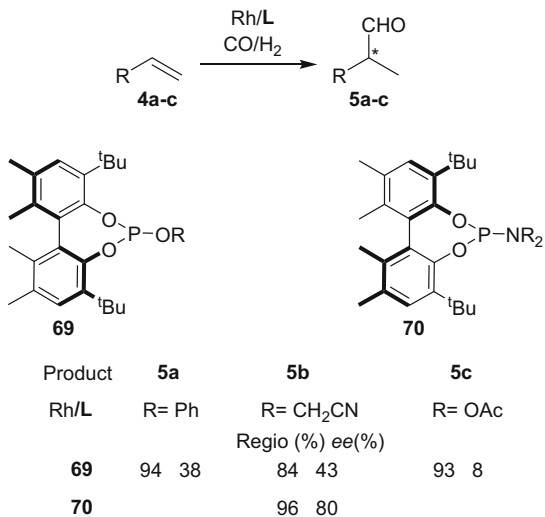
In this section, recent reports on the Rh-catalyzed asymmetric hydroformylation of “non-common” monosubstituted alkene substrates using chiral phosphorus donor ligands are presented.

The substrate scope for the hydroformylation of dialkylacrylamides **4d₁–d₄** has so far been limited to methacrylamide, acrylamide, or *N*-benzylacrylamide, with low enantioinduction (20–50% ee’s) [138, 139].

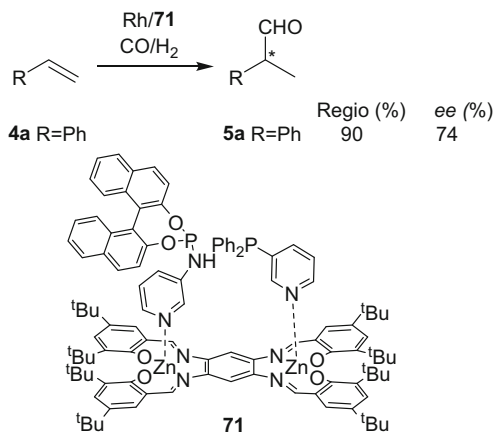
However, the use of a bis-diazaphospholane ligand (**61a**) in the Rh-catalyzed asymmetric hydroformylation of *N,N*-dialkylacrylamides was recently described achieving nearly total regioselectivity and ee’s up to 82% (Scheme 21) [140].

The use of the bis-3,4-diazaphospholane type ligands has also been reported in the rhodium-catalyzed hydroformylation of several 1,3-diene substrates (1,3-dienes, *N*-vinyl carboxamides, allyl carbamates, and allyl ethers) with excellent regio- and

Scheme 19 Rh-catalyzed asymmetric hydroformylation of monosubstituted alkenes using ligands **69** and **70**



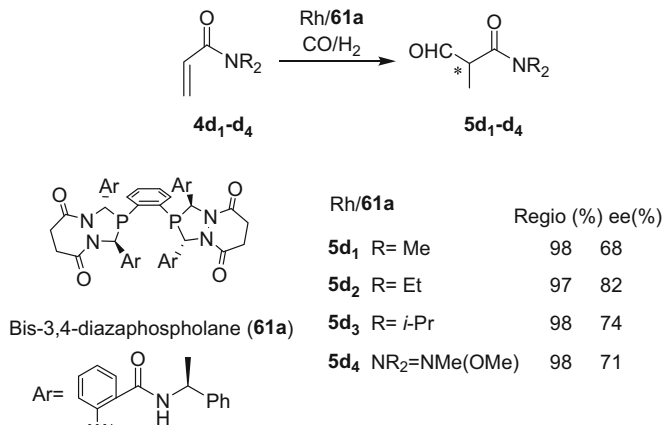
Scheme 20 Rh-catalyzed asymmetric hydroformylation of styrene using the templated ligand **71**



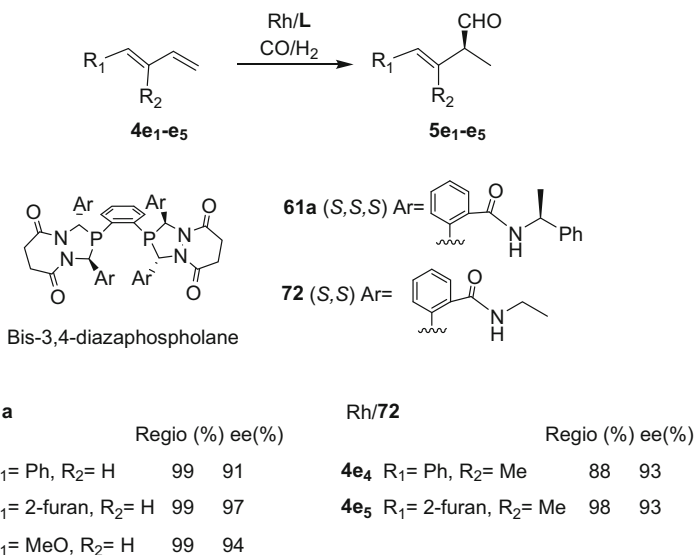
enantioselectivities by Landis et al. [141, 142]. Total conversions with good regioselectivities (>88%) and excellent enantioselectivities (91–97%) were achieved (Scheme 22).

The ligand **61a** was also successfully employed in the Rh-catalyzed asymmetric hydroformylation of other alkene substrates containing amine (**4f**) and ether (**4g**) substituents, with ee's up to 99% and 97%, respectively [142] (Scheme 23).

Recently, Leitner, Francio, and co-workers reported the highly regio- and enantioselective hydroformylation of vinyl esters using the bidentate phosphine, P-chiral

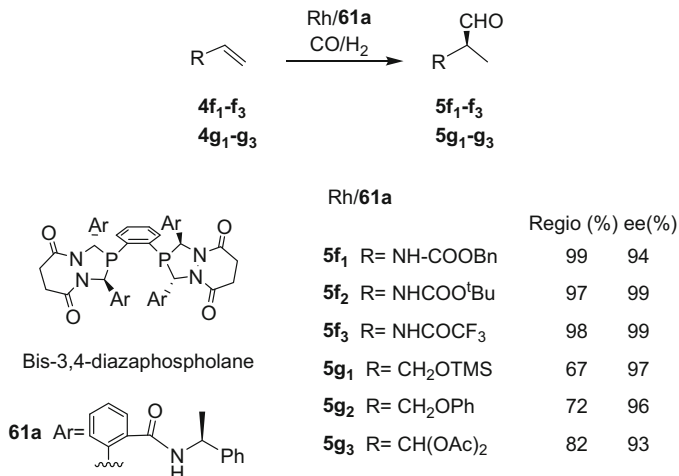


Scheme 21 Rh-catalyzed asymmetric hydroformylation of *N,N*-dialkylacrylamides



Scheme 22 Rh-catalyzed asymmetric hydroformylation of 1,3-dienes with ligands **61a** and **72**

phosphoramidate ligands [143]. The BettiPhos ligand **73** was particularly efficient and provided total regioselectivity and ee's up to 97% for a number of these substrates (Scheme 24).



Scheme 23 Rh-catalyzed asymmetric hydroformylation of monosubstituted enamides and other allylic substrates with the ligand **61a**

5 Rh-Catalyzed Asymmetric Hydroformylation of Disubstituted Alkenes

The Rh-catalyzed asymmetric hydroformylation of disubstituted alkenes has received much less attention than their monosubstituted counterparts. To the best of our knowledge, only a few examples of asymmetric Rh-catalyzed hydroformylation of 1,2-disubstituted and 1,1-disubstituted alkenes have been reported so far (Scheme 2) [26, 143–180].

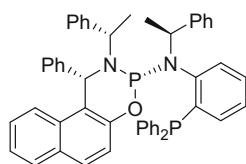
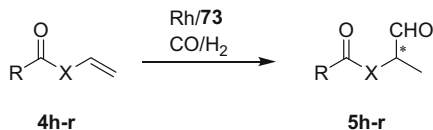
5.1 Linear 1,2-Disubstituted Alkenes

The 1,3-diphosphite ligand **29** was used in the Rh-catalyzed asymmetric hydroformylation of *trans*-anethole **8a** and estragole **8b** (Scheme 25) but moderate to low enantioselectivities were achieved (*ee* up to 15%) [145].

Nozaki and co-workers reported the asymmetric Rh-catalyzed hydroformylation of *trans*-anethole **8a** into **9a** using the BINAPHOS ligand **44** with excellent regioselectivity (98%) and a remarkable 80% *ee* [146, 147].

In the Rh-catalyzed asymmetric hydroformylation of 1,2-alkyl-disubstituted alkenes (Scheme 26) as substrates, the BINAPHOS ligand **44** provided high *ee* values [146, 147]. Interestingly, it was reported that the *E*-isomers **11b** and **11d** yielded lower enantioselectivity than their *Z*-counterparts **11a** and **11c**.

More recently, a monodentate phosphoramidite template ligand was used in the asymmetric Rh-catalyzed hydroformylation of *trans*-2-octene (Scheme 27). This

BettiPhos (**73**)

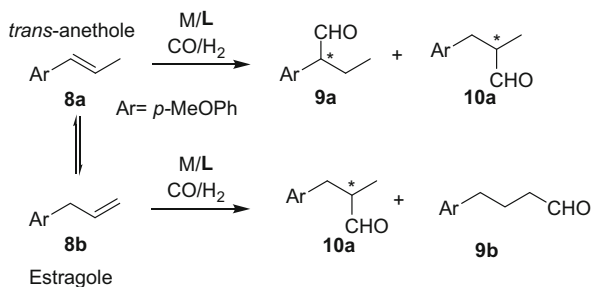
Product	Regio %	ee %
5h R = Et; X = O	>99	94
5i R = ^t Bu; X = O	>99	95
5j R = Ph; X = O	>99	94
5k R = 4-MeOC ₆ H ₄ ; X = O	>99	91
5l R = 4-FC ₆ H ₄ ; X = O	>99	92
5m R = naphthyl; X = O	98	88
5n R = CH ₃ (CH ₂) ₁₀ ; X = O	>99	95
5o	>99	96
5p	-	5
5q R = CH ₃ ; X = NH	96	82
5r R = CH ₃ ; X = NCH ₃	86	83

Scheme 24 Rh-catalyzed asymmetric hydroformylation of vinyl esters using the BettiPhos ligand **73**

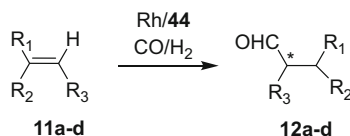
ligand (**74**) exhibits a supramolecular control over the Rh center, due to the presence of two pyridine functions in the bis(naphthol) skeleton that are bounded to zinc(II) porphyrins. With this ligand, useful conversions (up to 56%) with moderate ee's (up to 45%) were achieved. When the BINAPHOS ligand **44** was used in the same reaction, similar conversion (55%) was obtained although without significant enantioinduction [148]. More recently, a new supramolecular ligand **75** (Scheme 27) containing two phosphoramidite moieties was reported, providing remarkable enantioselectivities in the asymmetric hydroformylation of internal alkenes [149].

Very recently, Landis and co-workers showed that the diazaphospholane ligand **61a** could provide high enantioselectivity in the hydroformylation of *Z*-enamides and enol esters, providing excellent enantioselectivities for a broad range of these substrates (Scheme 28) [150].

Scheme 25 Isomerization processes and asymmetric hydroformylation of *trans*-anethole and estragole



Scheme 26 Rh-catalyzed asymmetric hydroformylation of disubstituted alkenes



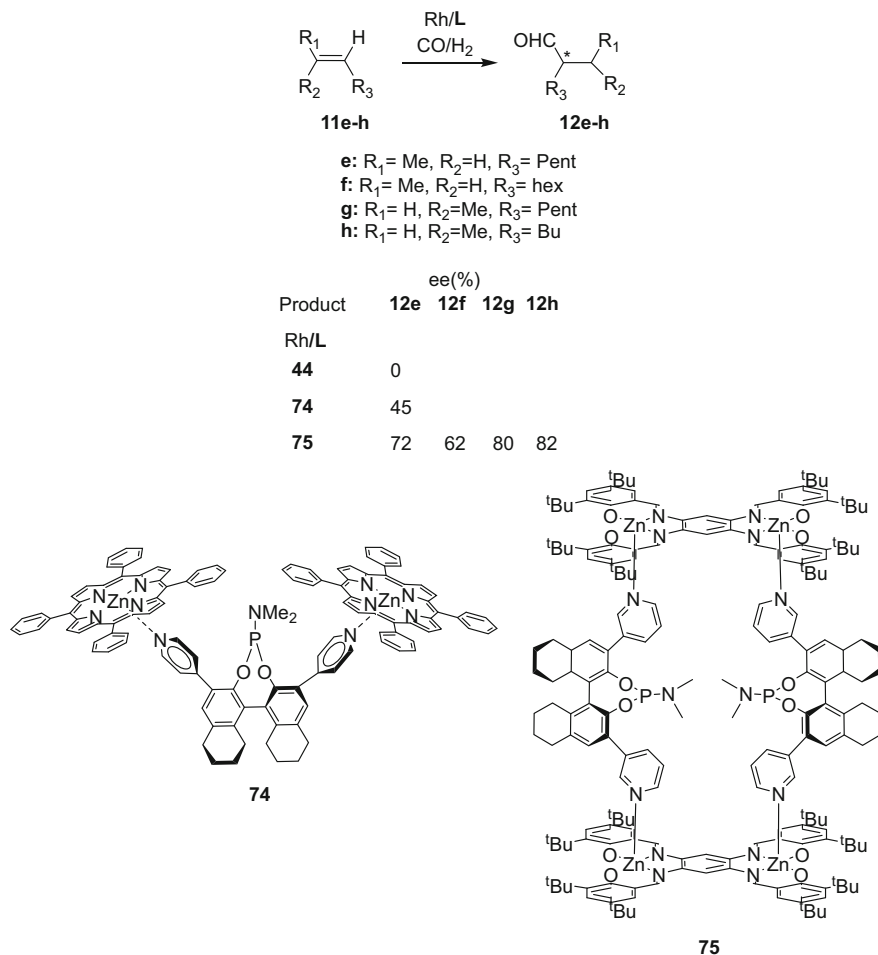
Product	ee (%)
12a R ₁ = H, R ₂ =R ₃ = Me	85
12b R ₁ = Me, R ₂ = H, R ₃ = Me	48
12c R ₁ = H, R ₂ =R ₃ = Et	79
12d R ₁ = Et, R ₂ = H, R ₃ = Et	69

Using the same ligand **61a**, Burke and Risi reported the total synthesis of (+)-patulolide C, which exhibits both antifungal and antibacterial activities [151, 152], through a methodology based upon Rh-catalyzed asymmetric hydroformylation (Scheme 29) [153]. This synthetic method included an Rh-catalyzed hydroformylation/intramolecular Wittig olefination to set the C₄-hydroxyl stereochemistry and *E*-olefin geometry and form the macrolactone, which afforded a very short, high-yielding synthesis of this compound, which usually required over 14 steps. The hydroformylation substrate is therefore an *E*-1,2-disubstituted alkene bearing an acetate and an alkyl substituent.

More recently, the same authors also employed this ligand in the synthesis of other biologically relevant molecule using asymmetric hydroformylation as the key step [55, 154].

5.2 Scaffolding [156] Ligands

The term “catalyst-directing groups” was defined for organocatalysts that are able to form simultaneously covalent bonds with a substrate and dative bonds with a metal catalyst, which allow them to direct metal-catalyzed transformations [157]. In general, these “scaffolding ligands” were named by analogy with scaffolding proteins, which promote biological processes [158].



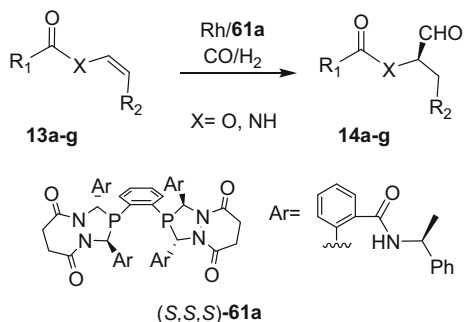
Scheme 27 Rh-catalyzed asymmetric hydroformylation of internal alkenes with the ligands **44**, **74**, and **75**

Using such methodology, the groups of Tan and Breit reported the highly regioselective Rh-catalyzed hydroformylation of homoallylic alcohols [157, 159]. Tan et al. designed the alkoxy benzoazaphophole ligand **76** derived from *N*-methylaniline that undergo facile exchange with other alcohols or secondary amines (Scheme 30) [141, 142].

The asymmetric hydroformylation of several alkene substrates was performed by Tan and co-workers using scaffolding ligands containing a tetrahydroisoquinoline group on the alkoxy benzoazaphosphole yielding the scaffolding ligand **78** (Scheme 31).

More recently, the group of Tan reported the use of ligands containing an oxazoline moiety able to bind alcohols (Scheme 32) [160]. They applied these ligands

Scheme 28 Rh-catalyzed asymmetric hydroformylation of *Z*-enamides and enol esters with the (*S,S,S*)-bis diazaphos ligand **61a** reported Landis and co-workers



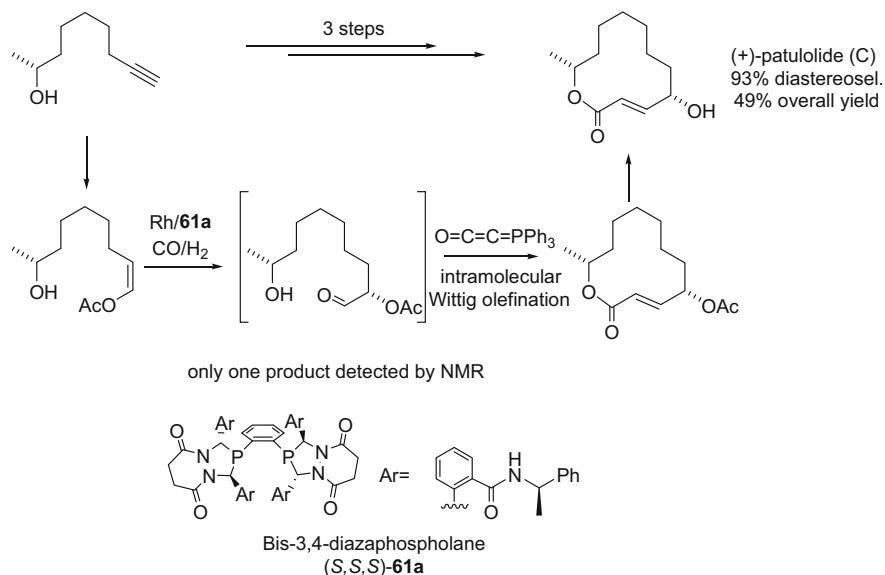
Product	Regio(%)	ee(%)
14a X=O, R ₁ = Ph, R ₂ = Bu	>99	97
14b X=O, R ₁ = <i>p</i> -C ₆ H ₄ -OH, R ₂ = Bu	>99	99
14c X=O, R ₁ = Me, R ₂ = CH ₂ -CH ₂ -Ph	>99	93
14d X=NH, R ₁ = Ph, R ₂ = Bu	>99	85
14e X=NH, R ₁ = Ph, R ₂ = CH ₂ -CH ₂ Ph	>99	90
14f X=NH, R ₁ = Ph, R ₂ = CH ₂ -CH ₂ Cl	93	92
14g X=NH, R ₁ = Ph, R ₂ = CH ₂ -CH ₂ CN	>99	94
14h X=NH, R ₁ = Ph, R ₂ = CH ₂ -C ₆ H ₁₁	>99	84
14i X=NH, R ₁ = Ph, R ₂ = Ph	86	98
14j X=NH, R ₁ = CF ₃ , R ₂ = Ph	92	90

in the diastereoselective hydroformylation of homoallylic alcohols to afford β -lactams with excellent regio- and diastereoselectivities.

The Breit research group demonstrated that Ph₂POMe was a suitable catalytic directing group for hydroformylation [157]. Notably, the functionalization of 1,2-disubstituted olefins and other substrates containing stereocenters proceeded with excellent regio- and stereoselectivity. Additionally, the chemoselective hydroformylation of homoallylic alcohols over unactivated alkenes was observed.

5.3 Monocyclic 1,2-Disubstituted Alkenes

Among monocyclic 1,2-disubstituted alkene substrates, 5-membered ring heterocycles such as dihydrofurans and dihydropyrroles have been the most studied. With these substrates, the simultaneous control of the chemo-, regio-, and enantioselectivity is a key issue since the presence of a heteroatom in the cycle favors in some cases an isomerization process in the presence of a metal-hydride species. Previous studies using achiral ligands demonstrated that the reaction conditions highly affected the chemo- and regioselectivity of this reaction [161, 162]. Indeed, allyl

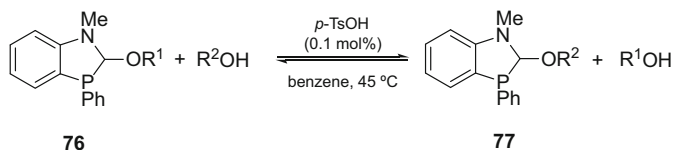
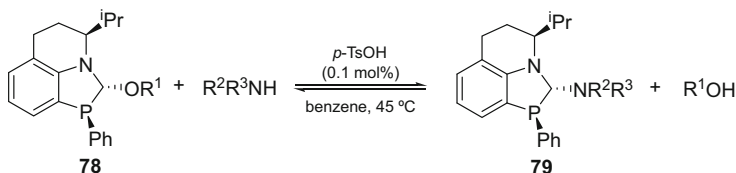
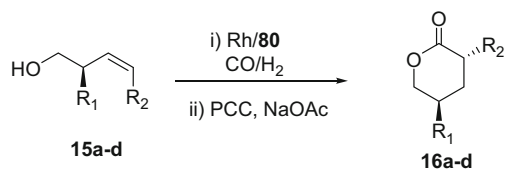


Scheme 29 Synthesis of (+)-patulolide **C** via Rh-catalyzed asymmetric hydroformylation/macro-cyclization cascade using ligand **61a**

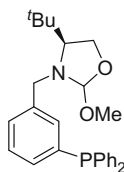
ethers were shown to rapidly isomerize into its vinyl analogue under hydroformylation conditions (Scheme 33). This isomerization process is of critical importance since it has a direct influence not only on the regioselectivity of the reaction, but also on the enantioselectivity since the opposite enantiomers of tetrahydro-3-carbaldehyde are formed from the allylic **17a** and vinylic **17b** isomers of the substrate [163]. It is therefore required to limit the isomerization in order to obtain high selectivities.

In the Rh-catalyzed asymmetric hydroformylation of 2,5-dihydrofuran **17a**, Nozaki and co-workers reported the first successful results using the BINAPHOS ligand **44** which yielded total regioselectivity to the tetrahydro-3-carbaldehyde **18a** with 68% *ee* (*R*) (Scheme 34) [146, 147, 164]. However, when the 2,3-dihydrofuran **17b** was tested with the same catalyst, no regioselectivity was observed and the *ee* obtained for the aldehyde **18b** decreased to 38% with *S* configuration. This catalytic system was thus suitable to avoid isomerization of **17a** into **17b** but not selective for the hydroformylation of **17b**. In the same study, the amine analogues **17c,d** and **17e** were also tested as substrates using the same catalytic system (Scheme 34) and similar results were obtained.

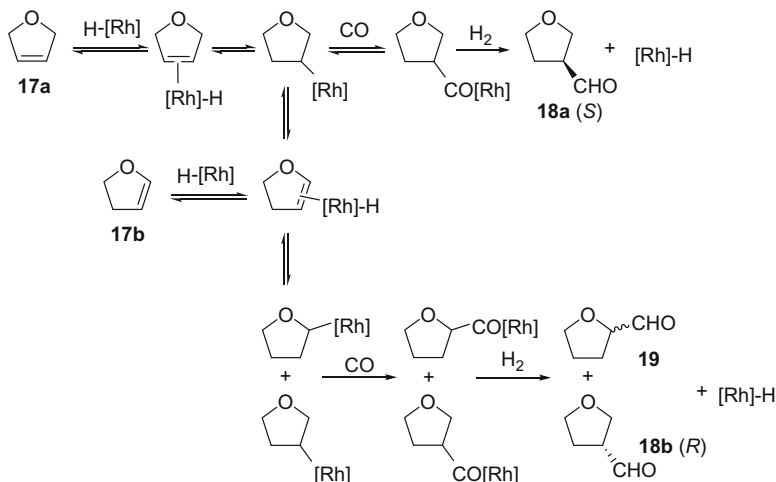
Recently, the previously mentioned 1,3-diphosphites **30**, **40** (Scheme 6) derived from carbohydrates were successfully applied in the Rh-catalyzed hydroformylation of these substrates [72, 165, 166]. The results indicated that ligands **30**, **38–40**, which have a glucose configuration, are the most appropriate to obtain high enantioselective induction in the hydroformylation of these substrates. In the case of the 2,5-dihydrofuran **17a**, the highest enantioselectivity in the aldehyde **18a** was obtained using ligand **38b** (88% *S*). Using this ligand, no isomerization was

**Scheme 30** Alkoxy benzoazaphosphole catalytic directing group**Scheme 31** Tetrahydroisoquinoline alkoxy benzoazaphosphole scaffolding ligand

	regio(%) anti/syn	
16a: R ₁ = Me; R ₂ = Bu	91	87/13
16b: R ₁ = iPr; R ₂ = Bu	95	91/9
16c: R ₁ = Me; R ₂ = Ph	88	83/17
16b: R ₁ = TBSO; R ₂ = Pent	85	89/11

**80****Scheme 32** Rh-catalyzed diastereoselective hydroformylation of homoallylic alcohols using the scaffolding ligand **80**

observed under hydroformylation conditions. Interestingly, the presence of bulky substituents at C-5 such as in ligands **39b–40b** was shown to increase the degree of isomerization. When the 2,3-dihydrofuran (**17b**) was used as substrate, *ee*'s up to 84% (*R*) in aldehyde **18b** were achieved using ligands **39b–40b**, together with a regioselectivity of 80%. The 2,5-dihydropyrrole **17d** was also tested with the Rh/**30b** system, achieving comparable results to those previously reported using ligand **44** (71 and 66%, respectively) (Scheme 9).



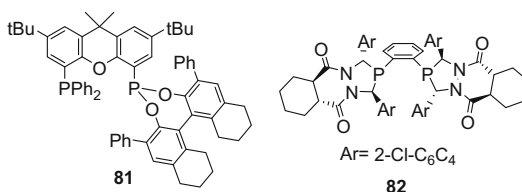
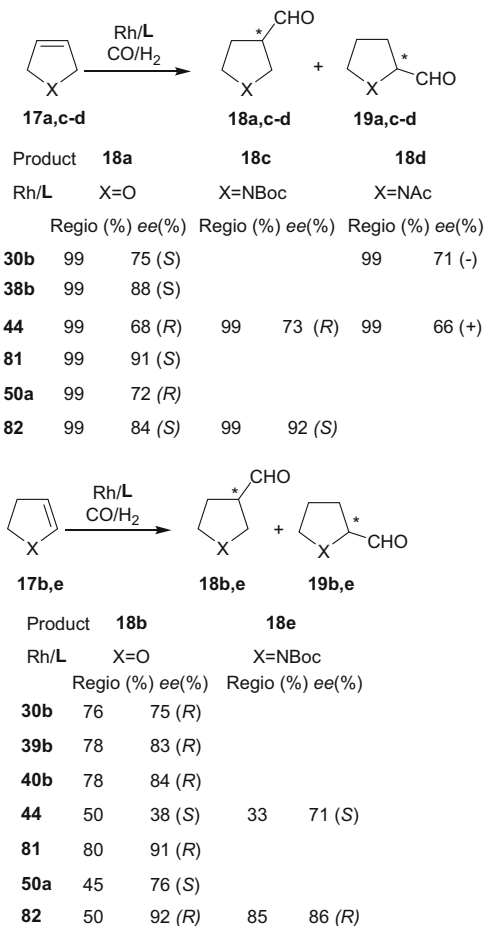
Scheme 33 Isomerization processes observed during the Rh-asymmetric hydroformylation of five-membered heterocyclic alkenes

Reek and co-workers described the synthesis and application of the ligand **81**, containing a skeleton related to the Xantphos diphosphine ligand, in the Rh-catalyzed asymmetric hydroformylation of the dihydrofurans **17a** and **17b** (Scheme 34). This system provided regioselectivities of 99 and 80%, respectively, and very high enantioselectivities (up to 91%) for these substrates [167, 168]. Recently, Zhang and co-workers reported the Rh-asymmetric hydroformylation of five-membered heterocyclic alkenes using a derivative of the diazaphospholane ligand **82** developed by Landis (Scheme 34) [169]. This system provided excellent regio- and enantioselectivities (up to 92%) for several of these substrates. Vidal-Ferran and co-workers also reported the use of the small bite angle phosphine phosphite ligand **50a** (Scheme 11) in the same reaction [109]. When the dihydrofuran **17a** was the substrate, they obtained total regioselectivity and *ee*'s up to 72%, while moderate regioselectivity and *ee*'s up to 76% were obtained when **17b** was tested.

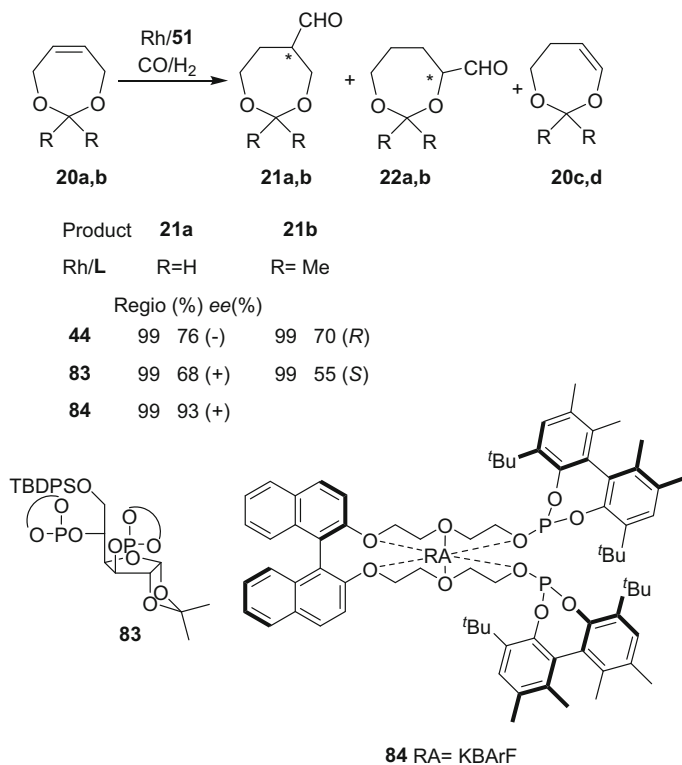
More recently, the same authors reported the use of conformationally transformable α,ω -bisphosphite ligands combined with an alkali metal BArF salt as a regulation agent (RA) [77]. These ligands provide enantioselectivities up to 82% in the asymmetric hydroformylation of 2,5-dihydrofuran **17a** and 2,3-dihydrofuran **17b**.

The asymmetric Rh-catalyzed hydroformylation of dioxapines **20a,b** was reported using the BINAPHOS ligand **44** and 1,3-diphosphite ligands derived from carbohydrates **83** (Scheme 35) [146–166]. Using the ligand **44**, total regioselectivity to **21a,b** was achieved, together with *ee*'s up to 76%. Among the carbohydrate derived ligands that were tested, the ligand **83** provided the best results (Scheme 35), affording total regioselectivity to **21a,b** and up to 68% *ee* and thus indicating that no isomerization of **20a,b** had occurred. More recently, Vidal-Ferran and co-workers reported the highest *ee* in the asymmetric hydroformylation of the dioxapines **20a** by using an Rh-complex bearing the diphosphite **84** (Scheme 35) [77].

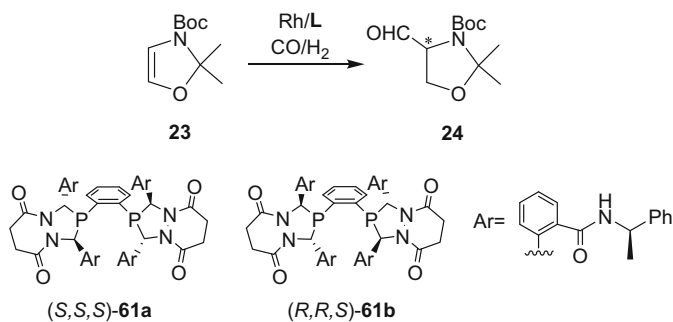
Scheme 34 Rh-catalyzed asymmetric hydroformylation of five-membered heterocyclic alkenes **17a–e**



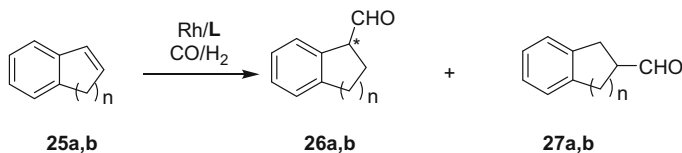
In 2012, the application of the asymmetric hydroformylation of cyclic disubstituted olefins was employed to provide useful chiral molecules like the Garner's aldehyde, a popular building block [170, 171]. Both enantiomers of this molecule were prepared through this reaction using catalytic systems bearing the diastereoisomeric bis-diazaphospholane ligands **61a** and **61b** (Scheme 36) [172]. The *S* enantiomer can



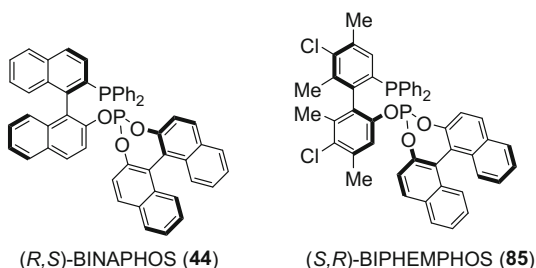
Scheme 35 Rh-catalyzed asymmetric hydroformylation of **20a,b**



Scheme 36 Synthesis of Garner's aldehyde through Rh-catalyzed asymmetric hydroformylation of the cyclic disubstituted olefin *N*-Boc-2,2-dimethyl-2,3-dihydrooxazole **23**



Product	L	Regio (%)	ee(%)
26a n=1	85	92	88
	44	92	83
26b n=2	85	96	97
	44	96	96



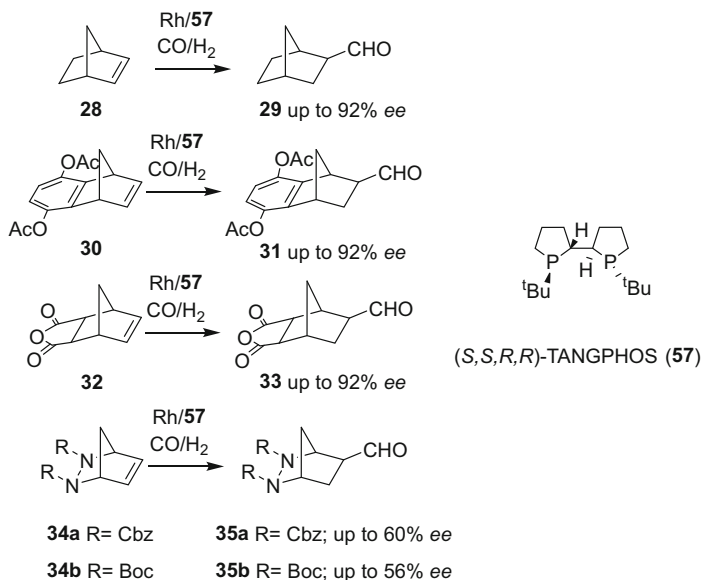
Scheme 37 Rh-catalyzed asymmetric hydroformylation of bicyclic alkenes using the ligands (R, S)-BINAPHOS (**44**) and BIPHEMPHOS (**85**)

be produced in 97% ee in the presence of (*S,S,S*)-**61a** while the *R* product is formed with a slightly lower ee's (94%), using the ligand (*R,R,S*)-**61b**. The reactions were run on a *ca.* 5 mmol scale at 55°C under 10 bar of syngas (1:1) using 2 mol% Rh catalyst.

5.4 Bicyclic 1,2-Disubstituted Alkenes

The Rh-catalyzed asymmetric hydroformylation of substrates **25a** and **25b** was reported by Nozaki and co-workers using the ligands **44** and **85** (Scheme 37) [146, 147]. The results are really remarkable, in particular with substrate **25b**, for which compound **26b** was obtained with practically total regio- and enantioselectivity (Scheme 37). The corresponding products **26a** and **26b** are of interest since the aldehyde **26a** can be converted in a single step into the corresponding amine which exhibits hypotensive activity and the product **26b** is a synthetic intermediate to produce a vasoconstrictor tetrahydrozoline [173].

Another bicyclic alkene substrate of interest for carbonylation reactions is the norbornene **28** and its derivatives. The first reports on the asymmetric Rh-hydroformylation of norbornene afforded low enantiomeric induction with ee's below 25% [174, 175]. In



Scheme 38 Rh-catalyzed asymmetric hydroformylation of norbornene derivatives using the diphospholane ligand **57**

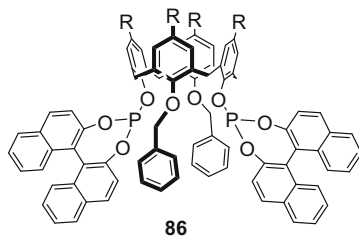


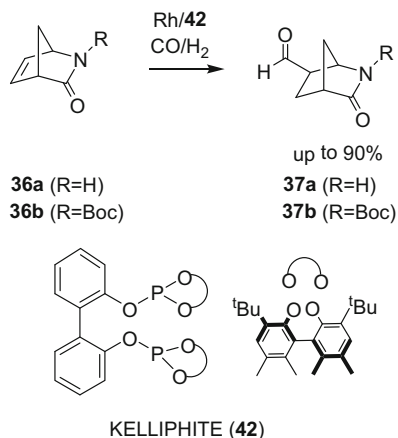
Fig. 1 Hemispherical diphosphite ligands **86** with a conical calixarene skeleton

2005, Bunel and co-workers reported the first highly enantioselective Rh-catalyzed hydroformylation of norbornene into the *exo* aldehyde using diphospholane ligands, reaching *ee*'s up to 92% with the TANGPHOS ligand **50** [176]. Using the same ligand, they also reported the hydroformylation of several derivatives of this substrate with similar enantioselectivities (Scheme 38).

Recently, the hemispherical diphosphite ligands **86** (Fig. 1) with a conical calixarene skeleton was used in the asymmetric Rh-hydroformylation of norbornene, achieving enantioselectivities up to 61% with the *exo* aldehyde being the major product [177].

More recently, the KELLIPHITE ligand (**42**) was employed in the Rh-catalyzed asymmetric hydroformylation of bicyclic lactam azabicyclo-[2.2.1]hept-5-en-3-

Scheme 39 Rh-catalyzed asymmetric hydroformylation of bicyclic lactam azabicyclo-[2.2.1]hept-5-en-3-ones using the KELLIPHITE ligand **42**



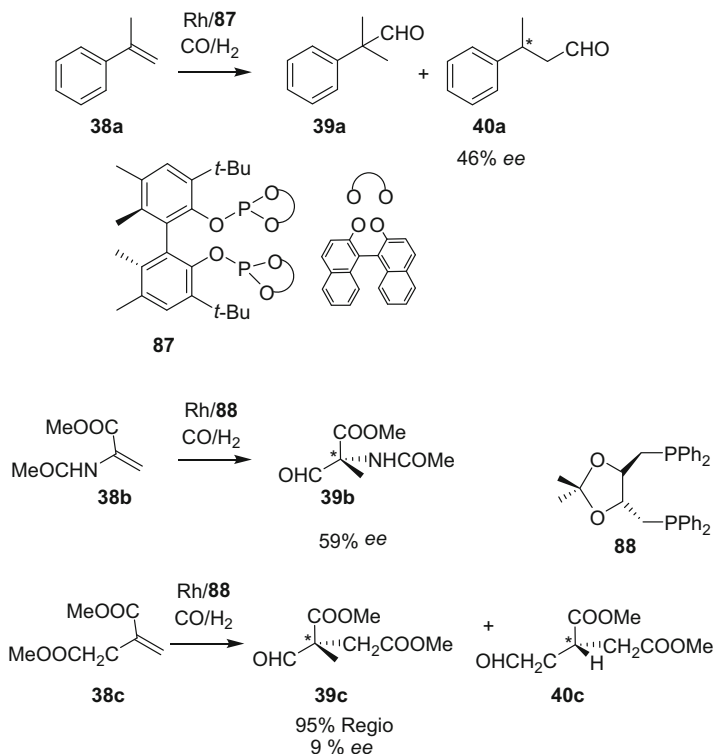
ones with very good results. The reaction was completely *exo*-selective, yielding total conversions and excellent regioselectivities (up to 90%) [178] (Scheme 39).

5.5 1,1'-Disubstituted Alkenes

The asymmetric hydroformylation of 1,1'-disubstituted alkenes differs from the classical asymmetric hydroformylation of monosubstituted terminal alkenes since the desired product is the linear aldehyde (Scheme 2) [179].

Indeed, the Rh-catalyzed asymmetric hydroformylation of 1,1-methylstyrene (**38a**) using diphosphite ligand **87** (Scheme 40) to form the linear product (**40a**) was recently patented. The enantioselectivity was, however, moderate (*ee* up to 46%) [180].

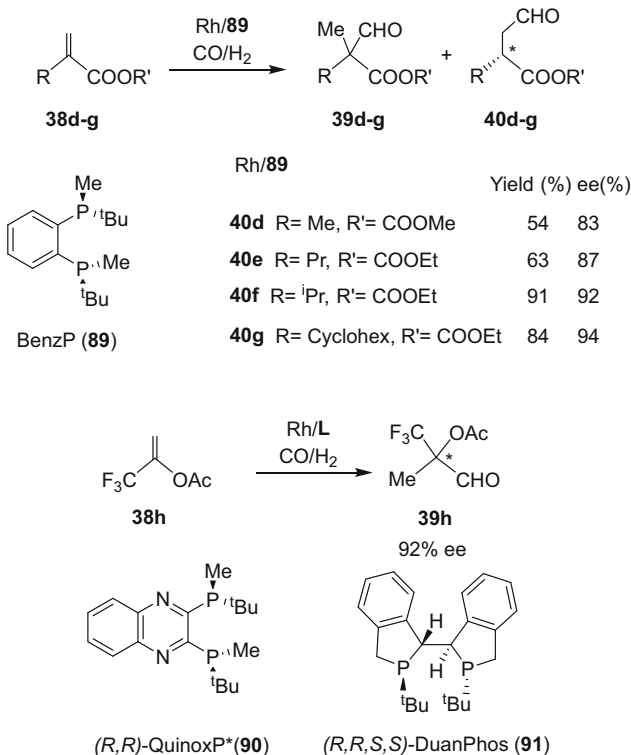
Interestingly, when dehydro amino acid derivatives **38b** and dimethyl itaconate **38c** were used as substrates (Scheme 40) in the presence of $[\text{RhH}(\text{CO})(\text{PPh}_3)_3]$ and 1–6 equivalents of the (R,R)-DIOP ligand **88**, the formation of the branched products was largely favored with moderate enantioselectivity (*ee*'s up to 59%). In this process highly functionalized quaternary carbons are easily obtained from common products. This interesting reaction deserves more attention by researchers in the field. It should be noted that when the α,β -unsaturated carboxylic compounds such as **38c** are hydroformylated in the presence of the $[\text{PtCl}(\text{SnCl}_3)]$, the only hydroformylation product obtained was the linear aldehyde with *ee*'s up to 82% [26].



Scheme 40 Rh-catalyzed asymmetric hydroformylation of 1,1'-disubstituted alkenes

Recently, Buchwald et al. reported the Rh-catalyzed asymmetric hydroformylation of 1,1-disubstituted alkenes (α -alkylacrylates) using the 1,3-diphosphine ligand BenzP (**89**). With this ligand, good regio- (up to 91%) and enantioselectivities (up to 94%) were achieved (Scheme 41) [181]. The fine-tuning of the partial pressures of CO/H₂ minimizes the problem of the side reactions; in fact, the mild reaction conditions make it safe for general laboratory use (10 bar 1:5 CO/H₂, 100°C).

More recently, the same authors reported the asymmetric hydroformylation of 3,3,3-trifluoroprop-1-en-2-yl acetate **39h** using the P-stereogenic ligands QuinoxP (**90**) and DuanPhos (**91**) with 92% ee [182]. After oxidation of the resulting aldehyde and hydrolysis, crystallization provided enantiomerically pure 2-trifluoromethylallylic acid.



Scheme 41 Rh-catalyzed asymmetric hydroformylation of α -alkylacrylates

6 Conclusions

Rhodium is currently the metal of choice to achieve high enantioselectivities in the hydroformylation of a relatively large variety of alkene substrates. The elucidation of the different steps of the catalytic cycle and the characterization of the resting state, together with the discovery of several types of ligands that are able to provide high enantioselectivities, have made the rhodium-catalyzed hydroformylation a synthetically useful tool.

In the catalytic cycle, the complex **16** has been identified as the resting state of the process. An important feature for bidentate ligands is their possible coordination to the rhodium center in eq–eq or eq–ax fashions. Indeed, although the enantioface discrimination occurs at the alkene coordination step from the square-planar species **17**, experimental observations showed that high enantioselectivity in asymmetric hydroformylation of alkenes is obtained using ligands that lead to the formation of only one isomer of the resting state **16**. This fact could be attributed to the similitude in the structures of the Rh hydride species **16** and **18**. The co-existence of the two possible isomers in solution was shown to always provide lower enantioselectivity.

Commonly, the synthesis of a chiral compound by asymmetric hydroformylation involves the introduction of a formyl group in a substituted olefinic carbon. This process has been widely studied mainly for monosubstituted alkenes. However, since the favored process is usually the introduction of this group in the less substituted carbon, this transformation is only useful for substrates containing electron-withdrawing group(s) ($R = Ph$, heteroatom) which direct the introduction of the formyl group in the most substituted carbon. Consequently, a regioselectivity problem must be first considered. The presence of a functional group at the allylic position, which contributes to stabilize the double bond, always supposes an additional issue, since isomerization takes place easily. This isomerization can be controlled by the appropriate choice of ligand and reaction conditions. For instance, increasing the CO pressure and/or decreasing the reaction temperature reduce the degree of isomerization.

Furthermore, low temperatures ($<70^{\circ}\text{C}$) are usually required to achieve high enantioselectivities although under these conditions, the reaction rate is usually low. A way to partially circumvent this problem is increasing the H_2 pressure thus shifting the equilibrium from the inactive complex **23** towards the active species **16**.

1,2-Disubstituted substrates are particularly challenging when similar substituents such as alkyl substituents are present in both positions. However, higher regio- and enantioselectivity can be achieved when one of the substituents direct the regioselectivity, as is the case of 2,3-dihydrofuran, dihydropyrrol, indene, or 1,2-dihydronaphthalene. In the case of symmetrically substituted alkenes such as 2,5-dihydrofuran and norbornene, no regiocontrol is required and high activities and enantioselectivities have been achieved in asymmetric hydroformylation.

1,1-Disubstituted or 1,1,2-trisubstituted are more challenging substrates. The general trend is the introduction of the formyl group onto the less substituted carbon, thus creating the chiral center at the more substituted carbon atom. This trend is respected in the hydroformylation of such substrates using Pt catalysts, achieving high regio- and enantioselectivities. Interestingly, it is also possible to introduce the formyl group at the more substituted carbon using Rh catalysts, thus creating a highly functionalized chiral quaternary center.

For years, ligands containing phosphite moieties such as diphosphites and phosphine–phosphites were considered as the most successful ligands to achieve high enantioselectivities. For instance, diphosphite ligands **24**, **30**, and **42** are highly effective in the asymmetric Rh-catalyzed hydroformylation of several alkene substrates and the phosphite–phosphine BINAPHOS (**44**) or its derivatives **46** and **47** have been very successful ligands in terms of selectivity and scope. Recently, however, diphosphines in which the P atoms are incorporated in a ring (**56–59**) have also shown to induce high levels of enantioselectivity in this process. Furthermore, diazaphospholane ligands **61a**, **61b**, and **72** are currently the most efficient ligand in the asymmetric hydroformylation of alkenes, with exceptional results in terms of regio- and enantioselectivity. These ligands have also been successfully immobilized onto solid support in order to recycle and reuse the corresponding catalysts and employ them under continuous conditions. Over the last years, these ligands were also applied in the enantioselective hydroformylation of specific substrates for the synthesis of various organic molecules of biological and/or synthetic interest.

It can consequently be concluded that the key to achieve high enantioselectivities is not the type of phosphorus function involved in the coordination to the metal, but the particular spatial arrangement of the coordinated ligand. Furthermore, recently, supramolecular strategies have also been very successful in asymmetric hydroformylation, clearly indicating that the control of the second coordination sphere could be key to reach selectivity for challenging substrates.

Nowadays, a variety of chiral products incorporating a formyl unit can be enantioselectively prepared by Rh-catalyzed asymmetric hydroformylation and this process can therefore be considered as a powerful and useful tool in organic synthesis.

Recently, an Rh catalyst was reported to convert alkenes to aldehydes without the need of gases through transfer hydroformylation [183, 184]. In this promising process, the catalyst transfers the equivalent of H₂ and CO between a sacrificial aldehyde and an alkene under mild conditions without evolving gases. Although this reaction is still at a very early stage, the development of efficient catalysts for the control of the selectivity could provide a general method for the formation of chiral aldehydes without the need of syngas.

References

1. Roelen O (1994) Chem Abstr 38:550
2. Roelen O (1938/1952) Chemische Verwertungsgesellschaft, mBH Oberhausen, DE Patent 849-584
3. Roelen O (1943) US Patent 2,317,066
4. Cornils B, Hermann WA (eds) (2002) Applied homogeneous catalysis with organometallic compounds, vol 1. Wiley-VCH, Weinheim
5. Weissermel K, Arpe JP (2003) Industrial organic chemistry. Wiley-VCH, Weinheim
6. Klosin J, Landis CR (2007) Acc Chem Res 40:1251–1259
7. Breit B (2007) Top Curr Chem 279:139–172
8. Ungvári F (2007) Coord Chem Rev 251:2087–2102
9. Ungvári F (2007) Coord Chem Rev 251:2072–2086
10. Wiese KD, Obst D (2006) Top Organomet Chem 18:1–33
11. Gual A, Godard C, Castillón S, Claver C (2010) Tetrahedron Asymmetry 21:1135–1146
12. van Leeuwen PWNM, Kamer PCJ, Claver C, Pàmies O, Diéguez M (2011) Chem Rev 111:2077–2118
13. Börner A, Franke R (2016) Hydroformylation: fundamentals, processes, and applications in organic synthesis. Wiley-VCH, Weinheim
14. Taddei M, Mann A (eds) (2013) Hydroformylation for organic synthesis. Springer, Heidelberg
15. Breit B (2007) Aldehydes: synthesis by hydroformylation of alkenes. In: Brückner R (ed) Science of synthesis, vol 25. Thieme, Stuttgart
16. van Leeuwen PWNM (2004) Homogeneous catalysis: understanding the art. Kluwer, Dordrecht and references therein
17. Trost BM (1991) Science 254:1471–1477
18. Breit B (2003) Acc Chem Res 36:264–275
19. Eilbracht P, Schmidt AM (2006) Top Organomet Chem 18:65–95
20. Evans D, Osborn JA, Wilkinson G (1968) J Chem Soc A 1968:3133–3142
21. Evans D, Yagupsky G, Wilkinson G (1968) J Chem Soc A 1968:2660–2665

22. Young JF, Osborn JA, Jardine FH, Wilkinson G (1965) *J Chem Soc Chem Commun* 1965:131–132
23. van Leeuwen PWNM, Claver C (2000) Rhodium catalysed hydroformylation. Kluwer, Dordrecht and references therein
24. Consiglio G, Nefkens SCA, Borer A (1991) *Organometallics* 10:2046–2051
25. Stille JK, Su H, Brechot P, Parrinello G, Hegedus LS (1991) *Organometallics* 10:1183–1189
26. Agbossou F, Carpentier JF, Mortreux A (1995) *Chem Rev* 95:2485–2506
27. Gladiali S, Bayón JC, Claver C (1995) *Tetrahedron Asymmetry* 6:1453–1474
28. Jongsma T, Challa G, van Leeuwen PWNM (1991) *J Organomet Chem* 421:121–128
29. Selent D, Wiese KD, Röttger D, Börner A (2000) *Angew Chem Int Ed* 39:1639–1641
30. Breit B, Winde R, Mackewitz T, Paciello R, Harms K (2001) *Chem Eur J* 7:3106–3121
31. Siegbahn PEM (1993) *J Am Chem Soc* 115:5803–5812
32. Matsubara T, Koga N, Ding Y, Musaev DG, Morokuma K (1997) *Organometallics* 16:1065–1078
33. Schmid R, Herrmann WA, Frenking G (1997) *Organometallics* 16:701–708
34. Gonzalez-Blanco O, Branchadell V (1997) *Organometallics* 16:5556–5562
35. van der Veen LA, Boele MDK, Bregman FR, Kamer PCJ, van Leeuwen PWNM, Kees G, Fraanje J, Schenck H, Bo C (1998) *J Am Chem Soc* 120:11616–11626
36. Gleich D, Schmid R, Herrmann WA (1998) *Organometallics* 17:4828–4834
37. Gleich D, Schmid R, Herrmann WA (1998) *Organometallics* 17:2141–2143
38. Gleich D, Schmid R, Herrmann WA (1999) *Organometallics* 18:4354–4361
39. van der Veen LA, Keeven PH, Schoemaker GC, Reek JNH, Kamer PCJ, van Leeuwen PWNM, Lutz M, Spek AL (2000) *Organometallics* 19:872–883
40. Versluis L, Ziegler T, Fan L (1990) *Inorg Chem* 29:4530–4536
41. Rocha WA, De Almeida WB (2000) *Int J Quantum Chem* 78:42–51
42. Carbó JJ, Maseras F, Bo C, van Leeuwen PWNM (2001) *J Am Chem Soc* 123:7630–7637
43. Alagona G, Ghio C, Lazzaroni R, Settambolo R (2001) *Organometallics* 20:5394–5404
44. Decker SA, Cundari TR (2002) *New J Chem* 26:129–135
45. Landis CR, Uddin J (2002) *J Chem Soc Dalton Trans* 47:729–742
46. Gleich D, Hutter J (2004) *Chem Eur J* 10:2435–2444
47. Zuidema E, Escorihuela L, Eichelsheim T, Carbó JJ, Bo C, Kamer PCJ, van Leeuwen PWNM (2008) *Chem Eur J* 14:1843–1853
48. Lazzaroni R, Settambolo R, Alagona G, Ghio C (2010) *Coord Chem Rev* 254:696–706
49. Kumar M, Subramaniam B, Chaudhari RV, Jackson TA (2014) *Organometallics* 33:4183–4191
50. Kumar M, Chaudhari RV, Subramaniam B, Jackson TA (2015) *Organometallics* 34:1062–1073
51. Keulemans AIM, Kwantes A, van Bavel T (1948) *Recl Trav Chim Pays-Bas* 67:298–308
52. Heck RF (1969) *Acc Chem Res* 2:10–16
53. Kamer PCJ, van Rooy A, Schoemaker GC, van Leeuwen PWNM (2004) *Coord Chem Rev* 248:2409–2424
54. Deutsch PP, Eisenberg R (1990) *Organometallics* 9:709–718
55. Castellanos-Páez A, Castellón S, Claver C, van Leeuwen PWNM, de Lange WGJ (1998) *Organometallics* 17:2543–2552
56. Jacobs I, de Bruin B, Reek JNH (2015) *ChemCatChem* 7:1708–1718
57. Masdeu-Bultó AM, Orejon A, Castellón S, Claver C (1996) *Tetrahedron Asymmetry* 7:1829–1834
58. Chen C, Dong X-Q, Zhang X (2016) *Chem Rec* 16:2674–2686
59. Diéguez M, Pàmies O, Claver C (2004) *Tetrahedron Asymmetry* 15:2113–2122
60. Babin JE, Whiteker GT (1993) Asymmetric synthesis world patent, WO 9303839
61. Whiteker GT, Briggs JR, Babin JE, Barne GA (2003) Asymmetric catalysis using biphosphite ligands in chemical industries, vol 89. Marcel Dekker, New York
62. van Leeuwen PWNM, van Roy A, Jongma T, Orije EEN, Kamer PCJ (1992) 203rd Meeting of the American Chemical Society, New York, Abstract I&EC 104
63. Buisman GJH, Vos EJ, Kamer PCJ, van Leeuwen PWNM (1995) *J Chem Soc Dalton Trans* 1995:409–417

64. Buisman GJH, van der Veen LA, Klootwijk A, de Lange WGJ, Kamer PCJ, van Leeuwen PWNM, Vogt D (1997) *Organometallics* 16:2929–2939
65. Cserépi-Szűcs S, Tóth I, Párkányi L, Bakos J (1998) *Tetrahedron Asymmetry* 9:3135–3142
66. Abdallah R, Breuzard JAJ, Bonet MC, Lemaire M (2006) *J Mol Catal A: Chem* 249:218–222
67. Buisman GJH, van der Veen LA, Kamer PCJ, van Leeuwen PWNM (1997) *Organometallics* 16:5681–5687
68. Buisman GJH, Martin ME, Vos EJ, Klootwijk A, Kamer PCJ, van Leeuwen PWNM (1995) *Tetrahedron Asymmetry* 6:719–738
69. Pàmies O, Net G, Ruiz A, Claver C (2000) *Tetrahedron Asymmetry* 11:1097–1108
70. Diéguez M, Pàmies O, Ruiz A, Castillón S, Claver C (2001) *Chem Eur J* 7:3086–3094
71. Diéguez M, Pàmies O, Ruiz A, Claver C (2002) *New J Chem* 26:827–833
72. Gual A, Godard C, Castillón S, Claver C (2010) *Adv Synth Catal* 352:463–477
73. Gual A, Godard C, Claver C, Castillón S (2009) *Eur J Org Chem* 2009:1191–1201
74. Cogley CJ, Klosin J, Qin C, Whiteker GT (2004) *Org Lett* 6:3277–3280
75. Cogley CJ, Gardner K, Klosin J, Praquin C, Hill C, Whiteker GT, Zanotti-Gerosa A (2004) *J Org Chem* 69:4031–4040
76. Vidal-Ferran A, Mon I, Bauzá A, Frontera A, Rovira L (2015) *Chem Eur J* 21:11417–11426
77. Rovira L, Vaquero M, Vidal-Ferran A (2015) *J Org Chem* 80:10397–10403
78. Sakai N, Mano S, Nozaki K, Takaya H (1993) *J Am Chem Soc* 115:7033–7034
79. Nozaki K (2005) *Chem Rec* 5:376–384 and references therein
80. Tanaka R, Nakano K, Nozaki K (2007) *J Org Chem* 72:8671–8676
81. Nakano K, Tanaka R, Nozaki K (2006) *Helv Chim Acta* 89:1681–1686
82. Shibahara F, Nozaki K, Hiyama T (2003) *J Am Chem Soc* 125:8555–8560
83. Nozaki K, Matsuo T, Shibahara F, Hiyama T (2003) *Organometallics* 22:594–600
84. Shibahara F, Nozaki K, Matsuo T, Hiyama T (2002) *Bioorg Med Chem Lett* 12:1825–1827
85. Nozaki K, Matsuo T, Shibahara F, Hiyama T (2001) *Adv Synth Catal* 343:61–63
86. Horiuchi T, Ohta T, Shirakawa E, Nozaki K, Takaya H (1997) *Tetrahedron* 53:7795–7780
87. Nozaki K, Nanno T, Takaya H (1997) *J Organomet Chem* 527:103–108
88. Nozaki K, Li WG, Horiuchi T, Takaya H (1996) *J Org Chem* 61:7658–7659
89. Horiuchi T, Ohta T, Nozaki K, Takaya H (1996) *Chem Commun* 1996:155–156
90. Nanno T, Sakai N, Nozaki K, Takaya H (1995) *Tetrahedron Asymmetry* 6:2583–2591
91. Lambers-Verstappen MMH, de Vries JG (2003) *Adv Synth Catal* 345:478–482
92. Nozaki K, Sakai N, Nanno T, Higashijima T, Mano S, Horiuchi T, Takaya H (1997) *J Am Chem Soc* 119:4413–4423
93. Nozaki K, Ito Y, Shibahara F, Shirakawa E, Ohta T, Takaya H, Hiyama T (1998) *J Am Chem Soc* 120:4051–4052
94. Aguado-Ullate S, Saureu S, Guasch L, Carbó JJ (2012) *Chem Eur J* 18:995–1005
95. Yan Y, Zhang X (2006) *J Am Chem Soc* 128:7198–7202
96. Wei B, Chen C, You C, Lv H, Zhang X (2017) *Org Chem Front* 4:288–291
97. Zhang X, Cao B, Yan Y, Yu S, Ji B, Zhang X (2010) *Chem Eur J* 16:871–877
98. Zhang X, Cao B, Yu S, Zhang X (2010) *Angew Chem Int Ed* 49:4047–4050
99. Aguado-Ullate S, Guasch L, Urbano-Cuadrado M, Bo C, Carbó JJ (2012) *Catal Sci Technol* 2:1694–1704
100. Deerenberg S, Kamer PCJ, van Leeuwen PWNM (2000) *Organometallics* 19:2065–2072
101. Pàmies O, Net G, Ruiz A, Claver C (2001) *Tetrahedron Asymmetry* 12:3441–3445
102. Arena CG, Faraone F, Graiff C, Tiripicchio A (2002) *Eur J Inorg Chem* 2002:711–716
103. Rubio M, Suárez A, Álvarez E, Bianchini C, Oberhauser W, Peruzzini M, Pizzano A (2007) *Organometallics* 26:6428–6436
104. Robert T, Abiri Z, Wassenaar J, Sandee AJ, Meeuwissen J, Sandee AJ, de Bruin B, Siegler MA, Spek AL, Reek JNH (2010) *Organometallics* 29:2413–2421
105. Arribas I, Vargas S, Rubio M, Suárez A, Domene C, Alvarez E, Pizzano A (2010) *Organometallics* 29:5791–5804
106. Doro F, Reek JNH, Leeuwen PWNM (2010) *Organometallics* 29:4440–4447

107. Robert T, Abiri Z, Wassenaar J, Sandee AJ, Romanski S, Neudörfel J-M, Schmalz H-G, Reek JNH (2010) *Organometallics* 29:478–483
108. Wassenaar J, de Bruin B, Reek JNH (2010) *Organometallics* 29:2767–2776
109. Fernández-Pérez H, Benet-Buchholz J, Vidal-Ferran A (2013) *Org Lett* 15:3634–3637
110. Lao JR, Benet-Buchholz J, Vidal-Ferran A (2014) *Organometallics* 33:2960–2963
111. Fee Czauderna C, Cordes DB, Slawin AMZ, Müller C, van der Vlugt JI, Kamer PCJ (2014) *Eur J Inorg Chem* 2014:1797–1810
112. Jouffroy M, Sémeril D, Armspach D, Matt D (2013) *Eur J Org Chem* 2013:6069–6077
113. Bellini R, Reek JNH (2012) *Chem Eur J* 18:13510–13519
114. Noonan GM, Fuentes JA, Cobley CJ, Clarke ML (2012) *Angew Chem Int Ed* 51:2477–2480
115. Axtell AT, Klosin J, Abboud KA (2006) *Organometallics* 25:5003–5009
116. Tan R, Zheng X, Qu B, Sader CA, Fandrick KR, Senanayake CH, Zhang X (2016) *Org Lett* 18:3346–3349
117. Axtell AT, Colbey CJ, Klosin J, Whiteker GT, Zanotti-Gerosa A, Abboud KA (2005) *Angew Chem Int Ed* 44:5834–5838
118. Axtell AT, Klosin J, Whiteker GT, Cobley CJ, Fox ME, Jackson M, Abboud KA (2009) *Organometallics* 28:2993–2999
119. Morimoto T, Fujii T, Miyoshi K, Makado G, Tanimoto H, Nishiyama Y, Kakiuchi K (2015) *Org Biomol Chem* 13:4632–4636
120. Yu Z, Eno MS, Annis AH, Morken JP (2015) *Org Lett* 17:3264–3267
121. Clarkson GJ, Ansell JR, Cole-Hamilton DJ, Pogorzelec PJ, Whittell J, Wills M (2004) *Tetrahedron Asymmetry* 15:1787–1792
122. Clark TP, Landis CR, Freed SL, Klosin J, Abboud KA (2005) *J Am Chem Soc* 127:5040–5042
123. Adint TT, Landis CR (2014) *J Am Chem Soc* 136:7943–7953
124. Nelsen ER, Brezny AC, Landis CR (2015) *J Am Chem Soc* 137:14208–14219
125. Johnson MD, May SA, Calvin JR, Lambertus GR, Kokitkar PB, Landis CR, Jones BR, Abrams ML, Stout JR (2016) *Org Process Res Dev* 20:888–900
126. Abrams ML, Buser JY, Calvin JR, Johnson MD, Lambertus GR, Landis CR, Martinelli JR, May SA, McFarland AD, Stout JR (2016) *Org Process Res Dev* 20:901–910
127. Miles KC, Abrams ML, Landis CR, Stahl SS (2016) *Org Lett* 18:3590–3593
128. Zhao B, Peng X, Wang W, Xia C, Ding K (2008) *Chem Eur J* 14:7847–7857
129. Peng X, Wang Z, Xia C, Ding K (2008) *Tetrahedron Lett* 49:4862–4864
130. Allmendinger S, Kinuta H, Breit B (2015) *Adv Synth Catal* 357:41–45
131. Hammerer T, Weisgerber L, Schenk S, Stelzer O, Englert U, Leitner W, Franciò G (2012) *Tetrahedron Asymmetry* 23:53–59
132. García-Simóm C, Gramage-Doria R, Raoufoghaddam S, Parella T, Costas M, Ribas X, Reek JNH (2015) *J Am Chem Soc* 137:2680–2687
133. Hua Z, Vassar VC, Choi H, Ojima I (2004) *Proc Natl Acad Sci* 101:5411–5416
134. Mazuela J, Pàmies O, Diéguez M, Palais L, Rosset S, Alexakis A (2010) *Tetrahedron Asymmetry* 21:2153–2157
135. Breit B, Seiche W (2005) *Angew Chem Int Ed* 44:1640–1643
136. Kuil M, Goudriaan PE, van Leeuwen PWNM, Reek JNH (2006) *Chem Commun* 2006:4679–4681
137. Kuil M, Goudriaan PE, Kleij AW, Tooke DM, Spek AL, van Leeuwen PWNM, Reek JNH (2007) *Dalton Trans* 2007:2311–2320
138. Consiglio G, Kollar L, Kolliker R (1990) *J Organomet Chem* 396:375–383
139. García L, Claver C, Dieguez M, Masdeu-Bulto AM (2006) *Chem Commun* 2006:191–193
140. Noonan GM, Newton D, Cobley CJ, Suárez A, Pizzano A, Clarke ML (2010) *Adv Synth Catal* 352:1047–1104
141. Watkins AL, Landis CR (2011) *Org Lett* 13:164–167
142. McDonald RI, Wong GW, Neupane RP, Stahl SS, Landis CR (2010) *J Am Chem Soc* 132:14027–14029
143. Schmitz C, Holthusen K, Leitner W, Franciò G (2016) *ACS Catal* 6:584–1589
144. Kollar L, Farkas E, Batiu J (1997) *J Mol Catal A: Chem* 115:283–288
145. Axet MR, Castellón S, Claver C (2006) *Inorg Chim Acta* 359:2973–2979

146. Nozaki K, Takaya H, Hiyama T (1997) *Top Catal* 4:175–185
147. Sakai N, Nozaki K, Takaya H (1994) *J Chem Soc Chem Commun* 1994:395–396
148. Bellini R, Chikkali SH, Berthon-Gelloz G, Reek JNH (2011) *Angew Chem Int Ed* 50:7342–7345
149. Gadzikwa T, Bellini R, Dekker HL, Reek JNH (2012) *J Am Chem Soc* 134:2860–2863
150. Leigh Abrams M, Foarta F, Landis CR (2014) *J Am Chem Soc* 136:14583–14588
151. Rodphaya D, Sekiguchi J, Yamada Y (1986) *J Antibiot* 5:629–635
152. Mori K, Sakai T (1988) *Liebigs Ann Chem* 1:13–17
153. Risi MR, Burke SD (2012) *Org Lett* 14:1180–1182
154. Risi RM, Maza AM, Burke SD (2015) *J Org Chem* 80:204–216
155. Foarta F, Landis CR (2016) *J Org Chem* 81:11250–11255
156. Yeung CS, Dong VM (2011) *Angew Chem Int Ed* 50:809–812
157. Grünanger CU, Breit B (2008) *Angew Chem Int Ed* 47:7346–7349
158. Hardie RC (2007) *Nature* 450:37–39
159. Lightburn TE, Dombrowski MT, Tan KL (2008) *J Am Chem Soc* 130:9210–9211
160. Joe CL, Blaisdell TP, Geoghan AF, Tan KL (2014) *J Am Chem Soc* 136:8556–8559
161. Polo A, Real J, Claver C, Castellón S, Bayón JC (1990) *J Chem Soc Chem Commun* 1990:600–601
162. Polo A, Claver C, Castellón S, Ruiz A, Bayón JC, Real J, Mealli C, Masi D (1992) *Organometallics* 11:3525–3533
163. del Río I, van Leeuwen PWNM, Claver C (2001) *Can J Chem* 79:560–565
164. Horiuchi T, Otha T, Shirakawa E, Nozaki K, Takaya H (1997) *J Org Chem* 62:4285–4292
165. Diéguez M, Pàmies O, Claver C (2005) *Chem Commun* 2005:1221–1223
166. Mazuela J, Coll M, Pàmies O, Diéguez M (2009) *J Org Chem* 74:5440–5445
167. Chikkali SH, Bellini R, Berthon-Gelloz G, Van der Vlugt JI, de Bruin B, Reek JNH (2010) *Chem Commun* 46:1244–1246
168. Chikkali SH, Bellini R, de Bruin B, Van der Vlugt JI, Reek JNH (2012) *J Am Chem Soc* 134:6607–6616
169. Zheng X, Xu K, Zhang X (2015) *Tetrahedron Lett* 56:1149–1152
170. Liang X, Andersch J, Bols M (2001) *J Chem Soc Perkin Trans* 1:2136–2157
171. Hoffman T, Kolleth A, Rigby JH, Arseniyadis S, Cossy J (2010) *Org Lett* 12:3348–3351
172. Clemens AJL, Burke SD (2012) *J Org Chem* 77:2983–2985
173. Botteghi C, Paganelli S, Schionato A, Marchetti M (1991) *Chirality* 3:355–369
174. Consiglio G, Rama FJ (1991) *J Mol Catal* 66:1–5
175. Lu S, Li X, Wang A (2000) *Catal Today* 63:531–536
176. Huang J, Bunel E, Allgeier A, Tedrow J, Storz T, Preston J, Correl T, Manley D, Soukup T, Jensen R, Syed R, Moniz G, Larsen R, Martinelli M, Reider PJ (2005) *Tetrahedron Lett* 46:7831–7834
177. Sémeril D, Matt D, Toupet L (2008) *Chem Eur J* 14:7144–7155
178. Noonan GM, Copley CJ, Lebl T, Clarke ML (2010) *Chem Eur J* 16:12788–12791
179. Deng Y, Wang H, Sun Y, Wang X (2015) *ACS Catal* 5:6828–6837
180. Ojima I, Takai M, Takahashi T (2004) *Patent WO* 2004-078766
181. Wang X, Buchwald SL (2011) *J Am Chem Soc* 133:19080–19083
182. Wang X, Buchwald SL (2013) *J Org Chem* 78:3429–3433
183. Murphy SK, Park J-W, Cruz FA, Dong VM (2015) *Science* 347:56–60
184. Landis CR (2015) *Science* 347:29–30

Rhodium Catalyzed Decarbonylation

Eduardo J. García-Suárez, Klara Kahr, and Anders Riisager

Abstract Rhodium catalyzed decarbonylation has developed significantly over the last 50 years and resulted in a wide range of reported catalyst systems and reaction protocols. Besides experimental data, literature also includes mechanistic studies incorporating Hammett methods, analysis of kinetic isotope effects as well as computational studies of model systems, which give an indication of the scope of the process. In this chapter, fundamental applications of Rh-catalyzed decarbonylation reactions are surveyed and discussed, including cross-coupling reactions, tandem reactions, and alternative methodologies for process intensification.

Keywords Aldehydes • Aryl-aryl coupling • Continuous-flow systems • Cross-coupling • Decarbonylation • Heck coupling • Ionic liquids • Oppenauer oxidation • Pauson–Khand • Rhodium • Sugars • Tandem reaction

Contents

1	Introduction	146
2	Early Work	147
3	Cross-Couplings	149
3.1	Cross-Coupling of Arenes with Olefins	150
3.2	Heck Coupling	152
3.3	Aryl-Aryl Cross-Coupling	154
4	Tandem Reactions	157
4.1	Oppenauer Oxidation	157
4.2	Enantioselective Decarbonylation	159
4.3	Pauson–Khand Cycloaddition	160
5	Alternative Processes	161
5.1	Aldoses	161

5.2 Ionic Liquids	162
5.3 Continuous-Flow Systems	163
6 Summary	164
References	164

1 Introduction

Carbon monoxide (CO) is a versatile and inexpensive gas, which is industrially produced in large scale by steam reforming of natural gas, incomplete combustion of other carbon containing materials or by gasification of coal [1]. In bulk chemical manufacturing CO is widely used as C1 building block [2], but its colorless and odorless properties combined with a high toxicity makes handling and storage potentially dangerous [3]. For this reason, there is a great interest – in especially smaller scale applications – to supply the CO equivalents through “in situ” generation instead of via external CO supply. This makes the overall processing less dangerous, thus contributing to generate a safer manufacture and working environment. An approach whereby CO can be generated “in situ” is to apply molecules containing carbonyl groups as source of CO via a decarbonylation reaction. Such reactions can be facilitated both thermally and catalytically, and especially the catalytic approach is attractive for aldehydes which liberate CO much easier than other functionalities, e.g., ketones [4]. In general terms, decarbonylation reactions are the reverse of CO insertion reactions, i.e., carbonylation reactions. Even though carbonylation reactions are significantly more widely applied in industrial applications, the decarbonylation reaction is a key methodology in organic synthetic chemistry, mainly in the preparation of biaryl motifs in natural products, advanced materials, and pharmaceuticals [4].

The current chapter surveys the use of rhodium metal complexes in catalytic decarbonylation. The first section describes early work on the topic and mechanistic aspects on the Rh-catalyzed decarbonylation reaction. The following sections describe potential applications of decarbonylation processes in cross-coupling reactions and tandem reaction protocols, e.g., the Oppenauer oxidation, enantioselective, and Pauson–Khand cascade decarbonylation reactions. Focus is also on the use of biomass derived compounds (sugars) as CO source, the use of ionic liquids (ILs) as alternative solvents for the decarbonylation reaction, catalyst recycling as well as process intensification by use of fixed-bed reactor technology for continuous-flow systems.

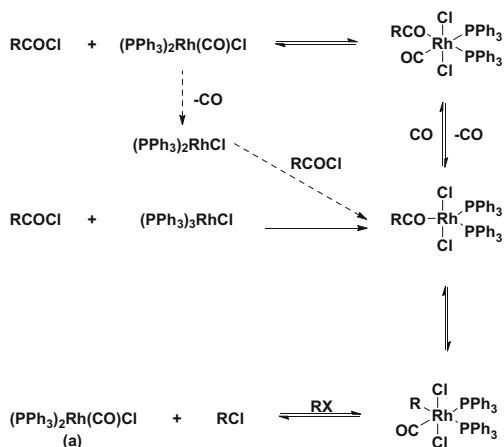
2 Early Work

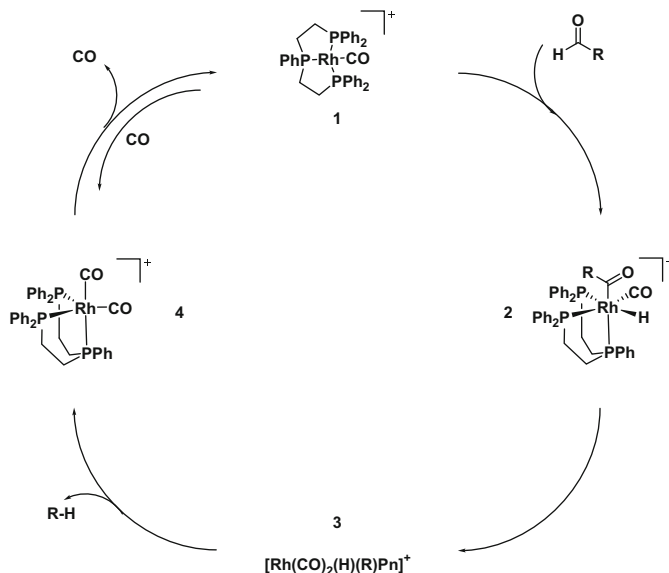
The first decarbonylation reaction for aldehydes and the associated mechanism was described in 1965–1966 by Tsuji and Ohno with a stoichiometric amount of the Wilkinson's catalyst $\text{RhCl}(\text{PPh}_3)_3$ (PPh_3 = triphenylphosphine) [5] (Scheme 1). In a first reaction step, the catalyst is in presence of the aldehyde converted to $\text{RhCl}(\text{CO})(\text{PPh}_3)_2$ (a), which is the true catalyst in the carbonylation reaction. Complex (a) is a stable, four-coordinated complex that easily can be expanded to form a six-coordinated complex as intermediate in the reaction.

In 1982 Pignolet et al. proposed a mechanism for the decarbonylation of aldehydes using cationic catalyst complexes with chelating diphosphines as ligands, such as $[\text{Rh}(\text{dppp})_2]\text{Cl}$ (dppp = diphenylpropanephosphine) [6]. The rationale for using chelating diphosphine ligands instead of monodentate phosphines (e.g., PPh_3) was that dissociation of coordinated CO to regenerate the active catalyst was a key step during the reaction. In this regard, it was showed that cationic complexes with chelating diphosphine ligands bind CO less strongly to the metal center than $\text{RhCl}(\text{CO})(\text{PPh}_3)_2$ complex due to a decrease in the Rh-CO π back-bonding and consequently, CO release is facilitated [6].

In 1999 Crabtree and co-workers suggested a mechanism for the decarbonylation of aldehydes by using the cationic Rh-triphos catalyst (triphos = bis(diphenylphosphinoethyl)phenylphosphine), $[\text{Rh}(\text{CO})(\text{triphos})][\text{SbF}_6]$ [7]. The proposed mechanism consists of four steps as depicted in Scheme 2. The first step is the oxidative addition of the aldehyde C–H bond to complex **1** generating a metal acyl complex similar to **2**. Then complex **2** undergoes retro-migratory insertion of the R group to generate an alkyl/aryl hydride complex **3**. The reductive elimination of complex **3** yields the alkane or arene and complex **4** that is supposed to be in equilibrium with complex **1**, which close the catalytic cycle. The possibility that the reaction involved a radical mechanism was excluded by using an aldehyde

Scheme 1 The mechanism for the decarbonylation of aldehydes proposed by Ohno et al. using Wilkinson's catalyst in stoichiometric amounts [5]



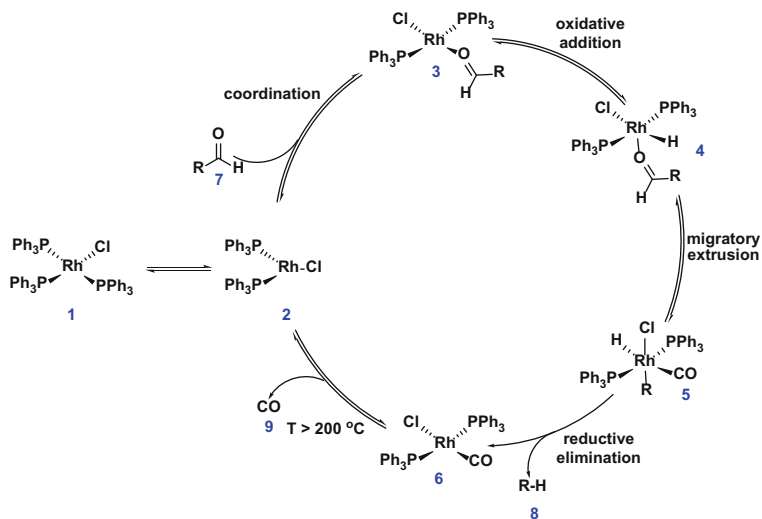


Scheme 2 Decarbonylation mechanism proposed by Crabtree et al. [7]

(citronellal) that served as radical trap, since cyclic species such as menthone or isomenthone would be expected to form which was not the case.

In 2008 Madsen et al. presented a combined experimental and theoretical study of the mechanism for the Rh-catalyzed decarbonylation of para-substituted benzaldehydes. In line with earlier work from the group, the experimental part incorporated Hammett studies and kinetic isotope effects in order to characterize the selective-determining step. In addition, the data was used to differentiate between several mechanistic proposals and used as starting point for the computational studies [8].

In the studies by Pignolet et al. the proposed mechanism was related to systems with chelating diphosphines ligands like dppp. However, the DFT calculations performed by Madsen et al. using a model ligand (dppp where Ph = H) revealed that the coordination of benzaldehyde to $\text{Rh}(\text{dppp})_2^+$ was unfavorable. The calculations were confirmed by measuring the energy minimization of different distances between the benzaldehyde oxygen atom and the Rh(I) center. Based on the previous studies by Pignolet, $\text{Rh}(\text{dppp})(\text{CO})_2^+$ was suggested as the optimal catalyst, which indicates an exchange of CO for benzaldehyde as the first step in the catalytic cycle [8]. The Hammett studies of benzaldehyde and phenyl acetaldehyde derivatives revealed a buildup of negative charge in the selectivity-determining step. In contrast, the kinetic isotope effects of the two substrates were comparable, indicating that the two mechanisms had to be identical. Furthermore, the computational studies of the catalytic cycle revealed that the oxidative addition into the formyl bond was followed by a rate-determining extrusion of CO and a reductive elimination. The proposed theoretical kinetic isotope effects were in compliance with the



Scheme 3 The mechanism for decarbonylation of aldehydes proposed by Kappe and co-workers using the Wilkinson's catalyst [9]

experimental values for both substrates, but only when the rate-determining step was selected as the migratory extrusion of CO.

In 2014 Kappe and co-workers proposed a plausible mechanism for Rh-catalyzed decarbonylation of aldehydes using Wilkinson's catalyst [9]. The catalytic cycle shown in Scheme 3 took into account results obtained from earlier experimental and computational mechanistic studies. The catalytic cycle includes a pre-step in which the square-planar Wilkinson's catalyst **1** is converted to an unsaturated d^8 complex **2**. The coordinately unsaturated complex **2** coordinates with the aldehyde **7** via the oxygen atom to form **3**, which reacts by a reversible oxidative addition into the formyl group of the aldehyde to form an acyl Rh(III) hydride complex **4**. The cycle continues by a rate-limiting migratory extrusion of CO, in which the vacant coordination site of the complex is occupied to give the $18e^-$ alkyl or aryl Rh(III) hydride **5**. The migratory extrusion is then followed by an irreversible reductive elimination, which produces the $16e^-$ carbonyl complex *trans*-[RhCl(CO)(PPh₃)₂] **6** and the decarbonylated product **8**. Finally the unsaturated d^8 complex **2** regenerates after dissociation of the extruded CO (**9**).

3 Cross-Couplings

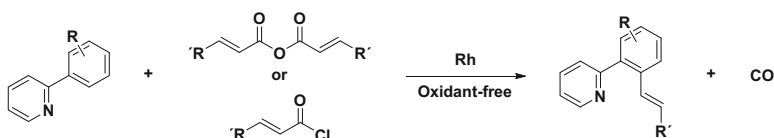
Grignard reagents have traditionally been used as stoichiometric reagents in coupling reactions with electrophilic carbon atoms, e.g., esters, ketones, hetero-atoms halides. However, transition metal catalyzed cross-couplings now play an essential role in both carbon–carbon and carbon–hetero bond formation, and the nature of the

ligand coordinating to the transition metal is important in determining the selectivity and the rate of the reaction.

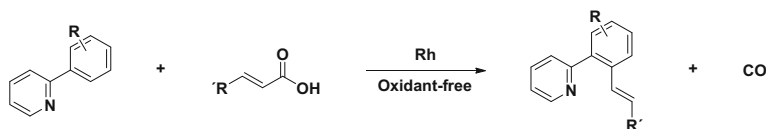
3.1 Cross-Coupling of Arenes with Olefins

Within the last decade, transition metal catalyzed cross-couplings have been developed in which unreactive arene C–H bonds are coupled with olefins to generate arylated olefins. Fujiwara and Moritani were the first to demonstrate that arenes could be applied as coupling partners with olefins by using a Pd-catalyst [10], but since then more active and selective catalytic systems have been developed. Hence, recent studies have demonstrated that certain directing groups facilitate regioselective C–H *ortho*-olefination [11]. Carboxylic acids and derivatives have also been recognized as effective coupling partners in decarbonylative cross-coupling reactions [12, 13]. Further research has been performed by applying vinyl carboxylic acids and their derivatives as olefins. With this approach, it has been possible to accomplish decarbonylation of vinyl carboxylates with direct functionalization of C–H bonds for improving the catalytic efficiency [14].

Yu and co-workers have investigated the direct olefination of arene C–H bonds by applying an Rh complex catalyst and a proper base. The direct olefination of cinnamoyl chlorides and cinnamic anhydrides tolerate a variety of functional groups (Scheme 4) and the pre-studied vinyl carboxylic acid has revealed to act as an effective reagent [15–17]. Further research of the decarbonylation reaction by arenes has been performed by Li and co-workers. A protocol for the decarbonylative direct olefination of arylpyridines with different vinyl carboxylic acids under mild conditions has been developed in presence of an Rh(I) catalyst in absence of an oxidant. The method provides a general and convenient procedure for Rh-catalyzed cross-coupling reactions (Scheme 5) [14].



Scheme 4 Direct olefination with cinnamoyl and cinnamic aldehyde by Yu and co-workers [15]

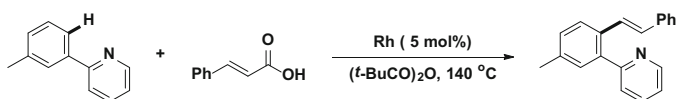


Scheme 5 Direct olefination of arylpyridines by Li and co-workers [14]

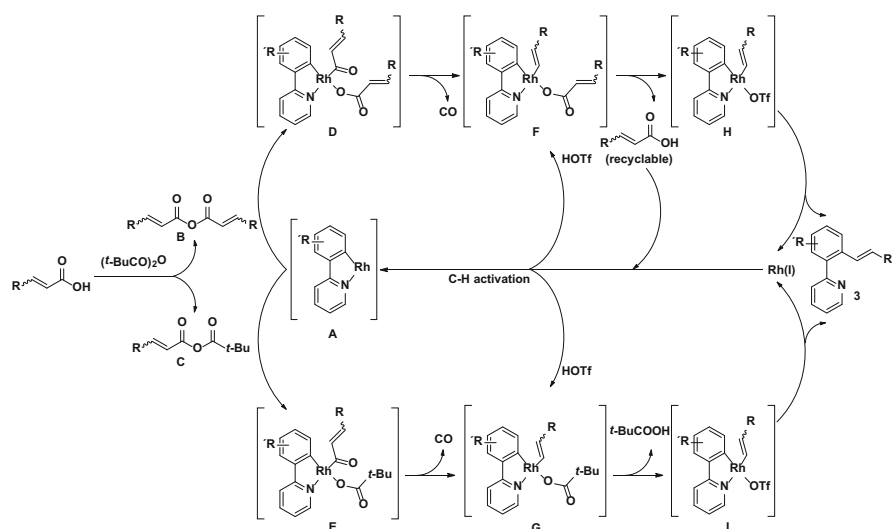
The catalytic activity of different rhodium complexes for direct olefination has been studied in a model system using 2-(*meta*-tolyl)pyridine and cinnamic acid with the additive pivalic anhydride ((*t*-BuCO)₂O) in toluene (Scheme 6) [14]. The catalyst [Rh(COD)₂]OTf (COD = 1,5-cyclooctadiene) showed the highest catalytic activity affording (*E*)-2-(5-methyl-2-styrylphenyl)pyridine. Almost similar activity was observed by applying [Rh(NBD)₂]BF₄ (NBD = norbornadiene) and [Rh(CO)₂Cl]₂, while other used Rh complexes showed no reactivity and negligible yield. Using other solvents, e.g., chlorobenzene, *para*-xylene, anisole, *N,N*-dimethylformamide, and dimethyl sulfoxide resulted in a reduced yield. Other tested additives were all inferior to the (*t*-BuCO)₂O.

A wide range of substrates with substituents on the benzene ring revealed to be effectively transformed to the *E* stereochemistry. Substrates with *meta*- or *ortho*-substituted aryl rings were also efficiently coupled to form the *ortho*-alkenylated products.

The mechanism for the decarbonylative direct olefination of aryl pyridines has been suggested by Li and co-workers (Scheme 7) [14]. In the first step, the aryl pyridine **3** reacts with the Rh(I) complex to form the aryl coordinated Rh complex **A** through C–H activation. The anhydrides **B** and **C** and the additive (*t*-BuCO)₂O react with complex **A** forming the acyl intermediates **D** and **E**, which decarbonylates



Scheme 6 Direct olefination of 2-(*meta*-tolyl)pyridine with cinnamic acid [14]



Scheme 7 Proposed mechanism for the decarbonylative direct olefination of aryl pyridines [14]

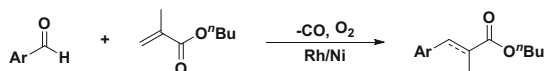
to form the allyl complexes **F** and **G**. Addition of trifluoromethanesulfonic acid (HOTf) generates complexes **H** and **I** in which the carboxylic acids are released. Product **3** is finally produced as the reductive elimination of **H** and **I** occurs and the rhodium(I) complex is regenerated to start another catalytic cycle [14].

3.2 Heck Coupling

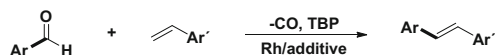
The Heck cross-coupling reaction was first reported by Mizoroki and Heck [18, 19], and is a fundamental method in organic synthesis for the direct arylation of terminal alkenes. The Heck reaction does not involve Grignard reagents, and accordingly carboxylic acids and their derivatives, such as acyl chloride, anhydrides, and esters, can be used in decarbonylative arylation of terminal alkenes [20]. Arylsulfonyl hydrazides and aroyl hydrazides can also be applied as aryl electrophiles in the reaction [21, 22].

In 2009 Li and co-workers presented a route for Rh/Ni co-catalyzed decarbonylative Heck-type coupling of aromatic aldehydes and conjugate alkenes using dioxygen as oxidant (Scheme 8). The reaction was accompanied by the formation of conjugate addition products [23]. In 2015 Yang and co-workers developed a general Rh-catalyzed oxidative decarbonylative Heck-type coupling of aromatic aldehydes by the use of terminal alkenes and acyl chlorides as additives (Scheme 9) [20].

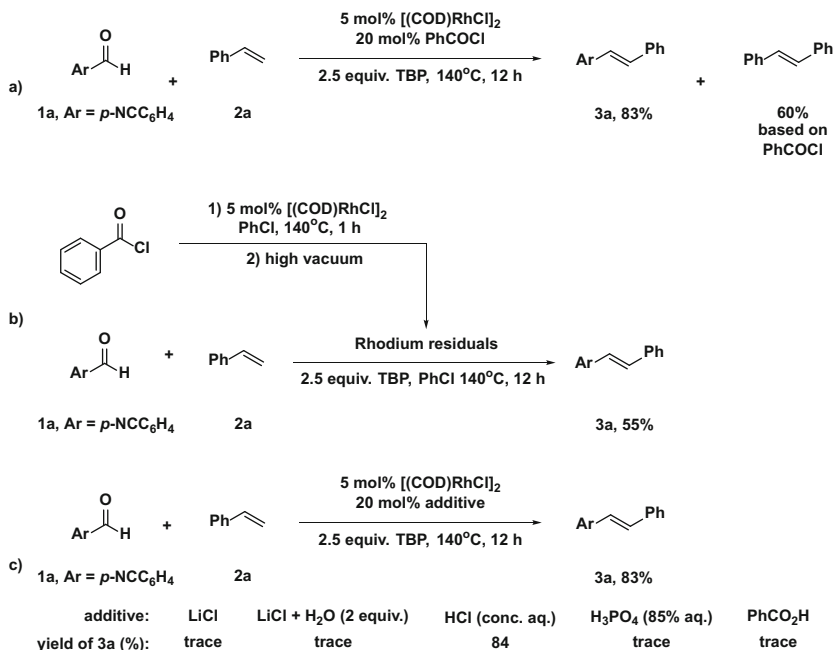
Mechanistic experiments to understand the role of the acyl chloride has been performed in the studies by Miura and co-workers [24, 25]. The reaction mixture consisting of $[(\text{COD})\text{RhCl}]_2$ catalyst and benzoyl chloride showed formation of styrene **2** to stilbene **3a** (Scheme 10a), while absence of the acyl chloride resulted in low yield. The Rh-catalyst precursor was activated in the catalytic cycle as stilbene was generated. This was supported by a reaction (Scheme 10b) in which the Rh-catalyst reacted with benzoyl chloride in the absence of styrene, which under high vacuum evaporated to afford Rh residual, which didn't catalyze the oxidative decarbonylative Heck-type coupling of aldehydes. However, generally when catalyst loading was increased a higher product yield was obtained, and the *trans* isomers was by ^1H NMR found to be the dominant reaction product [20]. In control



Scheme 8 Rh/Ni co-catalyzed oxidative decarbonylative arylation of conjugate alkene [20]



Scheme 9 Rh-catalyzed oxidative decarbonylative arylation of terminal alkene [20]

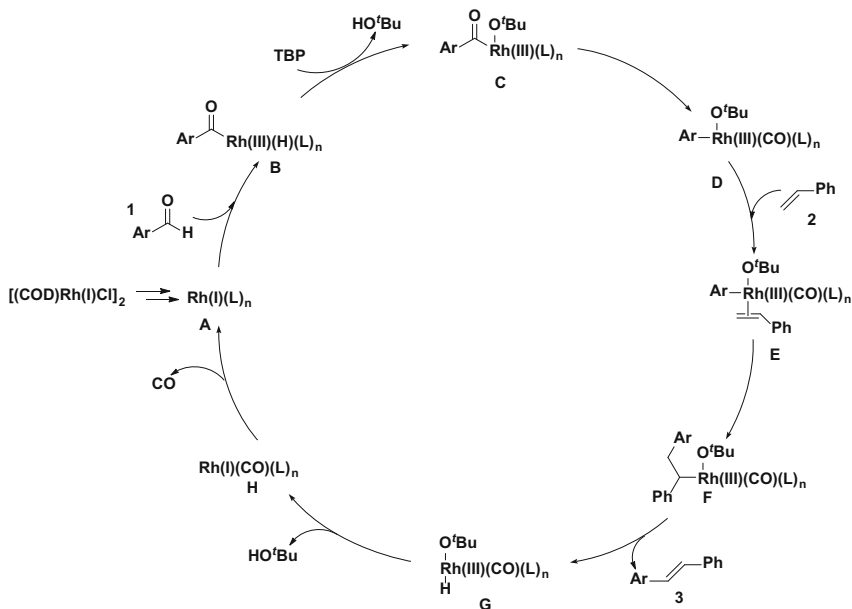


Scheme 10 Mechanistic experiments to understand the role of acyl chloride (a) without activation, (b) with activation and (c) with other additives [20]

experiments the benzoyl chloride was replaced with benzoic acid in presence of, e.g., lithium chloride (LiCl) and phosphoric acid (H₃PO₄) and no reaction product was formed (Scheme 10c).

Aryl aldehydes with electron withdrawing or donating substitutes have been found to afford a moderate yield of the products in the decarbonylation Heck-type coupling with no significant influence of steric effects by *ortho*-, *meta*-, and *para*-position substituents. In contrast, aliphatic aldehydes did not result in coupling products and aliphatic carboxylic acid was observed as product [20].

Based on literature reports Yang and co-workers proposed a mechanism for the oxidative decarbonylative coupling of aldehydes with alkenes which is illustrated in Scheme 11 [20]. An initial step in the mechanism is the oxidative addition of the aldehyde C–H bond to the activated Rh(I)-catalyst **A** to afford the acyl hydride Rh(III) complex **B**. Next, this complex is converted by tributyl phosphate (TBP) (upon liberation of Bu^tOH) to Rh(III) complex **C** and further to the aryl Rh(III) complex **D** by CO migration. Then styrene is coordinated to yield the π -bonded Rh(III) complex **E**, which after C = C insertion to the alkyl Rh(III) complex **F**, forms the oxidative decarbonylative Heck-type coupling product **3** and Rh(III) hydride complex **G** after successive β -hydride elimination. The active Rh(I) catalyst **A** is regenerated by reductive elimination of Bu^tOH to form Rh(I) complex **H** from which CO is dissociated.

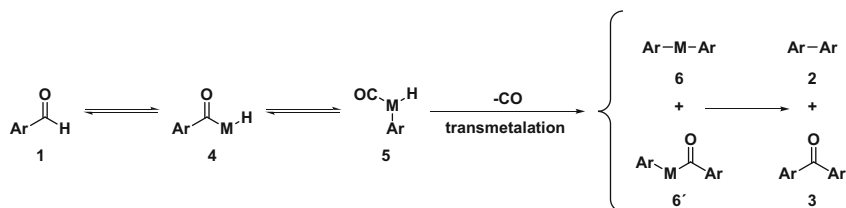


Scheme 11 Proposed mechanism for the oxidative decarbonylative coupling of aldehydes with alkenes [20]

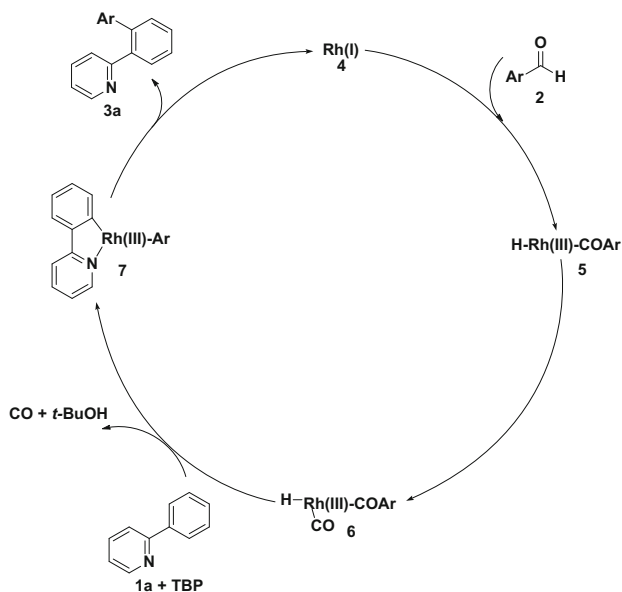
The Rh-catalyzed oxidative decarbonylative Heck-type coupling of aromatic aldehydes with terminal alkenes has been presented as an efficient procedure. Acyl chlorides have revealed to be a poor additive for the reaction to proceed and activate the Rh-catalyst precursor by coupling with styrene [26].

3.3 Aryl-Aryl Cross-Coupling

Protocols to form aryl-aryl bonds have been one of the core interests in organic chemistry for over a century due to the importance of biaryl motifs in natural products as well as pharmaceutical industry [27]. The most common procedure for constructing the aryl-aryl union is by far the homo- and cross-coupling of (pseudo) aryl halides and aryl metalloids via C–H bond activation. Recently, more challenging oxidative cross-coupling of simple arenes have been achieved and developed, affording biaryl products with high atom economy [28]. Based on previous studies of cross-dehydrogenative-coupling (CDC) reactions [29, 30] and decarbonylative coupling of different aldehydes and terminal alkynes [31, 32], Li and co-workers have suggested that aromatic aldehydes can be applied in CDC reactions with arenes in the presence of an oxidant (Scheme 12) [26]. The acyl metal complex **4** is generated by oxidative addition of the aldehyde to the transition metal. CO insertion to form complex **5** is then followed by reductive elimination to form a



Scheme 12 Aldehyde C–H bond activation and decarbonylative homocoupling [26]



Scheme 13 Mechanism for the oxidative arylation of 2-phenylpyridine with aryl aldehydes [33]

simple arene (Ar-H). The aryl metal hydride complex **5** is also capable of reacting with an alkene, alkyne, or arene [33–35] to obtain the decarbonylative coupling product. Furthermore, the arylmetal hydride forms the diaryl-metal complex **6** and the acyl-aryl-metal complex **6'**, which results in the C–C bond formation of biaryl and biarylketones after the reductive elimination.

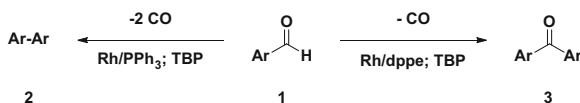
The optimal conditions for the decarbonylative homocoupling reaction include the catalyst $\text{Rh}(\text{acac})(\text{CO})_2$ (acac = acetylacetonate), the oxidant TBP when using PhCl as solvent [33]. Electron-rich aromatic aldehydes with methoxy-substitution in *para*- or *meta*-position were found to give a good yield of biaryls. However, even higher yield was obtained with 2-arylpyridine derivatives [33].

Li and co-workers proposed a mechanism for the homo-coupling of aryl aldehydes with 2-phenylpyridines (Scheme 13) [33]. Initially, oxidative addition of the aldehyde **2** to the Rh(I) center **4** generates Rh(III) acyl hydride complex **5**, which undergoes insertion of CO at elevated temperature to give Rh(III) hydride complex

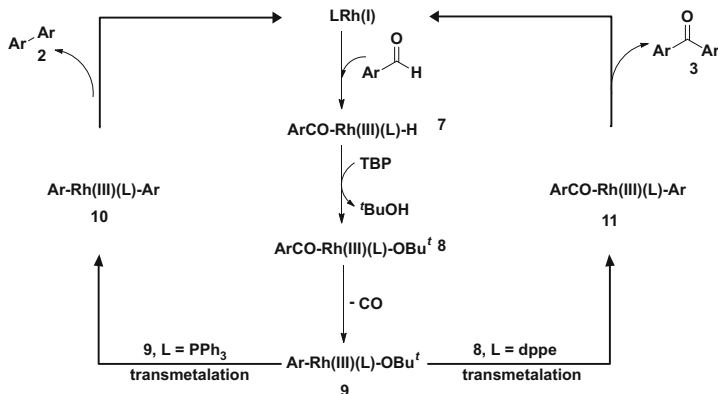
6. Next, **6** reacts with the pyridine compound **1a** through C–H bond activation, which is followed by dehydrogenation promoted by TBP to give Rh(III) complex **7**. Finally, reductive elimination of intermediate **7** affords the target biaryl product **3a** and regenerates the Rh(I) catalyst **4**.

Another method for oxidative decarbonylative homocoupling of aromatic aldehydes with phosphine ligands has also been developed to produce biaryl and diarylketones (Scheme 14). Different ligands have been tested in the method and $[\text{RhCl}(\text{CO})_2]_2$ in presence of PPh_3 showed the highest yield with the ratio of biaryl:diarylketones being 72:28. Changing the phosphine ligand with *dppp* showed no formation of biaryl. Aldehydes with weak electron-withdrawing substituents such as fluoro and chloro also showed a high yield of the biaryl product [26].

The proposed mechanism for the Rh-catalyzed oxidative decarbonylative homocoupling with phosphines is depicted in Scheme 15. First, the oxidative addition of the Rh(I) complex forms the acyl Rh(III) hydride complex **7**. This complex is then converted by TBP to Rh(III) complex **8**, which is decarbonylated to aryl Rh(III) complex **9**. By using the ligand PPh_3 , the transmetalation between two aryl Rh(III) **9** complexes forms the diaryl Rh(III) complex **10**, which releases the biaryl product **2** after the reductive elimination to the initial Rh(I) complex. Similar, by using the *dppp* ligand the transmetalation between acyl Rh(III) complex **8** and aryl Rh(III) complex **9** forms the Rh(III) complex **11**, which releases the diarylketones **3** after the reductive elimination. The dissociation rate for the



Scheme 14 Phosphine ligand triggered oxidative decarbonylative homocoupling of aldehydes [26]



Scheme 15 Proposed mechanism for the oxidative decarbonylative homocoupling [26]

Rh-complex **8** decreases when dppp is applied instead of PPh₃, and as a result the decarbonylation of **8** is more difficult for obtaining the aryl complex [26].

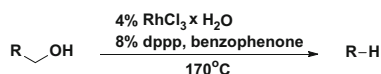
4 Tandem Reactions

Tandem reactions consist of at least two sequential steps in which the second step occurs in virtue of the functionality from the previous reaction [36]. Tandem reactions can reduce the number of steps required to form a complex molecule, increase the atom economy as well as reduce generation of waste from the reactions [37, 38]. Recently, main focus has been on the development of asymmetric catalyzed tandem reactions by applying chiral transition metal complexes [37, 39–41].

4.1 Oppenauer Oxidation

In tandem reaction protocols Oppenauer oxidation of primary alcohols to aldehydes followed by decarbonylation can be combined within the same reaction mixture. The reaction protocol allows the removal of hydroxymethyl group in one step, as illustrated in Scheme 16 for the tandem Oppenauer oxidation and decarbonylation of 2-naphthaldehyde reported by Madsen and co-workers using aluminum tri(*tert*-butoxide) as the Oppenauer catalyst under optimized conditions [42]. Importantly, long-chain aliphatic alcohol also showed generation of the desired product, however, along with olefin byproducts.

The optimal conditions for the tandem Oppenauer oxidation and decarbonylation reaction were found after exploration of different phosphine ligands (Fig. 1) for the decarbonylation in various solvents [42]. Use of monodentate ligands (i.e., PPh₃, PCy₃ (Cy = tricyclohexyl), P(*o*-furyl)₃, and PCy₂(2-biphenyl)) resulted in low conversion and the tridentate ligands **1** and **2** gave almost no conversion. The bidentate ligand dppp was more reactive than dppe (1,2-bis(diphenylphosphino)ethane) and dppb (1,4-bis(diphenylphosphino)butane). The diphosphines **3** and **4**, having a more rigid backbone and a smaller bite angle compared to the other tested biphosphines, yielded only minor products amounts, while the reactivity increased for biphosphines with bite angles of 104–107°, such as the Xantphos [43]. The P,N ligand Davephos [44] gave also only a minor amount of the product, while dppf (1,1'-ferrocenediyl-bis(diphenylphosphine)) and Binap (2,2'-bis(diphenylphosphino)-1,1'-binaphthyl) gave high and similar activity for the decarbonylation, albeit the stability of the former



Scheme 16 Rhodium-catalyzed decarbonylation of 2-naphthaldehyde using different solvents [42]

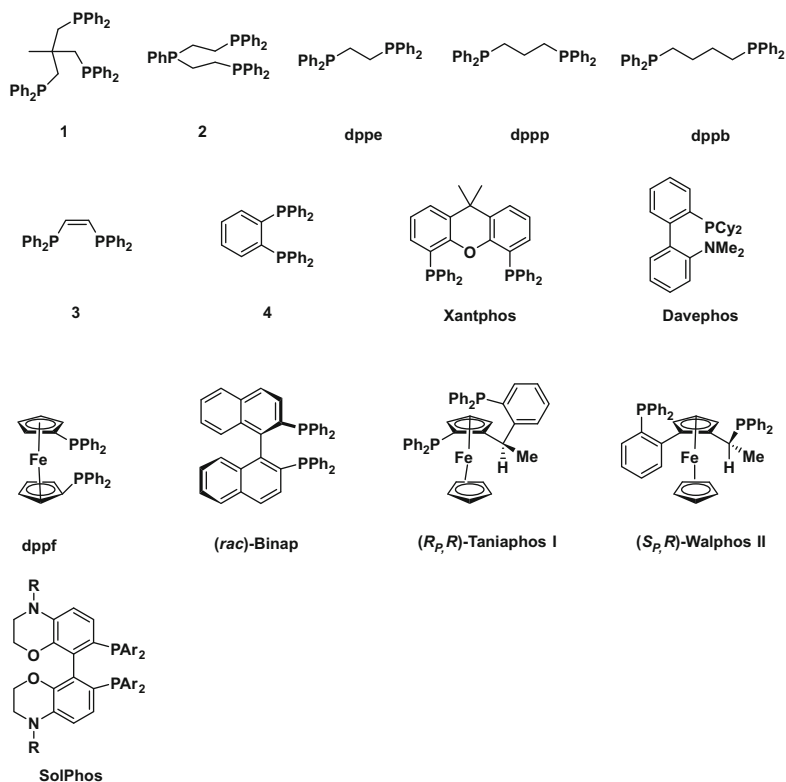
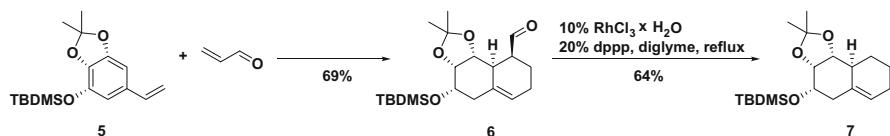


Fig. 1 Phosphine ligands tested [42]



Scheme 17 Diels–Alder decarbonylation reaction [42]

catalyst system was quite low (resulted in black coloration of the reaction mixture). In contrast, the quite similar ligand SolPhos (7,7'-bis(diarylpophosphino)-3,3',4,4'-tetrahydro-4,4'-dimethyl-8,8'-bis-2H-1,4-benzoxazine) resulted only in traces of the product and the Walphos II and Taniaphos I ligands revealed a reactivity comparable to dppp. Hence, the best ligands – dppp, dpfp, Binap, and Taniaphos I – were observed to have bite angles between 91 and 96° and a more flexible backbone, while both smaller bite angle (i.e., ligand 3 and 4) and larger bite angle (e.g., Xantphos and dppb) showed almost no conversion or a very slow reaction [43].

The synthetic utility of decarbonylation in tandem reactions involving a Diels–Alder reaction has also been demonstrated by Madsen et al. (Scheme 17) [45]. Here

aldehyde **6** was prepared in a Diels–Alder reaction between diene **5** and acrolein and decarbonylated to the unsaturated decalin compound **7** in good yield using the Rh-dppp complex catalyst system. Notably, this two-step protocol yielded product **7**, which was not possible to obtain by the direct one-step cycloaddition of ethylene and diene **5** due to a large HOMO-LUMO gap between the reagents [42].

4.2 Enantioselective Decarbonylation

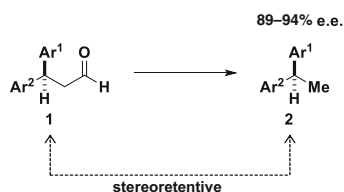
The demand for optically active building blocks is important for especially asymmetric synthesis in the drug-discovery industry [46]. Earlier study has demonstrated that optically active diarylalkanes can be formed by different procedures, including asymmetric alkylations of lithiated diarylmethanes and metal-catalyzed cross-coupling of benzylsilanes with aryl triflates [47]. The cross-coupling requires an optically active precursor, which led to investigations on enantioselective alkene reductions [48].

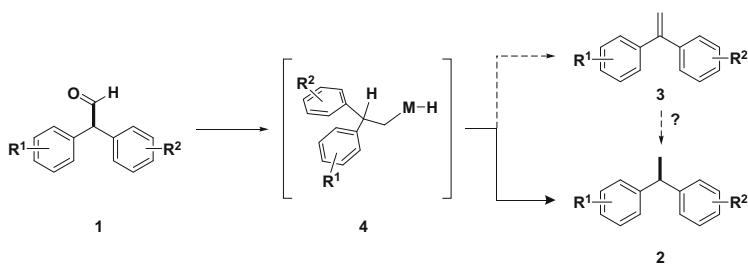
Carreira and co-workers have developed a one-pot protocol for the preparation of optically active 1,1-diarylethanes from 2,2-diarylpropanealdehydes involving enantioselective tandem 1,4-addition decarbonylation (Scheme 18) [47]. Hence, the protocol is a new procedure for asymmetric synthesis where the aldehyde is a removable steering group [49]. A range of functional groups such as ethers, halides, esters, and nitro groups were found to be compatible for the reaction and furans, thiophenes, and indoles provided the decarbonylated products. It was suggested that compound **3** is formed as a result of β -hydride elimination of the intermediate **4** during the reaction, despite the presence of **3** could lead to erosion of the optical purity of product **2** (Scheme 19).

The one-pot protocol using $[\text{Rh}(\text{C}_2\text{H}_4)_2\text{Cl}_2]$ and olefin ligands allowed also conversion of cinnamaldehyde derivatives without isolating the intermediate aldehyde [50]. Despite very low yields, it is so far the first example of aldehyde decarbonylation with Rh-diene complexes in absence of phosphine ligands [47].

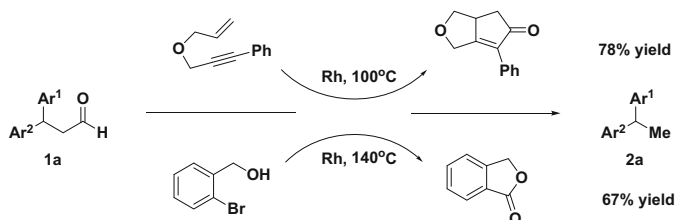
The conditions for the decarbonylation investigated by Carreira and co-workers have shown to be difficult for small-scale reactions or with volatile aldehydes, and the opportunity for coupling the decarbonylation to a process that consumes CO has been examined [47]. Two cyclization procedures have been developed utilizing aldehydes as a source of CO; the first involves a cascade Pauson–Khand reaction

Scheme 18 1,1-diarylethanes from 2,2-diarylpropanealdehydes [47]





Scheme 19 Metal-mediated decarbonylation versus dehydroformylation [47]



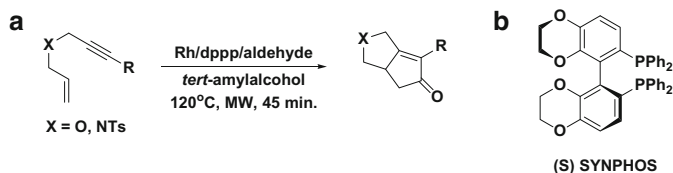
Scheme 20 Chemical traps for CO lead to catalytic decarbonylation [47]

of alkyne and alkene to form substituted cyclopentenones [51] and the other involves a cascade lactonization of benzylic alcohols to form benzofuranone (Scheme 20) [52].

4.3 Pauson–Khand Cycloaddition

Gedye [53] and Giguere [54] reported in 1986 microwave-accelerated organic synthesis (MAOS) which has been applied in Pauson–Khand decarbonylation reactions [55, 56]. The first microwave-assisted Rh-catalyzed cascade decarbonylation Pauson–Khand reaction (PKR) was reported by Kwong and co-workers in 2008 using aromatic aldehydes and $[\text{Rh}(\text{COD})\text{Cl}]_2/\text{dppp}$ as superior bisphosphine ligand system [57] (Scheme 21). Various enynes were successfully converted except *ortho*-substituted aromatic enynes which provided low yield due to steric hindrance. Remarkably, the use of CO surrogates (aldehydes) revealed better results than gaseous CO under the same reaction conditions. On the other hand, the use of oil-bath heating instead of microwave yielded only trace amount of product.

Besides the achiral cascade PKR, the possibility of achieving the first enantioselective microwave-assisted cascade transformation was examined with various substrates including O-, N-, and C-tethered enynes. Chiral diphosphine ligands were examined in place of dppp and (*S*)-SYNPHOS (BisbenzodioxanPhos) provided the best results in terms of product yield and enantioselectivity [57].



Scheme 21 (a) Microwave-assisted Rh-catalyzed cascade PKR; (b) (S) SYNPHOS [57]

5 Alternative Processes

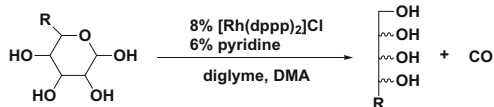
Rh-based decarbonylation catalyst systems have proved tolerant towards a wide range of functional groups when employed in total synthesis, thus making selective decarbonylation a potential strategy for upgrading carbohydrates (aldoses) and furfurals into biofuels and chemical building blocks in bio-refineries [58]. Alternative processes have also been developed with the aim of optimizing the recovery and recycling of the catalyst. The interest in new recyclable approaches has resulted in examination of ionic liquids as reaction media. Further process intensification has also been achieved by applying continuous-flow systems.

5.1 Aldoses

Procedures for altering the carbon chain length in unprotected aldoses has been a main focus area in carbohydrate chemistry the last century, but only few methods for shortening the carbon chain are actually developed [59]. In 1898 Ruff published a method for shortening the carbon chain, known as the Ruff degradation, which converts salts of aldonic acids into aldoses with one less carbon atom [60]. Another procedure for shortening the carbon chain is by oxidative degradation of aldoses into salts of aldonic acids with loss of one carbon atom [61, 62]. Notably, both reactions require stoichiometric amount of inorganic salts.

Aldoses are aldehydes that can undergo a C–H insertion reaction with a metal followed by decarbonylation. This transformation converts C_n aldoses into C_{n-1} alditols [63]. The conversion of aldoses to alditols was investigated by Andrew and co-workers using stoichiometric amounts of the Wilkinson's catalyst. Alditols were isolated in yields from 37 to 87% using *N*-methyl-2-pyrrolidinone (NMP) as solvent at 130°C [64].

In 2007 Madsen and co-workers developed a catalytic procedure with Rh-dppp for decarbonylation of unprotected aldoses, which resulted in new opportunities for using aldoses as chiral starting compound in synthetic chemistry [63]. Screening of different additives and solvents revealed that the optimal conditions were achieved by using pyridine as additive and a mixture of diglyme and DMA as solvent (Scheme 22). The applied catalyst $\text{Rh}(\text{dppp})\text{Cl}_2$ – prepared in two steps from $\text{RhCl}_3 \cdot 3\text{H}_2\text{O}$ – was found to show the best catalytic performance. In contrast, the



Scheme 22 Decarbonylation of aldoses into alditols [63]

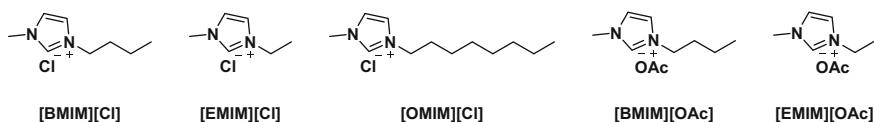
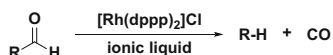


Fig. 2 ILs tested in the studied decarbonylation reaction [68]



Scheme 23 Decarbonylation reaction with IL catalyst system [68]

analogous in situ prepared catalyst mainly resulted in decomposition of the carbohydrate due to Rh(III) to Rh(I) reduction by the ligand followed by further reduction to Rh(0) by the carbohydrate (glucose) [42].

5.2 Ionic Liquids

Catalyst recovery and recycling are persisting challenges in homogeneous catalysis [65], but ionic liquids (ILs) have demonstrated potential to efficiently immobilize catalysts and separate the product phase in reactions such as Rh-catalyzed alkene hydroformylation [66] and methoxycarbonylation [67]. Furthermore, ILs can provide greener processes compared to traditional organic solvent systems due to their negligible vapor pressure, thermal stability, and coordination properties [66].

In 2014 Riisager et al. examined the use of different ILs (Fig. 2) as reaction media in Rh-phosphine catalyzed decarbonylation of aromatic and aliphatic aldehydes to produce benzene derivatives and alkanes (Scheme 23) [68]. The pre-catalyst $[\text{Rh}(\text{dppp})_2]\text{Cl}$ was chosen in the study as it earlier had been reported to facilitate decarbonylation of aldehydes with different solvents and various temperatures.

The IL [BMIM]Cl (BMIM: 1-butyl-3-methylimidazolium) showed the best catalytic activity, while change of the IL cation to [EMIM]⁺ (EMIm: 1-ethyl-3-methylimidazolium) decreased the yield. Similar results were observed by changing the chloride anion to acetate. The better performance of the chloride-based IL could be associated with the higher thermal stability and complex dissolution. Steric and electronic influence of the tested substrates revealed that *o*- and *m*-

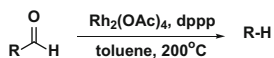
substituted aldehydes provided a higher yield of the product due to the induced steric hindrance, as it improved the migratory extrusion step and the reductive elimination step in the catalytic cycle [68]. Furthermore, it was demonstrated that the use of ILs as reaction media resulted in a biphasic system where the IL-catalyst phase could be easily recovered and reused in three catalytic cycles [68].

5.3 Continuous-Flow Systems

Continuous-flow systems are often preferred in industrial settings as catalyst-product separation is generally easy compared to homogeneous batch catalyzed reactions. In decarbonylation of aldehydes, CO is released and vaporized from the liquid phase into the gas phase and stripped from the reaction mixture carried by an inert gas. This feature may also prevent catalyst poisoning.

Kappe and co-workers have investigated biphasic gas-liquid continuous-flow decarbonylation of aldehydes in the presence of Rh-dppp catalyst (Scheme 24). It was found that benzaldehydes without electron-withdrawing groups reacted slower than cyanobenzaldehyde, and the efficiency of the annular flow regime was highlighted by synthesis of chromenes which are a significant category of natural products, e.g., cannabinoids, anthocyanides, and flavors [9]. Different chromene derivatives were also synthesized in a flow protocol by Bräse and co-workers utilizing Michael addition/aldol condensation followed by Rh-catalyzed decarbonylation [69]. The decarbonylation reaction was performed by a procedure developed by Madsen and co-workers [42].

Riisager et al. have reported the use of a solid, silica-supported $[\text{Rh}(\text{dppp})_2]\text{Cl}$ catalyst for gas-liquid continuous-flow decarbonylation of aromatic and aliphatic aldehydes [70]. Aromatic aldehydes with electron-withdrawing groups were poorly soluble in the applied solvents, which gave rise to low product yields. Higher yields and catalyst activity were obtained with electronically activated *o*- and *p*-substituted aldehydes, which – in the former case – were related to an induced steric hindrance [8]. Preservation of intact metal-ligand centers played a pivotal role for the catalytic performance, since ligand dissociation led to catalyst deactivation and formation of less active metal nanoparticles.



Scheme 24 Decarbonylation of aldehydes under continuous-flow conditions [9]

6 Summary

Compiled in the present chapter are a variety of Rh-catalyzed decarbonylation reactions that have been developed over the last 50 years using different ligands and substrates. The reported experimental studies incorporate Hammett studies, kinetic isotope effects as well as different computational analysis, which are also very important for improvement and development of catalytic reactions through understanding of reaction mechanisms. Approaches for in situ generation of CO have found use in a wide range of tandem reactions, whereby the use of hazardous CO as an external reagent is avoided. Furthermore, it has been possible to carry out aldehyde decarbonylation under mild reaction conditions. The development of Rh-catalyzed decarbonylation has also resulted in new, alternative reaction approaches using ILs and continuous-flow aiming towards process intensification and eased catalyst recovery and recycling. Such progress may be of importance for possible future industrial implementation.

References

1. Bierhals J (2012) Carbon monoxide. In: Ullmann's encyclopedia of industrial chemistry. Wiley-VCH, Weinheim
2. Elschenbroich C, Salzer A (2006) Organometallics: a concise introduction. Wiley-VCH, Weinheim
3. Omaye ST (2002) Toxicology 180:139
4. Necas D, Kotora M (2007) Curr Org Chem 11:1566
5. Tsuji J, Ohno K (1965) Tetrahedron Lett 44:3969
6. Doughty DH, Pignolet LH (1978) J Am Chem Soc 100:7083
7. Beck CM, Rathmill SE, Park YJ, Chen J, Crabtree RH, Liable-Sands LM, Rheingold AL (1999) Organometallics 18:5311
8. Fristrup P, Kreis M, Palmelund A, Norrby P-O, Madsen R (2008) J Am Chem Soc 130:5206
9. Gutmann B, Elsner P, Glasnov T, Roberge DM, Kappe CO (2014) Angew Chem Int Ed 53:11557
10. Moritani I, Fujiwara Y (1968) Tetrahedron Lett 24:4819
11. Ueura K, Satoh T, Miura M (2007) Org Lett 9:1407
12. Baudoin O (2007) Angew Chem Int Ed 46:1373
13. Goossen LJ, Rodriguez N, Goossen K (2008) Angew Chem Int Ed 47:3100
14. Qiu R, Zhang L, Xu C, Pan Y, Pang H, Xu L, Li H (2015) Adv Synth Catal 357:1229
15. Jin W, Yu Z, He W, Ye W, Xiao W-J (2009) Org Lett 11:1317
16. Zhao XD, Yu ZJ (2008) J Am Chem Soc 130:8136
17. Ye W, Luo N, Yu Z (2010) Organometallics 29:1049
18. Heck FR, Nolley JP (1972) J Org Chem 37:2320
19. Mizoroki T, Mori K, Ozaki A (1971) Bull Chem Soc Jpn 44:581
20. Kang L, Zhang F, Ding L-T, Yang L (2015) RSC Adv 5:100452
21. Yang F-L, Ma X-T, Trian S-K (2012) Chem Eur J 18:1582
22. Zhang Y-G, Liu X-L, He Z-Y, Li X-M, Kang H-J, Tian S-K (2014) Chem Eur J 20:2765
23. Yang L, Correia CA, Guo X, Li CJ (2010) Tetrahedron Lett 51:5486
24. Sugihara T, Satoh T, Miura M, Nomura M (2003) Angew Chem Int Ed 42:4672
25. Sugihara T, Satoh T, Miura M, Nomura M (2004) Adv Synth Catal 346:1765

26. Yang L, Zeng T, Shuai Q, Guo X, Li C-J (2011) *Chem Commun* 47:2161
27. Hassan J, Sévignon M, Gozzi C, Schulz E, Lemaire M (2002) *Chem Rev* 102:1359
28. Ashenhurst JA (2010) *Chem Soc Rev* 39:540
29. Li C-J (2009) *Acc Chem Res* 42:335
30. Baslé O, Bidange J, Shuai Q, Li C-J (2010) *Adv Synth Catal* 352:1145
31. Guo X, Wang J, Li C-J (2009) *J Am Chem Soc* 131:15092
32. Guo X, Wang J, Li C-J (2010) *Org Lett* 12:3176
33. Shuai Q, Yang L, Guo X, Baslé O, Li C-J (2010) *J Am Chem Soc* 132:12212
34. Yang L, Guo X, Li C-J (2010) *Adv Synth Catal* 352:2899
35. Guo X, Wang J, Li C-J (2009) *J Am Chem Soc* 131:15092
36. Tietze LF, Beifuss U (1993) *Angew Chem Int Ed* 32:131
37. Pellissier H (2006) *Tetrahedron* 26:1619
38. Nicolaou KC, Edmonds DJ, Bulger PG (2006) *Angew Chem Int Ed* 45:7134
39. Pellissier H (2006) *Tetrahedron* 62:2143
40. Enders D, Grondal C, Hüttl MRM (2007) *Angew Chem Int Ed* 46:1570
41. Grondal C, Jeanty M, Enders D (2010) *Nat Chem* 2:167
42. Kreis M, Palmelund A, Bunch L, Madsen R (2006) *Adv Synth Catal* 348:2148–2154
43. Dierkes P, van Leeuwen PWNM (1999) *J Chem Soc Dalton Trans* 1519
44. Old DW, Wolfe JP, Buchwald SL (1998) *J Am Chem Soc* 120:9722
45. Poulsen CS, Madsen R (2002) *Org Chem* 67:4441
46. Burke MD, Schreiber SL (2004) *Angew Chem Int Ed* 43:46
47. Fessard TC, Andrews SP, Motoyoshi H, Carreira EM (2007) *Angew Chem Int Ed* 46:9331
48. Bell S, Wuestenberg B, Kaiser S, Menges F, Pfaltz A (2006) *Science* 311:5761
49. Fessard TC, Motoyoshi H, Carreira EM (2007) *Angew Chem Int Ed* 46:2078
50. Paquin JF, Defieber C, Stephenson CRJ, Carreira EM (2005) *J Am Chem Soc* 127:10850
51. Morimoto T, Fuji K, Tsutsumi K, Kakiuchi K (2002) *J Am Chem Soc* 124:3806
52. Morimoto T, Fujioka M, Fuji K, Tsutsumi K, Kakiuchi K (2007) *J Organomet Chem* 692:625
53. Gedye R, Smith F, Westaway K, Ali H, Baldisera L, Laberge L, Rousell J (1986) *Tetrahedron Lett* 27:279
54. Giguere RJ, Bray TL, Duncan SM, Majetich G (1986) *Tetrahedron Lett* 27:4945
55. Kappe CO (2004) *Angew Chem Int Ed* 43:6250
56. Kappe CO, Dallinger D (2006) *Nat Rev Drug Discov* 5:51
57. Lee H-W, Lee L-N, Chan ASC, Kwong F-Y (2008) *Eur J Org Chem* 19:3403
58. Monard RN, Madsen R (2007) *J Org Chem* 72:9782
59. Györgydeák Z, Pelyvás IF (1998) *Monosaccharide sugars: chemical synthesis by chain elongation, degradation and epimerization*. Academic Press, San Diego
60. Ruff O (1898) *Chem Ber* 31:1573
61. Hendriks HEJ, Kuster BFM, Marin GB (1991) *Carbohydr Res* 214:71
62. Humphlett WJ (1967) *Carbohydr Res* 4:157
63. Monrad RN, Madsen R (2007) *J Org Chem* 72:9782
64. Andrews MA, Gould GL, Klaeren SA (1989) *J Org Chem* 54:5257
65. Cole-Hamilton DJ, Tooze RP (2006) *Homogeneous catalysis – advantages and problems*. In: Cole-Hamilton DJ, Tooze RP (eds) *Catalyst separation, recovery and recycling, Catalysis by metal complexes*, vol 30. Springer, Dordrecht
66. Haumann M, Riisager A (2008) *Chem Rev* 108:1474
67. Garcia-Suarez EJ, Khokarale SG, Van Buu ON, Fehrmann R, Riisager A (2014) *Green Chem* 16:161
68. Malcho P, Garcia-Suarez EJ, Riisager A (2014) *RSC Adv* 4:58151
69. Bröhmer MC, Volz N, Bräse S (2009) *Synlett* 1383–1386
70. Malcho P, Garcia-Suarez EJ, Mentzel UV, Engelbrekt C, Riisager A (2014) *Dalton Trans* 43:17230

Recent Developments in Rhodium-Catalyzed Cyclocarbonylation Reactions

Andrew J. Burnie and P. Andrew Evans

Abstract Rhodium-catalyzed cyclocarbonylation reactions, which include the Pauson–Khand-type or [2+2+1] reactions, represent a powerful strategy for the synthesis of cyclic ketones through the combination of relatively simple unsaturated groups; namely, alkenes, alkynes, allenes, dienes, heterocumulenes, nitriles, and strained rings with carbon monoxide derived from either CO gas or through the decarbonylation of aldehydes. This chapter examines a variety of methods for the synthesis of carbo- and heterocyclic rings of different sizes, including diastereoselective and enantioselective approaches, and will also present the application of these reactions in the total synthesis of important natural products, as exemplified by (+)-asteriscanolide and (–)-ingenol.

Keywords Asymmetric catalysis • Carbocyclizations • Carbon monoxide • Natural products • Pauson–Khand-type reaction • Rhodium catalysis • Tandem/sequential reactions

Contents

1	Introduction to Transition Metal-Catalyzed Carbocyclization Reactions	168
2	The Rhodium-Catalyzed Pauson–Khand Reaction	169
3	Rhodium-Catalyzed [n+1] Carbocyclization Reactions	169
3.1	[4+1] Carbocyclizations	169
3.2	[5+1] Carbocyclizations	172
3.3	[6+1] Carbocyclizations	176
3.4	[7+1] Carbocyclizations	176
4	Rhodium-Catalyzed [m+n+1] Carbocyclization Reactions	177
4.1	[2+2+1] Carbocyclizations	177

4.2	[(3+2)+1] Carbocyclizations	201
4.3	[(3+3)+1] Carbocyclizations	207
4.4	[5+2+1] Carbocyclizations	208
5	Rhodium-Catalyzed [$m+n+o+1$] Reactions	210
5.1	[(2+2+2)+1] Carbocyclizations	210
5.2	[2+2+1+1] Carbocyclizations	211
5.3	[5+1+2+1] Carbocyclizations	212
6	Alternatives to Carbon Monoxide in Rhodium-Catalyzed Cyclocarbonylation Reactions	213
7	Total Synthesis of Natural Products Using Rhodium-Catalyzed Cyclocarbonylation Reactions	217
8	Conclusions and Outlook	225
	References	226

1 Introduction to Transition Metal-Catalyzed Carbocyclization Reactions

The atom-economical construction of multiple carbon–carbon bonds with predictable chemo-, regio-, and stereoselectivity in a single synthetic operation remains a key objective for modern synthetic organic chemistry. While classical thermal or photochemical cycloaddition reactions demonstrate more than ample capability for the preparation of new (poly)cyclic compounds, much of the utility of these processes relies on the inherent polarization of the starting materials to promote the reaction and thereby achieve the desired product [1].

Recent decades have witnessed a significant shift in focus toward the use of various transition metal species to catalyze new cycloaddition reactions between unactivated alkenes, alkynes, and other unsaturated molecules, using the “tunability” of the metal complex to influence the selectivity in the reaction [2–5]. The key distinction between these carbocyclization reactions and the more classical approaches is that there is at least one carbometalation step. Among the most important features of these reactions is the high atom economy, as multiple carbon–carbon or carbon–heteroatom bonds can be formed in a single operation, making carbocyclization strategies a highly attractive approach for the reduction of chemical waste in synthetic applications. In addition, the ability to readily assemble structurally intriguing cyclic molecules, which contain a variety of ring sizes, degrees of unsaturation, and substitution patterns, from acyclic substrates under relatively mild conditions is also appealing for target-directed synthesis, because these intermediates would be difficult to prepare via classical pericyclic reactions.

While offering numerous advantages, the optimization of new carbocyclization reactions is not without its challenges. Most notably, the chemo- and regioselectivity of a fully *intermolecular* reaction can be very difficult to control in the absence of significant electronic or steric bias present in the substrates and/or the catalyst [6]. Tethering some (or all) of the components, thereby controlling the proximity of the reactive functionalities and reducing the likelihood of the

formation of undesired regioisomers, is by far the most popular approach for addressing this issue. Although this requirement often leads to an increase in the synthetic complexity of the substrates, it readily permits the selective synthesis of polycyclic products. Hence, this approach represents a convenient method for preparing the core structure of many natural products, which contain fused carbo- and heterocyclic rings of various sizes and degrees of unsaturation. While numerous 2C-components are widely available and readily undergo reactions of this type, the scope of 1C-components is primarily dominated by carbon monoxide (CO). Though highly toxic, CO is quite easy to handle and can be applied to various reaction manifolds with different transition metals, since it readily undergoes migratory insertion to install a carbonyl group in the final product, a process exemplified by the well-known Pauson–Khand reaction (PKR).

2 The Rhodium-Catalyzed Pauson–Khand Reaction

Since its initial discovery in 1973 by Pauson and Khand at the University of Strathclyde, the formal [2+2+1] cycloaddition of an alkene with an alkyne using CO derived from stoichiometric $\text{Co}_2(\text{CO})_8$ to afford cyclopentenones is among the most extensively studied of all transition metal-mediated reactions [7]. The historical development of the PKR will not be discussed in detail in this chapter, since there are already several excellent reviews available on the subject [8–12]. Rather, we wish to highlight the advent of rhodium catalysis in the field of carbonylative carbocyclizations, given the ability of rhodium to readily coordinate a wide variety of ligands and substrates, which has demonstrably broadened the scope of carbocyclization chemistry in the last 20 years and provides new strategies for the synthesis of (poly)cyclic compounds.

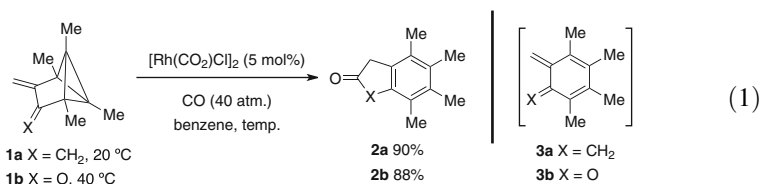
While the majority of the work using rhodium has focused on the [2+2+1] process in various guises, interchangeably referred to in the literature as the rhodium-catalyzed PKR or the PK-type reaction, the relative ease with which rhodium complexes can be applied to various reaction manifolds has facilitated the development of new two-, three-, and even four-component cyclocarbonylation methods, some of which in fact predate the rhodium-catalyzed PKR by several years, which afford five- to eight-membered rings with varying degrees of structural complexity and unsaturation.

3 Rhodium-Catalyzed [n+1] Carbocyclization Reactions

3.1 [4+1] Carbocyclizations

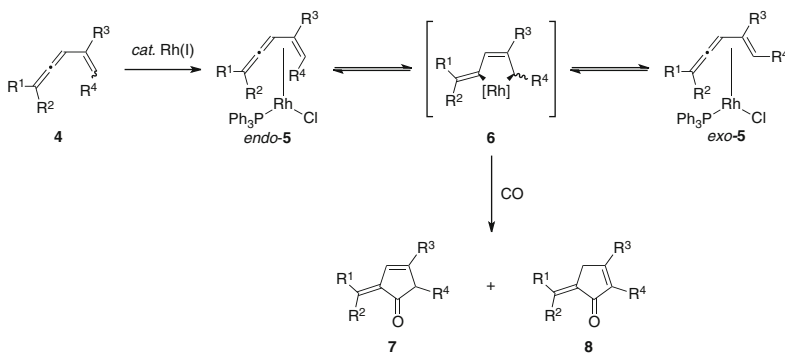
The first rhodium-catalyzed carbonylative [4+1] carbocyclization was reported by Heldeweg and Hogeveen in 1976 [13, 14]. The highly strained diene **1a** and enone **1b** can be transformed into the corresponding aromatic products **2a** and **2b** using

two equivalents of $[\text{Rh}(\text{CO})_2\text{Cl}]_2$ under mild conditions. Interestingly, in the course of these studies, they also discovered that treatment of the substrates with catalytic $[\text{Rh}(\text{CO})_2\text{Cl}]_2$ at high CO pressure (*ca.* 40 atm.) for several days also affords the desired products in excellent yields (Eq. 1). The reaction is proposed to involve the in situ formation of the reactive *ortho*-xylylene or *ortho*-benzoquinone methide intermediates **3a** and **3b**, by thermal rearrangement of **1a** and **1b**, respectively, which serve as the 4π -components in this reaction.

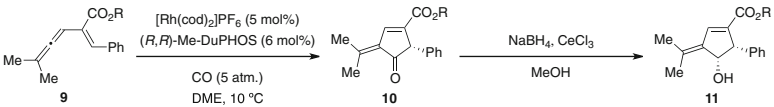


Murakami et al. later reported a [4+1] reaction of vinylallenes that contain di- and trisubstituted allenes [15]. The development of the reaction was driven by the initial discovery that substrate **4** provides a mixture of the *endo*-**5** and *exo*-**5** η^4 -coordinated rhodium complexes when treated with stoichiometric $\text{Rh}(\text{PPh}_3)_3\text{Cl}$ (Scheme 1). Interestingly, the two complexes are proposed to interconvert via the intermediate **6**, a pathway supported by the isolation and X-ray crystallographic analysis of a related complex of this type ($\text{R}^1 = \text{R}^2 = \text{Me}$, $\text{R}^3 = \text{Ph}$, $\text{R}^4 = \text{H}$), wherein the rhodacyclopentene ring was shown to be almost perfectly planar [16]. This intermediate can subsequently undergo migratory insertion with an equivalent of CO to provide mixtures of the cyclopentenone isomers **7** and **8**.

In a follow-up study, the same group also described an asymmetric variant of the [4+1] carbocyclization using the (*R,R*)-Me-DuPHOS ligand, wherein the CO pressure has a profound effect on the selectivity of the reaction [17, 18]. For instance, high CO pressure is optimal (5 vs. 1 atm.) to suppress competing β -hydride elimination from the rhodacycle intermediate, whereas at lower pressure (1 atm.), a conjugated triene is formed in an almost 1:1 ratio with the intended cyclopentenone



Scheme 1 Coordination of rhodium to vinylallenes and trapping with CO

Table 1 Synthesis of enantioenriched cyclopentenols via [4+1] carbocyclization


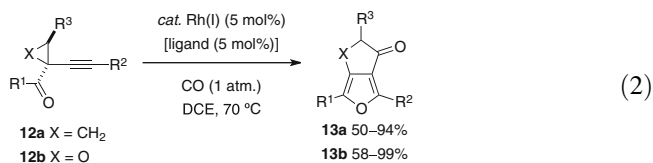
Entry	Product 11	R	Yield from 9 (%)	<i>ee</i> (%) ^a
1	a	Et	93	92
2	b	ⁱ Bu	96	92
3	c	Bn	94	95

^aDetermined by chiral HPLC analysis

product. Interestingly, the incorporation of an ester at the internal vinylic position of the alkene **9** leads to markedly improved stereoselectivity. The subsequent Luche reduction of the cyclopentenones **10** affords the *cis*-cyclopentenols **11** in almost quantitative yield and with excellent enantiomeric excess (Table 1).

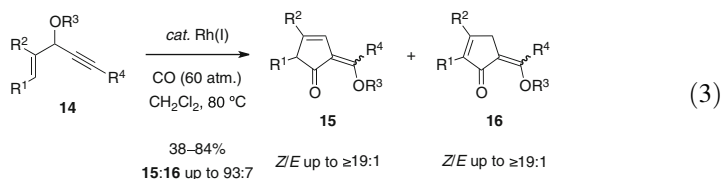
Furthermore, there are remarkable differences in the reactivity of the vinylallene species in the presence of other transition metals. For instance, a chiral platinum catalyst with (*R,R*)-Me-DuPHOS provides the cyclopentenones with the opposite absolute configuration at the α -position [19–21], whereas the corresponding palladium catalyst furnishes the corresponding [4+4+1] products at lower temperature, albeit extended conjugation is necessary for this reaction [22].

Recently, Zhang demonstrated the utility of cyclopropanes and epoxides in a rhodium-catalyzed [4+1] carbocyclization (Eq. 2). Treatment of 1-(1-alkynyl) cyclopropyl ketones **12a** (X = CH₂) with catalytic rhodium under 1 atm. of CO in DCE at 70 °C provides the bicyclic furanones **13a** bearing a variety of substitution patterns [23]. In a similar process, the analogous 1-(1-alkynyl)oxiranyl ketones **12b** (X = O) afford the corresponding oxacyclic derivatives **13b** in good to excellent yield [24]. In contrast to the cyclopropane substrates, the oxiranes require the addition of a biaryl phosphine ligand as they are otherwise inert.

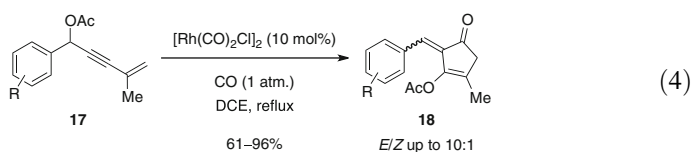


Malacria and coworkers reported the [4+1] carbocyclization of 3-acyloxy-1,4-enynes **14** containing internal alkynes using high CO pressure (Eq. 3) [25]. The reaction proceeds via an *intramolecular* 1,3-acyloxy migration (R³ = Piv, Bz, Ac), in which a variety of alkyl groups (R¹, R², R⁴) and alkene substitution patterns are tolerated, although the *endocyclic* olefin is prone to isomerization in all cases. In a concurrent study, Tang and coworkers reported an almost identical process under considerably milder conditions, requiring only 1 atm. of CO. In this case, the α,β -unsaturated isomer **16** was formed as the exclusive product in moderate to good

yield and with analogous geometrical selectivity via the treatment of the crude reaction mixture with two equivalents of triethylamine prior to purification [26].



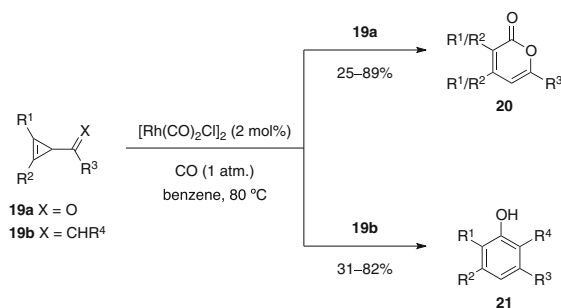
Yu and Pu also described the rhodium-catalyzed [4+1] reaction of acyloxy-substituted 1,3-enynes **17** with CO in refluxing DCE (Eq. 4) [27]. Although a variety of propargylic aryl substituents are tolerated, the *exocyclic* olefin product **18** is generally formed with modest geometric control.



3.2 [5+1] Carbocyclizations

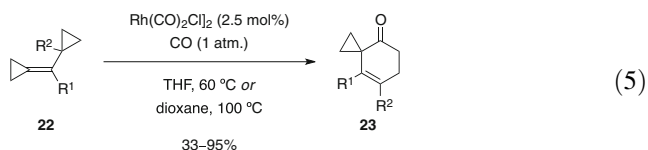
Cho and Liebeskind reported the first rhodium-catalyzed [5+1] reaction of cyclopropenyl esters and ketones **19a** (X=O) using low CO pressure to afford α -pyrone derivatives **20**, in which the product distribution is largely substrate dependent (Scheme 2) [28]. For example, cyclopropenyl esters (R³=OEt) derived from monosubstituted (R¹=H, R²=alkyl) and symmetrical alkynes (R¹=R²=Et) afford the 4,6-disubstituted α -pyrones exclusively, whereas cyclopropenyl ketones (R³=alkyl, aryl, vinyl, alkynyl) have a tendency to form furans as a result of premature reductive elimination. Additionally, treatment of symmetrical

Scheme 2 [5+1] Carbocyclizations affording α -pyrones **20** and phenols **21**

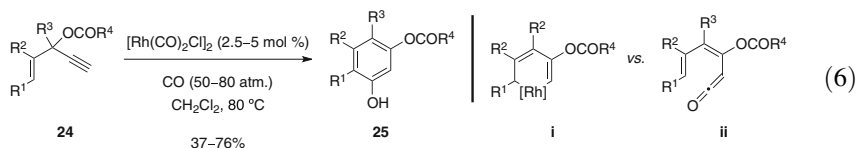


vinylcyclopropanes **19b** ($R^1 = R^2 = \text{Et}$, $R^3 = \text{Ph}$, $i\text{Pr}$, $X = \text{CHR}^4$, $R^4 = \text{H}$, Ph , $n\text{Pr}$) under the optimized reaction conditions affords the corresponding phenols **21** with varying efficiency because of the formation of cyclopentadiene by-products.

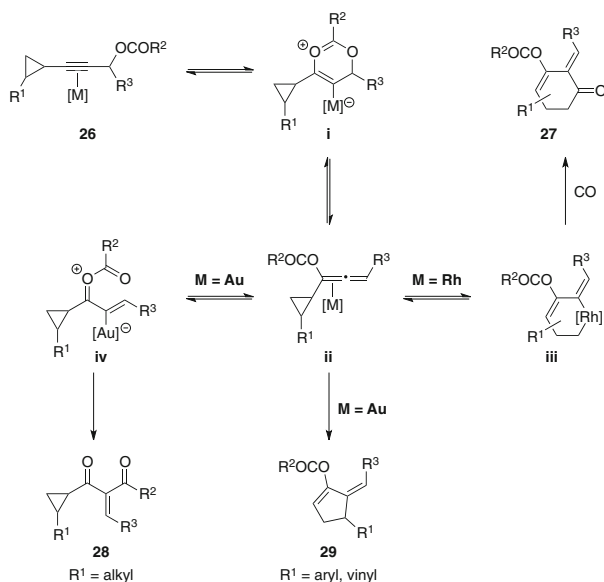
Kurahashi and de Meijere described the [5+1] reaction of (cyclopropylmethylene)cyclopropanes **22** with CO to afford substituted cyclohexenones **23** (Eq. 5) [29]. Interestingly, this transformation proceeds with moderate to excellent yield with either $\text{Co}_2(\text{CO})_8$ or $[\text{Rh}(\text{CO})_2\text{Cl}]_2$ as a catalyst in tetrahydrofuran (THF) at 60°C , albeit the latter provides higher yields in all cases. The reaction tolerates double bond and cyclopropane substitution ($R^1 = \text{Me}$, Ph , 1-cyclopropyl, $R^2 = \text{Me}$), which results in the incorporation of these substituents in the olefin in **23**. Nevertheless, the phenyl-substituted derivative ($R^1 = \text{Ph}$) is significantly less reactive, even after additional optimization of the solvent and temperature, which affords the requisite cyclohexenone **23** in poor yield (33%). Additionally, none of the desired products are formed from substrates without the cyclopropylmethylene functionality.



In an effort to develop a new strategy for the synthesis of functionalized resorcinols **25**, Malacria and coworkers described a carbonylative [5+1] reaction using 3-acyloxy-1,4-enynes **24** ($R^4 = \text{Piv}$, Ac) as the 5C-component (Eq. 6) [30]. The optimal conditions utilize high CO pressure in conjunction with dichloromethane, which afford the aromatic products **25** in 37–76% yield. Two mechanistic proposals were outlined, both of which invoke a 1,2-acyloxy migration, that is either followed by ring closure to a rhodacyclohexadiene **i** and carbonylation, or the formation of a ketene **ii** that can undergo a 6π -electrocyclization. Interestingly, the attempted trapping of the ketene **ii** with excess methanol affords almost equal amounts of the resulting acyclic methyl ester (not shown) and the resorcinol **25**, which presumably indicates that both of the proposed mechanisms may be operative. In related studies, Tang and coworkers reported that the use of a more electron-rich ester ($R^4 = 4\text{-Me}_2\text{NC}_6\text{H}_4$) facilitates the synthesis of **25** under significantly milder conditions, namely, at room temperature under 1 atm. of CO, albeit the substrate scope is quite limited [31].

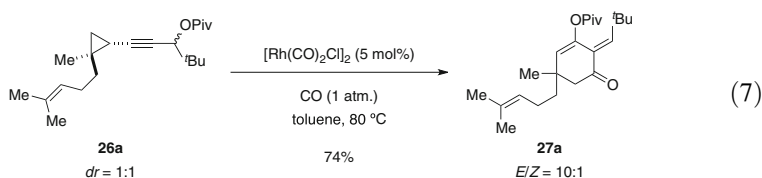


Cyclopropyl propargyl esters **26** are also suitable substrates for the rhodium-catalyzed [5+1] reaction, which provides access to substituted cyclohexenone



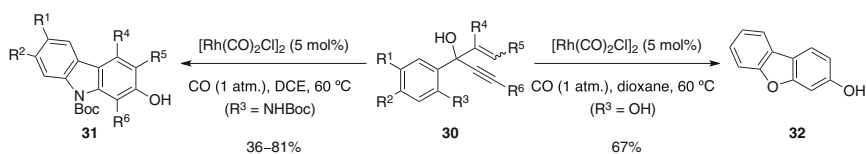
Scheme 3 Mechanism of the reactions of substituted cyclopropyl propargyl esters

derivatives in high yield [32]. The mechanism outlined in Scheme 3 accounts for the observed products, which depending on the metal catalyst employed results in a number of reaction pathways from the allenyl ester intermediate **ii**, which is derived from **26** by a 1,3-acyloxy migration (intermediate **i**). For instance, in the presence of a rhodium catalyst, oxidative ring opening of the cyclopropane affords the metallacycle **iii**, which under a CO atmosphere can undergo migratory insertion and reductive elimination to afford **27**, whereas a gold catalyst leads to the formation of **28** ($\text{R}^1 = \text{alkyl}$) or **29** ($\text{R}^1 = \text{aryl, vinyl}$) [33–35]. Interestingly, the stereochemistry in the cyclopropane **26a**, which is a 1:1 mixture of diastereoisomers at the propargylic position, is inconsequential since the cyclohexadienone **27a** is obtained with 10:1 *E/Z* selectivity (Eq. 7). The stereocontrol in this example is ascribed to the ability of the diastereomeric allene intermediates **ii** (Scheme 3) to interconvert to minimize steric interactions between the substituents and the coordinated rhodium catalyst [36].

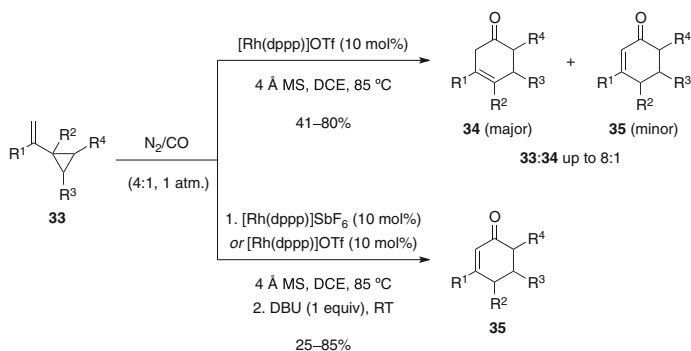


Tang et al. also reported an adaptation of the rhodium-catalyzed [5+1] carbocyclization of 3-hydroxy-1,4-enynes **30** to prepare substituted carbazole derivatives **31** ($R^3 = \text{NHBoc}$), by using a substrate that is able to participate in both an annulation and a cyclocarbonylation reaction (Scheme 4) [37]. A variety of substituents on the aryl ring (R^1 , R^2) and at the terminal position of the olefin (R^5) are well tolerated, albeit substitution of the internal position of the alkene ($R^4 = \text{Me}$) is problematic. In addition, the overall efficiency for an internal alkyne ($R^6 = \text{Me}$) can be dramatically improved using a fluorinated phosphite ligand and changing the solvent to THF. Furthermore, replacing the carbamate with a free phenol ($R^3 = \text{OH}$) and changing the solvent to dioxane permits the formation of the dibenzofuran **32**.

Yu and coworkers described the ring opening of VCPs **33** in the presence of a cationic rhodium catalyst to furnish cyclohexenone derivatives (Scheme 5), which is similar in concept to the process described by Kurahashi and de Meijere (cf. Eq. 5) [38]. Interestingly, the β,γ -unsaturated products **34** are formed as the major products, albeit the α,β -unsaturated products **35** can be formed exclusively upon treatment of the reaction mixture with DBU to mediate the conjugation of the olefin. Nevertheless, some of the unsymmetrical 1,2-disubstituted (e.g., $R^1 = R^2 = R^3 = \text{H}$, $R^4 = \text{trans-CH}_2\text{OH}$) and polysubstituted cyclopropane derivatives have a propensity to form regioisomeric mixtures.



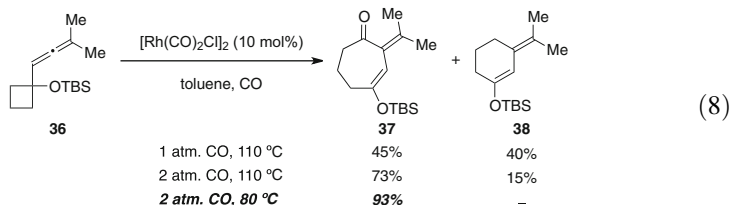
Scheme 4 [5+1] Carbocyclization reactions affording carbazoles and dibenzofurans



Scheme 5 [5+1] Carbocyclizations of VCPs affording substituted cyclohexenones

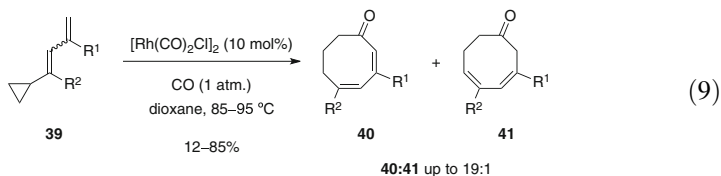
3.3 [6+1] Carbocyclizations

In contrast to the [5+1] reaction, only one example of a rhodium-catalyzed [6+1] carbocyclization has been reported, namely, the reaction of protected 1-allenylcyclobutanols **36** (Eq. 8) [39]. Although increasing the CO pressure to 2 atm. and reducing the reaction temperature from 110°C to 80°C provides complete selectivity for the cycloheptenone product **37** over the cyclohexene derivative **38**, which is formed by premature reductive elimination, these conditions are not general and require subtle modifications for each substrate. Interestingly, this substrate is effectively unreactive with the same iridium catalyst utilized for the [5+1] reaction of allenylcyclopropanes [40].

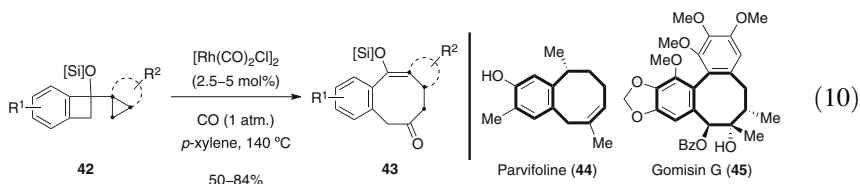


3.4 [7+1] Carbocyclizations

Yu and coworkers described the first rhodium-catalyzed carbonylative [7+1] carbocyclization reaction of the buta-1,3-dienylcyclopropanes **39**, which extended the conjugated π -system of the substrate used in the previous studies on the [5+1] carbocyclization reaction (cf. Scheme 5), to provide a mild method for the construction of eight-membered rings **40** (Eq. 9) [41]. This particular transformation appears to be unique to rhodium, since nickel [42] and palladium [43] catalysts promote a [1,3]-shift to afford 3-vinylcyclopentene derivatives. While the reaction is seemingly indiscriminate of the diene geometry, thereby allowing mixtures of isomers to be employed, the *Z*-isomer is generally more reactive. Furthermore, the fully conjugated cyclooctadienone product **40** is thermodynamically favored via the isomerization of the nonconjugated isomer **41** under the reaction conditions. Nevertheless, cyclopropane substitution is not tolerated; for example, 1,1-disubstituted examples undergo self-reaction to give cyclohexenone derivatives via an alternate pathway, whereas other substituted cyclopropane derivatives are unreactive under the conditions.



Yu et al. also reported the ability of the cyclopropyl-benzocyclobutenes **42** to act as 7C-components in the [7+1] carbocyclization reaction with CO (Eq. 10) [44]. A useful feature with this process is that the products **43** contain a fused benzocyclooctene ring system, which is present in the natural products parvifoline (**44**) and gomisin G (**45**). In contrast to the previously reported [7+1] reaction, cyclopropane rings with additional functionalization, including fusion to another cycloalkane, are nicely tolerated under the optimum conditions. However, in the absence of the silyl protecting group, an alternate C–C bond cleavage pathway predominates.



4 Rhodium-Catalyzed $[m+n+1]$ Carbocyclization Reactions

4.1 $[2+2+1]$ Carbocyclizations

The majority of the work on rhodium-catalyzed carbonylative carbocyclization reactions has focused on variations of the $[(2+2)+1]$ process, wherein a variety of tethered combinations of 2C-components have proven suitable substrates for this transformation. Hence, a number of different cyclic carbon skeletons have been prepared in a highly efficient fashion, through the careful design of substrates that incorporate suitably positioned π -components, which afford cyclopentenones that are fused to five-, six-, seven-, or even eight-membered rings with well-defined stereochemistry.

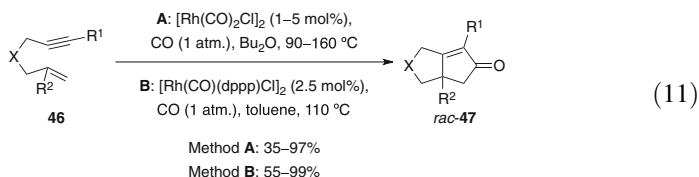
4.1.1 1, n -Enynes

Discovery and Initial Developments

Narasaka [45] and Jeong [46] independently reported the rhodium-catalyzed PK-type reaction of 1,6-enynes with CO and have also made significant contributions to the development of this reaction in the context of the scope and limitations. For instance, Narasaka and coworkers described the first rhodium-catalyzed $[(2+2)+1]$ carbocyclization in 1998, which laid the groundwork for nearly two decades of

innovation in the development of this particular class of reactions [47]. In the absence of ancillary phosphine ligands, low loadings of $[\text{Rh}(\text{CO})_2\text{Cl}]_2$ in dibutyl ether efficiently catalyze the carbonylation reaction of 1,6-enynes **46** containing different tethering atoms and various substitution patterns, albeit terminal and triorganosilyl-substituted alkynes ($\text{R}^1 = \text{H}, \text{SiMe}_3$) are considerably less efficient (Eq. 11, Method A). An additional report in 2001 outlined a fairly extensive study on the generality of the reaction, which resulted in the following observations:

- 1,2-Disubstituted alkenes react stereospecifically.
- Fused bicyclo[4.3.0] ring systems can be accessed by increasing the tether length or replacing the alkene with an allene.
- Electron-deficient alkynes, which had not been extensively employed in related PK-type reactions, are tolerated.
- The fully *intermolecular* rhodium-catalyzed PK-type reaction of alkenes and alkynes is possible but requires a reactive alkene such as norbornene.
- The CO pressure can be lowered to 0.1 atm. with minimal loss in efficiency, although high temperature and/or concentration is required.
- A key intermediate in Magnus' synthesis of *dl*-coriolin [48] can be prepared on gram-scale with high selectivity (*dr* = 9:1).



Jeong and coworkers concurrently reported the first rhodium-catalyzed PK-type reaction in 1998 using a phosphine-containing rhodium complex (Eq. 11, Method B) [49]. Interestingly, the optimum rhodium pre-catalyst that contains a bidentate ligand does not require the addition of a silver salt for activity, whereas pre-catalysts containing monodentate phosphine ligands require AgOTf in order to facilitate any type of conversion.

Sequential [(2+2)+1] Carbocyclization Reactions

Jeong and coworkers also described a one-pot synthesis of bicyclopentenones from propargyl pro-nucleophiles **48** and allylic acetates **49** via a palladium-catalyzed allylation in conjunction with a rhodium-catalyzed *intramolecular* PK-type reaction (Table 2) [50]. Interestingly, the two catalytic processes are independent of each other, i.e., palladium does not facilitate the PK reaction and rhodium does not facilitate either the allylation or an *intermolecular* PK reaction. The yields are generally excellent for the carbon and nitrogen tethers (entries 1, 2 and 4–6), whereas the process does not afford any of the oxygen-tethered PK products *rac*-**50** (entries 7 and 8).

Table 2 Sequential palladium-catalyzed allylation/rhodium-catalyzed PK-type reactions

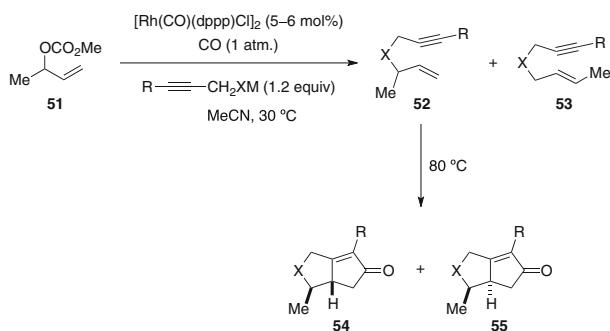
Entry	Substrate 48	X	R	Yield (%) ^a
1	a	C(CO ₂ Et) ₂	Ph	92
2	b	"	Me	73
3	c	"	H	0 ^b
4	d	NTs	Ph	90
5	e	"	Me	91
6	f	"	H	92
7	g	O	Ph	0 ^b
8	h	"	Me	0 ^b

^aIsolated yields^bA complex mixture was obtained

Based on their previous work in the area of rhodium-catalyzed allylic substitution reactions, Evans and Robinson devised a remarkable one-pot sequential allylic alkylation/PK-type reaction process, which requires a single rhodium catalyst (Table 3) [51]. The reaction required optimization of the pre-catalyst and solvent to achieve the optimal combination of branched/linear selectivity in the alkylation and diastereoselectivity in the annulation. An interesting dichotomy in selectivity was observed with the different tethers, namely, carbon- and nitrogen-tethered substrates (entries 1–6) provide excellent regioselectivity in the alkylation reaction compared to the oxygen-tethered derivatives (entries 7–9) but afford inferior diastereocontrol in the subsequent annulation.

Martin and coworkers later described a similar process also utilizing a single rhodium catalyst to mediate a sequential allylic alkylation/PK-type sequence [52, 53]. Interestingly, this process required a trifluoroacetate leaving group for optimal efficiency in the allylic substitution reaction.

In 2008, Zhang et al. reported an intriguing two-step PK-type reaction followed by a formal [3+3] cycloaddition, which provided the fused polycycles **58** (Eq. 12) [54]. Following an initial assessment of the reactivity of enediynes **56** in the [(2+2)+1] cyclocarbonylation, a number of substrates were then successfully transformed into the tricyclic products **58** by initial PK-type reaction, removal of the THF, then dissolving the crude cycloaddition products in DMF and adding two equivalents of a β -keto species **57** and substoichiometric potassium carbonate. Overall, the atom-economical sequence creates five new C–C bonds, three rings, and one quaternary stereocenter in moderate to good yields.

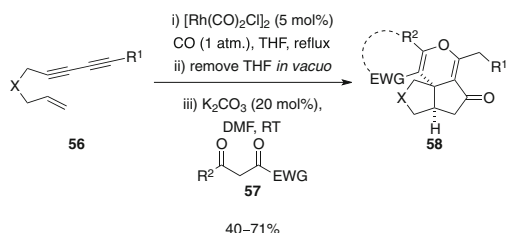
Table 3 Sequential rhodium-catalyzed allylic alkylation/PK-type reactions

Entry	Substrate 52	X	M	R	52:53 ^a	54:55 ^b	Yield (%) ^c
1	a	C(CO ₂ Me) ₂	Na	H	27:1	5:1	82
2	b	"	"	Me	19:1	6:1	80
3	c	"	"	Ph	11:1	9:1	78
4	d	NTs	Li	H	20:1	3:1	79
5	e	"	"	Me	32:1	6:1	84
6	f	"	"	Ph	57:1	7:1	81
7	g	O	Li	H	5:1	≥19:1	63
8	h	"	"	Me	7:1	≥19:1	73
9	i	"	"	Ph	8:1	≥19:1	81

^aRatios of regioisomers were determined by HPLC and capillary GLC

^bRatios of diastereomers were determined by 400 MHz ¹H NMR

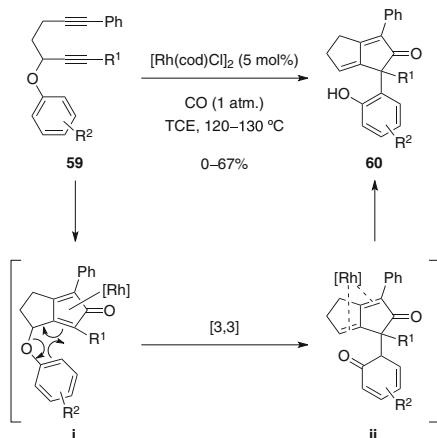
^cIsolated yields



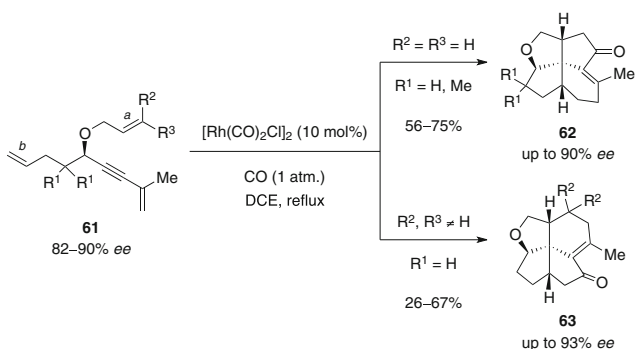
(12)

Chatani and coworkers combined the rhodium-catalyzed PK-type reaction with a Claisen rearrangement to convert the 1,6-enynes **59** to *ortho*-substituted phenols **60** (Scheme 6) [55]. Interestingly, the formation of the cyclopentadienone metal complex **i** is proposed to be critical for promoting the pericyclic reaction to afford **ii** at a significantly lower temperature than is generally the case for a thermal Claisen rearrangement with an aryl ring.

Pu and coworkers have described several examples of domino rhodium-catalyzed PK-type reactions/*intramolecular* Diels–Alder cycloadditions of optically active 1,6-enyne derivatives, which lead to fused polycyclic compounds with high enantiopurity [56, 57]. The domino reactions of trienynes **61** are sensitive



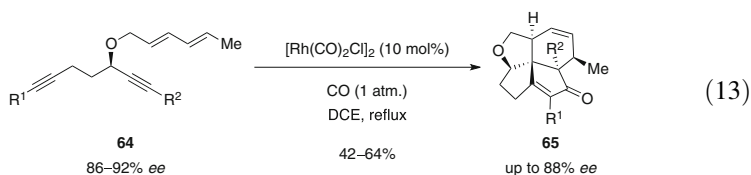
Scheme 6 Rhodium-catalyzed domino PK-type reaction/Claisen rearrangement



Scheme 7 Domino PK-type reaction/Diels–Alder cycloadditions of trienyne

to the substitution of the allylic ether olefin *a*, in which terminal olefins ($\text{R}^2 = \text{R}^3 = \text{H}$) readily participate in the PK-type reaction phase of the sequence to afford the tetracycles **62**, whereas 1,2-disubstituted ($\text{R}^2 = \text{H}$, $\text{R}^3 = \text{Me}$, Ph) and trisubstituted olefins ($\text{R}^2/\text{R}^3 \neq \text{H}$) are too sterically hindered and furnish the alternative tetracyclic adduct **63** via initial PK-type reaction between the alkyne and the less sterically encumbered terminal olefin *b* (Scheme 7).

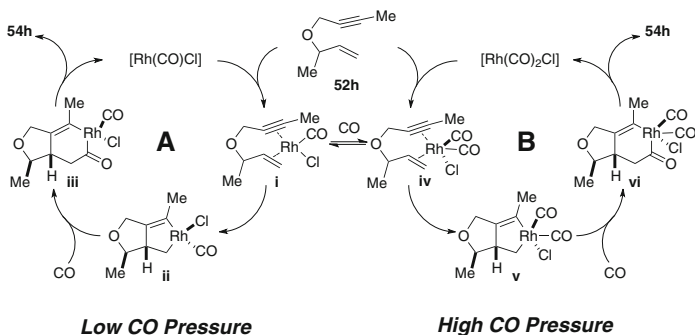
Furthermore, in a related process the structure of the fused tetracycles **65** is rationalized to be formed via a PK-type carbocyclization with the 1,6-diyne moiety of the dienediynes **64** and CO (Eq. 13) [57]. The resulting cyclopentadienone intermediate can then undergo a [4+2] cycloaddition with the pendent 1,3-butadiene to furnish the products in moderate yield. Although the diastereoselectivity of this transformation is excellent, some slight erosion of the enantiomeric excess was observed for two examples ($\text{R}^1 = \text{TMS}$, $\text{R}^2 = \text{Ph}$ or $(\text{CH}_2)_2\text{Ph}$) while values for the other substrates examined were not reported.



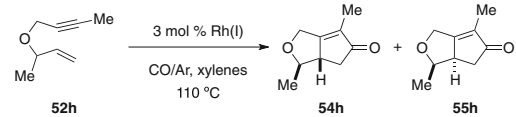
Origin of Diastereoselectivity in the [(2+2)+1] Reaction

More recently, Baik and Evans have reported several new insights into the mechanism of the diastereoselective rhodium-catalyzed PK-type reaction of 1,6-enynes in a collaborative approach that combines theoretical prediction with experimental verification. To this end, density functional theory (DFT) calculations predict a striking difference in the level of the diastereoselectivity in the oxidative addition of the four-coordinate species **ii** (Scheme 8, cycle A) versus the five-coordinate complex **iv** (cycle B), wherein the latter should provide the bicyclopentenone products with significantly improved diastereocontrol. [58]. Hence, they envisioned that this hypothesis could be tested experimentally by controlling the equilibrium between **i** and **iv** using CO concentration, since **i** is expected to be more prevalent at low CO concentration and **iv** should predominate at higher CO concentration.

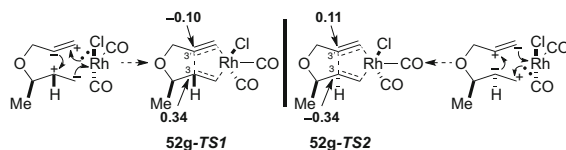
Interestingly, variation in the CO concentration led to a significant divergence in stereocontrol, in which higher CO concentration is indeed able to enforce a five-coordinate metal center and thereby garner the highest level of diastereocontrol (Table 4, entry 1 vs. 2 and 3). The prediction was further corroborated using a bidentate phosphine ligand, which enforces the five-coordinate geometry in the transition state (TS) to thereby attain similar levels of diastereocontrol for the formation of **55h** irrespective of CO pressure, albeit at the cost of efficiency at lower CO pressures due to competing side reactions (entry 4 vs. 5 and 6).



Scheme 8 Predicted catalytic cycles for the diastereoselective rhodium-catalyzed PK-type reaction under low and high CO pressures

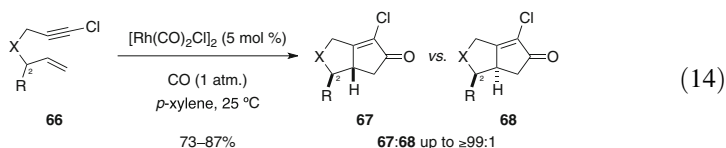
Table 4 Controlling diastereoselectivity in the PK-type reaction


Entry	Rhodium complex	Pressure (atm.)		Yield (%) ^a	54h:55h^b
		CO	Ar		
1	[Rh(CO)₂Cl]₂	1.00	0.00	81	22:1
2	''	0.10	0.90	64	10:1
3	''	0.05	0.95	57	6:1
4	[Rh(CO)(dppp)Cl]₂	1.00	0.00	88	≥99:1
5	''	0.10	0.90	51	58:1
6	''	0.05	0.95	44	57:1

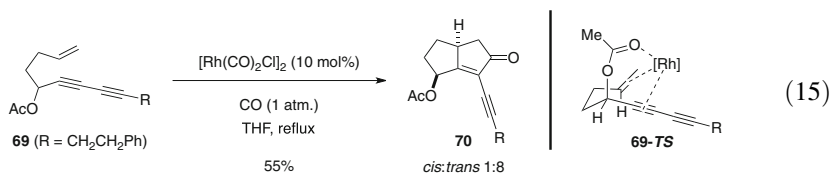
^aIsolated yields^bRatios of diastereomers were determined by capillary GLC analysis on the crude reaction mixtures**Fig. 1** Computed partial charges for the oxidative addition transition states in the rhodium-catalyzed PK-type reaction of 1,6-enynes

Further computational analysis of the diastereoselectivity obtained in this process led Baik and Evans to propose that pre-polarization of the 1,6-enyne would resemble the charge polarization of the desired transition state **52g-TS1**, which should lower the barrier for the rate-determining step and thereby permit the reactions to be conducted at lower temperature and thus improve the level of stereocontrol (Fig. 1) [59]. As indicated by the theoretical partial charges, both transition states **52g-TS1** and **52g-TS2** are highly charge-polarized but in opposite directions at the distal carbon atoms (C3, C3') in the metallacycles.

In accord with this hypothesis, chlorination of the alkyne terminus permits the cyclization of C2-substituted 1,6-chloroenynes **66** to proceed spontaneously at 25 °C and dramatically improves diastereoselectivity for this process (Eq. 14). For example, the reactions afford excellent yields of the chlorinated bicyclopentenone derivatives **67** at room temperature with almost perfect diastereoselectivities, including those for substrates with sulfonamide tethers (X = NTs), which is in contrast to previous studies (cf. Tables 3 and 6).



Pu and coworkers reported a variation of the rhodium-catalyzed PK-type reaction, wherein the omission of a chelating phosphine ligand leads to a reversal in diastereoselectivity [60]. For example, carbonylation of the enediyne **69** affords the bicyclopentenone **70** with a preference for the *trans*-stereoisomer (Eq. 15). To account for the observed selectivity, they proposed that the acetate substituent acts as a chelating group, thus directing the catalyst to the pseudoaxial face of the substrate as depicted in **69-TS** (cf. Table 6).



Enantioselective [(2+2)+1] Carbocyclizations

Jeong and coworkers described the first asymmetric *intramolecular* rhodium-catalyzed PK-type reaction, utilizing (*S*)-BINAP as the optimum chiral ligand (Table 5) [61]. In this case, the addition of AgOTf is necessary in order to initiate the process, by providing a cationic rhodium species with an open coordination site.

Table 5 The first asymmetric rhodium-catalyzed PK-type reaction

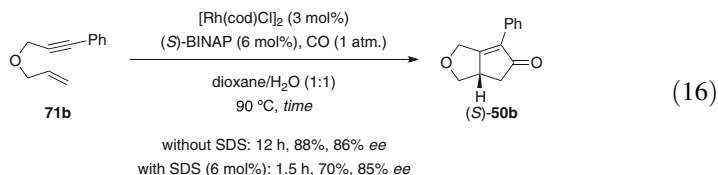
Entry	Substrate 71	CO (atm.)	Temp (°C)	Time (h)	Yield (%) ^a	<i>ee</i> (%) ^b
1	a	3	130	20	96	22
2	''	1	90	6	67	61
3	b	2	130	20	85	86
4	''	1	90	5	40	96
5	c	3	130	20	96	46
6	''	1	90	3	93	74

^aIsolated yields

^bDetermined by chiral HPLC analysis

Notably, tetrahydrofuran is crucial for obtaining the highest levels of stereocontrol, whereas the reaction is more efficient in toluene. The enantioselectivity can be further improved at lower temperature and under reduced CO pressure, albeit at the expense of the yield for most of the examples examined (entries 1, 3, and 5 vs. 2, 4, and 6). Jeong [62–64] and others [65, 66] have also reported alternative chiral ligands for the asymmetric rhodium-catalyzed [(2+2)+1] reaction of 1,6-enynes with CO, the impact of different solvents [67], the role of *intramolecular* chelation [68], desymmetrization reactions [69, 70], and kinetic resolutions [71].

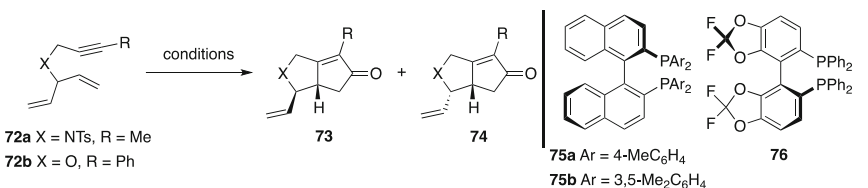
Chung and coworkers described the asymmetric *intramolecular* rhodium-catalyzed PK-type reaction using water as a cosolvent [72]. Treatment of the 1,6-enyne **71b** with [Rh(cod)Cl]₂ and (*S*)-BINAP in a 1:1 mixture of dioxane/H₂O furnished the bicyclopentenone (*S*)-**50b** in 88% yield and with 86% enantiomeric excess (Eq. 16). Interestingly, the addition of 6 mol% of the anionic surfactant SDS reduces the reaction time to 1.5 hours with minimal loss in enantioselectivity, albeit the yield is slightly reduced. Despite the moderate to excellent enantioselectivities (68–96% *ee*), the overall efficiency of this process is highly substrate dependent.



Schmid and Consiglio described the first asymmetric rhodium-catalyzed [(2+2)+1] cyclocarbonylation at room temperature in 2004, wherein slow release of CO into the reaction mixture from impregnated molecular sieves provides moderate yields and excellent enantioselectivities [73]. In 2008, Jeong and coworkers also reported an enantioselective room temperature [(2+2)+1] reaction, utilizing a chiral BINAP derivative in conjunction with a low partial pressure of CO to obtain the bicyclopentenones with generally high yields and enantioselectivities [74]. A striking feature with this process, is that under similar conditions, the sulfonamide-tethered prochiral dienyne **72a** provides the *trans*-diastereoisomer **74a** with moderate diastereo- and enantioselectivities (Table 6, entries 1–3) whereas the oxygen-tethered derivative **72b** favours the opposite diastereoisomer **73b** with analogous enantiocontrol (entries 4–6). The level of diastereocontrol for the oxygen tether is consistent with Evans' observations in the sequential diastereoselective rhodium-catalyzed allylic alkylation/PK-type reaction (cf. Table 3).

1,4-Enynes

In 2013, Shi and coworkers reported the PK-type reaction of 1,4-enynes, wherein the alkene and alkyne are tethered via a cyclopropyl ring (Scheme 9) [75]. For instance, treatment of the enynes **77** with 5 mol% [Rh(CO)₂Cl]₂ under 1 atm. of CO at elevated temperature affords the bicyclic indenones **78**, arising from the incorporation of two equivalents of CO, in moderate yield. The reaction is proposed to

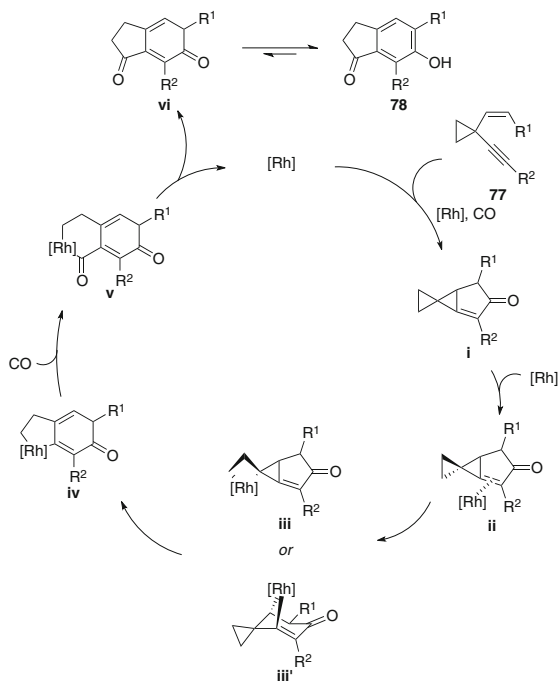
Table 6 Asymmetric desymmetrization of dienes by enantioselective PK-type reaction


72a X = NTs, R = Me
72b X = O, R = Ph

75a Ar = 4-MeC₆H₄
75b Ar = 3,5-Me₂C₆H₄

Entry	Substrate	Conditions ^a	Ligand	Ligand loading (mol%)	<i>t</i> (h)	73:74	ee 73/74 (%)
1	72a	A	75a	9	0.5	1:5.5	52/80
2	"	B	75b	20	1	1:3.4	56/71
3	"	"	76	20	"	1:4.2	42/86
4	72b	A	75a	9	2.5	≥19:1	86/–
5	"	"	75b	9	2	"	84/–
6	"	C	76	10	"	"	95/–

^aConditions: **A** [Rh(CO)₂Cl]₂ (3 mol%), ligand (9 mol%), AgOTf (12 mol%), CO (1 atm.), THF, 90 °C. **B** [Rh(CO)₂Cl]₂ (10 mol%), ligand (20 mol%), AgOTf (24 mol%), Ar:CO (10:1, 1 atm.), THF, 10 °C. **C** [Rh(CO)₂Cl]₂ (5 mol%), ligand (10 mol%), AgOTf (12 mol%), Ar:CO (10:1, 1 atm.), THF, 18–20 °C

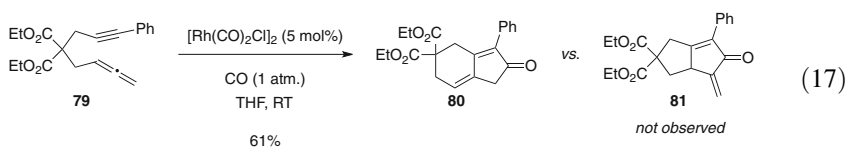
Scheme 9 Cyclopropyl-tethered [4+1] carbocyclization of 1,4-enynes

commence with a formal [(2+2)+1] reaction to form a spiro-pentane intermediate **i**, which is followed by oxidative addition with rhodium to form one of two possible metallacycles **iii** or **iii'** that β -carbon eliminate to afford intermediate **iv**. A second migratory insertion of CO and subsequent reductive elimination gives the cyclohexadienone **vi**, which then tautomerizes to the phenol **78**.

4.1.2 The Allenic Pauson–Khand-Type Reaction

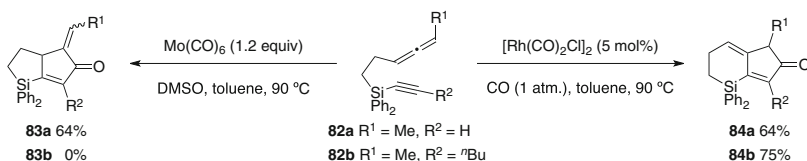
Allenynes

As previously discussed in Sect. 4.1.1, Narasaka reported the first rhodium-catalyzed allenic PK-type reaction with remarkable chemoselectivity, albeit with only a single example (Eq. 17) [45]. The carbocyclization of the allenyne **79** proceeds efficiently at room temperature with complete selectivity for bicyclopentenone **80** because of the selective reaction of rhodium with the distal bond of the allene, as opposed to the alternative reaction with the proximal bond to afford **81**.



In an effort to prepare the key cyclopentenone present in prostaglandins, Brummond and coworkers developed a silicon-tethered carbocyclization of allenynes, in which the tether can either be cleaved or functionalized following the cycloaddition [76]. Treatment of the silyl-tethered allenynes **82** with stoichiometric $\text{Mo}(\text{CO})_6$ or catalytic $[\text{Rh}(\text{CO})_2\text{Cl}]_2$ under 1 atm. of CO led to some interesting differences in reactivity (Scheme 10). For instance, molybdenum preferentially reacts at the proximal bond of the allene whereas rhodium reacts at the distal bond, to afford the structural isomers **83** and **84**, respectively [77]. Although the rhodium-catalyzed reactions proceed in moderate to good yield for both terminal and internal alkynes, the molybdenum-mediated process is completely intolerant of internal alkynes **82b**.

Further exploration of the substrate scope indicated that simple methylene tethers and a variety of allene substituents can be employed in the reaction,



Scheme 10 Mo-mediated and Rh-catalyzed reactions of allenynes

including a 1,1,3-trisubstituted derivative to form a spirocycle and a 1,3,3-trisubstituted allene bearing a free carboxylic acid (67%) [78]. Additionally, increasing the length of the tether affords fused bicyclo[5.3.0] derivatives in good yield.

Manku and Curran reported an adaptation of this process as the key ring-forming strategy in the preparation of a small library of highly functionalized bicyclopentenones via fluorous mixture synthesis [79]. Mixtures of allenynes bearing fluorous tags of different fluorine content were subjected to the cyclo-carbonylation reaction to provide the corresponding crude bicyclopentenones, which were then separated by fluorous HPLC according to the retention properties afforded by the different tags. Cleavage of the fluorous tags provided the desired bicyclopentenone derivatives in moderate to excellent yields and with high purity.

In 2002, Mukai et al. described the rhodium-catalyzed allenic PK-type reactions for the carbocyclization of 1,1-disubstituted phenylsulfonylallenes **85** and **87** (Scheme 11) [80, 81]. These substrates were chosen because of their relative ease of preparation from propargyl alcohol derivatives and the ability to readily transform the sulfone into other groups. Two different rhodium pre-catalysts were examined in the reaction, both of which afford the bicyclo[5.3.0] ring systems **86** and **88** exclusively. Conversely, a simple 1,8-enyne does not participate in the [(2+2)+1] reaction, highlighting the increased reactivity of allenes over alkenes.

Additional functionalization of the distal double bond of the allene relative to the sulfone in **89** proved more challenging, as higher CO pressures were required to favor the formation of the PK products **90** over crossed trienes **91** that result from β -hydride elimination (Table 7, entries 1 vs. 5 and 3 vs. 6). In contrast, utilizing internal alkynes provides a dramatic increase in yield (entry 1 vs. 2) [82, 83]. Moreover, larger groups (R^1) in conjunction with higher CO pressure completely suppress the formation of the triene product (entries 3 and 4).

In an adaptation of this approach, eight-membered ring containing bicyclo[6.3.0] derivatives **93** were accessed via the allenic PK-type reaction of **92** (Scheme 12A) [84]. In this case, a 1,2-disubstituted aromatic ring is required as the tether for

Scheme 11 Synthesis of bicyclo[5.3.0] compounds via [(2+2)+1] carbocyclization

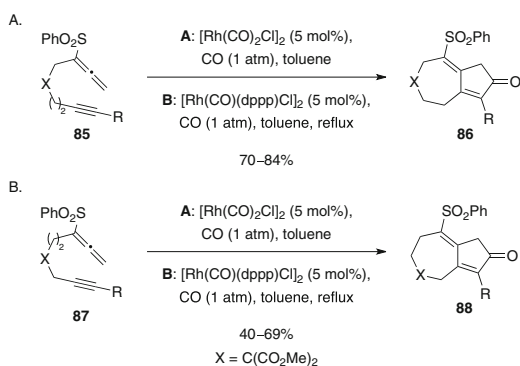
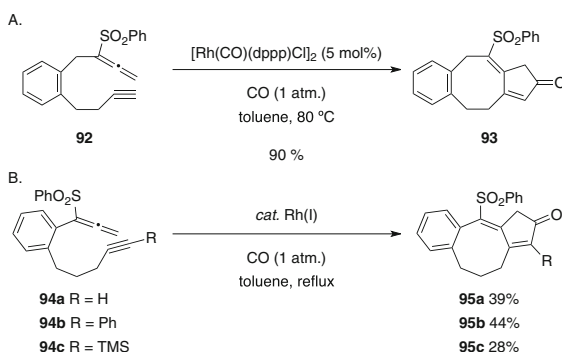


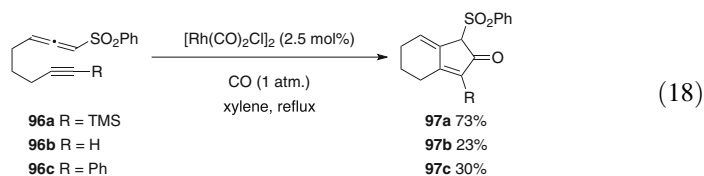
Table 7 Rhodium-catalyzed [(2+2)+1] carbocyclizations of trisubstituted allenynes

Entry	Substrate 89	R ¹	R ²	CO (atm.)	Time (h)	Product (% yield)	
1	a	H	H	10	3	90a (17)	91a (2)
2	b	H	TMS	"	13	90b (79)	91b (8)
3	c	ⁿ Pr	TMS	10 ^a	"	90c (67)	—
4	d	OBn	TMS	"	6	90d (91)	—
5	a	H	H	1 ^b	3	90a (4)	91a (77)
6	c	ⁿ Pr	TMS	1 ^c	5	90c (24)	91c (70) ^c

^a10 mol% of [Rh(CO)₂Cl]₂ was used^bRefluxed in toluene^cA mixture of (*E*)- and (*Z*)-isomers was obtained in a ratio of 4:1**Scheme 12** Synthesis of eight-membered rings via the allenic PK-type reaction

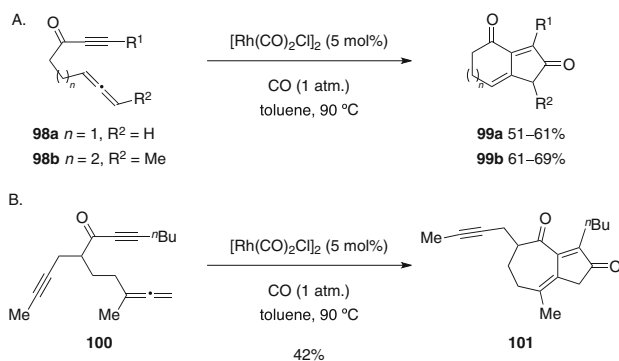
optimal efficiency, as both methylene and malonate tethers provide poor yields of the desired products. Although the isomeric 6,8,5-fused tricycles **95** can also be prepared using the isomeric substrate **94**, the reactions are considerably less efficient (Scheme 12B).

1,3-Disubstituted phenylsulfonylallenynes **96** have also been utilized as substrates in the [(2+2)+1] reaction for the synthesis of bicyclo[4.3.0] derivatives **97** (Eq. 18) [85]. In comparison to previously reported reactions of 1,1-disubstituted allenynes, the sulfonyl moiety is incorporated at the α -carbon of the cyclopentenone ring in the products. Although silylated internal alkynes are reasonably well tolerated under the optimum conditions, the aryl-substituted or terminal alkynes are less efficient (vide infra).

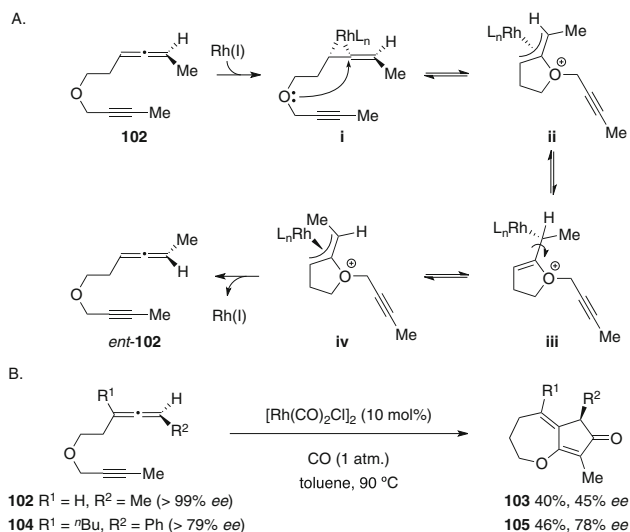


Brummond and Chen described the rhodium-catalyzed PK-type reaction of allenynes **98** to furnish bicyclic dienenediones **99** (Scheme 13A) [86]. Interestingly, the allene substitution determines the success of the cyclocarbonylation reaction, namely, a monosubstituted allene **98a** ($n = 1$, $R^2 = \text{H}$) is necessary for the formation of cyclohexenone **99a**, while a disubstituted allene **98b** ($n = 2$, $R^2 = \text{Me}$) is required for the synthesis of the seven-membered ring product **99b**. The carbonyl group plays a critical role in forming the seven-membered ring, since substrate **100**, which provides competition between two alkynes, affords **101** exclusively, albeit in modest yield (Scheme 13B).

Grillet and Brummond later reported the stereospecific construction of 5,7-bicyclic ring systems via the rhodium-catalyzed reaction of enantioenriched allenynes with CO in toluene at 90°C, using a relatively high catalyst loading to suppress the formation of the crossed triene side product observed by Mukai [87]. Nevertheless, the enantiomerically enriched 1,3-disubstituted allenenes **102** undergo varying degrees of stereochemical leakage, which is proposed to be the result of a bond rotation within cyclic intermediates **ii-iv** formed by initial *intra*-molecular attack of the etheral group in **i** and subsequent isomerization (Scheme 14A). Upon re-isomerization and reductive elimination, the opposite enantiomer *ent*-**102** can be formed and participate in the [(2+2)+1] process, thus eroding the enantiomeric excess. In contrast, the trisubstituted allene in **104** is too sterically congested to permit attack, thereby affording exclusive distal coordination and thus the ensuing cycloaddition occurs with significantly improved chirality transfer (Scheme 14B).

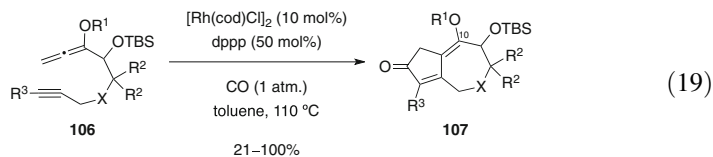


Scheme 13 [(2+2)+1] Carbocyclization reactions of allenynes with CO



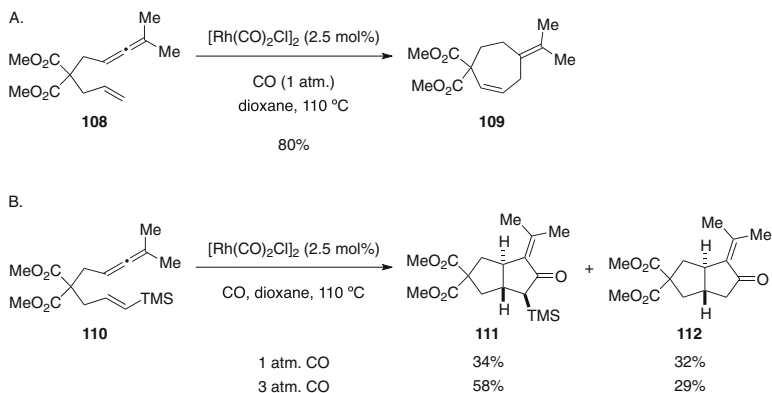
Scheme 14 Mechanistic rationale for erosion of enantiomeric excess and reactions of di- and trisubstituted allenynes

Ardisson and coworkers recently reported an intriguing contribution to this particular substrate class by employing 1,1-disubstituted alkoxyallenynes **106** as substrates, which permits entry into the guaiane skeleton **107** containing the requisite oxygenation at C10 that is present in a number of guaiane natural products (Eq. 19) [88]. Interestingly, the carbon-tethered substrates ($X = \text{CR}_2$, $\text{R}^2 = \text{H}$) generally provide higher yields than their nitrogen- ($X = \text{NTs}$, $\text{R}^2 = \text{H}$) and oxygen-tethered ($X = \text{O}$, $\text{R}^2 = \text{Me}$) counterparts, in which for each series of tethers the efficiency decreases in accord with the nature of the protecting group ($\text{R}^1 = \text{CON}(\text{tPr})_2 > \text{Bn} > \text{PMB}$). Moreover, the triorganosilyl-substituted alkynes ($\text{R}^3 = \text{TMS}$) are less efficient than the terminal and alkyl-substituted counterparts ($\text{R}^3 = \text{H}, \text{Me}, \text{Et}, \text{CH}_2\text{OBn}$) and in some cases fail to provide any of the corresponding products **107**.



Allenenes

In 2004, Makino and Itoh outlined the striking difference in the reactivity of tethered allenenes in a rhodium-catalyzed cyclocarbonylation, which was based on the substitution of the olefin (Scheme 15) [89]. For instance, with the



Scheme 15 Effect of a vinyl triorganosilane on cyclization reactions of allenenes

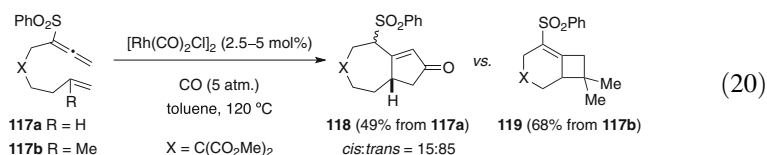
terminal olefin **108**, the cycloheptene product **109** is obtained in excellent yield (Scheme 15A), whereas the vinyl triorganosilane derivative **110** affords a mixture of the [(2+2)+1] carbocyclization product **111** and its desilylated derivative **112** with the formation of a *trans*-fused ring junction in both cases (Scheme 15B). Although the yield of the α -silyl bicyclopentenone **111** can be significantly improved at higher CO pressure, the formation of **112** remains problematic. The dichotomy in reactivity between **108** and **110** is attributed to increased stabilization of the silicon substituted rhodacycle intermediate, which thus favors CO insertion.

Inagaki and Mukai also reported an *intramolecular* rhodium-catalyzed PK-type [(2+2)+1] carbocyclization reaction of allenenes with CO [90]. As with their previous studies with allenes, 1,1-disubstituted phenylsulfonylallenes were employed, and depending on the tether length, either bicyclo[4.3.0] or bicyclo[5.3.0] compounds can be accessed. Nevertheless, the ratios of *cis*- and *trans*-isomers of the bicyclo[4.3.0] products are generally difficult to control (Table 8, entries 1, 3, and 6), albeit with the exception of reactions with 1,1-disubstituted alkenes **113** ($R^1 \neq H$), which stereoselectively afford the *trans*-bicyclo[4.3.0] adducts **115** with an angular substituent (entries 2, 4 and 5). For the larger bicyclo[5.3.0] ring systems, increasing the catalyst loading and CO pressure increases the preference for the formation of the *cis*-isomer, albeit complete stereocontrol is only observed in a single example. In general, 1,1-disubstituted alkenes are not suitable substrates for the preparation of the bicyclo[5.3.0] derivatives. For instance, the carbon-tethered substrate **117a** provides the bicyclopentenone **118** in 49% yield, whereas the 1,1-disubstituted derivative **117b** participates in a thermal [(2+2)] cycloaddition to afford **119** in 68% yield (Eq. 20).

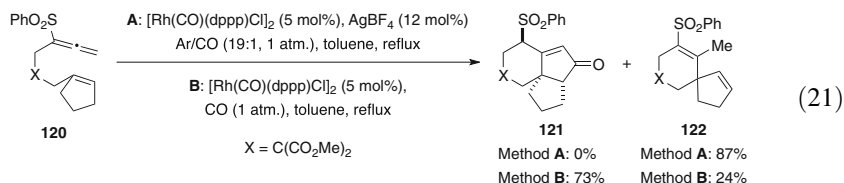
Table 8 Representative substrate scope for the cyclocarbonylation of allenenes **113**

Entry	Substrate 113	X	R ¹	R ²	Yield (%)	114:115
1	a	NTs	H	H	89	71:29
2	b	NTs	Me	''	58	0:100
3	c	O	H	''	63	82:18
4	d	C(CO ₂ Me) ₂	Me	''	85	0:100
5	e	''	(CH ₂) ₂ OMe	''	69	0:100
6	f	''	H	Me	51 ^a	33:67

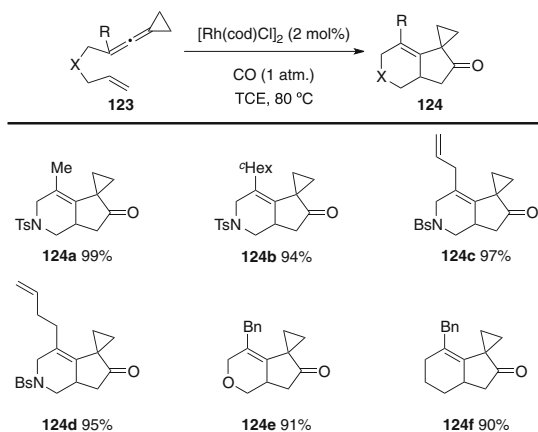
^aCompound **116** was also obtained in 36 % yield



Mukai and coworkers further examined the *intramolecular* rhodium-catalyzed [(2+2)+1] carbocyclization of 1,1-disubstituted allenenes with 1,1-disubstituted alkenes [91]. A very low partial pressure of CO and the addition of AgBF₄ is required for the optimal synthesis of the bicyclic products. A striking difference was observed with the cyclopentene containing derivative **120**, which under the optimum conditions affords exclusively the non-carbonylated spirocyclic adduct **122** in 87% yield (Eq. 21). Interestingly, the omission of the silver salt and switching to a higher CO pressure (1 atm.) was required to obtain the desired angular tricyclic **121** in 73% yield, albeit significant quantities of the spirocyclic **122** (24%) are formed.



Shi and Li reported the rhodium-catalyzed [(2+2)+1] carbocyclization of ene-vinylidencyclopropanes (ene-VDCPs) with CO, to afford products that contain an α -spiro-cyclopropane [92]. Treatment of the ene-VDCPs **123** with 2 mol% [Rh(cod)Cl]₂ under 1 atm. CO in 1,1,2,2-tetrachloroethane (TCE) at 80 °C promotes the formation of the carbonylated cycloadducts **124** in excellent yield, for a variety of allene substituents (Table 9). Nevertheless, the reaction with a homologated tether does not provide the analogous cycloadduct, limiting the application of this methodology to the synthesis of smaller rings.

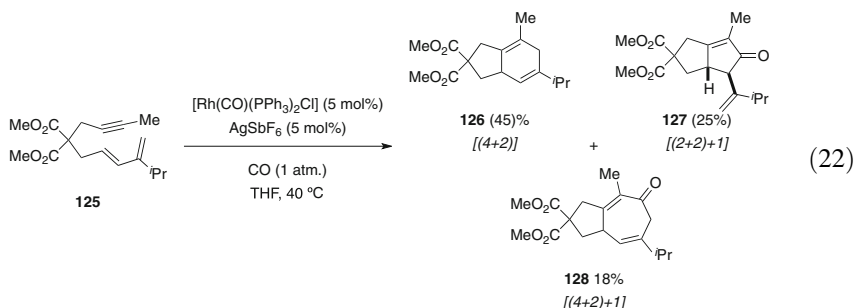
Table 9 Representative substrate scope of the [(2+2)+1] reaction of ene-VDCPs^{a,b}

^aReactions were carried out at 80 °C within 1 h

^bIsolated yields

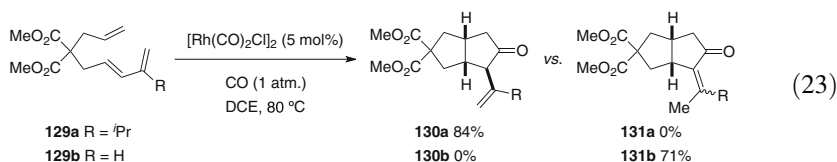
4.1.3 The Dienyl Pauson–Khand-Type Reaction

In 2003, Wender and coworkers described the first rhodium-catalyzed PK-type reaction using a diene as a 2C-component [93, 94]. The optimization of the reaction probed the impact of solvent, temperature, CO pressure, and catalyst loading, in which the modification of the catalyst with AgSbF_6 was required to suppress the formation of the undesired *intramolecular* [(4+2)] and [(4+2)+1] pathways (Eq. 22). Interestingly, the formation of the bicyclohexadienone **128** via the latter process is unique and to the best of our knowledge has not been further investigated. A variety of diene-ynes participate in the desired [(2+2)+1] carbocyclization, although terminal alkynes are poor substrates and afford low yields.



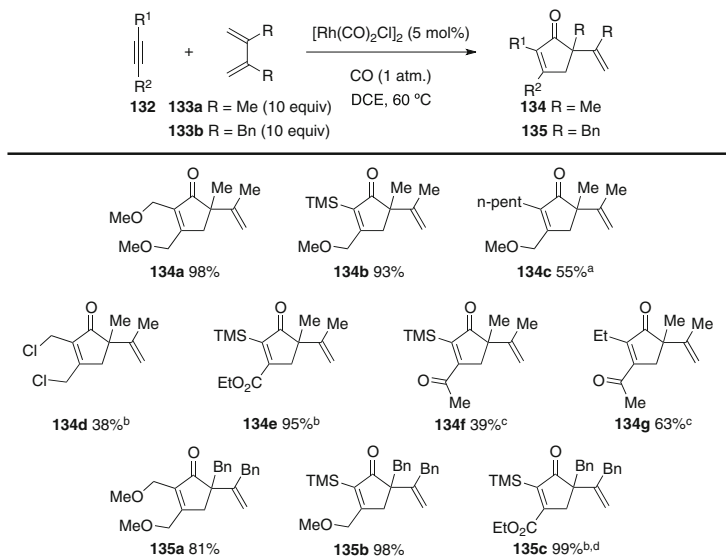
Alkenes tethered to dienes can also participate in a cyclocarbonylation reaction. Interestingly, the neutral complex $[\text{Rh}(\text{CO})_2\text{Cl}]_2$ provides the optimal catalyst for this process [95], which contrasts the alternate cationic pre-catalyst

[Rh(cod)(naph)]SbF₆ that leads to the exclusive formation of the corresponding [(4+2)] product. Furthermore, simple 1,6-dienes do not react via the [(2+2)+1] pathway, even with substrates that contain coordinating heteroatoms and extended conjugation in the form of a phenyl group. Alkyl substitution at the 2-position of the diene is critical to obtain the desired products in high yield, for example, the ene-diene **129a** (R = *i*Pr) affords the all-*cis*-bicyclopentanone **130a** in 84% yield, whereas the unsubstituted derivative **129b** (R = H) leads to the exclusive formation of the isomeric product **131b** (Eq. 23). A particularly impressive feature with this strategy is the ability to facilitate the fully *intermolecular* reaction between a strained cyclic alkene and a substituted 1,3-butadiene, albeit over an extended reaction time [95].



The PK-type reaction of ene-dienes was also examined using DFT studies to understand the precise role of the diene in the reaction mechanism and thus identify why these substrates are more reactive than simple 1,6-dienes [96]. The calculations suggest that following coordination of the active rhodium catalyst to the internal olefin of the diene and the pendent allyl group, the diene is able to undergo rearrangement from an η^2 -complex to the corresponding η^4 -coordination mode with concomitant thermoneutral expulsion of one of the CO ligands. The overall effect of these two events is that the rhodium center is more electron rich and therefore oxidative addition becomes much more facile, with a reasonable energy barrier of 21.7 kcal/mol. In contrast, the barrier for oxidative addition for the simple 1,6-diene is significantly higher (36.7 kcal/mol) since the rhodium center in this scenario is already relatively electron deficient, which means that the loss of a CO ligand prior to oxidative addition and the lack of an available *intramolecular* π -ligand to occupy the vacant coordination site make this process much less favorable.

Armed with the knowledge that dienes are more reactive than alkenes in the rhodium-catalyzed [(2+2)+1] process and that a fully *intermolecular* reaction between a strained alkene and a diene proceeds in high yield, Wender and coworkers expanded the scope of the rhodium-catalyzed dienyl PK-type reaction to the *intermolecular* reaction between diene **133a** with both symmetrical and unsymmetrical alkynes **132** (Table 10) [97]. Interestingly, some unsymmetrical alkynes afford a single regioisomer of the product **134**, whereas others bearing alkyl chains afford mixtures and terminal alkynes are unreactive. Nevertheless, the TMS-protected counterparts are able to participate in this process, which permits deprotection and access to the product derived from the terminal alkyne. Additionally, the dibenzyl analog **133b** provides the corresponding cycloadducts **135** in high yields. Remarkably, only 1.2 equivalents of **133b** are sufficient to provide **135c** in 82% yield, which is presumably because of the significantly reduced volatility of **133b** relative to the dimethyl derivative **133a**.

Table 10 Representative substrate scope of the fully *intermolecular* rhodium-catalyzed [2+2+1] carbocyclization of alkynes, 1,3-butadienes and CO

^aThe regioisomer from opposite alkyne insertion was also isolated in 35% yield

^b1:1 DCE:TCE employed as solvent

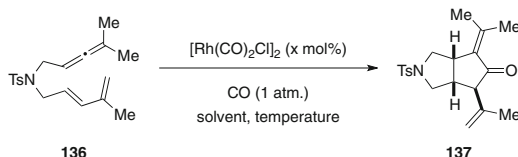
^cTCE employed as solvent instead of DCE

^dWith 1.2 equivalents of the diene: 82% yield

Allenes have also been tethered to dienes in the *intramolecular* rhodium-catalyzed [(2+2)+1] reaction to circumvent the limitations with the analogous reaction with ene-allenes developed by Brummond [98] and Itoh [89], which generally favor non-carbonylative cycloaddition reactions. Notably, there is a remarkable solvent effect on the reaction efficiency with diene-allenes **136** (Table 11) [99]. For instance, trifluoroethanol (TFE) provides the optimal medium to afford the cycloadduct **137** in 92% yield after *ca.* 15 minutes (entry 7), which is in sharp contrast to the other solvents even after extended reaction times. This substantial effect on the reaction rate was ascribed to the increased acidity of this solvent, since similar efficiency can be achieved by the simple addition of an acid additive. Notably, the analogous process in neat acetic acid affords the bicyclopentenone product **137** in 93% yield after *ca.* 2 hours.

4.1.4 Bis(allene)s

The rhodium-catalyzed [(2+2)+1] carbocyclization reaction with bis(allene) substrates is relatively limited, in that the majority of the research in this area focuses almost exclusively on tether lengths, and, consequently, substituent effects have not

Table 11 Optimization of the rhodium-catalyzed [(2+2)+1] carbocyclization of allene-dienes with CO

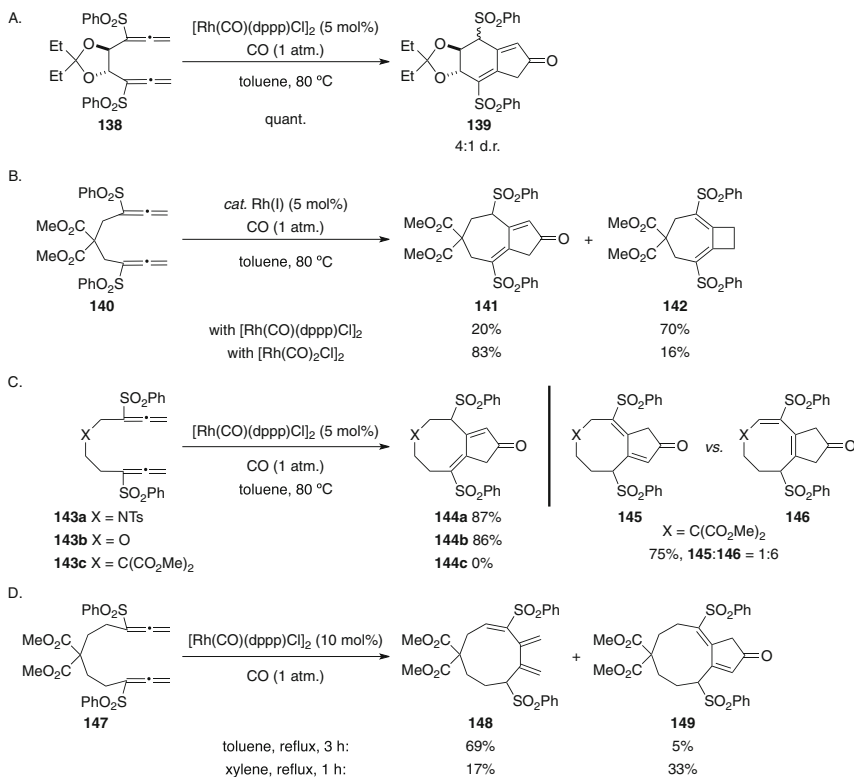
Entry	Solvent	Temp (°C)	Time (h)	Rh loading (mol%)	Yield (%)
1	DCE	80	1	5	43
2	"	RT	7	5	99
3	Toluene	"	24.5	10	38
4	Dioxane	"	21.5	"	64
5	MeCN	"	45	"	77
6	MeOH	"	12	"	96
7	TFE	"	0.25	"	92
8	TFE	RT	8	0.1	97

been extensively investigated [100–103]. Nevertheless, these substrates provide efficient access to medium-sized rings under relatively mild conditions; notably, the efficient construction of eight-membered rings, which had previously only been accessible in low yield via the rhodium-catalyzed PK-type reaction (see Scheme 12B).

Mukai et al. utilized this approach for the construction of bicyclo[4.3.0], [5.3.0] and [6.3.0] systems, in which substitution of both allenes with a sulfone is required for optimal formation of the carbonylated products (Scheme 16) [100, 101]. Bis(allene)s with only one sulfone are also tolerated, albeit the reactions generally lead to mixtures of products arising from olefin isomerization. (Scheme 16) [100, 101]. A single example of a PK-type reaction to afford a nine-membered ring **149** has also been described utilizing the homologated tether **147** (Scheme 16D).

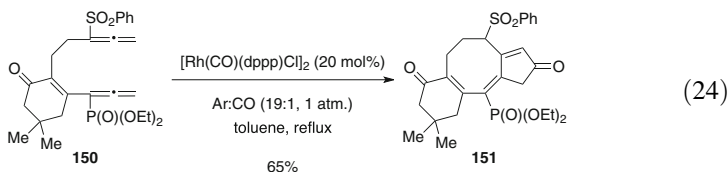
In general, the presence of two sulfones dramatically improves the efficiency, which is presumably the result of their ability to suppress the undesired cyclo-metalation of the internal olefins. The overall efficiency for the synthesis of bicyclo [5.3.0] derivatives appears to be somewhat catalyst dependent, since there is significant variation in the optimal pre-catalyst (Scheme 16B). In the case of the bis(allene) **140**, an unavoidable [(2+2)] side reaction that furnishes the bicyclobutadiene **142** competes with the intended cyclocarbonylation.

In the synthesis of bicyclo[6.3.0] derivatives **144** (Scheme 16C), the sulfonamide (**143a**) and oxygen (**143b**) tethers provide exclusively one product in high yield, whereas the carbon-tethered substrate **143c** does not provide the analogous product **144c** but instead affords an inseparable mixture of regioisomers arising from [1,3]- and [1,5]-hydrogen shifts, namely, **145** and **146**, respectively. Nevertheless, embedding a functionalized cyclohexene ring in the tether and replacing one of the sulfonyl groups with a phosphonate permits the extension of this strategy



Scheme 16 Rhodium-catalyzed PK-type reactions of bis(allenes)

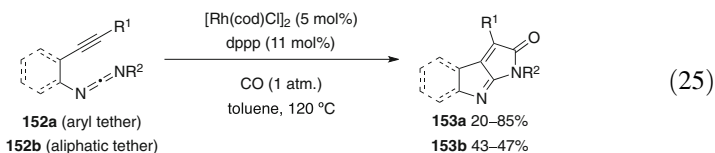
to the synthesis of 6,8,5-fused tricyclic scaffolds present in a number of natural products, as exemplified by the conversion of **150** to the tricycle **151** (Eq. 24) [102]. Furthermore, trisubstituted bis(allene)s permit the introduction of functionalization at the α -position(s) in the cyclopentenone ring, albeit with poor levels of stereocontrol [103].



4.1.5 The Rhodium-Catalyzed Hetero-Pauson–Khand-Type Reaction

Heterocycles are ubiquitous in natural products, pharmaceuticals, agrochemicals, and other high-value chemicals, which provide the impetus to develop new

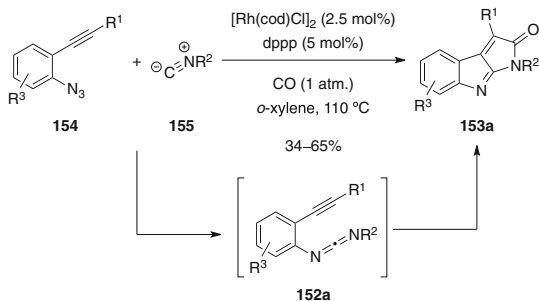
strategies for their de novo construction from acyclic starting materials in an efficient and atom-economical manner. The first rhodium-catalyzed PK-type reaction, where one of the reacting components contained a heteroatom, was reported in 2007. Saito and coworkers described the *intramolecular* reaction of aryl-tethered carbodiimides **152a** with internal alkynes under low CO pressure for the construction of fused bicyclic and tricyclic lactams **153a** in moderate to good yields (Eq. 25) [104]. Although aryl and linear alkyl substituents (R^2) are tolerated, cyclohexyl substitution provides significantly lower yields. Furthermore, the ethylene-tethered derivatives **152b** appear limited to aryl-substituted carbodiimides ($R^2 = \text{Ar}$), since an example of a carbodiimide with alkyl groups ($R^1 = \text{Me}$, $R^2 = \text{''Pr}$) failed to provide any of the corresponding cyclocarbonylated product **153b**.



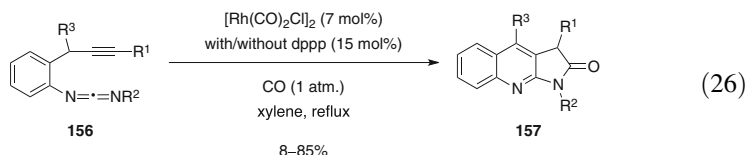
Zhang et al. recently reported an alternative strategy to access heterocycles **153a** using “self-relay” rhodium catalysis [105]. Treatment of aryl azides **154** with isonitriles **155** in the presence of the complex derived from $[\text{Rh}(\text{cod})\text{Cl}]_2$ and dppp at 110°C under CO atmosphere in *o*-xylene facilitates the initial formation of carbodiimides **152a** in situ, which are then subjected to a [(2+2)+1] cyclocarbonylation to afford the PK adducts **153a** in modest yield (Scheme 17). The process is compatible with a variety of aryl and heteroaryl substituents (R^1 , R^3), with higher yields obtained for more electron-rich substituents at both positions. In contrast, a single example of an alkyl substituent ($R^1 = (\text{CH}_2)_3\text{Cl}$) provided only a trace of the desired product. Moreover, only limited isonitrile scope is explored, which encompasses two examples ($R^2 = \text{''Bu}$, ${}^t\text{Hex}$). Nevertheless, the process can be modified to incorporate a second, different isonitrile in place of CO to provide the analogous pyrrolo[2,3-*b*]indol-2(*1H*)-imines.

Interestingly, the hetero-PK reaction with carbodiimide **156**, which has a homologated tether, facilitates rapid entry into the pyrrolo[2,3-*b*]quinolone skeleton **157** in good yield, albeit with increased catalyst loading (Eq. 26) [106]. A range of

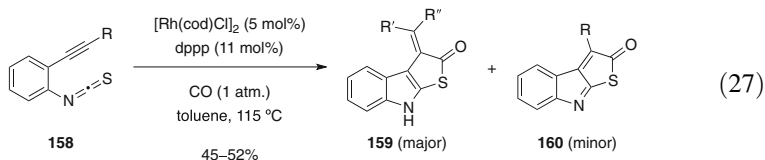
Scheme 17 “Self-relay” rhodium catalysis in the [(2+2)+1] carbocyclization reaction



substituted alkynes ($R^1 = \text{alkyl, Ph, TBS}$) are tolerated, in which the carbodiimide component ($R^2 = \text{Pr, Bn, } ^i\text{Hex, Ph}$) and benzylic position ($R^3 = \text{Me}$) also permit various substituents that increase the scope of this process. An interesting feature with this reaction is that the bidentate phosphine ligand is only required in some cases, in which a rationale for its inclusion or omission in reactions with relatively similar substrates is unclear.

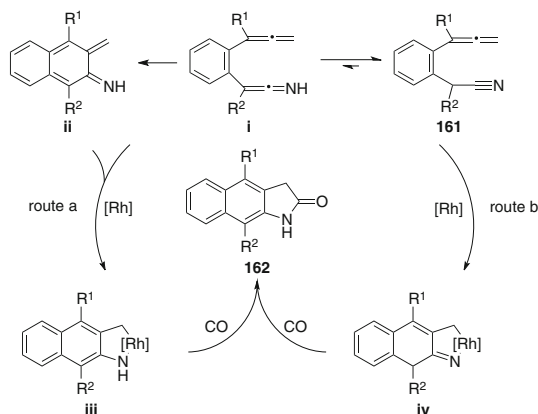


Saito and coworkers also explored the utility of isothiocyanates in the rhodium-catalyzed [(2+2)+1] carbocyclization reaction, which relies on the 1,2-disubstituted aromatic template **158** to afford the fused heterocycles **159** in moderate yield (Eq. 27) [107]. Primary and secondary alkyl substituents on the alkyne are well tolerated, including an example of a benzyl group, which leads to the formation of the *exocyclic* olefins **159** as the major products over the *endocyclic* thiophenones **160**, with the exception of a *tert*-butyl substituted derivative ($R = ^t\text{Bu}$) that exclusively provides **160**, albeit in only 5% yield.



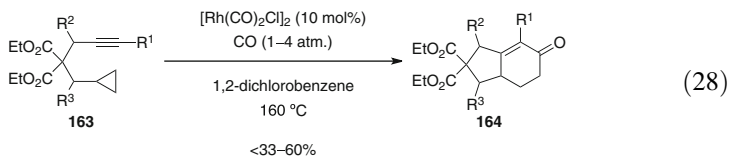
Nitriles have proven particularly challenging π -components for rhodium-catalyzed cyclocarbonylation reactions, which is presumably because of their ability to competitively coordinate the metal center and suppress catalysis. Nevertheless, Mukai and coworkers recently reported the first example of this type of process, wherein *ortho*-allenyl phenylacetone nitrile derivatives **161** are converted to the benzo[*f*]oxindoles **162** in moderate to good yield (Scheme 18) [108]. Although both electron-donating and electron-withdrawing substituents on the aryl ring (R^2 or $R^3 = \text{OMe, Cl, NO}_2$) are generally well tolerated, a monosubstituted allene ($R^1 = \text{H}$) furnished the corresponding product in very low yield (15%). Furthermore, aliphatic nitrile derivatives are also competent substrates provided a suitable electron-withdrawing substituent is adjacent to the nitrile. The reaction is proposed to be initiated via the isomerization of the nitrile **161** to a ketenimine **i** (route a), which is supported by control experiments using substrates that either cannot isomerize or react via direct oxidative addition of the nitrile group (route b). The ketenimine **i** may then either undergo oxidative addition with rhodium to afford intermediate **iii** or it may first undergo a 6π -electrocyclization reaction to give the bicyclic intermediate **ii** before coordination of the metal. From **iii**, migratory insertion of CO and reductive elimination furnishes the products **162**.

Scheme 18 Mechanistic rationale for the [(2+2)+1] carbocyclization of *ortho*-allenyl phenylacetonitriles



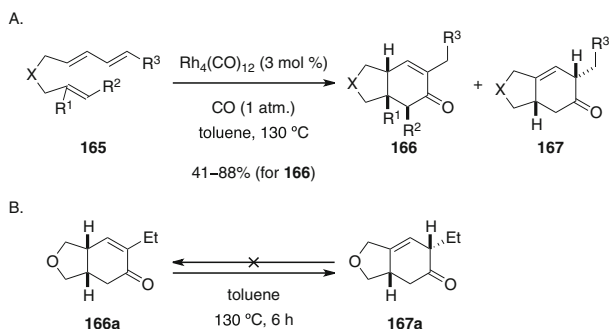
4.2 [(3+2)+1] Carbocyclizations

The rhodium-catalyzed [3+2+1] carbonylative carbocyclization, which is often referred to as the homologous PK-type reaction, has been the subject of significant attention since it provides an attractive method for the synthesis of cyclohexenone derivatives. Koga and Narasaka demonstrated the first example in 1999 with conversion of alkynyl-tethered cyclopropanes **163** to the corresponding bicyclohexenones **164** in modest yield due to the formation of several by-products (Eq. 28) [109]. In contrast to the related [2+2+1] reactions, the scope of three-carbon components is almost entirely restricted to cyclopropane derivatives.

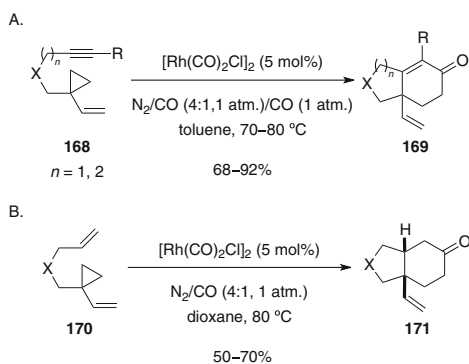


Following this initial report, the rhodium-catalyzed [(3+2)+1] reaction was not further developed until Chung and coworkers described an unusual variation using ene-dienes **165**, wherein the dienes provide novel three-carbon components (Scheme 19A) [110]. The reaction is tolerant of a number of different tethering groups ($X = O$, NTs, $C(CO_2Et)_2$) as well as terminal and internal dienes ($R^3 = H$, Me), albeit 1,1- ($R^1 = Me$) and 1,2-disubstituted ($R^2 = Me$) olefins provide lower yields of the products **166**. In addition, the isomerized derivatives **167** are also isolated as minor products in most cases. Interestingly, the α,β -unsaturated enone product **166a** isomerizes irreversibly to the β,γ -unsaturated isomer **167a** when heated at $130^\circ C$ in toluene for 6 hours (Scheme 19B).

Yu and coworkers recently described a homologous PK-type reaction, wherein alkyne- and alkene-tethered VCPs **168** and **170** undergo a facile cycloaddition



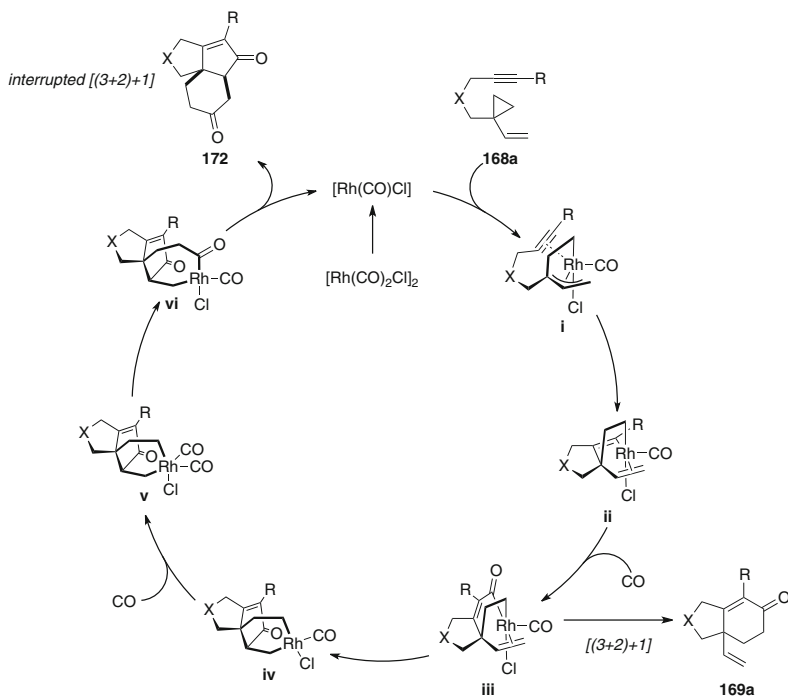
Scheme 19 Rhodium-catalyzed [(3+2)+1] carbocyclization of ene-dienes and product isomerization



Scheme 20 Synthesis of bicyclohexenones and bicyclohexanones with angular vinyl substituents

under low CO pressure to afford bicyclohexenones **169** and bicyclohexanones **171** in good to excellent yields (Scheme 20) [111]. Notably, the vinyl unit is crucial for the reaction to proceed under such mild conditions, as none of the [(3+2)+1] cycloadduct was generated in the absence of this moiety. Terminal ($R = \text{H}$) and internal ($R = \text{Me, Ph}$) alkynes **168** are well tolerated in the reaction, albeit some of the methyl-substituted analogs ($n = 1$) require higher CO pressure (1 atm. vs. 0.2 atm.), and the homologation of the tether ($n = 2$) permits the synthesis of 6,6-fused bicyclic products (Scheme 20A). In contrast, only two examples of ene-VCPs **170** were studied, and homologation of the tether led to a complex mixture (Scheme 20B).

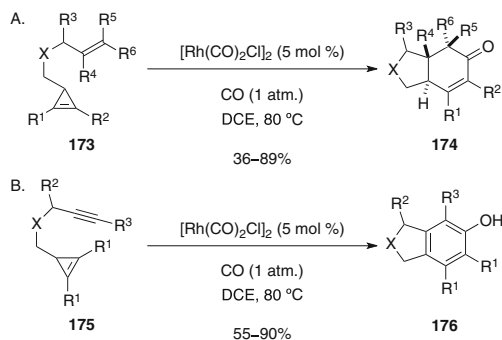
Additional studies identified a remarkable difference in the reactivity for yne-VCPs **168a** ($n = 1$) that contain alkyl-substituted internal alkynes ($R \neq \text{H, Ph}$), which permits an unprecedented carbocyclization to furnish fused angular tricycles **172** [112] (Scheme 21). The reaction is described as a formal [(5+1)]/[2+2)+1] cascade; however, control experiments do not support this pathway.



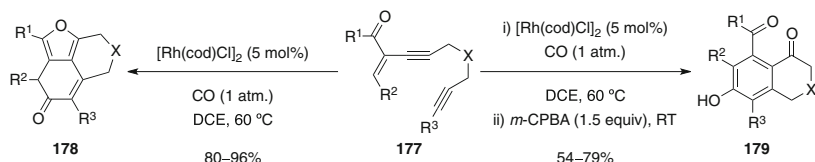
Scheme 21 Proposed catalytic cycle for the interrupted [(3+2)+1] carbocyclization

Moreover, DFT calculations reveal that for smaller alkyne substituents ($R = H, Me$), the activation energies for the formation of **169a** and intermediate **iv** are almost equal, which leads to the formation of mixtures of products. In contrast, larger groups ($R = TMS, ^iPr, ^tBu, ^cHex$) reduce the barrier for insertion of the pendent olefin, which permits a second migratory insertion of CO (intermediate **v** \rightarrow **vi**) and subsequent reductive elimination to afford **172**. As such, the reaction would be better described as an *interrupted* [(3+2)+1] carbocyclization. Although the yields of **172** are generally good to excellent, the pathway affording the bicyclohexenones **169a** is difficult to suppress, especially for the nitrogen-tethered substrates ($X = NTs$).

Wang and coworkers recently reported two new variations of the rhodium-catalyzed [(3+2)+1] carbocyclization of ene- and yne-cyclopropenes **173** and **175** with CO, which afford the corresponding bicyclohexenones **174** and bicyclic phenols **176**, respectively (Scheme 22) [113]. Remarkably, the bicyclohexenone products **174** have *trans*-fused ring junctions (Scheme 22A), while substitution of the alkyne terminus of **175** (R^3) allows for the formation of hexasubstituted aromatic rings in moderate to excellent yield (Scheme 22B). Nevertheless, many of the examples for both reactions utilize symmetrical cyclopropene derivatives to



Scheme 22 [(3+2)+1] Carbocyclizations of ene- and yne-cyclopropenes

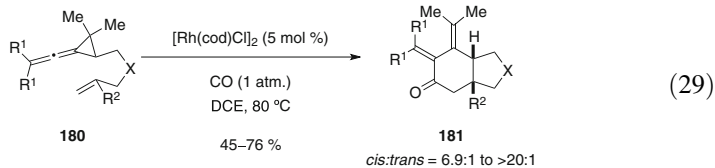


Scheme 23 [(3+2)+1] Carbocyclization reactions affording furan and phenol derivatives

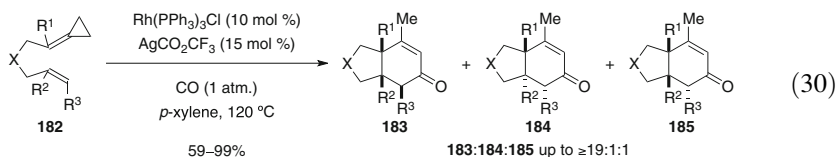
circumvent the formation of constitutional isomers. Interestingly, substitution of the cyclopropene moiety with alkyl groups ($\text{R}^1, \text{R}^2 = \text{}^n\text{Bu}$) greatly accelerates the reaction rate relative to the diphenyl analogs, which may be due to the increased reactivity of these species as a result of the loss of conjugation.

Zhao and Zhang reported a sequential rhodium-catalyzed heterocyclization/[3+2]+1 cyclocarbonylation of enediynes **177**, to afford tricyclohexenone derivatives **178** containing a tetrasubstituted furan ring system in excellent yield (Scheme 23) [114]. Interestingly, the addition of a slight excess of a peracid at room temperature after completion of the carbocyclization reaction furnished the phenols **179** as the major products via oxidative ring opening of the furan and tautomerization of the cyclohexenone. The scope of alkyne substituents is relatively broad ($\text{R}^3 = \text{H}, \text{}^n\text{Bu}, \text{TMS}, \text{Ar}$), albeit most of the examples employ phenyl ketone ($\text{R}^1 = \text{Ph}$) and styrene ($\text{R}^2 = \text{Ph}$) derivatives.

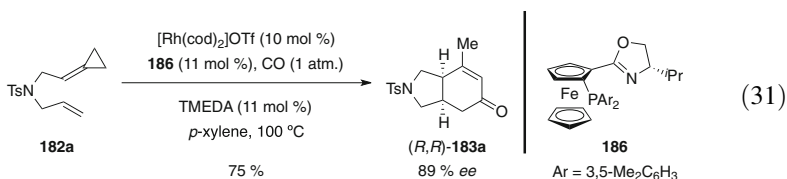
Shi et al. demonstrated that vinylidenecyclopropanes (VDCPs) **180** serve as 3C-components in the regio- and stereoselective [(3+2)+1] carbocyclization reaction, which affords the bicyclic hexadienones **181** in 45–76% yield with *exocyclic* alkenes at the α - and β -positions (Eq. 29) [115]. Although the reaction favors the formation of the *cis*-fused bicyclic products, the selectivity is quite variable. In addition, while cyclic and acyclic substituents (R^1) at the terminus of the allene are tolerated, substitution of the pendent alkene (R^2) with groups other than a proton or methyl group leads to complex mixtures of products.



Evans and coworkers concurrently disclosed the stereoselective rhodium(I)-catalyzed [(3+2)+1] carbocyclization of alkenylidene-cyclopropanes **182** with CO, which affords *cis*-fused bicyclohexenones **183** with high efficiency (Eq. 30) [116]. Experimental work was initiated following theoretical studies that provided a number of important insights into the mechanism of the reaction and most notably suggested that a cationic rhodium species would provide optimal catalytic efficiency. These studies also predicted that the reaction likely proceeds via a six-coordinate 18-electron rhodium(III)-trimethylenemethane complex, which was proposed to be the resting state for the catalytic cycle.

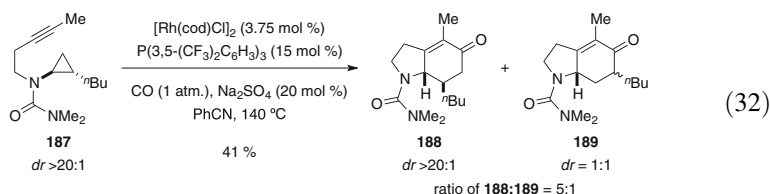


Remarkably, the experimental findings are in very good agreement with the mechanistic hypothesis delineated by the theoretical studies, which permits broad substrate scope with excellent diastereoselectivities, in addition to bridgehead quaternary carbon stereogenic centers (when R^1 and $R^2 \neq \text{H}$). Additionally, the asymmetric reaction of **182a** with a chiral bidentate *P,N*-ligand **186** provides (*R,R*)-**183a** in 75% yield and with 89% enantiomeric excess, which represents the first highly enantioselective reaction involving an ACP (Eq. 31).



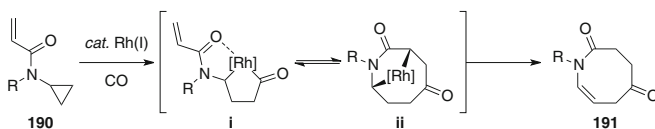
Bower and coworkers have recently demonstrated that aminocyclopropanes are also amenable to carbonylative [(3+2)+1] carbocyclization reactions, provided the nitrogen atom is protected with a directing group. Preliminary studies demonstrated that a neutral rhodium pre-catalyst in the presence of a π -acidic ligand promotes the [(3+2)+1] carbocyclization reaction of aminocyclopropanes with a pendant internal alkyne, to afford bicyclic enones in modest yield and good stereospecificity [117]. Nevertheless, the reaction requires very long reaction times, albeit it was subsequently shown that a cationic pre-catalyst both accelerates the rate of reaction and significantly improves the efficiency [118]. The process is limited to

internal alkynes, since the terminal derivatives afford only trace amounts of the desired products. However, the reaction does tolerate substitution at both the homopropargylic position and on the cyclopropane ring, in which the latter is exemplified by the transformation of the *n*-butyl-substituted aminocyclopropane **187** into the *N*-heterobicyclic enone **188** with high diastereofidelity (Eq. 32).

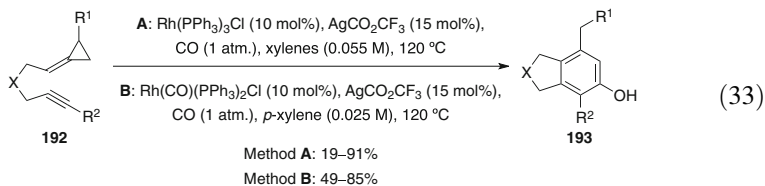


Additional studies demonstrated that the corresponding bicyclohexanone derivatives are accessible with moderate to high diastereoselectivities by simply replacing the alkyne with an alkene and using a carbamate directing group with suitable additives to promote the reaction [119]. Remarkably, the benzyl-protected *N*-cyclopropyl acrylamides **190** ($R = \text{Bn}$) are readily transformed into azocanes **191** at slightly higher temperatures (Scheme 24) [120]. Although all of these examples are formally [(3+2)+1] processes, the reactivity of the aminocyclopropane substrates is unique in that the migratory insertion of CO (intermediate **i**) is proposed to occur *prior* to the carbometalation of the respective 2π -components (intermediate **ii**); hence, a more accurate description of these reactions would be [3+1+2] carbocyclizations.

Chung and Evans independently reported the rhodium-catalyzed [(3+2)+1] carbocyclization reaction of alkyneidenecyclopropanes **192**, which afford poly-substituted phenols **193** (Eq. 33) [121, 122]. Interestingly, despite the fact that the processes are similar, there are distinct differences in the optimum reaction conditions. For instance, Chung et al. employ conditions that are almost identical to those previously reported for the synthesis of bicyclohexenones **183** (Eq. 33, Method A vs. Eq. 30), whereas Evans and coworkers demonstrated that $\text{Rh}(\text{CO})(\text{PPh}_3)_2\text{Cl}$ at a higher dilution provides optimal efficiency (Eq. 33, Method B). To this end, the utility of the products was illustrated with some useful synthetic transformations and it was also shown that substitution of the ACP ring ($R^1 = \text{Me}$) affords homologated derivatives. In contrast, Chung described some of the limitations of the reaction, namely, that increasing the tether length is detrimental to the reaction efficiency, while the presence of a *gem*-dimethyl group at the propargylic position completely suppresses carbonylation.



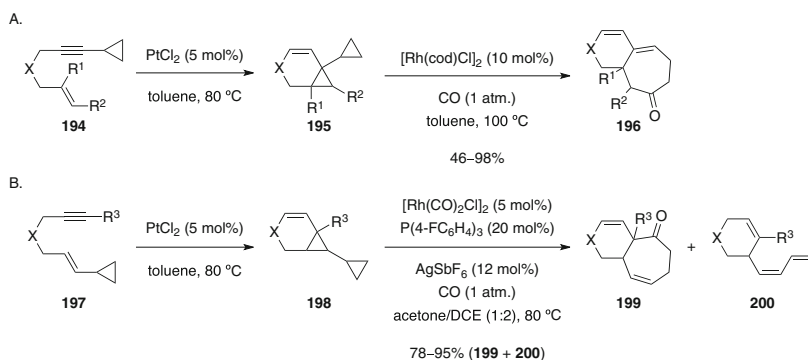
Scheme 24 General reaction for the synthesis of azocane derivatives



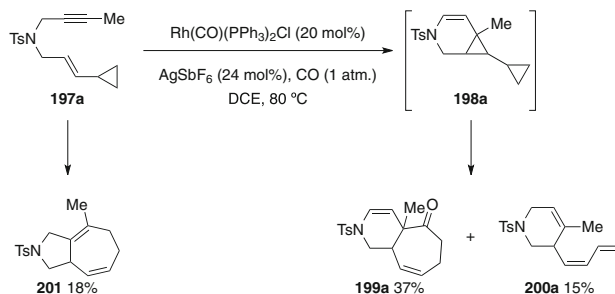
4.3 [(3+3)+1] Carbocyclizations

To the best of our knowledge, there is only a single example of the rhodium-catalyzed [(3+3)+1] carbonylative carbocyclization, which was reported by Chung and coworkers in 2008 [123]. This process is somewhat unusual since it involves the rhodium-catalyzed rearrangement and carbonylation of 1- and 7-cyclopropylbicyclo[4.1.0]hept-2-enes **195** and **198**, which were prepared from the 1,6-enynes **194** and **197** via platinum-catalyzed cycloaddition reactions, to afford the 6,7-fused bicycloheptenones **196** and **199** in moderate to high yield (Scheme 25). Interestingly, the substrates have different catalyst requirements, namely, the 1-cyclopropyl-substituted derivative **195** prefers a neutral catalyst (Scheme 25A), whereas a cationic system with an electron-deficient phosphine is optimal for the 7-cyclopropyl isomer **198** (Scheme 25B). However, in the latter case, the monocyclic trienes **200** are also isolated as minor products.

This work was later expanded to a sequential rhodium-catalyzed cycloisomerization/[(3+3)+1] process with the 1,6-enyne **197a** using a relatively high catalyst loading under 1 atm. of CO, to furnish the bicycloheptenone product **199a** in 37% yield, along with the corresponding [(5+2)] product **201** and the monocyclic triene **200a** (Scheme 26) [124]. The tricycle **198a** is proposed to be an intermediate in this process, albeit there is no direct evidence for its involvement.



Scheme 25 Rhodium-catalyzed [(3+3)+1] carbocyclizations

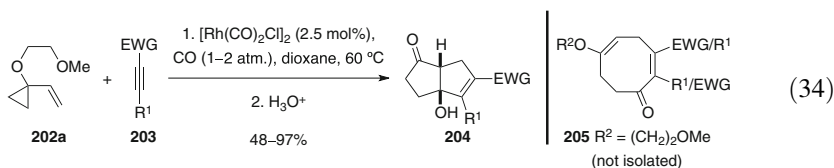


Scheme 26 Sequential rhodium-catalyzed cycloisomerization/[3+3+1] carbocyclization

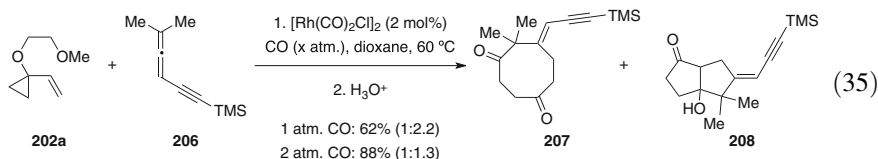
4.4 [5+2+1] Carbocyclizations

The ability to efficiently prepare cyclooctanoid derivatives remains an important and challenging area of research, which can be primarily ascribed to the plethora of important bioactive natural products that contain an eight-membered ring in their molecular framework. Nevertheless, much of the work in the area of carbonylative rhodium-catalyzed carbocyclizations designed to access this particular ring size has centered on the use of vinylcyclopropanes as 5C-components, in combination with various 2C-components and CO in [5+2+1] reactions [125].

Wender and coworkers reported the first example of the rhodium-catalyzed [5+2+1] reaction in 2002, through the combination of protected vinylcyclopropanols **202a**, electron-deficient alkynes **203**, and CO in a fully *intermolecular* manner (Eq. 34) [126]. Interestingly, the cyclooctanoids **205** were not isolated, but the structurally isomeric bicyclo[3.3.0]octenones **204**, which arise from a transannular aldol reaction upon acidic work-up, were instead obtained as the major products. The reaction is markedly more efficient with activated alkynes, in which ketones, amides, aldehydes, and esters (EWG) are all tolerated to furnish a single regio-isomer in each case, albeit with the exception of one substrate.



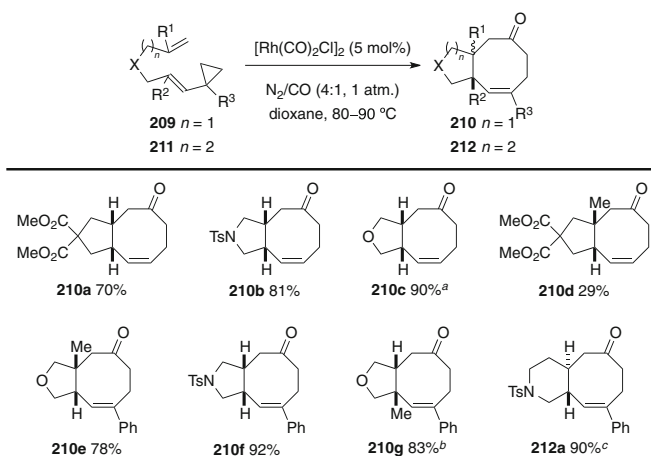
In a subsequent study, Wender illustrated that the allene **206** is also a suitable 2C-component in the [5+2+1] reaction with the VCP **202a** and CO (Eq. 35) [127]. Although a mixture of the eight-membered cyclic diketone **207** and the transannular aldol product **208** is formed in 62% overall yield using 1 atm. of CO, increasing the CO pressure improves the yield at the detriment of the product ratio. Notably, under both sets of conditions, the *E*-isomeric products are obtained exclusively and allene activation is not required.



Yu and Wender also reported a *semi-intermolecular* reaction of ene-VCPs with CO (Table 12) [128]. Treatment of the ene-VCPs **209** ($n = 1$) with 5 mol% of $[\text{Rh}(\text{CO})_2\text{Cl}]_2$ under low CO pressure (0.2 atm.) in dioxane at elevated temperatures provides the 5,8-fused bicyclooctenones **210** with good to excellent yield and with excellent diastereoselectivity. A variety of tethers and substitution patterns including the installation of angular methyl groups at either bridgehead position (R^1 , $\text{R}^2 = \text{Me}$) can be employed, including one example with a homologated tether (**211**; $\text{X} = \text{NTs}$, $\text{R}^1 = \text{R}^2 = \text{H}$, $\text{R}^3 = \text{Ph}$) that, interestingly, favors the *trans*-fused product **212a** (*trans/cis* = 5:1). In order to provide the necessary insight for the [(5+2)+1] reaction over the analogous [(5+2)] pathway, DFT calculations were utilized to demonstrate that the barrier for CO insertion into the intermediate rhodacycle is lower than that for direct reductive elimination [129].

Yu and coworkers extended this strategy to the construction of the 5,8,5-fused tricyclic ring systems **214** by fusing a cyclopentane ring to the VCP (Eq. 36) [130]. To this end, DFT calculations indicate that cleavage of the desired C–C bond of the cyclopropane in **213** (Scheme 27, bond *a*) is preferred (free energy of activation = 9.3 kcal/mol) to the intermediate derived from the cleavage of the internal bond (bond *b*) to afford the 6,8-fused ring structure **215** present in taxol,

Table 12 Representative substrate scope for the [(5+2)+1] carbocyclization of ene-VCPs

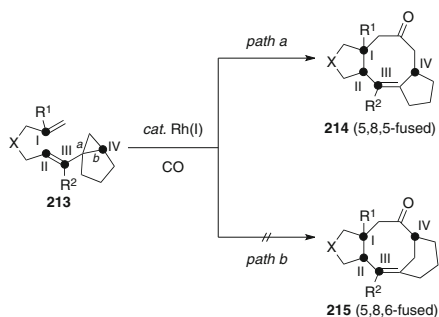


^aGC yield; isolated yield is 44% owing to the volatility of the product

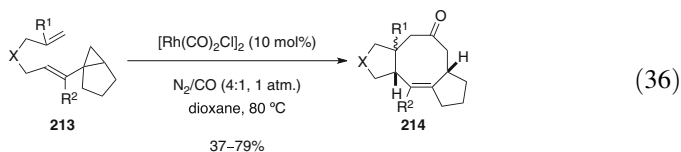
^bA [(5+2)] product was obtained in 11% yield

^cCombined yield of diastereomers (*trans/cis* = 5:1)

Scheme 27 Proposed pathways for a [(5+2)+1] carbocyclization reaction



which is presumably because the disfavored intermediate rhodacycle contains a bridgehead olefin. The calculations also predicted that substituents at positions II and III in the VCPs **213** would have a *cis*-relationship in the products and the stereochemistry of the tethered 5,8-fused ring junction in **214** would be controlled by the presence of a substituent at position IV. Gratifyingly, these predictions were confirmed experimentally, albeit the reaction efficiency is relatively modest.



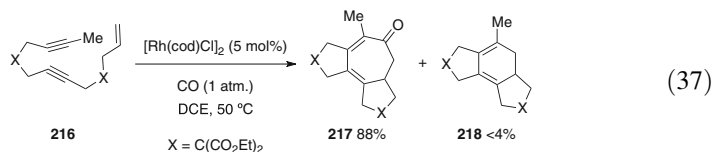
5 Rhodium-Catalyzed $[m+n+o+1]$ Reactions

Four-component coupling reactions are relatively rare in comparison to two- and three-component reactions. This is primarily due to the challenges in controlling chemoselective carbometalation steps without premature reductive elimination at any stage prior to CO incorporation, in addition to dealing with the higher entropy in the case of fully *intermolecular* processes. Nevertheless, there are a few notable examples of this class of reaction, in which these difficulties have been successfully addressed.

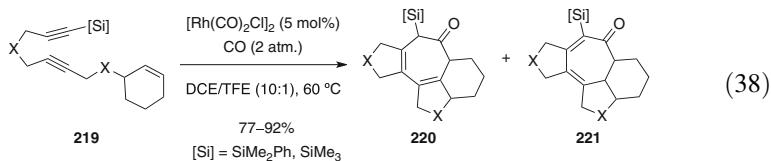
5.1 $[(2+2+2)+1]$ Carbocyclizations

Ojima and coworkers serendipitously discovered the first rhodium-catalyzed $[(2+2+2)+1]$ carbocyclization reaction, which involves the reaction of the enediynes with CO to afford tricycloheptadienones [131–133]. Prior to this work, the same group

described a hydrosilane-initiated carbonylative cycloaddition reaction of enediynes containing one internal and one terminal alkyne [134]. Interestingly, while exploring the scope and limitations of this process, they discovered that substrates containing two internal alkynes participate in a [(2+2+2)+1] cyclocarbonylation reaction when the hydrosilane is omitted. This process is exemplified by the reaction of the carbon-tethered enediyne **216**, which upon treatment with 5 mol% of $[\text{Rh}(\text{cod})\text{Cl}]_2$ under 1 atm. CO in DCE at 50°C, furnished the tricyclic product **217** in 88% yield with the corresponding [(2+2+2)] product **218** also formed as a minor by-product (Eq. 37).

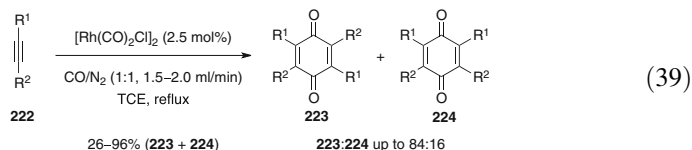


Additional studies demonstrated that the scope of the reaction could be further extended to the synthesis of tetracycles by simply using a cyclic alkene, albeit with slightly modified reaction conditions [135]. Furthermore, these reaction conditions tolerate silylated alkynes **219**, which provide the [(2+2+2)+1] products **220** and **221** in excellent yield as *ca.* 1:1 mixtures of diene regioisomers (Eq. 38).



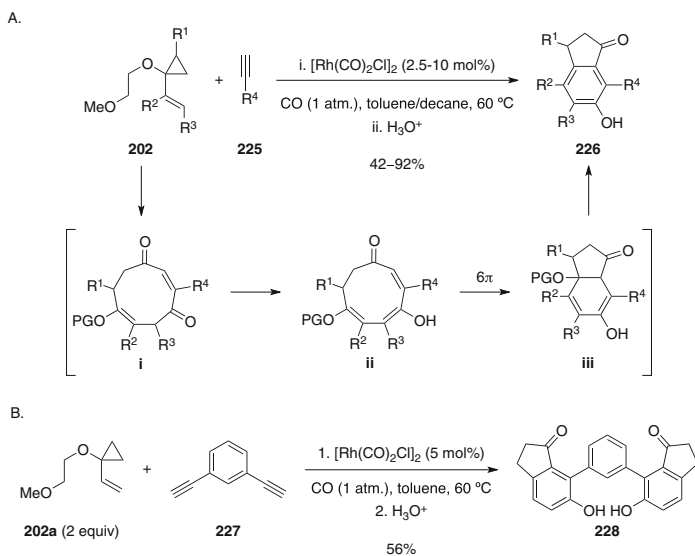
5.2 [2+2+1+1] Carbocyclizations

Huang and Hua further exemplified the relative scarcity of $[m+n+o+1]$ reactions with the first rhodium-catalyzed [2+2+1+1] cyclocarbonylation reaction, which involves the combination of two equivalents of the internal alkyne **222** with two equivalents of CO to afford tetrasubstituted *para*-benzoquinones **223** and **224** (Eq. 39) [136]. A critical element to the success of this process was the discovery that slowly bubbling a 1:1 mixture of CO/N₂ through the reaction medium provides the optimum conditions, as higher CO pressures lead to significantly lower efficiency. The reaction is able to incorporate a range of dialkyl and aryl-alkyl alkynes, including a broad variety of aryl substituents, albeit unsymmetrical alkynes (R¹ ≠ R²) provide poor regiocontrol.



5.3 [5+1+2+1] Carbocyclizations

Wender and coworkers also described a unique four-component, fully *intermolecular* [5+1+2+1] carbocyclization reaction, which involves the combination of VCPs **202** with terminal alkynes **225** and two equivalents of CO to form hydroxyindanones **226** (Scheme 28A) [137]. The initial product of the reaction is proposed to be the nine-membered diketone **i**, which tautomerizes to the trienone **ii** to permit a subsequent 6π -electrocyclization reaction and elimination to afford the observed products. Although the reaction suffers from product inhibition, this is nicely circumvented by the addition of decane as a cosolvent to precipitate the products from the reaction mixture. A key and striking feature with this work is the use of 1,3-bis-ethynylbenzene **227** as the alkyne component, which allows a bidirectional seven-component [5+1+2+1] reaction and thus creates ten new C–C bonds in a single operation (Scheme 28B).

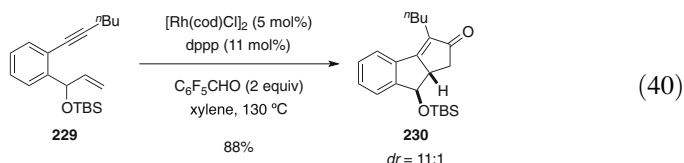


Scheme 28 Four-component and bi-directional seven-component [5+1+2+1] carbocyclization reactions (PG = (CH₂)₂OMe)

6 Alternatives to Carbon Monoxide in Rhodium-Catalyzed Cyclocarbonylation Reactions

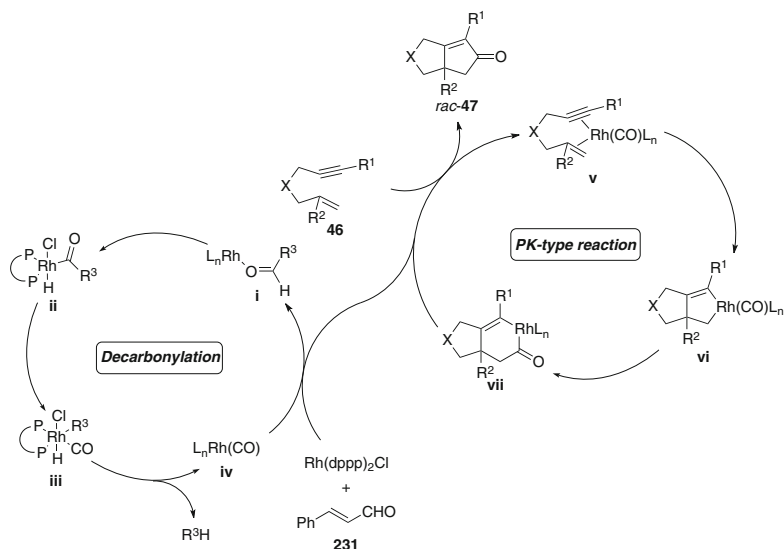
Although the synthetic utility of the rhodium-catalyzed PK-type reaction and its many variations cannot be overstated, the most obvious limitation of any and all of the processes described thus far is the requirement for toxic CO gas. Despite being an essential component of the reaction manifold, its use requires adherence to strict safety guidelines, which makes these reactions less appealing particularly for industrial applications. In order to circumvent this issue, several groups have developed methods that provide in situ sources of CO in the presence of a rhodium catalyst, thereby eliminating the need for CO gas.

Morimoto and Shibata independently described the first examples of rhodium-catalyzed cyclocarbonylation using aldehydes as a latent source of CO in 2002. Morimoto et al. elected to employ two equivalents of pentafluorobenzaldehyde in a solution-phase reaction, which is tolerant of various tethers and substitution patterns, and thus permits the diastereoselective reaction of the 1,6-enyne **229** to afford the *cis*-product **230** (Eq. 40) [138].



In contrast, Shibata and coworkers discovered that a solvent-free process using a large excess of cinnamaldehyde as the CO source also affords the desired bicyclopentenone products in high yields [139]. Two catalytic cycles are proposed to operate in concert to permit this reaction (Scheme 29). For instance, in one cycle, CO is abstracted from cinnamaldehyde (**231**) by rhodium to give a Rh–CO intermediate **iv**, which can then react with the 1,6-enyne **46** as *per* the generally accepted mechanism for the rhodium-catalyzed PKR to give a rhodacyclopentene **vi**. Migratory insertion of the abstracted CO to give intermediate **vii** and subsequent reductive elimination furnishes the product *rac*-**47**. This decarbonylation pathway is supported by various mechanistic studies, including evidence suggesting that free CO is not present in the reaction mixture [140]. Additionally, cinnamaldehyde can be used as a CO source for the enantioselective rhodium-catalyzed PKR, albeit the selectivities have some dependence on the substrate [58, 59].

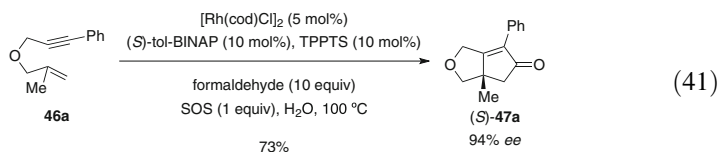
The cyclocarbonylation using formaldehyde as a source of CO in aqueous media has also been described [141]. By addition of the surfactant SDS, a “microscopically biphasic system” is generated, consisting of a micellar phase containing the organic substrate surrounded by an aqueous phase. The process requires a hydrophobic and a hydrophilic phosphine, which are proposed to generate two



Scheme 29 Dual catalytic cycles for the rhodium-catalyzed cyclocarbonylation of 1,6-enynes with CO derived from aldehydes

different rhodium complexes, in which the Rh–TPPTS complex performs the decarbonylation of formaldehyde in the aqueous phase to afford a Rh–CO species. This species can then supply CO at the micellar interface to the Rh–dppp complex for the PK-type reaction to proceed.

Additional studies demonstrated the feasibility of the asymmetric cyclocarbonylation by simply replacing the achiral ligand with (*S*)-tol-BINAP and using a different surfactant [142]. Nevertheless, the isolated yields are generally lower than those for reactions conducted under CO atmosphere with identical substrates. In addition, terminal alkynes are unreactive under these conditions, whereas the 1,1-disubstituted olefin **46a** is transformed into the bicyclopentenone (*S*)-**47a** bearing an angular methyl substituent in 73% yield with 94% enantiomeric excess (Eq. 41).



Kwong and coworkers described a surfactant-free version of this process using cinnamaldehyde (**231**) as the CO source in an aqueous medium [143]. The substrate scope is largely limited to oxygen-tethered 1,6-enynes **232**; however, a striking correlation between the electronic properties of the alkyne and the enantioselectivity was observed (Table 13). For instance, relatively electron-rich alkynes provide

Table 13 Electronic effects of the alkyne on enantioselectivity in aqueous CO gas-free PK-type reactions

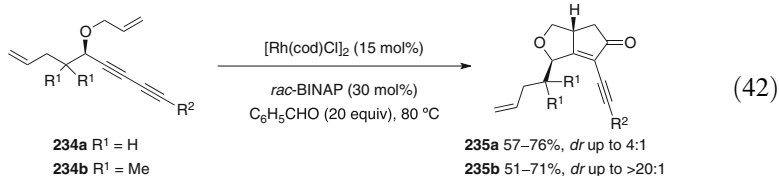
Entry	Substrate 232	R	Yield (%) ^a	ee (%) ^b
1	a	4-OMe	93	93
2	b	4-Me	92	88
3	c	H	82	84
4	d	4-F	90	82
5	e	3-OMe	88	81
6	f	4-Cl	91	77

^aIsolated yield^bDetermined by chiral HPLC

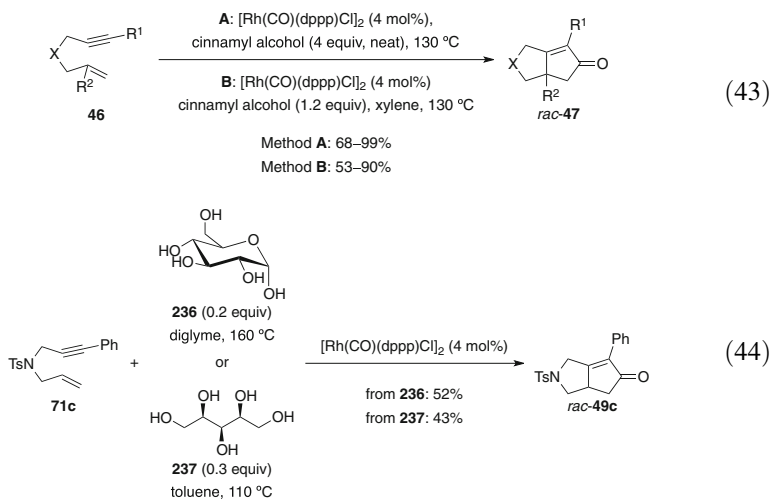
excellent enantioselectivities relative to the unsubstituted derivative (entries 1 and 2 vs. 3), whereas the enantioselectivity is reduced with increasingly electron-deficient alkynes (entries 4–6). A Hammett plot was used to illustrate that this correlation obeys a linear free-energy relationship. The effect of the electronic properties of the alkyne on the enantioselectivity is ascribed to the ability of electron-rich substrates to coordinate more closely to the rhodium center, thus enabling a higher degree of stereocontrol to be imparted in the transition state by being in closer proximity to the chiral environment. A similar effect was also observed in related CO gas-free carbocyclization reactions in alcoholic solvents [144].

An asymmetric PK-type reaction utilizing an aldehyde as the CO source was also described by Morimoto et al. using both neutral and cationic rhodium pre-catalysts in THF at 50°C [145]. They propose that the neutral catalyst impacts aldehyde decarbonylation and that the cationic species facilitates the cyclocarbonylation. Under the optimum conditions, the product yields are modest; however, the enantioselectivities are generally very high.

Pu and coworkers recently employed the PK-type reaction of 1,6-enynes with CO derived from aldehydes as one of the key steps for the construction of interesting polycyclic compounds [146]. Although the reaction is somewhat limited by high catalyst loadings and modest diastereocontrol in most cases, treatment of the requisite enantiomerically enriched dienediynes **234** with the complex derived from [Rh(cod)Cl]₂/*rac*-BINAP and a large excess of benzaldehyde at 80°C affords chemoselective access to oxygen-tethered bicyclopentenones **235** favoring the *cis*-isomer as the major product (Eq. 42). Notably, the diastereoselectivity can be dramatically improved by increasing the steric bulk adjacent to the stereogenic center (**234b**, R¹ = Me vs. H).



As rhodium is also known to dehydrogenate primary alcohols to aldehydes, Chung and coworkers hypothesized that benzylic alcohols could be used as latent CO sources in the rhodium-catalyzed PKR [147]. To this end, treatment of the 1,6-enynes **46** with $[\text{Rh}(\text{CO})(\text{dppp})\text{Cl}]_2$ using cinnamyl alcohol as the CO source either under solvent-free conditions (Method A) or in xylene (Method B) afforded the corresponding bicyclopentenones *rac*-**47** in good yields (Eq. 43). It was also shown that carbohydrates may also act as CO donors in substoichiometric quantities, as exemplified by *D*-glucose (**236**) and xylitol (**237**), which provide relatively modest overall yields of the cycloadducts *rac*-**49c** (Eq. 44).



Morimoto and coworkers concurrently described a similar process employing acetate-protected aldoses in asymmetric [(2+2)+1] transformations, wherein trace amounts of the ring-opened aldehyde form of the aldose present at equilibrium act as CO donors, albeit the yields and enantioselectivities were generally modest [148]. With a similar emphasis on the use of carbohydrates as the CO source in asymmetric PK-type reactions, they also reported the use of glyceraldehyde, prepared either from glycerol or *D*-mannitol, with a chiral catalyst derived from $[\text{Rh}(\text{cod})\text{Cl}]_2$ and (*S*)-tol-BINAP to provide the bicyclopentenone products in good to excellent yield and with moderate enantioselectivity [149].

Kwong and coworkers have also reported the use of formate derivatives as CO surrogates in asymmetric rhodium-catalyzed PK-type carbocyclizations of 1,6-enynes, which are proposed to operate via a dual catalytic process analogous

to that for aldehydes [150–152]. Under conventional heating, the products are afforded in moderate yield and with good to excellent enantioselectivities, albeit very long reaction times of up to three days are required. However, under microwave irradiation, similar yields and enantioselectivities can be obtained in under one hour.

In contrast to the aforementioned reactions, wherein the catalytic rhodium species are similar and the CO source varies, there are examples of different rhodium sources that facilitate the PK-type reactions with aldehydes. In this context, Park and Chung reported immobilized heterobimetallic Co_2Rh_2 nanoparticles as suitable pre-catalysts for the [(2+2)+1] carbocyclizations between alkenes, alkynes, and aldehydes as the CO source [153, 154]. Nevertheless, the *intermolecular* reactions between cyclic alkenes and terminal alkynes are somewhat less efficient than the *semi-intramolecular* reactions of 1,6-enynes containing internal alkynes. In addition, the analogous process with a chiral bidentate phosphine ligand converts the 1,6-enynes to the bicyclopentenones in excellent yield and with moderate to good enantioselectivities. Furthermore, these nanoparticles have also been used for more conventional PK-type reactions under CO atmosphere [155, 156].

More recently, Lin et al. have described the synthesis of BINAP-based metal-organic frameworks (MOFs), which can be metalated with rhodium complexes to provide efficient single-site catalysts for a number of asymmetric cyclization reactions, including the rhodium-catalyzed PK-type reaction of 1,6-enynes with cinnamaldehyde as a CO source [157]. Notably, this particular reaction manifold can operate with very low rhodium loadings (0.5 mol%), to afford the products in good yield and with good enantioselectivities.

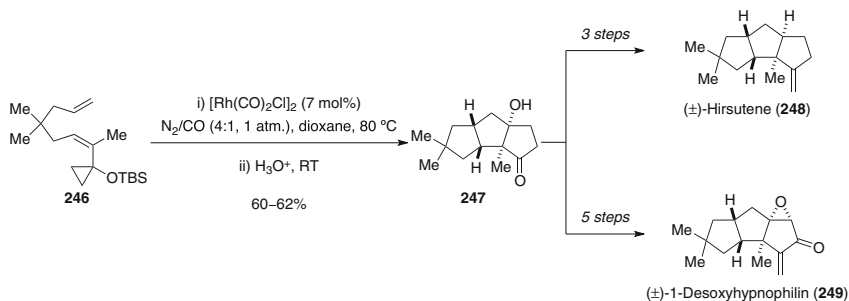
7 Total Synthesis of Natural Products Using Rhodium-Catalyzed Cyclocarbonylation Reactions

The synthetic utility of rhodium-catalyzed cyclocarbonylation reactions is highlighted in a number of key stereoselective ring-forming reactions in the total synthesis of bioactive natural products [158, 159]. Moreover, the ability to selectively generate seven- and eight-membered rings by careful substrate design makes this a particularly attractive and versatile strategy for target-directed synthesis, particularly given the prevalence of these ring sizes in important synthetic targets and the difficulties associated with their construction using classical methods.

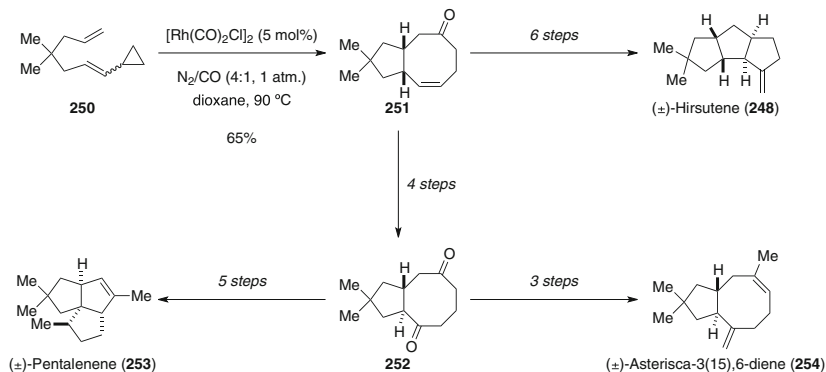
Guanacastepene A (**240**), the active component of fungal extracts isolated from *Daphnopsis americana*, has excellent activity against both MRSA and VREF (Eq. 45) [160]. Brummond recognized that the skeleton of this intriguing target could be accessed using the rhodium-catalyzed allenic [(2+2)+1] carbocyclization reaction, which would facilitate the construction of both the five- and seven-membered rings present in the natural product [161]. The allenyne **238** was prepared in 10 steps, utilizing Smith's modification of Stork's vinylogous ester-1,3-dicarbonyl transposition [162, 163]. The key step in the synthesis is the

Yu and coworkers adapted their previous work on the *semi-intermolecular* rhodium-catalyzed [(5+2)+1] carbocyclization of ene-VCPs and Wender's fully *intermolecular* [5+2+1] reaction of VCPs with alkynes and CO, to provide the key step in the total syntheses of (\pm)-hirsutene (**248**) and (\pm)-desoxyhyphnophilin (**249**) (Scheme 31) [166]. Treatment of the ene-VCP **246** with catalytic $[\text{Rh}(\text{CO})_2\text{Cl}]_2$ under a low partial pressure of CO followed by hydrolysis with mild acid promotes an *intramolecular* aldol reaction (cf. Eq. 34) to furnish the triquinane scaffold **247**, which provides a common intermediate for the synthesis of the aforementioned natural products. Model reactions and a combination of DFT calculations and nOe studies were ultimately utilized to design a suitable substrate to establish the desired stereochemistry in the transannular aldol reaction.

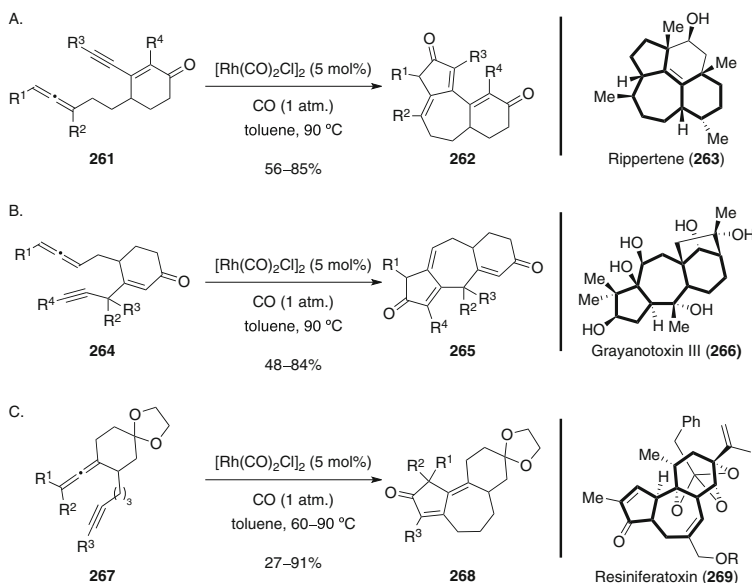
Yu and coworkers have also utilized the [(5+2)+1] carbocyclization reaction of ene-VCPs for the formal synthesis of several other natural products, three of which can be accessed from the bicyclic intermediate **251** (Scheme 32) [167–169]. For instance, the carbocyclization of the VCP **250** permits the relatively rapid construc-



Scheme 31 Key [(5+2)+1] carbocyclization reaction in the syntheses of (\pm)-hirsutene and (\pm)-1-desoxyhyphnophilin

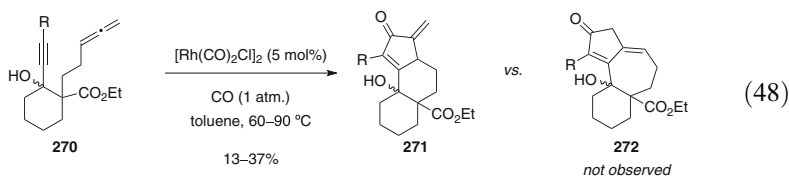


Scheme 32 Formal syntheses of (\pm)-hirsutene, (\pm)-pentalenene, and (\pm)-asterisca-3(15),6-diene via a common intermediate

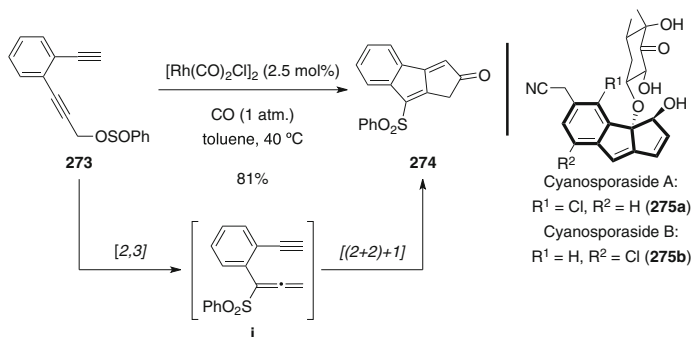


Scheme 34 Syntheses of the 6,7,5-fused ring skeletons found in some natural products

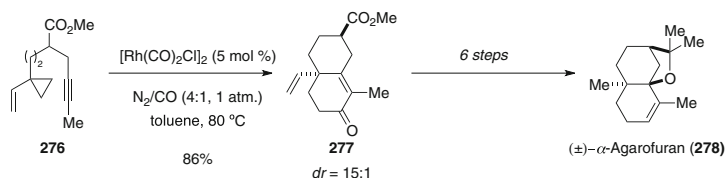
Brummond and coworkers further illustrated the potential utility of the allenic rhodium-catalyzed PK-type reaction for the synthesis of natural products. In this context, a series of three allenynes were prepared, which were designed to access different carbon skeletons found in the natural products rippertene (**263**), grayanotoxin III (**266**), and resiniferatoxin (**269**) (Scheme 34) [171]. Although the reactions of the allenynes **261** with CO afforded the cyclopentenones **262** in good yields for a range of substitution patterns (Scheme 34A), only a few allenynes of type **264** were examined (Scheme 34B), and the allenynes **267** provided the respective cyclocarbonylation products **268** with varying efficiency (Scheme 34C). Remarkably, the allenynes **270** that contain a tertiary propargylic alcohol preferentially react at the proximal bond of the allene, which is not typically observed with rhodium and is thus ascribed to the directing effect of the free hydroxyl group (Eq. 48).



Mukai et al. devised a strategy for the synthesis of the core tricyclic scaffold present in cyanosporasides A and B (**275**), which were isolated from *Salinispora pacifica* in 2006 by Fenical and coworkers (Scheme 35) [172, 173]. Treatment of



Scheme 35 Sequential [2,3]-sigmatropic rearrangement and cyclocarbonylation

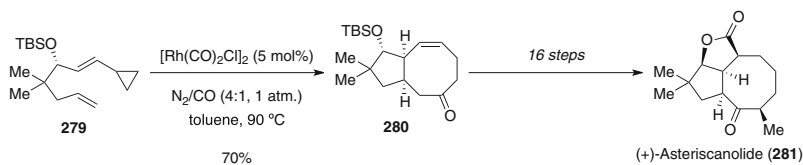


Scheme 36 Rhodium-catalyzed [(3+2)+1] carbocyclization of an yne-VCP in the total synthesis of (±)-α-agarofuran

273 with $[\text{Rh}(\text{CO})_2\text{Cl}]_2$ under 1 atm. CO at 40°C facilitates an in situ [2,3]-sigmatropic rearrangement to afford the intermediate allenyne **i**, which undergoes a [(2+2)+1] cyclocarbonylation reaction to furnish the tricyclopentenone **274**. Interestingly, the desulfonylated analog of **273** undergoes a similar rhodium-catalyzed carbocyclization to afford the corresponding tricycle, albeit 2-methylnaphthalene is formed as a side product [174].

The rhodium-catalyzed carbonylative [(3+2)+1] carbocyclization reaction has also been utilized in target-directed synthesis. For instance, Yu and coworkers recently applied their previously discussed methodology (cf. Scheme 20A) to the total synthesis of (±)-α-agarofuran (**278**), which was accomplished in 12 steps from ethyl cyclopropylideneacetate [111]. The key step in the sequence is the rhodium-catalyzed [(3+2)+1] carbocyclization of the alkyne-tethered VCP (±)-**276** with CO to furnish the 6,6-fused bicyclohexenone **277** in 86% yield and with 15:1 diastereoselectivity favoring the *trans*-isomer (Scheme 36).

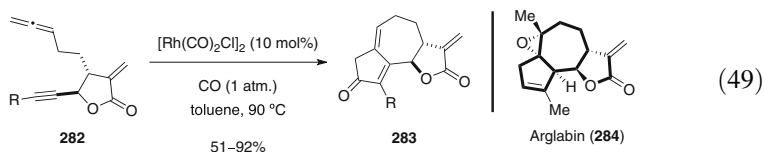
The natural sesquiterpene lactone, (+)-asteriscanolide (**281**), has been the target of several synthetic efforts since its initial isolation in 1985, largely owing to its intriguing structure, which consists of a complex tricyclic skeleton bearing five stereocenters. Yu and coworkers applied the rhodium-catalyzed [(5+2)+1] reaction of ene-VCPs with CO developed in their group to the efficient and stereoselective construction of the 5,8-fused carbocycle **280** in only three steps, which enables the



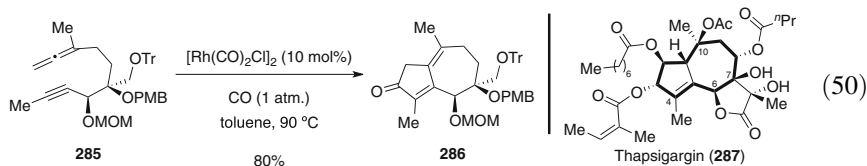
Scheme 37 A $[5+2]+1$ carbocyclization reaction utilized in the total synthesis of (+)-asteriscanolide

completion of a 19-step total synthesis of this agent (Scheme 37) [175, 176]. The key enantioenriched VCP **279** was prepared using a modified version of Carreira's protocol for the enantioselective addition of terminal alkynes to aldehydes [177], utilizing a chiral ligand developed by Jiang [178], followed by the reduction of the alkyne and protection of the chiral nonracemic secondary alcohol as a *tert*-butyldimethylsilyl ether.

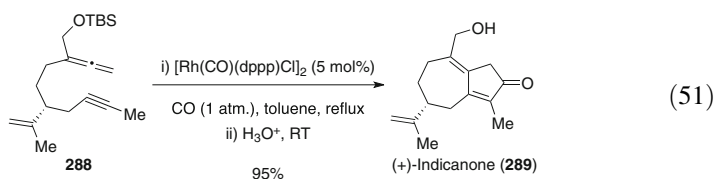
Brummond and coworkers utilized the rhodium-catalyzed allenic PK-type reaction of allenyne **282** with CO in the synthesis of the ring system present in 6,12-guaianolides, such as arglabin (**284**) (Eq. 49) [179]. Their approach to this skeleton is particularly noteworthy, since it contrasts the lengthy 10-step sequence required by Mukai et al. to install the lactone ring and complete the synthesis of (+)-achalensolide (**245**) (cf. Scheme 31). For instance, they demonstrated that both **282** and its *cis* epimer are relatively stable under the reaction conditions, thereby affording the tricyclic products **283** in good to excellent yields (67–90% from *cis*-**282**), thus indicating that the construction of this motif early in the sequence may be a viable strategy for target-directed synthesis [180]. Furthermore, a range of internal and terminal alkynes are tolerated, in which complete conversion of the substrates was achieved in 30 minutes in most cases.



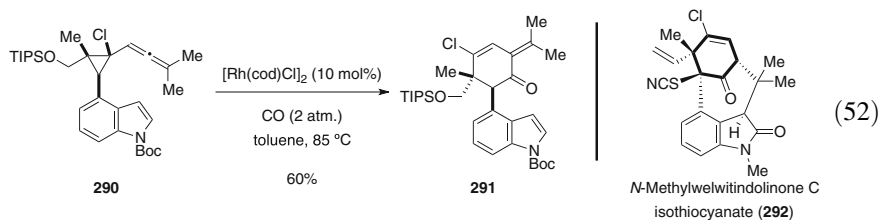
The complex guaianolide, thapsigargin (**287**), is a particularly challenging synthetic target, which consists of a highly functionalized 5,7,5-fused tricyclic core featuring eight stereogenic centers and bearing four different ester side chains. Ardisson and coworkers described an approach to the core structure of this natural product utilizing a rhodium-catalyzed PK-type reaction of the allenyl alkyne **285** with CO, to generate the bicyclic product **286** in 80% yield (Eq. 50) [181]. Although this strategy provides the seven-membered ring with the correct stereochemistry at C6 and C7, in addition to the installation of the methyl groups at C4 and C10 [182], the synthesis of **285** is relatively long (17 steps from triethyl phosphonoacetate) and the carbocyclization reaction requires a relatively high rhodium loading.



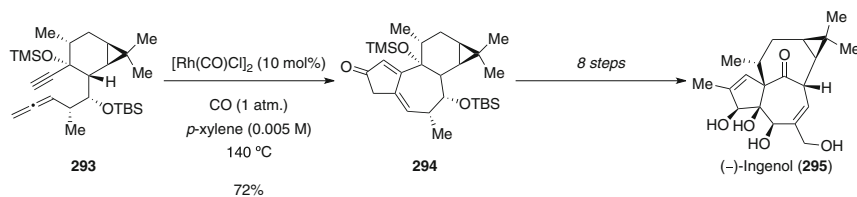
Mukai and coworkers reported the first total synthesis of the guaiene-type sesquiterpene, (+)-indicanone (**289**), the active component of a traditional medicine used in China for the treatment of pneumonia, rheumatism, and bronchitis (Eq. 51) [183]. The synthesis was initiated with the preparation of 1,8-allenylne **288** in 13 steps from (+)-limonene. Treatment of **288** with 5 mol% $[\text{Rh}(\text{CO})(\text{dppp})\text{Cl}]_2$ under 1 atm. of CO, followed by the addition of mild acid to cleave the TBS group, furnished the natural product in 95% yield. Interestingly, the natural product can be prepared directly from the free alcohol derivative of **288**, albeit the reaction is stoichiometric in rhodium.



In 2012, Zhang and Tang devised a strategy to access the functionalized cyclohexenone core present in the various derivatives of welwitindolinone C (**292**), using a [5+1] carbocyclization reaction of an allenylcyclopropane (Eq. 52) [184]. The allenylcyclopropane **290** was prepared in seven steps from 4-cyanoindole utilizing Du Bois' $\text{Rh}_2(\text{esp})_2$ catalyst [185] to catalyze the key *intramolecular* cyclopropanation step between a trisubstituted alkene and a chlorodiazoacetate, which was followed by the installation of the allene moiety. Treatment of **290** with 10 mol% $[\text{Rh}(\text{cod})\text{Cl}]_2$ under 2 atm. of CO afforded **291** in 60% yield in a highly stereospecific manner. Nevertheless, subsequent attempts to elaborate this intermediate and form the seven-membered ring were unsuccessful.



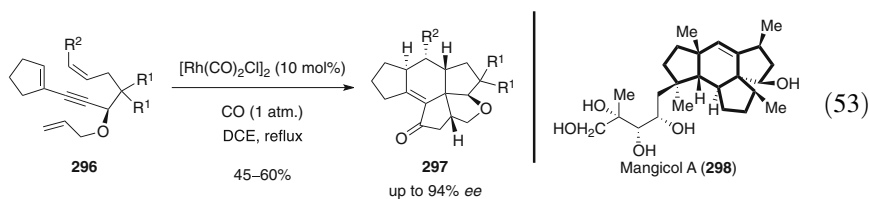
Baran and coworkers completed a concise total synthesis of the diterpenoid, (–)-ingenol (**295**), which was first isolated from *Euphorbia peplus* in 1968 (Scheme 38) [186, 187]. The synthetic strategy is divided into two phases: a “cyclase phase” to build up a tigliane skeleton, which concludes at an intermediate from which other



Scheme 38 Key [(2+2)+1] carbocyclization reaction in the total synthesis of (–)-ingenol

interesting analogs could be prepared, and an “oxidase phase” to install four hydroxyl groups and promote a skeletal rearrangement to the ingenane scaffold. The rhodium-catalyzed *intramolecular* allenic PK-type reaction between the allene **293** and CO provides the 5,7,6,3-fused tetracyclic ring system **294** in 72% yield, which enables the synthesis to be completed in 14 steps from (+)-3-carene. Notably, the cyclization requires high dilution in degassed anhydrous solvent for optimal efficiency. More recently, **294** was utilized by the same group in a 19-step total synthesis of (+)-phorbol [188].

Ying and Pu reported a domino PK-type reaction/Diels–Alder cycloaddition of enantioenriched trienyne **296** with CO to afford the fused pentacycles **297**, a strategy which represents a possible entry into the core of mangicol A (**298**) (Eq. 53) [189]. Treatment of the trienyne **296** with 10 mol% $[\text{Rh}(\text{CO})_2\text{Cl}]_2$ under 1 atm. of CO in refluxing DCE furnished **297** in moderate yield and with excellent stereoselectivity, generating four new stereocenters and five new C–C bonds, albeit a longer alkyl chain ($\text{R}^2 = n$ -pentyl) afforded a mixture of diastereoisomers with reduced enantiopurity.



8 Conclusions and Outlook

The rhodium-catalyzed Pauson–Khand-type reaction and related rhodium-catalyzed carbonylative carbocyclization processes have been major focal points in synthetic organic and organometallic chemistry for the last 20 years. An impressive array of cyclic and polycyclic targets can be readily assembled from simple substrates, which has been advantageous in the preparation of several important natural products. Moreover, many of these reactions are highly diastereo- and enantioselective, which provides a convenient approach to the construction of cyclic ketones that represent important synthons for target-directed synthesis. By

conducting these cyclocarbonylations in tandem with allylic substitution, rearrangements, or other cycloaddition reactions, other more complex targets can be prepared in an efficient manner from simpler starting materials. Additionally, rings up to eight and even nine atoms in size can be prepared via this strategy, and carbon monoxide gas-free reactions are attainable due to the impressive ability of rhodium to transfer “CO” from aldehydes and alcohols to metallacycle intermediates. It is expected that the utility of rhodium-catalyzed cyclocarbonylation reactions will continue to expand in the future, with the discovery of new reaction manifolds to access other complex targets with different ring sizes that would be difficult to prepare via a more classical methodology.

References

1. Davies HML, Sorensen EJ (eds) (2009) *Chem Soc Rev* 38:2969
2. Lautens M, Klute W, Tam W (1996) *Chem Rev* 96:49
3. Ojima I, Tzamarioudaki M, Li Z, Donovan RJ (1996) *Chem Rev* 96:635
4. Inglesby PA, Evans PA (2010) *Chem Soc Rev* 39:2791
5. Broere DLJ, Ruijter E (2012) *Synthesis* 44:2639
6. Reppe W, Schweckendiek WJ (1948) *Liebigs Ann Chem* 560:104
7. Khand IU, Knox GR, Pauson PL, Watts WE, Foreman MI (1973) *J Chem Soc Perkin Trans 1* 977
8. Strübing D, Beller M (2006) *Top Organomet Chem* 18:165
9. Pérez-Castells J (2006) *Top Organomet Chem* 19:207
10. Lee H-W, Kwong F-Y (2010) *Eur J Org Chem* 789
11. Shibata T (2011) In: De Vries JG, Molander GA, Evans PA (eds) *Science of synthesis*, vol 3. Thieme, Stuttgart, p 125
12. Lam FL, Lee HW, Wang J, Kwong FY (2012) Recent advancement of catalytic Pauson–Khand-type reactions. In: Rios Torres R (ed) *The Pauson–Khand reaction: scope, variations and applications*, 1st edn. Wiley, Chichester, pp 181–210
13. Heldeweg RF, Hogeveen H (1976) *J Am Chem Soc* 98:19
14. Chen J-R, Hu X-Q, Lu L-Q, Xiao W-J (2015) *Chem Rev* 115:5301
15. Murakami M, Itami K, Ito Y (1995) *Angew Chem Int Ed* 34:2691
16. Murakami M, Itami K, Ito Y (1996) *J Am Chem Soc* 118:11672
17. Murakami M, Itami K, Ito Y (1997) *J Am Chem Soc* 119:2950
18. Meng Q, Li M, Zhang J (2005) *J Mol Struct Theochem* 726:47
19. Murakami M, Itami K, Ito Y (1999) *J Am Chem Soc* 121:4130
20. Murakami M, Itami K, Ito Y (1999) *Organometallics* 18:1326
21. Mazumder S, Crandell DW, Lord RL, Baik M-H (2014) *J Am Chem Soc* 136:9414
22. Murakami M, Itami K, Ito Y (1998) *Angew Chem Int Ed* 37:3418
23. Zhang Y, Chen Z, Xiao Y, Zhang J (2009) *Chem Eur J* 15:5208
24. Wang T, Wang C-H, Zhang J (2011) *Chem Commun* 47:5578
25. Fukuyama T, Ohta Y, Brancour C, Miyagawa K, Ryu I, Dhimane A-L, Fensterbank L, Malacria M (2012) *Chem Eur J* 18:7243
26. Li X, Huang S, Schienebeck CM, Shu D, Tang W (2012) *Org Lett* 14:1584
27. Chen W, Tay J-H, Yu X-Q, Pu L (2012) *J Org Chem* 77:6215
28. Cho SH, Liebeskind LS (1987) *J Org Chem* 52:2631
29. Kurahashi T, de Meijere A (2005) *Synlett* 2619
30. Brancour C, Fukuyama T, Ohta Y, Ryu I, Dhimane A-L, Fensterbank L, Malacria M (2010) *Chem Commun* 46:5470

31. Schienebeck CM, Song W, Smits AM, Tang W (2015) *Synthesis* 47:1076
32. Shu D, Li X, Zhang M, Robichaux PJ, Tang W (2011) *Angew Chem Int Ed* 50:1346
33. Mauleón P, Krinsky JL, Toste FD (2009) *J Am Chem Soc* 131:4513
34. Garayalde D, Gómez-Bengoá E, Huang X, Goeke A, Nevado C (2010) *J Am Chem Soc* 132:4720
35. Wang S, Zhang L (2006) *J Am Chem Soc* 128:8414
36. Shu D, Li X, Zhang M, Robichaux PJ, Guzei IA, Tang W (2012) *J Org Chem* 77:6463
37. Li X, Song W, Tang W (2013) *J Am Chem Soc* 135:16797
38. Jiang G-J, Fu X-F, Li Q, Yu Z-X (2012) *Org Lett* 14:692
39. Wender PA, Deschamps NM, Sun R (2006) *Angew Chem Int Ed* 45:3957
40. Murakami M, Itami K, Ubukata M, Tsuji I, Ito Y (1998) *J Org Chem* 63:4
41. Yao Z-K, Li J, Yu Z-X (2011) *Org Lett* 13:134
42. Murakami M, Nishida S (1979) *Chem Lett* 927
43. Morizawa Y, Oshima K, Nozaki H (1982) *Tetrahedron Lett* 23:2871
44. Fu X-F, Xiang Y, Yu Z-X (2015) *Chem Eur J* 21:4242
45. Kobayashi T, Koga Y, Narasaka K (2001) *J Organomet Chem* 624:73
46. Jeong N, Sung BK, Kim JS, Park SB, Seo SD, Shin JY, In KY, Choi YK (2002) *Pure Appl Chem* 74:85
47. Koga Y, Kobayashi T, Narasaka K (1998) *Chem Lett* 249
48. Exon C, Magnus P (1983) *J Am Chem Soc* 105:2477
49. Jeong N, Lee S, Sung BK (1998) *Organometallics* 17:3642
50. Jeong N, Seo SD, Shin JY (2000) *J Am Chem Soc* 122:10220
51. Evans PA, Robinson JE (2001) *J Am Chem Soc* 123:4609
52. Ashfield BL, Miller KA, Martin SF (2004) *Org Lett* 6:1321
53. Ashfield BL, Miller KA, Smith AJ, Tran K, Martin SF (2005) *Org Lett* 7:1661
54. Fan L, Zhao W, Jiang W, Zhang J (2008) *Chem Eur J* 14:9139
55. Lee SI, Fukumoto Y, Chatani N (2010) *Chem Commun* 46:3345
56. Chen W, Tay J-H, Ying J, Yu X-Q, Pu L (2013) *J Org Chem* 78:2256
57. Ying J, Brown KB, Sandridge MJ, Hering BA, Sabat M, Pu L (2015) *J Org Chem* 80:3195
58. Wang H, Sawyer JR, Evans PA, Baik M-H (2008) *Angew Chem Int Ed* 47:342
59. Baik M-H, Mazumder S, Ricci P, Sawyer JR, Song Y-G, Wang H, Evans PA (2011) *J Am Chem Soc* 133:7621
60. Turlington M, Pu L (2011) *Org Lett* 13:4332
61. Jeong N, Sung BK, Choi YK (2000) *J Am Chem Soc* 122:6771
62. Kim DE, Choi C, Kim IS, Jeulin S, Ratovelomanana-Vidal V, Genêt J-P, Jeong N (2006) *Synthesis* 4053
63. Kim DE, Choi C, Kim IS, Jeulin S, Ratovelomanana-Vidal V, Genêt J-P, Jeong N (2007) *Adv Synth Catal* 349:1999
64. Kim DE, Ratovelomanana-Vidal V, Jeong N (2010) *Adv Synth Catal* 352:2032
65. Fan B-M, Xie J-H, Li S, Tu Y-Q, Zhou Q-L (2005) *Adv Synth Catal* 347:759
66. Cristóbal-Lecina E, Constantino AR, Grabulosa A, Riera A, Verdaguer X (2015) *Organometallics* 34:4989
67. Choi YH, Kwak J, Jeong N (2009) *Tetrahedron Lett* 50:6068
68. Kim DE, Park SH, Choi YH, Lee S-G, Moon D, Seo J, Jeong N (2011) *Chem Asian J* 6:2009
69. Jeong N, Kim DH, Choi JH (2004) *Chem Commun* 1134
70. Kim DE, Lee BH, Rajagopalararma M, Genêt J-P, Ratovelomanana-Vidal V, Jeong N (2008) *Adv Synth Catal* 350:2695
71. Kim DE, Kwak J, Kim IS, Jeong N (2009) *Adv Synth Catal* 351:97
72. Suh WH, Choi M, Lee SI, Chung YK (2003) *Synthesis* 2169
73. Schmid TM, Consiglio G (2004) *Chem Commun* 2318
74. Kim DE, Kim IS, Ratovelomanana-Vidal V, Genêt J-P, Jeong N (2008) *J Org Chem* 73:7985
75. Chen G-Q, Shi M (2013) *Chem Commun* 49:698
76. Brummond KM, Sill PC, Rickards B, Geib SJ (2002) *Tetrahedron Lett* 43:3735

77. Brummond KM, Mitasev B (2004) *Org Lett* 6:2245
78. Brummond KM, Chen H, Fisher KD, Kerekes AD, Rickards B, Sill PC, Geib SJ (2002) *Org Lett* 4:1931
79. Manku S, Curran DP (2005) *J Comb Chem* 7:63
80. Mukai C, Nomura I, Yamanishi K, Hanaoka M (2002) *Org Lett* 4:1755
81. Mukai C, Nomura I, Kitagaki S (2003) *J Org Chem* 68:1376
82. Mukai C, Inagaki F, Yoshida T, Kitagaki S (2004) *Tetrahedron Lett* 45:4117
83. Mukai C, Inagaki F, Yoshida T, Yoshitani K, Hara Y, Kitagaki S (2005) *J Org Chem* 70:7159
84. Mukai C, Hirose T, Teramoto S, Kitagaki S (2005) *Tetrahedron* 61:10983
85. Inagaki F, Kawamura T, Mukai C (2007) *Tetrahedron* 63:5154
86. Brummond KM, Chen D (2008) *Org Lett* 10:705
87. Grillet F, Brummond KM (2013) *J Org Chem* 78:3737
88. Tap A, Lecourt C, Dhambri S, Arnould M, Galvani G, Nguyen van Buu O, Jouanneau M, Férézou J-P, Ardisson J, Lannou M-I, Sorin G (2016) *Chem Eur J* 22:4938
89. Makino T, Itoh K (2004) *J Org Chem* 69:395
90. Inagaki F, Mukai C (2006) *Org Lett* 8:1217
91. Inagaki F, Itoh N, Hayashi Y, Matsui Y, Mukai C (2011) *Beilstein J Org Chem* 7:404
92. Yuan W, Dong X, Shi M, McDowell P, Li G (2012) *Org Lett* 14:5582
93. Wender PA, Deschamps NM, Gamber GG (2003) *Angew Chem Int Ed* 42:1853
94. Croatt MP, Wender PA (2010) *Eur J Org Chem* 19
95. Wender PA, Croatt MP, Deschamps NM (2004) *J Am Chem Soc* 126:5948
96. Pitcock WH Jr, Lord RL, Baik M-H (2008) *J Am Chem Soc* 130:5821
97. Wender PA, Deschamps NM, Williams TJ (2004) *Angew Chem Int Ed* 43:3076
98. Brummond KM, Chen H, Mitasev B, Casarez AD (2004) *Org Lett* 6:2161
99. Wender PA, Croatt MP, Deschamps NM (2006) *Angew Chem Int Ed* 45:2459
100. Inagaki F, Narita S, Hasegawa T, Kitagaki S, Mukai C (2009) *Angew Chem Int Ed* 48:2007
101. Kawamura T, Inagaki F, Narita S, Takahashi Y, Hirata S, Kitagaki S, Mukai C (2010) *Chem Eur J* 16:5173
102. Shafawait MTS, Inagaki F, Kawamura T, Mukai C (2013) *Tetrahedron* 69:1509
103. Mukai C, Takahashi Y, Ogawa K, Hayashi Y, Inagaki F (2014) *Chem Pharm Bull* 62:84
104. Saito T, Sugizaki K, Otani T, Suyama T (2007) *Org Lett* 9:1239
105. Zhang Z, Xiao F, Huang B, Hu J, Fu B, Zhang Z (2016) *Org Lett* 18:908
106. Saito T, Furukawa N, Otani T (2010) *Org Biomol Chem* 8:1126
107. Saito T, Nihei H, Otani T, Suyama T, Furukawa N, Saito M (2008) *Chem Commun* 172
108. Iwata T, Inagaki F, Mukai C (2013) *Angew Chem Int Ed* 52:11138
109. Koga Y, Narasaka K (1999) *Chem Lett* 705
110. Lee SI, Park JH, Chung YK, Lee S-G (2004) *J Am Chem Soc* 126:2714
111. Jiao L, Lin M, Zhuo L-G, Yu Z-X (2010) *Org Lett* 12:2528
112. Lin M, Li F, Jiao L, Yu Z-X (2011) *J Am Chem Soc* 133:1690
113. Li C, Zhang H, Feng J, Zhang Y, Wang J (2010) *Org Lett* 12:3082
114. Zhao W, Zhang J (2011) *Org Lett* 13:688
115. Lu B-L, Wei Y, Shi M (2012) *Organometallics* 31:4601
116. Mazumder S, Shang D, Negru DE, Baik M-H, Evans PA (2012) *J Am Chem Soc* 134:20569
117. Shaw MH, Melikhova EY, Kloer DP, Whittingham WG, Bower JF (2013) *J Am Chem Soc* 135:4992
118. Shaw MH, Whittingham WG, Bower JF (2016) *Tetrahedron* 72:2731
119. Shaw MH, McCreanor NG, Whittingham WG, Bower JF (2015) *J Am Chem Soc* 137:463
120. Shaw MH, Croft RA, Whittingham WG, Bower JF (2015) *J Am Chem Soc* 137:8054
121. Kim S, Chung YK (2014) *Org Lett* 16:4352
122. Evans PA, Burnie AJ, Negru DE (2014) *Org Lett* 16:4356
123. Kim SY, Lee SI, Choi SY, Chung YK (2008) *Angew Chem Int Ed* 47:4914
124. Kim SY, Chung YK (2010) *J Org Chem* 75:1281
125. Wang Y, Yu Z-X (2015) *Acc Chem Res* 48:2288

126. Wender PA, Gamber GG, Hubbard RD, Zhang L (2002) *J Am Chem Soc* 124:2876
127. Wegner HA, de Meijere A, Wender PA (2005) *J Am Chem Soc* 127:6530
128. Wang Y, Wang J, Su J, Huang F, Jiao L, Liang Y, Yang D, Zhang S, Wender PA, Yu Z-X (2007) *J Am Chem Soc* 129:10060
129. Yu Z-X, Wender PA, Houk KN (2004) *J Am Chem Soc* 126:9154
130. Huang F, Yao Z-K, Wang Y, Wang Y, Zhang J, Yu Z-X (2010) *Chem Asian J* 5:1555
131. Bennacer B, Fujiwara M, Ojima I (2004) *Org Lett* 6:3589
132. Montero-Campillo MM, Rodríguez-Otero J, Cabaleiro-Lago E (2008) *J Phys Chem A* 112:2423
133. Bennacer B, Fujiwara M, Lee S-Y, Ojima I (2005) *J Am Chem Soc* 127:17756
134. Ojima I, Lee S-Y (2000) *J Am Chem Soc* 122:2385
135. Kaloko JJ, Teng Y-HG, Ojima I (2009) *Chem Commun* 4569
136. Huang Q, Hua R (2007) *Chem Eur J* 13:8333
137. Wender PA, Gamber GG, Hubbard RD, Pham SM, Zhang L (2005) *J Am Chem Soc* 127:2836
138. Morimoto T, Fuji K, Tsutsumi K, Kakiuchi K (2002) *J Am Chem Soc* 124:3806
139. Shibata T, Toshida N, Takagi K (2002) *Org Lett* 4:1619
140. Shibata T, Toshida N, Takagi K (2002) *J Org Chem* 67:7446
141. Fuji K, Morimoto T, Tsutsumi K, Kakiuchi K (2003) *Angew Chem Int Ed* 43:2409
142. Fuji K, Morimoto T, Tsutsumi K, Kakiuchi K (2004) *Tetrahedron Lett* 45:9163
143. Kwong FY, Li YM, Lam WH, Qiu L, Lee HW, Yeung CH, Chan KS, Chan ASC (2005) *Chem Eur J* 11:3872
144. Kwong FY, Lee HW, Qiu L, Lam WH, Li Y-M, Kwong HL, Chan ASC (2005) *Adv Synth Catal* 347:1750
145. Furusawa T, Morimoto T, Ikeda K, Tanimoto H, Nishiyama Y, Kakiuchi K, Jeong N (2015) *Tetrahedron* 71:875
146. Turlington M, Du Y, Ostrum SG, Santosh V, Wren K, Lin T, Sabat M, Pu L (2011) *J Am Chem Soc* 133:11780
147. Park JH, Cho Y, Chung YK (2010) *Angew Chem Int Ed* 49:5138
148. Ikeda K, Morimoto T, Kakiuchi K (2010) *J Org Chem* 75:6279
149. Ikeda K, Morimoto T, Tsumagari T, Tanimoto H, Nishiyama Y, Kakiuchi K (2012) *Synlett* 393
150. Lee HW, Chan ASC, Kwong FY (2007) *Chem Commun* 2633
151. Lee HW, Kwong FY, Chan ASC (2008) *Synlett* 1553
152. Lee HW, Lee LN, Chan ASC, Kwong FY (2008) *Eur J Org Chem* 3403
153. Park KH, Jung IG, Chung YK (2004) *Org Lett* 6:1183
154. Park KH, Chung YK (2005) *Adv Synth Catal* 347:854
155. Park JH, Kim SY, Kim SM, Lee SI, Chung YK (2007) *Synlett* 453
156. Park JH, Kim E, Kim H-M, Choi SY, Chung YK (2008) *Chem Commun* 2388
157. Sawano T, Thacker NC, Lin Z, McIsaac AR, Lin W (2015) *J Am Chem Soc* 137:12241
158. Van Ornum SG, Hoerner S, Cook JM (2012) Recent adventures with the Pauson–Khand reaction in total synthesis. In: Rios Torres R (ed) *The Pauson–Khand reaction: scope, variations and applications*, 1st edn. Wiley, Chichester, pp 211–238
159. Gehrtz PH, Hirschbeck V, Ciszek B, Fleischer I (2016) *Synthesis* 48:1573
160. Brady SF, Singh MP, Janso JE, Clardy J (2000) *J Am Chem Soc* 122:2116
161. Brummond KM, Gao D (2003) *Org Lett* 5:3491
162. Stork G, Danheiser RL (1973) *J Org Chem* 38:1775
163. Smith AB III, Dorsey BD, Ohba M, Lupo AT Jr, Malamas MS (1988) *J Org Chem* 53:4314
164. Kim DH, Kim K, Chung YK (2006) *J Org Chem* 71:8264
165. Hirose T, Miyakoshi N, Mukai C (2008) *J Org Chem* 73:1061
166. Jiao L, Yuan C, Yu Z-X (2008) *J Am Chem Soc* 130:4421
167. Fan X, Tang M-X, Zhuo L-G, Tu YQ, Yu Z-X (2009) *Tetrahedron Lett* 50:155
168. Fan X, Zhuo L-G, Tu YQ, Yu Z-X (2009) *Tetrahedron* 65:4709
169. Yuan C, Jiao L, Yu Z-X (2010) *Tetrahedron Lett* 51:5674

170. Hayashi Y, Miyakoshi N, Kitagaki S, Mukai C (2008) *Org Lett* 10:2385
171. Brummond KM, Chen D, Davis MM (2008) *J Org Chem* 73:5064
172. Oh D-C, Williams PG, Kauffman CA, Jensen PR, Fenical W (2006) *Org Lett* 8:1021
173. Aburano D, Inagaki F, Tomonaga S, Mukai C (2009) *J Org Chem* 74:5590
174. Datta S, Liu R-S (2005) *Tetrahedron Lett* 46:7985
175. Liang Y, Jiang X, Yu Z-X (2011) *Chem Commun* 47:6659
176. Liang Y, Jiang X, Fu X-F, Ye S, Wang T, Yuan J, Wang Y, Yu Z-X (2012) *Chem Asian J* 7:593
177. Frantz DE, Fässler R, Carreira EM (2000) *J Am Chem Soc* 122:1806
178. Jiang B, Chen Z, Xiong W (2002) *Chem Commun* 1524
179. Grillet F, Huang C, Brummond KM (2011) *Org Lett* 13:6304
180. Wen B, Hexum JK, Widen JC, Harki DA, Brummond KM (2013) *Org Lett* 14:2644
181. Tap A, Jouanneau M, Galvani G, Sorin G, Lannou M-I, Férézou J-P, Ardisson J (2012) *Org Biomol Chem* 10:8140
182. Wells SM, Brummond KM (2015) *Tetrahedron Lett* 56:3546
183. Hayashi Y, Ogawa K, Inagaki F, Mukai C (2012) *Org Biomol Chem* 10:4747
184. Zhang M, Tang W (2012) *Org Lett* 14:3756
185. Espino CG, Fiori KW, Kim M, Du Bois J (2004) *J Am Chem Soc* 126:15378
186. Jørgensen L, McKerrall SJ, Kuttruff CA, Ungeheuer F, Felding J, Baran PS (2013) *Science* 341:878
187. McKerrall SJ, Jørgensen L, Kuttruff CA, Ungeheuer F, Baran PS (2014) *J Am Chem Soc* 136:5799
188. Kawamura S, Chu H, Felding J, Baran PS (2016) *Nature* 532:90
189. Ying J, Pu L (2014) *Chem Eur J* 20:16301

Rhodium-Catalysed Hydrogenations Using Monodentate Ligands

Mattia Cettolin, Pim Puylaert, and Johannes G. de Vries

Abstract The use of monodentate phosphorus ligands, such as phosphonites, phosphites and phosphoramidites, in the rhodium-catalysed asymmetric hydrogenation of a range of mostly alkene type substrates was reported for the first time in 2000. Not only are these ligands cheap and easy to prepare in one or two steps, their use has also created new opportunities, such as their robotic parallel synthesis and the use of complexes containing two different monodentate ligands, which tremendously increases the available diversity. This review covers the period between 2006 and 2016. Many new ligands have been made during this time; not only new variants on the three ligand types that were earlier reported, but also monodentate phosphines and secondary phosphine oxides. These were mostly tested on the usual *N*-acetyl-dehydroamino acids, itaconic esters and enamide type substrates. Other more novel substrates were *N*-formyl-dehydroamino acids, all the variants of the beta-dehydroamino acid family, enol esters, 2-methylidene-1,2,3,4-tetrahydro- β -carboline, alkenes containing phosphonate or thioether substituents, several substituted acrylic acids as well as substituted cinnamic acids. The mechanism of the rhodium-catalysed hydrogenation with phosphites, phosphonites, phosphoramidites as well as phosphepines has been reported. A common theme in these mechanisms is the formation of a dimeric bimetallic complex after subjecting the $[\text{RhL}_2(\text{cod})]\text{X}$ or $[\text{RhL}_2(\text{nbd})]\text{X}$ ($\text{X} = \text{BF}_4, \text{PF}_6, \text{SbF}_6$) complexes to hydrogen. Since these hydrogenations are usually carried out in non-polar solvents,

M. Cettolin

Dipartimento di Chimica, Università degli Studi di Milano, via C. Golgi 19, 20133 Milan, Italy
Leibniz Institut für Katalyse e. V., Albert-Einstein-Strasse 29a, 18059 Rostock, Germany

P. Puylaert

Leibniz Institut für Katalyse e. V., Albert-Einstein-Strasse 29a, 18059 Rostock, Germany

J.G. de Vries (✉)

Leibniz Institut für Katalyse e. V., Albert-Einstein-Strasse 29a, 18059 Rostock, Germany
Stratingh Institute for Chemistry, Nijenborgh 4, 9747 AG, Groningen, The Netherlands
e-mail: Johannes.deVries@catalysis.de

the formation of the expected $\text{RhL}_2(\text{Solvent})_2$ complexes does not occur after the removal of the diene and instead each rhodium atom in these dimeric complexes coordinates not only to two monodentate ligands, but also in η^6 fashion to an aromatic ring of one of the ligands that is bound to the other rhodium atom. These complexes can react with the substrate to form the substrate complex that is hydrogenated. Other studies also found that it is possible to form rhodium hydride complexes first, which react with the substrate to form product. There is one well-described industrial application on large scale in which a substituted 2-isopropylcinnamic acid is hydrogenated using a rhodium complex with a mixture of 2 eq. of 3,3'-dimethyl-PipPhos and 1 eq. of triphenylphosphine. The addition of the non-chiral triarylphosphine not only accelerated the reaction 50-fold, also the enantioselectivity was much improved. The product was used as a building block for AliskirenTM, a blood-pressure lowering agent.

Keywords Asymmetric hydrogenation • Homogeneous catalysis • Mechanism • Monodentate ligands • Phosphines • Phosphites • Phosphonites • Phosphoramidites • Production • Secondary phosphineoxides • Supramolecular catalysis

Contents

1	Introduction	232
2	New Monodentate Ligands	235
2.1	Phosphonites, Phosphites, Phosphoramidites	235
2.2	Phosphines and Secondary Phosphine Oxides	239
3	New Hydrogenation Reactions	240
4	Reaction Mechanism	245
5	Supramolecular Catalysis Using Monodentate Ligands	249
6	Industrial Application	258
	References	259

1 Introduction

After the invention of the use of $\text{RhCl}(\text{PPh}_3)_3$ as hydrogenation catalyst by Wilkinson, Knowles [1, 2] and Horner [3] independently arrived at the idea of using chiral versions of triphenylphosphine in such a complex, to allow the hydrogenation reaction of prochiral substrates to take place with enantioselection. Initial attempts using chiral at phosphorus ligand **1** (Fig. 1) were successful, but enantioselectivity was rather low. Horner retired after his first attempts, but Knowles continued, initially guided by the desire to develop a catalyst that would enable the production of L-phenylalanine (for the production of the sweetener aspartame) via asymmetric hydrogenation of the dehydroderivative **6b** (Scheme 1, **1**). The ligand PAMP (**2**) already was much better than **1** in this reaction as the product was obtained in 55% ee. Knowles reasoned that the many degrees of freedom in the rhodium

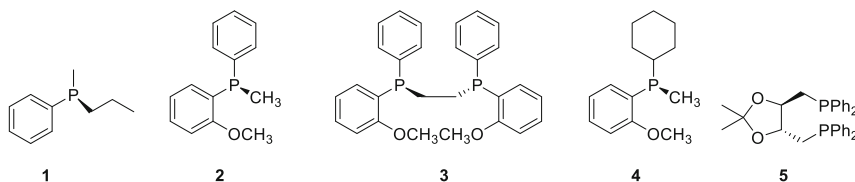
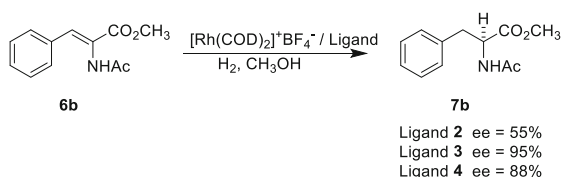


Fig. 1 Early chiral monodentate and bidentate phosphorus ligands



Scheme 1 Asymmetric hydrogenation of methyl 2-acetamido-cinnamate using PAMP, di-PAMP and CAMP as ligand

complex made from **2** were detrimental for the stereoselection and based on this designed the bidentate analogue di-PAMP (**3**). Indeed, the use of this ligand led to formation of the product **7** in 95% ee [4]. These ligands took a rather large number of steps to make, but later Kagan invented DIOP (**5**) which has chirality in the backbone instead of on phosphorus [5, 6]. These types of ligands were much easier to synthesise starting from a rather large pool of commercially available chiral starting materials and thus started the highly successful era of the bidentate phosphine ligands. The complexes could be prepared in situ, simply by adding the bisphosphine to $[\text{Rh}(\text{COD})_2]\text{BF}_4$ ($\text{COD} = 1,5\text{-cyclooctadiene}$). The bidentate ligand displaces one of the dienes and the other diene would be hydrogenated off, whereas methanol (the usual solvent) would occupy the remaining two vacant positions to give $[\text{Rh}(\text{PP})_2(\text{MeOH})_2]\text{BF}_4$. In spite of the fact that Knowles later showed that the monodentate ligand CAMP (**4**) induced 88% ee in the asymmetric hydrogenation of **6** [7], no more research was reported on the use of monodentate ligands in asymmetric hydrogenation for the next 30 years.

In the year 2000, suddenly three papers appeared that reported that BINOL-based monodentate phosphonites [8, 9], phosphites [10] and phosphoramidites [11, 12] were actually excellent ligands in the rhodium-catalysed asymmetric hydrogenation of substituted alkenes (Fig. 2). Enantioselectivities and reaction rates obtained in the hydrogenation of *N*-acetyl-dehydroamino acids and esters and a range of other alkene substrates were actually comparable to those obtained with bidentate phosphines. Not only that, but these ligands were easily obtained from cheap enantiopure BINOL (1,1'-Bi-2-naphthol) in just one or two synthetic steps, without the need for a further resolution. This also makes them at least an order of magnitude cheaper than the bidentate bisphosphines.

The advent of the monodentate ligands created more opportunities that would have been impossible to achieve with the bidentate bisphosphines. Since the active

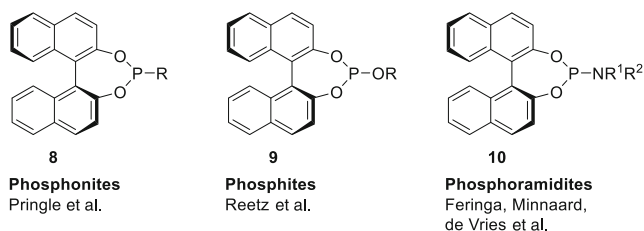


Fig. 2 Monodentate BINOL-based ligands for asymmetric hydrogenation

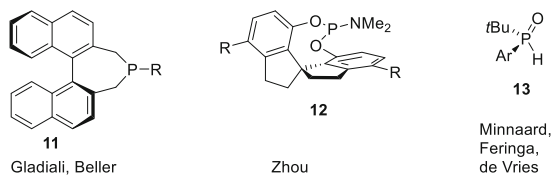


Scheme 2 Equilibrium mixture of rhodium complexes based on two different monodentate ligands

hydrogenation complex usually contains two monodentate ligands, it is possible in principle to create complexes based on two different ligands [13–18]. In practice, this is somewhat more problematic as ligand exchange tends to be fast in these complexes, so in the end a statistical mixture of three complexes is obtained, the ratio of which is determined by thermodynamics (Scheme 2). Nevertheless, the concept could work if the mixed complex is thermodynamically much more stable than the two homo-complexes or if it is kinetically superior.

In addition, it is possible to influence the ratio of complexes by varying the ratio of the two monodentate ligands. For instance, by using an L^1/L^2 ratio of 2, formation of $[\text{RhL}^2\text{L}^2]^+$ would be largely suppressed [16]. In screening large libraries of these combinations, it is usually found that the majority of combinations lead to worse results; however, there are always a few combinations that lead to better results, and hence, this is an attractive way to further increase the available diversity.

The easy synthesis of the monodentate ligands offers another opportunity: robotised parallel ligand synthesis. Methodology was developed by Lefort and co-workers at DSM in the Netherlands for the fully automated parallel synthesis of monodentate phosphoramidites (and phosphites) [19]. This was based on the fact that reaction between the BINOL-based phosphochloridate, which can be prepared in quantitative yield by refluxing the (substituted) BINOL with PCl_3 and stored indefinitely, and the amine (or alcohol) gives the phosphoramidites (phosphites) in between 90 and 98% purity based on the phosphorus NMR. However, it is very important that the Et_3NHCl salt formed in this reaction is quantitatively removed, as chloride not only inhibits the hydrogenation, but it also reduces the enantioselectivity. This was accomplished by performing the reaction in toluene, which leads to full precipitation of the salt. Using a simple liquid-dispensing robot and a 96-well oleophobic titre well plate, 96 ligands could be prepared in a few hours, and after filtration of the salts, the slightly impure ligands were combined with the metal precursor and the substrate in a vial and subjected to a parallel hydrogenation reaction overnight. Although the enantioselectivity of these reactions is slightly

Fig. 3 Non-BINOL-based monodentate ligands

reduced, the relative order of the enantioselectivity induced by the impure ligands is the same as those from the pure ligands [19]. This has remarkably reduced the time necessary to find a ligand that induces high enantioselectivity in combination with a high enough reaction rate.

The development of the BINOL-based monodentate ligands also spurred the development of other new non-BINOL-based monodentate ligands. The reader is referred to the earlier reviews for a detailed overview. Three ligand classes will be mentioned, in view of the many publications documenting their use. These are the 1,1'-binaphthyl-based phosphines (**11**) [20–24]; the spirobiindane diol (SPINOL)-based ligands, such as SIPHOS (**12**) [25–27]; and the secondary phosphine oxides (**13**) [28, 29] (Fig. 3).

The first 5 years of these developments from 2000 to 2005 have been well documented in several reviews [12, 23, 24, 30–32]. In this review we will paint the new developments of the period 2006–2016.

2 New Monodentate Ligands

2.1 Phosphonites, Phosphites, Phosphoramidites

Bondarev and Goddard reacted (*S*)- α,α -diphenylprolinol first with PCl_3 and next with aliphatic alcohols or phenols [33]. The bicyclic phosphoramidites **14** (Fig. 4) thus obtained were tested in the rhodium-catalysed enantioselective hydrogenation of **6b**, **27b** and **29b** in CH_2Cl_2 (Scheme 3). Depending on the chosen substituents, enantioselectivities between 22 and 95% were obtained. In a similar vein, (*S*)- α,α -diphenylprolinol was reacted with RPCl_2 in which R were aliphatic groups or phenyl to give the bicyclic aminophosphonates **15a**. The aliphatic analogues performed poorly and conversion was incomplete after overnight reaction, but the phenyl derivative performed well with ee's between 62 and 81%. Reaction of (*S*)- α,α -diphenylprolinol with $\text{P}(\text{NMe}_2)_3$ or $\text{P}(\text{NEt}_2)_3$ led to formation of the bicyclic diaminophosphites **15b**. The use of the dimethyl analogue led to full conversion and ee's between 61 and 91%. Armspach, Matt and co-workers synthesised four novel phosphoramidites **16** in which not only the diol but also the diamine contains a chiral 1,1'-binaphthyl structure [34]. These ligands were used for the rhodium-catalysed hydrogenation of substituted and unsubstituted methyl 2-acetamidocinnamates. The products were obtained quantitatively with ee's between 79 and

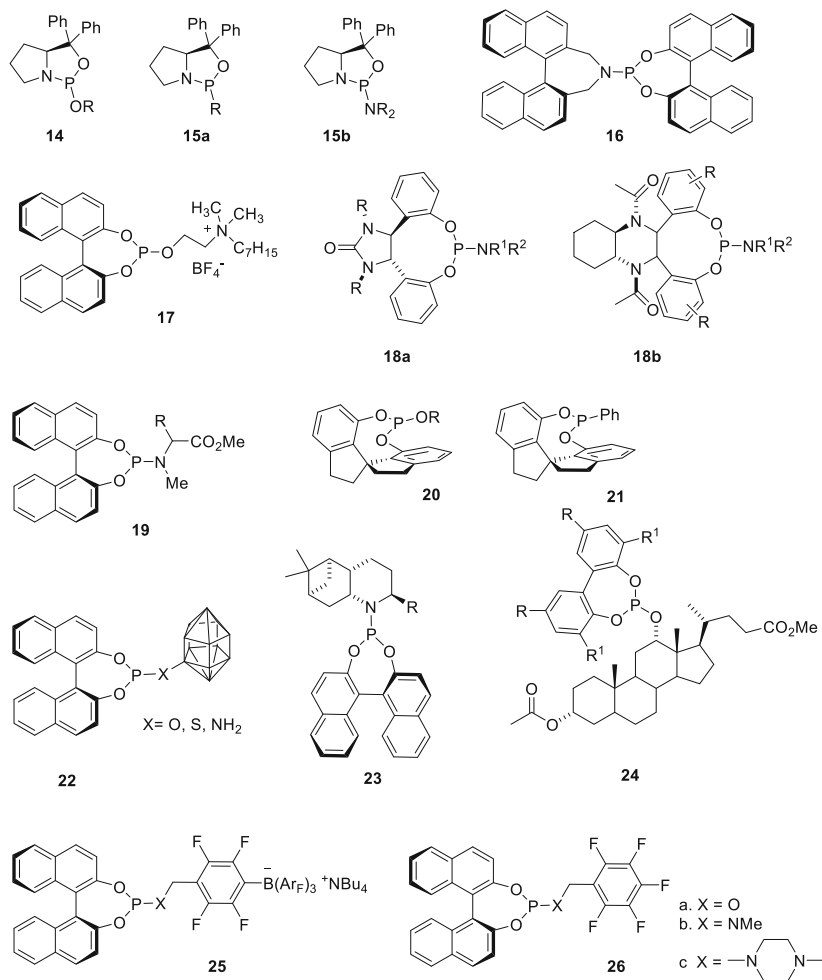
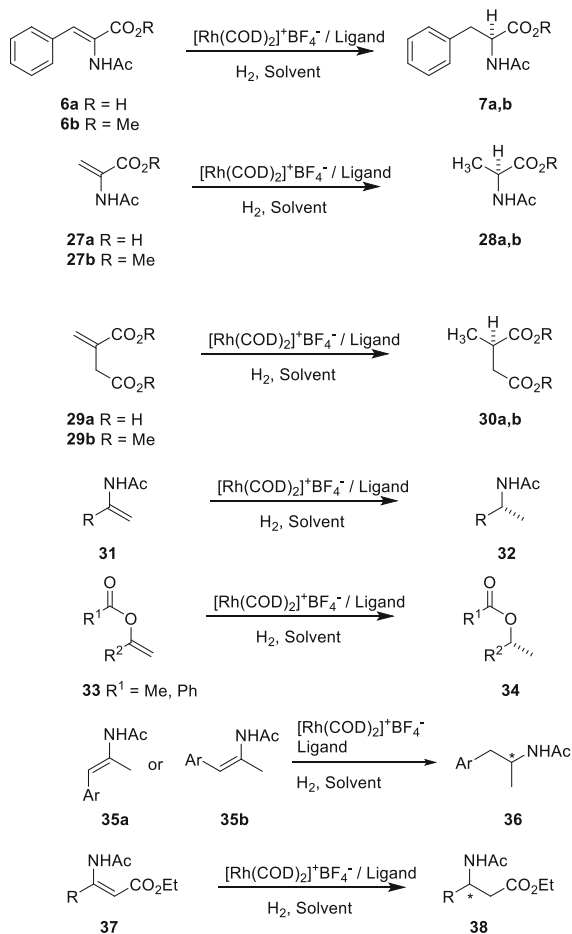


Fig. 4 Monodentate phosphonites, phosphites and phosphoramidites

99%. The *R,S*- and the *S,R*-ligands induced much higher enantioselectivity than the *R,R*- and the *S,S*-ligands.

Bondarev synthesised BINOL-based phosphite **17** containing a quaternary ammonium salt in the side chain (Fig. 4) [35]. This creates opportunities for attachment to solid supports or for using ionic liquids in two-phase hydrogenations. The resulting rhodium catalyst carries three positive charges that were compensated by three eq. of BF_4^- . The catalyst was used for the hydrogenation of **6b** and **29b** in CH_2Cl_2 . The products were obtained in excellent yields with ee's of 92 and 99%, respectively. Ding and co-workers created a new class of phosphoramidite ligands based on a chiral bisphenol, backbone [36, 37]. The backbone of these ligands, DpenPhos **18a** and CydamPhos **18b**, was prepared in three steps from the chiral

Scheme 3 Rhodium-catalysed hydrogenation reactions with monodentate ligands



diamine, and the resulting bisphenols were reacted with $\text{P}(\text{NMe}_2)_3$ or $\text{P}(\text{NEt}_2)_3$ to form the ligands. Both ligands were used for the rhodium-catalysed enantioselective hydrogenation of **6b** and **31** (Scheme 3).

Full conversion was obtained at S/C 100 with very high enantioselectivities, between 96 and 99.9%. DpenPhos was also used in the rhodium-catalysed hydrogenation of terminal enol carboxylates **33** [38]. Several aliphatic enol benzoates were reduced quantitatively with ee's between 87 and 90%, whereas aromatic ($\text{R}^2 = \text{aryl}$) enol acetates were reduced with ee's between 88 and 95%. Many groups have reported on BINOL-based phosphoramidite ligands in which the effect of the substituents on nitrogen was investigated. The area has been reviewed by Armspach, Matt and co-workers [39]. They have reported themselves on BINOL-based phosphoramidites **19** in which the nitrogen atom was part of an *N*-methyl-amino acid ester in which the amino acid was either alanine or phenylalanine [40]. These ligands were examined in the rhodium-catalysed enantioselective

hydrogenation of a **6b** and a number of analogues that carried halide substituents on the aromatic ring. The products were obtained in varying yield with ee's ranging from 67 to 92%. Zhou and co-workers continued their work on the spirobiindane diol-based monodentate ligands and introduced the phosphites **20** and the phosphonate **21** [41]. These ligands were applied in the asymmetric hydrogenation of *E*- and *Z*-aromatic enamides (**35a**, **b**). They were able to find ligands for the hydrogenation of both substrates with ee's up to 94–95%. Lyubimow and co-workers have tried to increase the size of the substituent in the BINOL-based phosphites and phosphoramidites by using *ortho*- and *meta-closo*-dodecacarboranes carrying a hydroxyl, a thiol or an amino-substituent in the 9-position (**22**) [42–45]. Substrates **6**, **27**, **29**, several substituted 2-acetamido-cinammic esters and β -dehydroamino acid esters **37** (Scheme 3) were subjected to rhodium-catalysed hydrogenation with these ligands. Most substrates could be hydrogenated with ee's between 80 and 98%; however, the β -dehydroamino acid esters were more stubborn substrates. They needed the use of hexafluoro-2-propanol as solvent which raised the ee to 69–85% for the aliphatic substrates, but the phenyl-substituted substrate was reduced with 46% ee only.

The idea to introduce extra chirality into the side chain of these ligands has fascinated many groups.

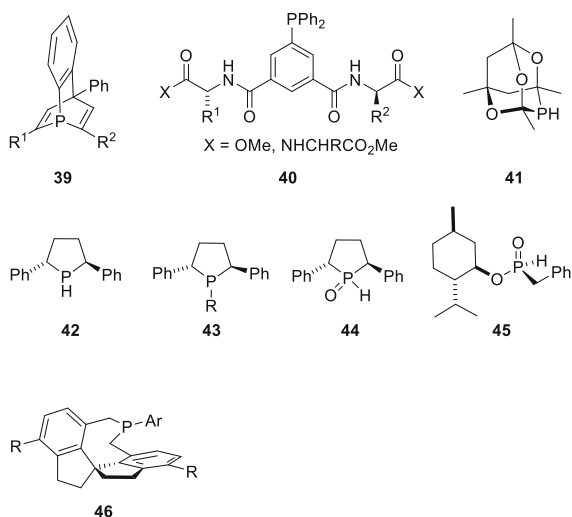
Franciò and co-workers converted enantiopure pinene into a decahydrobenzoquinoline, which was used as the amine in the synthesis of a BINOL-based phosphoramidite (**23** R = H, Me, Cy) [46]. A range of substituted alkenes was hydrogenated using these ligands with ee's varying from 49 to 99%. Iuliano and co-workers synthesised a *tropos* phosphite ligand **24** based on a 3,3'- or 5,5'-disubstituted biphenyl and methyl 3-acetyldeoxy-cholate [47]. Here the bisphenol is free to rotate, but either one of the two diastereomeric conformations is formed preferentially in the catalyst, or one of the diastereomers forms a much faster catalyst than the other. This principle was earlier developed by Reetz and co-workers [48], and by Gennari and Piarulli and co-workers [49]. In the rhodium-catalysed hydrogenation of **29b**, the product was obtained quantitatively with 52–94% ee.

Pfaltz and co-workers developed phosphoramidites **25** containing an anionic group in the side chain (Fig. 4). They compared the efficacy of these ligands with the analogous non-ionic ligands **26** in the rhodium-catalysed hydrogenation of **6b** [50]. There was no general trend: sometimes the anionic ligands gave better results and sometimes the neutral ligands. Interestingly, these ligands perform very well in a mixture with neutral ligands. Since the homocatalyst with two anionic ligands is energetically less favourable because of charge repulsion, the equilibrium is shifted strongly towards the heterocatalyst. This effect was further amplified when a phosphoric acid diester was used as the neutral ligand as here a hydrogen bond may form between the phosphoramidite and the proton of the phosphoric acid diester.

2.2 Phosphines and Secondary Phosphine Oxides

Breit and Fuchs reported the synthesis of chiral phosphabarrelenes **39** in which R¹ and R² are two different aryl groups [51]. The racemic ligands were separated by chiral chromatography. In the rhodium-catalysed hydrogenation of **6b** and **29b** using these ligands, the products were obtained with ee's between 14 and 31% ee. Kokan and Kirin synthesised a series of triphenylphosphines **40** in which one of the phenyl groups is decorated in the 3- and 5-positions with chiral amides, amino acid esters or dipeptide esters (Fig. 5) [52]. These ligands were used in the enantioselective rhodium-catalysed hydrogenation of **6b** (37–77% ee) and **27b** (12–80% ee) In addition, the latter substrate was hydrogenated using binary mixtures of these ligands (12–78% ee). Pringle and co-workers extensively investigated the use of the phosphadamantane motif originally developed by Epstein and Buckler in the design of several classes of ligands. They were able to obtain phosphine **41** in enantiopure form via a resolution [53]. The ligands were used in the asymmetric hydrogenation of **6b** (60% ee) and **27b** (54% ee). Enantiopure phospholanes obtained notoriety in their bidentate variety as DuPhos. Fiaud, Toffano and co-workers synthesised enantiopure monodentate phospholane **42** and used it in the asymmetric hydrogenation of **6a**, **6b**, **27a**, **29a**, **29b** and a number of other enamides and enol ethers [54]. The products were obtained quantitatively in most cases with ee's between 8 and 82%. Toffano and co-workers have synthesised the monodentate alkylated and arylated phospholanes **43** [55]. These ligands were tested in the rhodium-catalysed enantioselective hydrogenation of **6b**. The alkylated ligand performed disappointingly with ee's between 34 and 62%. However, the arylated phospholanes gave much better results, and enantioselectivities up to 93% (R = Ph) were obtained. The same group also synthesised the phospholane-based secondary phosphine oxide **44** [54]. This ligand was tested

Fig. 5 Monodentate phosphines and secondary phosphine oxides



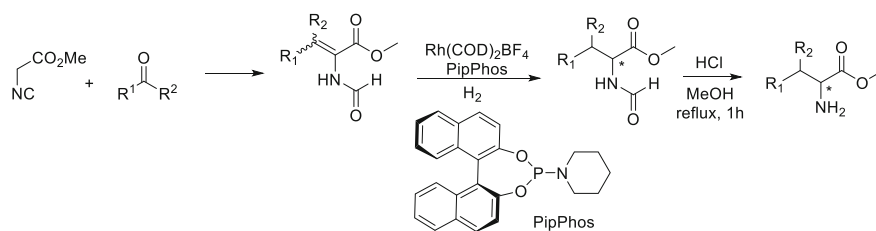
in the rhodium-catalysed asymmetric hydrogenation of **6b**. The enantioselectivity was highly solvent dependent. Whereas with most monodentate ligands, best results are obtained in non-protic solvents, such as CH_2Cl_2 ; in this case the result obtained in methanol (82% ee) was much better than that in CH_2Cl_2 (24%).

Han and co-workers synthesised a series of (*R*)-menthol-based H-phosphinates of which the benzyl derivative **45** performed best [56]. Asymmetric hydrogenation of **6b** and a number of ring-substituted analogues proceeded with excellent ee's between 93 and 99%. Hydrogenation of **29b** proceeded in 53% ee. Zhou and co-workers synthesised the SPINOL-based phosphines **46** (Ar = Ph, 4- $\text{CF}_3\text{C}_6\text{H}_4$, 4- MeOC_6H_4 , 3,5- Me_2 -4- MeOC_6H_4 , 3,5-*t*Bu-4- MeOC_6H_4). These ligands were applied successfully in the rhodium-catalysed hydrogenation of **35a**. Best results (ee = 81–97%) were obtained with the ligand in which Ar = 3,5-*t*Bu-4- MeOC_6H_4 .

3 New Hydrogenation Reactions

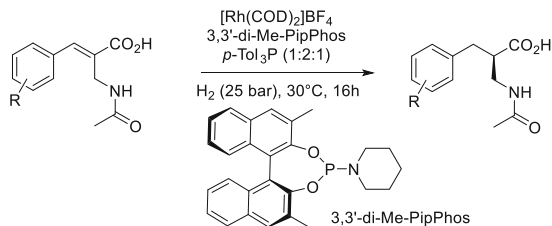
Most of the initial applications of the monodentate ligands concentrated on the hydrogenation of the *N*-acetyl dehydroamino acids and esters. In most applications the amino acid is needed without the protecting group on nitrogen. In practice it is not so easy to remove the *N*-acetyl group by hydrolysis. For this reason Feringa, de Vries, Minnaard and co-workers have investigated the use of other protecting groups for these hydrogenation substrates (Scheme 4). In practice the *N*-formyl group turns out to be a very good choice. The *N*-formyl-protected dehydroamino acid esters were readily prepared in one or two steps by condensation between methyl isocyanoacetate and an aldehyde or ketone using different protocols, depending on the substrates. In the rhodium-catalysed asymmetric hydrogenation, the use of PipPhos (**10**, $\text{R}^1, \text{R}^2 = -(\text{CH}_2)_5^-$) gave the best results, and the *N*-formyl amino acid esters were obtained with ee's around 99% for the substrates that were prepared from the aldehydes (Scheme 4). The ketone-derived substrates reacted more sluggishly, and here the ee's did not exceed 85%.

Asymmetric hydrogenation is of particular importance for the production of non-natural amino acids as these are often used in new drugs. Beta-amino acids have been used many times as they have the advantage not to be recognised by peptide hydrolysing enzymes, thus conferring metabolic stability to a peptide-like

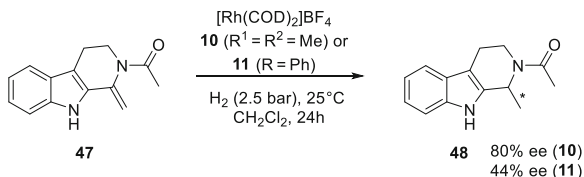


Scheme 4 Asymmetric hydrogenation of *N*-formyl-dehydroamino acid esters

Scheme 5 Asymmetric hydrogenation of 2-acetamidomethyl-cinnamic acids using mixtures of ligands



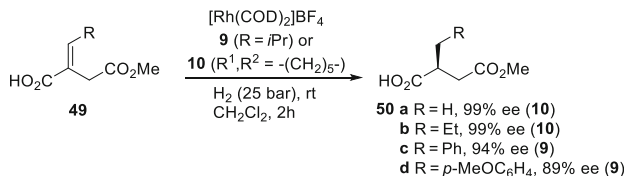
Scheme 6 Enantiopure 1,2,3,4-tetrahydro- β -carbolines via asymmetric hydrogenation



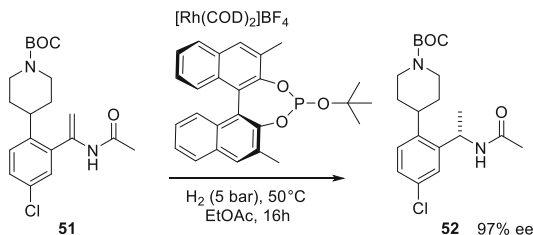
drug. Examples of β^3 -amino acids had already been reported earlier and this area has been reviewed [57]. More recently, Minnaard, Feringa and co-workers reported an asymmetric hydrogenation approach to access the β^2 -amino acids [58]. The substrates were prepared in a three-step sequence entailing a Baylis-Hillman reaction between methyl acrylate and a range of substituted benzaldehydes, followed by a Ritter reaction with acetonitrile and finally hydrolysis of the ester. In order to find a good catalyst, the high-throughput facilities at DSM were used. Not only was a library of monodentate phosphoramidites screened, but additionally also a library in which these monodentate phosphoramidites were combined with monodentate triaryl- or trialkylphosphine ligands. In the end 3,3'-dimethyl-PipPhos in combination with either tri-*para*-tolylphosphine or tri-1-naphthylphosphine gave the best results (ee's 90–91%) in the rhodium-catalysed hydrogenation of a number of methyl 3-acetamido-2-arylidene-propionates (Scheme 5).

Beller and co-workers reported a new approach towards enantiopure 1,2,3,4-tetrahydro- β -carbolines. A range of ligands was tested. Best results, up to 99% ee, were obtained using bidentate phospholane-type ligands. Nevertheless, using MonoPhos **10** ($R^1 = R^2 = \text{Me}$) or phosphepine **11** ($R = \text{Ph}$) on the same substrate gave the product with enantioselectivities of 80 and 44%, respectively (Scheme 6).

Many publications have appeared on the asymmetric hydrogenation of either itaconic acid (**29a**) or its diester (**29b**). Although these substrates serve as useful model compounds, the products are of little synthetic use, also in view of the fact that it is virtually impossible to discriminate between the two carboxylic acid functionalities. For this reason, the monoesters are more interesting substrates since either the acid or the ester functionality can be reduced selectively to the alcohol after hydrogenation of the double bond. De Vries, Rutjes and co-workers were able to synthesise a number of 4-substituted itaconic acid monoesters and screened a range of monodentate phosphoramidites and phosphites in their rhodium-catalysed hydrogenation [59]. Excellent results were obtained with the



Scheme 7 Asymmetric hydrogenation of substituted itaconic half-esters

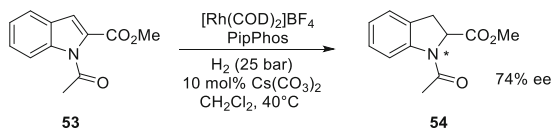


Scheme 8 Asymmetric hydrogenation of a bulky enamide

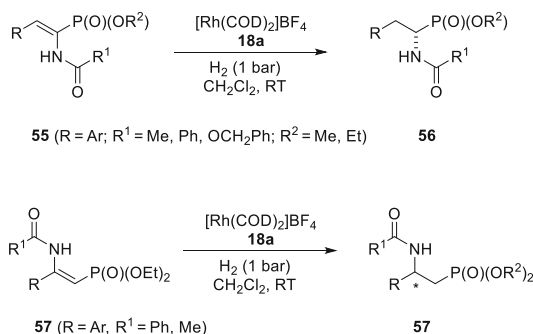
phosphoramidite PipPhos (**10**, $\text{R}^1, \text{R}^2 = -(\text{CH}_2)_5^-$) and monodentate phosphite ligand **9** ($\text{R} = i\text{Pr}$) (Scheme 7).

In the first 5 years after the discovery of the use of monodentate ligands for asymmetric hydrogenation, many groups have reported on the successful enantioselective hydrogenation of a range of enamides. These reactions have potential for the production of enantiopure pharma intermediates that often contain amines and amides. However, these “real-life” substrates often contain a range of other functional groups that may inhibit or slow down substantially the catalysis, either through interaction of the heteroatoms with the metal or through its steric bulk. The latter case was reported by Lefort and co-workers who were faced with the task to achieve both high enantioselectivity as well as high rate in the asymmetric hydrogenation of bulky enamide **51** (Scheme 8) [60]. They initially screened a library of 96 phosphoramidite ligands based on 3 different BINOL backbones and found that useful conversion and enantioselectivity was only obtained with phosphoramidites based on 3,3'-dimethyl-BINOL. For this reason a smaller library of 16 ligands was screened based on this scaffold and 14 amines and 2 alcohols. In the end the phosphite ligand based on *t*-BuOH gave the best results. It was possible to hydrogenate the substrate with a S/C ratio of 521. After 17 h the reaction was complete and the product was obtained in 97% ee. After treatment with activated charcoal and two recrystallisations, **52** was obtained with 99.6% chemical purity, 99.9% ee and a residual rhodium content of only 3 ppm.

Asymmetric hydrogenation of a range of heterocycles has been reported using monodentate phosphoramidites or phosphites usually with ruthenium- or iridium-based catalysts. One class of heterocycles that has been reduced successfully using rhodium catalysts based on monodentate ligands are the 2-substituted indoles. Minnaard, Feringa, de Vries and co-workers reported the rhodium-catalysed



Scheme 9 Asymmetric hydrogenation of methyl *N*-acetyl 2-indolecarboxylate



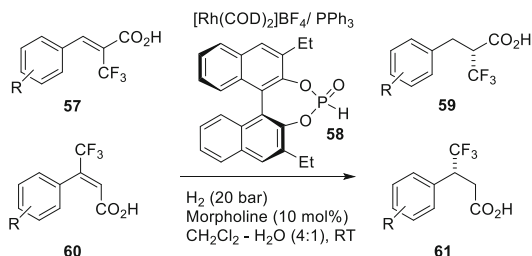
Scheme 10 Rhodium-catalysed asymmetric hydrogenation of α - and β -enamido phosphonates

asymmetric hydrogenation of methyl *N*-acetyl indole-2-carboxylate (Scheme 9) [61]. The best ligand was PipPhos, but it was necessary to use 10 mol% of Cs(CO₃)₂ as additive. They were able to show that high enantioselectivity was obtained only with the doubly protected derivative; the unprotected indole-2-carboxylic acid, its ester and its *N*-acetyl compound were all hydrogenated with poor enantioselectivity.

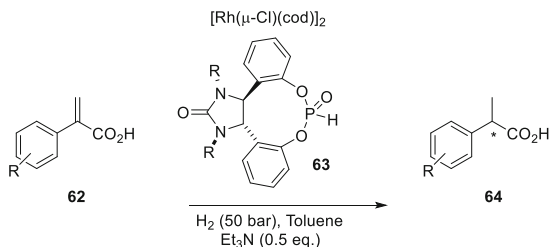
Minnaard and co-workers investigated the rhodium-catalysed asymmetric hydrogenation of thio-ethers that were obtained by the addition of thiols to dimethyl acetylenedicarboxylate [62]. The resulting sulfur-substituted fumarate and maleate esters were subjected to rhodium-catalysed hydrogenation using a range of different ligands. Good yields of the hydrogenated products could be obtained with moderate enantioselectivity using bidentate phosphine ligands. In contrast, the use of monodentate phosphoramidite ligands gave very slow reactions and mainly desulfurisation.

Ding and co-workers subjected α - and β -enamido phosphonates to rhodium-catalysed asymmetric hydrogenation using phosphoramidite ligands (Scheme 10) [63]. Interestingly, only phosphoramidite ligands containing a proton on the nitrogen atom such as **18a** (R¹ = H, R² = PhCH₂ or *i*Pr) were active in this reaction. The (*E*)- α -enamido phosphonates could all be hydrogenated with very good rates and in exceptionally high ee (97–99%) at 1 bar H₂. One *Z*-alkene (R = Ph, R¹ = R² = Me) was also hydrogenated and in this case the ee was lower (88%). Hydrogenation of the (*Z*)- β -enamido phosphonates proceeded much more sluggishly, with TOF's in the single digits; nevertheless, the ee was again very high (95–99%). In this series the (*E*)-substrates were hydrogenated with lower enantioselectivity.

Scheme 11 Asymmetric hydrogenation of trifluoromethyl-substituted cinnamic acids



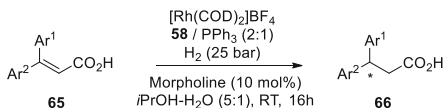
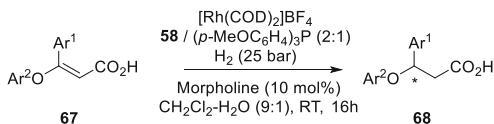
Scheme 12 Asymmetric hydrogenation of α -arylated acrylic acids



Ding and co-workers extensively investigated the asymmetric hydrogenation of substituted acrylic acids. They screened a range of mixed ligand catalysts based on secondary phosphine oxide (SPO)-type monodentate ligands and triphenylphosphine in the rhodium-catalysed asymmetric hydrogenation of (*Z*)- α -trifluoromethyl-cinnamic acid (Scheme 11) [64]. The SPO based on 3,3'-diethyl-BINOL together with triphenylphosphine (2:1) turned out to be the best combination, and with 1 mol% of catalyst full conversion was achieved after 16 h, and the product was obtained with 98% ee. A range of similar substrates with substituted aromatic or heteroaromatic rings were also hydrogenated with excellent enantioselectivities (96–99% ee). Even trifluoro-methacrylic acid was hydrogenated with 96% ee. Next, the asymmetric hydrogenation of (*E*)- β -trifluoromethyl-cinnamic acid was examined, and here the same catalyst combination gave excellent results. A range of aryl-substituted and heterocyclic derivatives were also hydrogenated with full conversions and ee's between 92 and 99%.

The same group also reported the rhodium-catalysed asymmetric hydrogenation of α -arylated acrylic acids [65]. This is of particular relevance as it potentially offers an entry towards enantiopure ibuprofen, naproxen, flurbiprofen as well as ketoprofen. A number of SPOs was screened in combination with different catalyst precursors. Surprisingly, the use of the chlorine containing precursor $[\text{Rh}(\mu\text{-Cl})(\text{cod})]_2$ induced the highest enantioselectivities. Normally speaking chloride is considered a catalyst poison, and halide-containing catalyst precursors are avoided. The best ligands were **63** in which R was either benzyl or ethyl. The products were obtained in over 99% yield with ee's ranging from 90 to 96% (Scheme 12).

A much more challenging class of substrates which was tackled by the same group are the β,β -diaryl-substituted acrylic acids, in which the two aryl groups are only slightly different as a result of the presence of substituents. Here the authors

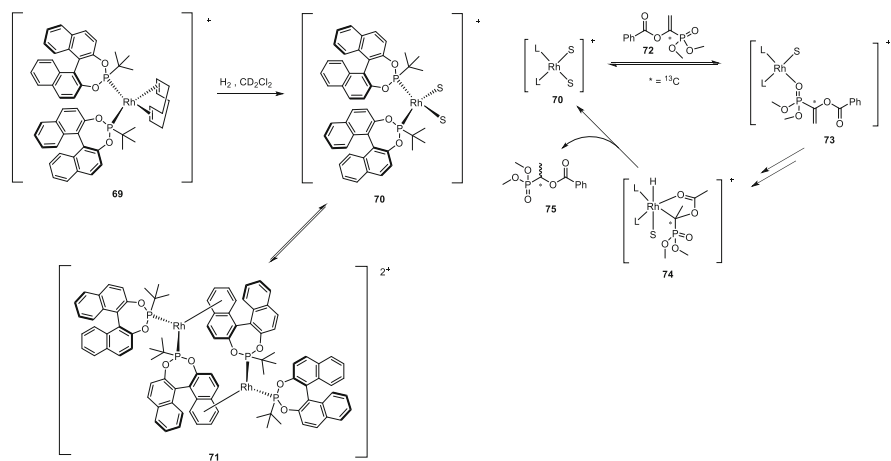
Scheme 13 Asymmetric hydrogenation of β,β -diaryl-substituted acrylic acids**Scheme 14** Asymmetric hydrogenation of β -aryloxy-cinnamic acid derivatives

screened the combination of a small library of SPO ligands in combination with triarylphosphines. Surprisingly high enantioselectivities were achieved using a combination of **58** (see Scheme 11) and PPh_3 (2:1), and a range of substrates was hydrogenated with *ee*'s ranging from 85 to 96% (Scheme 13).

The asymmetric hydrogenation of β -aryloxy-cinnamic acid derivatives is not unproblematic as the hydrogenation is accompanied by hydrogenolysis to the 3-phenylpropionic acids. The group of Ding found that whereas rhodium in combination with SPOs led to poor conversions and enantioselectivities, a mixed ligand approach in which a combination of an SPO and a triarylphosphine was used worked much better and hydrogenolysis was reduced to about 10% [66]. A small library of six SPOs and seven triarylphosphines was screened leading to the finding that a combination of SPO **58** with tri-(*p*-methoxyphenyl)phosphine (2:1) gave the 3-aryl-3-aryloxypropionic acids in 92–99% enantioselectivity (Scheme 14). These compounds can be converted into a number of interesting products, such as the psychopharmaceuticals duloxetine and atomoxetine.

4 Reaction Mechanism

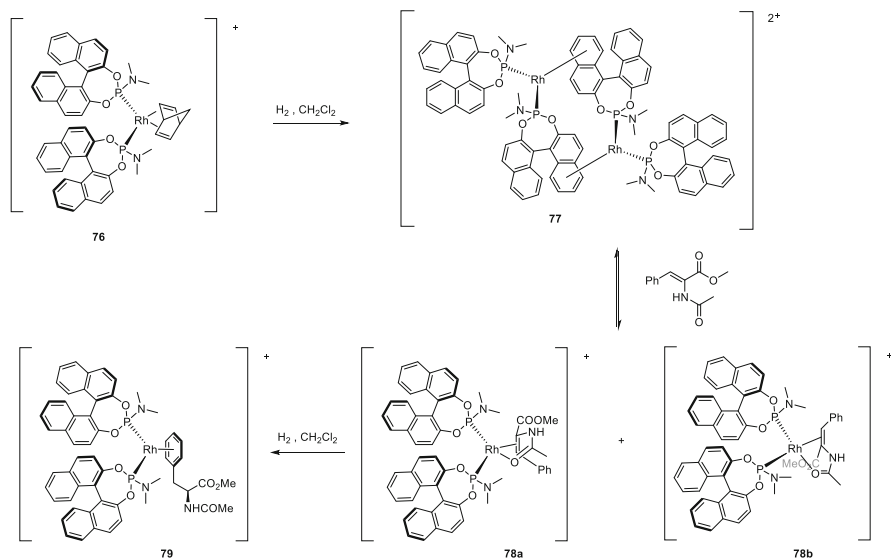
There are some marked differences in the mechanism of the rhodium-catalysed asymmetric hydrogenation of olefins employing monodentate ligands, when compared to the bidentate case. If the reaction were to proceed in a similar fashion, two equivalents of ligand should be coordinated in a *cis* fashion, resembling the coordination geometry of a rhodium-diphosphine complex, which may be the case if the substrate binds in a chelating fashion. In 2005, Reetz et al. showed, for monophosphonites specifically, that in the optimal case, two equivalents of ligand are available to coordinate to rhodium, and a positive non-linear effect ((+)-NLE) was observed in the benchmark hydrogenation of **29b**. The non-linear effect, which corroborates the presence of two monodentate ligands in the active hydrogenation catalyst, was already observed earlier by de Vries and co-workers in the asymmetric hydrogenation with rhodium/MonoPhos (**10**, $\text{R}^1, \text{R}^2 = \text{Me}$) [67]. In contrast to chiral diphosphines, DFT calculations showed that the reaction with monodentate phosphite ligands obeys the lock-and-key principle, i.e. that the thermodynamically



Scheme 15 Mechanism of rhodium-catalysed hydrogenation with a rhodium-bisphosphonite catalyst precursor

more stable catalyst-substrate complex leads to the formation of the enantiomer that is formed in large excess [68]. They proceeded to investigate NLEs of mixtures of chiral monodentate ligands **8** (R = Me) and **8** (R = *t*Bu). At least three complexes should be expected when considering two different ligands, namely, the two homo-combinations, as well as the hetero-combination. They showed that the ee of the hydrogenation of **29b** was enhanced to 96% for the mixture, from 90 and 57% for the exclusively homo-complexes. Additionally, using a racemate of one of the ligands still gave around 90% ee when keeping the other ligand enantiopure, whereas purposefully mismatching the ligand enantiomers showed a drop in enantioselectivity as well as rate. These findings indicated the second monodentate ligand does not necessarily have to be chiral for high enantioselectivity, which was later used to good effect in combinatorial studies [69].

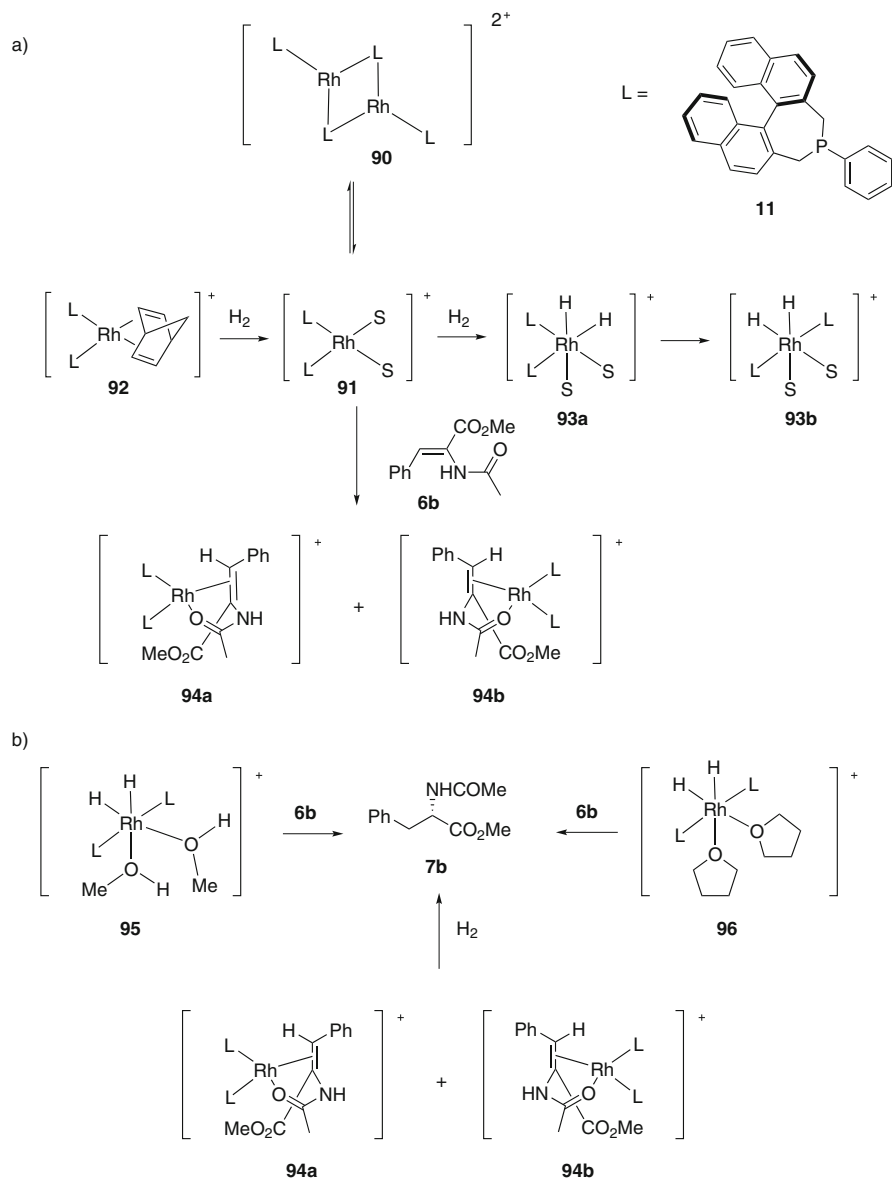
Gridnev et al. hydrogenated a solution of $[\text{Rh}(\text{L})_2(\text{cod})]^+$ in CD_2Cl_2 , where L = **8** (R = *t*Bu) (Fig. 2) and observed two species in equilibrium by ^{31}P -NMR spectroscopy (Scheme 15) [70]. Based on $J_{\text{P-Rh}}$ values and the nonequivalence of both phosphorus atoms for one of the species, these signals were assigned to the solvento complex $[\text{Rh}(\text{L})_2(\text{S})_2]^+$ (**70**) and the η -arene dimeric complex **71**. Addition of methyl 2-acetamido-cinnamate **6b** led to formation of a new doublet in the ^{31}P NMR; however, the expected chelating substrate complex could not be identified. At temperatures below 243 K, they observed a small concentration of the coordination complex of rhodium with labelled substrate **72**, containing a ^{13}C -label at the α -olefin position, as well as a phosphonate instead of the methyl ester moiety. Interestingly, no olefin coordination was observed from either the olefin protons or the α - ^{13}C , in contrast to the analogous Rh-BINAP complex. Applying a hydrogen atmosphere gave rise to the formation of monohydride **74**, with the α -carbon bound to rhodium. Based on comparison with analogous monohydride rhodium-bidentate complexes, this was concluded to be an intermediate in the catalytic cycle,



Scheme 16 Mechanism of asymmetric hydrogenation of methyl 2-acetamido-cinnamate with rhodium/MonoPhos

establishing that two monophosphonites are coordinated to rhodium during at least part of the reaction [70]. At first glance, this contrasts with the finding that the asymmetric hydrogenation of methyl (*Z*)-2-acetamido-cinnamate **27b** proceeded faster, but without a decrease in enantioselectivity, when the rhodium to ligand ratio was reduced to 1:1. However, this can be explained in terms of an equilibrium between different $[\text{RhL}_n]^+$ species, where catalytically inactive $[\text{RhL}_3]^+$ and $[\text{RhL}_4]^+$ species are less likely to form at lower ligand to metal ratios [67].

Alberico et al. set out to identify catalytic intermediates that form upon hydrogenating the norbornadiene ligand in $[\text{Rh}(\mathbf{10})_2(\text{nb})]^+$ (**76**), and elucidate why the high enantioselectivity of rhodium-monodentate systems seems to depend on the use of non-protic solvents, considering that the bidentate phosphine catalysts typically form solvento complexes with protic solvents (Scheme 16) [71]. Replacing the more usual precursor cod (1,5-cyclooctadiene) with nbd (norbornadiene), they obtained a complex containing two MonoPhos ligands (**10**, $\text{R}^1, \text{R}^2 = \text{Me}$) as well as the nbd. In contrast to the cod complexes, these complexes have well-resolved ³¹P NMR and ¹H NMR spectra. Catalytically inactive $[\text{Rh}(\mathbf{10})_4]^+$ was observed as well, which, by increasing the ligand stoichiometry, was isolated for full characterisation and control experiments. Under hydrogenation conditions in the absence of substrate, **76** turned into the dimeric $[\text{Rh}_2(\mathbf{10})_4]^{2+}$ species **77**, without any indication of solvento complex formation. Addition of methyl (*Z*)-2-acetamido-cinnamate (**27b**) to a solution of the dimer gave rise to a mixture of the dimer **77** and a single chelating substrate complex as observed in ³¹P NMR. After lowering the temperature, a few hours later, all **77** had disappeared, and now a minor substrate complex



Scheme 17 Mechanistic studies of the rhodium-catalysed asymmetric hydrogenation using monodentate phosphine ligand **11**; (a) Formation of hydride as well as substrate complexes are feasible; (b) Both hydride complex and substrate complex can lead to product formation

was observed as well. After application of hydrogen, these two complexes disappeared, and a new complex **79** showed up which was identified as the rhodium complex in which the product **7b** was bound via its aromatic ring to the rhodium.

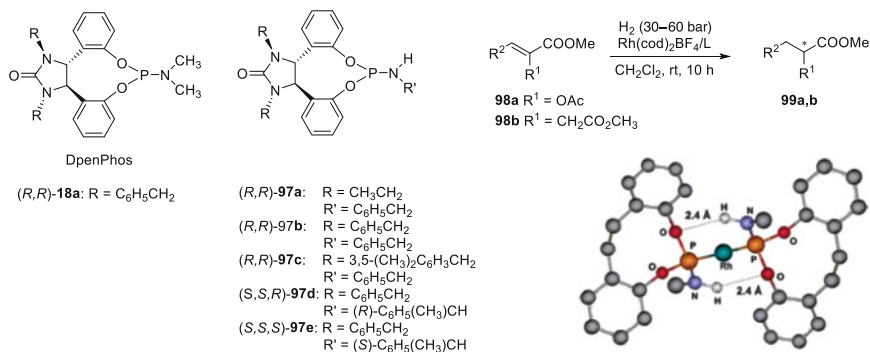
Addition of 5 eq. of **27b** to **79** fully converted this complex back to the mixture of substrate complexes **78**. Their findings suggest an anti-lock-and-key mechanism, in contrast to what Reetz et al. concluded for the phosphite case.

In a similar study from Alberico and Gridnev, the behaviour of the rhodium complex based on the chiral phosphine **11** ($R = \text{Ph}$) was studied (Scheme 17). Here also a mixture of the dimer (**90**) and the solvato complex $[\text{RhL}_2\text{S}_2]^+$ (**91**) was observed upon hydrogenation of the catalyst precursor (Scheme 17a). Upon addition of substrate, they could clearly observe the formation of the two diastereomeric chelating substrate adducts (**94a, b**). Reaction of this mixture with hydrogen at -90°C gave rise to formation of the product **7b** with 99% ee. If however the catalyst precursor was hydrogenated in a mixture of CD_2Cl_2 and a polar solvent such as CD_3OH or THF-d_8 , the dihydride complexes $[\text{RhL}_2\text{S}_2\text{H}_2]^+$ (**95, 96**) were observed (Scheme 17b). Oxidative addition of hydrogen to $[\text{RhL}_2\text{S}_2]^+$ must initially lead to the *cis*(H)-*cis*(P) structure **93a**, but as indicated by $J_{\text{P-P}}$ and ^1H chemical shift values for the hydrides, only *cis*(H)-*trans*(P) $[\text{RhH}_2\text{L}_2\text{S}_2]^+$ **93b** was observed. Stoichiometric, low-temperature addition of the substrate again led to formation of the product in $>99\%$ ee. Upon raising the temperature, the substrate reappeared coordinated to rhodium, suggesting the reaction steps remain reversible until a late stage [72].

The observation of *trans*-diphosphines is somewhat surprising, as Schiaffino and Ercolani argued that these could be left out of the equation. Their DFT studies indicated that, while thermodynamically more stable, the formation of *trans*-(PMe_3)₂ species is essentially blocked with respect to all possible *cis* isomers [73].

5 Supramolecular Catalysis Using Monodentate Ligands

Ding and co-workers first recognised the effect of hydrogen bonding in catalysts bearing two monodentate phosphoramidite ligands in which the amine contains only a single substituent (Scheme 18) [74]. These ligands were used in the rhodium-catalysed enantioselective hydrogenation of several (*Z*)-methyl α -(acetoxy)acrylates (**98a**) and (*E*)- β -aryl itaconate (**98b**) derivatives with ee's between 96 and $>99\%$, whereas catalysts using phosphoramidite ligands based on the corresponding secondary amine did not show any reaction with **98a**. Moreover, the asymmetric hydrogenation of substrate **98b** proceeded 1,000 times faster with **97b** as compared to DpenPhos **18a**. They showed in $^1\text{H-NMR}$ studies that a downfield shift of almost 2 ppm was observed for the NH protons of **97b** upon complexation to rhodium in CD_2Cl_2 . The addition of CD_3OD left the complex unchanged, whereas the NH signal of the free ligand shifted 0.31 ppm downfield. These findings showed hydrogen-bonding interactions between the ligands, indicating that self-assembly of a chelate complex is the basis for the improved catalytic activity in this type of ligands. A calculated structure of the rhodium complex showing the hydrogen bonds is shown in Scheme 18.



Scheme 18 Primary amine-based phosphoramidites form chelates through hydrogen bond formation. The calculated structure is reproduced from Liu et al. [74] with permission from the American Chemical Society

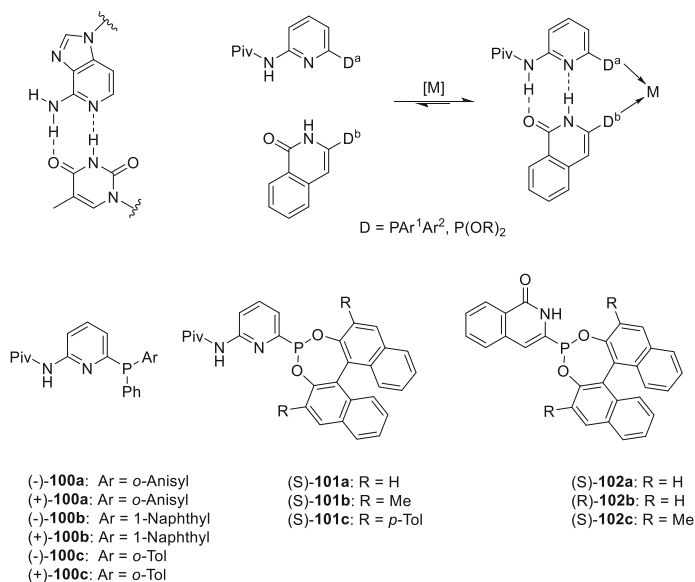
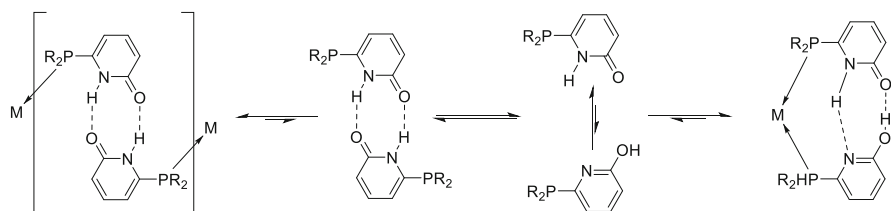
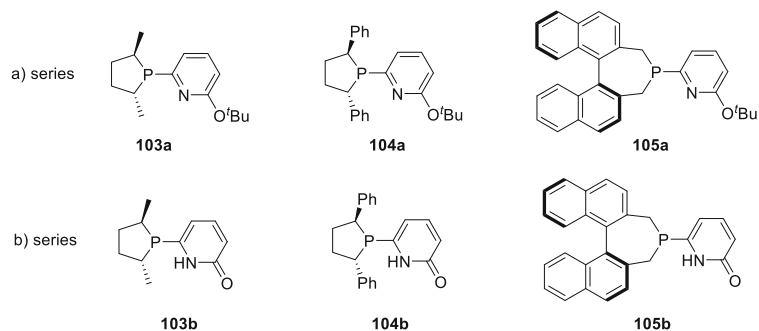


Fig. 6 Supramolecular library of ligands

Inspired by Watson-Crick base pairing, Breit and co-workers described a combinatorial approach towards the Rh-catalysed asymmetric hydrogenation. A library of chiral amidopyridines and isoquinolin-1(2*H*)-one's equipped with phosphine and phosphinite donor moieties was synthesised (Fig. 6). Supramolecular heterobidentate complexes readily formed upon mixing with [Rh(cod)₂]BF₄ (Scheme 19). The optimal combination resulted in full conversion and an ee of 99% when applied in the hydrogenation of methyl 2-acetamido-acrylate **27b** under mild conditions. With different combinations, quantitative conversions and ee's >90% were also obtained

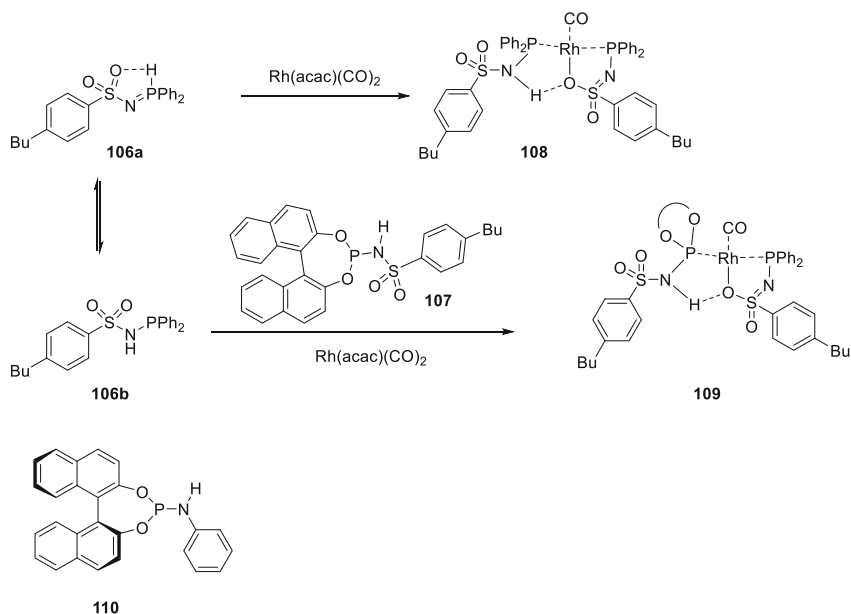


Scheme 19 Supramolecular phospholane and phosphepine ligands

in the rhodium-catalysed hydrogenation of methyl 2-acetamido-cinnamate (**6b**) and dimethyl itaconate (**29b**) (Scheme 3) [75].

Breit, Börner and co-workers prepared three sets of chiral phospholanes and phosphepines linked to a pyridone, and investigated the complexation behaviour of these ligands with several metals and co-ligands, shown schematically in Scheme 19 [76]. Self-assembly towards a chelate complex was possible with two equivalents of the pyridone ligands, where tautomerisation of the pyridone system to hydroxypyridine is key. In the hydrogenation of the benchmark substrates **6b**, **27b** and **29b** (Scheme 3), low enantioselectivities were obtained with the ligands from the a series, which cannot engage in such a supramolecular interaction, whereas hydrogenation using the ligands of series b gave much higher enantioselectivities with the phosphepine ligand clearly as the best one. However, hydrogenation with the ligands of series b was much slower than with the ligands of series a. The authors explained this by assuming the formation of polymeric ensembles.

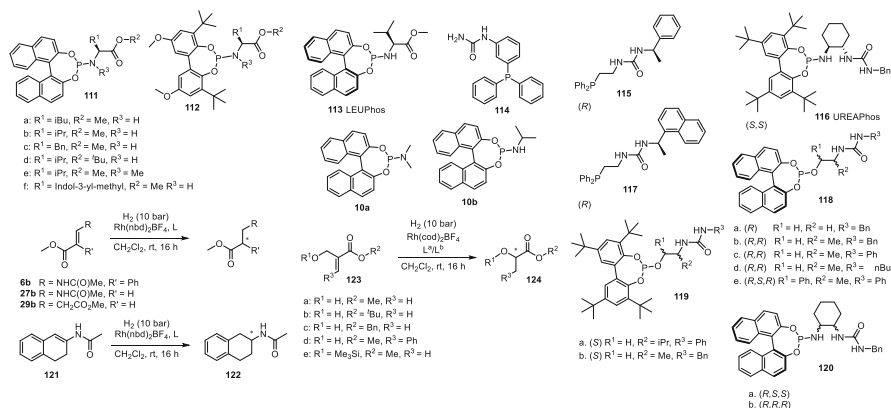
The group of Reek has reported extensively on the development of supramolecular chiral ligands. The so-called METAMORPhos ligands are based on arylsulfonamido-phosphines, such as **106** and phosphoramidites such as **107** (Scheme 20) [77]. When reacted with a rhodium precursor, a homo-bisligated complex, i.e. **108** was obtained through hydrogen bonding of one ligand with its tautomerised form. However, when a 1:1 mixture of **106** and **107** was used, the hetero-complex **109** was formed exclusively. This is a clear advantage of these supramolecular ligands over the classical monodentate ligands were always a mixture of homo- and hetero-complexes is formed. The neutral complexes were inactive in hydrogenation reactions, but could be activated by treatment with



Scheme 20 METAMORPhos ligands

$\text{HBF}_4 \cdot \text{OMe}_2$. Catalytic hydrogenations of **27b** were carried out starting from $[\text{Rh}(\text{nbd})_2]\text{BF}_4$, however. The homo-complex based on **106**, being non-chiral, showed no ee, and the homo-complex based on **107** induced 99% ee, whereas the hetero-complex based on **106** and **107** induced 91.7% ee, but was reported to be twice as active as the homo-complex based on **107**. Interestingly, the use of the mixture of **106** and **110** led to formation of a mixture of the two homo-complexes.

Reek and co-workers developed another generation of supramolecular ligands by synthesising phosphoramidite ligands based on amino acids **111**, where hydrogen-bonding behaviour can also be expected [78]. Rhodium catalysts based on these ligands enabled full conversions and ee's up to 89% in the hydrogenation of dimethyl itaconate **29b**. It was found that the larger steric bulk of the chiral centre R^1 had a positive effect on the ee. Interestingly, the *N*-methylated valine-based ligand **111d**, which should not give rise to hydrogen bonding, outperformed the others in the hydrogenations of methyl 2-acetamido-acrylate (**27b**) (97% ee) and 2-acetamido-cinnamate (**6b**) (84%), whereas it was a poor ligand in the case of dimethyl itaconate (**29b**) (43% conversion, 3% ee.) None of the ligands enabled more than 50% conversion in the conversion of **121**. In a similar vein, the same authors reported the amino acid-based LEUPhos **113**, which was used in combination with achiral phosphines, most notably ureaphosphine **114** [79]. Hydrogen bonding between these two ligands led to the exclusive formation of the hetero supramolecular complex upon mixing with $[\text{Rh}(\text{cod})_2]\text{BF}_4$. This complex catalysed the hydrogenation of **123** with ee's of 92–99%, outperforming the control experiments with co-ligands without the urea moiety. Furthermore, they highlighted the



Scheme 21 Urea-based supramolecular ligands

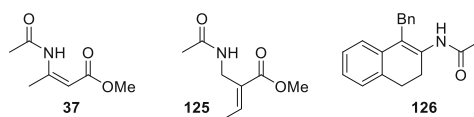


Fig. 7 Substrates tested with a UREAphos ligand library

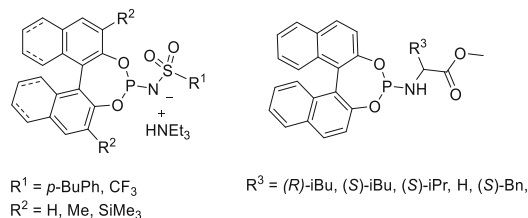
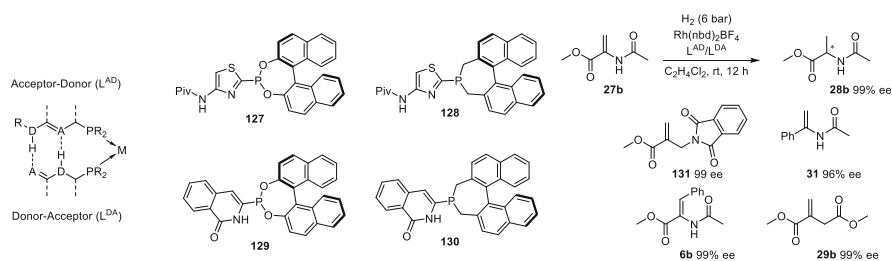


Fig. 8 Combination of anionic METAMORPhos ligands with amino acid-based phosphoramidites

importance of hydrogen bonding between the substrate and the ligand by DFT calculations, as further evidenced by the trimethylsilyl-protected substrate (**123e**) only giving 52% ee. When the phosphine and urea moieties are separated by a short linker, urea-based ligands such as UREAphos (**116**) may also be used to self-assemble into homo-bisligated complexes, as shown by Meeuwissen et al. [80] They synthesised a library of 12 phosphoramidites and phosphines (Scheme 21, **115–120**) decorated with a urea group and investigated them in a high-throughput setup for the hydrogenation of substrates **37**, **121**, **123a**, and **125–126** (Fig. 7). An optimisation screen was performed for substrates **125** (84% conversion, 96% ee) and **126** (84% conversion, 83% ee) using ligand **118b**.

More recently, both paths converged when anionic METAMORPhos ligands were combined with neutral amino acid-based phosphoramidites (Fig. 8),



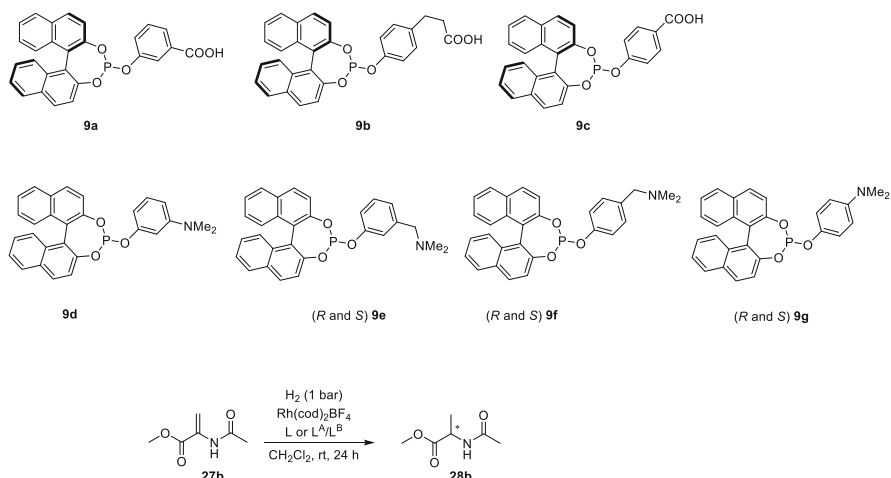
Scheme 22 Library of donor-acceptor ligands for supramolecular catalysis

increasing the combinatorial scope further [81]. Homo-combinations of anionic METAMORPhos ligands naturally led to negatively charged complexes $[Rh(L)_2(nbd)]HNEt_3$, which dimerised to $[Rh_2(L)_4](HNEt_3)_2$ under hydrogen atmosphere, except for those cases where steric bulk was introduced on the 3,3' positions of the BINOL. Hetero-combinations with amino acid-based phosphoramidites led to a range of different complexes. Importantly, the dimeric complexes were also active hydrogenation catalysts. A combinatorial screening for a series of substrates led to the conclusion that the hetero-complexes were most active and selective, and ee's around 90% could typically be obtained.

An elegant alternative to high-throughput screening was reported by Wieland and Breit [82]. They performed a diversity-oriented synthesis to generate a library of 12 acceptor-donor and 10 donor-acceptor monodentate ligands (Scheme 22). Enantioselective olefin hydrogenation catalysts were identified by dividing their library into subgroups and identifying the best-performing subgroup in the rhodium-catalysed hydrogenation of **27b** and then iterating this process by dividing the subgroup into further subgroups and repeating the process. The combinations L^{AD}/L^{DA} shown below all induced full conversions and 98–99% ee and were identified after 17 experiments instead of performing the reaction for all 120 combinations. The approach was expanded to give optimal ligand combinations for four more substrates (Scheme 22).

The combination of BINOL-based phosphites equipped with acidic and basic moieties, as described by Gennari and co-workers, only had a modest effect on the enantioselectivity in the rhodium-catalysed hydrogenation of **27b** (Scheme 23) [83]. Homo-combinations induced ee's of 80–87% at full conversion, whereas the hetero-combinations resulted in ee's up to 90%. Use of ligands **9e** and **9f**, containing a benzylic amine, led to reduced conversions of 30% and 89%, respectively. Their strongly basic group possibly acts as a catalyst poison. This effect was partially cancelled out upon mixing with a carboxylic acid-containing ligand. Notably, only 30% ee was obtained in the rhodium-catalysed hydrogenation of **27b** when intentionally mismatching (*R*)-**9a** with (*S*)-**9e**.

The same group designed a library of BINOL-based phosphites connected to a phthalic acid bisamide (Phthalaphos) using several different amino alcohol spacers (Fig. 9) [84, 85]. From this library, highly enantioselective ligands were identified



Scheme 23 Library of acidic and basic ligands

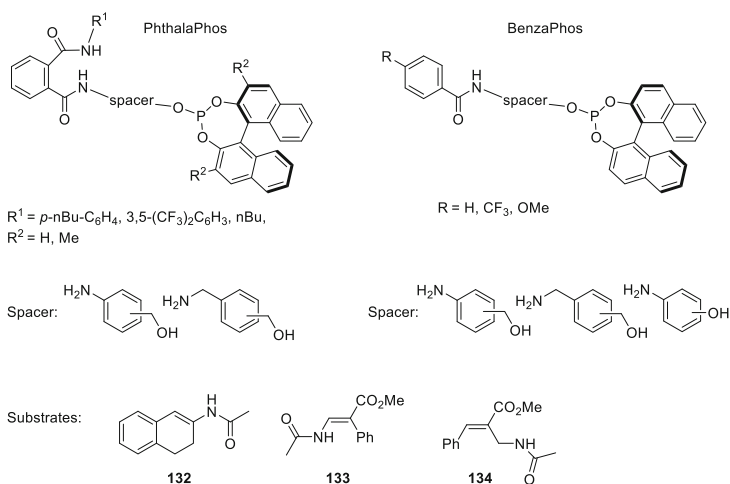
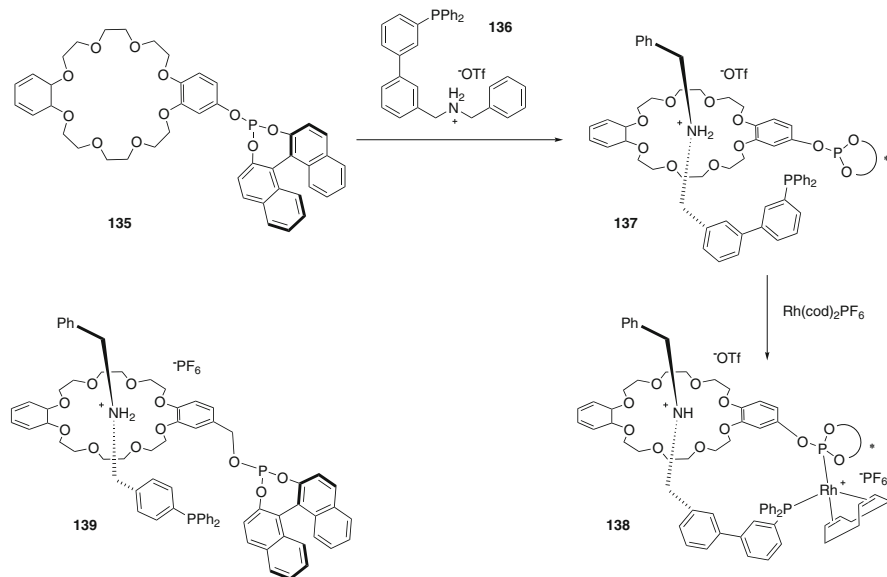


Fig. 9 PhthalaPhos and BenzaPhos ligand libraries

for substrates **6b**, **27b**, **31** ($R = \text{Ph}$), **121** and **134**; however, for substrates **37**, **123a**, **132** and **133**, only moderate to poor results were obtained. Computational studies and control experiments confirmed the importance of hydrogen bridges between two equivalents of ligand in the homo-bisligated complex, as well as suggesting the formation of ligand-substrate hydrogen bridges in catalytic intermediates. They further simplified these ligands by replacing the phthalic bisamide with benzamides, leading to another library that was dubbed BenzaPhos (Fig. 9) [86]. The first-generation BenzaPhos ligands, i.e. those with unsubstituted benzamides, already led to ee values from 76 to >99% for substrates **6b**, **27b**, **31** ($R = \text{Ph}$), **121** and **123**, thus identifying the optimal spacer. The three most suitable



Scheme 24 Rotaxane-based supramolecular ligands

ligands were modified by including a *p*-CF₃- or *p*-MeO-substituent on the benzamide, further improving the enantioselectivity in these hydrogenations. The influence of hydrogen bridging was again supported by computational studies and control experiments.

Nishibayashi and co-workers [87], as well as Fan and co-workers [88], investigated supramolecular chiral ligands based on the rotaxane principle, i.e. an interaction between a phosphine-linked dibenzyl ammonium salt (the 'axle' moiety) and a phosphite-linked crown ethers (dibenzo[24]crown-8; the 'wheel' moiety) (Scheme 24). These were then employed with $[\text{Rh}(\text{cod})_2]\text{PF}_6$ or $[\text{Rh}(\text{cod})_2]\text{BF}_4$ for the room temperature, 1 bar hydrogenation of **6b**, **27b**, several *para*-substituted methyl 2-acetamido-cinnamates as well as two naphthyl analogues of **6b**. In the Nishibayashi work, some variations of the position of the phosphine on the axle unit were included, showing that the phosphine-phosphite distance in the resulting supramolecular ligand was crucial for obtaining quantitative conversions and *ee*'s >90%. Replacing the phosphite group on the wheel moiety with a chiral oxazoline dropped the *ee* to only 15%. In Fan's work, full conversions were also obtained with a range of substituted methyl 2-acetamido-cinnamates, albeit with more modest *ee* values, varying from 69 to 84%.

Based on the ability of benzene-1,3,5-tricarboxamides (BTA) to form helical rods through π - π stacking as well as hydrogen bridging, Raynal et al. designed several phosphine-functionalised BTAs with zero (**142**), one (**141**, **143**) or two remote chiral centres (**140**) in the side chains (Fig. 10) [89]. These were shown to self-assemble into chiral helices and in combination with $[\text{Rh}(\text{cod})_2]\text{BAR}_f$ catalysed

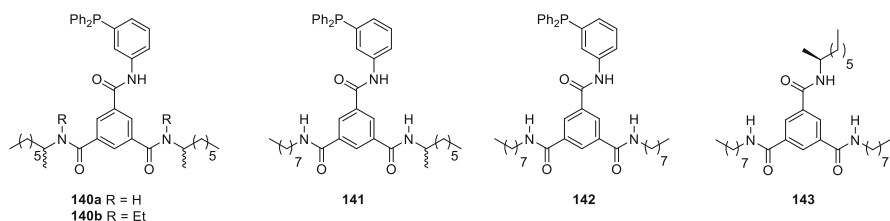


Fig. 10 Precursors for helical supramolecular ligands

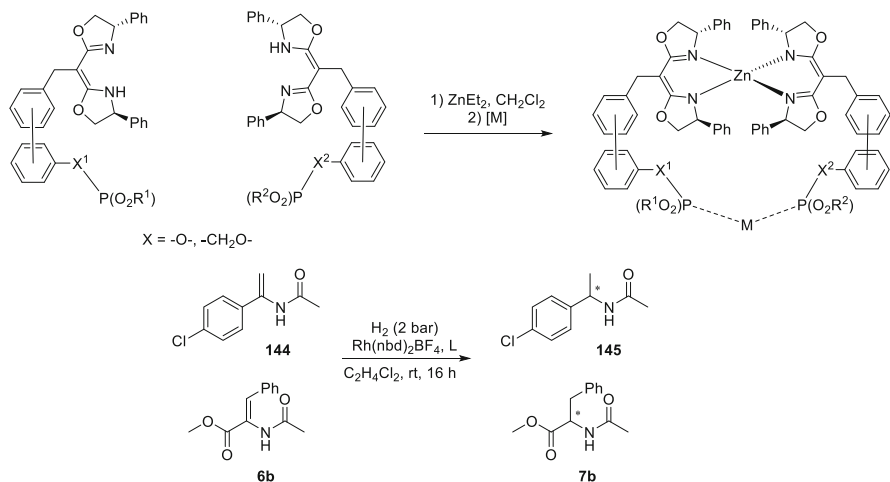
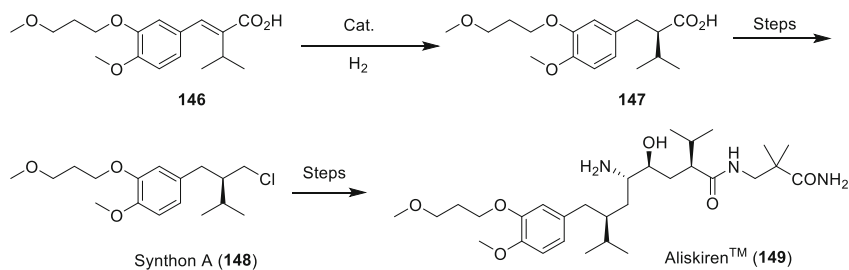


Fig. 11 Supramolecular ligands linked by zinc

the asymmetric hydrogenation of **29b** in hexane. Up to 88% ee was obtained, but only where all amides in the side chain contained an N-H functionality. Additionally, when the reactions were repeated in increasingly polar solvents or with more polar counterions, enantioselectivity was lost, presumably through breaking up the chiral assemblies.

Instead of hydrogen bridging, Takacs and co-workers used complexation of chiral bisoxazolines to Zn(II) for the self-assembly of modular supramolecular ligands [90]. The bisoxazolines were connected to bisphenol- or bis-naphthol-based phosphites via varying spacers (Fig. 11). In combination with $[\text{Rh}(\text{nbd})_2]\text{BF}_4$ as rhodium source, this led to a library of >150 catalysts, which were then screened in the hydrogenation of **6b** and **144** as model substrates. In general, most catalysts containing a flexible linker gave nearly quantitative conversions and ee's around 90%, whereas the more constrained linkers performed worse than control experiments with two equivalents of the monodentate phosphite ligand **9** (Fig. 2, R = Ph).

In summary, the self-assembly of monodentate ligands to form de facto supramolecular chiral bidentate ligands has been investigated mainly from a

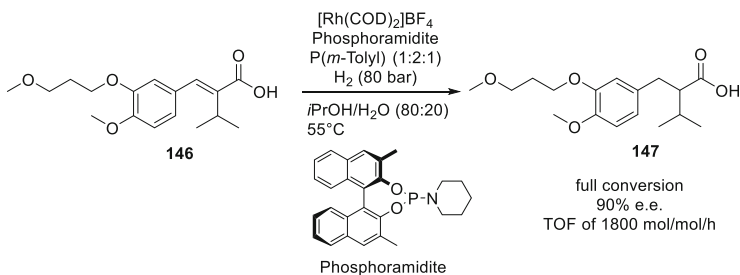


Scheme 25 Asymmetric hydrogenation step in the production of Aliskiren™

combinatorial point of view. Several different strategies for self-assembly have been highlighted. Monodentate ligands are often easier to synthesise than, especially unsymmetrical, bidentate ones, and self-assembly lends itself well for generating large libraries of catalyst combinations. Considering the difficulty of rationally designing catalysts for a given substrate, such a combinatorial approach may well prove successful, as was shown in the asymmetric hydrogenation of a range of acrylates and enamides.

6 Industrial Application

Although there were probably several processes where monodentate ligands have been used on the 10–100 kg scale, we are aware of only one ton-scale process. At DSM a process was developed for the production of Synthon A (147), an intermediate for the production of the renin-inhibitor Aliskiren™ (149), a blood pressure-lowering agent developed by Novartis and Speedel (Scheme 25) [91]. In the medicinal chemistry route, the asymmetric hydrogenation was performed with rhodium and Walphos, a ferrocene-based bidentate phosphine ligand. At DSM the high-throughput screening equipment was used to screen libraries of monodentate phosphoramidite ligands. In a first screen, it became obvious that the catalysts not only delivered the product in a rather low ee, but far worse, the rate of the reaction was so low that an industrial process seemed impossible. Since it is known that the rate determining step in rhodium-catalysed homogeneous hydrogenation is the oxidative addition of hydrogen, the researcher screened combinations of phosphoramidite ligands with electron-rich phosphine ligands as electron-rich ligands are known to accelerate oxidative addition reactions. This strategy paid off. After a number of screens, a ligand combination was found of 3,3'-dimethyl-PipPhos and tri-*m*-tolylphosphine, which allowed hydrogenation of the substrate with a turnover frequency of 1,800 h⁻¹ (Scheme 26). In addition, the product was formed in 90% ee, which could be easily upgraded by crystallisation in the subsequent steps. This process was implemented at DSM on ton scale.



Scheme 26 Ton-scale rhodium-catalysed asymmetric hydrogenation using a mixed monodentate ligand catalyst

References

- Knowles WS, Sabacky MJ (1968) *J Chem Soc Chem Commun* 1445
- Knowles WS (1983) *Acc Chem Res* 16:106
- Horner L, Siegel H, Büthe H (1968) *Angew Chem Int Ed Engl* 7:942
- Vineyard BD, Knowles WS, Sabacky MJ, Bachman GL, Weinkauff DJ (1977) *J Am Chem Soc* 99:5946
- Dang TP, Kagan HB (1971) *J Chem Soc Chem Commun* 481
- Kagan HB, Dang TP (1972) *J Am Chem Soc* 94:6429
- Knowles WS, Sabacky MJ, Vineyard BD (1972) *J Chem Soc Chem Commun* 10
- Claver C, Fernandez E, Gillon A, Heslop K, Hyett DJ, Martorell A, Orpen AG, Pringle PG (2000) *Chem Commun* 961
- Reetz MT, Sell T (2000) *Tetrahedron Lett* 41:6333
- Reetz MT, Mehler G (2000) *Angew Chem Int Ed* 39:3889
- van den Berg M, Minnaard AJ, Schudde EP, van Esch J, de Vries AHM, de Vries JG, Feringa BL (2000) *J Am Chem Soc* 122:11539
- Minnaard AJ, Feringa BL, Lefort L, de Vries JG (2007) *Acc Chem Res* 40:1267
- Reetz MT, Sell T, Meiswinkel A, Mehler G (2003) *Angew Chem Int Ed* 42:790
- Reetz MT, Mehler G (2003) *Tetrahedron Lett* 44:4593
- Pena D, Minnaard AJ, Boogers JAF, de Vries AHM, de Vries JG, Feringa BL (2003) *Org Biomol Chem* 1:1087
- Hoen R, Boogers JAF, Bernsmann H, Minnaard AJ, Meetsma A, Tiemersma-Wegman TD, de Vries AHM, de Vries JG, Feringa BL (2005) *Angew Chem Int Ed* 44:4209
- Gennari C, Monti C, Piarulli U, de Vries JG, de Vries AHM, Lefort L (2005) *Chem Eur J* 11:6701
- Reetz MT, Li X (2006) *Chem Commun* 2159
- Lefort L, Boogers JAF, de Vries AHM, de Vries JG (2004) *Org Lett* 6:1733
- Junge K, Oehme G, Monsees A, Riermeier T, Dingerdissen U, Beller M (2002) *Tetrahedron Lett* 43:4977
- Enthaler S, Erre G, Junge K, Michalik D, Spannenberg A, Marras F, Gladiali S, Beller M (2007) *Tetrahedron Asymmetry* 18:1288
- Enthaler S, Erre G, Junge K, Holz J, Börner A, Alberico E, Nieddu I, Gladiali S, Beller M (2007) *Org Proc Res Dev* 11:568
- Gladiali S, Alberico E, Junge K, Beller M (2011) *Chem Soc Rev* 40:3744
- Erre G, Enthaler S, Junge K, Gladiali S, Beller M (2008) *Coord Chem Rev* 252:471
- Hu A-G, Fu Y, Xie J-H, Zhou H, Wang L-X, Zhou Q-L (2002) *Angew Chem Int Ed* 41:2348
- Fu Y, Xie J-H, Hu A-G, Zhou H, Wang L-X, Zhou Q-L (2002) *Chem Commun* 480
- Zhu S-F, Fu Y, Xie J-H, Liu B, Xing L, Zhou Q-L (2003) *Tetrahedron Asymmetry* 14:3219

28. Jiang X-B, Minnaard AJ, Hessen B, Feringa BL, Duchateau ALL, Andrien JGO, Boogers JAF, de Vries JG (2003) *Org Lett* 5:1503
29. Jiang X-B, van den Berg M, Minnaard AJ, Feringa BL, de Vries JG (2004) *Tetrahedron Asymmetry* 15:2223
30. Jerphagnon T, Renaud J-L, Bruneau C (2004) *Tetrahedron Asymmetry* 15:2101
31. de Vries JG (2005) In: Ager DJ (ed) *Handbook of chiral chemicals*, 2nd edn. CRC Press, Boca Raton, pp 269–286
32. van den Berg M, Feringa BL, Minnaard AJ (2007) In: de Vries JG, Elsevier CJ (eds) *Handbook of homogeneous hydrogenation*, vol 2. Wiley-VCH, Weinheim, p 995
33. Bondarev OG, Goddard R (2006) *Tetrahedron Lett* 47:9013
34. Eberhardt L, Armspach D, Matt D, Toupet L, Oswald B (2007) *Eur J Org Chem* 5395
35. Lyubimov SE, Davankov VA, Valetskii PM, Petrovskii PV, Maksimova MG, Gavrilov KN (2006) *Russ Chem Bull Int Ed* 55:1448
36. Liu Y, Ding K, Am J (2005) *Chem Soc* 127:10488
37. Zhao B, Wang Z, Ding K (2006) *Adv Synth Catal* 348:1049
38. Liu Y, Wang Z, Ding K (2012) *Tetrahedron* 68:7581
39. Eberhardt L, Armspach D, Harrowfield J, Matt D (2008) *Chem Soc Rev* 37:839
40. Eberhardt L, Armspach D, Matt D, Toupet L, Oswald B (2007) *Eur J Inorg Chem* 4153
41. Zhu S-F, Liu T, Yang S, Song S, Zhou Q-L (2012) *Tetrahedron* 68:7685
42. Lyubimov SE, Tyutyunov AA, Kalinin VN, Said-Galiev EE, Khokhlov AR, Petrovskii PV, Davankov VA (2007) *Tetrahedron Lett* 48:8217
43. Lyubimov SE, Davankov VA, Petrovskii PV, Hey-Hawkins E, Tyutyunov AA, Rys EG, Kalinin VN (2008) *J Organomet Chem* 693:3689
44. Lyubimov SE, Kuchurov IV, Tyutyunov AA, Petrovskii PV, Kalinin VN, Zlotin SG, Davankov VA, Hey-Hawkins E (2010) *Catal Commun* 11:419
45. Lyubimov SE, Rastorguev EA, Verbitskaya TA, Petrovskii PV, Hey-Hawkins E, Kalinin VN, Davankov VA (2011) *Polyhedron* 30:1258
46. Schmitz C, Leitner W, Franciò G (2015) *Eur J Org Chem* 2889
47. Iuliano A, Losi D, Facchetti S (2007) *J Org Chem* 72:8472
48. Reetz MT, Li X (2005) *Angew Chem Int Ed* 44:2959
49. Monti C, Gennari C, Piarulli U, de Vries JG, De Vries AHM, Lefort L (2005) *Chem Eur J* 11:6701
50. Frank DJ, Franzke A, Pfaltz A (2013) *Chem Eur J* 19:2405
51. Breit B, Fuchs E (2006) *Synthesis* 2121
52. Kokan Z, Kirin SI (2013) *Eur J Org Chem* 8154
53. Hopewell J, Jankowski P, McMullin CL, Orpen AG, Pringle PG (2010) *Chem Commun* 46:100
54. Galland A, Dobrota C, Toffano M, Fiaud J-C (2006) *Tetrahedron Asymmetry* 17:2354
55. Dobrota C, Fiaud J-C, Toffano M (2015) *ChemCatChem* 7:144
56. Wang X-B, Goto M, Han L-B (2015) *Chem Eur J* 20:3631
57. Bruneau C, Renaud J-L, Jerphagnon T (2008) *Coord Chem Rev* 252:532
58. Hoen R, Tiemersma-Wegman T, Procuranti B, Lefort L, de Vries JG, Minnaard AJ, Feringa BL (2007) *Org Biol Chem* 5:267
59. Hekking KFW, Lefort L, de Vries AHM, van Delft FL, Schoemaker HE, de Vries JG, Rutjes FPJT (2008) *Adv Synth Catal* 350:85
60. Lefort L, Boogers JAF, Kuilman T, Vijn RJ, Janssen J, Straatman H, de Vries JG, De Vries AHM (2010) *Org Proc Res Dev* 14:568
61. Mršić N, Jerphagnon T, Minnaard AJ, Feringa BL, de Vries JG (2010) *Tetrahedron Asymmetry* 21:7
62. Meindersma AF, Pollard MM, Feringa BL, de Vries JG, Minnaard AJ (2007) *Tetrahedron Asymmetry* 18:2849
63. Zhang J, Li Y, Wang Z, Ding K (2011) *Angew Chem Int Ed* 50:11743
64. Dong K, Li Y, Wang Z, Ding K (2013) *Angew Chem Int Ed* 52:14191

65. Dong K, Li Y, Wang Z, Ding K (2014) *Org Chem Front* 1:155
66. Li Y, Wang Z, Ding K (2015) *Angew Chem Int Ed* 21:16387
67. van den Berg M, Minnaard AJ, Haak RM, Leeman M, Schudde EP, Meetsma A, Feringa BL, de Vries AHM, Elizabeth C, Maljaars P, Willans CE, Hyett D, Boogers JAF, Henderickx HJW, de Vries JG (2003) *Adv Synth Catal* 345:308
68. Reetz MT, Meiswinkel A, Mehler G, Angermund K, Graf M, Thiel W, Mynott R, Blackmond DG (2005) *J Am Chem Soc* 127:10305
69. Reetz MT, Fu Y, Meiswinkel A (2006) *Angew Chem Int Ed* 45:1412
70. Gridnev ID, Fan C, Pringle PG (2007) *Chem Commun* 1319
71. Alberico E, Baumann W, de Vries JG, Drexler H-J, Gladiali S, Heller D, Henderickx HJW, Lefort L (2011) *Chem Eur J* 17:12683
72. Gridnev ID, Alberico E, Gladiali S (2012) *Chem Commun* 48:2186
73. Schiaffino L, Ercolani G (2011) *J Phys Org Chem* 24:257
74. Liu Y, Sandoval CA, Yamaguchi Y, Zhang X, Wang Z, Kato K, Ding K (2006) *J Am Chem Soc* 128:14212
75. Weis M, Waloch C, Seiche W, Breit B (2006) *J Am Chem Soc* 128:4188
76. Birkholz M-N, Dubrovina NV, Jiao H, Michalik D, Holz J, Paciello R, Breit B, Börner A (2007) *Chem Eur J* 13:5896
77. Patureau FW, Kuil M, Sandee AJ, Reek JNH (2008) *Angew Chem Int Ed* 47:3180
78. Breuil P-AR, Reek JNH (2009) *Eur J Org Chem* 6225
79. Breuil P-AR, Patureau FW, Reek JNH (2009) *Angew Chem Int Ed* 48:2162
80. Meeuwissen J, Kuil M, van der Burg AM, Sandee AJ, Reek JNH (2009) *Chem Eur J* 15:10272
81. Terrade FG, Kluwer AM, Detz RJ, Abiri Z, van der Burg AM, Reek JNH (2015) *ChemCatChem* 7:3368
82. Wieland J, Breit B (2010) *Nat Chem* 2:832
83. Pignataro L, Lynikaite B, Cvengroš J, Marchini M, Piarulli U, Gennari C (2009) *Eur J Org Chem* 2539
84. Pignataro L, Carboni S, Civera M, Colombo R, Piarulli U, Gennari C (2010) *Angew Chem Int Ed* 49:6633
85. Pignataro L, Boghi M, Civera M, Carboni S, Piarulli U, Gennari C (2012) *Chem Eur J* 18:1383
86. Pignataro L, Bovio C, Civera M, Carboni S, Piarulli U, Gennari C (2012) *Chem Eur J* 18:10368
87. Hattori G, Hori T, Miyake Y, Nishibayashi Y (2007) *J Am Chem Soc* 129:12930
88. Li Y, Feng Y, He YM, Chen F, Pan J, Fan Q-H (2008) *Tetrahedron Lett* 49:2878
89. Raynal M, Portier F, van Leeuwen PWHM, Bouteiller L (2013) *J Am Chem Soc* 135:17687
90. Thacker NC, Moteki SA, Takacs JM (2012) *ACS Catal* 2:2743–2752
91. Boogers JAF, Felfer U, Kotthaus M, Lefort L, Steinbauer G, de Vries AHM, de Vries JG (2007) *Org Proc Res Dev* 11:585–591

CO₂ Reduction Reactions by Rhodium-Based Catalysts

Danilo Bonincontro and Elsje Alessandra Quadrelli

Abstract Reduction reactions of CO₂ using chemicals obtained from renewable energy sources (as for example, dihydrogen obtained using renewable-issued electricity) or using directly renewable energy sources can contribute to store and use renewable energies in our current infrastructures. Rh-based catalysts have been playing a key role in the field of CO₂ reduction. From its very first application as homogeneous catalyst to now, several Rh-based catalytic systems have been successfully tested. This chapter gives the reader an overview as well as a mechanistic insight where possible into the Rh-catalysed CO₂ reduction reductions: production of formic acid and higher carboxylic acids with homogeneous catalysts, methane, CO and various oxygenated compounds via heterogeneous catalysis, and various products by means of electro- and photocatalysis.

Keywords Carbon dioxide • Electrocatalysis • Formic acid • Heterogeneous catalysis • Homogenous catalysis • Mechanism • Photocatalysis • Rhodium

Contents

1	Introduction	264
2	Molecular Catalysts	266
2.1	Formic Acid	266
2.2	Higher Carboxylic Acids	269

D. Bonincontro

Université de Lyon, C2P2, UMR 5265, CNRS – Univeristé de Lyon1 UCBL – CPE Lyon, 43
Bvd du 11 Novembre 1918, 69616 Villeurbanne, France

Dipartimento di Chimica Industriale “Toso Montanari”, Viale Risorgimento 4, Bologna, Italy

E.A. Quadrelli (✉)

Université de Lyon, C2P2, UMR 5265, CNRS – Univeristé de Lyon1 UCBL – CPE Lyon, 43
Bvd du 11 Novembre 1918, 69616 Villeurbanne, France

e-mail: quadrelli@cpe.fr

3	Heterogeneous Catalysts	272
3.1	Methanation	272
3.2	Dry Reforming	274
3.3	Oxygenated Compounds	275
4	Electro- and Photocatalysis	276
5	Conclusion	278
	References	279

1 Introduction

Carbon dioxide emissions are emerging as a towering side effect of fossil fuel utilization. As a major energy provider, accounting for 81% of our 2013 global consumption, fossil fuels are responsible for a big share of the year's – 31.6 GT of CO₂ emissions [1, 2]. Despite considerable efforts to reduce such consumption and curb CO₂ emissions, the predicted increase in overall energy consumption, and the expected continued dominance of fossil fuels in the energy mix for the next decades, explains in part why, regardless the scenario envisaged [3], CO₂ emissions are expected to raise continuously for at least the next decade (see Fig. 1) [2]. Albeit nature provides very efficient carbon cycles, capable mainly through photosynthesis and ocean capture to absorb back about half of the anthropogenic emissions [4], the CO₂ buildup cannot be curbed unless major dedicated efforts are directed to this aim [5–11].

Carbon dioxide has long been considered an intractable waste, due, inter alia, to its very high thermodynamic stability. The rare – yet very established and industrially relevant – applications of carbon dioxide utilization, production of urea to

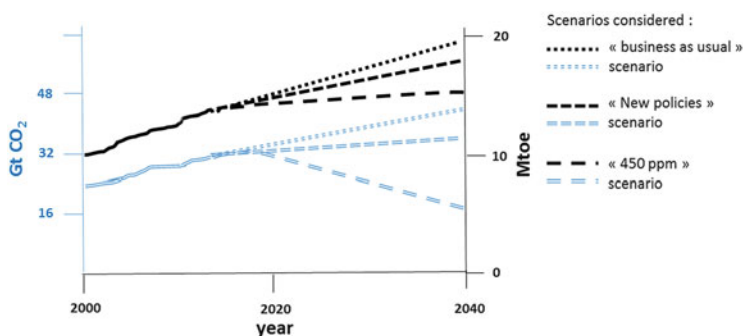
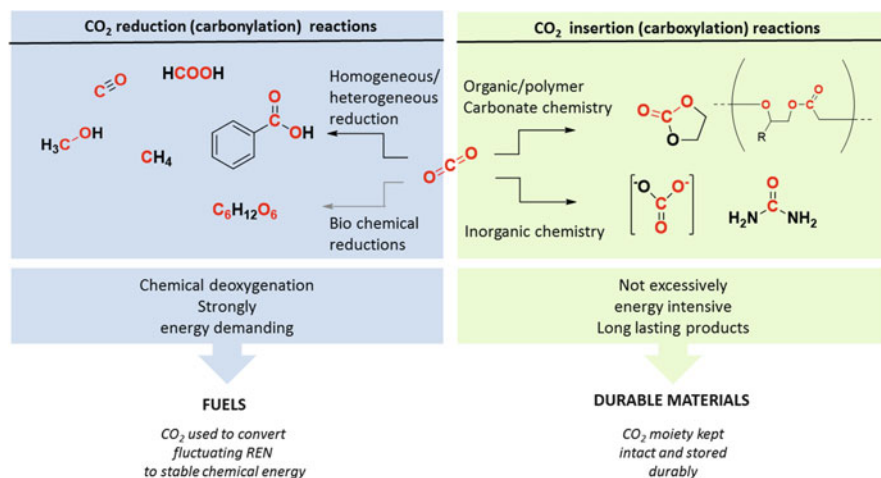


Fig. 1 World energy demand (right axis and black lines) and CO₂ anthropogenic emissions (left axis and blue lines) between 2000 and 2040 measured and forecasted according to different scenarios: the “business-as-usual” scenario (i.e., no dedicated change in energy policy), the “new policies” scenario which takes into account the environmental pledges announced by the countries in October 2015 before the COP21, and the “450 scenario ppm” (officially named Scenario 450) developed with the goal to maintain the greenhouse gases concentration in atmosphere under 450 ppm of CO₂ [2]

name one, typically do not change the carbon oxidation number or at least do not require large energy input due to the favorable thermodynamic parameters of the carbonylation reactions [5–8]. The capacity to synthesize from CO₂ sufficiently long-lived materials (ex polymers or building blocks from carbonylation of waste) are some of the examples that show how carbon dioxide utilization (CDU) reactions are emerging as an important complement/alternative to carbon capture storage [5–8].

At the opposite end of such carboxylation reactions, reactions aiming at breaking (and hence reducing) one of these very stable C = O bonds imply substantial energy supply (see Scheme 1). CO₂ thermodynamic stability explains the need for very large quantities of energies to jolt the carbon atom back into a reduced valence state and thus removing one C = O bond and/or forming new C–C or C–H bonds such as in CO, HCOOH (+II oxidation number), CH₃OH (–II oxidation number) or CH₄ (–IV). This energetic hurdle has made CO₂ unattractive for reduction reactions until recently. Now, with the overarching desire to find ways to store renewable energy as chemical energy, this very same thermodynamic stability makes CO₂ a suitable molecule to store energy. Indeed, CO₂ is asserting itself as a crucial vector molecule for the injection of renewable energy in our current infrastructure thus providing a key technology for avoidance of fossil fuel [9, 10]. This review will focus on these CO₂ reduction reactions.

In the chemical industry, over 90% of the processes involve at least one catalytic step [11]. Catalysis plays a similar fundamental role in the chemistry enabling the reduction of CO₂ in added-value products [5–10]. Among the several catalytic systems, we will here review the role of rhodium-based catalysts in the CO₂ reduction reactions.



Scheme 1 Overview of two major types of CDU reactions: *left*, reduction reactions as mean to provide an energy vector for fossil fuel avoidance, see text; *right*, in CO₂ insertion reaction as mean to chemical storage of CO₂ molecules

2 Molecular Catalysts

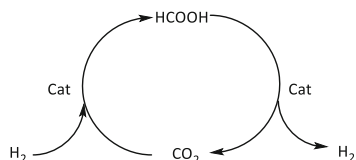
2.1 Formic Acid

World formic acid (FA) production was 950,000 t in 2014, and its industrial applications are very wide, ranging from silage manufacturing, leather and tanning production, to pharmaceutical industry [12]. More than 80% of FA world production comes from the hydrolysis of methyl formate which is obtained through the reaction between CO and methanol (which is recycled after the hydrolysis). A more sustainable approach for its production could become the direct reduction of CO₂ with H₂ produced with renewable energy, *r*-H₂ (see Scheme 2) [10, 13].

To estimate the impact of such potential technology switch, one could first propose the following upper boundary: replacing the entire traditional production with CO₂-based technologies could lead to a consumption of 1 Mt y⁻¹ of CO₂ (around 0.003% of the overall annual CO₂ emission). At the same time, this estimate does not take into account the major role that CO₂-based formic acid production could make: store and transport hydrogen through the cycle reported in Scheme 2 [5–9, 13–15]. Such approach is claimed to be CO₂-emission neutral if the dihydrogen is “renewable” hydrogen, *r*-H₂, and permits easier and safer transportability of liquid fuel with respect to compressed molecular hydrogen. In this case of formic acid formation (Eq. 2), the role of CO₂ reaction would not be about storing (or consuming) CO₂, but rather about avoiding later CO₂ emissions through fossil fuel replacement with renewable energy (REN)-based fuels (see column 1, Scheme 1). In this latter case, the volume of formic acid produced from CO₂ depends on the penetration of such energy vector in the infrastructures, which, if successful, could largely overpass the figures cited above.

The first work which showed CO₂ reduction into formic acid following Eq. (2) was through rhodium-based catalysis into the spotlight. Inoue reported in 1976 that RhCl(PPh)₃ was among the best catalysts to achieve formic acid production directly from CO₂ and H₂ [16]. The screening of different transition metal complexes was performed in nonaqueous medium (benzene) and in the presence of a base and water (typical molar ratio base/water 1/10). Among the different complexes tested, the Wilkinson’s complex, RhCl(PPh)₃, in the presence of trimethylamine as base was found active, second only to ruthenium-based system. A deep insight into the catalytic behavior of Wilkinson’s complex was reported by

Scheme 2 Reaction scheme for current industrial route to formic acid (Eq. 1) and alternative route directly from CO₂ (Eq. 2), which is part the proposed CO₂-mediated storage and release of H₂ [10, 13–15]



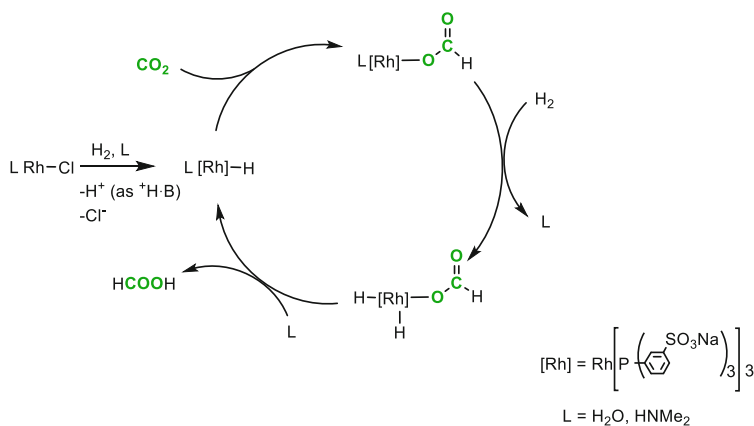
Ezhova [17]. This work highlighted the effect of different parameters on the catalytic behavior of the complex. A predominant role is played by the solvent: heptane, benzene, and THF were found to repress the activity of the complex, while DMSO and MeOH have been found to be suitable solvents for this reaction, even though when MeOH is used the presence of methyl formate is detected at the end of the reaction. The study of the catalytic properties of other Rh(I)-containing species demonstrated the importance of phosphine ligands: all complexes containing a phosphine ligand were found to be active in the conversion of CO₂ into formic acid; on the other hand, the complex without a phosphine ligand are inactive, and some of them showed activity only after the addition of phosphine ligands. The ³¹P-NMR study reported in the same paper suggested that RhCl(PPh₃)₂(NEt₃) is the precursor of the active complex, and its decomposition is inhibited by the excess of phosphine.

The conversion of CO₂ in nonaqueous solvents is also catalyzed by RhH (diphosphine) complexes [18]. The diphosphines are prepared in situ using the bidentate phosphine 1,4-bis(diphenylphosphino)butane (dppb, Ph₂P-(CH₂)₄-PPh₂) and two different Rh-containing precursors: [RhCl(cod)₂]₂ and [RhH(cod)₄] (cod = 1,5-cyclooctadiene). The first system suffers from an “induction time” that could be overcome by an activation with H₂ or HCOOH, which is necessary to obtain RhH(dppb), the postulated active species. In order to understand which of the effects are structural changes in phosphine ligands on the catalytic activity of Rh (I) precursors, Leitner’s group synthesized and tested the catalytic activity of a series of [(P₂)Rh(hfacac)] (hfacac = 1,1,1,5,5,5-hexafluoroacetylacetonate) complexes. It was found that the larger the P-Rh-P bite angle, the greater the ¹⁰³Rh NMR chemical shift and the higher the reaction rate [19]. Further studies were focused on the determination of the accessible molecular surface (AMS) [20] of such complexes and their correlation with the activity, and it was found that the AMS inversely correlated with the reaction rate.

In order to obtain water-soluble Rh(I)-based complexes, the already mentioned [RhCl(cod)₂]₂ and [RhH(cod)₄] precursors were modified using the water-soluble sodium trisulfonated triphenylphosphine ligand (C₆H₄-m-SO₃⁻Na⁺)₃P, TPPTS in a ratio P:Rh = 2.6:1 [21]. Both complexes were found active in the reduction of CO₂ into selective formic acid using NEt₃ as base. The complex RhCl(TPPTS)₃ was also successfully tested. Amine variation sensibly affected the catalytic performances. NEt₃ and HNEt₂ showed the best performances, while ethanolamines reduced the catalytic activity. The base is indeed believed to play a crucial role in the catalytic cycle, since monohydridorhodium complex, RhH(TPPTS)₃L, is formed only in the presence of a base (see Scheme 3).

All the catalytic cycles reported so far involve CO₂ insertion into Rh(I)-H bonds. A DFT calculation showed that the energy associated to the CO₂ insertion into the Rh-H bond is higher for Rh(III) than for Rh(I) [23]. This different behavior could explain why Rh(III)-containing complexes are not commonly used. However, as it will be discussed in Sect. 4, a Rh(III) complex were found to be active as an electrocatalyst in the conversion of CO₂ into formate.

A recent development in the field of formic acid production with rhodium-based catalysts in the context of carbon capture and utilization (CCU) was proposed by Li



Scheme 3 Catalytic cycle for CO₂ conversion into formic acid catalyzed by ClRh(TPPTS)₃L in the presence of a base, B (e.g., NEt₃, HNEt₂, ethanolamine) [22]

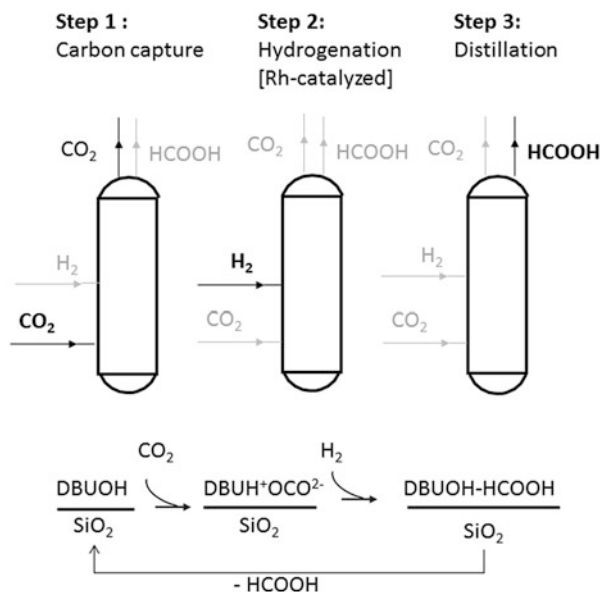


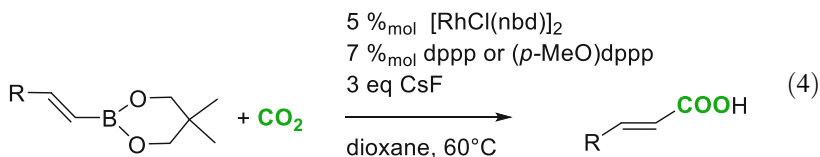
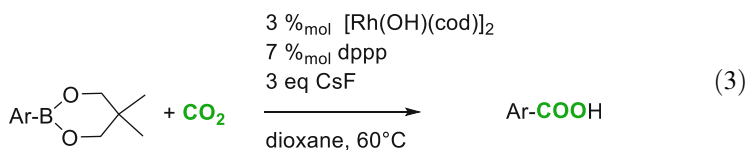
Fig. 2 Proposed CCU process for the conversion of CO₂ into formic acid mediated by silica-supported DBU and Rh-based catalyst [24]

[24] with an integrated carbon capture and utilization (CCU) process for the in situ conversion of CO₂ into formate. According to the authors, 99% of the CO₂ captured can be converted into formate using suitable amidine derivative 1,8-diazabicyclo [5.4.0]-undec-7-ene (DBU) as CO₂ capturing agent and RhCl₃ as catalyst precursor. The immobilization of the amidine derivative over silica gave rise to the formation of solid capturing agent which was equally found to be effective in the process. Such solid could be regenerated yielding a three-step chemical process (see Fig. 2).

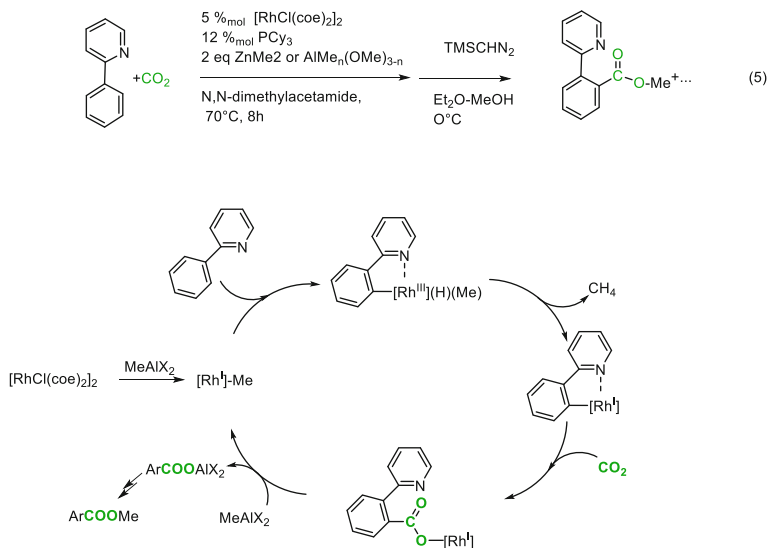
In summary, formic acid has been one of the first catalytic targets of Rh-based CO₂ conversion and has continued to attract considerable interest in the context of coupling with CO₂ capture but also to other longer carbon chain targets (see below).

2.2 Higher Carboxylic Acids

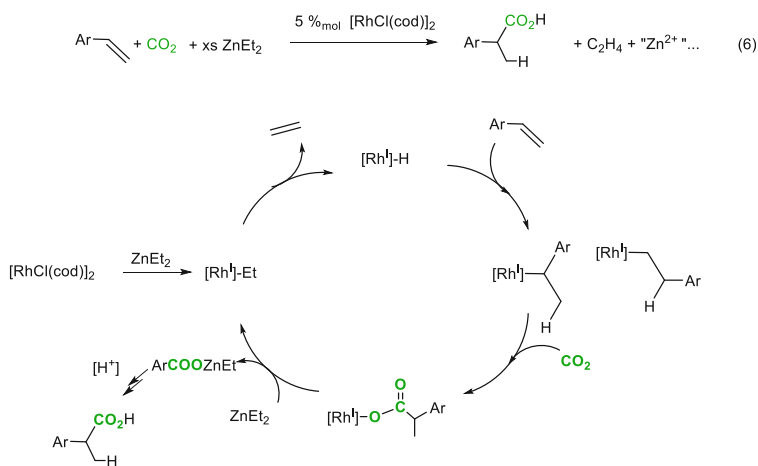
An attractive target for the CO₂ conversion is the production of carboxylic acids, which are very widely used chemicals [5–8]. The use of CO₂ as electrophile reagent in the carboxylation reaction requires high nucleophile reactants, such as organolithiums or Grignard reagents. Alongside these classical approaches, different catalytic cycles involving transition metal complexes have been developed, among which are Rh(I) species [25]. For example, [Rh(OH)(cod)]₂ was found to be an effective precursor in the carboxylation of the ester of a wide range of arylboronic acid under mild conditions (1 atm of CO₂ at 60°C in dioxane as solvent in the presence of 1,3-bis(diphenylphosphino)propane, dppp, see Eq. 3) [26], which makes this reaction particularly useful when the Grignard reagent route is not available. The analogous precursor [RhCl(nbd)]₂ (nbd = norbornadiene) was used in the carboxylation of alkenylboronic acids in the already mentioned operative conditions (Eq. 4).



The rhodium (I) complex [RhCl(cyclooctene)]₂, activated in situ by an alkylating agent such as AlMe₂(OMe) and in the presence of tricyclohexylphosphine, PCy₃, catalyzes the direct carboxylation of phenylpyridines and phenylpyrazoles (see Eq. 5) [27]. In the proposed catalytic cycle, the Rh(I) catalyst activates the C–H bond; then, after methane reductive elimination from the resulting Rh(III) aryl intermediates, the complex undergoes the nucleophilic insertion of the CO₂ moiety in the Rh^I–Ar bond; the final transmetalation step with the aluminum alkylating agent releases the carboxylated species regenerating the active catalytic species (see Scheme 4). The direct carboxylation of benzene and its derivatives (toluene, xylenes, and others) could also be achieved using 1,2-bis(dicyclohexylphosphino)ethane–rhodium(I) chloride complex as precursor [28]. The catalytic cycle proposed for such reaction is the same as the one showed in Scheme 4, and kinetic



Scheme 4 Proposed catalytic cycle for the carboxylation of phenylpyridine using $[\text{RhCl}(\text{coe})_2]_2$ as precursor and PCY_3 as ligand [27]

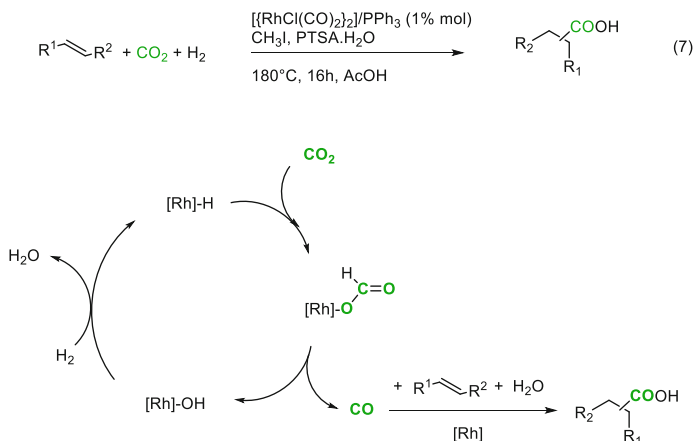


Scheme 5 Rh-catalyzed ($[\text{RhCl}(\text{cod})]_2$ as precursor) olefin carboxylation pathway [29]

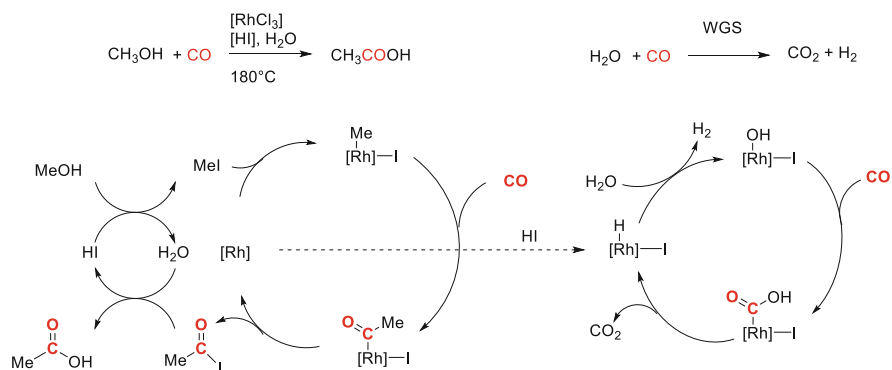
isotopic labeling experiments suggested that the rate determining step is the C–H bond activation.

Following a proposed reaction mechanism related to the previous one (Scheme 5), the bimetallic system combining catalytic $[\text{RhCl}(\text{cod})]_2$ and stoichiometric ZnEt_2 achieves hydrocarboxylation of aryl olefins with carbon dioxide (see Eq. 6) [29].

A markedly different mechanistic route was assessed for $[\text{RhCl}(\text{CO})_2]_2$ -catalyzed hydrocarboxylation of linear and cyclic olefins with CO_2 and H_2 (Eq. 7) in the



Scheme 6 Hydrocarboxylation reaction of olefin with CO₂ and H₂, and underpinning catalytic cycles: *r*-WGS and hydroxycarbonylation reactions [30]

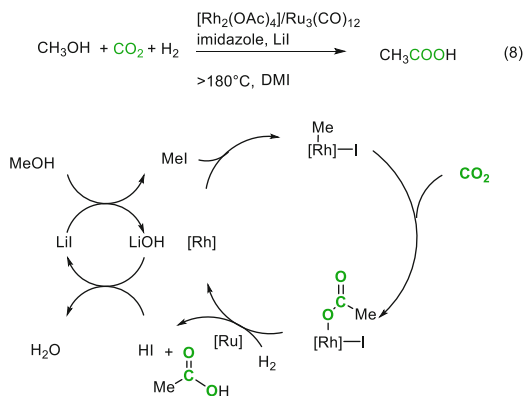


Scheme 7 Catalytic cycles involved in Monsanto acetic acid production by Rh/iodide-based system: *left*, methanol carbonylation; *right*, water-gas shift (WGS) cycle

presence of methyl iodide as promoter in acid conditions (see Scheme 6) [30]. Unlike the aforementioned proposed direct carboxylation routes, the detailed mechanistic studies showed that, in this case at least, the CO₂ is not directly incorporated in the substrate. Robust isotopic labeling studies showed that the products of Eq. (6) are obtained through an intermediary reverse water-gas shift reaction (*r*-WGSR), which acts as the “upstream” cycle for the subsequent hydroxycarbonylation mechanism which involves CO and water as reactants.

The two-cycle mechanism reported in Scheme 6 relies on the catalytic competence of Rh complexes to promote water-gas shift reaction (WGS). Such behavior is in line with the well-established reactivity of the industrial Monsanto catalyst $[\text{Rh}(\text{CO})_2\text{I}_2]^-$, which, beside catalyzing the carbonylation of methanol (its primary goal), can serve as entry point to water-gas shift activities (see Scheme 7) necessary to rhodium solubilization in the reaction media [31, 32].

Scheme 8 Direct acid acetic production from methanol, CO₂ and H₂ using a Ru/Rh catalytic couple



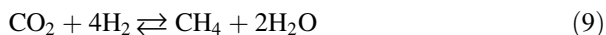
A Ru–Rh bimetallic catalyst, obtained from Ru₃(CO)₁₂ and Rh₂(OAc)₄ in the presence of LiI and imidazole ligand, seems to bypass such rWGS activity and converts methanol to acetic acid with CO₂ and H₂ (Eq. 8) via a proposed direct hydrocarboxylation route (see Scheme 8) [33]. The proposed cycles involve indeed a direct CO₂ insertion in the Rh–Me bond and subsequent ruthenium-catalyzed hydrogenation of the ensuing Rh-carboxylate. The roles of Rh-/Ru-based catalysts are to be assessed also in view of the reported Ru-only hydroformylation/reduction of alkenes, the hydroxymethylation reaction or the alkoxy carbonylation [34], and the WGS (and *r*-WGS) ability of Rh centers [30–32].

Regardless of these mechanistic considerations, this capacity of CO₂ to act as a CO surrogate (either as an existing intermediate product of the process of just formally) is emerging as a very timely and productive field, where Rh, alongside Ru, appears to play a crucial catalytic role [30, 34].

3 Heterogeneous Catalysts

3.1 Methanation

The CO₂ conversion into methane (known as Sabatier reaction; see Eq. 9) is a well-known route for the CO₂ reduction and can be an attractive way to produce substitute natural gas [8].



Supported metals are well-known catalysts for the methanation of CO₂ [35–40], and these included Rh-based catalysts supported over metal oxides such as γ-Al₂O₃ [37–39] and TiO₂ [37, 40].

Rhodium supported over γ -Al₂O₃ has been reported to be an active catalyst for the transformation of CO₂ into methane even in mild condition (room temperature and atmospheric pressure) [38], although CO₂ conversion increases with temperature [41]. In order to obtain a catalytic active species, the catalyst must be reduced with H₂ before the reaction [41], and this reduction leads to an increase of Rh(0) species present over the surface as measured by XPS technique [39]. Mechanistically, DRIFTS analysis [39] showed that CO₂ is dissociated into CO and O over the Rh surface; this process leads to the formation of two different C-containing species bonded over the catalyst surface: Rh(I)-(CO)₂ (also called gem-dicarbonyl species) and Rh(0)-CO. When a pulse of H₂ is introduced inside the chamber, the peaks of the gem-dicarbonyl species disappear rapidly; meanwhile, the intensity of the peak related to the mono-carbonyl species does not change. According to this analysis, it appears that the oxidation state of the Rh has a predominant role in the catalytic process. Karelovic and Ruiz [42] prepared and tested different catalysts with different Rh particles and showed that larger particles are more active than smaller ones between 135 and 150°C, while at higher temperature, the reaction rate is independent from the particle size. A similar study was conducted over TiO₂-supported Rh catalysts [40]. For metal particles smaller than 7 nm, the rate of methane production increases as metal particles size increases; for bigger particles the rate seems to be independent from the size.

Because of the high cost of the Rh (around 20\$/g in 2016) and its lower activity compared to Ni (which suffers from more rapid deactivation than Rh but costs less than 0.01\$/g), several attempts to improve the catalytic properties of the Rh/ γ -Al₂O₃ system were proposed by coupling this system with other supported metal species. For instance, the catalytic properties of the Rh(0.3%)/ γ -Al₂O₃ were improved by addition of the (presumably catalytically inactive) Mn (0.5%). Such catalyst showed the same catalytic properties as the Rh(0.5%)/ γ -Al₂O₃ catalyst [43]. The 1:1 mechanical mixture of the inert Pd(5%)/ γ -Al₂O₃ with the active Rh(2%)/ γ -Al₂O₃ possesses higher activity than the Rh-based catalyst alone [44]. This higher activity is thought to be the result of a synergistic effect between the two different catalysts: the hydrogenation of strongly activated carbonyl species adsorbed over Pd surfaces (mostly bridge-bonded CO, at odds with carbonyl hydride species for Rh-only catalyst) is performed by the H species originated by the Rh-containing catalyst. An analogous synergistic effect was found by coupling Rh/ γ -Al₂O₃ and Ni-loaded activated carbon (AC) [45]. In this case, the synergistic effect is due to the high capacity of the Ni/AC system to absorb and activate hydrogen. The migration of such activated hydrogen species to the Rh surface reduces the carbonyl species to methane. At the same time, the hydrogen species keeps the rhodium into a reduced state which is, as already mentioned before, a key feature in the activity of Rh-based system.

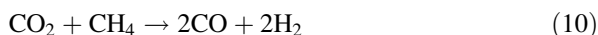
Several metal-promoted mesostructured silica nanoparticles (MSN) have been tested [46]. Among these, the Rh-containing one showed the best catalytic activity at 623 K. Differently from the already mentioned metal oxides supports which do not have any role in the mechanism cycle, the MSN support interacts with the

species activated by the metal promoter, leading to the formation of bridged carbonyl, linear carbonyl, and bidentate formate, which are converted into methane.

Rhodium was mentioned among the metals associated with nickel to form “liquid catalyst” for methanation reaction but was not among the most performing co-catalysts [47].

3.2 Dry Reforming

A further reaction in which Rh-containing catalysts are widely used is the CO₂ reforming of methane (also known as methane dry reforming, MDR, Eq. 10) [5–8, 48].



The interest that this reaction has been receiving by the scientific community is justified by the possibility to use this reaction as starting step in the on-site conversion of natural gas into liquid or gaseous fuels through the syngas intermediary [9, 10, 49].

γ -Al₂O₃-supported Rh and Ru were found to be active in the CO₂ reforming of methane [50]. The catalytic tests showed that for reaction temperatures higher than 600°C the Rh-containing catalyst outperforms Ru-based ones in terms of both reactant conversion and deactivation trend. From this first work, different metal oxides have been tested as support for the Rh in order to understand the effect of the interaction between metallic sites and support [51, 52]. Catalytic results showed that irreducible supports (γ -Al₂O₃, La₂O₃, MgO, SiO₂, and Y₂O₃) are more suitable than the reducible ones (CeO₂, Nb₂O₅, Ta₂O₅, TiO₂, and ZrO₂) [52]. Among the former, γ -Al₂O₃, MgO, and La₂O₃ provided stable activities for more than 50 h. The authors suggested that strong interaction between Rh and the support induces high stability of the catalytic system. The lower activity of the catalysts having reducible supports was attributed to the fact that the Rh-metal particles could be partially covered by islets of partially reduced species leading to a decrease of the metal surface area.

The effect of the support in the catalytic performance of Rh-containing catalysts is also significant when Rh is supported with Ni, which is known to have high activity toward the MDR but suffers from severe deactivation due to carbon deposition [53]. Rhodium can limit such carbon deposition [54]. In detail, the bimetallic-loaded boron nitride (BN) showed higher CH₄ conversion and H₂ yield than the analogous γ -Al₂O₃. This enhancement was attributed to the easier formation of Rh–Ni clusters over the BN surface than over γ -Al₂O₃. In fact the metal support affinity is higher for γ -Al₂O₃, and this hinders the formation of such clusters. The synergic effect between Rh and Ni was also found when the two metals were supported over NaY-type zeolite [55].

Rh-containing crystalline materials have been tested in DRM reaction. Hydrotalcite-derived Rh₁Mg₇₁Al₂₈ was found to be active in the MDR reaction without any deactivation during 50 h of reaction [56], and the catalyst does not show any change of structure at the end of the reaction. More recent approaches suggested the use of Rh containing pyrochlores [57]. It was showed that replacing Zr by Rh in low amount (2 and 5% wt.) in the lanthanum zirconate pyrochlore structure leads to the formation of catalytic active species. In fact, the catalytic results showed that the unmodified pyrochlore is not able to convert both CO₂ and CH₄; meanwhile, the conversion of both reactants occurs when the two modified pyrochlores are used. Moreover, modified catalysts activity increased during the time: since no preactivation is performed, it was suggested that the reduction of the catalyst is crucial for their activities.

3.3 Oxygenated Compounds

Oxygenated compounds such as ethanol, acetic acid, and oxalate can be obtained from CO₂ using Rh-containing catalysts. The selectivity of CO₂ reduction with H₂ (H₂/CO₂ = 3) of Rh/SiO₂-based catalyst is strongly affected by the presence of a metal promoter [58]. While unmodified Rh/SiO₂ catalyst is highly selective (99.7%) for methane production, the presence of a promoter can induce the formation of oxygenated compounds. A screening of 30 different promoters (in 1:1 Rh/M atomic ratio) showed that four additives (Li, Fe, Sr and Ag) can give rise to rhodium-catalyzed ethanol production. Among these additives, Li is the most selective (15.5%, yield 1.0%). The FT-IR study showed that CO, that comes from the CO₂ dissociation, is adsorbed over the Rh surface as linear and bridged species over the surface of both Li-containing and unpromoted Rh/SiO₂ catalyst. Nevertheless, the comparison between the relative intensities of the two peaks for the two different samples showed that over the Li-containing surface, there is a higher amount of bridged species than over the unmodified Rh/SiO₂. The authors suggest that the higher amount of CO species could hinder the H₂ adsorption, leading to a lower methane selectivity of the Li-containing catalyst. Higher selectivity (16.0%) and yield (4.3%) could be reached tuning the operative conditions and the metal loading of the Fe-containing Rh/SiO₂ catalyst [59].

Ag-modified Rh/SiO₂ was found to convert a CO₂/H₂ mixture into different hydrogenated compounds in low yield, since more than 90% of the fed CO₂ is converted into CO. Among the hydrogenated compounds, acetic acid is the most abundant one at 463 K [60]. Using unpromoted Rh/SiO₂, Ding [61] proposed a different path to convert CO₂ into acetic acid; it was proposed a stepwise route in which CH₄ is used instead of H₂.

4 Electro- and Photocatalysis

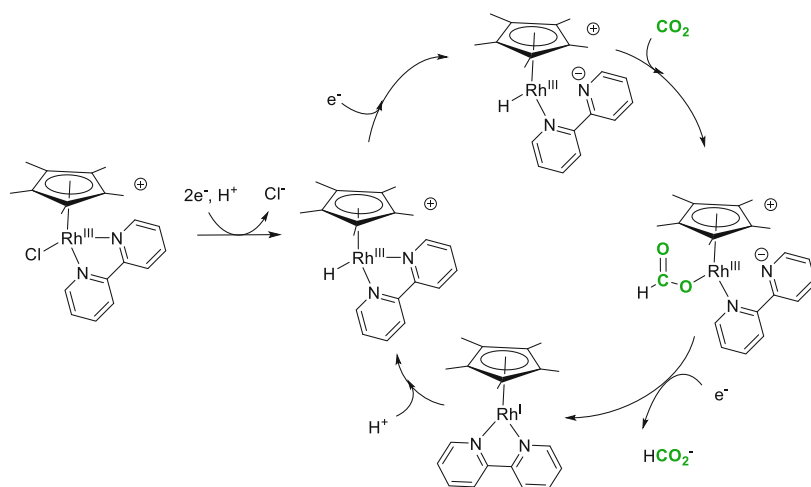
Electrochemical CO₂ reduction is a key technology for the introduction of “green electrons”, that is, electricity produced from renewable resources in our current energy infrastructure [62].

Over two decades ago, Rh(III) complexes Cp*RhCl(2,2'-phenanthroline) and *cis*-[Rh(III)(bpy)₂(TFMS)₂]⁺ (bpy = 2,2'-bipyridine, TFMS = trifluoromethanesulfonate) were found to be active in the electrochemical conversion of CO₂ into formate [63, 64]. One by-product was molecular hydrogen. The faradaic efficiency in selective CO₂ reduction is generally a key issue: already in one of these first systems [63], the catalytic tests showed that the selectivity in formate decreases as the number of coulomb passed increases, and for hydrogen the trend is the opposite. The authors suggested that the protons required for both formate and hydrogen production come from the tetra-*n*-butylammonium ions of the supporting electrolyte [63].

Another Rh(III)-containing complex that has been successfully tested is [(η⁵-Me₅Cp₅)Rh(bpy)Cl]⁺ [64]. This work gave the opportunity to have an insight over the mechanism for the electrocatalytic cycle (see Scheme 9).

Beside formate, oxalate can also be obtained from another use in [(RhCp*)₃(μ₃-S)₂]²⁺ electrocatalyzed reduction of CO₂ in the presence of LiBF₄, under controlled potential electrolysis at -1.50 V in CO₂-saturated CH₃CN [65].

Following short- and medium-term electrocatalysis deployment, photo-based catalysis appears as the necessary (longer-term) next step in the forecast deployment of CDU-based technologies toward more sustainable energy production and resource consumption [8, 62]. Albeit several major technologic forward leaps are



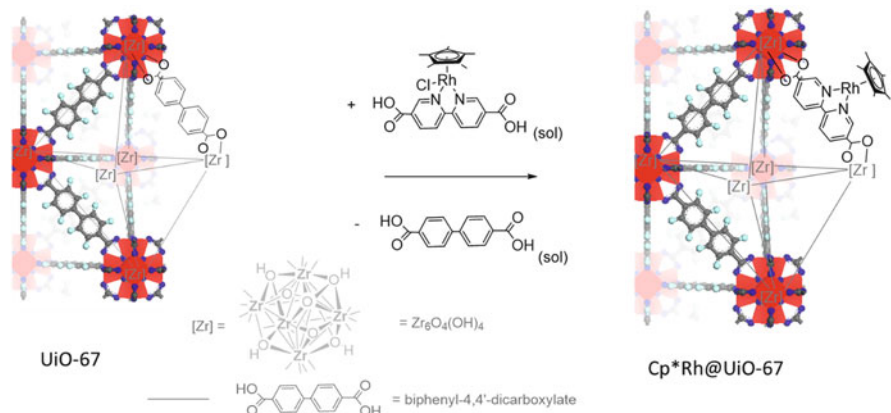
Scheme 9 Electrocatalytic conversion of CO₂ into formate using [(η⁵-Me₅Cp₅)Rh(bpy)Cl]⁺ as electrocatalyst [64]

necessary to achieve large-scale utilization of photo catalyst, the field already has decade-old precedents as far as Rh-based systems are concerned. The use of Rh-based photocatalysts was firstly disclosed in 1994, when Rasko and Solymosi found that CO₂ photoactivation is stronger over Rh/TiO₂ than over the bare oxide, since the cleavage of a C–O bond was observed only for the test performed over Rh-loaded TiO₂ [66]. Such feature is in agreement with the use of Rh/TiO₂ as catalyst for the CO₂ photo-induced reduction reported the same year [67]. The comparison between TiO₂ and Rh-loaded TiO₂ catalytic behavior in the photoreduction of CO₂ in water showed that the deposition of Rh on TiO₂ leads to an enhancement of the conversion of CO₂ and to a change of the selectivity. In fact when the reaction is performed using pure TiO₂, formic acid and formaldehyde are the only products; using Rh-loaded titania catalysts, methanol was also detected. Eventually, W⁺⁶-doped titania and optimized pretreatment, enabled a near-selective production of methanol [67].

The Rh/TiO₂ catalyst was also tested in the gas phase reduction of CO₂ with H₂ [68]. The catalytic results showed that both activity and selectivity strongly depend on the rhodium loading. The 0.5–4% Rh-loading range was investigated, and it was found that low loading of Rh leads to high conversion of CO₂ and high selectivity into CO. On the contrary, high Rh loading suppresses the production of CO, giving rise to a small CH₄ production. The X-Ray absorption spectroscopy (XAS) characterization of the different Rh-loaded catalyst showed that rhodium oxidation state depends on the metal amount: the higher the metal amount the higher the Rh-metal/Rh-oxide ratio. Comparing the catalytic results and XAS experiments, it was stated that more the Rh is reduced, the higher the CH₄ selectivity. It was also seen that this catalyst is mildly affected by deactivation. This slow deactivation was firstly ascribed to the formation of rhodium carbonyl compounds, but further studies [69] disproved this hypothesis, since no carbonylic species were detected by IR tests. Hence, it was suggested that the deactivation is due to the CO reduction into CH_x species, which stay over the Rh/TiO₂ and could be not detected by IR means.

Recently, it was found that the use of light-harvesting complexes (LHC) enhance the catalytic activity of Rh-doped TiO₂ in the aqueous phase reduction of CO₂ [70]. In fact, the catalytic results showed that the yields in acetaldehyde and methyl formate are ten and four times higher, respectively, when the LHC is used. A Rh-containing species (Rh_{1.32}Cr_{0.66}O₃) has been used as co-catalyst in the CO₂ reduction into methanol, while the catalyst is a solid solution of Cu, Ag, In, Zn, and S [71]. However, the catalytic performances of such couple are lower than those when the Rh co-catalyst is replaced with RuO₂.

Recently, the very same rhodium-based electrocatalysts discovered by the end of the twentieth century (see Scheme 9) were reported to be active photocatalyst for the reduction of CO₂ into formic acid [72]. By careful engineering of the 2,2'-bipyridine moiety, it was possible to enchain this molecular Rh(III) arrangements in a solid crystalline scaffold, namely, metal-organic framework MOF UiO-67 (see Scheme 10). Interestingly, the catalytic behavior of Cp*Rh(bpydc)Cl₂ (bpydc = 2,2'-bipyridine-5,5'-dicarboxylic acid) in solution and supported in MOF UiO-67 is similar as demonstrated by the similar TON values (42 and 47 for



Scheme 10 UiO-67 functionalization with the active photocatalytic species: $\text{Cp}^*\text{Rh}(\text{bpydc})\text{Cl}_2$ [72]

the unsupported and for the MOF-supported, respectively) [72], thus providing an example of a Rh-based solid system en route to the artificial leaf objective [73].

5 Conclusion

In conclusion, rhodium has a very well-established track record as an early key player in the catalytic reduction of carbon dioxide. The first examples reported in molecular chemistry were almost concomitant with that of several Rh-based Wilkinson-type catalyst deployments which contributed to several major industrial milestones; rhodium was indeed a key element in the Monsanto process for acetic acid production, in the asymmetric hydrogenation in L-DOPA production and is still very present in the three-way catalytic converter for deNO_x activity or in the asymmetric isomerization en route to menthol [32]. The activation of CO₂ was therefore one among of the several landmark achievements for this metal with many industrial applications.

As a member of the platinum group metals (PGM) cluster, rhodium also suffers from the same cost issues of its congeners. This aspect explains in part the subsequent research effort dedicated at its substitution by more accessible and possibly even more active alternative. Nevertheless, rhodium continues to play a key role, either because its content has been successfully diluted rather than fully removed (e.g., Ni–Rh systems) or because it is active in cutting edge applications where the frontier is more about finding some activity at all, rather than improving existing ones. Photocatalysis is a paragon of this strategy, since it aims at the blue sky objective of injecting REN in our current infrastructure. In this area, rhodium-based catalysts are among the key molecular species. This exemplifies well that rhodium is still front and center in many crucial field of catalysis, among which carbon dioxide utilization.

Acknowledgments DB and EAQ gratefully acknowledge the SINCHEM Joint Doctorate program selected under the Erasmus Mundus Action 1 Program – FPA 2013–0037. EAQ acknowledges support from French CNRS, University Claude Bernard Lyon and CPE Lyon. DB thanks Fondazione “Toso Montanari” from Bologna (Italy).

References

1. Lawrence Livermore National Laboratory. https://flowcharts.llnl.gov/content/assets/images/charts/Energy/ENERGY_2011_WORLD.png. Accessed 26 June 2016
2. International Energy Agency (2015) World Energy Outlook 2015
3. International Energy Agency. <http://www.iea.org/publications/scenariosandprojections/>. Accessed 29 June 2016
4. DePaolo DJ, Cole DR (2013) Geochemistry of geologic carbon sequestration: an overview. *Rev Mineralogy Geochem* 77(1):1–14
5. Aresta M, Dibenedetto A, Quaranta E (2016) *J Catalysis*. <http://dx.doi.org/10.1016/j.jcat.2016.04.003>
6. Liu Q, Wu L, Jackstell R, Beller M. Using carbon dioxide as a building block in organic synthesis
7. Styring P, Armstrong K, Quadrelli EA (eds) (2014) Carbon dioxide utilisation: closing the carbon cycle, 1st ed. Elsevier, Amsterdam, ISBN: 978-0-444-62746-9, 311 pp
8. Quadrelli EA, Centi G, Duplan J-L, Perathoner S (2011) Carbon dioxide recycling: emerging large-scale technologies with industrial potential. *ChemSusChem* 4(9):1194–1215
9. Centi G, Quadrelli EA, Perathoner S (2013) Catalysis for CO₂ conversion: a key technology for rapid introduction of renewable energy in the value chain of chemical industries. *Energy Environ Sci* 6(6):1711–1731
10. Klankermayer J, Leitner W (2016) Harnessing renewable energy with CO₂ for the chemical value chain: challenges and opportunities for catalysis. *Philos Trans A Math Phys Eng Sci* 374 (2016)
11. Dechema Gesellschaft für Chemische Technik und Biotechnologie e. V International Energy Agency (IEA) and International Council of Chemical Associations (ICCA) Technology Roadmap. https://www.iea.org/publications/freepublications/publication/Chemical_Roadmap_2013_Final_WEB.pdf. Accessed 24 June
12. Hietala J, Vuori A, Johnsson P, Pollari I, Reutemann W, Kieczka H (2000) Formic acid. In: Ullmann’s encyclopedia of industrial chemistry. Wiley-VCH Verlag GmbH & Co. KGaA
13. Joó F (2008) Breakthroughs in hydrogen storage—formic acid as a sustainable storage material for hydrogen. *ChemSusChem* 1(10):805–808
14. Loges B, Boddien A, Junge H, Beller M (2008) Controlled generation of hydrogen from formic acid amine adducts at room temperature and application in H₂/O₂ fuel cells. *Angew Chem Int Ed* 47(21):3962–3965
15. Fellay C, Dyson PJ, Laurency G (2008) A viable hydrogen-storage system based on selective formic acid decomposition with a ruthenium catalyst. *Angew Chem Int Ed* 47(21):3966–3968
16. Inoue Y, Izumida H, Sasaki Y, Hashimoto H (1976) Catalytic fixation of carbon dioxide to formic acid by transition-metal complexes under mild conditions. *Chem Lett* 5(8):863–864
17. Ezhova NN, Kolesnichenko NV, Bulygin AV, Slivinskii EV, Han S (2002) Hydrogenation of CO₂ to formic acid in the presence of the Wilkinson complex. *Russ Chem Bull* 51 (12):2165–2169
18. Leitner W, Dinjus E, Gaßner F (1994) Activation of carbon dioxide. *J Organomet Chem* 475 (1):257–266
19. Fornika R, Gorls H, Seemann B, Leitner W (1995) Complexes [(P₂)Rh(hfacac)] (P₂ = bidentate chelating phosphane, hfacac = hexafluoroacetylacetonate) as catalysts for

- CO₂ hydrogenation: correlations between solid state structures, 103Rh NMR shifts and catalytic activities. *J Chem Soc Chem Commun* (14):1479–1481
20. Angermund K, Baumann W, Dinjus E, Fornika R, Görls H, Kessler M, Krüger C, Leitner W, Lutz F (1997) Complexes [(P2)Rh(hfacac)] as model compounds for the fragment [(P2)Rh] and as highly active catalysts for CO₂ hydrogenation: the accessible molecular surface (AMS) model as an approach to quantifying the intrinsic steric properties of chelating ligands in homogeneous catalysis. *Chem Eur J* 3(5):755–764
 21. Gassner F, Leitner W (1993) Hydrogenation of carbon dioxide to formic acid using water-soluble rhodium catalysts. *J Chem Soc Chem Commun* (19):1465–1466
 22. Jessop PG, Joó F, Tai C-C (2004) Recent advances in the homogeneous hydrogenation of carbon dioxide. *Coord Chem Rev* 248(21–24):2425–2442
 23. Musashi Y, Sakaki S (2002) Theoretical study of Rhodium(III)-catalyzed hydrogenation of carbon dioxide into formic acid. Significant differences in reactivity among Rhodium(III), Rhodium(I), and Ruthenium(II) complexes. *J Am Chem Soc* 124(25):7588–7603
 24. Li Y-N, He L-N, Lang X-D, Liu X-F, Zhang S (2014) An integrated process of CO₂ capture and in situ hydrogenation to formate using a tunable ethoxyl-functionalized amidine and Rh/bisphosphine system. *RSC Adv* 4(91):49995–50002
 25. Sakakura T, Choi J-C, Yasuda H (2007) Transformation of carbon dioxide. *Chem Rev* 107(6):2365–2387
 26. Ukai K, Aoki M, Takaya J, Iwasawa N (2006) Rhodium(I)-catalyzed carboxylation of aryl- and alkenylboronic esters with CO₂. *J Am Chem Soc* 128(27):8706–8707
 27. Mizuno H, Takaya J, Iwasawa N (2011) Rhodium(I)-catalyzed direct carboxylation of arenes with CO₂ via chelation-assisted C–H bond activation. *J Am Chem Soc* 133(5):1251–1253
 28. Suga T, Mizuno H, Takaya J, Iwasawa N (2014) Direct carboxylation of simple arenes with CO₂ through a rhodium-catalyzed C–H bond activation. *Chem Commun* 50(92):14360–14363
 29. Kawashima S, Aikawa K, Mikami K (2016) Rhodium-catalyzed hydrocarboxylation of olefins with carbon dioxide. *Eur J Org Chem*
 30. Ostapowicz TG, Schmitz M, Krystof M, Klankermayer J, Leitner W (2013) Carbon dioxide as a C1 building block for the formation of carboxylic acids by formal catalytic hydrocarboxylation. *Angew Chem Int Ed* 52(46):12119–12123
 31. Maitlis PM, Haynes A, Sunley GJ, Howard MJ (1996) Methanol carbonylation revisited: thirty years on. *J Chem Soc Dalton Trans* (11):2187–2196
 32. Gian Paolo Chiusoli PMM (2006) Metal-catalysis in industrial organic processes
 33. Qian Q, Zhang J, Cui M, Han B (2016) Synthesis of acetic acid via methanol hydrocarboxylation with CO₂ and H₂. *Nat Commun* 7
 34. Wu L, Liu Q, Jackstell R, Beller M (2014) Carbonylations of alkenes with CO surrogates. *Angew Chem Int Ed* 53(25):6310–6320
 35. Aziz MAA, Jalil AA, Triwahyono S, Ahmad A (2015) CO₂ methanation over heterogeneous catalysts: recent progress and future prospects. *Green Chem* 17(5):2647–2663
 36. Wei W, Jinlong G (2011) Methanation of carbon dioxide: an overview. *Front Chem Sci Eng* 5(1):2–10
 37. Solymosi F, Erdöhelyi A, Bánsági T (1981) Methanation of CO₂ on supported rhodium catalyst. *J Catal* 68(2):371–382
 38. Ruiz P, Jacquemin M, Blangenois N (2010) Catalytic CO₂ methanation process. Google Patents
 39. Beuls A, Swalus C, Jacquemin M, Heyen G, Karelovic A, Ruiz P (2012) Methanation of CO₂: further insight into the mechanism over Rh/γ-Al₂O₃ catalyst. *Appl Catal B Environ* 113–114:2–10
 40. Karelovic A, Ruiz P (2013) Mechanistic study of low temperature CO₂ methanation over Rh/TiO₂ catalysts. *J Catal* 301:141–153
 41. Jacquemin M, Beuls A, Ruiz P (2010) Catalytic production of methane from CO₂ and H₂ at low temperature: insight on the reaction mechanism. *Catal Today* 157(1–4):462–466

42. Karelavic A, Ruiz P (2012) CO₂ hydrogenation at low temperature over Rh/ γ -Al₂O₃ catalysts: effect of the metal particle size on catalytic performances and reaction mechanism. *Appl Catal Environ* 113–114:237–249
43. Ichikawa S (1995) Chemical conversion of carbon dioxide by catalytic hydrogenation and room temperature photoelectrocatalysis. *Energy Conversion Manag* 36(6–9):613–616
44. Karelavic A, Ruiz P (2013) Improving the hydrogenation function of Pd/ γ -Al₂O₃ catalyst by Rh/ γ -Al₂O₃ addition in CO₂ methanation at low temperature. *ACS Catal* 3(12):2799–2812
45. Swalus C, Jacquemin M, Poleunis C, Bertrand P, Ruiz P (2012) CO₂ methanation on Rh/ γ -Al₂O₃ catalyst at low temperature: “In situ” supply of hydrogen by Ni/activated carbon catalyst. *Appl Catal Environ* 125:41–50
46. Aziz MAA, Jalil AA, Triwahyono S, Sidik SM (2014) Methanation of carbon dioxide on metal-promoted mesostructured silica nanoparticles. *Appl Catal Gen* 486:115–122
47. Zhang Y, Zhan X, Zheng X, Wang Z, Fang Z, Xue Y, Tao L (2015) Liquid catalyst for methanation of carbon dioxide. US 20150126626
48. Pakhare D, Spivey J (2014) A review of dry (CO₂) reforming of methane over noble metal catalysts. *Chem Soc Rev* 43(22):7813–7837
49. Havran V, Duduković MP, Lo CS (2011) Conversion of methane and carbon dioxide to higher value products. *Ind Eng Chem Res* 50(12):7089–7100
50. Richardson JT, Paripatyadar SA (1990) Carbon dioxide reforming of methane with supported rhodium. *Appl Catal* 61(1):293–309
51. Zhang ZL, Tshipouriaris VA, Efstathiou AM, Verykios XE (1996) Reforming of methane with carbon dioxide to synthesis gas over supported rhodium catalysts: I. Effects of support and metal crystallite size on reaction activity and deactivation characteristics. *J Catal* 158(1):51–63
52. Wang HY, Ruckenstein E (2000) Carbon dioxide reforming of methane to synthesis gas over supported rhodium catalysts: the effect of support. *Appl Catal A Gen* 204(1):143–152
53. Asencios YJO, Assaf EM (2013) Combination of dry reforming and partial oxidation of methane on NiO–MgO–ZrO₂ catalyst: effect of nickel content. *Fuel Process Technol* 106:247–252
54. Józwiak WK, Nowosielska M, Rynkowski J (2005) Reforming of methane with carbon dioxide over supported bimetallic catalysts containing Ni and noble metal: I. Characterization and activity of SiO₂ supported Ni–Rh catalysts. *Appl Catal Gen* 280(2):233–244
55. Estephane J, Ayoub M, Safieh K, Kaydoun M-N, Casale S, Zakhem HE (2015) CO₂ reforming of CH₄ over highly active and stable γ RhNix/NaY catalysts. *Comptes Rendus Chimie* 18(3):277–282
56. Basile F, Fornasari G, Poluzzi E, Vaccari A (1998) Catalytic partial oxidation and CO₂-reforming on Rh- and Ni-based catalysts obtained from hydrotalcite-type precursors. *Appl Clay Sci* 13(5–6):329–345
57. Pakhare D, Wu H, Narendra S, Abdelsayed V, Haynes D, Shekhawat D, Berry D, Spivey J (2013) Characterization and activity study of the Rh-substituted pyrochlores for CO₂ (dry) reforming of CH₄. *Appl Petrochem Res* 3(3–4):117–129
58. Kusama H, Okabe K, Sayama K, Arakawa H (1996) CO₂ hydrogenation to ethanol over promoted Rh/SiO₂ catalysts. *Catal Today* 28(3):261–266
59. Kusama H, Okabe K, Sayama K, Arakawa H (1997) Ethanol synthesis by catalytic hydrogenation of CO₂ over Rh-Fe/SiO₂ catalysts. *Energy* 22(2–3):343–348
60. Ikehara N, Hara K, Satsuma A, Hattori T, Murakami Y (1994) Unique temperature dependence of acetic acid formation in CO₂ hydrogenation on Ag-promoted Rh/SiO₂ catalyst. *Chem Lett* 23(2):263–264
61. Ding Y-H, Huang W, Wang Y-G (2007) Direct synthesis of acetic acid from CH₄ and CO₂ by a step-wise route over Pd/SiO₂ and Rh/SiO₂ catalysts. *Fuel Process Technol* 88(4):319–324
62. Quadrelli EA (2016) 25 years of energy and green chemistry: saving, storing, distributing and using energy responsibly. *Green Chem* 18(2):328–330
63. Bolinger CM, Story N, Sullivan BP, Meyer TJ (1988) Electrocatalytic reduction of carbon dioxide by 2,2′-bipyridine complexes of rhodium and iridium. *Inorg Chem* 27(25):4582–4587

64. Caix C, Chardon-Noblat S, Deronzier A (1997) Electrocatalytic reduction of CO₂ into formate with [(η⁵-Me₅C₅)M(L)Cl] + complexes (L = 2,2'-bipyridine ligands; M = Rh(III) and Ir(III)). *J Electroanal Chem* 434(1–2):163–170
65. Kushi Y, Nagao H, Nishioka T, Isobe K, Tanaka K (1994) Oxalate formation in electrochemical CO₂ reduction catalyzed by rhodium-sulfur cluster. *Chem Lett* 23(11):2175–2178
66. Rasko J, Solymosi F (1994) Infrared spectroscopic study of the photoinduced activation of CO₂ on TiO₂ and Rh/TiO₂ catalysts. *J Phys Chem* 98(29):7147–7152
67. Solymosi F, Tombácz I (1994) Photocatalytic reaction of H₂O + CO₂ over pure and doped Rh/TiO₂. *Catal Lett* 27(1):61–65
68. Kohno Y, Hayashi H, Takenaka S, Tanaka T, Funabiki T, Yoshida S (1999) Photo-enhanced reduction of carbon dioxide with hydrogen over Rh/TiO₂. *J Photochem Photobiol A Chem* 126(1–3):117–123
69. Kohno Y, Yamamoto T, Tanaka T, Funabiki T (2001) Photoenhanced reduction of CO₂ by H₂ over Rh/TiO₂: characterization of supported Rh species by means of infrared and X-ray absorption spectroscopy. *J Mol Catal A Chem* 175(1–2):173–178
70. Lee C-W, Antoniou Kourounioti R, Wu JCS, Murchie E, Maroto-Valer M, Jensen OE, Huang C-W, Ruban A (2014) Photocatalytic conversion of CO₂ to hydrocarbons by light-harvesting complex assisted Rh-doped TiO₂ photocatalyst. *J CO₂ Utilization* 5:33–40
71. Liu J-Y, Garg B, Ling Y-C (2011) Cu_xAg_yIn_zZn_kSm solid solutions customized with RuO₂ or Rh_{1.32}Cr_{0.66}O₃ co-catalyst display visible light-driven catalytic activity for CO₂ reduction to CH₃OH. *Green Chem* 13(8):2029–2031
72. Chambers MB, Wang X, Elgrishi N, Hendon CH, Walsh A, Bonnefoy J, Canivet J, Quadrelli EA, Farrusseng D, Mellot-Draznieks C, Fontecave M (2015) Photocatalytic carbon dioxide reduction with rhodium-based catalysts in solution and heterogenized within metal-organic frameworks. *ChemSusChem* 8(4):603–608
73. Centi G, Perathoner S (2000) Artificial leaves. In: Kirk-Othmer encyclopedia of chemical technology. Wiley

Index

A

- Acetaldehyde, 277
- Acetalization, 78–81
- 2-Acetamidomethylcinnamic acids,
 - asymmetric hydrogenation, 241
- Acetic acid, 70, 196, 271, 272, 278
- Achalensolide, 218, 223
- Acylguanidyldiphenylphosphine, 77
- 3-Acyloxy-1,4-enynes, 171
- Aflatoxins, 80
- Agarofuran, 222
- Alcohols, 70, 75, 157, 216, 235, 242
 - benzylic, 160
 - homoallylic, 82, 126–129
 - hydroformylation, 79
- Aldehydes, 19, 43, 70, 99, 145, 167, 208, 213, 223, 240
 - decarbonylation, 149, 167, 215
- Alditols, 161
- Aldonic acids, 161
- Aldoses, 161
- Alkenediols, 79
- Alkenes, cyclic, 15
 - diboration, 13
 - disubstituted, 123
 - hydroboration, 2
 - hydroformylation, 70, 101, 104
- Alkenylboronate, 7
- Alkenylboronic acids, 269
- Alkenylidenecyclopropanes, 205
- Alkenyl pinacolboronates, 3
- Alkoxyallenynes, 191
- Alkoxybenzoazaphosphole, 129
- α -Alkylacrylates, asymmetric hydroformylation, 137
- Alkylarenes, 21
- Alkylboronate esters, 21
- 3-Alkylideneoxindoles, 15
- Alkylthiolation, 42
- Alkynes, 31, 43
 - 2-Alkynylaryl isocyanates, 15, 17
- Allene(s), 31, 34, 53, 60, 61, 167, 197
- Allenes, 191–193, 220
- Allenylcyclobutanols, 176
- Allenylcyclopropanes, 176, 224
- Allenylphenylacetoneitriles, 201
- Allenynes, 187–192, 217–225
- Allenynones, 190
- Allyl carbamates, 120
- Allyl cyanide, hydroformylation, 106
- Amino acid derivatives, 135
- α -Aminoalkylboronates, 2
- 3-Amino-1,2-diols, 14
- Anethole, 123
- Aroyl hydrazides, 152
- Arylalkenes, hydroaminomethylation, 92
- Aryl-aryl coupling, 145
- Aryl-aryl cross-coupling, 154
- 3-aryl-3-aryloxypropionic acids, 245
- α -Arylenamides, 4
- Arylethylamines, 92
- Aryl halides, borylation, 22
- Arylpyridines, olefination, 150
- Aryl 2-pyridyl ethers, 25
- Arylsulfonyl hydrazides, 152
- Asterisca-3(15),6-diene, 219

Asteriscanolide, 167, 222
 Asymmetric catalysis, 99, 167
 Asymmetric hydroformylation using
 rhodium catalysts, 99–139
 Asymmetric hydrogenation, 231
 Azababicyclo-[2.2.1]hept-5-en-3-ones, 134
 Azaborines, 3
 Azocanes, 206

B

Benzaldehyde, 148, 163, 215, 241
 decarbonylation, 148
 BenzaPhos, 255
 Benzene, borylation, 20
 carboxylation, 269
 Benzene-1,3,5-tricarboxamides (BTA), 256
 Benzonitriles, borylation, 24
 1,3-Benzothiazoles, 43
 Benzothiophene, 43
 1,3-Benzoxazoles, 43
 BettiPhos, 122
 BIBOP, 115
 Bicyclohexanones, 202
 Bicyclo[3.3.0]octenones, 208
 Bicyclopentenone, 192, 214
 BINAP, 157, 184, 214, 246
 BINAPHANE, 36
 BINAPHOS, 108–111, 123, 130, 133, 138
 BINAPINE, 111, 114, 116
 BINOL, 117, 233–238, 242, 244, 254
 BIPHEMPHOS, 133
 Biphephos, 74, 82, 87
 Bis(allene)s, 196
 Bis(boronate) compounds, 11
 1,2-Bis(diphenylphosphino)butane (dppb),
 55, 157, 158, 179
 2,2'-Bis(dipyrrolylphosphinoxy)
 1,1'-binaphthyl, 73
 Bis(neopentyl glycolato)diboron, 9, 18
 Bis-phosphinite ligands, 117–118
 Bis-phosphonite ligands, 117
 Bis(pinacolato)diboron, 4
 Bisborylrhodium, 5
 Bisdiazaphospholane, 82
 Bisoxazolines, 257
 Bisphosphacyclic ligands, 114–117
 Bisphospholane, 114
 BMIM, 162
 BOBPHOS, 115
N-Boc-2,2-dimethyl-2,3-dihydrooxazole, 132
 Boronate esters, 2
 Borylation, 1–26
N-Boryl-1,2-dihydropyridine, 3
 Butanal, 100

Butanediol, 76, 105
 Butene, 72
 (*t*-Butylthio)acetylene, 55
 Butyraldehyde, 100

C

Calixarene, 134
 Camphene, 94
 Carbocyclizations, 167–225
 Carbohydrates, 108, 128, 130, 161, 216
 Carbon capture and utilization (CCU), 268
 Carbon dioxide, 263–278
 methanation, 272
 Carbon monoxide, 70, 100, 146, 167,
 169, 213
 Carbonyl(s), 55, 63, 70, 146, 169, 274, 277
 α,β -unsaturated, 18
 Carbonylation, 69, 133, 146, 271
 Carbothiolation, 31, 34, 53–56
 Carboxylic acids, 70, 77, 95, 117, 150,
 263, 269
 Carene, 225
 Catalysis, 1
 asymmetric, 89, 99, 167
 heterogeneous, 272
 homogeneous, 231, 263
 Catecholborane, 2
 C–B bond, 1
 C–H activation, 31, 39
 Chiral ligands, 99
 CHIRAPHITE, 111
 Chromenes, 162
 Cinnamaldehyde, 159, 213, 214, 217
 Cinnamic acids, 151, 231
 Cinnamic aldehyde, olefination, 150
 Cinnamyl alcohol, 216
 Cinnamyl sulfide, 36
 Citronellal, 148
 Citronellene, 79
 Continuous-flow systems, 145, 163
 Coupling, aryl-aryl, 145
 Cross-coupling, 31, 35, 145, 149
 Crown ethers, 256
 C–S bond, formation, 31
 Cyanoindole, 224
p-Cyano- α -methylthioacetophenone, 42
 Cyanosporasides, 221
 2-Cyanothiophene, 43
 Cycloaddition, 159, 168, 179, 196, 201, 207
 Diels–Alder, 180, 225
 Pauson–Khand, 145, 160
 Cyclocarbonylation, 167–226
 Cyclohexene, 78
 Cyclopentadiene, 173

Cyclopentadienone, 180, 181
Cyclopentane, 209
Cyclopentene, 78, 91, 193
Cyclopentenols, 171
Cyclopentenones, 160, 169, 171, 177, 187, 189, 198, 221
Cyclopropylbicyclo[4.1.0]hept-2-enes, 207

D

Decarbonylation, 145–163
 enantioselective, 159
1-Decyne, 55
Dehydroformylation, 160
Deoxy-1,2-*O*-
 isopropylidene- α -D-glucopyranose, 106
Desoxyhypnophilin, 219
Dialkylacrylamides, hydroformylation, 120
1,1-Diarylethanes, 159
1,8-Diazabicyclo[5.4.0]undec-7-ene
 (DBU), 268
Diazaphospholane, 111, 115
 α -Diazoesters, 4
Diboration, Rh-catalyzed, 11
Diboron, reagents, 1–25
 Rh-activation, 5
Didodecyl disulfide, 36
Diels–Alder, cycloadditions, 180, 225
 decarbonylation, 158
1,3-Dienes, 109
 hydroformylation, 122
1,6-Dienes, 195
Diényl Pauson–Khand-type reaction, 194
Dienynes, 186
2,7-Di-*n*-hexyl-9,9-dimethyl-4,5-bis
 (10-dimethyl-phenoxaphosphino)
 xanthene, 73
Dihydrofurans, 130
Diisoproamine, 93
Dimethyl itaconate, asymmetric
 hydrogenation, 117
Dimethylacetylenedicarboxylate, 243
DIOP, 76, 135, 253
Dioxapines, 130
Diphenylamines, 93
1,2-Diphenyl-2-methylthio-1-ethanone, 43
o-Diphenylphosphanylbenzene
 (*o*-DPPB), 81
Disphosphite, 104
Dithiaparacyclophanes, 36
Dodecane, 90
Dodecene, 90, 91, 115
Dodecyne, 57
Dry reforming, 274
DuPHOS, 115, 170, 239

E

Electrocatalysis, 263, 276
Enamides, 123, 127, 231, 242, 258
Enamido phosphonates, 243
Enantioselectivity, 5, 60, 99, 242, 257
Ene-dienynes, 179, 184, 204, 210
Enynes, 160, 177, 185, 218
ESPHOS, 115
Estragole, 94, 123
Ethanalamine, 74, 91, 267
Ethylenedithioethers, 35
Ethylhexanol, 100
Ethyl oleate, 95

F

Fatty acids, hydroaminomethylation, 93
Fenpiprane, 93
Flurbiprofen, 244
Formaldehyde, 35, 115, 213, 214, 277
 dithioacetals, 35
Formic acid, 263, 266, 277
N-Formyl-dehydroamino acid esters,
 asymmetric hydrogenation, 240
Furanones, 171

G

Glutathione disulfide, 50
Grayanotoxin, 221
Guaianolide, 218
Guanacastepene A, 217

H

Halides, 22, 31, 149, 154, 159, 238, 244
Heck coupling, 145, 152–154
N-Heterocyclic carbene (NHC), 8, 13, 60–64
Heterogeneous catalysis, 263, 272
Hexane-2,4-diol, 105
Hexylamine, 95
Hirsutene, 219
Hirsutic acid C, 220
Homogeneous catalysis, 231, 263
Hydroaminomethylation (HAM), 84
Hydroboration, Rh-catalyzed, 2
Hydrocarboxylation, 270–272
Hydroformylation, 69–139, 162, 272
Hydroformylation-acetalization, 78
Hydroformylation-hydrogenation, 75
Hydroformylation-Wittig olefination, 81
Hydrogenations, 75, 231, 240–259, 272
Hydrotalcite, 275
Hydrothiolation, 31, 34, 42, 53, 55–64
7-Hydroxyenoates, 82

I

Ibuprofen, 244
Indicanone, 224
Indolines, 48, 49
Ingenol, 167, 224
Ionic liquids (ILs), 79, 145, 146, 162, 236
Iphos, 73
Isolimonene, 78
Isomenthone, 148
Isomerization-hydroformylation, 72–75
Isopropyliden- α -D-xylofuranose, 106
Itaconic acid, 241
Itaconic esters, 231

K

KELLIPHITE, 109, 134
Ketazines, 47
Ketoprofen, 244

L

LEUPhos, 252
Ligands, chiral, 99
 monodentate, 231
Light-harvesting complexes (LHC), 277
Limonene, 79, 93
Linalool, 79, 80
Lutidine, 79

M

Markovnikov selectivity, 62
Menthone, 148
Mesostructured silica nanoparticles (MSN), 273
Metal–organic frameworks (MOFs),
 BINAP-based, 217
METAMORPhos, 251
Metathesis, 10
Methanation, 272
Methane dry reforming (MDR), 274
4-Methoxy styrene, 5
Methoxycarbonylation, 162
Methyl 2-acetamido-acrylate, 250
Methyl 2-acetamido-cinnamate, 233, 247
Methyl *N*-acetyl 2-indolecarboxylate, 243
3-Methylpentanal, 77
Methylstyrene, asymmetric
 hydroformylation, 135
1-Methyltetrazole, 43
Methylthiolation, 42–44
Molecular cage, 120
Monoborylalkane, 6

Monodentate ligands, 231
Monoterpenes, 79
Morpholine, 94

N

Naphos, 73, 74, 91
2-Naphthaldehyde, 157
Naproxen, 244
Natural products, 167
Neopentylborane, 2
Nitriles, borylation, 24
Nitroalkanes, 42
Nonanal, 74

O

Oct-4-ene, 74
Olefins, carboxylation, 270
Oppenauer oxidation, 145, 157
Oxalate, 276

P

PAMP, 232
Patulolide C, 83, 128
Pauson–Khand reactions, 145, 146, 159, 160,
 167, 169, 187, 194
Penicillamine, 78
Pent-2-ene, hydroformylation, 73
Pentafluorobenzaldehyde, 213
Pentafluorobenzenes, 38
Pentafluoropyridine, 22
Pentalenene, 219, 220
Pentamidine, 93
Pentane, 13
Pentane-1,2-diol, 105, 106
Perhydrofuro[2,3-*b*]furans, 80
Phenylalanine, 232
2-Phenylbenzodioxaborole, 20
Phenylpyridines, 269
Phenylpropyl sulfide, 36
Phenylpyrazoles, 269
Phenylpyridine, oxidative arylation, 155
 sulfenylation, 47
7-(Phenylthio)-1*H*-indole, 48
 α -(Phenylthio)isobutyrophenone, 44
Phenylthiolation, 44
Phorbol, 225
Phosphanylpyridone, 77
Phosphepines, 251
Phosphine–phosphite ligands, 108
Phosphine–phosphoramidite, 114

- Phosphines, 51, 59, 147, 156, 231, 233, 239, 253
Phosphine oxides, 239
Phosphites, 75, 101, 104, 110, 231–249, 254, 257
Phospholanes, 251
Phosphonites, 231, 235
Phosphonium ylide, 81
Phosphoramidites, 231, 235, 258
Phosphorus, 99
Phosphorus ylides, 81
Phosphorus-based ligands, monodentate, 118
Phosphineoxides, secondary, 231
Photocatalysis, 263, 276
PhthalaPhos, 255
Pinacolborane, 3
Pinene, 78
PipPhos, 258
Prelog–Djerassi lactone, 117
Propene, 75, 100
Prozapine, 93
Pyridines, 3, 60–63, 79, 124, 156
Pyridyl boronic esters, 22
Pyrochlores, 275
Pyrrolidine-2-carboxylic acid, 95
Pyrrolidines, 82
- Q**
Quinolinolate, 62
- R**
Raffinate II, 72
Regioselectivity, 99
Renin inhibitor, 258
Rh–PBP pincer, 4
Rh–NHC catalysts, 60–64
Rhodium, 1, 69, 31, 99, 167, 263
Rhodium–bisoxazolinyphenyl (Rh(Phebox)), 18
Rippertene, 221
Rotaxanes, 256
- S**
Sabatier reaction, 272
Scaffolding ligands, 125
Sesquiterpenoids, 220
SIPHOS, 235
SolPhos, 158
- SPINOL, 235, 240
Stereoselectivity, 1
Styrene, 78, 92, 103, 106–121, 152–154, 204
 hydroformylation, 106, 121
Styrylboronate esters, 14
Sugars, 145
Supramolecular catalysis, 231
SYNPHOS, 160, 161
Synthon A, 258
- T**
Tandem reactions, 145, 157
 hydroformylation, 69
Tandem/sequential reactions, 167
TANGPHOS, 114, 116, 134
Taniaphos I, 158
Terpinene, 79
Terpinolene, 79
Tetra(alkoxy)diboron, 6
Tetrafluoropyridyl boronic ester, 22
Tetrahydro- β -carboline, 231, 241
Tetrahydroisoquinoline, 126, 129
Tetrahydroquinoline, 89
Tetrahydrozoline, 133
Tetraphos, 74, 75
Tetrahydro-3-carbaldehyde, 128
Thiocamphor, 18
Thioethers, 31
 metathesis, 49
Thiolation, 31, 34, 55
Thiophenes, 110, 159
 hydroformylation, 110
Thiosulfenylation, 48
Tigliane, 224
2-(*m*-tolyl)pyridine, olefination, 150
Tri-*O*-acetyl-D-glucal, 79
Tricycloheptadienones, 210
2-Trifluoromethylallylic acid, 136
Trifluoromethylthiolation, 48
N-(Trifluoromethylthio)saccharin, 48
Trifluoroprop-1-en-2-yl acetate, 136
Triphenylphosphines, 239
Triphos, 147
- U**
UREAPhos, 253
Ureaphosphine, 252
Ureas, 21

V

- Valinol, 95
- Vinyl acetate, 78, 83
 - hydroformylation, 106, 118
- Vinylallenes, 170
- 4-Vinylanisole, diboration, 14
- Vinylarenes, 7, 11, 12, 15
 - hydroformylation, 105, 106
- N*-Vinyl carboxamides, 120
- Vinyl carboxylic acids, 150
- 3-Vinylcyclopentene, 176
- Vinylcyclopropenes, 173
- Vinylidenecyclopropanes (VDCPs), 193, 204, 208
- 2-Vinylnaphthalene, 92
- Vinyl sulfide, 57–62
- Vinyl thioethers, 51

W

- Walphos, 158, 258
- Water-gas shift reaction (WGS), 271
- Welwitindolinone C, 224
- Wilkinson's catalyst, 147, 149, 161, 232, 278
 - dissociative mechanism, 102
- Wittig olefination, 81, 125, 128

X

- Xantphos, 23, 76, 82, 86, 130, 157

Y

- YANPHOS, 110–112